

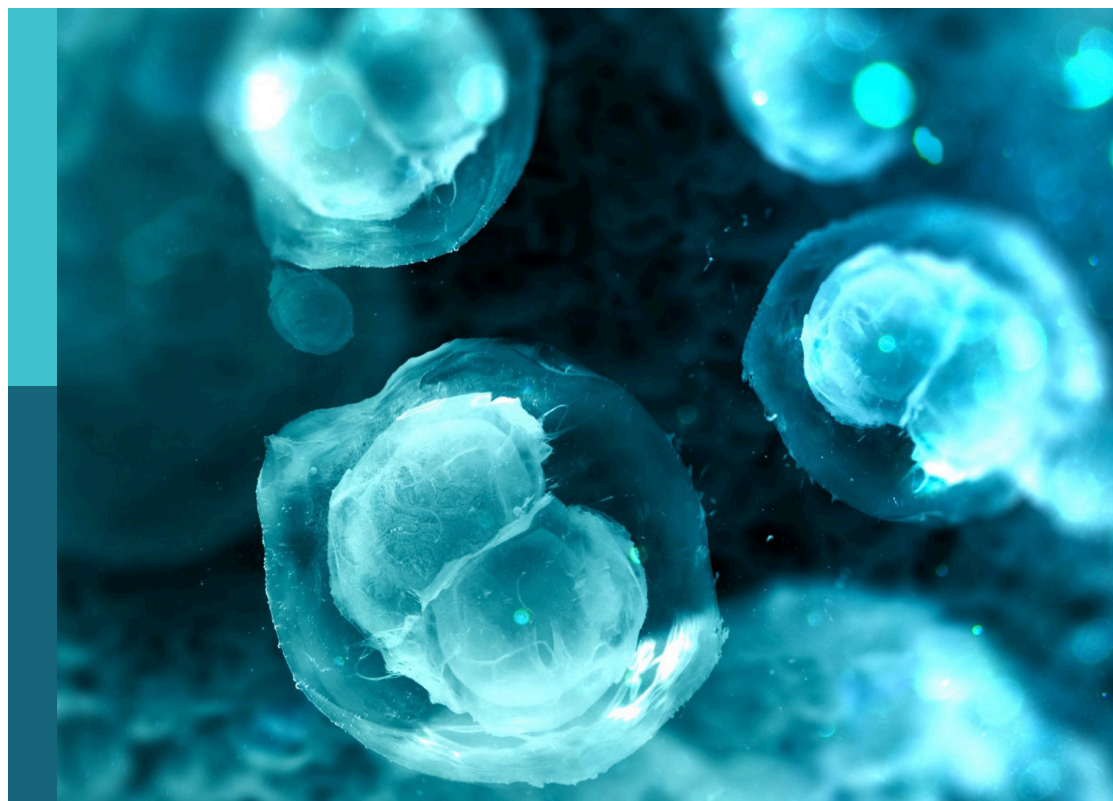
# Plasticity of cell polarity across scales in development and disease

**Edited by**

Eurico Morais-de-Sá, Josana Rodriguez, Alexander Ludwig and Jens Januschke

**Published in**

Frontiers in Cell and Developmental Biology  
Frontiers in Microbiology



## FRONTIERS EBOOK COPYRIGHT STATEMENT

The copyright in the text of individual articles in this ebook is the property of their respective authors or their respective institutions or funders. The copyright in graphics and images within each article may be subject to copyright of other parties. In both cases this is subject to a license granted to Frontiers.

The compilation of articles constituting this ebook is the property of Frontiers.

Each article within this ebook, and the ebook itself, are published under the most recent version of the Creative Commons CC-BY licence. The version current at the date of publication of this ebook is CC-BY 4.0. If the CC-BY licence is updated, the licence granted by Frontiers is automatically updated to the new version.

When exercising any right under the CC-BY licence, Frontiers must be attributed as the original publisher of the article or ebook, as applicable.

Authors have the responsibility of ensuring that any graphics or other materials which are the property of others may be included in the CC-BY licence, but this should be checked before relying on the CC-BY licence to reproduce those materials. Any copyright notices relating to those materials must be complied with.

Copyright and source acknowledgement notices may not be removed and must be displayed in any copy, derivative work or partial copy which includes the elements in question.

All copyright, and all rights therein, are protected by national and international copyright laws. The above represents a summary only. For further information please read Frontiers' Conditions for Website Use and Copyright Statement, and the applicable CC-BY licence.

ISSN 1664-8714  
ISBN 978-2-8325-3712-1  
DOI 10.3389/978-2-8325-3712-1

## About Frontiers

Frontiers is more than just an open access publisher of scholarly articles: it is a pioneering approach to the world of academia, radically improving the way scholarly research is managed. The grand vision of Frontiers is a world where all people have an equal opportunity to seek, share and generate knowledge. Frontiers provides immediate and permanent online open access to all its publications, but this alone is not enough to realize our grand goals.

## Frontiers journal series

The Frontiers journal series is a multi-tier and interdisciplinary set of open-access, online journals, promising a paradigm shift from the current review, selection and dissemination processes in academic publishing. All Frontiers journals are driven by researchers for researchers; therefore, they constitute a service to the scholarly community. At the same time, the *Frontiers journal series* operates on a revolutionary invention, the tiered publishing system, initially addressing specific communities of scholars, and gradually climbing up to broader public understanding, thus serving the interests of the lay society, too.

## Dedication to quality

Each Frontiers article is a landmark of the highest quality, thanks to genuinely collaborative interactions between authors and review editors, who include some of the world's best academicians. Research must be certified by peers before entering a stream of knowledge that may eventually reach the public - and shape society; therefore, Frontiers only applies the most rigorous and unbiased reviews. Frontiers revolutionizes research publishing by freely delivering the most outstanding research, evaluated with no bias from both the academic and social point of view. By applying the most advanced information technologies, Frontiers is catapulting scholarly publishing into a new generation.

## What are Frontiers Research Topics?

Frontiers Research Topics are very popular trademarks of the *Frontiers journals series*: they are collections of at least ten articles, all centered on a particular subject. With their unique mix of varied contributions from Original Research to Review Articles, Frontiers Research Topics unify the most influential researchers, the latest key findings and historical advances in a hot research area.

Find out more on how to host your own Frontiers Research Topic or contribute to one as an author by contacting the Frontiers editorial office: [frontiersin.org/about/contact](https://frontiersin.org/about/contact)

# Plasticity of cell polarity across scales in development and disease

## Topic editors

Eurico Morais-de-Sá — Universidade do Porto, Portugal

Josana Rodriguez — Newcastle University, United Kingdom

Alexander Ludwig — Nanyang Technological University, Singapore

Jens Januschke — University of Dundee, United Kingdom

## Citation

Morais-de-Sá, E., Rodriguez, J., Ludwig, A., Januschke, J., eds. (2023). *Plasticity of cell polarity across scales in development and disease*.

Lausanne: Frontiers Media SA. doi: 10.3389/978-2-8325-3712-1

## Table of contents

- 04 **GFP-Tagged Protein Detection by Electron Microscopy Using a GBP-APEX Tool in *Drosophila***  
Fred Bernard, Julie Jouette, Catherine Durieu, Rémi Le Borgne, Antoine Guichet and Sandra Claret
- 17 **ERM-1 Phosphorylation and NRFL-1 Redundantly Control Lumen Formation in the *C. elegans* Intestine**  
Jorian J. Sepers, João J. Ramalho, Jason R. Kroll, Ruben Schmidt and Mike Boxem
- 34 **Insights Into Mechanisms of Oriented Division From Studies in 3D Cellular Models**  
Federico Donà, Susanna Eli and Marina Mapelli
- 44 **Emerging Cnidarian Models for the Study of Epithelial Polarity**  
Lindsay I. Rathbun, Coralee A. Everett and Dan T. Bergstralh
- 60 **Polarity Events in the *Drosophila melanogaster* Oocyte**  
Ana Milas and Ivo A. Telley
- 73 **Won't You be My Neighbor: How Epithelial Cells Connect Together to Build Global Tissue Polarity**  
Lauren E. Cote and Jessica L. Feldman
- 83 **Epithelial Cell Polarity During *Drosophila* Midgut Development**  
Jia Chen and Daniel St Johnston
- 96 **Rho and Rab Family Small GTPases in the Regulation of Membrane Polarity in Epithelial Cells**  
Klaus Ebnet and Volker Gerke
- 110 **Emerging concepts on the mechanical interplay between migrating cells and microenvironment *in vivo***  
Guilherme Ventura and Jakub Sedzinski
- 119 **Cell polarity signalling at the birth of multicellularity: What can we learn from the first animals**  
Bree A. Wright, Marc Kvensakul, Bernd Schierwater and Patrick O. Humbert
- 138 **Pleiotropy drives evolutionary repair of the responsiveness of polarized cell growth to environmental cues**  
Enzo Kingma, Eveline T. Diepeveen, Leila Iñigo de la Cruz and Liedewij Laan





# GFP-Tagged Protein Detection by Electron Microscopy Using a GBP-APEX Tool in *Drosophila*

Fred Bernard<sup>1\*†</sup>, Julie Jouette<sup>1†</sup>, Catherine Durieu<sup>2</sup>, Rémi Le Borgne<sup>2</sup>, Antoine Guichet<sup>1\*</sup> and Sandra Claret<sup>1\*</sup>

<sup>1</sup> Polarity and Morphogenesis Team, Institut Jacques Monod, CNRS, UMR 7592, University of Paris, Paris, France,

<sup>2</sup> ImagoSeine Platform, Institut Jacques Monod, CNRS, UMR 7592, University of Paris, Paris, France

## OPEN ACCESS

### Edited by:

Alexander Ludwig,  
Nanyang Technological University,  
Singapore

### Reviewed by:

Nicholas Ariotti,  
University of New South Wales,  
Australia  
Markus Affolter,  
University of Basel, Switzerland

### \*Correspondence:

Fred Bernard  
frederic.bernard@ijm.fr  
Antoine Guichet  
antoine.guichet@ijm.fr  
Sandra Claret  
sandra.claret@ijm.fr

<sup>†</sup> These authors have contributed  
equally to this work

### Specialty section:

This article was submitted to  
Morphogenesis and Patterning,  
a section of the journal  
Frontiers in Cell and Developmental  
Biology

**Received:** 02 June 2021

**Accepted:** 12 July 2021

**Published:** 12 August 2021

### Citation:

Bernard F, Jouette J, Durieu C,  
Le Borgne R, Guichet A and Claret S  
(2021) GFP-Tagged Protein Detection  
by Electron Microscopy Using  
a GBP-APEX Tool in *Drosophila*.  
Front. Cell Dev. Biol. 9:719582.  
doi: 10.3389/fcell.2021.719582

In cell biology, detection of protein subcellular localizations is often achieved by optical microscopy techniques and more rarely by electron microscopy (EM) despite the greater resolution offered by EM. One of the possible reasons was that protein detection by EM required specific antibodies whereas this need could be circumvented by using fluorescently-tagged proteins in optical microscopy approaches. Recently, the description of a genetically encodable EM tag, the engineered ascorbate peroxidase (APEX), whose activity can be monitored by electron-dense DAB precipitates, has widened the possibilities of specific protein detection in EM. However, this technique still requires the generation of new molecular constructions. Thus, we decided to develop a versatile method that would take advantage of the numerous GFP-tagged proteins already existing and create a tool combining a nanobody anti-GFP (GBP) with APEX. This GBP-APEX tool allows a simple and efficient detection of any GFP fusion proteins without the needs of specific antibodies nor the generation of additional constructions. We have shown the feasibility and efficiency of this method to detect various proteins in *Drosophila* ovarian follicles such as nuclear proteins, proteins associated with endocytic vesicles, plasma membranes or nuclear envelopes. Lastly, we expressed this tool in *Drosophila* with the UAS/GAL4 system that enables spatiotemporal control of the protein detection.

**Keywords:** APEX, nanobody, green fluorescent protein, ovarian follicle, electronic microscopy, GBP, *Drosophila melanogaster*

## INTRODUCTION

In cell biology studies, protein localization is crucial to understand the cellular functions of proteins and for understanding the dysfunction of proteins in diseases. For years, the technique used for this purpose was immunohistochemistry. It requires specific antibodies directed against each of the proteins of interest (POI). However, the production of good quality primary antibodies is random and labor-intensive. Once obtained, it remains a resource with limited availability.

The advent of genetically targetable fluorescent protein tags has offered a possibility to bypass the requirement of antibody production against each POI. In addition, fluorescent tags have further expanded the field of possibilities to *in vivo* localization in living tissues or cells. Therefore, in

*Drosophila*, where large scale projects are regularly conducted, various programs and consortiums have developed systematic approaches with the objective of creating lines expressing a fluorescent version of each protein of the proteome. Different approaches have been used to generate protein trap lines where an artificial exon encoding GFP is inserted into the genome (Morin et al., 2001; Clyne et al., 2004; Kelso et al., 2004; Buszczak et al., 2007; Quiñones-Coello et al., 2007; Lowe et al., 2014; Nagarkar-Jaiswal et al., 2015). Currently, the CRISPR technique better facilitates the creation of fusion proteins regulated by their endogenous environment, thereby the number of fluorescently tagged proteins generated by individual labs continuously increases.

In the vast majority of studies, the experiments described above are performed using light microscopes, which are fast, cheap and simple. The conventional fluorescence microscopy has a spatial resolution within a 200–300 nm range and it reaches a maximum of 10 nm in super-resolution microscopy but requires specialized equipment and/or fluorophores. In these conditions, intracellular localization often requires the co-localization with a fluorescent marker of organelles or compartments, although the size of many organelles is below the resolution limit of these microscopes.

Due to the imprecision of this approach, a high-resolution analysis becomes necessary through, for example, electron microscopy (EM)-based detection. Although EM achieves much higher spatial resolution (~1 nm in biological samples), the localization of proteins by EM approaches remains rare. Several reasons lead to this situation. High quality results by EM immunolocalizations are difficult to obtain. Indeed, when performed on whole tissue, immunolocalization protocols include permeabilization steps that degrade intracellular structures. Alternatively, immunolocalizations performed on ultra-thin sections have only little epitope accessible to antibodies (Sosinsky et al., 2007; Schnell et al., 2012). Moreover, contrasting agents have a negative impact on the antigen-antibody binding, therefore protocols aim at maintaining them at low levels. This leads to images with poor contrast and makes the subsequent identification of ultrastructures difficult. Another alternative is then to perform ultrathin sections of cryoprotected samples infiltrated by 2.3 M sucrose followed by an immunolabeling of each section, which is both technically challenging and time consuming (Tokuyasu, 1986). Thus, there have been attempts to develop genetically encoded tags to circumvent these limitations, however, they either require light (mini-SOG) (Shu et al., 2011) or are not usable in most cellular compartments (HRP) (Porstmann et al., 1985). It is only the recent development of an engineered ascorbate peroxidase (APEX) that has allowed the use of tags in EM to be expanded (Martell et al., 2012). The APEX tag, derived from soybean ascorbate peroxidase (Lam et al., 2014), is a 28 kDa enzyme that converts the diffusible 3,3'-diaminobenzidine (DAB) into an insoluble osmiophilic polymer in the presence of H<sub>2</sub>O<sub>2</sub>. This polymer becomes EM-visible upon treatment by osmium tetroxide (OsO<sub>4</sub>). APEX has the advantage to retain activity after fixation with glutaraldehyde, a fixative that very well preserves the ultrastructure of the sample. APEX has been used as a tag in many studies and has largely proven its efficiency, making it

now a tag of choice for the detection of fusion proteins in EM (Martell et al., 2012, 2017; Ariotti et al., 2015; Chen et al., 2015; Lee et al., 2016; Lin et al., 2016; Ludwig, 2020; Tan et al., 2020).

Here we have chosen to use the APEX2, a version of APEX (K14D, W41F, and E112K) with an additional mutation (A134P) (Lam et al., 2014). It has the same advantages of APEX while producing the DAB polymer with faster kinetics and incorporating the heme cofactor more efficiently. Similarly to an approach that has been reported to work successfully in zebrafish (Ariotti et al., 2015), we have created a GBP-APEX2 tool that combines the APEX2 with a GFP binding protein (GBP). The GBP corresponds to the coding sequence of an anti-GFP nanobody which is a single-domain polypeptide derived from the variable heavy chain (Vhh) of the heavy chain-only antibodies of camelids (Kirchhofer et al., 2010; Kubala et al., 2010). This GBP domain will allow the association of APEX with any GFP-tagged protein *in vivo*. In previous studies, it has been shown that individual intermediate filaments can be resolved (Ariotti et al., 2015) indicating that APEX-GBP allows a spatial resolution of ~10 nm.

The APEX-GBP strategy avoids the need to create new APEX-tagged transgenic lines for each new POIs, and takes advantage of all the GFP-tagged lines already available in the *Drosophila* community. In addition, to further increase the adaptability and the versatility of our tool, we placed this fusion construct under the regulatory region of UAS sequences. These sequences trigger the expression of coding sequences placed downstream, when they are bound by the GAL4 transcription factor. Numerous *Drosophila* strains, with different expression patterns of GAL4 are available and thus, spatiotemporal control of expression can be achieved (Brand and Perrimon, 1993; Duffy, 2002).

As a proof of principle, we present here the localization of several GFP-tagged proteins and describe a detailed protocol applicable to the *Drosophila* ovarian follicle (Figure 1).

## MATERIALS AND EQUIPMENT

### Preliminary Notes

Many of the chemicals used during the APEX reaction and EM steps are hazardous to humans and the environment. Therefore, pay attention to the attached Material Safety Data Sheets and handle these reagents with care: glutaraldehyde (toxic), paraformaldehyde (carcinogen, toxic), DAB (carcinogen), cacodylate buffer (toxic, arsenic), hydrogen peroxide (corrosive), uranyl acetate (radioactive), lead citrate (toxic) and osmium tetroxide (highly volatile, toxic and highly reactive). Wearing gloves as well as adapted personal protective equipment and manipulating under a fume hood are essential.

### Fly Stocks

Fly strains and crosses were raised on standard cornmeal food at 25°C. To overexpress UAS transgenes specifically in germline cells, *nos-GAL4<sup>VP16</sup>* [*P(mw, GAL4:VP16-nos.UTR) CG6325(MVD1)*] (DGRC Kyoto #107955) and *mat-Tub-Gal4<sup>VP16</sup>* [*P(mw, mat-alpha4-Gal4-VP16)*]

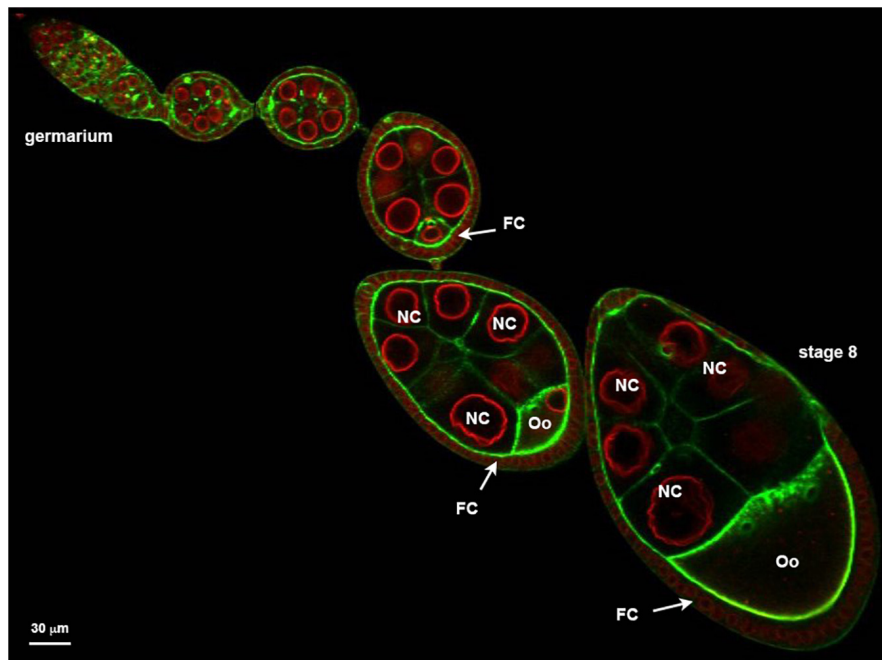


**FIGURE 1 |** Ovariole organized in a succession of developing follicle. Nuclear envelopes (red) are stained with alexa594-WGA and the cortical actin (green) revealed with Alexa448-Phalloidin. Follicles are developmental subunits in which the oocyte (Oo) develops. The oocyte is located at the posterior of the follicle and is associated with 15 additional germ cells named nurse cells (NC). A monolayer of follicular cells (FC) surrounds the germline. On the example presented here, the ovariole exhibits at its anterior extremity (left) a region called germarium in which the stem cells proliferate. At the other extremity (right) a stage 8 showing an oocyte that represents almost one half of the follicle.

(Januschke et al., 2002) were used. To overexpress UAS transgenes in somatic follicular cells, *Tj-GAL4* [*y,w;* *P(GawB)NP1624*] (DGRC Kyoto #104055) was used. The strains *UASp-APEX2-GBP* and *UASp-6myc-APEX2-GBP* are from this study. The following GFP strains were used: *P(Baz<sup>BAC.GFP</sup>)* aka *P[w + , FRT9-2]18E, f, baz [815.8]*, *P{CaryP;PB[BAC Baz-sfGFP2]attP18}* (Besson et al., 2015); *P(mud<sup>BAC.GFP</sup>)* (Bosveld et al., 2016); *UASp-Baz-GFP* (Benton and St Johnston, 2003); *UASp-Rab5-GFP* (Dong and Wu, 2013); *hsp-flp; FRT79D ubi-nlsGFP* (gift from JR Huynh); *Tub-GFP-Rab6* (Januschke et al., 2007), *RanBP2-GFP* (Hampoelz et al., 2019).

## Generation of Transgenic Flies

APEX2-GBP from pCSDST2 APEX2-GBP (Plasmid #67651, Addgene) was subcloned in pENTR<sup>TM</sup>/D-Topo. Using the Gateway<sup>TM</sup> recombination cloning, APEX2-GBP sequence was inserted in pPMW (promotor UASp with a N-terminal 6myc tag), in pPW (promotor UASp without tag) from the *Drosophila* Gateway<sup>TM</sup> Collection. The transgenic flies have been generated by random insertion by the BestGene Company (United States).

## Reagents and Equipment for Ovary Dissection and Immunostaining

- Bovine Serum Albumin (Thermo Fisher Scientific, BP1600).
- Chicken Anti-APEX2 antibody (Innovagen PA-APX2-100) raised against AA126-146.

- Mouse anti-Myc/c-Myc 9E10 antibody (SantaCruz, sc40).
- Anti-Mouse Secondary antibody, Alexa Fluor 546.
- Goat anti-Chicken IgY (H + L) Secondary Antibody, Alexa Fluor 546.
- Phosphate buffered saline pH 7.4 (PBS).
- Tween 20 (Sigma-Aldrich, P1379-1L).
- Triton X-100 (Sigma-Aldrich, T8787-100ML).
- Paraformaldehyde 16% (w/v) in sealed 10 mL glass ampules (Avantor, 43368.9L).
- Citifluor<sup>TM</sup> Mountant Solution AF1 (Electron Microscopy Sciences, 17970-25).
- Forceps Dumont #5 (Carl Roth, K342.1).
- Stainless steel needles (Entosphinx, 20).
- Colorimetric 8 cell tray (Kartell Labware, 357).

## Reagents and Equipment for EM Sample Preparation and Detection

- Methylene blue staining solution (Richardson et al., 1960) (Methylene blue 0.5%, azur II 0.5%, Sodium borate 0.5%).
- Glass microscopy slides (Fisher Scientific, 1018049).
- Glutaraldehyde EM grade 25%, in sealed 10-ml glass ampules (EMS 16220).
- 3,3'-Diaminobenzidine tetrahydrochloride (DAB; Sigma-Aldrich, D5905).
- Hydrogen peroxide (H<sub>2</sub>O<sub>2</sub>), 3% (Boster Immunoleader AR1108).
- Sodium cacodylate buffer 0.2 M pH 7.4 (EMS 11652).

- Agar Low Viscosity resin Kit (Agar scientific, AGR1078).
- Fluoropolymer film 199  $\mu\text{m}$  thickness (EMS, 50425).
- Formvar powder (Agar scientific AGR1202).
- Single slot grids (oval hole) (EMS, G2010-Cu).
- Osmium tetroxide 4%, in sealed 2-mL glass ampules (EMS, 19150).
- Potassium hexacyanoferrate(II) trihydrate (Sigma-Aldrich 244023).
- Ethanol.
- Uranyl acetate (AnalaaR 10288).
- Lead citrate (Deltamicroscopies 11300).

## STEPWISE PROCEDURE

### Fly Handling

In food vials, cross 5–10 virgin females with 3–5 males of the desired genotype and hold the vial at 25°C. After fly hatching select the females of the correct genotype, transfer them with few males in fresh food vials supplemented with dry yeast for their ovaries to fatten up and leave them for one or 2 days before dissection.

### Microdissection

- 1- Anesthetize the flies on a pad, with carbon dioxide.
- 2- Under the dissecting microscope, pick up one female with a pair of forceps and immerse it in a large drop (50–100  $\mu\text{L}$ ) of PBT (PBS with 0.1% Tween 20) at room temperature.
- 3- Hold the fly by the thorax with one pair of tweezers, and pull the dorsal abdominal cuticle around the A4–A5 segmental boundary with another pair of forceps.
- 4- Isolate and detach the pair of ovaries, which can fill up to 2/3 of the female abdomen, and should be readily available upon cuticle removal.
- 5- Tease apart the ovarioles of each ovary. While holding the posterior end of the ovaries (older stages) with a forceps, pass a needle in between the ovarioles toward the germarium at the anterior end of the ovary.
- 6- Transfer the ovaries into a 2 mL centrifuge tube containing 200  $\mu\text{L}$  of PBT at room temperature and continue the experiment quickly.

### Fixation and DAB Reaction

- 7- Remove the PBT and add 500  $\mu\text{L}$  of the fixative solution (2.5% paraformaldehyde, 1% glutaraldehyde in 0.1 M sodium cacodylate buffer).
- 8- Keep it 20 min at RT then move to 4°C.
- 9- Keep it at 4°C for 1 h, in the dark.  
*During this time, prepare the DAB solution.*
- 10- Wash three times 5 min in 0.1 M sodium cacodylate buffer at 4°C.
- 11- Prepare the DAB solution (1 mg/ml DAB, 0.1 M sodium cacodylate buffer). 1.5 mL per sample is required:
  - Dissolve one tablet of 10 mg DAB in 5 ml of  $\text{H}_2\text{O}$  with 5 min vigorous vortexing.

- Dilute 1:1 the DAB/ $\text{H}_2\text{O}$  with 0.2 M sodium cacodylate buffer.
- Remove undissolved precipitates with syringe filtration using a 0.2  $\mu\text{m}$  filter (Millipore).

- 12- Add 500  $\mu\text{L}$  of the final solution to the sample.
- 13- Allow to react for 30 min (*Increased time reduces background*).
- 14- Replace the solution with a DAB/Cacodylate + 5.88 mM  $\text{H}_2\text{O}_2$  solution.
- 15- Incubate for 20 min at RT.
- 16- Stop the reaction with 3 min  $\times$  2 min washes with 0.1 M sodium cacodylate buffer.

### Post-Fixation

- 17- Prepare post-fixative solution.
  - (a) 1% osmium tetroxide (prepared from 4% stock solution).
  - (b) 1.5% Potassium hexacyanoferrate(II) trihydrate (prepared from stock powder).
  - (c) 0.1 M cacodylate buffer (prepared from 0.2 M stock solution).
- 18- Incubate for 1 h at 4°C.
- 19- Wash three times 2 min in 0.1 M cacodylate buffer.
- 20- Wash three times 2 min in  $\text{H}_2\text{O}$ .

### Dehydration

- 21- Incubate 10 min in 30% EtOH solution.
- 22- Incubate 10 min in 50% EtOH solution.
- 23- Incubate 10 min in 70% EtOH solution.
- 24- Incubate 10 min in 90% EtOH solution.
- 25- Incubate twice 10 min in 100% EtOH solution.

### Resin

- 26- Incubate in resin LV agar/EtOH (1/1) overnight.
- 27- Incubate twice in resin for 1 h.
- 28- Mount the samples between two sheets of fluoropolymer film, separated by a fluoropolymer film spacer.  
This step is important because it allows the ovarioles to be laid out flat in order to select the right stage of development and to orientate them.
  - 28.1: Three pieces of fluoropolymer film embedding film are cut in the dimensions of a microscopy slide (75 mm  $\times$  25 mm).
  - 28.2: In the center of one of the three pieces of fluoropolymer film a square of 20 mm  $\times$  20 mm is cut out.
  - 28.3: Place the first piece of fluoropolymer film on a microscopy slide.
  - 28.4: Superimpose the hollowed film.
  - 28.5: Pipet the samples in resin.
  - 28.6: Spread out the ovarioles.
  - 28.7: Carefully apply the third piece of fluoropolymer film to minimizing the formation of bubbles.
  - 28.8: Put a microscopy slide on top to make a sandwich.



- 29- Leave the samples at 60°C for 18 h.
- 30- Select the stage of interest that will be subsequently processed using a light microscope.
- 31- Cut around the selected ovarian follicle and stick it flat on a block of resin with a drop of resin.
- 32- Leave the blocks at 60°C for 18 h.

## Cutting Sections and Contrasting

The samples are cut with an ultramicrotome. Select the area of interest in *z* by staining semi-thin sections (400 nm) with methylene blue solution. Then collect 70 nm ultra-thin sections on slot grids with an oval hole covered with formvar film. Classic grids with a square mesh can also be used depending on the cell model. In the case of the ovarian follicle, the object is too large and is partially hidden by the bars during the acquisition. Post-stain sections in 4% aqueous uranyl acetate in the dark for 15 min and lead citrate for 8 min in a CO<sub>2</sub>-depleted atmosphere created by the vicinity of sodium hydroxide tablets.

## Electron Microscopy Analysis

Observe the grids at 120 kV with a transmission electron microscope Tecnai12 (Thermo Fisher Scientific).

## RESULTS

### Method Validation

When the method is performed for the first time or to troubleshoot the experiment, we recommend optimizing each step beforehand, including interaction between GBP-APEX2 and the GFP tagged POI, enzymatic activity of APEX2 and quality of the sample preparation.

### Validating APEX2-GBP and GFP Expressions and Co-localization by Fluorescent Microscopy

We first verified that the GBP-APEX2 construction colocalized with the GFP tagged POI. This can be verified in the tissue using an immunofluorescence approach. Depending on the GBP-APEX2 strain used, immunostaining can be performed with the anti-APEX2 and/or anti-myc antibodies. Furthermore, this allows one to verify that the binding of APEX-GBP does not alter the localization of the GFP-tagged protein.

After microdissection (as described above), the ovaries should be treated according to the following protocol:

- 1- Fix with 4% paraformaldehyde (in PBS) for 12 min.
- 2- Wash twice 10 min with PBT2 (PBS + 0.1% Triton X-100).
- 3- Block in PBT2 + BSA 2% for 1 h.
- 4- Incubate in PBT2 + primary antibody overnight at 4°C. Anti-Myc antibody is used at 1/250 at anti-Apex2 at 1/500.
- 5- Wash three times 10 min with PBT2.
- 6- Incubate with secondary antibody in PBT2 for 2 h at room temperature.
- 7- Wash three times 10 min with PBT2.
- 8- Mount samples between slide and coverslip in a drop of citifluor<sup>TM</sup>.

As a first example, we have performed immunofluorescence on ovaries expressing both a GFP version of the Mud/NuMA protein encoded by a BAC transgene and the UAS-myc-GBP-APEX2 construct expressed under the control of the *mat-Tub-Gal4<sup>VP16</sup>* driver. Both GFP and anti-myc signals are colocalized at the nuclear envelope of the *Drosophila* oocyte (**Figure 2A**). This confirms that the GBP-APEX construct is able to correctly detect the GFP tagged protein. Similar results have been obtained when we undertook to detect the plasma membrane associated protein PAR3/Baz with the UAS-GBP-APEX construct and anti-APEX2 antibodies (**Figure 2B**).

It is noteworthy that the non-visualization of APEX signal at the exact localization of GFP fusion protein is not harmful for the rest of the experiment. Also, in some cases, a diffuse localization of the GBP-APEX can be detected in the cytoplasm without any consequence on subsequent precise detection of the GFP fusion protein (**Supplementary Figure 1**).

### Validating APEX2 Activity by Light Microscopy

A critical step in this protocol is the ability of APEX2 to convert the DAB into a polymer. The polymer produced by the APEX enzymes is osmophilic and thus can be visualized in EM, but it can also be visualized using light microscopy appearing as light brown stain (**Figures 3A,B**). Usually, the subcellular localization of APEX in the tissue can be roughly distinguished and bodes well for visualization in transmission EM (TEM). As an illustration, we decided to detect Baz-GFP with the GBP-APEX2 construct and look at the DAB product with a transmission light microscope. When the GBP-APEX2 is specifically expressed in the germline, under the regulatory sequences of *nanos-GAL4 (nos-GAL4<sup>VP16</sup>)*, a brown precipitate is accumulated only in the nurse cells and the oocyte (**Figure 3A**). Moreover, we could clearly see a stronger accumulation at the anterior of the oocyte where PAR3/Baz is normally enriched. Alternatively, when the GBP-APEX2 is specifically driven in the follicular cells with the *traffic-jam-GAL4 (tj-GAL4)*, we observed a strong staining in the follicular epithelium that surrounds the ovarian follicle. The brown labeling is, as expected, more intense at the apical side of the cells (**Figure 3B**). The light brown staining observed over the germ cells corresponds to signals accumulated in the follicular cells above them. These experiments show that the fixation procedure does not alter the enzymatic activity of the APEX, nor the specificity of the DAB precipitate accumulation in cells expressing the GBP-APEX construct.

Of note the absence of accurate staining in transmission light microscopy does not indicate that no signal will be detected in TEM. However, if there is no staining at all, it is necessary to verify first that APEX is genetically present in the tissue/cell, and then that the labeling procedure with DAB is correctly performed.

### Validating Sample Preparation

The quality of TEM preparation is a function of the correct completion of several crucial steps i.e., fixation, dehydration and embedding in a resin. The quality of embedding is very important and can be checked by the analysis of semi-thin sections of the sample under a light microscope. For thick samples like

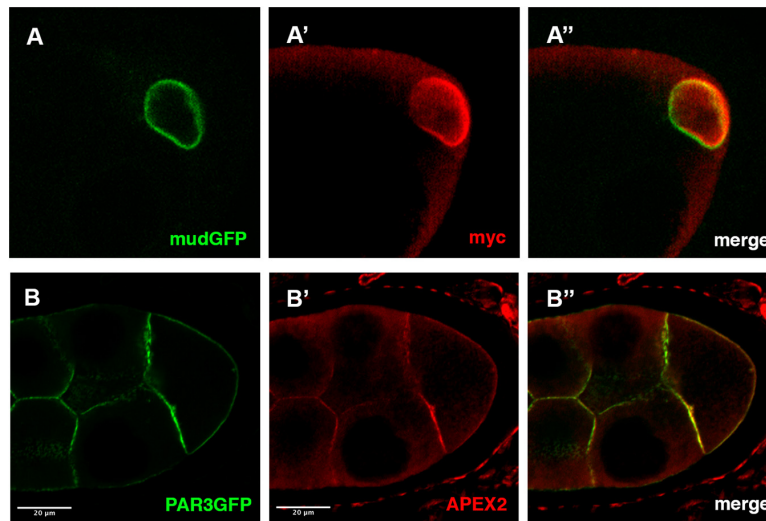


**FIGURE 2 |** Detection APEX2-GFP protein by immunofluorescence. **(A,B)** In *mud-GFP; mat-Tub-Gal4<sup>VP16</sup>, UAS-mycAPEX2-GBP* ovarian follicle, the GFP signal is detected around the nucleus of the oocyte **(A)**. With anti-myc antibodies **(A')**, we observe a similar pattern that overlaps with the GFP fluorescence **(A'')**. Similarly, in *nos-Gal4<sup>VP16</sup>, UAS-APEX2-GBP, UAS-Par3-GFP* egg chamber, we observe the GFP **(B)** associated with the membranes. Anti-APEX antibodies **(B')** reveal an overlapping staining **(B'')**.

the *Drosophila* oocyte, this step can also be used to screen for adapted z-position before collecting ultra-thin sections for TEM. Semi-thin sections (0.4  $\mu\text{m}$  thick) can be colored with methylene blue in order to better visualize cell morphology. Methylene blue staining allows one to recognize cell nuclei (**Figure 3C**) but also to reveal potential issues with the fixation step that could affect tissue morphology (**Figure 3D**).

After inclusion in resin (see above), we proceed to the following steps:

- 1- Semi-thin sections are generated with an ultramicrotome (Leica Microsystems UC6).
- 2- Two or three sections are deposited within a drop of water onto a glass slide.
- 3- Slides are placed 15–30 s on a preheated hot plate to dry the sections.
- 4- When the water is totally evaporated, apply a drop of the methylene blue staining solution onto the sections to cover the entire surface.
- 5- Incubate for 30 s on the hot plate.
- 6- Remove the staining solution by rinsing with distilled water.
- 7- Last traces of water are removed by placing the slide for 30 s back on the hot plate.
- 8- Observation under a dissecting microscope.

It should be noted that various polychromatic staining techniques can be used for embedded tissue sections (Toluidine blue, Basic fuchsin, and Malachite green).

## Proof of Principles

In order to validate our APEX tool in *Drosophila*, we have chosen to test, in the ovarian follicle, different GFP-tagged

proteins associated with various subcellular compartments. These proteins are either overexpressed with the UAS/GAL4 system or expressed under the control of their own promoters with transgenes, or directly tagged in the genome by CRISPR mediated GFP insertion. For each condition, GFP was visualized by confocal microscopy, in parallel to the treatment for TEM observation. The APEX2-GBP construction is expressed under the control of UAS promoter and *nos-GAL4<sup>VP16</sup>* driver in the germline cells or *tj-GAL4* driver in the follicle cells.

In a first attempt, we detected DE-Cadherin (DE-Cad) encoded by the *shotgun* gene in *Drosophila*. DE-Cad is a component of the adherens junction that localizes at the plasma membrane. Using a DE-Cad-GFP knockin line (Huang et al., 2009), we observed by fluorescence a signal at the oocyte plasma membrane with patches of higher intensity (**Figures 4A,A'**). Similarly, APEX detection and visualization by TEM revealed electron dense patches associated with plasma membranes (**Figure 4A''**).

We then addressed whether this approach is suitable to detect protein involved in cellular trafficking, such as the GTPases RAB5 and RAB6. Fluorescence detection of the RAB5-GFP tagged protein, expressed under the control of UAS sequence, displays a cortical signal along the plasma membrane of the oocyte (**Figures 4B,B'**) as expected with the previously described RAB5 association with early endosomes (Zerial and McBride, 2001; Compagnon et al., 2009). With our detection method by TEM, we have observed signals associated with vesicles near the plasma membrane (**Figure 4B''**). Interestingly the DAB precipitate seems to be organized in nanodomains on the endosomes as it has been proposed previously (Franke et al., 2019). Concerning RAB6, this GTPase is known to be associated with medial Golgi and *Trans* Golgi Network (Antony et al., 1992) and it has been shown to regulate

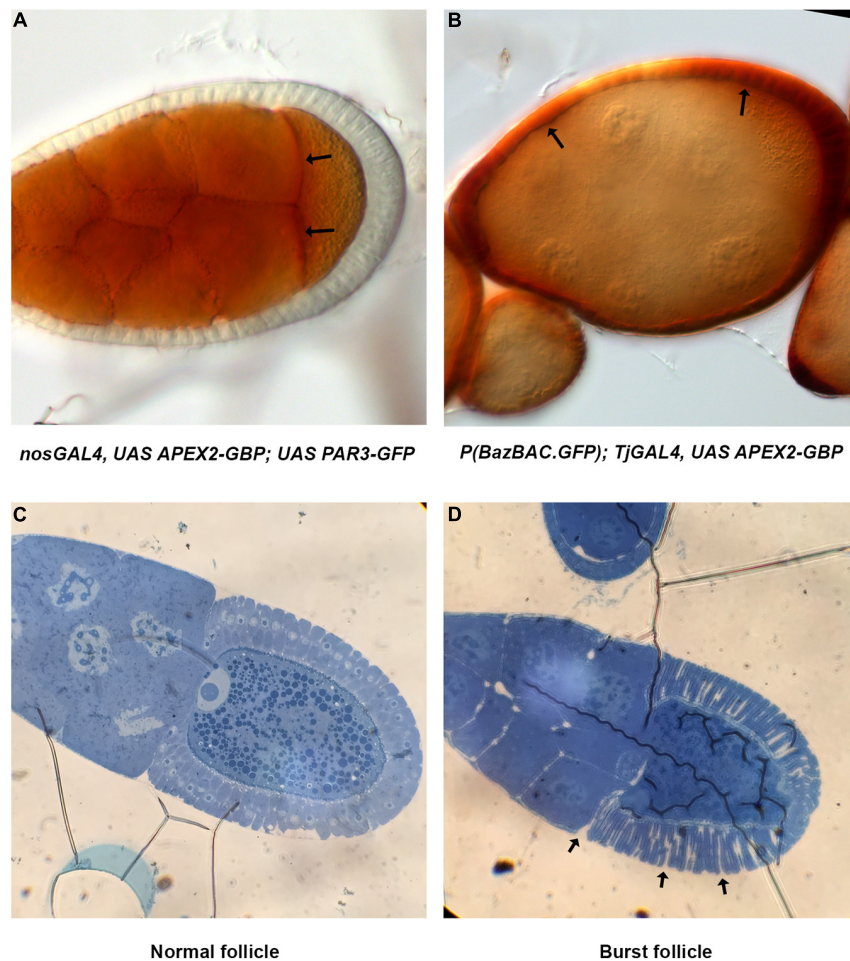


**FIGURE 3 |** Method validation. **(A)** Images of *nos-Gal4<sup>VP16</sup>*, *UAS-APEX2-GBP*, *UAS-Par3-GFP* ovarian follicle acquired on transmission light microscope reveal DAB precipitates specifically in the germline. Stronger accumulation at the anterior of the oocyte (arrows) is coherent with Par3 distribution profile. **(B)** In *P(Baz<sup>BAC.GFP</sup>); UAS-APEX2-GBP/Tj-GAL4*, DAB staining is only observed in follicular cells (arrows). Note that the brown shade over the germline staining is due to surrounding follicular cells. **(C,D)** Methylene blue staining reveals morphology of the follicle and allows visualization of nuclei. Thereby, we can also verify the developmental stage of the egg chamber **(C)**. In addition, issue with fixation is also revealed by burst ovarian follicles [arrows, **(D)**].

transport between early and late Golgi compartments and to sustain Golgi morphology (White et al., 1999; Januschke et al., 2007). With fluorescence we observed a diffuse staining pattern, with a few more intense dots, scattered within the cytoplasm (**Figures 4C,C'**). APEX-GBP revealed by TEM highly contrasted dots in the close vicinity of Golgi apparatus, a location consistent with the previously described role of RAB6 (**Figure 4C''**).

To monitor the versatility of the UAS-GBP-APEX2 tool, we tested the use of this tool in the somatic cells surrounding the ovarian follicle. For this purpose, we monitored the localization of the PAR3/Baz polarity protein tagged with GFP and expressed at endogenous levels. Upon APEX detection and visualization by TEM, dense patches were easily identified at the level of the adherens junctions as expected for PAR3/Baz (**Figures 5A,A'** and **Supplementary Figure 1**). The APEX-GBP system is therefore effective in tracking the EM localization of GFP-tagged proteins independently of their expression level.

To test, if the method is sensitive enough to reflect differences in protein quantity, we chose to follow the nuclear envelope repartition of the Mud/NuMA protein, that is known to be asymmetrically distributed at the oocyte nuclear envelope (Yu et al., 2006; Tissot et al., 2017; **Figures 5B,B'**). Accordingly, the ultra-thin sections observed in TEM exhibit more dense signals on the portion of the nuclear envelope facing the posterior membrane of the oocyte (**Figure 5B''**). DAB precipitates on the opposite side of the nucleus are much less present showing that our conditions can detect different quantities of proteins.

One limit of the APEX approach is the diffusion of the DAB precipitate formed by the enzymatic activity. We thus decided to estimate this diffusion by looking at a protein with a precise location, i.e., the RanBP2/Nup358 protein that is an outer component of nuclear pore complexes (Bernad et al., 2004). Strikingly, the diffusion observed with the detection of RanBP2-GFP is restricted outside of the nucleus according to the known location of the protein (**Figure 5C**). Furthermore, we do not



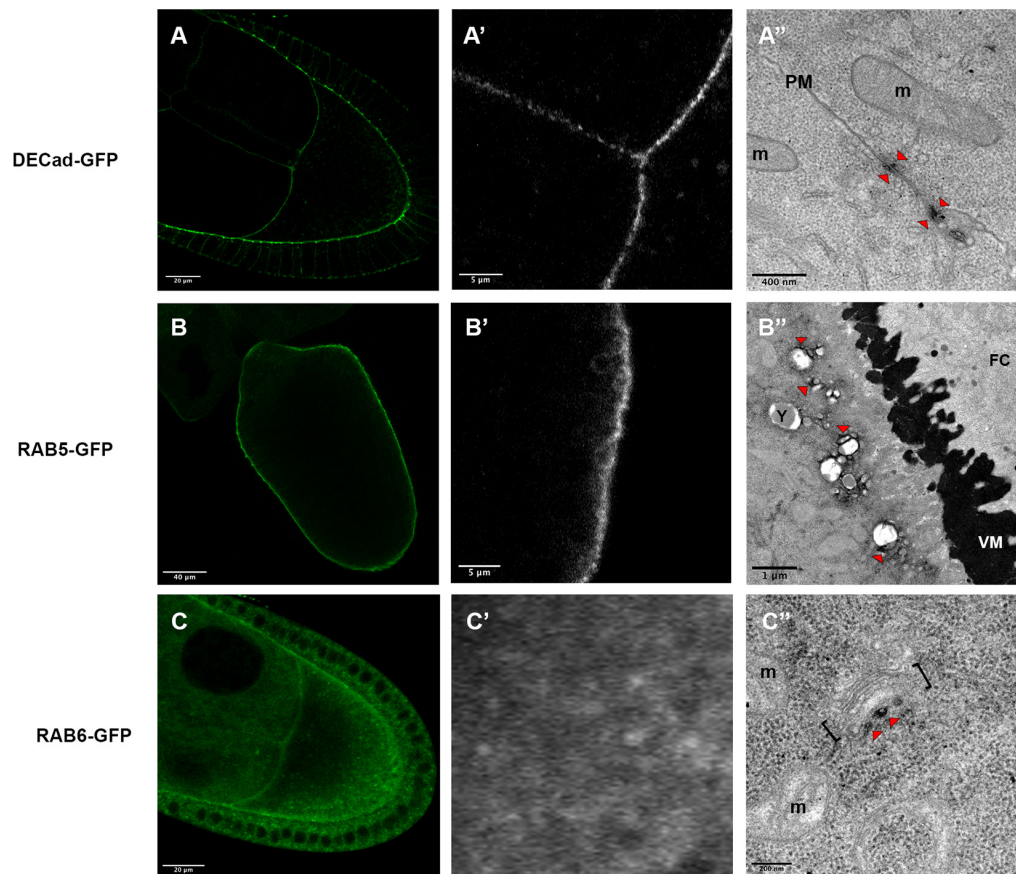


**FIGURE 4 |** Expression profiles of *DE-Cad-GFP* (A–A''), *Rab5-GFP* (B–B'') and *Rab6-GFP* (C–C''), revealed by fluorescent microscopy (A,A',B,B',C,C') or by electron microscopy (A'',B'',C''). *DE-Cad* localizes at the plasma membrane [(A), higher magnification (A')]. DAB precipitates are visualized (arrowheads) near plasma membranes (PM) separating the oocyte and a nurse cell (A''). *Rab5* that has a cortical localization revealed by fluorescence [(B), higher magnification (B')], is detected at a small distance of the plasma membrane at the surfaces of vesicles [(B''), arrowheads]. *Rab6-GFP* displays a diffuse cytoplasmic signal (C) with some dots revealed at higher magnification (C'). By electron microscopy, DAB precipitates are detected in the vicinity of Golgi apparatus [(C''), arrowhead]. (m) mitochondria, brackets highlight a Golgi unit, (VM) vitelline membrane, (FC) follicular cells. Number of observations *DE-Cad-GFP* ( $n = 4$ ), *Rab5-GFP* ( $n = 2$ ) and *Rab6-GFP* ( $n = 6$ ).

detect staining when large portions of NE devoid of visible nuclear pores are observed. In this case, no diffusion could be detected inside the nucleus, showing that this method is suitable to decipher if a given protein is associated with the inner or outer membrane of the NE.

This observation prompted us to test if the UAS-GBP-APEX2 tool could be used to detect protein within the nucleus, despite our choice not to include a nuclear localization sequence in our GBP-APEX construct. In order to address if a nucleus-resident protein could nevertheless be monitored in TEM using our APEX-GBP tool, we expressed a nls-GFP transgene concomitantly with APEX-GBP in the ovarian follicle (Figure 6). In Figure 6A, the APEX-GBP is expressed only in the germline and we can observe a more intense staining in the germline nuclei (Figure 6, white N). Note that a weak staining in the germline cytoplasm can also be observed indicating the presence of APEX-GBP not associated with GFP. Importantly, in the follicle cells that serve as a control condition, the nucleus is lighter than the surrounding cytoplasm (Figures 6A,B, black n),

unlike the germline where the nucleus is more strongly stained (Figures 6A,B, white N) than the cytoplasm.

## DISCUSSION: CRITICAL PARAMETERS AND TROUBLESHOOTING

### Driver/APEX-GBP Couple

Having a bi-partite system where the APEX is uncoupled from the POI has many advantages as mentioned previously. However, in this system APEX is expressed throughout the whole cell independently of the POI's subcellular location and thereby induces a background signal. Therefore, it is important to perform control experiments when studying a protein for the first time (see below). This is also exemplified by the detection of signals unspecific to our protein when immunofluorescence experiments are performed with anti-APEX antibodies (see Figure 2). However, in TEM, this does not prevent an accurate detection of Mud only at the nuclear envelope of the oocyte. It

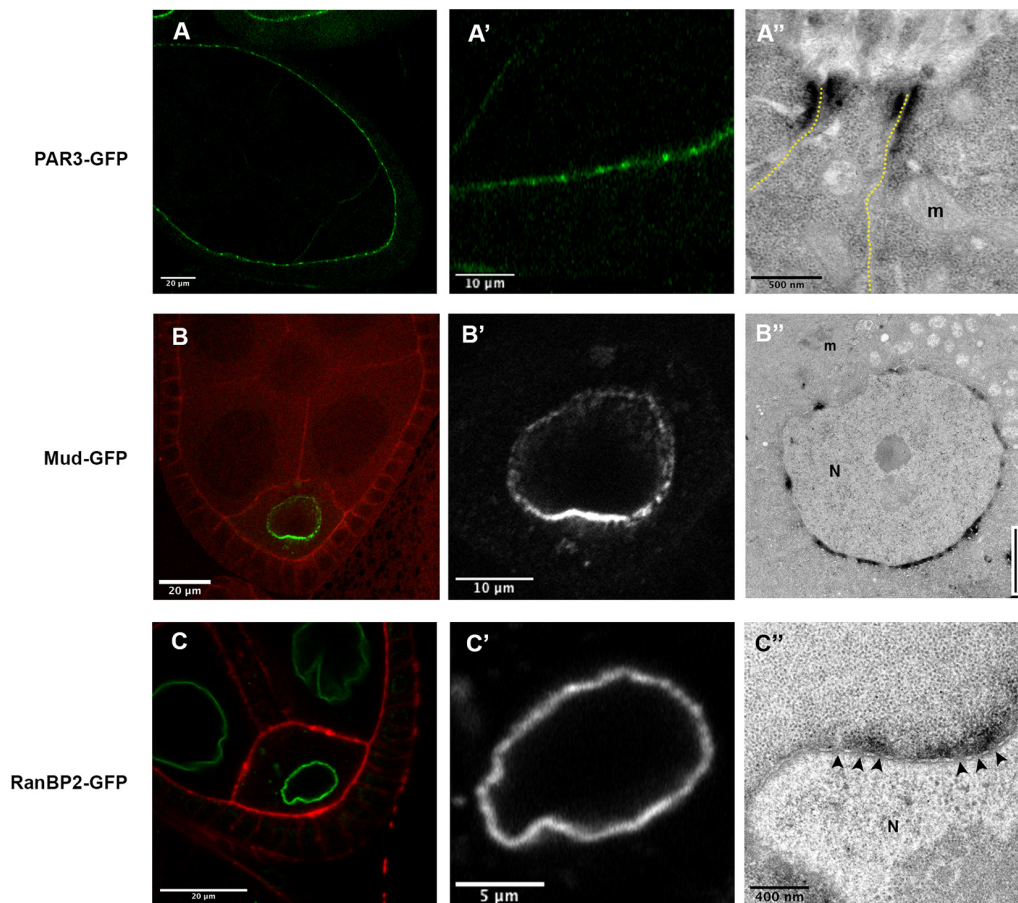


**FIGURE 5 |** (A) In  $P(\text{Baz}^{\text{BAC.GFP}}); Tj\text{-GAL4}, UAS\text{-APEX2-GBP}$  egg chambers, Baz-GFP accumulate apically in the follicular cells, with a stronger accumulation at the junctional level (A,A'). Consistently, a dense signal is revealed at the level of the junction between two follicular cells (A'). (B) In  $\text{mud}^4/\text{mud}^4; P(\text{mud}^{\text{BAC.GFP}})/P(\text{mud}^{\text{BAC.GFP}}); nos\text{-GAL4}^{VP16}, UAS\text{-APEX2-GBP}$  follicles, an asymmetric distribution of Mud-GFP is observed at the nuclear envelope of the oocyte (B,B'). This accumulation, more important on the hemisphere facing the posterior membrane of the oocyte, is also revealed by the APEX-GBP tool by electron microscopy. (C) In  $\text{RanBP2-GFP}; nos\text{-GAL4}^{VP16}, UAS\text{-APEX2-GBP}$  egg chamber the GFP signal is detected at the nuclear envelope [(C'), zoom on oocyte nucleus (N) in panel (C'')]. By electron microscopy, we can observe that the accumulation of DAB precipitate is outside the nucleus and correlates with the presence of nuclear pores (arrowheads). (N) nucleus, (m) mitochondria. Number of observations (A): ( $n = 5$ ), (B,C) ( $n = 2$ ).

is noteworthy that negative controls display much lower global signal, indicating that a significant but acceptable level of noise is induced by this condition. We can speculate that the local concentration of APEX protein is higher when bound to the POI and thereby create a signal/noise ratio in favor of the detection.

When we used the *Tj-GAL4* driver to detect the nls-GFP in the follicular cells, we observed a cytoplasmic background of a similar level to the nuclear signal associated with the nls-GFP transgene (Figure 6E). It is then difficult without control to distinguish between specific and non-specific labeling. Nonetheless, in the same cells and with the same driver, the signal of PAR3/Baz-GFP, expressed at endogenous levels with a BAC transgene, was strong enough to be unambiguously identified (Figure 5A''). These examples reveal that the driver/APEX-GBP couple has to be carefully chosen in order to maximize the signal to noise ratio. It is noteworthy that several methods have recently been reported to improve the signal-noise ratio, i.e., the use of conditionally stable nanobodies for GFP fused to APEX, that

favor degradation of unbound nanobodies by the proteasome reduces background APEX signals (Ariotti et al., 2018), or the possibility to convert the oxidized diaminobenzidine reaction product of APEX into a silver/gold particle that in addition provides a readily quantifiable particulate signal (Rae et al., 2021). Both approaches have been proven successful in cell cultures and remain to be tested and adapted *in vivo* to thicker tissue like *Drosophila* follicles.

## Negative Controls

Transmission EM images are displayed in gray levels that reflect the density of the structure encountered by the electron beam. In order to help visualize cellular structures and increase the contrast, the samples must be incubated with osmium tetroxide, uranyl acetate and/or potassium ferricyanide. DAB precipitates also appear as dense structures, thereby it could be challenging to identify the osmiophilic precipitate produced by APEX especially when the POI has an unknown location. Therefore,



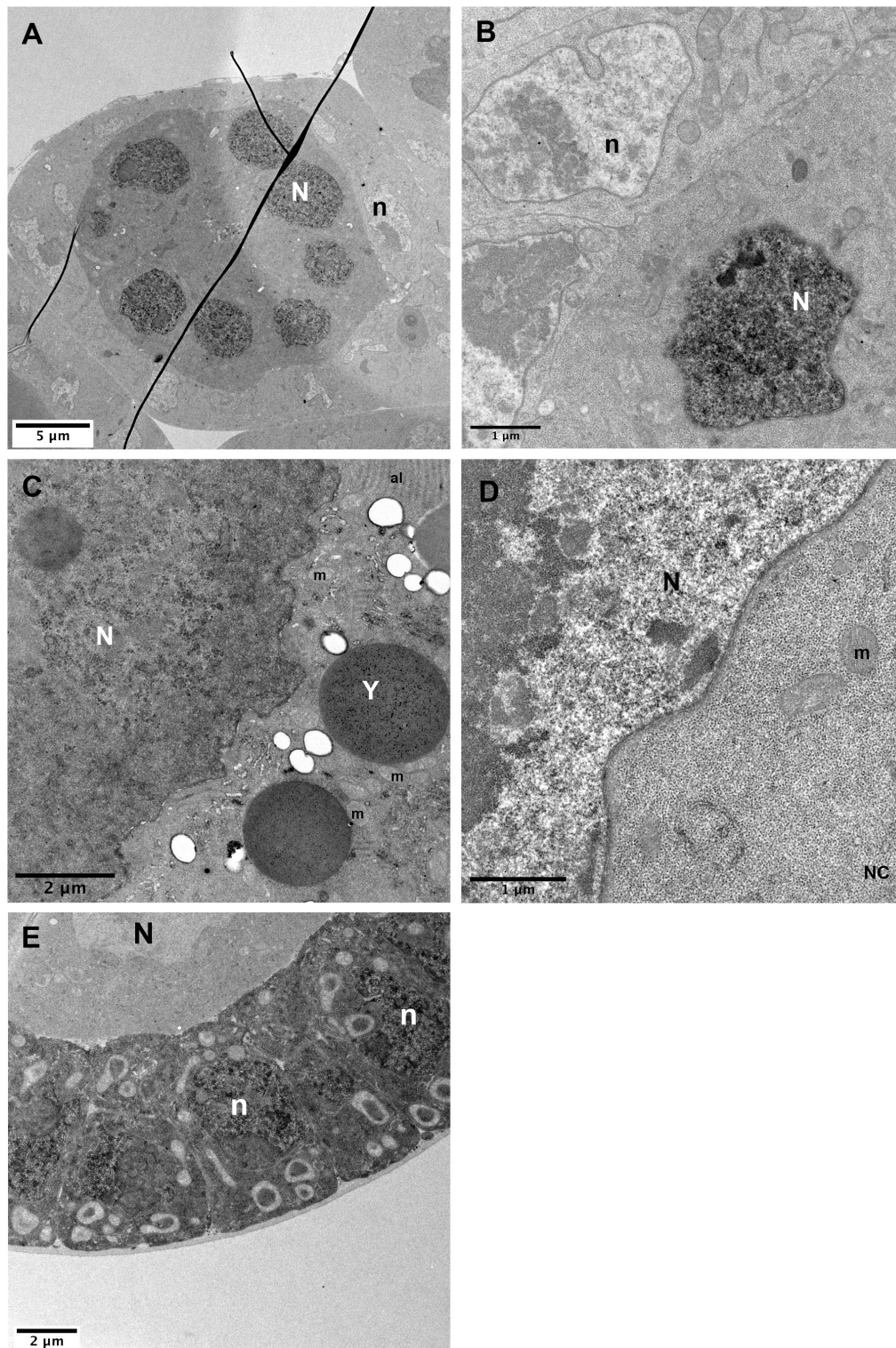


**FIGURE 6 |** Nuclear detection of APEX2. **(A–C)** In *hsp-flp; FRT79D ubi-nlsGFP/nos-GAL4<sup>VP16</sup>, UAS-APEX2-GBP* follicles, strong DAB staining is observed in germline nuclei (N) **(A)**, higher magnifications in panels **(B,C)**. **(D)** Control sample without the APEX2-GBP transgene exhibits a strong difference between the contrasts of the nucleus that is lighter than the cytoplasm. Comparison of the contrasts between panels **(C,D)** clearly shows that the stronger signal in the nucleus of *hsp-flp; FRT79D ubi-nlsGFP/nos-GAL4<sup>VP16</sup>, UAS-APEX2-GBP* ovarian follicles is specific. **(E)** In *hsp-flp; Tj-GAL4; FRT79D ubi-nlsGFP/UAS-APEX2-GBP*, nuclei of the follicular cells display strong accumulation of DAB precipitates. (N) germline nuclei, (n) follicle cells nuclei, (Y) yolk vesicle, (m) mitochondria, (al) annulate lamellae. Number of observations **(A–C)**: (*n* = 5), **(D)** (*n* = 2), **(E)** (*n* = 2).

we suggest performing negative controls with samples devoid of APEX-GBP proteins (no GAL4 transgene or no UAS-APEX2-GBP transgenes) and samples lacking GFP proteins. If a staining is reproducibly observed in APEX expressing tissue and never observed in controls, we can be confident about the specificity of the staining. In the case of nls-GFP localization with APEX, we thus compared the contrasts existing in the oocyte nucleus in the presence (**Figure 6C**) or absence (**Figure 6D**) of the APEX2 transgene. We also observed APEX-related contrast in the absence of GFP-labeled proteins (**Supplementary Figure 2**).

## Golgi Apparatus

In the *Drosophila* ovarian follicle, we often visualized an electron dense staining, independently of the presence of APEX, within the Golgi cisternae (**Supplementary Figure 2**). We believe that it depends on a glutathione peroxidase (PHGPx) located in the Golgi apparatus (Missirlis et al., 2003). The visualization of this staining is not fully penetrant but the APEX-GBP tool is probably not appropriate for the detection of POI located in this organelle.

## Weak APEX Signal

H<sub>2</sub>O<sub>2</sub> is necessary for the oxidation reaction to occur, however, it has also been reported that long incubation could inhibit the reaction (Ludwig, 2020). Therefore, in case of weak signal, the DAB labeling can not very easily be adjusted by changing its duration. Instead it has been suggested that lowering H<sub>2</sub>O<sub>2</sub> concentration to 0.5 mM greatly enhances APEX2 activity and sensitivity, and results in an increased contrast in TEM (Ludwig, 2020). It is therefore possible that small amounts of APEX protein can be detected by adjusting the H<sub>2</sub>O<sub>2</sub> concentration within the 10–0.5 mM range. Here we used in routine an intermediate concentration of 5.9 mM.

## Time Considerations

Dissection, fixation and washing procedures take around 4 h and are followed by 1 h post-fixation incubation, 1 h dehydration before an overnight incubation in the resin. Embedding takes a further 24 h, followed by an additional day required for resin polymerization. The embedded sample can be stored indefinitely before sectioning.

## CONCLUSION

The use of APEX has recently gained momentum in the scientific community as it offers an easy, cheap and rapid way of localizing a POI with the resolution of EM. This peroxidase has already been used in *Drosophila* in its original version (Chen et al., 2015; Lin et al., 2016).

By coupling APEX2 to the GBP nanobody, we have created a new tool that can be used in any cell type and for any GFP (and derivatives) labeled protein in *Drosophila*. We show here the flexibility of this tool to identify the nanometric localization of proteins in different compartments by TEM. Notably, proteins either expressed by their endogenous promoters or over-expressed have been detected with the exact same conditions, showing that this protocol does not need too much adaptation

from one POI to another. We have tested our protocol with classical TEM, but there have been reports showing that EM volume imaging such as SBF (serial block face) technology could also be successfully combined with APEX approaches (data not shown and Ariotti et al., 2015; Ludwig, 2020).

The bi-partite detection of APEX also offers the possibility for a reliable technique of correlative light and EM (CLEM) whereby the GFP-tagged POI can be visualized using fluorescence microscopy, and the DAB precipitate generated by APEX can be identified by EM at the place of the GFP-tag (For review, see Ariotti et al., 2015; Ludwig, 2020).

Finally, another popular use of APEX are the proteomic approaches. Indeed, in addition to DAB, APEX can use biotin-phenol as substrate. In presence of H<sub>2</sub>O<sub>2</sub>, APEX then catalyzes the formation of biotin-phenoxyl, which can covalently bind electron-rich amino acids such as tyrosine in the proteins located in close proximity. It is estimated that modified proteins are within a radius of 20 nm. Biotinylated proteins are subsequently identified by mass spectrometry. Several studies have successfully developed this approach including in *Drosophila* (Markmiller et al., 2018; Marmor-Kollet et al., 2020) and the *Drosophila* oocyte (Mannix et al., 2019; Gerdes et al., 2020). In addition, as APEX can also biotinylate guanosine in RNA, a recent study has used this property to determine subcellular transcriptome after RNA sequencing (Fazal et al., 2019). All these studies have been performed by using direct fusion of APEX to a POI. Theoretically, our APEX-GBP tool could also be suitable for these approaches and would prevent labs from generating new constructs given all the already existing GFP-tagged proteins.

## DATA AVAILABILITY STATEMENT

The original contributions presented in the study are included in the article/**Supplementary Material**, further inquiries can be directed to the corresponding author/s.

## AUTHOR CONTRIBUTIONS

JJ and SC designed the project and performed the cloning and transgenic analysis. SC and FB performed *Drosophila* experiments. CD and RB performed the TEM experiments. SC and FB conducted data interpretation and writing. All authors contributed to manuscript revision, read, and approved the submitted version.

## FUNDING

This work was supported by the CNRS, by the ARC (PJA 20161204931 and PJA 20191209724), by the “Ligue Contre le Cancer” (grant RS20/75-17), the Association des Entreprises contre le Cancer (Grant Gefluc 2020 #221366), and by an Emergence grant from IdEx Université de Paris (ANR-18-IDEX-0001). JJ was supported by a fellowship from “Ministère de l'Éducation Nationale, de la Recherche et de



la Technologie" (MENRT) and by a 4th year Ph.D. fellowship from Fondation "Ligue Contre le Cancer".

## ACKNOWLEDGMENTS

We would like to thank the ImagoSeine core facility of the Institut Jacques Monod, member of IBI SA and the France-BioImaging (ANR-10-INBS-04) infrastructure. We would also like to thank P. Conduit for critical comments on the manuscript; A. Ludwig, J. M. Verbavatz, and lab members for the critical discussions; the Bloomington Stock Center for fly stocks; and BestGene Inc Service for *Drosophila* embryo injections.

## REFERENCES

- Antony, C., Cibert, C., Geraud, G., Santa Maria, A., Maro, B., Mayau, V., et al. (1992). The small GTP-binding protein rab6p is distributed from medial Golgi to the trans-Golgi network as determined by a confocal microscopic approach. *J. Cell Sci.* 103, 785–796. doi: 10.1242/jcs.103.3.785
- Ariotti, N., Hall, T. E., Rae, J., Ferguson, C., McMahon, K. A., Martel, N., et al. (2015). Modular detection of GFP-labeled proteins for rapid screening by electron microscopy in cells and organisms. *Dev. Cell* 35, 513–525. doi: 10.1016/j.devcel.2015.10.016
- Ariotti, N., Rae, J., Giles, N., Martel, N., Sieracki, E., Gambin, Y., et al. (2018). Ultrastructural localisation of protein interactions using conditionally stable nanobodies. *PLoS Biol.* 16:e2005473. doi: 10.1371/journal.pbio.2005473
- Benton, R., and St Johnston, D. (2003). *Drosophila* PAR-1 and 14-3-3 inhibit Bazooka/Par-3 to establish complementary cortical domains in polarized cells. *Cell* 115, 691–704. doi: 10.1016/s0092-8674(03)00938-3
- Bernad, R., van der Velde, H., Fornerod, M., and Pickersgill, H. (2004). Nup358/RanBP2 attaches to the nuclear pore complex via association with Nup88 and Nup214/CAN and plays a supporting role in CRM1-mediated nuclear protein export. *Mol. Cell. Biol.* 24, 2373–2384. doi: 10.1128/mcb.24.6.2373-2384.2004
- Besson, C., Bernard, F., Corson, F., Rouault, H., Reynaud, E., Keder, A., et al. (2015). Planar cell polarity breaks the symmetry of PAR protein distribution prior to mitosis in *Drosophila* sensory organ precursor cells. *Curr. Biol.* 25, 1104–1110. doi: 10.1016/j.cub.2015.02.073
- Bosveld, F., Markova, O., Guirao, B., Martin, C., Wang, Z., Pierre, A., et al. (2016). Epithelial tricellular junctions act as interphase cell shape sensors to orient mitosis. *Nature* 530, 495–498. doi: 10.1038/nature16970
- Brand, A. H., and Perrimon, N. (1993). Targeted gene expression as a means of altering cell fates and generating dominant phenotypes. *Development* 118, 401–415. doi: 10.1242/dev.118.2.401
- Buszczak, M., Paterno, S., Lighthouse, D., Bachman, J., Planck, J., Owen, S., et al. (2007). The carnegie protein trap library: a versatile tool for *drosophila* developmental studies. *Genetics* 175, 1505–1531. doi: 10.1534/genetics.106.065961
- Chen, C. L., Hu, Y., Udeshi, N. D., Lau, T. Y., Wirtz-Peitz, F., He, L., et al. (2015). Proteomic mapping in live *Drosophila* tissues using an engineered ascorbate peroxidase. *Proc. Natl. Acad. Sci. U.S.A.* 112, 12093–12098. doi: 10.1073/pnas.1515623112
- Clyne, P. J., Brotman, J. S., Sweeney, S. T., and Davis, G. (2004). Erratum: green fluorescent protein tagging *drosophila* proteins at their native genomic loci with small P elements. *Genetics* 167:2143. doi: 10.1093/genetics/167.4.2763a
- Compagnon, J., Gervais, L., San Roman, M., Chamot-Bœuf, S., and Guichet, A. (2009). Interplay between Rab5 and PtdIns(4,5)P2 controls early endocytosis in the *Drosophila* germline. *J. Cell Sci.* 122, 25–35. doi: 10.1242/jcs.033027
- Dong, C., and Wu, G. (2013). G-protein-coupled receptor interaction with small GTPases. *Methods Enzymol.* 522, 97–108. doi: 10.1016/b978-0-12-407865-9.00006-6
- Duffy, J. B. (2002). GAL4 system in *Drosophila*: a fly geneticist's Swiss army knife. *Genesis* 34, 1–15. doi: 10.1002/gene.10150
- Fazal, F. M., Han, S., Parker, K. R., Kaewsapsak, P., Xu, J., Boettiger, A. N., et al. (2019). Atlas of Subcellular RNA localization revealed by APEX-Seq. *Cell* 178, 473–490. doi: 10.1016/j.cell.2019.05.027
- Franke, C., Repnik, U., Segeletz, S., Brouilly, N., Kalaidzidis, Y., Verbavatz, J. M., et al. (2019). Correlative single-molecule localization microscopy and electron tomography reveals endosome nanoscale domains. *Traffic* 20, 601–617. doi: 10.1111/tra.12671
- Gerdes, J. A., Mannix, K. M., Hudson, A. M., and Cooley, L. (2020). HtsRc-mediated accumulation of f-actin regulates ring canal size during *drosophila* melanogaster oogenesis. *Genetics* 216, 717–734. doi: 10.1534/genetics.120.303629
- Hampel, B., Schwarz, A., Ronchi, P., Bragulat-Teixidor, H., Tischer, C., Gaspar, I., et al. (2019). Nuclear pores assemble from nucleoporin condensates during oogenesis. *Cell* 179, 671–686. doi: 10.1016/j.cell.2019.09.022
- Huang, J., Zhou, W., Dong, W., Watson, A. M., and Hong, Y. (2009). Directed, efficient, and versatile modifications of the *Drosophila* genome by genomic engineering. *Proc. Natl. Acad. Sci. U.S.A.* 106, 8284–8289. doi: 10.1073/pnas.0900641106
- Januschke, J., Gervais, L., Dass, S., Kaltschmidt, J. A., Lopez-Schier, H., St Johnston, D., et al. (2002). Polar transport in the *Drosophila* oocyte requires dynein and kinesin I cooperation. *Curr. Biol.* 12, 1971–1981. doi: 10.1016/s0960-9822(02)01302-7
- Januschke, J., Nicolas, E., Compagnon, J., Formstecher, E., Goud, B., and Guichet, A. (2007). Rab6 and the secretory pathway affect oocyte polarity in *Drosophila*. *Development* 134, 3419–3425. doi: 10.1242/dev.008078
- Kelso, R. J., Buszczak, M., Quiñones, A. T., Castiblanco, C., Mazzalupo, S., and Cooley, L. (2004). Flytrap, a database documenting a GFP protein-trap insertion screen in *Drosophila melanogaster*. *Nucleic Acids Res.* 32, D418–D420. doi: 10.1093/nar/gkh014
- Kirchhofer, A., Helma, J., Schmidhals, K., Frauer, C., Cui, S., Karcher, A., et al. (2010). Modulation of protein properties in living cells using nanobodies. *Nat. Struct. Mol. Biol.* 17, 133–139. doi: 10.1038/nsmb.1727
- Kubala, M. H., Kovtun, O., Alexandrov, K., and Collins, B. M. (2010). Structural and thermodynamic analysis of the GFP-GFP-nanobody complex. *Protein Sci.* 19, 2389–2401. doi: 10.1002/pro.519
- Lam, S. S., Martell, J. D., Kamer, K. J., Deerinck, T. J., Ellisman, M. H., Mootha, V. K., et al. (2014). Directed evolution of APEX2 for electron microscopy and proximity labeling. *Nat. Methods* 12, 51–54. doi: 10.1038/nmeth.3179
- Lee, S.-Y., Kang, M.-G., Park, J.-S., Lee, G., Ting, A. Y., and Rhee, H.-W. (2016). APEX Fingerprinting reveals the subcellular localization of proteins of interest. *Cell Rep.* 15, 1837–1847. doi: 10.1016/j.celrep.2016.04.064
- Lin, T. Y., Luo, J., Shinomiya, K., Ting, C. Y., Lu, Z., Meinertzhagen, I. A., et al. (2016). Mapping chromatic pathways in the *Drosophila* visual system. *J. Comp. Neurol.* 524, 213–227. doi: 10.1002/cne.23857
- Lowe, N., Rees, J. S., Roote, J., Ryder, E., Armean, I. M., Johnson, G., et al. (2014). Analysis of the expression patterns, subcellular localisations and interaction partners of *drosophila* proteins using a pigp protein trap library. *Development* 141, 3994–4005. doi: 10.1242/dev.111054

## SUPPLEMENTARY MATERIAL

The Supplementary Material for this article can be found online at: <https://www.frontiersin.org/articles/10.3389/fcell.2021.719582/full#supplementary-material>

**Supplementary Figure 1** | Immunostaining anti-APEX2 on *P(Baz<sup>BAC</sup>.GFP)*; *Tj-GAL4*, *UAS-APEX2-GBP* ovarian follicles. Specific but diffuse staining is revealed in follicular cells.

**Supplementary Figure 2** | (A) Examples of non-specific staining independent of APEX in Golgi apparatus. (B) Negative control of APEX experiment. The APEX procedure was realized on *mud<sup>4</sup>/mud<sup>4</sup>; P(mud<sup>BAC</sup>.GFP)/P(mud<sup>BAC</sup>.GFP)*. In absence of APEX2-GBP, we revealed only the cell structures. (G) Golgi apparatus, (N) nuclei, (m) mitochondria, (PM) plasma membrane, (ER) endoplasmic reticulum.

- Ludwig, A. (2020). "Selective visualization of caveolae by tem using apex2," in *Methods in Molecular Biology*, ed. C. Blouin (New York, NY: Humana Press Inc), 1–10. doi: 10.1007/978-1-0716-0732-9\_1
- Mannix, K. M., Starble, R. M., Kaufman, R. S., and Cooley, L. (2019). Proximity labeling reveals novel interactomes in live *Drosophila* tissue. *Development* 146:dev176644. doi: 10.1242/dev.176644
- Markmiller, S., Soltanieh, S., Server, K. L., Mak, R., Jin, W., Fang, M. Y., et al. (2018). Context-dependent and disease-specific diversity in protein interactions within stress granules. *Cell* 172, 590–604. doi: 10.1016/j.cell.2017.12.032
- Marmor-Kollet, H., Siany, A., Kedersha, N., Knafo, N., Rivkin, N., Danino, Y. M., et al. (2020). Spatiotemporal proteomic analysis of stress granule disassembly using APEX reveals regulation by SUMOylation and links to ALS pathogenesis. *Mol. Cell* 80, 876–891. doi: 10.1016/j.molcel.2020.10.032
- Martell, J. D., Deerinck, T. J., Lam, S. S., Ellisman, M. H., and Ting, A. Y. (2017). Electron microscopy using the genetically encoded APEX2 tag in cultured mammalian cells. *Nat. Protoc.* 12, 1792–1816. doi: 10.1038/nprot.2017.065
- Martell, J. D., Deerinck, T. J., Sancak, Y., Poulos, T. L., Mootha, V. K., Sosinsky, G. E., et al. (2012). Engineered ascorbate peroxidase as a genetically encoded reporter for electron microscopy. *Nat. Biotechnol.* 30, 1143–1148. doi: 10.1038/nbt.2375
- Missirlis, F., Rahlfs, S., Dimopoulos, N., Bauer, H., Becker, K., Hilliker, A., et al. (2003). A putative glutathione peroxidase of *Drosophila* encodes a thioredoxin peroxidase that provides resistance against oxidative stress but fails to complement a lack of catalase activity. *Biol. Chem.* 384, 463–472. doi: 10.1515/BC.2003.052
- Morin, X., Daneman, R., Zavortink, M., and Chia, W. (2001). A protein trap strategy to detect GFP-tagged proteins expressed from their endogenous loci in *Drosophila*. *Proc. Natl. Acad. Sci. U.S.A.* 98, 15050–15055. doi: 10.1073/pnas.261408198
- Nagarkar-Jaiswal, S., Lee, P. T., Campbell, M. E., Chen, K., Anguiano-Zarate, S., Gutierrez, M. C., et al. (2015). A library of MiMICs allows tagging of genes and reversible, spatial and temporal knockdown of proteins in *Drosophila*. *Elife* 4:e05338. doi: 10.7554/eLife.05338
- Porstmann, B., Porstmann, T., Nugel, E., and Evers, U. (1985). Which of the commonly used marker enzymes gives the best results in colorimetric and fluorimetric enzyme immunoassays: horseradish peroxidase, alkaline phosphatase or  $\beta$ -galactosidase? *J. Immunol. Methods* 79, 27–37. doi: 10.1016/0022-1759(85)90388-6
- Quiñones-Coello, A. T., Petrella, L. N., Ayers, K., Melillo, A., Mazzalupo, S., Hudson, A. M., et al. (2007). Exploring strategies for protein trapping in *drosophila*. *Genetics* 175, 1089–1104. doi: 10.1534/genetics.106.065995
- Rae, J., Ferguson, C., Ariotti, N., Webb, R. I., Cheng, H. H., Mead, J. L., et al. (2021). A robust method for particulate detection of a genetic tag for 3D electron microscopy. *Elife* 10:e64630. doi: 10.7554/ELIFE.64630
- Richardson, K. C., Jarett, L., and Finke, E. H. (1960). Embedding in epoxy resins for ultrathin sectioning in electron microscopy. *Biotech. Histochem.* 35, 313–323. doi: 10.3109/10520296009114754
- Schnell, U., Dijk, F., Sjollem, K. A., and Giepmans, B. N. G. (2012). Immunolabeling artifacts and the need for live-cell imaging. *Nat. Methods* 9, 152–158. doi: 10.1038/nmeth.1855
- Shu, X., Lev-Ram, V., Deerinck, T. J., Qi, Y., Ramko, E. B., Davidson, M. W., et al. (2011). A genetically encoded tag for correlated light and electron microscopy of intact cells, tissues, and organisms. *PLoS Biol.* 9:1001041. doi: 10.1371/journal.pbio.1001041
- Sosinsky, G. E., Giepmans, B. N. G., Deerinck, T. J., Gaietta, G. M., and Ellisman, M. H. (2007). Markers for correlated light and electron microscopy. *Methods Cell Biol.* 2007, 575–591. doi: 10.1016/S0091-679X(06)79023-9
- Tan, B., Yatim, S. M. J. M., Peng, S., Gunaratne, J., Hunziker, W., and Ludwig, A. (2020). The mammalian crumbs complex defines a distinct polarity domain apical of epithelial tight junctions. *Curr. Biol.* 30, 2791–2804. doi: 10.1016/j.cub.2020.05.032
- Tissot, N., Lepesant, J. A., Bernard, F., Legent, K., Bosveld, F., Martin, C., et al. (2017). Distinct molecular cues ensure a robust microtubule-dependent nuclear positioning in the *Drosophila* oocyte. *Nat. Commun.* 8:15168. doi: 10.1038/ncomms15168
- Tokuyasu, K. T. (1986). Application of cryoultramicrotomy to immunocytochemistry. *J. Microsc.* 143, 139–149. doi: 10.1111/j.1365-2818.1986.tb02772.x
- White, J., Johannes, L., Mallard, F., Girod, A., Grill, S., Reinsch, S., et al. (1999). Rab6 coordinates a novel Golgi to ER retrograde transport pathway in live cells. *J. Cell Biol.* 147, 743–759. doi: 10.1083/jcb.147.4.743
- Yu, J. X., Guan, Z., and Nash, H. A. (2006). The mushroom body defect gene product is an essential component of the meiosis II spindle apparatus in *Drosophila* oocytes. *Genetics* 173, 243–253. doi: 10.1534/genetics.105.051557
- Zerial, M., and McBride, H. (2001). Rab proteins as membrane organizers. *Nat. Rev. Mol. Cell Biol.* 2, 107–117. doi: 10.1038/35052055

**Conflict of Interest:** The authors declare that the research was conducted in the absence of any commercial or financial relationships that could be construed as a potential conflict of interest.

**Publisher's Note:** All claims expressed in this article are solely those of the authors and do not necessarily represent those of their affiliated organizations, or those of the publisher, the editors and the reviewers. Any product that may be evaluated in this article, or claim that may be made by its manufacturer, is not guaranteed or endorsed by the publisher.

Copyright © 2021 Bernard, Jouette, Durieu, Le Borgne, Guichet and Claret. This is an open-access article distributed under the terms of the Creative Commons Attribution License (CC BY). The use, distribution or reproduction in other forums is permitted, provided the original author(s) and the copyright owner(s) are credited and that the original publication in this journal is cited, in accordance with accepted academic practice. No use, distribution or reproduction is permitted which does not comply with these terms.



# ERM-1 Phosphorylation and NRFL-1 Redundantly Control Lumen Formation in the *C. elegans* Intestine

Jorian J. Sepers<sup>1†</sup>, João J. Ramalho<sup>1,2†</sup>, Jason R. Kroll<sup>1</sup>, Ruben Schmidt<sup>1</sup> and Mike Boxem<sup>1\*</sup>

<sup>1</sup>Division of Developmental Biology, Department of Biology, Faculty of Science, Institute of Biodynamics and Biocomplexity, Utrecht University, Utrecht, Netherlands, <sup>2</sup>Laboratory of Biochemistry, Wageningen University and Research, Wageningen, Netherlands

## OPEN ACCESS

### Edited by:

Alexander Ludwig,  
Nanyang Technological University,  
Singapore

### Reviewed by:

Martha Soto,  
Rutgers, The State University of New  
Jersey, United States  
Maureen Peters,  
Oberlin College, United States

### \*Correspondence:

Mike Boxem  
m.boxem@uu.nl

<sup>†</sup>These authors have contributed  
equally to this work

### Specialty section:

This article was submitted to  
Morphogenesis and Patterning,  
a section of the journal  
Frontiers in Cell and Developmental  
Biology

**Received:** 02 September 2021

**Accepted:** 04 January 2022

**Published:** 07 February 2022

### Citation:

Sepers JJ, Ramalho JJ, Kroll JR,  
Schmidt R and Boxem M (2022) ERM-  
1 Phosphorylation and NRFL-1  
Redundantly Control Lumen Formation  
in the *C. elegans* Intestine.  
Front. Cell Dev. Biol. 10:769862.  
doi: 10.3389/fcell.2022.769862

Reorganization of the plasma membrane and underlying actin cytoskeleton into specialized domains is essential for the functioning of most polarized cells in animals. Proteins of the ezrin-radixin-moesin (ERM) and Na<sup>+</sup>/H<sup>+</sup> exchanger 3 regulating factor (NHERF) family are conserved regulators of cortical specialization. ERM proteins function as membrane-actin linkers and as molecular scaffolds that organize the distribution of proteins at the membrane. NHERF proteins are PDZ-domain containing adapters that can bind to ERM proteins and extend their scaffolding capability. Here, we investigate how ERM and NHERF proteins function in regulating intestinal lumen formation in the nematode *Caenorhabditis elegans*. *C. elegans* has single ERM and NHERF family proteins, termed ERM-1 and NRFL-1, and ERM-1 was previously shown to be critical for intestinal lumen formation. Using CRISPR/Cas9-generated *nrfl-1* alleles we demonstrate that NRFL-1 localizes at the intestinal microvilli, and that this localization is depended on an interaction with ERM-1. However, *nrfl-1* loss of function mutants are viable and do not show defects in intestinal development. Interestingly, combining *nrfl-1* loss with *erm-1* mutants that either block or mimic phosphorylation of a regulatory C-terminal threonine causes severe defects in intestinal lumen formation. These defects are not observed in the phosphorylation mutants alone, and resemble the effects of strong *erm-1* loss of function. The loss of NRFL-1 did not affect the localization or activity of ERM-1. Together, these data indicate that ERM-1 and NRFL-1 function together in intestinal lumen formation in *C. elegans*. We postulate that the functioning of ERM-1 in this tissue involves actin-binding activities that are regulated by the C-terminal threonine residue and the organization of apical domain composition through NRFL-1.

**Keywords:** ezrin, radixin, moesin, ERM-1, NHERF, EBP50, E3KARP, NRFL-1

## INTRODUCTION

The establishment of molecularly and functionally distinct apical, basal, and lateral domains is a key feature of polarized epithelial cells. The outside-facing apical domain has a different lipid and protein composition than the basal and lateral domains and is often decorated by microvilli. The specialization of the apical domain and microvilli formation requires the activities of the ezrin/radixin/moesin (ERM) family of proteins. ERM proteins consist of an N-terminal band Four-point-one/ezrin/radixin/moesin (FERM) domain that mediates binding to the plasma membrane and



membrane-associated proteins, a C-terminal tail that mediates actin binding, and a central  $\alpha$ -helical linker region (Fehon et al., 2010; McClatchey, 2014). In the cytoplasm, ERM proteins are kept in an inactive, closed, conformation that masks most of regulatory and protein interaction motifs due to an intramolecular interaction between the N- and C-terminal domains (Gary and Bretscher, 1995; Magendantz et al., 1995; Pearson et al., 2000; Li et al., 2007). Binding to the plasma membrane lipid phosphatidylinositol-(4,5) bisphosphate (PIP<sub>2</sub>) as well as phosphorylation of a conserved C-terminal threonine residue (T567 in ezrin) promote the transition to an open and active conformation that can link the plasma membrane to the underlying actin cytoskeleton and control the spatial distribution of protein complexes at the membrane (Simons et al., 1998; Nakamura et al., 1999; Barret et al., 2000; Coscoy et al., 2002; Yonemura et al., 2002; Fievet et al., 2004; Hao et al., 2009; Roch et al., 2010).

The ability of ERM proteins to associate with other proteins can be extended by binding to the scaffolding proteins NHERF1 and NHERF2 (Na<sup>+</sup>/H<sup>+</sup> exchanger regulatory factors 1 and 2). NHERF1/2 were identified as co-regulators of the Na<sup>+</sup>/H<sup>+</sup> exchanger NHE3 in kidney epithelial cells (Weinman et al., 1993; Yun et al., 1997; Lamprecht et al., 1998). Independently, NHERF1 was identified as the ERM-binding phosphoprotein 50 (EBP50), based on its ability to interact with activated ezrin and moesin (Reczek et al., 1997). NHERF1/2 are closely related proteins that contain two postsynaptic density 95/disk large/zona occludens-1 (PDZ) domains and an ERM-binding (EB) C-terminal tail that can bind to the FERM domain of active ERM proteins. Since their discovery, a large variety of NHERF1/2 interactors have been identified, including transporters like the cystic fibrosis transmembrane conductance regulator (CFTR) (Seidler et al., 2009), growth factor receptors including EGFR and PDGFR (Maudsley et al., 2000; Lazar et al., 2004), and other scaffold proteins such as the NHERF family member PDZK1 (PDZ domain containing 1) (LaLonde and Bretscher, 2009).

The functional significance of the interaction of NHERF1/2 with ERM proteins is best understood for NHERF1/EBP50. In JEG3 cells, NHERF1/EBP50 promotes microvilli formation or stability by acting as a linker between ezrin and PDZK1, and mice lacking either ezrin or NHERF1/EBP50 show similar defects in microvilli formation and organization in the intestine (Morales et al., 2004; Saotome et al., 2004; Garbett et al., 2010; LaLonde et al., 2010). In a model of MDCK cells developing into 3D cysts, a complex of NHERF1/EBP50, ezrin, and Podocalyxin promotes apical identity and is required for lumen formation (Bryant et al., 2014). In a different 3D cyst model grown from Caco-2 colorectal cells, NHERF1/EBP50 is similarly required for apical-basal polarization and lumen formation, but in conjunction with moesin rather than ezrin (Georgescu et al., 2014).

In addition to extending the scaffolding capacity of ERM proteins, NHERF proteins have also been reported to regulate the activity of ERM proteins. In NHERF1/EBP50 knockout mice, levels of ERM proteins in membrane fractions of kidney and intestinal epithelial cells are decreased, suggesting that NHERF1/EBP50 stabilizes ERM proteins at the plasma membrane (Morales et al., 2004). In *Drosophila* follicle cells, the single NHERF1/2

ortholog Sip1 is thought to promote phosphorylation and activation of Moesin through recruitment of the Ste20-family kinase Slik (Hughes et al., 2010). In an ovarian cancer cell line, depletion of NHERF1/EBP50 led to reduced levels of phosphorylated ERM (pERM) upon stimulation with lysophosphatidic acid (LPA) (Oh et al., 2017). Similarly, NHERF2 was found to promote the phosphorylation of ERM in bovine pulmonary artery endothelial cells, possibly through an interaction with Rho kinase 2 (ROCK2) (Boratkó and Csontos, 2013). Finally, NHERF1/EBP50 may also indirectly affect the localization of ERM proteins, by promoting the local accumulation of PIP<sub>2</sub> through recruitment of lipid phosphatases or kinases (Ikenouchi et al., 2013; Georgescu et al., 2014). Thus, NHERF proteins may function both as ERM effectors and regulators.

Here, we make use of the nematode *Caenorhabditis elegans* to better understand how NHERF and ERM proteins function together to promote apical domain identity. The *C. elegans* genome encodes single orthologs of each protein family, termed NRFL-1 and ERM-1, that are highly similar in sequence and domain composition to their counterparts in other organisms (Figure 1A; Supplementary Figure S1A). ERM-1 localizes to the apical surface of several epithelial tissues and is essential for apical membrane morphogenesis in the intestine (Göbel et al., 2004; Van Fürden et al., 2004). Loss of *erm-1* in the intestine causes constrictions, loss of microvilli, severe reduction in the levels of apical actin, and defects in the accumulation of junctional proteins (Göbel et al., 2004; Van Fürden et al., 2004; Bernadskaya et al., 2011). Recently, we demonstrated that the functioning of ERM-1 critically depends on its ability to bind membrane phospholipids, while phosphorylation of a C-terminal regulatory threonine residue modulates ERM-1 apical localization and dynamics (Ramalho et al., 2020).

In contrast to ERM-1, little is known about the functioning of NRFL-1. A yeast-two hybrid screen identified the amino acid transporter (AAT) family protein AAT-6 as an interactor of NRFL-1 (Hagiwara et al., 2012). However, the effects of NRFL-1 loss are minor. In aging adults, AAT-6 is no longer retained at the luminal membrane of the intestine in *nrfl-1* mutants, while younger *nrfl-1* mutants show increased mobility of AAT-6 by fluorescence recovery after photobleaching (FRAP). Moreover, *nrfl-1* mutants are homozygous viable, demonstrating that NRFL-1 is not critical for intestinal development (Hagiwara et al., 2012).

To investigate the relationship between ERM-1 and NRFL-1, we used CRISPR/Cas9 engineering to generate an *nrfl-1* deletion mutant, a mutant lacking the ERM-1 binding domain, and fluorescently tagged NRFL-1 variants. We show that NRFL-1 localizes to the apical microvillar domain of the intestine, and that this localization depends on the ability of NRFL-1 to bind to ERM-1 via the C-terminal ERM-1 binding domain. The loss of *nrfl-1* did not affect the localization, phosphorylation status, or protein dynamics of ERM-1, indicating that *C. elegans* NRFL-1 does not control the activity of ERM-1. However, when we combined the *nrfl-1* null mutant with *erm-1* mutants that block or mimic phosphorylation of the C-terminal threonine

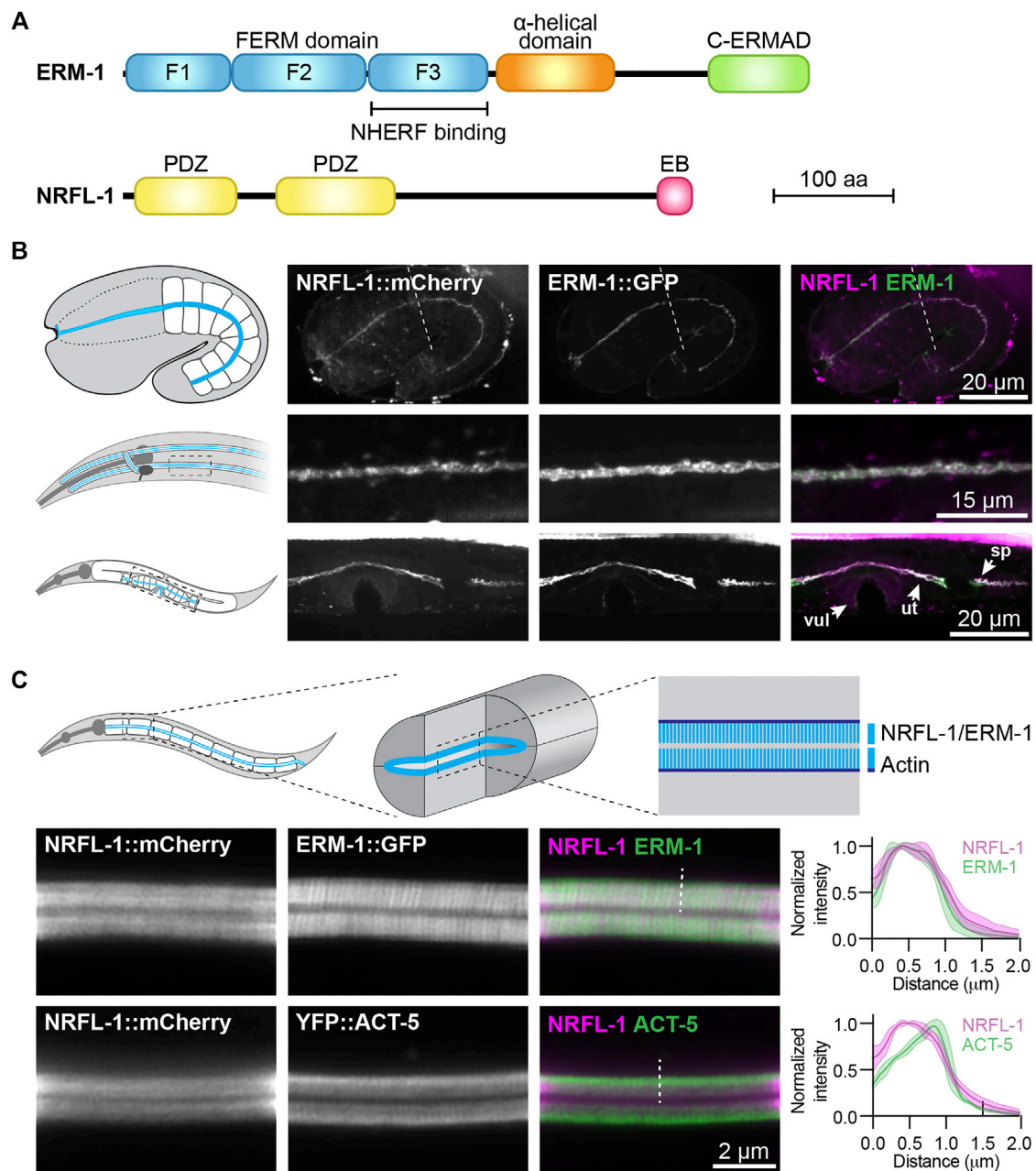


**FIGURE 1** | NRFL-1::mCherry localizes to the apical microvilli of intestinal cells. **(A)** Schematic representation of the domain organization of ERM-1 and NRFL-1. F1-F3 correspond to the three structural modules making up the FERM domain. FERM = Four-point-one, ezrin, radixin, moesin; C-ERMAD = C-terminal ezrin Radixin moesin (ERM) association domain; PDZ = Post-synaptic density-95, disks-large and zonula occludens-1; EB = ERM binding. **(B)** Distribution of NRFL-1::mCherry and ERM-1::GFP in embryos (top panels), the excretory canal in L1 larvae (middle panels), and the vulva (vul), uterus (ut) and spermatheca (sp) in L4 larvae (bottom panels). Dashed line in the embryo panels separates the pharynx (left) from the intestine (right). **(C)** Distribution of NRFL-1::mCherry relative to ERM-1::GFP and YFP::ACT-5 at the apical membrane of L4 larval intestines. Dashed line serves as an example of the line scan position used for the graphs on the right. Graphs plot the relative fluorescence intensity from the intestinal lumen to the cytoplasm. Solid line represents the mean and the shading lines the  $\pm$  SD.  $n = 6$  animals for both graphs. Images were taken using spinning-disk. **(B)** and Airyscan confocal microscopes **(C)**, and maximum intensity projections **(B)** or a single plane **(C)** are presented. Note that due to the longer wavelength emitted by mCherry compared to GFP, the microvilli are better resolved using ERM-1::GFP than using NRFL-1::mCherry.

544 residue, we observed severe intestinal defects, resembling the effects of strong loss of *erm-1* function. In mice, ezrin was shown to form distinct complexes with NHERF1/EBP50 and actin. As the ERM-1 phosphorylation mutants affect the ability

of ERM-1 to interact with actin, we postulate that the activities of ERM-1 in the intestine redundantly involve actin binding and the organization of apical domain composition through NRFL-1.

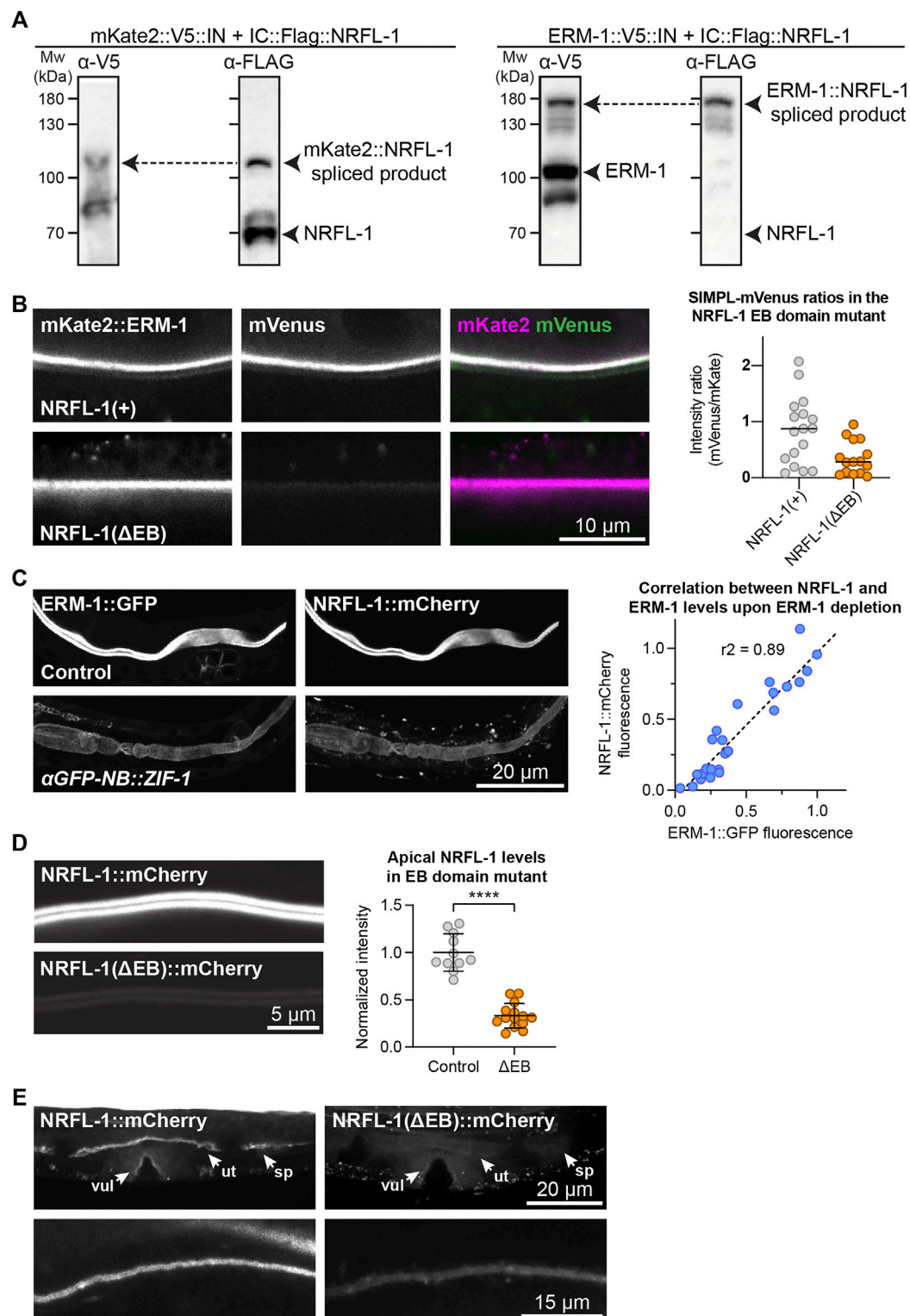


**FIGURE 2 |** NRFL-1 localizes to the apical domain through ERM-1 binding. **(A)** Detection of an ERM-1–NRFL-1 interaction using the SIMPL system. V5 and FLAG epitopes are detected by western blot. Arrowheads indicate both unspliced proteins and the higher molecular weight covalently linked fusion proteins, generated by Intein splicing activity. Little splicing of NRFL-1 is observed with the control mKate2::V5::IN protein, while all NRFL-1 is spliced to ERM-1 in animals expressing ERM-1::V5::IN **(B)** Detection of an interaction of ERM-1 with wild-type NRFL-1, but not with NRFL-1(ΔEB), using the SIMPL-mVenus system. NRFL-1a::InteinC-3xFLAG-VC155 [NRFL-1(+)] or NRFL-1a(ΔEB)::InteinC-3xFLAG-VC155 [NRFL-1(ΔEB)] are expressed with mKate2::ERM-1::VN155-HA-V5-InteinN (mKate2::ERM-1). *(Continued)*



**FIGURE 2** | Fluorescence micrographs show representative examples. Graphs show quantification of apical mVenus levels, expressed as a ratio over mKate2::ERM-1 to account for varying expression levels of the extrachromosomal array. Each data point represents a single intestinal cell. Lines indicate median.  $N = 17$  cells for NRFL-1(+) and 15 cells for NRFL-1( $\Delta$ EB). **(C)** Quantification of apical levels of NRFL-1::mCherry vs. ERM-1::GFP in L1 larval intestines upon different levels of ERM-1::GFP depletion by expression of an anti-GFP nanobody::ZIF-1 fusion protein. Fluorescence micrographs show representative examples, graph shows quantification of signal intensity at the apical membrane. Each data point in the graph represents a single animal, and the line a linear regression. Values are normalized to the mean intensity in control animals.  $n = 25$  animals. **(D)** Quantification of apical levels of NRFL-1( $\Delta$ EB)::mCherry relative to NRFL-1::mCherry at the apical membrane of L1 larval intestines. Fluorescence micrographs show representative examples, and the graph the quantification. Each data point in the graph represents a single animal, and values are normalized to the mean intensity in control animals. Error bars: mean  $\pm$  SD; Statistical test: Welch's Student's t-test; \*\*\*\* =  $p \leq 0.0001$ .  $n = 10$  animals for NRFL-1::mCherry and 14 animals for NRFL-1( $\Delta$ EB)::mCherry. **(E)** Localization of NRFL-1::mCherry and NRFL-1( $\Delta$ EB)::mCherry in the vulva (vul), uterus (ut) and spermatheca (sp) in L4 larvae (top panels), and the excretory canal in L1 larvae (bottom panels). Images of the same tissue were acquired and displayed with the same settings for comparison. All images were taken using a spinning disk confocal microscope, and a single plane **(B)** or maximum intensity projections **(C,D, and E)** are presented.

## RESULTS

### NRFL-1 Localizes to the Apical Domain Through ERM-1 Binding

To investigate the relationship between NRFL-1 and ERM-1, we first examined if NRFL-1 colocalizes with ERM-1. We used CRISPR/Cas9 to engineer an endogenous C-terminal NRFL-1::mCherry fusion, which tags all predicted isoforms. Animals homozygous for the *nrfl-1::mCherry* knock-in are viable and have a wild-type appearance. We detected expression of NRFL-1 in multiple epithelia including the intestine, excretory canal, pharynx, uterus, and spermatheca (**Figures 1B,C**). In each of these tissues, NRFL-1::mCherry co-localized with an endogenous ERM-1::GFP fusion protein at the cortex (**Figures 1B,C**). In the embryo, NRFL-1 localized to the nascent apical domain of intestinal cells, overlapping with ERM-1 (**Figure 1B**). Confocal super resolution imaging of the intestine in larval stages showed co-localization of NRFL-1 with ERM-1::GFP and YFP::ACT-5 at microvilli, apical to the more intense belt of YFP::ACT-5 at the terminal web (**Figure 1C**). The observed distribution of NRFL-1::mCherry is consistent with previous observations in *C. elegans* (Hagiwara et al., 2012), as well as with localization of EBP50 in mammalian epithelial tissues (Ingraffea, 2002; Morales et al., 2004; Kreimann et al., 2007).

We previously showed that ERM-1 and NRFL-1 interact in a yeast two-hybrid assay and in pull-downs from mammalian cultured cells (Koorman et al., 2016). To determine if these proteins interact in a more physiological setting, we used the recently developed split intein-mediated protein ligation (SIMPL) system that relies on protein splicing by split intein domains to detect protein-protein interactions (Yao et al., 2020). We ubiquitously expressed ERM-1 fused to the intein N-terminal fragment (IN) and the V5 epitope, and NRFL-1 fused to the C-terminal fragment (IC) and the FLAG epitope. We observed full splicing of NRFL-1 to ERM-1 by western blot of *C. elegans* lysates, apparent as a high molecular weight band that stains with both V5 and FLAG antibodies (**Figure 2A**). In contrast, a negative control pair consisting of IC-tagged NRFL-1 and IN-tagged mKate2 showed only limited splicing of NRFL-1 to mKate2 (**Figure 2A**). To visualize if splicing occurs *in vivo* in the intestine, we modified the SIMPL system by including a split mVenus tag. We added the mVenus N-terminal fragment (VN155) to ERM-1::V5-IN and mVenus C-terminal fragment (VC155) to IC-FLAG::NRFL-1, such that upon intein splicing the reconstituted mVenus becomes

linked to NRFL-1 (Kodama and Hu, 2010). We readily observed localization of mVenus at the apical domain of intestinal cells, indicating that NRFL-1 and ERM-1 interact in this tissue (**Figure 2B**).

We next investigated whether NRFL-1 distribution to the apical plasma membrane is dependent on ERM-1, by analyzing NRFL-1::mCherry upon tissue-specific depletion of ERM-1. To deplete ERM-1 in intestinal cells, we introduced an anti-GFP-nanobody::ZIF-1 fusion driven by the intestine-specific *elt-2* promoter as an extrachromosomal array in animals expressing endogenous ERM-1::GFP and NRFL-1::mCherry (Wang et al., 2017). Expression of the nanobody::ZIF-1 fusion resulted in variable levels of ERM-1::GFP depletion. The apical levels of ERM-1::GFP and NRFL-1::mCherry showed a linear correlation, indicating that apical recruitment of NRFL-1 in the intestine directly depends on ERM-1 (**Figure 2C**).

The interaction between mammalian EBP50 and ezrin requires the C-terminal EB domain (Reczek et al., 1997; Reczek and Bretscher, 1998; Finnerty et al., 2004), which is conserved in NRFL-1 (**Figures 1A; Supplementary Figure S1A**). To determine if the NRFL-1 EB domain is required for the interaction with ERM-1, we repeated the SIMPL-mVenus experiment using an NRFL-1( $\Delta$ EB) mutant that lacks the C-terminal 28 amino acids of NRFL-1. Compared to wild-type NRFL-1, we observed only residual apical localization of mVenus in intestinal cells, indicating that the interaction of NRFL-1 with ERM-1 depends on the presence of the EB domain (**Figure 2B**).

To determine if the EB domain is necessary for the apical localization of NRFL-1, we used CRISPR/Cas9 to engineer the 28 aa EB deletion in the *nrfl-1::mCherry* strain. The resulting *nrfl-1( $\Delta$ eb)::mCherry* animals are homozygous viable, consistent with the lack of severe defects in previously described *nrfl-1* mutants (Hagiwara et al., 2012; Na et al., 2017). We detected a dramatic reduction in apical levels of NRFL-1( $\Delta$ EB)::mCherry in intestinal cells when compared with NRFL-1::mCherry (**Figure 2D**). NRFL-1( $\Delta$ EB)::mCherry also failed to localize at the cortex in the uterus and spermatheca, while apical levels in the excretory canal were reduced (**Figure 2E**). These results indicate that apical recruitment of NRFL-1 is mediated by the EB domain. However, the presence of some residual apical NRFL-1( $\Delta$ EB)::mCherry in the intestine and excretory canal suggests the existence of alternative membrane-targeting mechanisms. Collectively, our results show that the interaction between ERM and NHERF

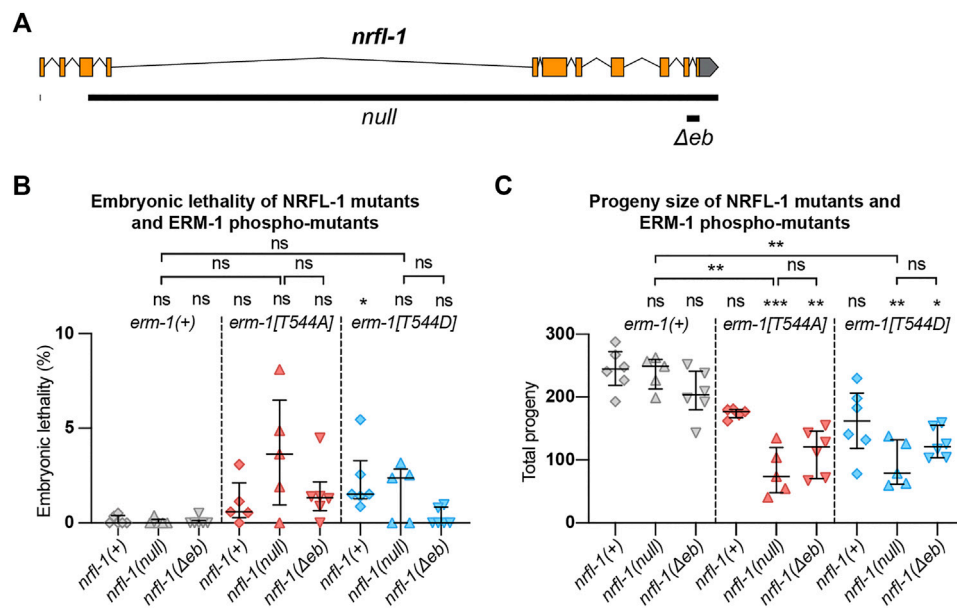


**FIGURE 3 |** NRFL-1 cooperates with ERM-1 C-terminal phosphorylation. **(A)** Gene model for *nrfl-1a*. Orange boxes represent exons and lines represent introns. Grey box represents 3' untranslated region. Black bars denote the regions deleted in *null* and  $\Delta eb$  alleles. **(B,C)** Quantification of embryonic lethality **(B)** and total progeny **(C)** from parents of indicated genotypes. Each data point represents the embryonic lethality **(B)** or progeny **(C)** of a single animal; N = 5 or 6. Error bars: mean  $\pm$  SD. Statistical test: Kruskal-Wallis test with Dunn's multiple comparison correction.

proteins is conserved in *C. elegans*, and that the localization of NRFL-1 is largely mediated by its interaction with ERM-1.

## NRFL-1 Cooperates with ERM-1 Phosphorylation in Regulating Intestinal Lumen Formation

We next wanted to investigate the effects of loss of NRFL-1 on intestinal lumen formation. Previous studies using partial deletion alleles of *nrfl-1* indicated that loss of NRFL-1 alone does not cause defects in the formation of the intestine (Hagiwara et al., 2012; Na et al., 2017). To rule out the possibility that the lack of severe defects is due to the production of truncated NRFL-1 proteins, we used CRISPR/Cas9 genome engineering to generate the *nrfl-1(mib59)* deletion allele. This allele lacks almost the entire *nrfl-1* locus and additionally causes a frameshift in the first exon of the long isoforms (Figure 3A). Hence, we refer to *mib59* as *nrfl-1(null)*. The *mib59* deletion also removes a candidate non-coding RNA and overlapping 21U-RNA located in the large 3<sup>rd</sup> exon of *nrfl-1a*. Animals homozygous for the *nrfl-1(null)* allele are viable, have a healthy appearance, and normal brood sizes, confirming that NRFL-1 is not essential for *C. elegans* development (Figure 3B,C).

One of the possible reasons for the lack of a severe intestinal phenotype in *nrfl-1(null)* animals is that NRFL-1 may only mediate part of the functions of ERM-1 in the intestine. To investigate this possibility, we made use of the non-phosphorylatable *erm-1[T544A]* and phosphomimetic *erm-1[T544D]* alleles we generated previously (Ramalho et al., 2020). Both mutants cause a delay in the apical recruitment of ERM-1

and actin during embryogenesis, and the appearance of constrictions along the course of the lumen that only occasionally persist to the L1 stage. In contrast to *erm-1* RNAi or strong loss-of-function alleles, however, these animals are viable. Thus, *erm-1[T544A]* and *erm-1[T544D]* represent partial loss-of-function alleles that may act as a sensitized background to reveal the contribution of NRFL-1 to ERM-1 functioning. We therefore generated double mutants that carry the *nrfl-1(null)* allele and either of the *erm-1[T544A]* or *erm-1[T544D]* alleles. As a first indicator of synthetic defects, we examined the double mutant strains for embryonic lethality or an increase in the mild brood size defect observed in *erm-1[T544A]* and *erm-1[T544D]* mutants. We did not observe strong embryonic lethality in any mutant combination (<5%, Figure 3B). However, combining *nrfl-1(null)* with either *erm-1* phosphorylation mutant resulted in a strongly reduced brood size (Figure 3C). In addition, many larvae in the double mutant combination had a sick appearance and developed slowly. Nevertheless, both double mutants can be maintained as homozygotes, unlike strong *erm-1* loss of function mutants.

We next examined the formation of the intestinal lumen and actin distribution using YFP::ACT-5 as a marker. We did not detect any defects in apical enrichment of ACT-5 or intestinal morphology in *nrfl-1(null)* embryos and larvae (Figures 4A–C). Combining the *erm-1[T544A]* and *erm-1[T544D]* alleles with the *nrfl-1(null)* allele significantly increased the frequency of intestinal constrictions and their persistence until larval development (Figures 4A,C). Intestines of early larval *nrfl-1(null); erm-1[T544A]* and *nrfl-1(null); erm-1[T544D]* animals were characterized by a cystic appearance and multiple

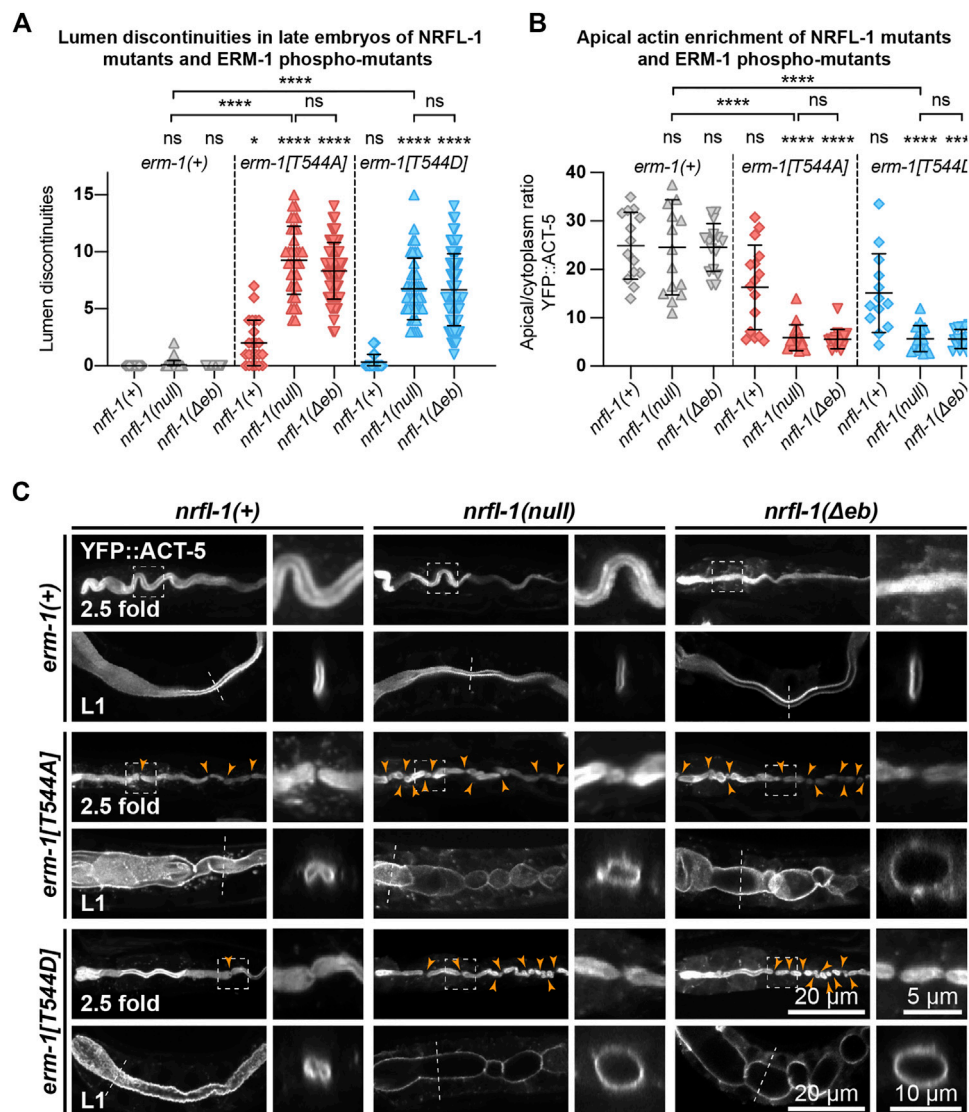


**FIGURE 4 |** ERM-1 phosphorylation and NRFL-1 redundantly contribute to intestinal morphology. **(A)** Quantification of lumen discontinuities in 2.5-fold stage embryos of indicated genotypes expressing YFP::ACT-5. Each data point represents a single animal. Error bars: mean  $\pm$  SD. Statistical test: Kruskal-Wallis test with Dunn's multiple comparison correction. *nrfl-1(+)*; *erm-1(+)*  $n = 19$ , *nrfl-1(null)*; *erm-1(+)*  $n = 35$ , *nrfl-1( $\Delta$ eb)*; *erm-1(+)*  $n = 48$ , *nrfl-1(+)*; *erm-1[T544A]*  $n = 23$ , *nrfl-1(null)*; *erm-1[T544A]*  $n = 35$ , *nrfl-1( $\Delta$ eb)*; *erm-1[T544A]*  $n = 61$ , *nrfl-1(+)*; *erm-1[T544D]*  $n = 28$ , *nrfl-1(null)*; *erm-1[T544D]*  $n = 41$ , *nrfl-1( $\Delta$ eb)*; *erm-1[T544D]*  $n = 69$ . **(B)** Quantification of the apical-cytoplasm ratio of YFP::ACT-5 in L1 larvae of indicated genotypes. Each data point represents a single animal. Error bars: mean  $\pm$  SD. Statistical test: Kruskal-Wallis test with Dunn's multiple comparison correction. *nrfl-1(+)*; *erm-1(+)*  $n = 14$ , *nrfl-1(null)*; *erm-1(+)*  $n = 15$ , *nrfl-1( $\Delta$ eb)*; *erm-1(+)*  $n = 16$ , *nrfl-1(+)*; *erm-1[T544A]*  $n = 16$ , *nrfl-1(null)*; *erm-1[T544A]*  $n = 16$ , *nrfl-1( $\Delta$ eb)*; *erm-1[T544A]*  $n = 16$ , *nrfl-1(+)*; *erm-1[T544D]*  $n = 13$ , *nrfl-1(null)*; *erm-1[T544D]*  $n = 16$ , *nrfl-1( $\Delta$ eb)*; *erm-1[T544D]*  $n = 16$ . **(C)** Representative images of intestinal defects in 2.5-fold stage embryos and L1 larvae of indicated genotypes, expressing YFP::ACT-5 as an apical marker. Images of the 2.5-fold stage embryos were computationally straightened, and the orange arrowheads indicate the constrictions in the lumen. Small panels to the right of each embryo panel show an enlargement of the region indicated by the dashed box, and small panels to the right of each L1 larva show a cross-section view of the intestine at the position indicated by the dotted line. All images are taken using a spinning-disk confocal microscope, and maximum intensity projections are presented.

constrictions that block intestinal flow as seen in feeding assays with fluorescent membrane-impermeable dextran (Supplementary Figure S2A). In surviving L2 or older animals, we only observed morphological defects but no lumen discontinuities, indicating that the early larval arrest in double mutants is due to a block of flow of food through the intestine (Supplementary Figure S2B). In addition to the

increase in intestinal constrictions, we also observe that loss of *nrfl-1* caused a further decrease in the apical levels of YFP::ACT-5 in *erm-1[T544A]* and *erm-1[T544D]* mutant animals (Figure 4B).

Finally, as the EB domain is essential for the apical localization of NRFL-1 and its interaction with ERM-1, we determined if loss of the EB domain results in similar synergistic phenotypes with the ERM-1 phosphorylation mutants as complete loss of NRFL-1.

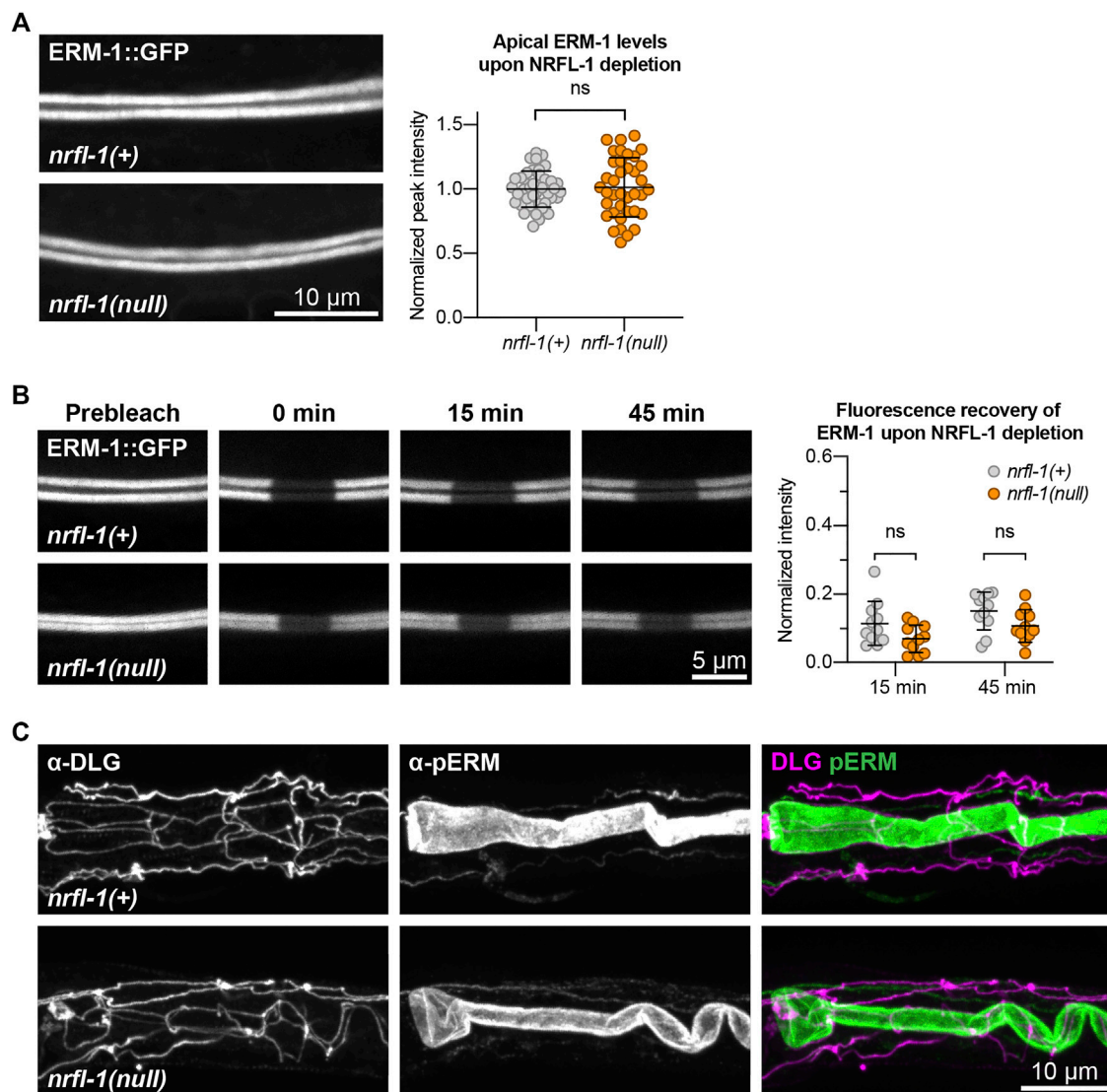


**FIGURE 5 |** NRFL-1 does not regulate ERM-1 apical accumulation, dynamics, or phosphorylation status. **(A)** Representative images and quantification of ERM-1::GFP levels at the apical membrane of intestines in *nrfl-1(+)* and *nrfl-1(null)* L4 larvae. Each data point represents a single animal, and values are normalized to the mean intensity in control animals. Error bars: mean  $\pm$  SD. Statistical test: Unpaired Student's t-test. *nrfl-1(+)*  $n = 40$ , *nrfl-1(null)*  $n = 38$ . **(B)** FRAP analysis of apical ERM-1::GFP in the intestine of *nrfl-1(+)* and *nrfl-1(null)* L4 larvae. Fluorescence micrographs show representative examples. Graph shows the fluorescence intensity of ERM-1 in the photobleached region at the apical intestinal domain during recovery. Each data point represents a single animal, and values are relative to prebleach levels. Error bars: mean  $\pm$  SD. Statistical test: Unpaired Student's t-test.  $n = 11$  for both genotypes and both timepoints. **(C)** Representative images of fixed *nrfl-1(+)* and *nrfl-1(null)* larvae stained with antibodies recognizing the junctional protein DLG-1 ( $\alpha$ -DLG) and phosphorylated ERM-1 ( $\alpha$ -pERM).

We used CRISPR/Cas9 genome engineering to generate a second *nrfl-1*( $\Delta eb$ ) allele, also removing the final 28 aa but lacking the mCherry tag used above (Figure 3A). Similar to our observations for the mCherry-tagged variant, homozygous *nrfl-1*( $\Delta eb$ ) mutants are viable and show no significant defects in brood size, intestinal development, or apical ACT-5 enrichment (Figures 3B,C; Figures 4A–C). However, when combined with *erm-1*[T544A] or *erm-1*[T544D], the resulting double mutants showed similar defects in viability, growth, brood size, intestinal development, and ACT-5 enrichment as observed using the *nrfl-1*(null) allele (Figures 3B,C; Figures 4A–C). Thus, the

*nrfl-1*( $\Delta eb$ ) allele behaves like a null allele of *nrfl-1*. Taken together, our data show that NRFL-1 and ERM-1 function together in promoting lumen formation in the *C. elegans* intestine, and the binding to ERM-1 is essential for the functioning of NRFL-1 in the intestine.

## NRFL-1 Does Not Directly Regulate ERM-1 Activity

NRFL-1 could function together with ERM-1 in at least two ways. It could act as a scaffold protein that is required for ERM-1 to



organize protein complexes at the membrane, or it could regulate the activity of ERM-1 itself. To distinguish between these possibilities, we investigated whether loss of NRFL-1 affects the distribution, mobility, or T544 phosphorylation status of ERM-1. We first analyzed the distribution of ERM-1::GFP in larval *nrfl-1(null)* mutants. We did not detect any change in ERM-1::GFP subcellular localization or levels at the apical membrane in the intestine (**Figure 5A**). Moreover, FRAP analysis demonstrated that the mobility of ERM-1::GFP at the apical intestinal membrane was not significantly altered in *nrfl-1(null)* larvae (**Figure 5B**). We next investigated whether NRFL-1 regulates ERM-1 C-terminal phosphorylation by staining *nrfl-1(null)* mutants with an antibody specific for the C-terminal phosphorylated form of ERM proteins (pERM). The residues used to raise this antibody are fully conserved between mammals and *C. elegans* (Ramalho et al., 2020). Nevertheless, we first confirmed the specificity of the antibody for T544 phosphorylated ERM-1 by immunostaining of ERM-1[T544A] mutant animals. We readily detected pERM staining of the intestinal lumen in wild-type larvae, while no staining was observed in ERM-1[T544A] animals (**Supplementary Figure S3A**). Moreover, treatment of embryos with a phosphatase abolished staining with the pERM antibody (**Supplementary Figure S3B**). Thus, the pERM antibody is specific for T544 phosphorylated ERM-1. We then stained *nrfl-1(+)* and *nrfl-1(null)* animals with the pERM antibody. In both backgrounds, the pERM antibody stained the lumen of the intestine, indicating that loss of *nrfl-1* does not significantly alter the phosphorylation status of the C-terminal regulatory threonine of ERM-1 (**Figure 5C**). Taken together, our results show that NRFL-1 does not regulate the distribution, dynamics, or phosphorylation of ERM-1, and therefore does not seem to directly regulate ERM-1.

## DISCUSSION

ERM and NHERF proteins function together in the specialization of polar membrane domains in several mammalian cell types. Here, we show that this cooperation is conserved in *C. elegans*, and that ERM-1 and NRFL-1 function together in lumen formation in the intestine. NRFL-1 physically interacts with ERM-1 through its C-terminal EB domain. The interaction with ERM-1 is responsible for the apical localization of NRFL-1 in the intestine, as depletion of ERM-1 or deletion of the EB domain results in a loss of NRFL-1 apical localization.

Loss of *nrfl-1* by itself did not cause overt defects in intestinal formation, animal development, or viability. Three previous partial deletion alleles of *nrfl-1* have been described: *ok2292*, *tm3501*, and *ok297* (Hagiwara et al., 2012, 1; Na et al., 2017). No severe defects in animal development were reported for *ok2292* or *tm3501* (Hagiwara et al., 2012). However, *nrfl-1(ok297)* animals were reported to have ruptured vulva and sterile phenotypes (Na et al., 2017). Given that neither of the other two previously characterized alleles nor our newly generated *nrfl-1* deletion allele display these phenotypes, we think it is likely that the *ok297* strain analyzed either contains additional background

mutations or that *ok297* represents a neomorphic allele of *nrfl-1*. The non-essential role of *nrfl-1* contrasts with data in mice, where NHERF1/EBP50 loss causes defects in intestinal microvilli formation (Morales et al., 2004), and in *Drosophila*, where *Sip1* mutants cause morphological defects in the follicle cells surrounding the oocytes and late embryonic lethality (Hughes et al., 2010).

Combining the *nrfl-1(null)* deletion mutant with phosphorylation-defective *erm-1[T544A]* or *erm-1[T544D]* mutants resulted in severe defects in intestinal lumen formation. Double mutant animals have a cystic intestinal lumen, characterized by distended regions and severe constrictions. These animals develop slowly or arrest during early larval development, likely due at least in part to the inability of luminal contents to travel through the digestive system. The double mutant intestinal phenotype is similar to that described for *erm-1(RNAi)* and the *erm-1(tm677)* deletion allele (Göbel et al., 2004; Van Fürden et al., 2004), and to an ERM-1 mutant unable to bind to the plasma membrane (ERM-1 [4 KN]) (Ramalho et al., 2020). Nevertheless, complete loss of *erm-1* functioning causes maternal effect L1 lethality, while *erm-1[T544A]*; *nrfl-1* and *erm-1[T544D]*; *nrfl-1* double mutant strains can be maintained homozygously despite the developmental defects.

In many other systems, the loss of NHERF proteins results in similar phenotypes as loss of ERM proteins. NHERF1/EBP50 and ezrin are both required for microvilli formation in mouse intestinal cells as well as in cultured epithelial cells (Bonilha et al., 1999; Morales et al., 2004; Saotome et al., 2004; Garbett et al., 2010; LaLonde et al., 2010; Viswanatha et al., 2012), and loss of NHERF1/EBP50 or moesin causes similar defects in the morphogenesis of 3D cysts grown from Caco-2 cells (Georgescu et al., 2014). This is likely due to positive effects of NHERF proteins on the localization, stability, or activity of ERM proteins (Morales et al., 2004; Hughes et al., 2010; Boratkó and Csontos, 2013; Oh et al., 2017). In *C. elegans* we found no evidence for such a role towards wild-type ERM-1. The loss of NRFL-1 did not cause any noticeable defects in the localization or levels of ERM-1 at the apical membrane, in the mobility of ERM-1 as examined by FRAP, or in the phosphorylation of T544. We also did not observe a decrease in apical actin levels in *nrfl-1* mutant animals. In organisms where NHERF loss affects the localization or activity of ERM proteins, the loss of NHERF would result in both a lack of protein scaffolding by NHERF and a reduction in actin organizing ability of ERM. Thus, the lack of a reciprocal relationship in *C. elegans* make it a unique model in which these different aspects of ERM protein function can be observed separately.

To explain our observations, we considered two possible models for the roles of ERM-1 and NRFL-1. In the first, the functioning of *C. elegans* ERM-1 involves at least two separable activities: one regulated by the phosphorylation of the C-terminal T544 residue, and one mediated via the recruitment of NRFL-1. The exact consequences of altering T544 phosphorylation are not known, but apical enrichment of the intestinal actin ACT-5 is clearly disrupted (Ramalho et al., 2020). This is in agreement with findings in other systems that C-terminal phosphorylation of

ERM proteins is required for apical recruitment of actin (Hipfner et al., 2004; Roch et al., 2010; Abbattiscianni et al., 2016). Interestingly, fractionation experiments from kidney epithelial cells indicated that ERM proteins interact with actin and NHERF1/EBP50 in distinct complexes (Morales et al., 2004). Together with the lack of ACT-5 defects in *nrfl-1* mutants, this presents a possible model in which T544 phosphorylation regulates actin binding, while the scaffolding activities of NRFL-1 mediate recruitment or local distribution of membrane-associated proteins by ERM-1. This model can, however, not account for the observation that loss of *nrfl-1* causes a further decrease of apical actin levels in *erm-1*[T544A] or *erm-1*[T544D] mutant animals, which indicates that NRFL-1 can contribute to the actin organizing activities of ERM-1.

In the second model, both the T544 phosphorylation cycle and binding of NRFL-1 promote an open, active, ERM-1 configuration. A redundant role for T544 phosphorylation and NRFL-1 binding in ERM-1 activation would account for the lack of effects of *nrfl-1* loss on wild-type ERM-1, and for our previous observations that T544 mutations in *C. elegans* have a relatively mild effect on ERM-1 activity compared to similar mutations in mammalian ERM proteins (Ramalho et al., 2020). Support for this model comes from the wedge mechanism that has been proposed for the mammalian kinase LOK, in which the C-terminal domain of LOK wedges apart the FERM and F-actin-binding domains of ezrin to gain access to the regulatory T567 site (Pelaseyed et al., 2017). A chimeric kinase in which the LOK C-terminal domain was replaced with the NRFL-1 ortholog EBP50t was able to phosphorylate ezrin, indicating that EBP50t harbors a similar wedging activity as the LOK C-terminal domain. However, the existence of a wedging mechanism has not been investigated in *C. elegans* nor independently confirmed in mammalian systems. Moreover, loss of *nrfl-1* alone did not affect apical actin levels. Together with the lack of effects of *nrfl-1* loss on ERM-1 localization and stability, this argues against this second model: if T544 phosphorylation and NRFL-1 performed similar roles in ERM-1 activation, their loss would be expected to result in similar defects as well.

Most likely, the activities of NRFL-1 and ERM-1 in *C. elegans* involve a combination of these two models. NRFL-1 may primarily mediate the scaffolding activities of ERM-1 but also promote the open and active conformation of ERM-1, while T544 phosphorylation is the dominant mechanism regulating actin organization by ERM-1. Only when T544 phosphorylation is disrupted does the positive effect of NRFL-1 binding on promoting an open ERM-1 conformation capable of actin binding become apparent. Regardless of the exact mechanism, our results demonstrate that ERM-1 phosphorylation and NRFL-1 redundantly control lumen formation in the *C. elegans* intestine.

There are important differences between our studies in *C. elegans* and studies of ERM proteins in other organisms. The first is that phosphorylation of the C-terminal threonine residue is generally considered to be a critical step in the activation of ERM proteins, while T544A and T544D mutations are tolerated in *C. elegans*. Importantly, the requirement for phosphorylation is not universal. Several studies have observed rescuing activity of Moesin-T559A or Moesin-T559D transgenes in *Drosophila*

(Speck et al., 2003; Hipfner et al., 2004; Roch et al., 2010), and phosphorylation of ERM proteins is not required for the formation of microvilli-like structures in A431 and MDCK II cells (Yonemura et al., 2002). The second major difference is that loss of *nrfl-1* by itself causes no severe defects in *C. elegans*, while loss of NHERF1/EBP50 causes intestinal abnormalities in mice (Morales et al., 2004; Broere et al., 2009) and flies lacking the NHERF ortholog Sip1 are not viable (Hughes et al., 2010). We think it is most likely that the activities and regulation of ERM proteins are conserved between organisms—involving lipid binding, regulatory phosphorylation on the C-terminal threonine residue, and the binding to adapter proteins—but that the relative importance of these events depends on the biological setting and experimental system used.

## MATERIALS AND METHODS

### *C. elegans* Strains and Culture Conditions

*C. elegans* strains were cultured under standard conditions (Brenner, 1974). Only hermaphrodites were used, and all experiments were performed with animals grown at 15 °C or 20 °C on standard Nematode Growth Medium (NGM) agar plates seeded with OP50 *Escherichia coli*. Table 1 contains a list of all the strains used.

### Cloning and Strain Generation for the SIMPL System

Bait and prey SIMPL constructs were generated using the SapI-based cloning strategy, as previously described (Yao et al., 2020). For the conventional SIMPL system, previously described intein inserts were used (Yao et al., 2020). For the SIMPL-mVenus system, the InteinC-3xFLAG-VC155 and VN155-HA-V5-InteinN inserts were codon-optimized for *C. elegans*, flanked by SapI sites and ordered as gBlocks (IDT). Primers containing the appropriate SapI overhangs were used to amplify *erm-1*, *nrfl-1* and *nrfl-1*( $\Delta$ eb) from a cDNA library, InteinC-3xFLAG-VC155 from the ordered gBlock and mKate from pDD375 (Addgene #91825). All gBlocks and PCR products were blunt-end cloned into the plasmid pHSG298. Bait or prey, intein, the *rps-0* promoter and the *unc-54* 3' UTR fragments were combined and inserted into the pMLS257 plasmid (Addgene #73716) using the SapTrap assembly method (Schwartz and Jorgensen, 2016; Yao et al., 2020). Finally for the SIMPL-mVenus system, an mKate2 sequence was integrated into the newly generated *Prps-0::erm-1::VN155-HA-V5-InteinN::unc-54* plasmid. The mKate2 sequence and the *Prps-0::erm-1::VN155-HA-V5-InteinN::unc-54* plasmid were amplified using primers with the appropriate overhangs to incorporate the mKate2 into the plasmid between the promoter and *erm-1* coding sequence using Gibson Assembly (GA). Constructs were verified by Sanger sequencing before injection (Macrogen Europe). Plasmids used for injection were purified using the PureLink HQ Mini Plasmid DNA Purification Kit (Thermo Fisher) using the extra wash step and buffer recommended for endA + strains. Final plasmid sequences are available in Genbank format in **Supplementary File S1**.

**TABLE 1 |** List of *C. elegans* strains used

Strain	Genotype
N2	Wild type
JM125	<i>cals107[Pges-1::YFP::act-5]</i>
BOX163	<i>erm-1(mib9[erm-1[p. T544D]] I</i>
BOX165	<i>erm-1(mib10[erm-1[p. T544A]] I</i>
BOX196	<i>erm-1(mib10[erm-1[p. T544A]] I; cals107[Pges-1::YFP::act-5]</i>
BOX197	<i>erm-1(mib9[erm-1[p.T544D]] I; cals107[Pges-1::YFP::act-5]</i>
BOX213	<i>erm-1(mib15[erm-1::GFP]) I</i>
BOX273	<i>mibls48[Pelt-2::TIR-1::tagBFP2-Lox511::tbb-2-3'UTR, IV::5014740-5014802 (cxTi10816 site)] IV</i>
BOX404	<i>nrfl-1(mib59[nrfl-1a(null = c.-1_8del; c.287_1404+703)] IV</i>
BOX422	<i>nrfl-1(mib73[nrfl-1::mCherry]) IV; mibls48[Pelt-2::TIR-1::tagBFP2-Lox511::tbb-2-3'UTR, IV::5014740-5014802 (cxTi10816 site)] IV</i>
BOX428	<i>erm-1(mib15[erm-1::GFP]) I; nrfl-1(mib73[nrfl-1::mCherry]) IV; mibls48[Pelt-2::TIR-1::tagBFP2-Lox511::tbb-2-3'UTR, IV::5014740-5014802 (cxTi10816 site)] IV</i>
BOX429	<i>nrfl-1(mib73[nrfl-1::mCherry]) IV; mibls48[Pelt-2::TIR-1::tagBFP2-Lox511::tbb-2-3'UTR, IV::5014740-5014802 (cxTi10816 site)] IV; cals107[Pges-1::YFP::act-5]</i>
BOX440	<i>nrfl-1(mib75[nrfl-1a(Δeb = c.1318_1401del)::mCherry]) IV; mibls48[Pelt-2::TIR-1::tagBFP2-Lox511::tbb-2-3'UTR, IV::5014740-5014802 (cxTi10816 site)] IV; cals107[Pges-1::YFP::act-5]</i>
BOX495	<i>erm-1(mib15[erm-1::GFP]) I; nrfl-1(mib59[nrfl-1a(null = c.-1_8del; c.287_1404+703)] IV; mibls48[Pelt-2::TIR-1::tagBFP2-Lox511::tbb-2-3'UTR, IV::5014740-5014802 (cxTi10816 site)] IV</i>
BOX597	<i>nrfl-1(mib104[nrfl-1a(Δeb = c.1318_1401del)] IV</i>
BOX670	<i>erm-1(mib10[erm-1[p.T544A]] I; nrfl-1(mib59[nrfl-1a(null = c.-1_8del; c.287_1404+703)] IV</i>
BOX671	<i>erm-1(mib9[erm-1[p.T544D]] I; nrfl-1(mib59[nrfl-1a(null = c.-1_8del; c.287_1404+703)] IV</i>
BOX672	<i>nrfl-1(mib59[nrfl-1a(null = c.-1_8del; c.287_1404+703)] IV; cals107[Pges-1::YFP::act-5]</i>
BOX673	<i>erm-1(mib10[erm-1[p.T544A]] I; nrfl-1(mib59[nrfl-1a(null = c.-1_8del; c.287_1404+703)] IV; cals107[Pges-1::YFP::act-5]</i>
BOX674	<i>erm-1(mib9[erm-1[p.T544D]] I; nrfl-1(mib59[nrfl-1a(null = c.-1_8del; c.287_1404+703)] IV; cals107[Pges-1::YFP::act-5]</i>
BOX675	<i>erm-1(mib10[erm-1[p.T544A]] I; nrfl-1(mib104[nrfl-1a(Δeb = c.1318_1401del)] IV</i>
BOX676	<i>erm-1(mib9[erm-1[p.T544D]] I; nrfl-1(mib104[nrfl-1a(Δeb = c.1318_1401del)] IV</i>
BOX677	<i>nrfl-1(mib104[nrfl-1a(Δeb = c.1318_1401del)] IV; cals107[Pges-1::YFP::act-5]</i>
BOX678	<i>erm-1(mib10[erm-1[p.T544A]] I; nrfl-1(mib104[nrfl-1a(Δeb = c.1318_1401del)] IV; cals107[Pges-1::YFP::act-5]</i>
BOX679	<i>erm-1(mib9[erm-1[p.T544D]] I; nrfl-1(mib104[nrfl-1a(Δeb = c.1318_1401del)] IV; cals107[Pges-1::YFP::act-5]</i>

Transgenic animals expressing bait and prey constructs were generated by microinjection in the gonads of young adult N2 animals using an inverted microinjection setup (Eppendorf) with 20 ng/μL of bait and prey plasmids, as well as the pDD382 plasmid (Addgene #91830) containing a visible dominant Rol marker and an hygromycin selection cassette. The DNA mix was spun at max speed on a tabletop centrifuge for 15 min prior to injection. Injected animals were incubated for 2–3 days at 20°C before addition of hygromycin B (250 μg/ml) to the plates. After 1–2 days, surviving Rol animals were singled, allowed to develop, and F2 progeny was screened for successful transmission of the transgenic extrachromosomal array. Multiple lines with successful transmission were saved and used for analysis.

## Western Blot SIMPL Analysis

Animals were grown on NGM plates supplemented with hygromycin B (250 μg/ml) until plates were full, washed off with M9 buffer (0.22 M KH<sub>2</sub>PO<sub>4</sub>, 0.42 M Na<sub>2</sub>HPO<sub>4</sub>, 0.85 M NaCl, 0.001 M MgSO<sub>4</sub>), washed three times with M9 buffer, and incubated at room temperature (RT) for 20 min. Samples were then pelleted and resuspended in 100–200 μL of lysis buffer (25 mM Tris-HCl pH 7.5, 150 mM NaCl, 1 mM EDTA, 0.5% IGEPAL CA-630 (Sigma-Aldrich), 1 tablet/50 ml cOmplete protease inhibitor cocktail (Sigma-Aldrich)), and sonicated with a Diagenode BioRupter Plus for 10 min with the high setting and on/off cycles of 30 s in a 4°C water bath. The lysates were spun at max speed for 15 min, an equal volume

of 2 × SDS buffer (100 mM Tris-HCl, 4% SDS, 0.2% bromophenol blue, 20% glycerol, and 10% β-mercaptoethanol) was added, and boiled 10 min. Depending on the experiment, 5–12 μL of protein lysate was loaded into pre-cast protein gels (4–12% Bolt Bis Tris Plus, ThermoFisher) together with 10 μL of the molecular marker (PageRuler prestained, ThermoFisher). Gels were run for 30–45 min at 200 V in NuPAGE MOPS SDS Running buffer (ThermoFisher), and transferred onto a PVDF membrane (Immobilon-P 0.45 μm, Millipore) at 4°C and 30 V overnight in Bolt transfer buffer (Thermo Fisher). For staining, membranes were rinsed in TBST (50 mM Tris-Cl, 150 mM NaCl, 0.1% Tween-20), blocked with 4% milk in TBST for 1 h at RT, and incubated with primary antibodies in milk for 1 h at RT. Membranes were washed three times for 10 min in TBST, incubated with secondary antibodies in milk for 1 h at RT, and washed again three times for 10 min in TBST before exposure using ECL (SignalFire Plus, Cell signaling). The following antibodies and concentrations were used: rabbit anti-V5, 1:1000 (Cell Signaling #13202); mouse anti-FLAG, 1:10000 (Sigma #F1804); goat anti-Rabbit and donkey anti-mouse HRP conjugates, 1:5000.

## CRISPR/Cas9 Genome Engineering

The *nrfl-1::mCherry*, *nrfl-1(Δeb)* and *nrfl-1(Δeb)::mCherry* strains were engineered by homology-directed repair of CRISPR/Cas9-induced DNA double-strand breaks (DSBs), while the *nrfl-1(null)* deletion was generated by imprecise repair of CRISPR/Cas9-induced DSBs. Delivery of components for CRISPR/Cas9

**TABLE 2 |** List of DNA and RNA sequences used

<i>SIMPL system</i>	
erm-1 SapI forward	CTGCTCTTCGAAGATGTCGAAAAAGCGATCAA
erm-1 SapI reverse	CTGCTCTTCGCGTCATATTTTCGATTGATCGA
nrfl-1 SapI forward	CTGCTCTTCGAAGATTGGTGACATTCGAGCGA
nrfl-1 SapI reverse	CTGCTCTTCGCGTCATGTTGCTGACCAATTGAT
nrfl-1( $\Delta$ eb) SapI reverse	AGGCTCTTCGCGTAGCTTCTCTTGCTGACAFAT
InteinC-3xFLAG-VC155 SapI forward	GAGCTCTTCGACGATGGACGAGCGTGAGCTTA
InteinC-3xFLAG-VC155 SapI reverse	GAGCTGCTCTTCGCGCACTTGTAGAGCTCATCCATTC
InteinC-3xFLAG-VC155 GA forward	TCGGACACCGTATGTCGAAAAAGCGATC
InteinC-3xFLAG-VC155 GA reverse	TCGGAGACCATATTACCTTAAAATTCAAAAATTAATTCAG
mKate2 GA forward	TTTTAAGGTAATATGGTCTCCGAGCTCATTAAAGAAAAC
mKate2 GA reverse	TTTTTTCGACATACGGTGTCCGAGCTTGGATG
<i>nrfl-1(null)</i>	
nrfl-1 sgRNA 5' forward oligo 1	TCTTGTGCTCGGAATGTGCACCA
nrfl-1 sgRNA 5' reverse oligo 1	AAACTGGTGACATTCGAGCGAC
nrfl-1 sgRNA 5' forward oligo 2	TCTTGTCAACGACACAAAGTCTTGG
nrfl-1 sgRNA 5' reverse oligo 2	AAACCCAAGACTTTGTGCTGTTGAC
nrfl-1 sgRNA 3' forward oligo 1	TCTTGCCCTTAACGAGAAGTATCAAT
nrfl-1 sgRNA 3' reverse oligo 1	AAACATTGATACTTCTCGTTAAGGC
nrfl-1 sgRNA 3' forward oligo 2	TCTTGCCAATTGATACTTCTCGTTA
nrfl-1 sgRNA 3' reverse oligo 2	AAACTAACGAGAAGTATCAATTGGC
Deletion forward primer	TGGACAGTTCGTTGGTACCG
Deletion reverse primer	TACACGCGCAAAGTGACCTA
<i>nrfl-1(<math>\Delta</math>eb)</i>	
nrfl-1 EB sgRNA 5'	UUUAAUCUUAUGCUGAACG
nrfl-1 EB sgRNA 3'	AUUGAUACUUCUGUUAAGG
ssODN repair template	ACGATGATATCTATCATTTGTCAGCAAGAGAAGCTACGATGATATCTATCATTTGTCAGCAAGAGAAGCT
Integration forward primer	ATGCATCACCTCGAGGCTG
Integration reverse primer	TGAGCGATTGTGAAATGGAAGG
<i>nrfl-1::mCherry</i> - Combined with both nrfl-1 sgRNAs 3' of <i>nrfl-1(null)</i>	
LH arm forward primer	ACGTTGTAAAACGACGGCCAGTCGCCGGCATTAAATGCGCATTGGTCTGC
LH arm reverse primer step 1	GACTAATTGATACTTCTCGTTAAGACTCATCTCGTGCCCTACAATT
LH arm reverse primer step 2	CCTGAGGCTCCCGATGCTCCCATGTTGCTGACTAATTGATACTTCTCGT
RH arm forward primer	AGGATGACGATGACAAAGAGATAATCTTTGCAACTTCTTCTATTTTCTTC
RH arm reverse primer	GGAAACAGCTATGACCATGTTATCGATTTACCTTCCAATGTCAGGTTCCC
Integration forward primer	TCAGGGAGCCGGATCTGATT
Integration reverse primer	CGGCTGAACAAAAGGAGCAG
<i>nrfl-1(<math>\Delta</math>eb)::mCherry</i> —Combined with nrfl-1 EB sgRNA 5' of <i>nrfl-1(<math>\Delta</math>eb)</i>	
nrfl-1 EB mCherry sgRNA	TCATAACATTGCATATTCAT
ssODN repair template	CCCCAGATCAAGAATTTGGTTTAATCTTCATGCTGTTGATAAGTATCATAAAGATCATAACATTGCTTACAGCTGGGATA ATGTTGAAAGAGTTGATACTCGTCCA
Integration forward primer	GATTTGGCGGGTTTTTCGAGG
Integration reverse primer	CGGCTGAACAAAAGGAGCAG

editing was done by microinjection in the gonads of young adult animals of different genetic backgrounds: *nrfl-1( $\Delta$ eb)* and *nrfl-1(mib59)* were generated in an N2 background; *nrfl-1::mCherry* was generated in BOX273 background, and *nrfl-1( $\Delta$ eb)::mCherry* in a BOX422 background. All sequences of the oligonucleotides and crRNAs used (synthesized by IDT) are listed in **Table 2**.

For the *nrfl-1::mCherry*, two plasmid-based sgRNAs were used, generated by ligation of annealed oligo pairs into the *pU6::sgRNA* expression vector pJJR50 (Addgene #75026) as previously described (Waaijers et al., 2016). To generate the *nrfl-1::mCherry* repair template we created a custom SEC

vector, pJJR83 (Addgene #75028), by replacing a fragment of pDD282 (Addgene #66823) containing the GFP sequence with a similar fragment containing a codon optimized mCherry sequence with synthetic introns using the flanking Bsu36I and BglII restriction sites. Homology arms of about  $\pm 750$  bp, flanking the DSB site, were amplified from genomic DNA and introduced into pJJR83 as previously described (Dickinson et al., 2015). The sgRNA (100 ng/ $\mu$ L) and SEC repair template (20 ng/ $\mu$ L) plasmids combined with *Peft-3::Cas9* (60 ng/ $\mu$ L; Addgene #46168) and *Pmyo-2::mCherry* co-injection marker (2.5 ng/ $\mu$ L; pCFJ90, Addgene #19327) were micro-injected in the gonad of young



adults. Two injected animals were pooled per plate, incubated for 3 days at 20°C, 500 µL of 5 mg/ml hygromycin was added per plate, and non-transgenic Rol animals were selected after 4–5 days. These selected animals were lysed and genotyped with primers flanking the homology arms and confirmed by Sanger sequencing. To eliminate the SEC selection cassette L1 progeny of homozygous Rol animals was heat shocked in a water-bath at 34°C for 1 h.

To generate the *nrfl-1*(null) deletion allele a mix containing *Peft-3::Cas9* (Addgene #46168; 50 ng/µL), two pairs of sgRNA plasmids targeting the 5' or 3' ends of the *nrfl-1* open reading frame (75 ng/µL each), and a *dpy-10* sgRNA plasmid (50 ng/µL) for co-CRISPR selection (Arribere et al., 2014) were micro-injected in the gonad of young adults. To select for deletions, injected animals were transferred to individual plates, incubated for 3–4 days at 20°C, and 96 non-transgenic F1 animals (wild-type, Dpy, or Rol) from 2–3 plates containing high numbers of Dpy and Rol animals were selected and transferred to individual plates. After laying eggs, F1 animals were lysed and genotyped with primers flanking the *nrfl-1* ORF. In all cases, deletions were confirmed by Sanger sequencing. Sanger sequencing was also used to determine the precise molecular lesion in selected animals. The *nrfl-1*(null) allele used in this paper, *nrfl-1*(*mib59*), consists of a 9 bp deletion starting 1 bp before the initial base of the start codon of long *nrfl-1* isoforms (a, c, d, h, j), and a second 11,537 bp deletion spanning part of the third exon (791 bp from start of *nrfl-1a*) until the downstream intergenic region, which includes the entire ORFs of the small *nrfl-1* isoforms (left flank 5'- atgcttgatctctgaagaaggag, right flank 5' aatatcacgaacaactctaggagc). The *mib59* allele also deleted an ncRNA (C01F6.16) and three piRNAs (C01F6.10, F32B2.25, and F23B2.28) located within *nrfl-1* introns.

The NRFL-1 EB domain deletions were generated using the Alt-R CRISPR-Cas9 system (IDT). A single-stranded oligodeoxynucleotide with about 35 bp homology arms was used as a repair template to fuse the flanks of a deletion spanning nucleotides 1390–1473 of *nrfl-1h*, as previously described (Dokshin et al., 2018). A mix of 250 ng/µL Cas9 protein, 2 µM repair template, 4.5 µM each *nrfl-1* crRNAs, 10 µM tracrRNA, as well as 1 µM *dpy-10* crRNA and ssODN repair for co-CRISPR selection (Arribere et al., 2014) was micro-injected into the gonads of young adults. Animals were selected as described above for the *nrfl-1*(null) allele and genotyped using two primers flanking the deletion.

## Microscopy and Image Analysis

Imaging of *C. elegans* was done by mounting embryos or larvae on a 5% agarose pad in 20 mM Tetramisole solution in M9 to induce paralysis. Spinning disk confocal imaging was performed using a Nikon Eclipse Ti-U manual microscope equipped with a Yokogawa CSU-X1 spinning disk using a 60× 1.4 NA objective, 488 and 561 nm lasers, Semrock 488 long-pass, 525/30 (green), 617/73 (red) & 512/630 (dual) emission filters, 600 Texas Red (EX540-580/DM595/BA600-660) filter blocks, and Andor iXON DU-885 camera. Imaging for FRAP and immunohistochemistry experiments was performed on a Nikon Eclipse-Ti with Perfect Focus System microscope

equipped with a Yokogawa CSU-X1-A1 spinning disk using 60× and 100× 1.4 NA objectives, Chroma ET-DAPI (49000), ET-GFP (49002), ET-mCherry (49008) emission filters, 355 nm, 488 nm, 491 nm, and 561 nm lasers, and a Photometrics Evolve 512 EMCCD camera. Targeted photobleaching was done using an ILas system (Roper Scientific France/PICT-IBiSA, Institut Curie). Spinning disk images were acquired using MetaMorph Microscopy Automation and Image Analysis Software. All stacks along the z-axis were obtained at 0.25 µm intervals. Super resolution images of the microvilli were obtained using a Zeiss AxioObserver 7 SP microscope with Definite Focus 2 operated by Zeiss ZEN software with an Airyscan 32-channel GaAsP-PMT area detector using a 100× 1.46 NA objective, and Laser Argon Multiline and 561 nm lasers. Maximum intensity Z projections were done in ImageJ (Fiji) software (Schindelin et al., 2012; Rueden et al., 2017). For quantifications, the same laser power and exposure times were used within experiments. Image scales were calibrated for each microscope using a micrometer slide. For display in figures, level adjustments, false coloring, and image overlays were done in Adobe Photoshop. Image rotation, cropping, and panel assembly were done in Adobe Illustrator. All edits were done non-destructively using adjustment layers and clipping masks, and images were kept in their original capture bit depth until final export from Illustrator for publication.

## Quantitative Image Analysis

Quantitative analysis of spinning disk images was done in Fiji. All values were corrected for background levels by subtracting the average of three regions within the field of view that did not contain any animals. For quantification of apical protein levels, measurements were done in intestinal cells forming int2 through int6, and where the opposing apical membranes could be clearly seen as two lines. Levels were obtained by averaging the peak values of intensity profiles from three 25 px-wide (10 px-wide for the SIMPL-mVenus system) line scans perpendicular to the membrane per animal. For YFP::ACT-5, which is expressed from a transgene with variable expression levels, we express apical enrichment as the ratio of apical/cytoplasmic. Cytoplasmic levels were measured by averaging three regions within the cytoplasm of intestinal cells. Intensity distribution profiles to analyze co-distribution of NRFL-1 with ERM-1 and ACT-5 were obtained by taking three 25 px-wide line scans perpendicular to the apical membrane in each animal. Before averaging these three values, they were aligned and normalized to the peak value. Measurements of multiple animals were again aligned based on the peak value. All presented graphs were made using GraphPad Prism and Adobe Illustrator.

## Protein Degradation

For protein degradation using the anti-GFP-nanobody::ZIF-1 approach (Wang et al., 2017), gonads of young adult BOX428 animals were microinjected with 30 ng/µL *Pelt-2::α-GFP-NB::ZIF-1* and 2.5 ng/µL *Pmyo-2::GFP* (#Addgene 26347) as a co-injection marker. Transgenic F1 animals were transferred to

individual plates, F2 progeny was screened for successful transmission of the extrachromosomal array and imaged using spinning disk microscopy.

## Brood Size

L4 animals were put on individual plates at 20°C and transferred to a new plate daily until they died. After the parent was removed from a plate, hatched animals and the unhatched eggs were counted 2–4 days later. The number of animals and unhatched eggs combined constitutes the total progeny size. The graph presented was made using GraphPad Prism and Adobe Illustrator.

## Texas Red-Dextran Assay

Mixed stage populations were collected in M9 and washed two times in M9. Animals were then pelleted, concentrated, resuspended in 1 mg/ml Texas Red-dextran 40,000 MW (ThermoFisher D1829) in egg buffer (118 mM NaCl, 48 mM KCl, 2 mM MgCl<sub>2</sub>, 2 mM CaCl<sub>2</sub>, 25 mM HEPES pH 7.3), and incubated for 60 min on a shaker at 500 rpm. The dye in solution was removed by washing the samples with M9 two times. Animals were paralyzed in 10 mM Tetramisole, transferred to an agarose pad on a glass slide, and imaged using spinning disk microscopy.

## FRAP Experiments and Analysis

For FRAP assays, laser power was adjusted in each experiment to avoid complete photobleaching of the selected area, as the time scale of experiments prevented assessment of photo-induced damage. Photobleaching was performed on a circular region with a diameter of 30 or 40 px at the cortex, and images were taken just before bleaching, directly after, after 15 min, and after 45 min. These images were analyzed using ImageJ. The size of the area for FRAP analysis was defined by the full width at half maximum of an intensity plot across the bleached region. For each time point, the mean intensity value within the bleached region was determined, and the background, defined as the mean intensity of a non-bleached region outside the animal, was subtracted. The mean intensities within the bleached region were corrected for acquisition photobleaching per frame using the background-subtracted mean intensity of a similar non-bleached region at the cortex, which was normalized to the corresponding pre-bleach mean intensity. FRAP recovery was calculated as the change in corrected intensity values within the bleached region from the first image after bleaching normalized to the mean intensity just before bleaching.

## Immunohistochemistry

For the staining of larval stages, embryos were obtained from gravid adults by bleaching and allowed to hatch and develop on plates at 15°C for 24 h. Animals were collected from plates and washed three times with M9 and once with MQ H<sub>2</sub>O before being transferred to poly-L-lysine-coated frosted slides. For the staining of embryos, embryos were obtained from gravid adults by dissection in MQ H<sub>2</sub>O on poly-L-lysine-coated frosted slides and allowed to develop at RT for 4 h. A coverslip (Carl Roth, #1) was lowered on top of larvae/embryos, followed by freezing in liquid nitrogen and snapping off of the coverslip. Fixation was performed in formaldehyde solution with

phosphatase inhibitors (3,7% formaldehyde (Sigma-Aldrich), 250 μM EDTA and 50 mM NaF in PBS (1,35 M NaCl, 27 mM KCl, 100 mM Na<sub>2</sub>HPO<sub>4</sub>, 18 mM KH<sub>2</sub>PO<sub>4</sub>)) at RT for 10 min. Samples were rinsed in PBS, permeabilized (PBS + 0,5% triton X-100 (Sigma-Aldrich)) for 30 min, washed four times in wash buffer (0,1% Triton X-100, 250 μM EDTA and 50 mM NaF in PBS) for 10 min each and then blocked (1% bovine serum albumin (Sigma-Aldrich) and 10% goat serum (Sigma-Aldrich)) for 1 h at RT. For the staining with protein phosphatase treatment, samples were treated with Lambda Protein phosphatase (NEB) for 30 min at 30°C followed with an additional four times washing step before they were blocked. Primary antibodies (anti-phospho-ezrin (Thr567)/radixin (Thr564)/moesin (Thr558) (48G2) rabbit mAb #3726 (Cell Signaling Technologies) 1:200 and mouse anti-DLG (Hybridoma bank) 1:50) in blocking solution were applied overnight at 4°C. Samples were then washed four times in wash buffer for 10 min each and stained with secondary antibodies (Alexa-Fluor 488 goat anti-rabbit and Alexa-Fluor 568 goat anti-mouse (Life Technologies, A-11008 and A11004), both 1:500) in blocking solution for 1 hour at RT. Samples were then washed four times in wash buffer and once in PBS for 10 min each and finally mounted with Prolong Gold Antifade with DAPI (ThermoFisher) under a coverslip and sealed with nail polish.

## Statistical Analysis

All statistical analyses were performed using GraphPad Prism 8. For population comparisons, a D'Agostino and Pearson test of normality was first performed to determine if the data was sampled from a Gaussian distribution. For data drawn from a Gaussian distribution, comparisons between two populations were done using an unpaired *t*-test, with Welch's correction if the SDs of the populations differed significantly, and comparisons between >2 populations were done using a one-way ANOVA, or a Welch's ANOVA if the SDs of the populations differed significantly. For data not drawn from a Gaussian distribution, a non-parametric test was used (Mann-Whitney for 2 populations and Kruskal-Wallis for >2 populations). ANOVA and non-parametric tests were followed up with multiple comparison tests of significance (Dunnett's, Tukey's, Dunnett's T3 or Dunn's). Tests of significance used and sample sizes are indicated in the figure legends. No statistical method was used to pre-determine sample sizes. No samples or animals were excluded from analysis. The experiments were not randomized, and the investigators were not blinded to allocation during experiments and outcome assessment.

## DATA AVAILABILITY STATEMENT

The original contributions presented in the study are included in the article/**Supplementary Material**, further inquiries can be directed to the corresponding author.

## AUTHOR CONTRIBUTIONS

Conceptualization: JS, JR, MB; Methodology: JS, JR, JK, RS; Formal analysis: JS, JR, JK; Investigation: JS, JR, JK, RS;

Writing—original draft: JS, JR, MB; Writing—review and editing: JK, RS; Visualization: JS, JR; Supervision: MB; Project administration: MB; Funding acquisition: MB.

## FUNDING

Some strains were provided by the *Caenorhabditis* Genetics Center, which is funded by NIH Office of Research Infrastructure Programs (P40 OD010440). This work was supported by the Netherlands Organization for Scientific Research (NWO)-ALW Open Program 824.14.021 and NWO-VICI 016.VICI.170.165 grants to MB, and Open Competition ENW grant XS3.087 to JK.

## ACKNOWLEDGMENTS

We thank V. Portegijs and S. van den Heuvel for the *Pelt-2::αGFP-NB::ZIF-1* plasmid, H.R. Pires for strain BOX273, and members of the S. van den Heuvel, S. Ruijtenberg, and MB groups for helpful discussions. We also thank Wormbase (Harris et al., 2020) and the Biology Imaging Center, Faculty of Sciences, Department of Biology, Utrecht University.

## REFERENCES

- Abbattiscianni, A. C., Favia, M., Mancini, M. T., Cardone, R. A., Guerra, L., Monterisi, S., et al. (2016). Correctors of Mutant CFTR Enhance Subcortical cAMP-PKA Signaling through Modulating Ezrin Phosphorylation and Cytoskeleton Organization. *J. Cel Sci.* 129, 1128–1140. doi:10.1242/jcs.177907
- Arribere, J. A., Bell, R. T., Fu, B. X. H., Artilles, K. L., Hartman, P. S., and Fire, A. Z. (2014). Efficient Marker-free Recovery of Custom Genetic Modifications with CRISPR/Cas9 in *Caenorhabditis elegans*. *Genetics* 198, 837–846. doi:10.1534/genetics.114.169730
- Barret, C., Roy, C., Montcourrier, P., Mangeat, P., and Niggli, V. (2000). Mutagenesis of the Phosphatidylinositol 4,5-Bisphosphate (Pip2) Binding Site in the Nh2-Terminal Domain of Ezrin Correlates with its Altered Cellular Distribution. *J. Cel Biol.* 151, 1067–1080. doi:10.1083/jcb.151.5.1067
- Bernadskaya, Y. Y., Patel, F. B., Hsu, H.-T., and Soto, M. C. (2011). Arp2/3 Promotes junction Formation and Maintenance in the *Caenorhabditis* Intestine by Regulating Membrane Association of Apical Proteins. *Mol. Biol. Cell.* 22, 2886–2899. doi:10.1091/mbc.e10-10-0862
- Bonilha, V. L., Finnemann, S. C., and Rodriguez-Boulton, E. (1999). Ezrin Promotes Morphogenesis of Apical Microvilli and Basal Infoldings in Retinal Pigment Epithelium. *J. Cel Biol.* 147, 1533–1548. doi:10.1083/jcb.147.7.1533
- Boratkó, A., and Csontos, C. (2013). NHERF2 Is Crucial in ERM Phosphorylation in Pulmonary Endothelial Cells. *Cell Commun. Signal. CCS* 11, 99. doi:10.1186/1478-811X-11-99
- Brenner, S. (1974). The Genetics of *Caenorhabditis* Elegans. *Genetics* 77, 71–94. doi:10.1093/genetics/77.1.71
- Broere, N., Chen, M., Cinar, A., Singh, A. K., Hillesheim, J., Riederer, B., et al. (2009). Defective Jejunal and Colonic Salt Absorption and altered Na<sup>+</sup>/H<sup>+</sup> Exchanger 3 (NHE3) Activity in NHE Regulatory Factor 1 (NHERF1) Adaptor Protein-Deficient Mice. *Pflugers Arch.* 457, 1079–1091. doi:10.1007/s00424-008-0579-1
- Bryant, D. M., Roignot, J., Datta, A., Overeem, A. W., Kim, M., Yu, W., et al. (2014). A Molecular Switch for the Orientation of Epithelial Cell Polarization. *Develop. Cel* 31, 171–187. doi:10.1016/j.devcel.2014.08.027
- Coscoy, S., Waharte, F., Gautreau, A., Martin, M., Louvard, D., Mangeat, P., et al. (2002). Molecular Analysis of Microscopic Ezrin Dynamics by Two-Photon FRAP. *Proc. Natl. Acad. Sci.* 99, 12813–12818. doi:10.1073/pnas.192084599

## SUPPLEMENTARY MATERIAL

The Supplementary Material for this article can be found online at: <https://www.frontiersin.org/articles/10.3389/fcell.2022.769862/full#supplementary-material>

**Supplementary Figure S1** | NRFL-1 is recruited to the apical domain by ERM-1 in different tissues. (A) Schematic representation of the domain organization of *C. elegans* NRFL-1, *D. melanogaster* Sip1 and *H. sapiens* NHERF1/EBP50 and NHERF2. Percentages above the domains represent the similarity between that domain and the corresponding domain of NRFL-1. For the single PDZ domain of Sip1, two percentages are presented corresponding to each NRFL-1 PDZ domain. In the EB domain alignment, amino acids that are important for the interaction with ERM proteins are shown in red (Terawaki et al., 2006). PDZ = Post-synaptic density-95, disks-large and zonula occludens-1; EB = ERM binding.

**Supplementary Figure S2** | Lumen discontinuities in *nrf1-1* and *erm-1* single and double mutants. (A) Representative images of the intestine in L2 larvae of the indicated genotypes expressing YFP::ACT-5 as an apical marker. (B) L1 larvae carrying the apical marker YFP::ACT-5 of the indicated genotypes fed with Texas-Red Dextran. The orange arrowhead indicates the constriction that prevents the flow of fluorescent dye along the intestine. All images are taken using a spinning-disk confocal microscope, and a single focal plane is shown.

**Supplementary Figure S3** | Validation of the specificity of the α-pERM for T544 phosphorylated ERM-1. (A,B) Representative images of fixed animals stained with antibodies recognizing the junctional protein DLG-1 (α-DLG) and phosphorylated ERM-1 (α-pERM). (A) shows *erm-1(+)* and *erm-1/T544A* larvae and (B) shows the intestine of wild-type 2.5-fold embryos that are untreated (-PP) and treated with protein phosphatase (+PP). All images are taken using a spinning-disk confocal microscope, and maximum intensity projections are presented.

- Dickinson, D. J., Pani, A. M., Heppert, J. K., Higgins, C. D., and Goldstein, B. (2015). Streamlined Genome Engineering with a Self-Excising Drug Selection Cassette. *Genetics* 200, 1035–1049. doi:10.1534/genetics.115.178335
- Dokshin, G. A., Ghanta, K. S., Piscopo, K. M., and Mello, C. C. (2018). Robust Genome Editing with Short Single-Stranded and Long, Partially Single-Stranded DNA Donors in *Caenorhabditis elegans*. *Genetics* 210, 781–787. doi:10.1534/genetics.118.301532
- Fehon, R. G., McClatchey, A. I., and Bretscher, A. (2010). Organizing the Cell Cortex: The Role of ERM Proteins. *Nat. Rev. Mol. Cel Biol.* 11, 276–287. doi:10.1038/nrm2866
- Fievet, B. T., Gautreau, A., Roy, C., Del Maestro, L., Mangeat, P., Louvard, D., et al. (2004). Phosphoinositide Binding and Phosphorylation Act Sequentially in the Activation Mechanism of Ezrin. *J. Cel Biol.* 164, 653–659. doi:10.1083/jcb.200307032
- Finnerty, C. M., Chambers, D., Ingraffea, J., Faber, H. R., Karplus, P. A., and Bretscher, A. (2004). The EBP50-Moesin Interaction Involves a Binding Site Regulated by Direct Masking on the FERM Domain. *J. Cel Sci.* 117, 1547–1552. doi:10.1242/jcs.01038
- Garbett, D., LaLonde, D. P., and Bretscher, A. (2010). The Scaffolding Protein EBP50 Regulates Microvillar Assembly in a Phosphorylation-dependent Manner. *J. Cel Biol.* 191, 397–413. doi:10.1083/jcb.201004115
- Gary, R., and Bretscher, A. (1995). Ezrin Self-Association Involves Binding of an N-Terminal Domain to a Normally Masked C-Terminal Domain that Includes the F-Actin Binding Site. *Mol. Biol. Cell.* 6, 1061–1075. doi:10.1091/mbc.6.8.1061
- Georgescu, M.-M., Cote, G., Agarwal, N. K., and White, C. L. (2014). NHERF1/EBP50 Controls Morphogenesis of 3D Colonic Glands by Stabilizing PTEN and Ezrin-Radixin-Moesin Proteins at the Apical Membrane. *Neoplasia* 16, 365–374.e2. doi:10.1016/j.neo.2014.04.004
- Göbel, V., Barrett, P. L., Hall, D. H., and Fleming, J. T. (2004). Lumen Morphogenesis in *C. elegans* Requires the Membrane-Cytoskeleton Linker Erm-1. *Dev. Cel* 6, 865–873. doi:10.1016/j.devcel.2004.05.018
- Hagiwara, K., Nagamori, S., Umemura, Y. M., Ohgaki, R., Tanaka, H., Murata, D., et al. (2012). NRFL-1, the *C. elegans* NHERF Orthologue, Interacts with Amino Acid Transporter 6 (AAT-6) for Age-dependent Maintenance of AAT-6 on the Membrane. *PLoS ONE* 7, e43050. doi:10.1371/journal.pone.0043050



- Hao, J.-J., Liu, Y., Kruhlak, M., Debell, K. E., Rellahan, B. L., and Shaw, S. (2009). Phospholipase C-Mediated Hydrolysis of PIP2 Releases ERM Proteins from Lymphocyte Membrane. *J. Cel Biol.* 184, 451–462. doi:10.1083/jcb.200807047
- Harris, T. W., Arnaboldi, V., Cain, S., Chan, J., Chen, W. J., Cho, J., et al. (2020). WormBase: a Modern Model Organism Information Resource. *Nucleic Acids Res.* 48, D762–D767. doi:10.1093/nar/gkz920
- Hipfner, D. R., Keller, N., and Cohen, S. M. (2004). Slik Sterile-20 Kinase Regulates Moesin Activity to Promote Epithelial Integrity during Tissue Growth. *Genes Dev.* 18, 2243–2248. doi:10.1101/gad.303304
- Hughes, S. C., Formstecher, E., and Fehon, R. G. (2010). Sip1, the Drosophila orthologue of EBP50/NHERF1, Functions with the Sterile 20 Family Kinase Slik to Regulate Moesin Activity. *J. Cel Sci.* 123, 1099–1107. doi:10.1242/jcs.059469
- Ikenouchi, J., Hirata, M., Yonemura, S., and Umeda, M. (2013). Spingomyelin Clustering Is Essential for the Formation of Microvilli. *J. Cel Sci.* 126, 3585–3592. doi:10.1242/jcs.122325
- Ingraffia, J., Reczek, D., and Bretscher, A. (2002). Distinct Cell Type-specific Expression of Scaffolding Proteins EBP50 and E3KARP: EBP50 Is Generally Expressed with Ezrin in Specific Epithelia, whereas E3KARP Is Not. *Eur. J. Cel Biol.* 81, 61–68. doi:10.1078/0171-9335-00218
- Kodama, Y., and Hu, C.-D. (2010). An Improved Bimolecular Fluorescence Complementation Assay with a High Signal-To-Noise Ratio. *BioTechniques* 49, 793–805. doi:10.2144/000113519
- Koorman, T., Klompstra, D., van der Voet, M., Lemmens, I., Ramalho, J. J., Nieuwenhuize, S., et al. (2016). A Combined Binary Interaction and Phenotypic Map of *C. elegans* Cell Polarity Proteins. *Nat. Cel Biol.* 18, 337–346. doi:10.1038/ncb3300
- Kreimann, E. L., Morales, F. C., de Orbata-Cruz, J., Takahashi, Y., Adams, H., Liu, T.-J., et al. (2007). Cortical Stabilization of  $\beta$ -catenin Contributes to NHERF1/EBP50 Tumor Suppressor Function. *Oncogene* 26, 5290–5299. doi:10.1038/sj.onc.1210336
- LaLonde, D. P., and Bretscher, A. (2009). The Scaffold Protein PDZK1 Undergoes a Head-To-Tail Intramolecular Association that Negatively Regulates its Interaction with EBP50. *Biochemistry* 48, 2261–2271. doi:10.1021/bi802089k
- LaLonde, D. P., Garbett, D., and Bretscher, A. (2010). A Regulated Complex of the Scaffolding Proteins PDZK1 and EBP50 with Ezrin Contribute to Microvillar Organization. *Mol. Biol. Cell.* 21, 1519–1529. doi:10.1091/mbc.e10-01-0008
- Lamprecht, G., Weinman, E. J., and Yun, C.-H. C. (1998). The Role of NHERF and E3KARP in the cAMP-Mediated Inhibition of NHE3. *J. Biol. Chem.* 273, 29972–29978. doi:10.1074/jbc.273.45.29972
- Lazar, C. S., Cresson, C. M., Lauffenburger, D. A., and Gill, G. N. (2004). The Na<sup>+</sup>/H<sup>+</sup> Exchanger Regulatory Factor Stabilizes Epidermal Growth Factor Receptors at the Cell Surface. *Mol. Biol. Cell.* 15, 5470–5480. doi:10.1091/mbc.e04-03-0239
- Li, Q., Nance, M. R., Kulikuskas, R., Nyberg, K., Fehon, R., Karplus, P. A., et al. (2007). Self-masking in an Intact ERM-merlin Protein: An Active Role for the Central  $\alpha$ -Helical Domain. *J. Mol. Biol.* 365, 1446–1459. doi:10.1016/j.jmb.2006.10.075
- Magendantz, M., Henry, M. D., Lander, A., and Solomon, F. (1995). Interdomain Interactions of Radixin *In Vitro*. *J. Biol. Chem.* 270, 25324–25327. doi:10.1074/jbc.270.43.25324
- Maudsley, S., Zahra, A. M., Rahman, N., Blitzer, J. T., Luttrell, L. M., Lefkowitz, R. J., et al. (2000). Platelet-Derived Growth Factor Receptor Association with Na<sup>+</sup>/H<sup>+</sup> Exchanger Regulatory Factor Potentiates Receptor Activity. *Mol. Cel Biol.* 20, 8352–8363. doi:10.1128/mcb.20.22.8352-8363.2000
- McClatchey, A. I. (2014). ERM Proteins at a Glance. *J. Cel Sci.* 127, 3199–3204. doi:10.1242/jcs.098343
- Morales, F. C., Takahashi, Y., Kreimann, E. L., and Georgescu, M.-M. (2004). Ezrin-radixin-moesin (ERM)-binding Phosphoprotein 50 Organizes ERM Proteins at the Apical Membrane of Polarized Epithelia. *Proc. Natl. Acad. Sci.* 101, 17705–17710. doi:10.1073/pnas.0407974101
- Na, K., Shin, H., Cho, J.-Y., Jung, S. H., Lim, J., Lim, J.-S., et al. (2017). Systematic Proteogenomic Approach to Exploring a Novel Function for NHERF1 in Human Reproductive Disorder: Lessons for Exploring Missing Proteins. *J. Proteome Res.* 16, 4455–4467. doi:10.1021/acs.jproteome.7b00146
- Nakamura, F., Huang, L., Pestonjamas, K., Luna, E. J., and Furthmayr, H. (1999). Regulation of F-Actin Binding to Platelet Moesin *In Vitro* by Both Phosphorylation of Threonine 558 and Polyphosphatidylinositides. *Mol. Biol. Cell.* 10, 2669–2685. doi:10.1091/mbc.10.8.2669
- Oh, Y.-S., Heo, K., Kim, E.-K., Jang, J.-H., Bae, S. S., Park, J. B., et al. (2017). Dynamic Relocalization of NHERF1 Mediates Chemotactic Migration of Ovarian Cancer Cells toward Lysophosphatidic Acid Stimulation. *Exp. Mol. Med.* 49, e351. doi:10.1038/emmm.2017.88
- Pearson, M. A., Reczek, D., Bretscher, A., and Karplus, P. A. (2000). Structure of the ERM Protein Moesin Reveals the FERM Domain Fold Masked by an Extended Actin Binding Tail Domain. *Cell* 101, 259–270. doi:10.1016/s0092-8674(00)80836-3
- Pelaseyed, T., Viswanatha, R., Sauvanet, C., Filter, J. J., Goldberg, M. L., and Bretscher, A. (2017). Ezrin Activation by LOK Phosphorylation Involves a PIP2-dependent Wedge Mechanism. *eLife* 6, e22759. doi:10.7554/eLife.22759
- Ramalho, J. J., Sepers, J. J., Nicolle, O., Schmidt, R., Cravo, J., Michaux, G., et al. (2020). C-terminal Phosphorylation Modulates ERM-1 Localization and Dynamics to Control Cortical Actin Organization and Support Lumen Formation during *Caenorhabditis elegans* Development. *Development* 147, dev188011. doi:10.1242/dev.188011
- Reczek, D., Berryman, M., and Bretscher, A. (1997). Identification of EBP50: A PDZ-Containing Phosphoprotein that Associates with Members of the Ezrin-Radixin-Moesin Family. *J. Cel Biol.* 139, 169–179. doi:10.1083/jcb.139.1.169
- Reczek, D., and Bretscher, A. (1998). The Carboxyl-Terminal Region of EBP50 Binds to a Site in the Amino-Terminal Domain of Ezrin that Is Masked in the Dormant Molecule. *J. Biol. Chem.* 273, 18452–18458. doi:10.1074/jbc.273.29.18452
- Roch, F., Polesello, C., Roubinet, C., Martin, M., Roy, C., Valenti, P., et al. (2010). Differential Roles of PtdIns(4,5)P2 and Phosphorylation in Moesin Activation during Drosophila development. *J. Cel Sci.* 123, 2058–2067. doi:10.1242/jcs.064550
- Rueden, C. T., Schindelin, J., Hiner, M. C., DeZonia, B. E., Walter, A. E., Arena, E. T., et al. (2017). ImageJ2: ImageJ for the Next Generation of Scientific Image Data. *BMC Bioinformatics* 18, 529. doi:10.1186/s12859-017-1934-z
- Saotome, I., Curto, M., and McClatchey, A. I. (2004). Ezrin Is Essential for Epithelial Organization and Villus Morphogenesis in the Developing Intestine. *Develop. Cel* 6, 855–864. doi:10.1016/j.devcel.2004.05.007
- Schindelin, J., Arganda-Carreras, I., Frise, E., Kaynig, V., Longair, M., Pietzsch, T., et al. (2012). Fiji: an Open-Source Platform for Biological-Image Analysis. *Nat. Methods* 9, 676–682. doi:10.1038/nmeth.2019
- Schwartz, M. L., and Jorgensen, E. M. (2016). SapTrap, a Toolkit for High-Throughput CRISPR/Cas9 Gene Modification in *Caenorhabditis elegans*. *Genetics* 202, 1277–1288. doi:10.1534/genetics.115.184275
- Seidler, U., Singh, A. K., Cinar, A., Chen, M., Hillesheim, J., Hogema, B., et al. (2009). The Role of the NHERF Family of PDZ Scaffolding Proteins in the Regulation of Salt and Water Transport. *Ann. N. Y. Acad. Sci.* 1165, 249–260. doi:10.1111/j.1749-6632.2009.04046.x
- Simons, P. C., Pietromonaco, S. F., Reczek, D., Bretscher, A., and Elias, L. (1998). C-terminal Threonine Phosphorylation Activates ERM Proteins to Link the Cell's Cortical Lipid Bilayer to the Cytoskeleton. *Biochem. Biophysical Res. Commun.* 253, 561–565. doi:10.1006/bbrc.1998.9823
- Speck, O., Hughes, S. C., Noren, N. K., Kulikuskas, R. M., and Fehon, R. G. (2003). Moesin Functions Antagonistically to the Rho Pathway to Maintain Epithelial Integrity. *Nature* 421, 83–87. doi:10.1038/nature01295
- Terawaki, S.-i., Maesaki, R., and Hakoshima, T. (2006). Structural Basis for NHERF Recognition by ERM Proteins. *Structure* 14, 777–789. doi:10.1016/j.str.2006.01.015
- Van Fürden, D., Johnson, K., Segbert, C., and Bossinger, O. (2004). The *C. elegans* Ezrin-Radixin-Moesin Protein ERM-1 Is Necessary for Apical junction Remodelling and Tubulogenesis in the Intestine. *Dev. Biol.* 272, 262–276. doi:10.1016/j.ydbio.2004.05.012
- Viswanatha, R., Ohouo, P. Y., Smolka, M. B., and Bretscher, A. (2012). Local Phosphocycling Mediated by LOK/SLK Restricts Ezrin Function to the Apical Aspect of Epithelial Cells. *J. Cel Biol.* 199, 969–984. doi:10.1083/jcb.201207047
- Waaijers, S., Muñoz, J., Berends, C., Ramalho, J. J., Goerdal, S. S., Low, T. Y., et al. (2016). A Tissue-specific Protein Purification Approach in *Caenorhabditis elegans* Identifies Novel Interaction Partners of DLG-1/Discs Large. *BMC Biol.* 14, 66. doi:10.1186/s12915-016-0286-x
- Wang, S., Tang, N. H., Lara-Gonzalez, P., Zhao, Z., Cheerambathur, D. K., Prevo, B., et al. (2017). A Toolkit for GFP-Mediated Tissue-specific Protein Degradation in *C. elegans*. *Development* 144, 2694–2701. doi:10.1242/dev.150094

- Weinman, E. J., Steplock, D., and Shenolikar, S. (1993). cAMP-mediated Inhibition of the Renal brush Border Membrane Na<sup>+</sup>-H<sup>+</sup> Exchanger Requires a Dissociable Phosphoprotein Cofactor. *J. Clin. Invest.* 92, 1781–1786. doi:10.1172/jci116767
- Yao, Z., Aboualizadeh, F., Kroll, J., Akula, I., Snider, J., Lyakisheva, A., et al. (2020). Split Intein-Mediated Protein Ligation for Detecting Protein-Protein Interactions and Their Inhibition. *Nat. Commun.* 11, 2440. doi:10.1038/s41467-020-16299-1
- Yonemura, S., Matsui, T., Tsukita, S., and Tsukita, S. (2002). Rho-dependent and -independent Activation Mechanisms of Ezrin/radixin/moesin Proteins: an Essential Role for Polyphosphoinositides *In Vivo*. *J. Cell Sci.* 115, 2569–2580. doi:10.1242/jcs.115.12.2569
- Yun, C. H. C., Oh, S., Zizak, M., Steplock, D., Tsao, S., Tse, C.-M., et al. (1997). cAMP-mediated Inhibition of the Epithelial brush Border Na<sup>+</sup>/H<sup>+</sup> Exchanger, NHE3, Requires an Associated Regulatory Protein. *Proc. Natl. Acad. Sci.* 94, 3010–3015. doi:10.1073/pnas.94.7.3010

**Conflict of Interest:** The authors declare that the research was conducted in the absence of any commercial or financial relationships that could be construed as a potential conflict of interest.

**Publisher's Note:** All claims expressed in this article are solely those of the authors and do not necessarily represent those of their affiliated organizations, or those of the publisher, the editors and the reviewers. Any product that may be evaluated in this article, or claim that may be made by its manufacturer, is not guaranteed or endorsed by the publisher.

Copyright © 2022 Sepers, Ramalho, Kroll, Schmidt and Boxem. This is an open-access article distributed under the terms of the Creative Commons Attribution License (CC BY). The use, distribution or reproduction in other forums is permitted, provided the original author(s) and the copyright owner(s) are credited and that the original publication in this journal is cited, in accordance with accepted academic practice. No use, distribution or reproduction is permitted which does not comply with these terms.



# Insights Into Mechanisms of Oriented Division From Studies in 3D Cellular Models

Federico Donà, Susanna Eli and Marina Mapelli\*

IEO, European Institute of Oncology IRCCS, Milan, Italy

## OPEN ACCESS

### Edited by:

Jens Januschke,  
University of Dundee, United Kingdom

### Reviewed by:

Salah Elias,  
University of Southampton,  
United Kingdom  
Dan Bergstralh,  
University of Rochester,  
United States  
Christopher A. Johnston,  
University of New Mexico,  
United States

### \*Correspondence:

Marina Mapelli  
marina.mapelli@ieo.it

### Specialty section:

This article was submitted to  
Morphogenesis and Patterning,  
a section of the journal  
Frontiers in Cell and Developmental  
Biology

**Received:** 03 January 2022

**Accepted:** 17 February 2022

**Published:** 09 March 2022

### Citation:

Donà F, Eli S and Mapelli M (2022)  
Insights Into Mechanisms of Oriented  
Division From Studies in 3D  
Cellular Models.  
Front. Cell Dev. Biol. 10:847801.  
doi: 10.3389/fcell.2022.847801

In multicellular organisms, epithelial cells are key elements of tissue organization. In developing tissues, cellular proliferation and differentiation are under the tight regulation of morphogenetic programs, that ensure the correct organ formation and functioning. In these processes, mitotic rates and division orientation are crucial in regulating the velocity and the timing of the forming tissue. Division orientation, specified by mitotic spindle placement with respect to epithelial apico-basal polarity, controls not only the partitioning of cellular components but also the positioning of the daughter cells within the tissue, and hence the contacts that daughter cells retain with the surrounding microenvironment. Daughter cells positioning is important to determine signal sensing and fate, and therefore the final function of the developing organ. In this review, we will discuss recent discoveries regarding the mechanistics of planar divisions in mammalian epithelial cells, summarizing technologies and model systems used to study oriented cell divisions *in vitro* such as three-dimensional cysts of immortalized cells and intestinal organoids. We also highlight how misorientation is corrected *in vivo* and *in vitro*, and how it might contribute to the onset of pathological conditions.

**Keywords:** mitotic spindle orientation, epithelial polarity, cysts, organoids, planar divisions

## INTRODUCTION

The mitotic spindle is a bipolar structure formed by microtubules (MTs) that in mitosis captures the duplicated chromosomes and segregates them equally between daughter cells. In unicellular and multicellular organisms the mitotic spindle can be regarded as a key player for the successful outcome of cell division (Pietro et al., 2016). In stem cells and progenitors, the mitotic spindle orientation contributes to define the fate choice of daughter cells and their positioning within the tissue, resulting in either symmetric or asymmetric division (Morin and Bellaïche, 2011). Oriented divisions have been extensively studied in invertebrate systems (Gönczy, 2008; Knoblich, 2008; Knoblich, 2010; Morin and Bellaïche, 2011; Pietro et al., 2016), however mechanistic insights into orientation mechanisms in vertebrates are still limited. Spindle positioning is known to impact on cell proliferation, cell fate and tissue development although a comprehensive understanding of the molecular details underlying these processes is just building (Pietro et al., 2016; Lechler and Mapelli, 2021). Timing and execution of spindle placement rely on intrinsic and extrinsic signals sensed by the dividing cell (Pietro et al., 2016).

In the epithelial tissues, contacts between the dividing cell and the adjacent ones are important factors determining the division orientation (Osswald and Morais-de-Sá, 2019). In polarized epithelial monolayers, cells divide by planar divisions with the mitotic spindle parallel to the epithelium, and the two daughter cells remain within the same monolayer, leading to tissue growth

and expansion (Nakajima, 2018). Studies on division orientation in 3D culture, including organoids derived from various tissues, are just starting to reveal interesting differences between orientation mechanisms and misorientation correction compared to what observed in 2D and in invertebrate systems. In this review, we summarize what is known about mitotic spindle dynamics and oriented cell divisions in vertebrate 3D cysts and organoids. In the first section, we will present an overview of spindle orientation effectors. Then, we will describe mechanisms of oriented cell divisions in cysts grown from mammalian cell lines, while in the end of the review we will focus on more complex 3D cellular structures such as organoids. Finally, the potential role of mitotic spindle proteins in disease associated with defective epithelial morphogenesis and homeostasis will be discussed, with a few examples from *Drosophila* studies.

## Mitotic Spindle Machinery: The Importance of the Gai/LGN/NuMA Complex

Division orientation depends on mitotic spindle positioning, that is generally attained in metaphase and sometime corrected in telophase (Morin and Bellaïche, 2011; Lough et al., 2019). In many epithelial systems, division orientation follows the Hertwig's rule, according to which the spindle aligns along the long axis of the dividing cell (Hertwig, 1884). To which extent spindle alignment to the long cell axis is guided by mechanosensing pathways responding to compressional cues exerted by neighbouring cells, or it is contributed by cytoskeletal forces exerted by MT motors is still debated. Elegant studies in MDCK (Madin–Darby Canine Kidney) Extra-Cellular-Matrix-free (ECM-free) monolayers “in suspension” showed that the division orientation occurs along the longest cell axis and is instructed by the interphase geometry (Wyatt et al., 2015). In these cells, components of the force generators complexes including NuMA and Gai accumulates at cortical polar sites. Consistently, studies in *Xenopus* epithelia indicate that cells divide according to interphase cellular shape that is defined by three-cell junction distribution, where LGN and E-cadherin accumulates (Nestor-Bergmann et al., 2019). Collectively, this evidence suggests that in mammalian epithelial cells interphase shape drives force generators distributions to orchestrate divisions along the longest cell axis. Notably, these findings in vertebrate cells are consistent with previous observations in *Drosophila* tissues (Bosveld et al., 2016), although do not seem to apply to the development of *Drosophila* follicular epithelium at early-stage egg chambers (Finegan et al., 2019).

Several studies elucidated the molecular mechanisms of orientation, in which a fundamental role is played by Gai/LGN/NuMA proteins, an evolutionarily conserved ternary complex. Gai is the subunit of heterotrimeric G-proteins that localizes at the plasma membrane, LGN acts as a molecular scaffold, and NuMA is the mitotic dynein-adaptor involved in MT-pulling force onset. The majority of studies addressing the mechanistics of orientation were conducted in adherent cells in isolation, such as HeLa cells (Du et al., 2001; Du and Macara, 2004; Zheng et al., 2010; Kiyomitsu and Cheeseman, 2012; Kotak

et al., 2012; Gallini et al., 2016; Pirovano et al., 2019; Takayanagi et al., 2019), or in a monolayers of MDCK cells, in which the spindle axis aligns parallel to the substratum in an integrin-dependent manner (Reinsch and Karsenti, 1994; Tuncay et al., 2015; Chishiki et al., 2017; Lázaro-Diéguez and Müsch, 2017).

In metaphase, the Gai/LGN/NuMA complex localizes at the plasma membrane above the spindle poles (Du et al., 2001; Du and Macara, 2004; Kotak et al., 2012; Gallini et al., 2016; Pirovano et al., 2019; Zheng et al., 2010; Machicoane et al., 2014) and recruits the MT motor dynein/dynactin (Kotak et al., 2012; Okumura et al., 2018; Woodard et al., 2010) (**Figure 1A**). Exploiting the minus-end directed movement of dynein, cortically localized dynein motors generate pulling forces on astral MTs branching from the spindle poles that in metaphase contribute to spindle placement (Théry et al., 2007; Kiyomitsu and Cheeseman, 2012; Kotak et al., 2012). Notably, ectopic recruitment of NuMA to the cell cortex by optogenetic techniques is necessary and sufficient to orient the spindle, while cortical targeting of dynein is not sufficient to generate enough pulling forces to place the spindle (Fielmich et al., 2018; Okumura et al., 2018), implying that the activity of MT motors requires a defined spatial cortical organization. In line with these findings, recent studies revealed that not only the levels of NuMA/dynein/dynactin motors present at the cortex, but also their spatial distribution plays a role in the onset of effective MT-pulling forces (Pirovano et al., 2019; Renna et al., 2020).

In mitosis Gai proteins are uniformly enriched at the cell cortex, but only a GDP-loaded pool of Gai (Gai<sup>GDP</sup>) accumulates above the spindle poles and is the one that selectively binds to LGN (Du et al., 2001; Willard et al., 2004; Mochizuki et al., 1996). The recruitment of LGN at the cortex by Gai is controlled by GAPs (GTPase activating proteins) and GEFs (Guanine Exchange Factors) that tune the GTP-state of Gai. An important Gai GEF implicated in spindle placement is Ric-8A, which appears to play a key role in targeting LGN to the cortex (Chishiki et al., 2017; Woodard et al., 2010). In metaphase, LGN is spatially restricted to the cortical side facing the spindle poles by direct binding to Gai (Zheng et al., 2010) (**Figure 1A**). Lateral recruitment of LGN and in turn NuMA/dynein motors promotes planar spindle orientation (Zheng et al., 2010). Notably, the conformation of LGN depends on its binding partners (Du and Macara, 2004; Pan et al., 2013): in the unliganded form LGN is kept in an inhibited conformation by intra-molecular interactions between the N-terminal TPR domain and the C-terminal GoLoco region. Cooperative binding of the four GoLoco motifs to cortical Gai<sup>GDP</sup> molecules recruits LGN to the cortex and induces a conformational change releasing the TPR domain that in turn associates with NuMA. These events result in the enrichment for NuMA/dynein/dynactin motors to specific cortical sites and onset of astral MT-pulling forces (Du and Macara, 2004; Pan et al., 2013) (**Figure 1A**). Notably, the TPR domain of LGN interacts not only with NuMA but also with Afadin and E-cadherin in a mutually exclusive manner, with functional implications that will be discussed below. NuMA shares the domain structures with other dynein-activator proteins (Kiyomitsu and Boerner, 2021), including a hook domain and a CC1-like box motifs, both at the N-terminus,



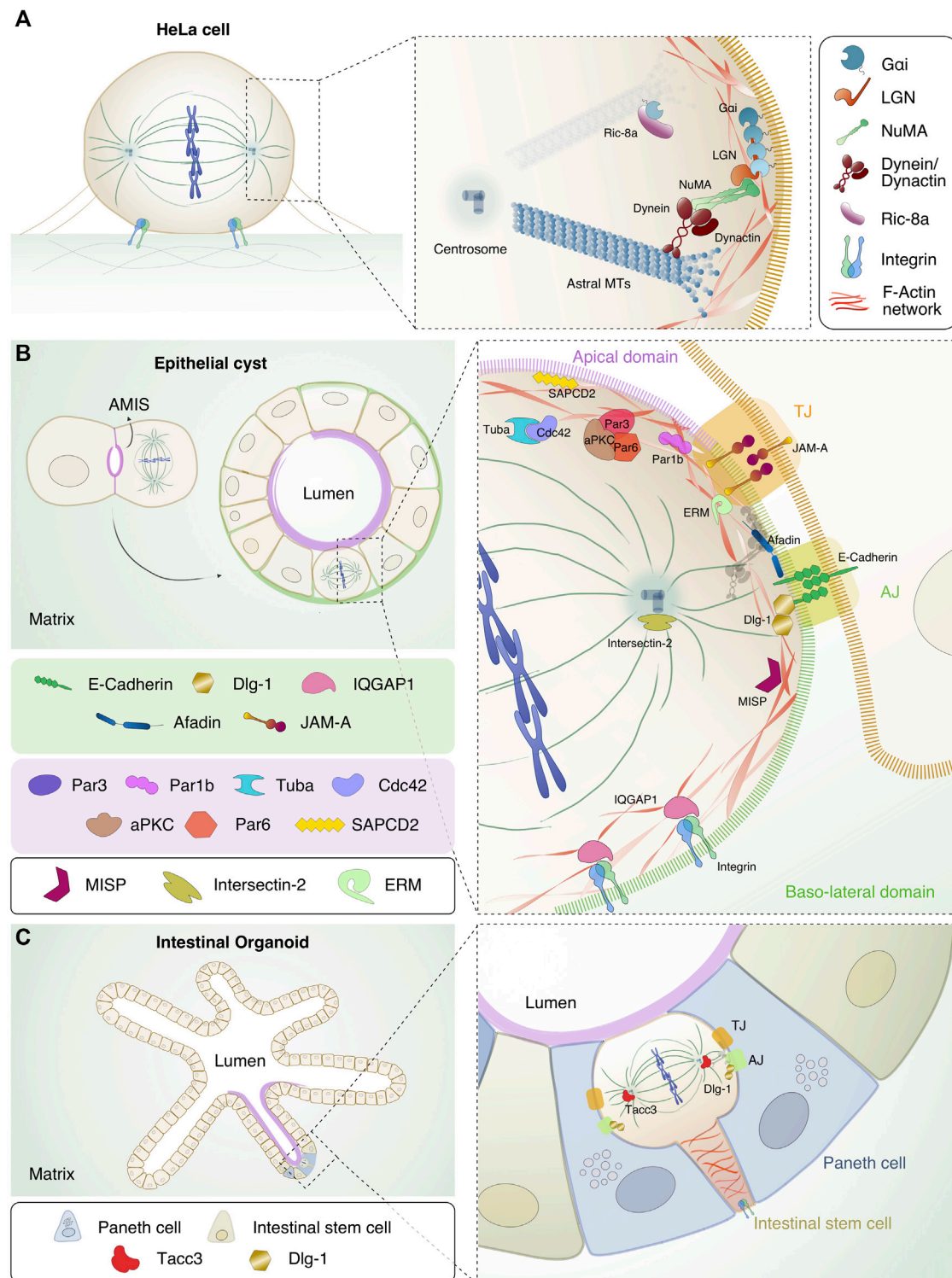


**FIGURE 1 |** Localization and interaction of the spindle orientation and polarity proteins in different model systems. **(A)** HeLa cell in metaphase. Chromosomes (in blue) are aligned at the metaphase plate in the centre of the cell, MTs (in dark green) form the mitotic spindle and integrins important for adhesion of the mitotic cell to the substratum, are shown in light blue and green. In the inset, the details of the interaction interfaces between orientation proteins Gai/LGN/NuMA, dynein/dynactin (in bordeaux) and astral MTs are shown. The Gai/NuMA/LGN complex is recruited at the lateral sides above spindle poles. NuMA is in green, LGN in orange and Gai in petrol blue. Ric-8-A (in purple) is shown in the cytoplasm, close to the plasma membrane-bound Gai. **(B)** Evolution from two-cell stage, in which the mitotic spindle orients parallel to the AMIS, to mature cyst with a single lumen. The diving cell in the mature cyst has the mitotic spindle parallel to the apical side. In the scheme, the apical domain is highlighted in purple (Continued)

**FIGURE 1** | while the basolateral side in green. In the close-up, the mitotic spindle proteins displayed in A are shown in relation with the polarity or junctional protein discussed in the text. At the level of cell-cell junctions, the tight junction (TJ, orange box) and the adherens junction (AJ, bright green box) are shown with key components highlighted. At the TJ, JAM-A (in rainbow orange), the polarity complex with Par3 (dark purple), Par6 (light red), aPKC (brown), Cdc42 (illac) and Tuba (cyan) are depicted. Par1b (fuchsia) and SAPCD2 (yellow) are pictured at the apical side. At the AJ levels, E-cadherin (in green), Afadin (in blue) and Dlg-1 (in gold) are shown. At the basal side of the cell, IQGAP1 (in pink) and integrins are depicted. Intersectin-2 (in olive green) is present at the centrosomes. F-actin is shown in red, and the interacting proteins MISP (in purple wine) and ERM (in aqua green) connecting the mitotic cortex to the plasma membrane are indicated. **(C)** Left: intestinal organoids showing the crypt-villi structure that recapitulates the intestine architecture. The apical side of the organoids is shown in purple, the intestinal stem cells (in ocre) and the Paneth cells (in blue) are highlighted. In the inset on the right, mitotic ISC located apically in the monolayer is shown with the actin cable connecting the dividing cells to the basal membrane. Dlg-1 and Tacc3 (in tomato) are shown.

responsible for the binding to dynein and dynactin. After a central 1500-residue long coiled-coil, NuMA codes for a C-terminal region binding to LGN, microtubules, as well as to the plasma membrane in anaphase (Kotak et al., 2013; Seldin et al., 2013; Carminati et al., 2016; Seldin et al., 2016; Pirovano et al., 2019; Renna et al., 2020). All these diverse functionalities of NuMA C-terminus contribute to spindle placement during mitotic progression, partly modulated by mitotic kinases' phosphorylation (Lechler and Mapelli, 2021).

## Polarity and Epithelial Junctions in Spindle Orientation in Polarized Monolayers and Cysts

In 2D systems such as polarized MDCK cells grown in monolayer, cells divide with the spindle axis aligned to the substratum by planar symmetric divisions that generate two daughter cells remaining in the same monolayer (Reinsch and Karsenti, 1994; Tuncay et al., 2015; Lázaro-Díéguez and Müsch, 2017). In this setting, spindle alignment is maintained by astral MTs captured by cortical cues localized at the lateral domains of the dividing cell, including cell-cell adhesion molecules (Gloerich et al., 2017; Lázaro-Díéguez and Müsch, 2017). Additional information has been obtained in more physiologically relevant 3D models, such as cysts.

The most common cells used to study oriented divisions in cysts are MDCK and Caco-2 (human colon adenocarcinoma) cells that, when plated on a substrate that mimics the ECM such as matrigel, grow as monolayered spheres by planar divisions occurring with the spindle axis perpendicular to the apico-basal polarity (Zegers et al., 2003; Jaffe et al., 2008). A cyst is characterized by a central lumen and a surrounding monolayer of polarized cells (Zegers et al., 2003) (**Figure 1B**). Notably, lumen formation in MDCK- or Caco-2-derived cysts relies on spindle orientation, as opposed to cysts obtained from MCF10A cells (human breast immortalized cells) where lumen forms by anoikis, i. e. apoptosis of inner cells after a full sphere is formed (Debnath et al., 2002). After the first division, MDCK single cells have been shown to form an apical membrane initiation site (AMIS) between the two daughter cells, in the position where the midbody was located (Overeem et al., 2015), that will later become the lumen of the nascent cyst (Rodríguez-Boulan and Macara, 2014) (**Figure 1B** left). Cells composing the mature cyst have two types of domains: the apical side facing the central lumen where the PAR (partitioning defective) family proteins localize, and the baso-lateral domain where adhesion proteins such as integrins are in contact with the ECM, and where adjacent cells are in contact with each other by adherens (AJ) and

tight junctions (TJ) (McCaffrey and Macara, 2011) (**Figure 1B** right). Importantly, each of these membrane domains is key for the localization of spindle orientation proteins instructing planar divisions including Gai, NuMA and LGN (see below) (Overeem et al., 2015; Nakajima, 2018). In **Table 1** we summarized the proteins involved in spindle orientation with their function, localization and defects occurring upon depletion.

One of the first proteins to be implicated in planar divisions in cysts was the GTPase Cdc42, whose depletion in Caco-2 cells results in multi-lumen cysts due to spindle misorientation (Jaffe et al., 2008). In MDCK cells, Cdc42 has been shown to be activated by the two GEFs Tuba, regulating cell-cell junctions and Cdc42 apical localization (Qin et al., 2010; Otani et al., 2006), and Intersectin-2, implicated in endocytosis and in the mitotic Cdc42 targeting at centrosomes (Rodríguez-Fraticelli et al., 2010; Okamoto et al., 1999; Hussain et al., 2001). Planar spindle orientation is also mediated by the apically-localized polarity complex composed by Par3, Par6 and the kinase aPKC (**Figure 1B**). Several studies in 3D systems have shown that depletion of Par3 leads to mislocalization of the kinase aPKC (Hao et al., 2010; Zheng et al., 2010; Durgan et al., 2011; Vorhagen and Niessen, 2014), which phosphorylates LGN on Ser401 to exclude it from the apical side ensuring its localization at the lateral cortex, possibly by direct association with the baso-lateral protein Dlg-1 (Saadaoui et al., 2014). An intriguing role has been described for the Par1b/MARK2 kinase that in MDCK cells monolayer with high Rho activity promotes LGN/NuMA recruitment at the lateral site and planar divisions with the spindle axis aligned to the substratum. Conversely, in hepatocytes, that in addition to apico-basal polarity also organize a lateral lumen for the development of bile canalicular networks and have reduced Rho activity, Par1b prevents NuMA/LGN lateral recruitment causing tilted spindles and asymmetric partitioning of the lateral lumen among daughter cells (Lázaro-Díéguez et al., 2013; Slim et al., 2013).

In addition to their cohesive role, also some junctional proteins have been shown to be involved in spindle orientation in cysts, including the Junctional adhesion molecule-A (JAM-A), Afadin (AF6), E-Cadherin and Dlg-1 (Discs large homolog 1) (**Figure 1B**). In MDCK cysts, JAM-A activates Cdc42 and PI(3)K (Phosphatidylinositol 3-kinases), generating a gradient of PtdIns(3,4,5)P3 enriched at the cortex area facing the spindle poles, which is required for correct localization of dynein/dynactin and for spindle orientation (Toyoshima et al., 2007; Tuncay et al., 2015). Consistently, JAM-A was shown to activate Cdc42 also in progenitors of the developing cerebral cortex this way contributing to spindle orientation (Fededa et al., 2016).

**TABLE 1 |** Proteins involved in division orientation, and model systems in which they were studied (fly and worm orthologues are reported, when present).

Protein	Cellular system	Function	Mitotic localization	Defects upon ablation	REFs
NuMA <i>dmMud</i> , <i>ceLIN-5</i>	HeLa, Caco-2/MDCK cyst	Dynein adaptor	Spindle poles Polar, cortex Centrosomes	Misorientation Multilumen	(Du et al., 2001; Du and Macara, 2004; Woodard et al., 2010; Kotak et al., 2012; Kotak et al., 2013; Seldin et al., 2013; Bañón-Rodríguez et al., 2014; Carminati et al., 2016; Gallini et al., 2016; Seldin et al., 2016; Kschonsak and Hoffmann, 2018; Okumura et al., 2018; Pirovano et al., 2019; Renna et al., 2020)
LGN, <i>dmPins</i> , <i>ceGPR-1/2</i>	HeLa, MDCK cyst/monolayer	Scaffold	Polar cortex	Misorientation Multilumen	(Mochizuki et al., 1996; Willard et al., 2004; Rodriguez-Fraticelli et al., 2010; Woodard et al., 2010; Zheng et al., 2010; Pan et al., 2013; Machicoane et al., 2014; Saadaoui et al., 2014; Carminati et al., 2016; Gloerich et al., 2017; Hart et al., 2017; Saadaoui et al., 2017; Wang et al., 2018; Pirovano et al., 2019; Takayanagi et al., 2019)
Gai, <i>dmGai/Goa</i> , <i>ceGPR-1/2</i>	HeLa, MDCK cyst	GTPase of G-proteins	Cell cortex	Misorientation Multilumen	(Du and Macara, 2004; Chishiki et al., 2017)
Ric-8a <i>dmRic8</i> , <i>ceRic8/synebrin</i>	HeLa, MDCK cyst	GEF	Cell cortex, TJ	Misorientation Multilumen	(Woodard et al., 2010; Chishiki et al., 2017)
Cdc42, <i>dmCdc42</i> , <i>ceCdc42</i>	Caco-2/MDCK cyst	GTPase	Cell cortex, Centrosomes	Misorientation Multilumen	(Otani et al., 2006; Jaffe et al., 2008; Qin et al., 2010; Rodriguez-Fraticelli et al., 2010; Vodicska et al., 2018)
Intersectin-2	MDCK cyst	GEF	Centrosomes	Misorientation Multilumen	Rodriguez-Fraticelli et al. (2010)
Tuba	MDCK cyst	GEF	Cell cortex	Misorientation Multilumen	(Otani et al., 2006; Qin et al., 2010)
PAR1b, <i>dmPar1b</i> , <i>cePAR1</i>	MDCK cyst, hepatocyte cells	Scaffold and adaptor	Apical cortex	Misorientation	(Lázaro-Diéguez et al., 2013; Slim et al., 2013)
PAR3, <i>dmBazooka</i> , <i>cePAR3</i>	Caco-2/MDCK cyst	Scaffold and adaptor	Apical cortex	Misorientation Multilumen	(Hao et al., 2010; Vorhagen and Niessen, 2014)
PAR6, <i>dmPAR6</i> , <i>cePAR6</i>	Caco-2/MDCK cyst	Scaffold and adaptor	Apical cortex	Misorientation Multilumen	(Durgan et al., 2011; Vorhagen and Niessen, 2014)
aPKC, <i>dmaPKC</i> , <i>cePKC-3</i>	Caco-2/MDCK cyst	Apical polarity	Apical cortex	Misorientation Multilumen	(Hao et al., 2010; Durgan et al., 2011; Vorhagen and Niessen, 2014)
SAPCD2	MDCK, Mouse retina epithelium	Apical polarity	Apical cortex	Misorientation Multilumen	Chiu et al. (2016)
Dlg1, SAP97, <i>dmDlg</i> , <i>ceDLG-1</i>	HeLa, Caco-2/MDCK cyst, Chick neuroepithelium, Intestinal organoids	Polarity protein	Basolateral Cell cortex	Misorientation Multilumen	(Saadaoui et al., 2014; Porter et al., 2019; Young et al., 2019)
JAM-A	HeLa, MDCK cyst, MDCK monolayer, Murine brain	Junction formation	TJ	Misorientation Multilumen, Fate defects	(Tuncay et al., 2015; Fededa et al., 2016)
Afadin, <i>dmCanoe</i> , <i>ceAFD-6</i>	HeLa, Caco-2/MDCK cyst Hepatocyte, Mice intestine	Junction formation Actin-binding	Lateral cortex, AJ	Misorientation Multilumen, Intestine defects	(Carminati et al., 2016; Gao et al., 2017; Rakotomamonjy et al., 2017; Lough et al., 2019; Bonucci et al., 2020)
E-Cadherin, <i>dmshg</i> , <i>ceHMR-1</i>	HeLa, MDCK cyst	AJ formation	Lateral cortex, AJ	Misorientation Multilumen	(Gloerich et al., 2017; Hart et al., 2017; Lázaro-Diéguez and Müsch, 2017; Wang et al., 2018)
IQGAP1, <i>cepes-7</i>	MDCK cyst	Adhesion, Actin-binding, MT-binding	Basolateral Cell cortex	Misorientation Multilumen	(Bañón-Rodríguez et al., 2014; Vodicska et al., 2018)
MISP	HeLa, Caco-2 cyst	Actin and MTs interactor	Cell cortex	Misorientation Multilumen	(Zhu et al., 2013; Kschonsak and Hoffmann, 2018; Vodicska et al., 2018)
ERM, <i>dmMoesin</i> , <i>ceERM-1</i>	HeLa, MDCK cyst	Linking Actin to cortex	Cell cortex	Misorientation Multilumen	(Hebert et al., 2012; Machicoane et al., 2014; Kschonsak and Hoffmann, 2018)
Tacc3, <i>dmTACC</i> , <i>ceTAC-1</i>	HeLa, Intestinal organoids, Murine intestine	MTs stabilization	Centrosomes, Spindle poles	Misorientation	(LeRoy et al., 2007; Burgess et al., 2015; Yao et al., 2016)

The actin-binding protein Afadin, localized at adherent junctions, mediates planar spindle orientation in Caco-2 cyst

by recruiting LGN to the lateral cortex via direct interactions with the LGN-TPR domain (Carminati et al., 2016; Gao et al., 2017;

Bonucci et al., 2020) (**Figure 1B**). Consistently, studies conducted in MDCK cysts (Gao et al., 2017), hepatocyte cells (Bonucci et al., 2020), and murine neuro glia (Rakotomamonjy et al., 2017) show that Afadin is crucial for spindle orientation as its depletion leads to an aberrant spindle placement (Lough et al., 2019; Carminati et al., 2016; Gao et al., 2017; Bonucci et al., 2020; Rakotomamonjy et al., 2017). In MDCK cysts, planar cell divisions also rely on the interaction between the intra-cellular domain of E-cadherin and LGN-TPR domain (Gloerich et al., 2017; Hart et al., 2017) (**Figure 1B**). As with Afadin, NuMA competes also with E-cadherin for LGN binding (Zhu et al., 2011; Carminati et al., 2016; Gloerich et al., 2017; Hart et al., 2017). This suggests that Afadin and E-cadherin might be needed for the initial LGN targeting at the cortex, when NuMA is still in the nucleus, and that these interactions dissociate later in mitosis. An alternative explanation envisions that the cortical Gai<sup>GDP</sup>-bound pool of LGN cycles between different mitotic binding partners associating with its TPR domain, including NuMA, Afadin and E-cadherin, in order to coordinate mechano-sensing junctional cues with spindle orientation and mitotic progression. Future live-imaging studies will clarify whether this is the case.

In addition to this role, E-cadherin was shown to be important for maintenance of cell polarity and spindle orientation in prostate epithelia by interacting with LGN, NuMA and Scrib at the lateral sites of mitotic cells, this way preserving correct apico-basal polarity, planar cell divisions and tissue integrity. Consistently, conditional loss of E-cadherin during murine prostate development leads to disorganized epithelia observed in early state prostate tumorigenesis (Wang et al., 2018). Spindle orientation functions have been reported also for the baso-lateral polarity protein Dlg-1, that belongs to the membrane-associated guanylate kinase (MAGUK) family and is required for adherens junction formation and maintenance (Su et al., 2012) (**Figure 1B**). In HeLa cells, in MDCK cysts and in the chick neuroepithelium, Dlg-1 promotes spindle orientation by binding to the phosphorylated LGN protein (Saadaoui et al., 2014; Saadaoui et al., 2017; Porter et al., 2019), fully in line with was previously shown in *Drosophila* epithelial systems (Morin and Bellaïche, 2011; Pietro et al., 2016). In turn, the correct localization of Dlg-1 is influenced by other factors including Gai (Saadaoui et al., 2014) and the tumor suppressor protein CASK (calcium/calmodulin-dependent serine protein kinase) (Porter et al., 2019). The binding of Dlg-1 to CASK and Gai is key to direct LGN to restricted cortical regions before metaphase, and ultimately to target LGN and NuMA-dynein appropriately (Saadaoui et al., 2014; Saadaoui et al., 2017; Porter et al., 2019).

Another polarity protein affecting LGN cortical recruitment is the suppressor APC domain containing 2 (SAPCD2), that has been shown to interact with Gai/LGN complexes to orchestrate mitotic spindle orientation in MDCK cyst and in mouse retina (Chiu et al., 2016). Specifically, SAPCD2 binding to the close conformation of LGN restricts LGN/NuMA accumulation at the lateral site providing a mechanism to balance the proportion of planar and vertical divisions, and hence the symmetric or

asymmetric outcome of retinal progenitor mitosis (Chiu et al., 2016).

We already reported the relevance of the Gai GEF Ric-8A for spindle orientation in HeLa cells (Woodard et al., 2010). Recent work highlighted a role for Ric-8A in tight junction formation in MDCK cysts and in LGN recruitment to the lateral cortex by generation of a localized Gai-GDP pool promoting planar cell divisions (Chishiki et al., 2017) (**Figure 1B**).

Beside junctional and polarity proteins, the actin cytoskeleton, as well as actin and microtubule-binding proteins, contribute actively to spindle orientation (Pietro et al., 2016), as described in invertebrate systems such as *Drosophila* neuroblasts (Kunda and Baum, 2009) and HeLa cells (Pietro et al., 2016; Rizzelli et al., 2020). However, the role of actin in planar division and cystogenesis is less clear. In MDCK cysts, the microtubule-associated protein IQGAP1, localized at the basal site, participates to MTs dynamics and promotes planar spindle orientation by interacting with the MT plus-ends and by targeting NuMA laterally (Bañón-Rodríguez et al., 2014) (**Figure 1B**). Notably, in HeLa cells the interaction between IQGAP1 and Cdc42 has been shown to allow the binding of Cdc42 to the actin-binding protein MISP (Mitotic Interactor and Substrate of PLK1) implicated in spindle positioning (Zhu et al., 2013; Cadart et al., 2014; Vodicska et al., 2018). MISP associates to members of the ERM (Ezrin, Radixin and Moesin) protein family, that connects the mitotic acto-myosin cortex to the plasma membrane, in this way assisting the correct localization of NuMA at the cortex for correct spindle positioning (Hebert et al., 2012; Zhu et al., 2013; Machicoane et al., 2014; Kschonsak and Hoffmann, 2018) (**Figure 1B**).

## Mitotic Spindle Orientation in Intestinal Organoids

Studies of oriented divisions in cysts provided great insights into the crosstalk between orientation pathways and epithelial polarity. However, cysts of immortalized cell lines do not entirely recapitulate the cell diversity and the signaling response of epithelial tissues *in vivo* (Lancaster and Knoblich, 2014; Clevers and Tuveson, 2019).

Tissue organoids, especially murine intestinal organoids, are becoming a relevant model to study division orientation in a more physiological setting. Organoids are model systems that recapitulate not only the morphology of the organ but also the cellular composition, from stem cells to differentiated lineages (Clevers, 2013; Sato and Clevers, 2013). Methods to grow, manipulate genetically and image intestinal organoids have been first established in the Clevers lab (Sato and Clevers, 2013; Sato et al., 2009), whose work revealed that the organoids grown from intestinal epithelial cells form crypt and villi-like domains mirroring the morphology of the intestinal epithelium, with an analogous composition and distribution of cell types (Sato and Clevers, 2013; Sato et al., 2009) (**Figure 1C**). These studies revealed that in intestinal organoids the proliferating cells reside at the bottom of the crypt, close to the stem cell niche compartment constituted by non-dividing Paneth cells, that generate a Wnt3 gradient decreasing along the crypt axis (**Figure 1C**). Intestinal



stem cells (ISCs) divide symmetrically moving toward the apical side of the monolayer that faces the organoid lumen, with the metaphase plate perpendicular to the apical side (**Figure 1C**). These ISC apical mitosis retain a connection to the basal site, and hence to the ECM, through an actin cable (Carroll et al., 2017; McKinley et al., 2018) (**Figure 1C**) that is essential for daughter cells to move back to the basal side of the monolayer upon cytokinesis (Carroll et al., 2017). As a matter of fact, the use of intestinal organoids to study oriented division is still in its infancy, contributed mainly by descriptive imaging experiments and a few mechanistical studies investigating the molecular mechanisms of mitosis. Little is known on molecules executing oriented divisions in organoid, but it is plausible that the same set of polarity and junctional proteins important for correct cystogenesis is implicated in division orientation also in these systems, with molecular details that remain to be explored.

Ablation of Dlg-1 from the murine intestinal crypts has been shown to result in misoriented divisions of the intestinal stem cells with a consequent delay in cell migration from the crypts bottom to the villi that promotes tumorigenic events (Young et al., 2019). Similarly, depletion from the murine crypts of the protein Tacc3, which is involved in MT crosslinking and stabilization of the Aurora-A dependent kinetochore-microtubules attachment (LeRoy et al., 2007; Burgess et al., 2015), blocks proliferation (Yao et al., 2016). Interestingly, knock-out of Tacc3 from intestinal organoids derived from APC (Adenomatous polyposis coli) mutated mice, models for colorectal cancer (Merenda et al., 2020), increases chromosome misalignment and hypomorphic mitotic spindles, leading to prolonged mitosis or mitotic arrest (Yao et al., 2016), to a certain extent mimicking what observed *in vivo*. Both findings open the possibility to target specific mitotic spindle proteins for chemotherapeutic therapy. In conclusion, although organoids hold the potential to allow more insightful analyses on the orientation pathways and their relevance for morphogenesis and disease, more studies are required to elucidate the molecular mechanisms accounting for oriented divisions in these systems.

## Spindle Misorientation: What Can Go Wrong and What Can be Done to Fix it

As discussed, oriented divisions are important for the regulation of epithelial morphogenesis and homeostasis. Consistently, their deregulation has been associated to several pathological conditions such as cancer, microcephaly, and developmental defects (Gillies and Cabernard, 2011; Nakajima, 2018; Lechler and Mapelli, 2021). However, not always the causal relationship between misorientation and diseases is clear. *In vivo* studies revealed that spindle misorientation is oftentimes corrected or is embryonic lethal (Nakajima, 2018; Lechler and Mapelli, 2021).

In murine hepatic epithelial cells *in vivo*, spindle misorientation leads to detachment of epithelial sheets from nephron epithelial tubules (Gao et al., 2017). Similarly, in stem cell systems, misorientation alters the balance between symmetric and asymmetric divisions resulting in defective changes in architecture and functioning. This has been documented for neuroepithelial progenitors during murine cortical

development, in which misorientation leads to the expansion of the radial glial compartment with a delay in neurogenesis (Fededa et al., 2016).

Tissues have developed different mechanisms to rescue the damage that a misoriented spindle can cause, that have been first discovered in *Drosophila* and still await to be confirmed in mammalian tissues. The first mechanism impinges on the ability of epithelial tissue to reintegrate cells that after misoriented cytokinesis are misplaced above the epithelial layer (Bergstrahl et al., 2015; Lough et al., 2019). As described for intestinal organoids (Carroll et al., 2017), in *Drosophila* imaginal disc the dividing cells have an actin protrusion that keeps them in connection to the basal side of the monolayer and assists the appropriate repositioning of daughters after cytokinesis (Nakajima et al., 2013). Parallel studies showed that also adhesive molecules, such as Fasciculin-2/3 and neuroglian, play a role in reintegrating in the epithelial layer the cells misplaced above the follicular epithelium due to orientation defects (Bergstrahl et al., 2015; Cammarota et al., 2020). In *Drosophila* imaginal discs, evidence was provided that upon misorientation, one of the two daughter cells loses connection with the basal side and is displaced in the lumen (Nakajima et al., 2013). In the absence of re-integration, the misplaced cells can encounter two different fates: it either remains in the wrong position, where proliferation causes morphological defects (Dekanty et al., 2012; Nakajima et al., 2013; Poulton et al., 2014), or it undergoes apoptosis due to lack of survival signals (Nakajima et al., 2013; Poulton et al., 2014). Whether any of these mechanisms for misorientation correction is in place in vertebrate epithelial tissues remains an interesting open question.

## CONCLUSION

Much is known about division orientation and how the spindle orientation components are recruited to the cortex in single cells in isolation and cysts. However, a clear picture of orientation mechanisms in more complex systems, such as organoids and tissues, is still missing. The complexity of cell-cell contacts and the presence of different cell populations in epithelial tissues contribute to determine the division orientation in ways that we do not fully grasp. We also still need to further understand the mechanisms that mammalian tissues have evolved to respond to misorientation in order to preserve tissue architecture. Some of the open questions that the field should address in the future are how the correction mechanisms work in mammalian systems and how we can leverage this knowledge to better understand physio-pathological processes associated with misoriented spindles in the presence or absence of other genetic lesions. We anticipate that the use organoids as model systems might be instrumental in these studies.

## AUTHOR CONTRIBUTIONS

FD and MM wrote the manuscript. SE illustrated the concepts covered by the review.

## FUNDING

FD is funded from AIRC and from the European Union's Horizon 2020 research and innovation program under the Marie Skłodowska-Curie grant agreement No. 800924. SE is a

## REFERENCES

- Bañón-Rodríguez, I., Gálvez-Santisteban, M., Vergarajauregui, S., Bosch, M., Borreguero-Pascual, A., and Martín-Belmonte, F. (2014). EGFR Controls IQGAP Basolateral Membrane Localization and Mitotic Spindle Orientation during Epithelial Morphogenesis. *Embo J.* 33 (2), 129–145. doi:10.1002/embj.201385946
- Bergstralh, D. T., Lovegrove, H. E., and St Johnston, D. (2015). Lateral Adhesion Drives Reintegration of Misplaced Cells into Epithelial Monolayers. *Nat. Cell Biol.* 17 (11), 1497–1503. doi:10.1038/ncb3248
- Bonucci, M., Kuperwasser, N., Barbe, S., Koka, V., de Villeneuve, D., Zhang, C., et al. (2020). mTOR and S6K1 Drive Polycystic Kidney by the Control of Afadin-dependent Oriented Cell Division. *Nat. Commun.* 11 (1), 3200. doi:10.1038/s41467-020-16978-z
- Bosveld, F., Markova, O., Guirao, B., Martin, C., Wang, Z., Pierre, A., et al. (2016). Epithelial Tricellular Junctions Act as Interphase Cell Shape Sensors to orient Mitosis. *Nature* 530 (7591), 495–498. doi:10.1038/nature16970
- Burgess, S. G., Peset, I., Joseph, N., Cavazza, T., Vernos, I., Pfuhl, M., et al. (2015). Aurora-A-Dependent Control of TACC3 Influences the Rate of Mitotic Spindle Assembly. *Plos Genet.* 11, e1005345. doi:10.1371/journal.pgen.1005345
- Cadart, C., Zlotek-Zlotkiewicz, E., Le Berre, M., Piel, M., and Matthews, H. K. (2014). Exploring the Function of Cell Shape and Size during Mitosis. *Dev. Cell* 29 (2), 159–169. doi:10.1016/j.devcel.2014.04.009
- Cammarota, C., Finegan, T. M., Wilson, T. J., Yang, S., and Bergstralh, D. T. (2020). An Axon-Pathfinding Mechanism Preserves Epithelial Tissue Integrity. *Curr. Biol.* 30 (24), 5049–5057. doi:10.1016/j.cub.2020.09.061
- Carminati, M., Gallini, S., Pirovano, L., Alfieri, A., Bisi, S., and Mapelli, M. (2016). Concomitant Binding of Afadin to LGN and F-Actin Directs Planar Spindle Orientation. *Nat. Struct. Mol. Biol.* 23 (2), 155–163. doi:10.1038/nsmb.3152
- Carroll, T. D., Langlands, A. J., Osborne, J. M., Newton, I. P., Appleton, P. L., and Näthke, I. (2017). Interkinetic Nuclear Migration and Basal Tethering Facilitates post-mitotic Daughter Separation in Intestinal Organoids. *J. Cell Sci.* 130 (22), 3862–3877. doi:10.1242/jcs.211656
- Chishiki, K., Kamakura, S., Hayase, J., and Sumimoto, H. (2017). Ric-8A, an Activator Protein of Gai, Controls Mammalian Epithelial Cell Polarity for Tight junction Assembly and Cystogenesis. *Genes Cells* 22 (3), 293–309. doi:10.1111/gtc.12477
- Chiu, C. W. N., Monat, C., Robitaille, M., Lacomme, M., Daulat, A. M., Macleod, G., et al. (2016). SAPCD2 Controls Spindle Orientation and Asymmetric Divisions by Negatively Regulating the Gai-LGN-NuMA Ternary Complex. *Dev. Cell* 36 (1), 50–62. doi:10.1016/j.devcel.2015.12.016
- Clevers, H. (2013). The Intestinal Crypt, A Prototype Stem Cell Compartment. *Cell* 154 (2), 274–284. doi:10.1016/j.cell.2013.07.004
- Clevers, H., and Tuveson, D. A. (2019). Organoid Models for Cancer Research. *Annu. Rev. Cancer Biol.* 3 (1), 223–234. doi:10.1146/annurev-cancerbio-030518-055702
- Debnath, J., Mills, K. R., Collins, N. L., Reginato, M. J., Muthuswamy, S. K., and Brugge, J. S. (2002). The Role of Apoptosis in Creating and Maintaining Luminal Space within normal and Oncogene-Expressing Mammary Acini. *Cell* 111 (1), 29–40. doi:10.1016/s0092-8674(02)01001-2
- Dekanty, A., Barrio, L., Muzzopappa, M., Auer, H., and Milan, M. (2012). Aneuploidy-induced Delaminating Cells Drive Tumorigenesis in Drosophila Epithelia. *Proc. Natl. Acad. Sci.* 109 (50), 20549–20554. doi:10.1073/pnas.1206675109
- Du, Q., and Macara, I. G. (2004). Mammalian Pins Is a Conformational Switch that Links NuMA to Heterotrimeric G Proteins. *Cell* 119 (4), 503–516. doi:10.1016/j.cell.2004.10.028
- Du, Q., Stukenberg, P. T., and Macara, I. G. (2001). A Mammalian Partner of Inscuteable Binds NuMA and Regulates Mitotic Spindle Organization. *Nat. Cell Biol.* 3 (12), 1069–1075. doi:10.1038/ncb1201-1069
- PhD student within the European School of Molecular Medicine (SEMM). This work was supported by a grant to MM. from the Italian Association for Cancer Research (AIRC) (IG 2020 ID 25098) and partially supported by the Italian Ministry of Health with Ricerca Corrente and 5x1000 funds.
- Durgan, J., Kaji, N., Jin, D., and Hall, A. (2011). Par6B and Atypical PKC Regulate Mitotic Spindle Orientation during Epithelial Morphogenesis. *J. Biol. Chem.* 286 (14), 12461–12474. doi:10.1074/jbc.m110.174235
- Fededa, J. P., Esk, C., Mierzwa, B., Stanyte, R., Yuan, S., Zheng, H., et al. (2016). Micro RNA -34/449 Controls Mitotic Spindle Orientation during Mammalian Cortex Development. *Embo J.* 35 (22), 2386–2398. doi:10.15252/embj.201694056
- Fielmich, L. E., Schmidt, R., Dickinson, D. J., Goldstein, B., Akhmanova, A., and van den Heuvel, S. (2018). Optogenetic Dissection of Mitotic Spindle Positioning *In Vivo*. *Elife* 7, 7. doi:10.7554/eLife.38198
- Finegan, T. M., Na, D., Cammarota, C., Skeeters, A. V., Nádasi, T. J., Dawney, N. S., et al. (2019). Tissue Tension and Not Interphase Cell Shape Determines Cell Division Orientation in the Drosophila Follicular Epithelium. *EMBO J.* 38, 38. doi:10.15252/embj.2018100072
- Gallini, S., Carminati, M., De Mattia, F., Pirovano, L., Martini, E., Oldani, A., et al. (2016). NuMA Phosphorylation by Aurora-A Orchestrates Spindle Orientation. *Curr. Biol.* 26 (4), 458–469. doi:10.1016/j.cub.2015.12.051
- Gao, L., Yang, Z., Hiremath, C., Zimmerman, S. E., Long, B., Brakeman, P. R., et al. (2017). Afadin Orients Cell Division to Position the Tubule Lumen in Developing Renal Tubules. *Development* 144 (19), 3511–3520. doi:10.1242/dev.148908
- Gillies, T. E., and Cabernard, C. (2011). Cell Division Orientation in Animals. *Curr. Biol.* 21, R599–R609. doi:10.1016/j.cub.2011.06.055
- Gloerich, M., Bianchini, J. M., Siemers, K. A., Cohen, D. J., and Nelson, W. J. (2017). Cell Division Orientation Is Coupled to Cell-Cell Adhesion by the E-Cadherin/LGN Complex. *Nat. Commun.* 8, 13996. doi:10.1038/ncomms13996
- Gönczy, P. (2008). Mechanisms of Asymmetric Cell Division: Flies and Worms Pave the Way. *Nat. Rev. Mol. Cell Biol.* 9 (5), 355–366. doi:10.1038/nrm2388
- Hao, Y., Du, Q., Chen, X., Zheng, Z., Balsbaugh, J. L., Maitra, S., et al. (2010). Par3 Controls Epithelial Spindle Orientation by aPKC-Mediated Phosphorylation of Apical Pins. *Curr. Biol.* 20 (20), 1809–1818. doi:10.1016/j.cub.2010.09.032
- Hart, K. C., Tan, J., Siemers, K. A., Sim, J. Y., Pruitt, B. L., Nelson, W. J., et al. (2017). E-cadherin and LGN Align Epithelial Cell Divisions with Tissue Tension Independently of Cell Shape. *Proc. Natl. Acad. Sci. U S A.* 114, E5845. doi:10.1073/pnas.1701703114
- Hebert, A. M., DuBoff, B., Casaleto, J. B., Gladden, A. B., and McClatchey, A. I. (2012). Merlin/ERM Proteins Establish Cortical Asymmetry and Centrosome Position. *Genes Dev.* 26 (24), 2709–2723. doi:10.1101/gad.194027.112
- Hertwig, O. (1884). *Untersuchungen zur Morphologie und Physiologie der Zelle*. Fisher, 1884
- Hussain, N. K., Jenna, S., Glogauer, M., Quinn, C. C., Wasiak, S., Guipponi, M., et al. (2001). Endocytic Protein Intersectin-L Regulates Actin Assembly via Cdc42 and N-WASP. *Nat. Cell Biol.* 3 (10), 927–932. doi:10.1038/ncb1001-927
- Jaffe, A. B., Kaji, N., Durgan, J., and Hall, A. (2008). Cdc42 Controls Spindle Orientation to Position the Apical Surface during Epithelial Morphogenesis. *Biomed. Lit.* 183 (4), 625–633. doi:10.1083/jcb.200807121
- Kiyomitsu, T., and Boerner, S. (2021). The Nuclear Mitotic Apparatus (NuMA) Protein: A Key Player for Nuclear Formation, Spindle Assembly, and Spindle Positioning. *Front. Cell Dev. Biol.* 9, 653801. doi:10.3389/fcell.2021.653801
- Kiyomitsu, T., and Cheeseman, I. M. (2012). Chromosome- and Spindle-Pole-Derived Signals Generate an Intrinsic Code for Spindle Position and Orientation. *Nat. Cell Biol.* 14 (3), 311–317. doi:10.1038/ncb2440
- Knoblich, J. A. (2010). Asymmetric Cell Division: Recent Developments and Their Implications for Tumour Biology. *Nat. Rev. Mol. Cell Biol.* 11 (12), 849–860. doi:10.1038/nrm3010
- Knoblich, J. A. (2008). Mechanisms of Asymmetric Stem Cell Division. *Cell* 132 (4), 583–597. doi:10.1016/j.cell.2008.02.007

- Kotak, S., Busso, C., and Gönczy, P. (2012). Cortical Dynein Is Critical for Proper Spindle Positioning in Human Cells. *J. Cell Biol.* 199 (1), 97–110. doi:10.1083/jcb.201203166
- Kotak, S., Busso, C., and Gönczy, P. (2013). NuMA Phosphorylation by CDK1 Couples Mitotic Progression with Cortical Dynein Function. *Embo J.* 32 (18), 2517–2529. doi:10.1038/emboj.2013.172
- Kschonsak, Y. T., and Hoffmann, I. (2018). Activated Ezrin Controls MISP Levels to Ensure Correct NuMA Polarization and Spindle Orientation. *J. Cell Sci.* 131, 131. doi:10.1242/jcs.214544
- Kunda, P., and Baum, B. (2009). The Actin Cytoskeleton in Spindle Assembly and Positioning. *Trends Cell Biol.* 19 (4), 174–179. doi:10.1016/j.tcb.2009.01.006
- Lancaster, M. A., and Knoblich, J. A. (2014). Organogenesis in a Dish: Modeling Development and Disease Using Organoid Technologies. *Science* 345 (6194), 1247125. doi:10.1126/science.1247125
- Lázaro-Díéguez, F., Cohen, D., Fernandez, D., Hodgson, L., van IJzendoorn, S. C. D., and Müsch, A. (2013). Par1b Links Lumen Polarity with LGN-NuMA Positioning for Distinct Epithelial Cell Division Phenotypes. *J. Cell Biol.* 203 (2), 251–264. doi:10.1083/jcb.201303013
- Lázaro-Díéguez, F., and Müsch, A. (2017). Cell-cell Adhesion Accounts for the Different Orientation of Columnar and Hepatocytic Cell Divisions. *J. Cell Biol.* 216 (11), 3847–3859. doi:10.1083/jcb.201608065
- Lechler, T., and Mapelli, M. (2021). Spindle Positioning and its Impact on Vertebrate Tissue Architecture and Cell Fate. *Nat. Rev. Mol. Cell Biol.* 22 (10), 691–708. doi:10.1038/s41580-021-00384-4
- LeRoy, P. J., Hunter, J. J., Hoar, K. M., Burke, K. E., Shinde, V., Ruan, J., et al. (2007). Localization of Human TACC3 to Mitotic Spindles Is Mediated by Phosphorylation on Ser558 by Aurora A: A Novel Pharmacodynamic Method for Measuring Aurora A Activity. *Cancer Res.* 67 (11), 5362–5370. doi:10.1158/0008-5472.can-07-0122
- Lough, K. J., Byrd, K. M., Descovich, C. P., Spitzer, D. C., Bergman, A. J., Beaudoin, G. M., et al. (2019). Telophase Correction Refines Division Orientation in Stratified Epithelia. *Elife* 8, 8. doi:10.7554/eLife.49249
- Machicoane, M., de Frutos, C. A., Fink, J., Rocancourt, M., Lombardi, Y., Garel, S., et al. (2014). SLK-dependent Activation of ERMs Controls LGN-NuMA Localization and Spindle Orientation. *Dev. Cell* 205 (6), 791–799. doi:10.1083/jcb.201401049
- McCaffrey, L. M., and Macara, I. G. (2011). Epithelial Organization, Cell Polarity and Tumorigenesis. *Trends Cell Biol.* 21 (12), 727–735. doi:10.1016/j.tcb.2011.06.005
- McKinley, K. L., Stuurman, N., Royer, L. A., Scharfner, C., Castillo-Azofeifa, D., Delling, M., et al. (2018). Cellular Aspect Ratio and Cell Division Mechanics Underlie the Patterning of Cell Progeny in Diverse Mammalian Epithelia. *Elife* 7, 7. doi:10.7554/eLife.36739
- Merenda, A., Fenderico, N., and Maurice, M. M. (2020). Wnt Signaling in 3D: Recent Advances in the Applications of Intestinal Organoids. *Trends Cell Biol.* 30 (1), 60–73. doi:10.1016/j.tcb.2019.10.003
- Mochizuki, N., Cho, G., Wen, B., and Insel, P. A. (1996). Identification and cDNA Cloning of a Novel Human Mosaic Protein, LGN, Based on Interaction with G Alpha I2. *Gene* 181 (1–2), 39–43. doi:10.1016/s0378-1119(96)00456-8
- Morin, X., and Bellaïche, Y. (2011). Mitotic Spindle Orientation in Asymmetric and Symmetric Cell Divisions during Animal Development. *Dev. Cell* 21 (1), 102–119. doi:10.1016/j.devcel.2011.06.012
- Nakajima, Y.-i., Meyer, E. J., Kroesen, A., McKinney, S. A., and Gibson, M. C. (2013). Epithelial Junctions Maintain Tissue Architecture by Directing Planar Spindle Orientation. *Nature* 500 (7462), 359–362. doi:10.1038/nature12335
- Nakajima, Y.-i. (2018). Mitotic Spindle Orientation in Epithelial Homeostasis and Plasticity. *J. Biochem.* 164 (4), 277–284. doi:10.1093/jb/mvy064
- Nestor-Bergmann, A., Stooke-Vaughan, G. A., Goddard, G. K., Starborg, T., Jensen, O. E., and Woolner, S. (2019). Decoupling the Roles of Cell Shape and Mechanical Stress in Orienting and Cueing Epithelial Mitosis. *Cell Rep.* 26 (8), 2088–2100. doi:10.1016/j.celrep.2019.01.102
- Okamoto, M., Schoch, S., and Südhof, T. C. (1999). EHS1/intersectin, a Protein that Contains EH and SH3 Domains and Binds to Dynamin and SNAP-25. *J. Biol. Chem.* 274 (26), 18446–18454. doi:10.1074/jbc.274.26.18446
- Okumura, M., Natsume, T., Kanemaki, M. T., and Kiyomitsu, T. (2018). Dynein-Dynactin-NuMA Clusters Generate Cortical Spindle-Pulling Forces as a Multi-Arm Ensemble. *Elife* 7, 7. doi:10.7554/eLife.36559
- Osswald, M., and Morais-de-Sá, E. (2019). Dealing with Apical-Basal Polarity and Intercellular Junctions: a Multidimensional challenge for Epithelial Cell Division. *Curr. Opin. Cell Biol.* 60, 75–83. doi:10.1016/j.cob.2019.04.006
- Otani, T., Ichii, T., Aono, S., and Takeichi, M. (2006). Cdc42 GEF Tuba Regulates the Junctional Configuration of Simple Epithelial Cells. *Biomed. Lit.* 175 (1), 135–146. doi:10.1083/jcb.200605012
- Overeem, A. W., Bryant, D. M., and van IJzendoorn, S. C. D. (2015). Mechanisms of Apical-Basal axis Orientation and Epithelial Lumen Positioning. *Trends Cell Biol.* 25 (8), 476–485. doi:10.1016/j.tcb.2015.04.002
- Pan, Z., Zhu, J., Shang, Y., Wei, Z., Jia, M., Xia, C., et al. (2013). An Autoinhibited Conformation of LGN Reveals a Distinct Interaction Mode between GoLoco Motifs and TPR Motifs. *Structure* 21 (6), 1007–1017. doi:10.1016/j.str.2013.04.005
- Pietro, F., Echard, A., and Morin, X. (2016). Regulation of Mitotic Spindle Orientation: an Integrated View. *EMBO Rep.* 17 (8), 1106–1130. doi:10.15252/embr.201642292
- Pirovano, L., Culurgioni, S., Carminati, M., Alfieri, A., Monzani, S., Cecatiello, V., et al. (2019). Hexameric NuMA: LGN Structures Promote Multivalent Interactions Required for Planar Epithelial Divisions. *Nat. Commun.* 10 (1), 2208. doi:10.1038/s41467-019-09999-w
- Porter, A. P., White, G. R. M., Mack, N. A., and Malliri, A. (2019). The Interaction between CASK and the Tumour Suppressor Dlg1 Regulates Mitotic Spindle Orientation in Mammalian Epithelia. *J. Cell Sci.* 132, 132. doi:10.1242/jcs.230086
- Poulton, J. S., Cuningham, J. C., and Peifer, M. (2014). Acentrosomal Drosophila Epithelial Cells Exhibit Abnormal Cell Division, Leading to Cell Death and Compensatory Proliferation. *Dev. Cell* 30 (6), 731–745. doi:10.1016/j.devcel.2014.08.007
- Qin, Y., Meisen, W. H., Hao, Y., and Macara, I. G. (2010). Tuba, a Cdc42 GEF, Is Required for Polarized Spindle Orientation during Epithelial Cyst Formation. *J. Cell Biol.* 189 (4), 661–669. doi:10.1083/jcb.201002097
- Rakotomamonjy, J., Brunner, M., Jüschke, C., Zang, K., Huang, E. J., Reichardt, L. F., et al. (2017). Afadin Controls Cell Polarization and Mitotic Spindle Orientation in Developing Cortical Radial Glia. *Neural Dev.* 12 (1), 7. doi:10.1186/s13064-017-0085-2
- Reinsch, S., and Karsenti, E. (1994). Orientation of Spindle axis and Distribution of Plasma Membrane Proteins during Cell Division in Polarized MDCKII Cells. *J. Cell Biol.* 126 (6), 1509–1526. doi:10.1083/jcb.126.6.1509
- Renna, C., Rizzelli, F., Carminati, M., Gaddoni, C., Pirovano, L., Cecatiello, V., et al. (2020). Organizational Principles of the NuMA-Dynein Interaction Interface and Implications for Mitotic Spindle Functions. *Structure* 28 (7), 820–829. doi:10.1016/j.str.2020.04.017
- Rizzelli, F., Malabarba, M. G., Sigismund, S., and Mapelli, M. (2020). The Crosstalk between Microtubules, Actin and Membranes Shapes Cell Division. *Open Biol.* 10 (3), 190314. doi:10.1098/rsob.190314
- Rodriguez-Boulán, E., and Macara, I. G. (2014). Organization and Execution of the Epithelial Polarity Programme. *Nat. Rev. Mol. Cell Biol.* 15 (4), 225–242. doi:10.1038/nrm3775
- Rodriguez-Fraticelli, A. E., Vergarajauregui, S., Eastburn, D. J., Datta, A., Alonso, M. A., Mostov, K., et al. (2010). The Cdc42 GEF Intersectin 2 Controls Mitotic Spindle Orientation to Form the Lumen during Epithelial Morphogenesis. *J. Cell Biol.* 189 (4), 725–738. doi:10.1083/jcb.201002047
- Saadaoui, M., Konno, D., Loulier, K., Goïame, R., Jadhav, V., Mapelli, M., et al. (2017). Loss of the Canonical Spindle Orientation Function in the Pins/LGN Homolog AGS 3. *EMBO Rep.* 18 (9), 1509–1520. doi:10.15252/embr.201643048
- Saadaoui, M., Machicoane, M., di Pietro, F., Etoc, F., Echard, A., and Morin, X. (2014). Dlg1 Controls Planar Spindle Orientation in the Neuroepithelium through Direct Interaction with LGN. *Biomed. Lit.* 206 (6), 707–717. doi:10.1083/jcb.201405060
- Sato, T., and Clevers, H. (2013). Growing Self-Organizing Mini-Guts from a Single Intestinal Stem Cell: Mechanism and Applications. *Science* 340 (6137), 1190–1194. doi:10.1126/science.1234852
- Sato, T., Vries, R. G., Snippert, H. J., van de Wetering, M., Barker, N., Stange, D. E., et al. (2009). Single Lgr5 Stem Cells Build Crypt-Villus Structures *In Vitro* without a Mesenchymal Niche. *Nature* 459 (7244), 262–265. doi:10.1038/nature07935
- Seldin, L., Muroyama, A., and Lechler, T. (2016). NuMA-microtubule Interactions Are Critical for Spindle Orientation and the Morphogenesis of Diverse Epidermal Structures. *Elife* 5, 5. doi:10.7554/eLife.12504

- Seldin, L., Poulson, N. D., Foote, H. P., and Lechler, T. (2013). NuMA Localization, Stability, and Function in Spindle Orientation Involve 4.1 and Cdk1 Interactions. *MBoC* 24 (23), 3651–3662. doi:10.1091/mbc.e13-05-0277
- Slim, C. L., Lázaro-Díéguez, F., Bijlard, M., Toussaint, M. J., de Bruin, A., Du, Q., et al. (2013). Par1b Induces Asymmetric Inheritance of Plasma Membrane Domains via LGN-dependent Mitotic Spindle Orientation in Proliferating Hepatocytes. *Plos Biol.* 11, e1001739. doi:10.1371/journal.pbio.1001739
- Su, W. H., Mruk, D. D., Wong, E. W., Lui, W. Y., and Cheng, C. Y. (2012). Polarity Protein Complex Scribble/Lgl/Dlg and Epithelial Cell Barriers. *Adv. Exp. Med. Biol.* 763, 149–170. doi:10.1007/978-1-4614-4711-5\_7
- Takayanagi, H., Hayase, J., Kamakura, S., Miyano, K., Chishiki, K., Yuzawa, S., et al. (2019). Intramolecular Interaction in LGN, an Adaptor Protein that Regulates Mitotic Spindle Orientation. *J. Biol. Chem.* 294 (51), 19655–19666. doi:10.1074/jbc.ra119.011457
- Théry, M., Jiménez-Dalmaroni, A., Racine, V., Bornens, M., and Jülicher, F. (2007). Experimental and Theoretical Study of Mitotic Spindle Orientation. *Nature* 447 (7143), 493–496. doi:10.1038/nature05786
- Toyoshima, F., Matsumura, S., Morimoto, H., Mitsushima, M., and Nishida, E. (2007). PtdIns(3,4,5)P3 Regulates Spindle Orientation in Adherent Cells. *Dev. Cel* 13 (6), 796–811. doi:10.1016/j.devcel.2007.10.014
- Tuncay, H., Brinkmann, B. F., Steinbacher, T., Schürmann, A., Gerke, V., Iden, S., et al. (2015). JAM-A Regulates Cortical Dynein Localization through Cdc42 to Control Planar Spindle Orientation during Mitosis. *Nat. Commun.* 6, 8128. doi:10.1038/ncomms9128
- Vodicska, B., Cerikan, B., Schiebel, E., and Hoffmann, I. (2018). MISF Regulates the IQGAP1/Cdc42 Complex to Collectively Orchestrate Spindle Orientation and Mitotic Progression. *Sci. Rep.* 8 (1), 6330. doi:10.1038/s41598-018-24682-8
- Vorhagen, S., and Niessen, C. M. (2014). Mammalian aPKC/Par Polarity Complex Mediated Regulation of Epithelial Division Orientation and Cell Fate. *Exp. Cel Res.* 328 (2), 296–302. doi:10.1016/j.yexcr.2014.08.008
- Wang, X., Dong, B., Zhang, K., Ji, Z., Cheng, C., Zhao, H., et al. (2018). E-cadherin Bridges Cell Polarity and Spindle Orientation to Ensure Prostate Epithelial Integrity and Prevent Carcinogenesis *In Vivo*. *Plos Genet.* 14, e1007609. doi:10.1371/journal.pgen.1007609
- Willard, F. S., Kimple, R. J., and Siderovski, D. P. (2004). Return of the GDI: the GoLoco Motif in Cell Division. *Annu. Rev. Biochem.* 73, 925–951. doi:10.1146/annurev.biochem.73.011303.073756
- Woodard, G. E., Huang, N.-N., Cho, H., Miki, T., Tall, G. G., and Kehrl, J. H. (2010). Ric-8A and Gai Recruit LGN, NuMA, and Dynein to the Cell Cortex to Help Orient the Mitotic Spindle. *Mol. Cel Biol* 30 (14), 3519–3530. doi:10.1128/mcb.00394-10
- Wyatt, T. P. J., Harris, A. R., Lam, M., Cheng, Q., Bellis, J., Dimitracopoulos, A., et al. (2015). Emergence of Homeostatic Epithelial Packing and Stress Dissipation through Divisions Oriented along the Long Cell axis. *Proc. Natl. Acad. Sci. USA* 112 (18), 5726–5731. doi:10.1073/pnas.1420585112
- Yao, R., Oyanagi, J., Natsume, Y., Kusama, D., Kato, Y., Nagayama, S., et al. (2016). Suppression of Intestinal Tumors by Targeting the Mitotic Spindle of Intestinal Stem Cells. *Oncogene* 35 (47), 6109–6119. doi:10.1038/ncr.2016.148
- Young, M. A., May, S., Damo, A., Yoon, Y. S., Hur, M.-W., Swat, W., et al. (2019). Epigenetic Regulation of Dlg1, via Kaiso, Alters Mitotic Spindle Polarity and Promotes Intestinal Tumorigenesis. *Mol. Cancer Res.* 17 (3), 686–696. doi:10.1158/1541-7786.mcr-18-0280
- Zegers, M. M. P., O'Brien, L. E., Yu, W., Datta, A., and Mostov, K. E. (2003). Epithelial Polarity and Tubulogenesis *In Vitro*. *Trends Cel Biol.* 13 (4), 169–176. doi:10.1016/s0962-8924(03)00036-9
- Zheng, Z., Zhu, H., Wan, Q., Liu, J., Xiao, Z., Siderovski, D. P., et al. (2010). LGN Regulates Mitotic Spindle Orientation during Epithelial Morphogenesis. *Fac. Opinions* 189 (2), 275–288. doi:10.1083/jcb.200910021
- Zhu, J., Wen, W., Zheng, Z., Shang, Y., Wei, Z., Xiao, Z., et al. (2011). LGN/mInsc and LGN/NuMA Complex Structures Suggest Distinct Functions in Asymmetric Cell Division for the Par3/mInsc/LGN and Gai/LGN/NuMA Pathways. *Mol. Cel* 43 (3), 418–431. doi:10.1016/j.molcel.2011.07.011
- Zhu, M., Settele, F., Kotak, S., Sanchez-Pulido, L., Ehret, L., Ponting, C. P., et al. (2013). MISF Is a Novel Plk1 Substrate Required for Proper Spindle Orientation and Mitotic Progression. *J. Cel Biol.* 200 (6), 773–787. doi:10.1083/jcb.201207050

**Conflict of Interest:** The authors declare that the research was conducted in the absence of any commercial or financial relationships that could be construed as a potential conflict of interest.

**Publisher's Note:** All claims expressed in this article are solely those of the authors and do not necessarily represent those of their affiliated organizations, or those of the publisher, the editors and the reviewers. Any product that may be evaluated in this article, or claim that may be made by its manufacturer, is not guaranteed or endorsed by the publisher.

Copyright © 2022 Donà, Eli and Mapelli. This is an open-access article distributed under the terms of the Creative Commons Attribution License (CC BY). The use, distribution or reproduction in other forums is permitted, provided the original author(s) and the copyright owner(s) are credited and that the original publication in this journal is cited, in accordance with accepted academic practice. No use, distribution or reproduction is permitted which does not comply with these terms.





# Emerging Cnidarian Models for the Study of Epithelial Polarity

Lindsay I. Rathbun, Coralee A. Everett and Dan T. Bergstralh\*

Department of Biology, University of Rochester, Rochester, NY, United States

## OPEN ACCESS

### Edited by:

Alexander Ludwig,  
Nanyang Technological University,  
Singapore

### Reviewed by:

Lucas Leclerc,  
UMR7009 Laboratoire de Biologie du  
Développement de Villefranche sur  
Mer, France  
Toshio Takahashi,  
Suntory Foundation for Life Sciences,  
Japan

### \*Correspondence:

Dan T. Bergstralh  
dan.bergstralh@rochester.edu

### Specialty section:

This article was submitted to  
Morphogenesis and Patterning,  
a section of the journal  
Frontiers in Cell and Developmental  
Biology

**Received:** 13 January 2022

**Accepted:** 01 March 2022

**Published:** 01 April 2022

### Citation:

Rathbun LI, Everett CA and  
Bergstralh DT (2022) Emerging  
Cnidarian Models for the Study of  
Epithelial Polarity.  
Front. Cell Dev. Biol. 10:854373.  
doi: 10.3389/fcell.2022.854373

Epithelial tissues are vital to the function of most organs, providing critical functions such as secretion, protection, and absorption. Cells within an epithelial layer must coordinate to create functionally distinct apical, lateral, and basal surfaces in order to maintain proper organ function and organism viability. This is accomplished through the careful targeting of polarity factors to their respective locations within the cell, as well as the strategic placement of post-mitotic cells within the epithelium during tissue morphogenesis. The process of establishing and maintaining epithelial tissue integrity is conserved across many species, as important polarity factors and spindle orientation mechanisms can be found in many phyla. However, most of the information gathered about these processes and players has been investigated in bilaterian organisms such as *C. elegans*, *Drosophila*, and vertebrate species. This review discusses the advances made in the field of epithelial polarity establishment from more basal organisms, and the advantages to utilizing these simpler models. An increasing number of cnidarian model organisms have been sequenced in recent years, such as *Hydra vulgaris* and *Nematostella vectensis*. It is now feasible to investigate how polarity is established and maintained in basal organisms to gain an understanding of the most basal requirements for epithelial tissue morphogenesis.

**Keywords:** cnidaria, epithelia, polarity, model organisms, apical-basal cell polarity

## INTRODUCTION

Cell polarity defines specific spatial and functional domains within a cell through the asymmetric positioning of cellular components such as proteins, organelles, and cytoskeletal components. Epithelia are polarized tissues that perform specialized functions, typically at the boundary between an organ and the external environment. Cell polarity establishment and maintenance is vital for these functions; directional processes such as secretion, nutrient uptake, and signaling require a defined apical and basal surface to occur successfully (Humbert et al., 2008; St Johnston and Ahringer 2010). The importance of epithelial polarity is also highlighted by the observation that its loss is a common feature of malignancy (Bergstralh and St Johnston 2012; Williams et al., 2017; Jung et al., 2019; Tennooren et al., 2019; Catterall, Lelarge, and McCaffrey 2020; Che et al., 2021; Tilston-Lunel et al., 2021).

For decades, studies of epithelialization and polarity establishment have focused largely on well-established bilaterian models, namely *C. elegans*, *Drosophila*, and mammalian systems. As with all biological model systems, however, each of these organisms comes with its own set of technical and genetic caveats. In this brief article we highlight the utility of cnidarian animals to study the process of epithelial polarity establishment and maintenance (Figure 1). We argue that these animals represent a promising yet under-utilized class of model organisms. Cnidaria and Bilateria are both phyla under

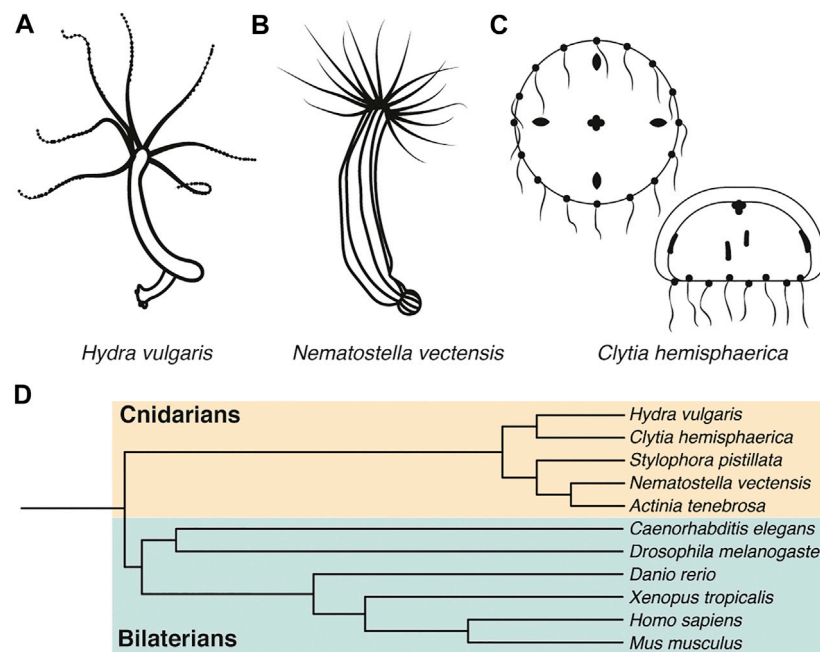


**FIGURE 1** | *H. vulgaris*, *N. vectensis*, and *C. hemisphaerica* are emerging model systems for polarity studies. **(A–C)** Representative drawings of *Hydra vulgaris*, *Nematostella vectensis*, and *Clytia hemisphaerica*. **(D)** Evolutionary tree depicting cnidarian and bilaterian model organisms.

the larger Eumetazoan subkingdom. Consistent with previous work, we show here that cnidarians share polarity establishment factors with bilaterians, within a simpler body plan. They also possess regenerative capabilities and a robust ability to reorganize upon dissociation, furthering their potential to push the field of polarity establishment and maintenance forward.

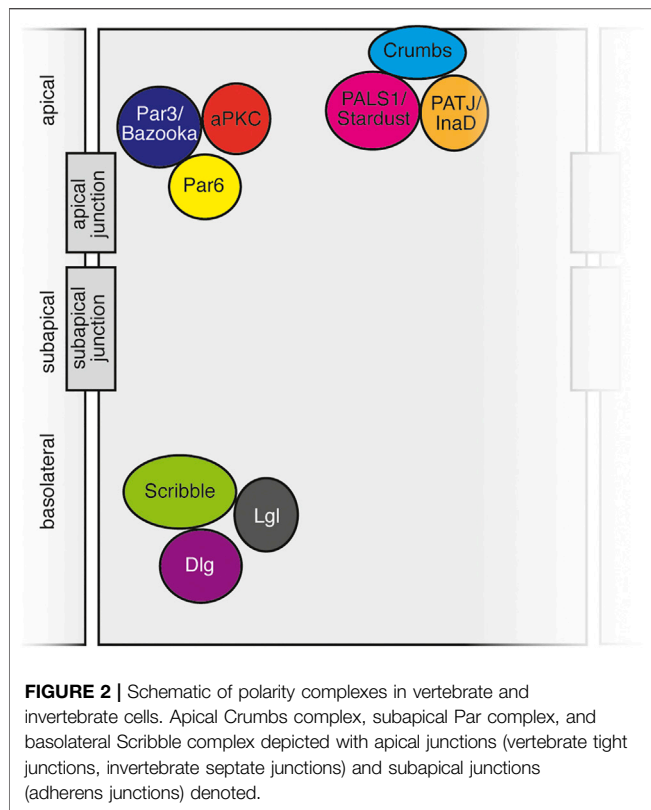
## Advantages to Phylogenetically Basal Model Organisms and Examples

There are some significant technical advantages to cnidarian models, an example of basal metazoans that diverged from bilaterians millions of years ago. Firstly, these simple organisms have robust regeneration capabilities that can be harnessed for use in studying polarity and cell sorting mechanisms (Seybold, Salvenmoser, and Hobmayer 2016; Cochet-Escartin et al., 2017; Skokan, Vale, and McKinley 2020). *Hydra vulgaris* and other cnidarians can completely regenerate from dissected tissue over the span of several days (Tucker and Adams 2014). Cnidarians are also able to reassemble from a completely dissociated cell suspension after mechanical or enzymatic dissociation (Tucker and Adams 2014; Cochet-Escartin et al., 2017). This provides an opportunity to follow the process of polarity establishment from a dissociated group of cells to a functional multicellular tissue in an *in vivo* animal context. This has previously been accomplished in polarized cell culture models such as MDCK cysts (Rodriguez-Boulant, Kreitzer, and Musch 2005; Martin-Belmonte et al., 2007; Mellman and Nelson 2008; Bryant et al., 2010) and three-dimensional organoid culture systems (Li et al., 2018; Serra et al., 2019; Lukonin et al.,

2020; Rosenbluth et al., 2020; Schuster et al., 2020; Hendriks et al., 2021), however these models would not develop into a fully functional organism like an animal model such as *Hydra vulgaris*.

Cnidarian model systems can also be tailored to investigate how polarity establishment mechanisms differ between tissues. In addition to total dissociation protocols, there are established techniques to isolate particular tissues for site-specific studies. For example, *Hydra* mesoglea has been isolated through a detergent extraction and freezing protocol in order to investigate the extracellular matrix proteins within (Tucker and Adams 2014). Since extracellular matrix proteins can influence polarity establishment (reviewed in (Manninen 2015)), this protocol could be used to determine how extracellular matrix influences polarity establishment in *Hydra*, and possibly modified to investigate additional structures within the *Hydra*. Additionally, primary cell cultures can be created from cnidarian tissues for more in-depth studies, such as those generated from the cnidarian *Anemonia viridis* for use in tissue-specific and pluripotency marker expression studies (Ventura et al., 2018), providing another manner in which to study polarity establishment in specific cnidarian tissues.

Lastly, cnidarians such as *Hydra vulgaris* (Chapman et al., 2010; Siebert et al., 2019), the anemone *Nematostella vectensis* (Putnam et al., 2007; Sebe-Pedros et al., 2018), and jellyfish *Clytia hemisphaerica* (Leclerc et al., 2019) have been genetically sequenced and/or transcriptionally characterized. This important factor increases the number of genetic tools available for use in these organisms such as CRISPR knockout technology (Ikmi et al., 2014; Lommel et al., 2017; Momose et al., 2018). Components of the Par, Crumbs, and Scribble polarity



complexes have been identified and characterized in cnidarian organisms (Figures 1–4), and their high level of conservation with bilaterian systems suggests that studies in cnidarian model systems could contribute to the field of polarity establishment.

Beyond technical advantages, choosing to utilize a cnidarian or other basal model organism provides a simplified setting to investigate research questions within the context of a whole, functional animal. For example, *Hydra vulgaris* features a body plan with two main tissue layers, the ectoderm and endoderm, separated by the mesoglea and interstitial cells. This provides a setting to study processes such as tissue morphogenesis (Hicklin and Wolpert 1973; Maroudas-Sacks et al., 2021), cell differentiation and lineage tracing (Plickert and Krohner 1988; Takashima, Gold, and Hartenstein 2013; Siebert et al., 2019), and asexual budding mechanisms (Clarkson and Wolpert 1967; Webster and Hamilton 1972) in a simplified, yet multi-tissue, context. Within the wide spectrum of biological research models to choose from, cnidarians and other basal animals represent an important niche between *ex vivo* cultured systems and more complicated *in vivo* bilaterian model organisms such as mouse, zebrafish, or *Drosophila*.

Cnidarians occupy an advantageous position within the evolutionary tree in a group historically referred to as Epitheliozoa. This subset of organisms is comprised of bilaterians, cnidarians, ctenophores, and placozoans, all of which are considered animals that have “true tissues” (Ax 1995). The exact definition of an epitheliozoan seems to be controversial in the literature. Some sources cite the presence of belt desmosomes as a requirement for this grouping (Ax 1995;

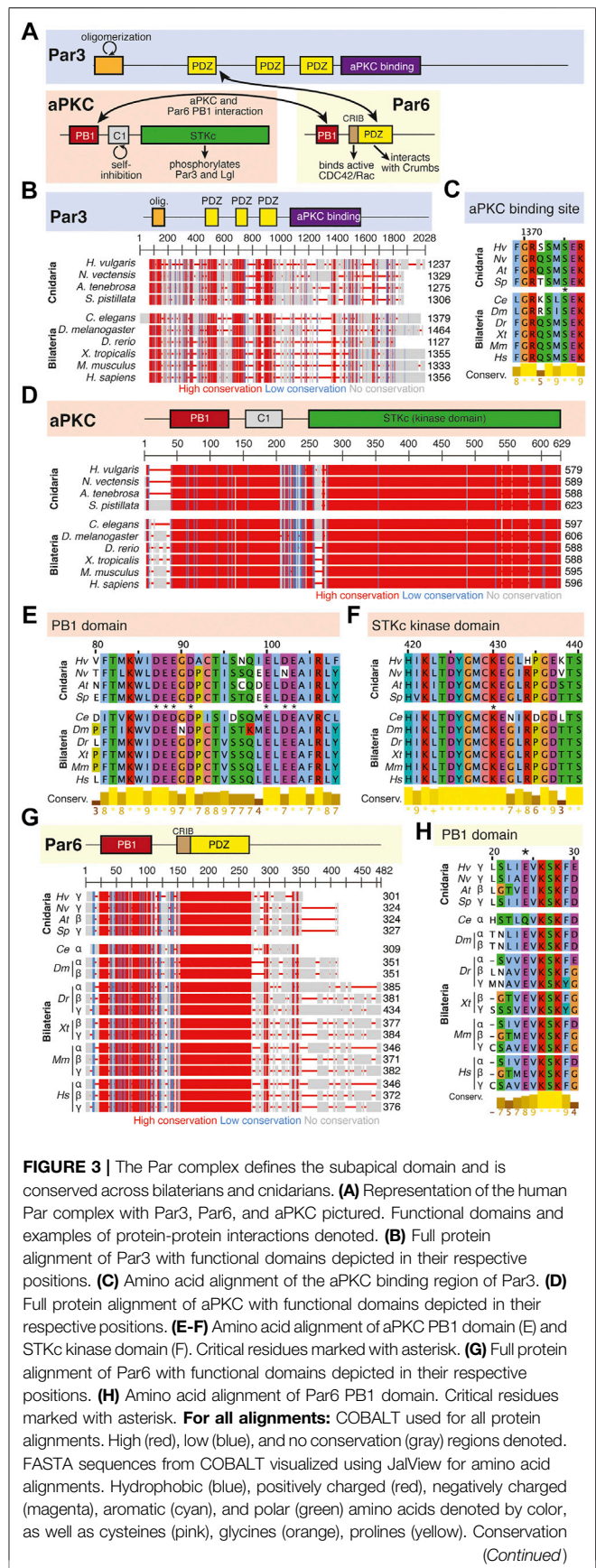




**FIGURE 3** | denoted on bottom of alignment. Cnidarians: *Hydra vulgaris* (Hv), *Nematostella vectensis* (Nv), *Actinia tenebrosa* (At), *Stylophora pistillata* (Sp). Bilaterians: *Caenorhabditis elegans* (Ce), *Drosophila melanogaster* (Dm), *Danio rerio* (Dr), *Xenopus tropicalis* (Xt), *Mus musculus* (Mm), *Homo sapiens* (Hs). Refer to **Tables 1–3** for information regarding sequences used in this figure.

Dohrmann and Worheide 2013), while others define “true tissues” as those that are connected by tight junctions (septate junctions in invertebrates) (Ganot et al., 2015). It is also debated whether they have the appropriate proteins or the ability to properly build these junctional complexes (Sperling, Peterson, and Pisani 2009). For example, sponges can be excluded since they do not have proper belt desmosomes (Leys and Riesgo 2012). Additionally, poriferans only have one tissue type within their body, raising the argument that they cannot have true epithelial tissues if they are not creating barriers between different tissue types. While the poriferan group is controversial when it comes to its relationship to epitheliozoans, cnidarians have been placed in this clade through a variety of genomic and phenotypic analyses (Ax 1995; Zrzavy et al., 1998; Sperling, Peterson, and Pisani 2009; Dohrmann and Worheide 2013; Ganot et al., 2015). Epithelia are therefore an ancient characteristic and important enough in biological evolution that a phylogenetic grouping has been created for organisms with epithelial tissues. Within this group, cnidarians are a more basal group of organisms, making them an option to study epithelial polarity establishment and maintenance in a simple epitheliozoan.

## Polarity and Epithelialization Studies in Cnidarian Models

Mechanisms controlling planar cell polarity are conserved in cnidarians. Briefly, the core planar cell polarity pathway involves the asymmetric distribution of several critical proteins to distinguish one side of the cell from the other along the larger-scale axis of the tissue and embryo. Some of these proteins include Frizzled, Strabismus/Van Gogh, Flamingo, Dishevelled, Prickle, and Diego (Devenport 2014). These evolutionarily conserved proteins are required for proper morphogenesis and development in several cnidarian species. For example, Strabismus, Frizzled, and Dishevelled are required for *Nematostella vectensis* invagination (Kumburegama, Wijesena, and Wikramanayake 2008; Kumburegama et al., 2011; Wijesena and Martindale 2018; Technau 2020; Wijesena et al., 2022), ciliated epithelium development in *Clytia hemispherica* (Momose and Houliston 2007; Momose, Derelle, and Houliston 2008; Momose, Kraus, and Houliston 2012; Lapebie et al., 2014), and tissue evagination dependent on Strabismus, Dishevelled, and Frizzled in *Hydra vulgaris* (Philipp et al., 2009). Additionally, the Fat-Dachsous polarity pathway utilizes an asymmetry in the localization of the protocadherins Fat and Dachsous to create cellular and tissue polarity (Devenport 2014), and these components have been similarly identified and studied in *Hydra* and *Nematostella* (Magie and Martindale 2008; Hulpiau and van Roy 2011;

Tucker and Adams 2014; Gul et al., 2017). While fewer studies concern the mechanisms driving apicobasal polarity in cnidarians, the conservation of PCP factors suggests that apicobasal polarity complexes and mechanisms are also likely to be conserved in cnidarians.

*Hydra vulgaris* *Hydra* are the oldest cnidarian model system used in research (Figure 1A), first studied by Abraham Trembley in 1744 (Trembley, 1744). The *Hydra* body column is largely comprised of two epithelial cell layers, the ectoderm and endoderm, with various types of interstitial cells positioned between. Additional cell types are interspersed between the epithelial cells, including gland cells in endoderm, nematocytes and nematoblasts in the ectoderm, and various neural cell types found in both layers (Technau and Steele 2011). The mesoglea is positioned between the two layers, composed of a thick extracellular matrix secreted by the endoderm and ectoderm (Epp, Smid, and Tardent 1986; Sarras et al., 1993). Basal myofibrils present in both cell layers run in orthogonal directions, with those in the endoderm running circumferentially around the body column, and those of the ectoderm running longitudinally along the body axis (Otto 1977). The endoderm is sometimes referred to as the gastrodermis due to the presence of gland cells that aid in digestion. *Hydra* is even referred to as a “living gut” due to their simple digestive system that spans the body column, and therefore much of the *Hydra* body plan in general (Vogg, Galliot, and Tsiairis 2019). *Hydra* feature a robust asexual reproduction process called budding, which has been used to study developmental programming and head determination. Epithelialization is an important process in both budding and regeneration, which is one of the main reasons that *Hydra* is a promising model for the study of polarity establishment and cell sorting (Seybold, Salvenmoser, and Hobmayer 2016).

One of the main advantages of the *Hydra* model system is their ability to reassemble after dissociation and subsequent reaggregation. This reaggregation can occur with minimal cell numbers, as only approximately 5–15 cells are necessary to create a head organizer within the population, allowing for a full *Hydra* to grow out of the small cell cluster (Technau et al., 2000). The patterning mechanism that defines the head, foot, and tentacle regions of the *Hydra* have been modelled using simulations such as the Meinhardt reaction-diffusion model, where these regions positioned with respect to one another by gradients of inhibitory or activating signals that determine the *Hydra* body axis (MacWilliams 1982; Meinhardt 1993).

*Hydra* reaggregation experiments have been used to understand how cells sort within a mixed population. Such studies suggest that factors such as the capacity for epithelialization (Skokan, Vale, and McKinley 2020), cell surface tension (Cochet-Escartin et al., 2017), interfacial tension and cell-cell adhesiveness (Technau and Holstein 1992) dictate how cells will sort into layers within an aggregate. Ectodermal engulfment of the endoderm in *Hydra* is compared to the morphogenetic process of epiboly in other organisms, where epithelial tissue undergoes a spreading process in the early development of vertebrates such as fish and amphibians (Piccolo 2013). Similarly, the *Hydra* ectodermal



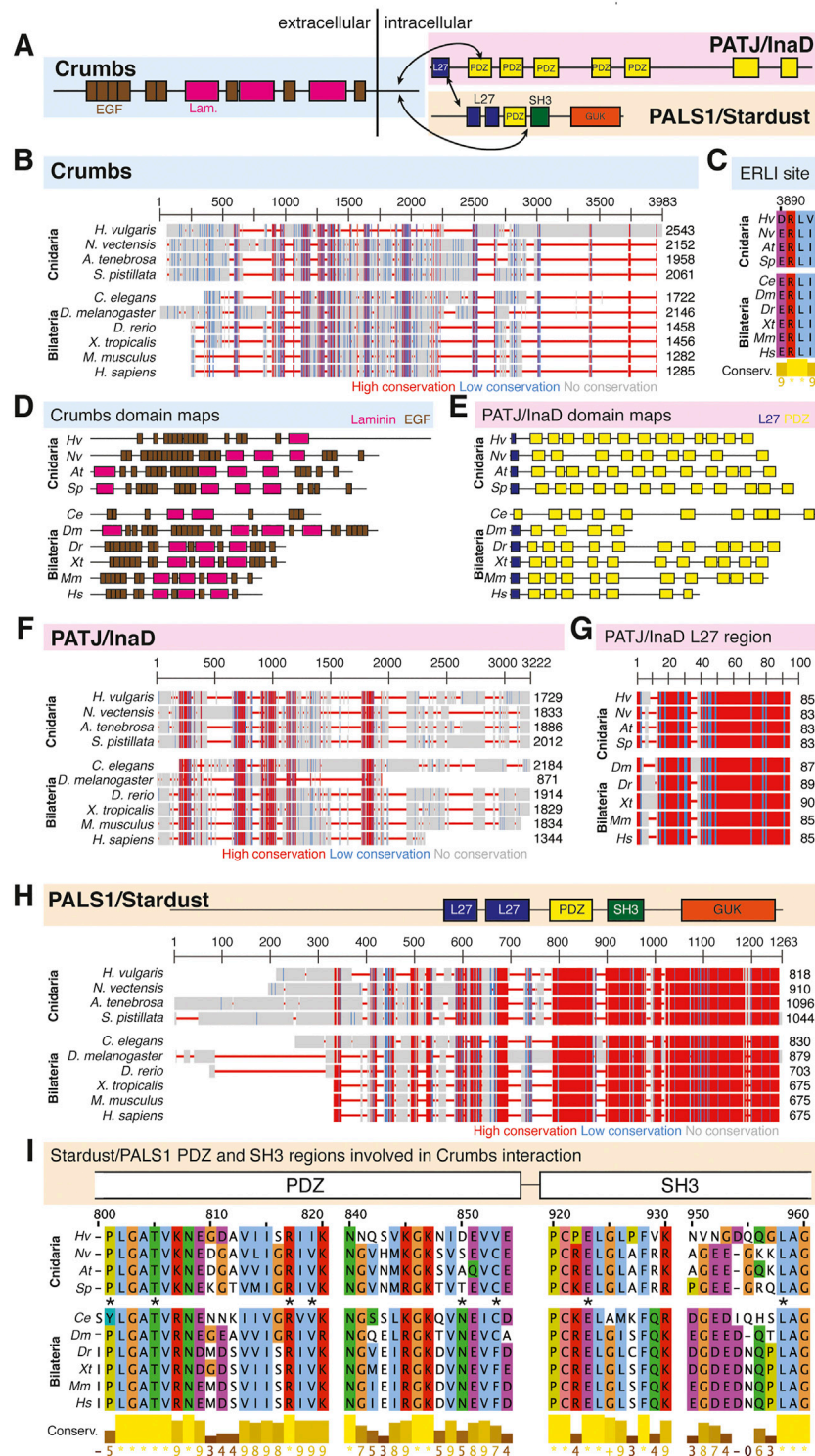


**FIGURE 4 |** The Crumbs complex defines the apical domain and is conserved across bilaterians and cnidarians. **(A)** Representation of the human Crumbs complex with Crumbs, PALS1/Stardust, PATJ/InaD pictured. Functional domains and examples of protein-protein interactions denoted. **(B)** Full protein alignment of Crumbs. **(C)** Amino acid alignment of the ERLI motif at the Crumbs C-terminus. **(D-E)** Domains maps of Crumbs (D) and PATJ/InaD (E) depicting laminin (magenta, D), EGF (brown, D), L27 (navy, E), and PDZ (yellow, E) domain positions. Protein lengths drawn to scale. **(F)** Full protein alignment of PATJ/InaD. **(G)** Protein alignment of PATJ/InaD L27 domain magnified from (F). **(H)** Full protein alignment of PALS1/Stardust with functional domains depicted in their respective positions. **(I)** Amino acid alignment of regions within PALS1/Stardust PDZ and SH3 domains. Critical residues involved in binding Crumbs marked with asterisk. **For all alignments:** COBALT used for all (Continued)

**FIGURE 4 |** protein alignments. High (red), low (blue), and no conservation (gray) regions denoted. FASTA sequences from COBALT visualized using JalView for amino acid alignments. Hydrophobic (blue), positively charged (red), negatively charged (magenta), aromatic (cyan), and polar (green) amino acids denoted by color, as well as cysteines (pink), glycines (orange), prolines (yellow). Conservation denoted on bottom of alignment. Cnidarians: *Hydra vulgaris* (Hv), *Nematostella vectensis* (Nv), *Actinia tenebrosa* (At), *Stylophora pistillata* (Sp). Bilaterians: *Caenorhabditis elegans* (Ce), *Drosophila melanogaster* (Dm), *Danio rerio* (Dr), *Xenopus tropicalis* (Xt), *Mus musculus* (Mm), *Homo sapiens* (Hs). Refer to **Tables 4–6** for information regarding sequences used in this figure.

cells engulfed the endodermal cell cluster when they came into contact, reforming the bilayer epithelium that is typically found in *Hydra* (Kishimoto, Murate, and Sugiyama 1996). As shown in these examples, the ability to completely dissociate *Hydra* tissues provides a setting to study the physical and biochemical characteristics of these cells to determine how they will behave when combined in a tissue with other cell populations, and how that multicellular tissue behaves as a whole during development.

Epithelialization as it relates to cell-cell adhesion establishment has also been extensively studied using *Hydra* reaggregation experiments. The process of cell-cell adhesion reestablishment was documented through electron microscopy to determine the order in which adhesion complexes are created. In this context, the apical-basal axis of developing epithelial cells elongates, followed by septate junction, gap junction, mesoglea, and hemidesmosome-like junction development. Interestingly, the process of planar cell polarity establishment begins before apical-basal polarity establishment has completed (Seybold, Salvenmoser, and Hobmayer 2016). Apicobasal polarity establishment both influences and is influenced by the setup of cell-cell adhesions, and these molecular players have been identified and studied in *Hydra* (Buzgariu et al., 2015).

***Nematostella vectensis*** The sea anemone *Nematostella vectensis* is one of the more commonly utilized cnidarian model systems outside of hydroids (**Figure 1B**). *Nematostella* was the first cnidarian to be genetically sequenced and while it has a relatively small genome, there are remarkable similarities to the genomes of humans and other bilaterian vertebrates (Putnam et al., 2007). For example, almost half of 27,000 predicted protein coding transcripts have clear orthologs to protostomes, deuterostomes, or both, and the number of exons and splice sites are nearly identical to humans (Tucker and Adams 2014). Interestingly, a comprehensive single-cell analysis of whole *Nematostella* animals found that many genetic similarities are shared between cnidarians and vertebrate bilaterians that are not present in invertebrate bilaterians, which include common model systems such as *C. elegans* and *Drosophila* (Putnam et al., 2007; Sebe-Pedros et al., 2018). For example, DNA methylation is absent in both *Drosophila* and *C. elegans* but occurs in *Nematostella* and other invertebrate organisms (Feng et al., 2010; Zemach et al., 2010; Zemach and Zilberman 2010; Schwaiger et al., 2014).

Synchronous cell divisions increase the cell mass of the embryo during early *Nematostella* development. The localization of Par3/Bazooka and Par6 oscillates in time with these cell divisions, moving to cell surfaces and cell-cell interfaces between divisions and away from this location during divisions (Ragkousi et al., 2017; Doerr and Ragkousi 2019). Par6 localizes to the apical cortex during interphase, and Par3/Bazooka can be found at subapical cell-cell contacts during this time. However,

consistent with previous work in *Drosophila* (Bergstrahl, Lovegrove, and St Johnston 2013), neither protein is detected at these sites during mitosis (Ragkousi et al., 2017; Doerr and Ragkousi 2019). This points to a mechanism that can quickly dismantle and reestablish epithelial polarity between cell divisions to preserve epithelial integrity during tissue growth. Interestingly, components of the Par system are not present in the endomesodermal epithelial tissue during gastrulation in *Nematostella*, despite being present in blastula cells earlier in development (Salinas-Saavedra et al., 2015; Salinas-Saavedra, Rock, and Martindale 2018; Salinas-Saavedra and Martindale 2020). This coincides with the absence of adherens junctions in this same tissue, suggesting different mechanisms of cell adhesion in these adjacent tissues (Salinas-Saavedra, Rock, and Martindale 2018). This loss of both cell polarity and cell-cell adhesions points to EMT occurring in this specific population of cells during this stage of development (Whiteman et al., 2008; Lim and Thiery 2012). Furthermore, apical polarity proteins such as Par1, Par3/Bazooka, Par6, aPKC, and Lgl only become asymmetrically distributed to their respective membrane domains later on in development, whereas they are localized along the cytoplasm and microtubule cytoskeleton during early developmental stages (Salinas-Saavedra et al., 2015).

Additional studies have determined the role of cadherins during *Nematostella* tissue morphogenesis. The cadherin-catenin complex is conserved in *Nematostella* and is required at the adherens junctions for proper embryo development and later tissue morphogenesis (Clarke et al., 2016; Nathaniel Clarke, Lowe, and James Nelson 2019). For example, Cadherin1 and Cadherin3 are expressed at different times during development, marking the transition from blastoderm to distinct germ layer formation. Disruption of this cadherin expression pattern results in a loss of tissue integrity and improper embryogenesis (Pukhlyakova et al., 2019).

***Clytia hemisphaerica*** The jellyfish *Clytia hemisphaerica* (**Figure 1C**) is an increasingly popular cnidarian model for the study of tissue development, wound healing, and regeneration (Kamran et al., 2017; Malamy and Shribak 2018; Kraus, Chevalier, and Houliston 2020; Sinigaglia et al., 2020). Its genome has been recently sequenced, and previous studies have also characterized the *Clytia* transcriptome through single cell RNA-sequencing (Leclerc et al., 2019; Chari et al., 2021). *Clytia* are frequently used to study wound healing, a component of which is epithelialization. The epithelial layer covering the surface of *Clytia medusa* is composed of a flat, squamous monolayer, allowing for imaging with DIC (differential interference contrast) microscopy (Malamy and Shribak 2018). As a result, the migration of epithelial cells during development, wound healing, and regeneration has been carefully analyzed to determine the physical steps and chemical mechanisms involved

(Malamy and Shribak 2018; Kraus, Chevalier, and Houliston 2020; Sinigaglia et al., 2020). These instances of epithelial-to-mesenchymal transitions, as well as the dedifferentiation events that occur in other jellyfish species (Lin, Grigoriev, and Spencer 2000; Estephane and Ancil 2010), make *Clytia* a promising model system for use in the study of both the establishment and breakdown of apical cell polarity. An additional advantage to this system is that *Clytia* components can be cultured outside the body for additional technical assays. For example, the female gonads of *Clytia* have been cultured to determine the mRNA gradients required to set up the body axes of the developing animal (Amiel and Houliston 2009).

Studies using *Clytia* have investigated the intersection between apicobasal polarity establishment and body axis establishment. Rapid synchronous cell divisions during early development increase embryonic cell mass prior to tissue layer specification. After the midblastula stage, cell divisions become asynchronous as cells begin to polarize and adopt a more columnar shape with nuclei that begin to localize towards the apical surface. At this point, ingression and gastrulation begin and the ectoderm and endoderm start to take form. This occurs through a population of cells called bottle cells that undergo EMT (epithelial to mesenchymal transition), change their shape to detach from the epithelial layer into the blastocoel, and adopt a mesenchymal morphology. These bottle cells do not undergo EMT and inward migration at the same time, allowing for many cells at varying stages of this process to be observed and characterized simultaneously. After 24 h post-ingression, these cells have reorganized to create the endodermal epithelial layer inside the developing embryo (Kraus, Chevalier, and Houliston 2020). This creates an opportunity to effectively study the process of polarity establishment in the early *Clytia* embryo, as well as its reverse process in EMT later during gastrulation.

## Apicobasal Polarity Establishment and Maintenance

While the exact mechanism of polarity establishment on a molecular level is not completely understood, there are a few important steps that are consistent across species. Firstly, three cortical polarity complexes (Par, Crumbs, and Scribble) interact to eventually localize properly to their respective domains (Figure 2). This triggers downstream pathways to continue setting up the necessary molecular components at each cellular surface. Secondly, cell-cell adhesions are established to attach cells to one another and provide tissue structural integrity, as well as an avenue for communication and materials transport between cells. This includes tight junctions (known as septate junctions in invertebrates), adherens junctions, and desmosomal junctions. The organization of polarity complexes and creation of cell-cell junctions are interconnected processes, with each process influencing and being influenced by the other (Rodriguez-Boulán and Macara 2014). While this review focuses mainly on the role of the Crumbs, Par, and Scribble complexes, a comprehensive review of cell-cell adhesion molecules has been published by Tepass et al. (2001).

Cell polarity in epithelia is driven by mutual antagonism between cortical factors. Work across multiple systems has demonstrated the

importance of at least three conserved protein complexes: the Par (Par6, aPKC, Par3/Bazooka) and Crumbs (Crumbs, Stardust, PATJ) complexes that are found at the apical and subapical surface, respectively, and the Scribble module (Discs Large, Lethal Giant Larvae, Scribble) that is sequestered to the basolateral membrane (Tepass, Theres, and Knust 1990; Knust, Tepass, and Wodarz 1993; Etemad-Moghadam, Guo, and Kemphues 1995; Tabuse et al., 1998; Bilder, Li, and Perrimon 2000; Bilder and Perrimon 2000). While the exact relationships between individual complex members continue to be elucidated, an emerging theme is that polarity is maintained by an exceedingly complex network of mutual antagonism. This also includes proteins outside the canonical Par, Crumbs, and Scribble complexes, such as Yurt (Laprise et al., 2006; Laprise et al., 2009) and Par1 (Benton and St Johnston 2003).

The Par complex includes Par6, Par3/Bazooka, and aPKC (atypical protein kinase C, Figure 3). The spatial relationship between Par proteins is conserved throughout animals, but interactions between the components are complex and historically have been difficult to parse out. In *Drosophila*, Par3/Bazooka, Par6, and aPKC localize apically (Kuchinke, Grawe, and Knust 1998; Wodarz et al., 2000; Petronczki and Knoblich 2001; Morais-de-Sa, Mirouse, and St Johnston 2010). The size of the apical domain is regulated through a negative feedback mechanism between Crumbs and Yurt, a basolateral protein that is recruited to apical membranes towards the end of epithelial development (Laprise et al., 2006; Laprise et al., 2009).

The Crumbs complex has four known components, Crumbs, Stardust/PALS1 (protein associated with Lin7 1), and PATJ/InaD (PALS1-associated tight junction protein/inactivation no afterpotential D, Figure 4) (Bachmann et al., 2001; Bachmann et al. 2004; Bachmann et al. 2008). Crumbs is partially responsible for the establishment of the apical domain in epithelial cells (Wodarz et al., 1995), and all components of the Crumbs complex are thought to be required for tight junction formation in mammals (Tan et al., 2020).

Scribble module factors localize to the basolateral membrane (Figure 5) (Bilder and Perrimon 2000; St Johnston and Ahringer 2010). In the *Drosophila* follicular epithelium, Discs Large (Dlg) localizes Scribble to the cortex via the Dlg SH3 domain. Lethal Giant Larvae (Lgl) is a known inhibitor of Par complex component aPKC, and this inhibition can occur here through the interaction of Lgl with Dlg and Scribble. This mechanism then confines the Scribble complex components to the basolateral domain, and aPKC along with other Par complex components to the apical domain above (Khouri and Bilder 2020; Ventura et al., 2020). Lgl is involved in mutual antagonism with aPKC, which phosphorylates Lgl to exclude it from the apical cortex. Conversely, Lgl inhibits aPKC from the lateral domain (Lee, Robinson, and Doe 2006; Atwood and Prehoda 2009; Ventura et al., 2020).

Cell-cell adhesion molecules also play an important role in polarity establishment and maintenance in cooperation with the three polarity complexes mentioned above. For example, adherens junctions can drive apical polarity establishment (Nejsum and Nelson 2007; Desai, Harmon, and Green 2009) in cells, but cell polarity can also govern adherens junction formation in other settings (Qin et al., 2005). While this complicated relationship is still being



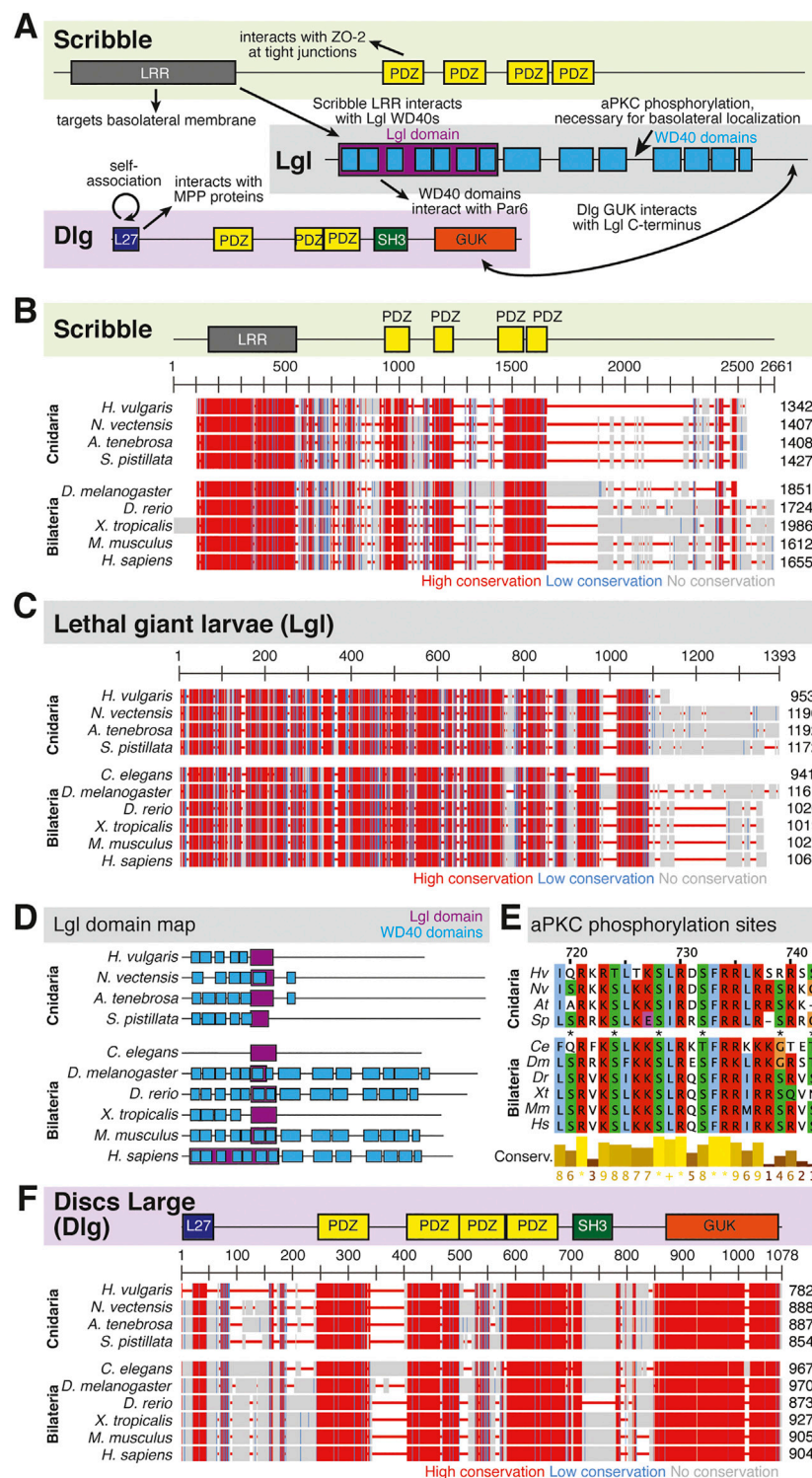


**FIGURE 5 |** The Scribble complex defines the basolateral domain and is conserved across bilaterians and cnidarians. **(A)** Representation of the human Scribble complex with Scribble, Discs Large (Dlg), and Lethal Giant Larvae (Lgl) pictured. Functional domains and examples of protein-protein interactions denoted. **(B,C)** Full protein alignments of Scribble (B) and Lethal Giant Larvae (Lgl, C). Scribble functional domains depicted in their respective positions within alignment. **(D)** Lgl domains maps depicting WD40 (cyan) and Lgl (violet) positions. Protein lengths drawn to scale. **(E)** Amino acid alignment of Lgl region phosphorylated by aPKC. Critical residues depicted with asterisks. **(F)** Full protein alignment of Discs Large (Dlg). functional domains depicted in their respective positions within alignment. **For all alignments:** COBALT used for all protein alignments. High (red), low (blue), and no conservation (gray) regions denoted. FASTA sequences from COBALT visualized (Continued)



**FIGURE 5 |** using JalView for amino acid alignments. Hydrophobic (blue), positively charged (red), negatively charged (magenta), aromatic (cyan), and polar (green) amino acids denoted by color, as well as cysteines (pink), glycines (orange), prolines (yellow). Conservation denoted on bottom of alignment. Cnidarians: *Hydra vulgaris* (Hv), *Nematostella vectensis* (Nv), *Actinia tenebrosa* (At), *Stylophora pistillata* (Sp). Bilaterians: *Caenorhabditis elegans* (Ce), *Drosophila melanogaster* (Dm), *Danio rerio* (Dr), *Xenopus tropicalis* (Xt), *Mus musculus* (Mm), *Homo sapiens* (Hs). Refer to **Tables 7–9** for information regarding sequences used in this figure.

**TABLE 1 |** aPKC.

Taxa	Organism	NCBI ref seq ID	name
Cnidaria	<i>Hydra vulgaris</i>	XP_012559790.1	Predicted: protein kinase C iota type-like
	<i>Nematostella vectensis</i>	XP_032242981.1	protein kinase C iota type
	<i>Actinia tenebrosa</i>	XP_031568621.1	protein kinase C iota type-like
	<i>Stylophora pistillata</i>	XP_022789559.1	protein kinase C iota type-like isoform X3
Bilateria	<i>Caenorhabditis elegans</i>	NP_495011.1	Protein kinase C-like 3
	<i>Drosophila melanogaster</i>	NP_001036541.1	atypical protein kinase C, isoform C
	<i>Danio rerio</i>	NP_571930.2	protein kinase C iota type
	<i>Xenopus tropicalis</i>	NP_001012707.1	protein kinase C iota type
	<i>Mus musculus</i>	NP_032883.2	protein kinase C iota type
	<i>Homo sapiens</i>	NP_002731.4	protein kinase C iota type

investigated, it is clear that both cell-cell adhesion and cell polarity establishment are interconnected processes during epithelial tissue morphogenesis and development (Coopman and Djiane 2016).

Most information in the field of polarity establishment and maintenance have come from studies in complex animal systems like *Drosophila* and *C. elegans*, or in cultured systems such as MDCK cells (Etemad-Moghadam, Guo, and Kempfues 1995; Wodarz et al., 1995; Kuchinke, Grawe, and Knust 1998; Tabuse et al., 1998; Wodarz et al., 2000; Petronczki and Knoblich 2001; Martin-Belmonte et al., 2007; Bryant et al., 2010; Morais-de-Sa, Mirouse, and St Johnston 2010; Bergstrahl, Lovegrove, and St Johnston 2013; Khoury and Bilder 2020; Ventura et al., 2020). While these studies have contributed a great amount of information to our understanding of epithelial polarization, the addition of more diverse model systems to this body of work would continue to push this field forward. Therefore, it is advantageous to consider cnidarian models and others outside the bilaterian group for future studies.

## Identification and Function of Polarity Regulators in Cnidarians

To demonstrate the utility of cnidarians as a model system for the study of polarity, we and others have undertaken phylogenetic analysis to test whether polarity regulators are conserved. Components of the Par, Crumbs, and Scribble complex have been identified in many organisms outside the bilaterian clade, including several cnidarian species such as *Hydra vulgaris* and *Nematostella vectensis* (Ragkousi et al., 2017; Doerr and Ragkousi 2019; Schiller and Bergstrahl 2021). Several important functional domains within these three polarity complexes are conserved between bilaterian and cnidarian organisms, making cnidarian organisms promising models for the study of polarity establishment and maintenance.

Within the Par Complex, aPKC, Par6, and Par3/Bazooka are highly conserved across several bilaterian and cnidarian species (**Figure 3**). Par3/Bazooka features a specific serine residue within the aPKC binding region that is the site of aPKC phosphorylation, which is vital for the function of the whole Par complex (Soriano et al., 2016; Nagai-Tamai et al., 2002). Although the rest of the protein alignment denotes increased variability, this specific serine residue is present in all organisms tested (**Figure 3B, C**, S1375). High levels of conservation were found across the alignment of aPKC (**Figure 3D**). Within aPKC, several specific residues are conserved that are required for the function of the PB1 domain, which interacts with Par6 (**Figure 3E**). Additionally, a specific lysine residue is required for the kinase function of the STKc (serine/threonine protein kinase catalytic) domain (Li et al., 1995). In addition to high levels of conservation across the whole domain (**Figure 3D**), this specific invariable lysine residue is conserved across the ten organisms investigated (**Figure 3F**). Par6 is also highly conserved across both the ten species investigated as well as multiple Par6 isoforms (**Figure 3G**), including the PB1 region required for interaction with aPKC (**Figure 3H**). This suggests that the molecular mechanisms driving Par complex function during polarity establishment are conserved across bilaterian and cnidarian organisms.

Overall, components of the Crumbs complex appear to be conserved between the bilaterian and cnidarian species investigated (**Figure 4A**). Although a protein alignment of Crumbs seems to suggest a low level of sequence conservation (**Figure 4B**), further examination revealed that the vital EGF and laminin G-like domains are present in all ten species, but in different locations and numbers (**Figure 4D**). These extracellular domains facilitate protein-protein interactions within the Crumbs complex (Tepass, Theres, and Knust 1990; Bulgakova and Knust 2009; Thompson, Pichaud, and Roper 2013; Rothberg

**TABLE 2 |** Par3.

Taxa	Organism	NCBI ref seq ID	Name
Cnidaria	<i>Hydra vulgaris</i>	XP_012559005.1	PREDICTED: uncharacterized protein LOC100212317 isoform X2
	<i>Nematostella vectensis</i>	XP_001637950.2	partitioning defective 3 homolog isoform X2
	<i>Actinia tenebrosa</i>	XP_031549913.1	partitioning defective 3 homolog isoform X1
	<i>Stylophora pistillata</i>	XP_022805323.1	partitioning defective 3 homolog isoform X1
Bilateria	<i>Caenorhabditis elegans</i>	NP_001022607.1	Partitioning defective protein 3
	<i>Drosophila melanogaster</i>	NP_001334669.1	bazooka, isoform A
	<i>Danio rerio</i>	NP_991298.1	par-3 family cell polarity regulator alpha, b
	<i>Xenopus tropicalis</i>	XP_004915521.1	partitioning defective 3 homolog isoform X2
	<i>Mus musculus</i>	NP_296369.2	partitioning defective 3 homolog isoform 3
	<i>Homo sapiens</i>	NP_062565.2	partitioning defective 3 homolog isoform 1

**TABLE 3 |** Par6.

Taxa	Organism	NCBI ref seq ID	Name
Cnidaria	<i>Hydra vulgaris</i>		Predicted: partitioning defective 6 homolog gamma-like
	<i>Nematostella vectensis</i>	XP_032231060.1	partitioning defective 6 homolog gamma
	<i>Actinia tenebrosa</i>	XP_031569341.1	partitioning defective 6 homolog beta-like
	<i>Stylophora pistillata</i>	XP_022786713.1	partitioning defective 6 homolog gamma-like
Bilateria	<i>Caenorhabditis elegans</i>	NP_001040687.1	Partitioning defective protein 6
	<i>Drosophila melanogaster</i>	NP_573238.1	par-6, isoform A
		>NP_728094.1	par-6, isoform B
	<i>Danio rerio</i>	NP_001093521.2	partitioning defective 6 homolog alpha
		NP_001096145.1	partitioning defective 6 homolog beta
		NP_997728.1	par-6 family cell polarity regulator gamma b
	<i>Xenopus tropicalis</i>	NP_001122111.1	partitioning defective 6 homolog beta
		NP_001017338.1	partitioning defective 6 homolog gamma
	<i>Mus musculus</i>	NP_062669.2	partitioning defective 6 homolog alpha isoform 1
		NP_067384.2	partitioning defective 6 homolog beta
		NP_444347.3	partitioning defective 6 homolog gamma
	<i>Homo sapiens</i>	NP_058644.1	partitioning defective 6 homolog alpha isoform 1
		NP_115910.1	partitioning defective 6 homolog beta
		NP_115899.1	partitioning defective 6 homolog gamma

**TABLE 4 |** Crumbs.

Taxa	Organism	NCBI ref seq ID	Name
Cnidaria	<i>Hydra vulgaris</i>	XP_012557050.1	Predicted: uncharacterized protein LOC100203132
	<i>Nematostella vectensis</i>	XP_032230278.1	protein crumbs isoform X2
	<i>Actinia tenebrosa</i>	XP_031551871.1	protein crumbs homolog 1-like
	<i>Stylophora pistillata</i>	XP_022801826.1	protein crumbs-like
Bilateria	<i>Caenorhabditis elegans</i>	NP_510822.1	CCD66913.1 <i>Drosophila</i> CRumBs homolog
	<i>Drosophila melanogaster</i>	NP_524480.2	crumbs, isoform A
	<i>Danio rerio</i>	NP_001038627.1	protein crumbs homolog 2b precursor
	<i>Xenopus tropicalis</i>	XP_002937280.2	protein crumbs homolog 2 isoform X1
	<i>Mus musculus</i>	NP_001157038.1	protein crumbs homolog 2 precursor
	<i>Homo sapiens</i>	NP_775960.4	protein crumbs homolog 2 precursor

et al., 1988; den Hollander et al., 1999; Sasaki et al., 1988; Omori and Malicki 2006). Additionally, the ERLI motif located at the C-terminus of the Crumbs protein is highly conserved across both cnidarians and bilaterians. This sequence allows for the interaction of Crumbs with the other components of the Crumbs complex, Stardust/PALS1 and PATJ/InaD. Similarly, PATJ/InaD features a highly conserved L27 domain, but the number of

subsequent PDZ domains differs from species to species (Figures 4E–G). Lastly, Stardust/PALS1 demonstrates high levels of protein conservation, especially in the region of the PDZ and SH3 domains that facilitate its interaction with Crumbs (Figures 4H, I). These results show that although there is variability between Crumbs isoforms in various species, the functional domains are largely conserved. Therefore, it is likely

**TABLE 5 |** PATJ/InaD.

Taxa	Organism	NCBI ref seq ID	Name
Cnidaria	<i>Hydra vulgaris</i>	XP_012558951.1	Predicted: multiple PDZ domain protein-like
	<i>Nematostella vectensis</i>	EDO33706.1	predicted protein
	<i>Actinia tenebrosa</i>	XP_031574464.1	multiple PDZ domain protein-like
	<i>Stylophora pistillata</i>	XP_022779809.1	multiple PDZ domain protein-like isoform X2
Bilateria	<i>Caenorhabditis elegans</i>	ABH03415.1	MPZ-1
	<i>Drosophila melanogaster</i>	NP_477342.1	patj, isoform C
	<i>Danio rerio</i>	XP_009294504.1	inaD-like protein isoform X1
	<i>Xenopus tropicalis</i>	XP_002931635.3	inaD-like protein isoform X1
	<i>Mus musculus</i>	NP_766284.2	inaD-like protein isoform 1
	<i>Homo sapiens</i>	XP_011538771.1	inaD-like protein isoform X12

**TABLE 6 |** Stardust/PALS1/MPP5.

Taxa	Organism	NCBI ref seq ID	Name
Cnidaria	<i>Hydra vulgaris</i>	XP_012557503.1	Predicted: MAGUK p55 subfamily member 5-like
	<i>Nematostella vectensis</i>	XP_032229010.1	MAGUK p55 subfamily member 5 isoform X1
	<i>Actinia tenebrosa</i>	XP_031565974.1	uncharacterized protein LOC116301110
	<i>Stylophora pistillata</i>	XP_022792787.1	MAGUK p55 subfamily member 5-like
Bilateria	<i>Caenorhabditis elegans</i>	NP_001355433.1	MAGUK family
	<i>Drosophila melanogaster</i>	NP_001245575.1	stardust, isoform K
	<i>Danio rerio</i>	XP_009291449.1	MAGUK p55 subfamily member 5-A isoform X1
	<i>Xenopus tropicalis</i>	XP_002937246.1	MAGUK p55 subfamily member 5
	<i>Mus musculus</i>	NP_062525.1	protein PALS1
	<i>Homo sapiens</i>	NP_071919.2	protein PALS1 isoform 1

**TABLE 7 |** Discs Large (Dlg).

Taxa	Organism	NCBI ref seq ID	Name
Cnidaria	<i>Hydra vulgaris</i>	XP_012556528.1	PREDICTED: disks large homolog 1-like
	<i>Nematostella vectensis</i>	XP_001638123.2	disks large homolog 1
	<i>Actinia tenebrosa</i>	XP_031552782.1	disks large homolog 1-like isoform X2
	<i>Stylophora pistillata</i>	XP_022791231.1	disks large homolog 1-like isoform X2
Bilateria	<i>Caenorhabditis elegans</i>	NP_001024431.1	Disks large homolog 1
	<i>Drosophila melanogaster</i>	NP_996406.1	discs large 1, isoform B
	<i>Danio rerio</i>	NP_955820.1	disks large homolog 1
	<i>Xenopus tropicalis</i>	NP_001039116.1	disks large homolog 1
	<i>Mus musculus</i>	NP_001239364.1	disks large homolog 1 isoform 4
	<i>Homo sapiens</i>	NP_001091894.1	disks large homolog 1 isoform 1

**TABLE 8 |** Lethal Giant Larvae (Lgl).

Taxa	Organism	NCBI ref seq ID	Name
Cnidaria	<i>Hydra vulgaris</i>	XP_012555599.1	PREDICTED: lethal (2) giant larvae protein homolog 1 isoform X1
	<i>Nematostella vectensis</i>	XP_032221124.1	lethal (2) giant larvae protein homolog 1 isoform X1
	<i>Actinia tenebrosa</i>	XP_031560162.1	lethal (2) giant larvae protein homolog 1-like isoform X1
	<i>Stylophora pistillata</i>	XP_022802656.1	lethal (2) giant larvae protein homolog 2-like
Bilateria	<i>Caenorhabditis elegans</i>	NP_508169.2	LLGL domain-containing protein
	<i>Drosophila melanogaster</i>	NP_001245801.1	lethal (2) giant larvae, isoform G
	<i>Danio rerio</i>	NP_997747.1	LLGL scribble cell polarity complex component
	<i>Xenopus tropicalis</i>	XP_012827183.1	LLGL scribble cell polarity complex component 2 isoform X1
	<i>Mus musculus</i>	NP_663413.2	LLGL scribble cell polarity complex component 2 isoform 1
	<i>Homo sapiens</i>	NP_004131.4	lethal (2) giant larvae protein homolog 1

**TABLE 9 |** Scribble.

Taxa	Organism	NCBI ref seq ID	Name
Cnidaria	<i>Hydra vulgaris</i>	XP_004209241.2	Predicted: protein scribble homolog isoform X1
	<i>Nematostella vectensis</i>	XP_032228868.1	protein scribble homolog isoform X1
	<i>Actinia tenebrosa</i>	XP_031556444.1	protein scribble homolog
	<i>Stylophora pistillata</i>	XP_022783798.1	protein scribble homolog isoform X1
Bilateria	<i>Caenorhabditis elegans</i>	CAB91651.1	LET-413 protein
	<i>Drosophila melanogaster</i>	NP_524754.2	scribble, isoform D
	<i>Danio rerio</i>	NP_001007176.1	protein scribble homolog
	<i>Xenopus tropicalis</i>	XP_031759452.1	protein scribble homolog isoform X1
	<i>Mus musculus</i>	NP_001297472.1	protein scribble homolog isoform 3
	<i>Homo sapiens</i>	NP_874365.3	protein scribble homolog isoform a

that Crumbs function in apical polarity establishment and maintenance is conserved as well.

Components of the Scribble complex are highly conserved across bilaterian and cnidarian organisms (Schiller and Bergstrahl 2021) (**Figure 5A**). Both Scribble and Dlg contain multiple PDZ domains with high levels of conservation. These PDZ domains are vital to protein-protein interactions that include Scribble and Dlg within the polarity establishment pathway and others (Kallay et al., 2006; Takizawa et al., 2006; How et al., 2019; Bilder 2003; Bilder, Li, and Perrimon 2000; Bilder, Schober, and Perrimon 2003; Sotelo et al., 2012; Matsumine et al., 1996; Makino et al., 1997; Subbaiah et al., 2012). Lgl displays varying positions of its LGL domain, as well as different numbers of WD40 domains between species (**Figures 5C,D**). Despite these differences, the aPKC phosphorylation site towards the middle of the protein is highly conserved (**Figure 5E**). Additionally, the domains of Dlg are highly conserved including the vital GUK domain, which facilitates interaction between Dlg and phosphorylated Pins/LGN/GPSM2 among other possible functions (Johnston et al., 2009; Johnston et al., 2011; Anderson et al., 2016; Schiller and Bergstrahl 2021) (**Figure 5F**). This suggests that both the polarity and spindle orientation mechanisms of Dlg are evolutionarily conserved, as well as the overall function of the Scribble complex.

## REFERENCES

- Amiel, A., and Houlston, E. (2009). Three Distinct RNA Localization Mechanisms Contribute to Oocyte Polarity Establishment in the Cnidarian *Clytia Hemisphaerica*. *Developmental Biol.* 327 (1), 191–203. doi:10.1016/j.ydbio.2008.12.007
- Anderson, D. P., Whitney, D. S., Hanson-Smith, V., Woznica, A., Campodonico-Burnett, W., Volkman, B. F., et al. (2016). Evolution of an Ancient Protein Function Involved in Organized Multicellularity in Animals. *Elife* 5, e10147. doi:10.7554/eLife.10147
- Atwood, S. X., and Prehoda, K. E. (2009). aPKC Phosphorylates Miranda to Polarize Fate Determinants during Neuroblast Asymmetric Cell Division. *Curr. Biol.* 19 (9), 723–729. doi:10.1016/j.cub.2009.03.056
- Ax, Peter. 1995. "Das System der Metazoa I. Ein Lehrbuch der phylogenetischen Systematik."
- Bachmann, A., Grawe, F., Johnson, K., and Knust, E. (2008). Drosophila Lin-7 Is a Component of the Crumbs Complex in Epithelia and Photoreceptor Cells and Prevents Light-Induced Retinal Degeneration. *Eur. J. Cell Biol.* 87 (3), 123–136. doi:10.1016/j.jecb.2007.11.002

## CONCLUSION

Despite the extensive number of epithelialization studies in the past several decades, the information obtained has come from a limited pool of model systems. While bilaterian systems have been incredibly useful in identifying the first polarity proteins and their respective pathways, the complexity of these organisms has mostly limited these studies to early embryogenesis. Alternatively, cultured settings have given a simplified model in which to test the role of these polarity factors during epithelialization, however these settings are not physiologically representative of what may occur in a whole, living organism. Therefore, it would be advantageous to look outside the bilaterian clade for candidate model systems in which to continue and supplement these existing studies. This review has highlighted the technical, genetic, and evolutionary evidence that supports the use of cnidarian model organisms in future studies of cell polarity establishment and maintenance.

## AUTHOR CONTRIBUTIONS

LR, CE: writing, editing, data collection and analysis, DB: editing.

- Bachmann, A., Schneider, M., Theilenberg, E., Grawe, F., and Knust, E. (2001). Drosophila Stardust Is a Partner of Crumbs in the Control of Epithelial Cell Polarity. *Nature* 414 (6864), 638–643. doi:10.1038/414638a
- Bachmann, A., Timmer, M., Sierralta, J., Pietrini, G., Gundelfinger, E. D., Knust, E., et al. (2004). Cell Type-specific Recruitment of Drosophila Lin-7 to Distinct MAGUK-Based Protein Complexes Defines Novel Roles for Sdt and Dlg-S97. *J. Cell Sci* 117 (Pt 10), 1899–1909. doi:10.1242/jcs.01029
- Benton, R., and Johnston, D. S. (2003). Drosophila PAR-1 and 14-3-3 Inhibit Bazooka/PAR-3 to Establish Complementary Cortical Domains in Polarized Cells. *Cell* 115 (6), 691–704. doi:10.1016/s0092-8674(03)00938-3
- Bergstrahl, D. T., Lovegrove, H. E., and St Johnston, D. (2013). Discs Large Links Spindle Orientation to Apical-Basal Polarity in Drosophila Epithelia. *Curr. Biol.* 23 (17), 1707–1712. doi:10.1016/j.cub.2013.07.017
- Bergstrahl, D. T., and St Johnston, D. (2012). Epithelial Cell Polarity: what Flies Can Teach Us about Cancer. *Essays Biochem.* 53, 129–140. doi:10.1042/bse0530129
- Bilder, D., Li, M., and Perrimon, N. (2000). Cooperative Regulation of Cell Polarity and Growth by Drosophila Tumor Suppressors. *Science* 289 (5476), 113–116. doi:10.1126/science.289.5476.113
- Bilder, D. (2003). PDZ Domain Polarity Complexes. *Curr. Biol.* 13 (17), R661–R662. doi:10.1016/s0960-9822(03)00599-2



- Bilder, D., and Perrimon, N. (2000). Localization of Apical Epithelial Determinants by the Basolateral PDZ Protein Scribble. *Nature* 403 (6770), 676–680. doi:10.1038/35001108
- Bilder, D., Schöber, M., and Perrimon, N. (2003). Integrated Activity of PDZ Protein Complexes Regulates Epithelial Polarity. *Nat. Cell Biol.* 5 (1), 53–58. doi:10.1038/ncb897
- Bryant, D. M., Datta, A., Rodríguez-Fraticelli, A. E., Peränen, J., Martín-Belmonte, F., and Mostov, K. E. (2010). A Molecular Network for De Novo Generation of the Apical Surface and Lumen. *Nat. Cell Biol.* 12 (11), 1035–1045. doi:10.1038/ncb2106
- Bulgakova, N. A., and Knust, E. (2009). The Crumbs Complex: from Epithelial-Cell Polarity to Retinal Degeneration. *J. Cell Sci.* 122 (Pt 15), 2587–2596. doi:10.1242/jcs.023648
- Buzgariu, W., Al Haddad, S., Tomczyk, S., Wenger, Y., and Galliot, B. (2015). Multi-functionality and Plasticity Characterize Epithelial Cells in Hydra. *Tissue Barriers* 3 (4), e1068908. doi:10.1080/21688370.2015.1068908
- Catterall, R., Lelarge, V., and McCaffrey, L. (2020). Genetic Alterations of Epithelial Polarity Genes Are Associated with Loss of Polarity in Invasive Breast Cancer. *Int. J. Cancer* 146 (6), 1578–1591. doi:10.1002/ijc.32691
- Chapman, J. A., Kirkness, E. F., Simakov, O., Hampson, S. E., Mitros, T., Weinmaier, T., et al. (2010). The Dynamic Genome of Hydra. *Nature* 464 (7288), 592–596. doi:10.1038/nature08830
- Chari, T., Weissbourd, B., Gehring, J., Ferraioli, A., Leclère, L., Herl, M., et al. (2021). Whole-animal Multiplexed Single-Cell RNA-Seq Reveals Transcriptional Shifts across Clytia Medusa Cell Types. *Sci. Adv.* 7 (48), eabh1683. doi:10.1126/sciadv.abh1683
- Che, J., Wang, J., Li, H., Zhen, H., Shang, K., Yang, Y., et al. (2021). Decreased Expression of Dlg5 Is Associated with a Poor Prognosis and Epithelial-Mesenchymal Transition in Squamous Cell Lung Cancer. *J. Thorac. Dis.* 13 (5), 3115–3125. doi:10.21037/jtd-21-752
- Clarke, D. N., Miller, P. W., Lowe, C. J., Weis, W. I., and Nelson, W. J. (2016). Characterization of the Cadherin-Catenin Complex of the Sea Anemone *Nematostella vectensis* and Implications for the Evolution of Metazoan Cell-Cell Adhesion. *Mol. Biol. Evol.* 33 (8), 2016–2029. doi:10.1093/molbev/msw084
- Clarkson, S. G., and Wolpert, L. (1967). Bud Morphogenesis in hydra. *Nature* 214 (5090), 780–783. doi:10.1038/214780a0
- Cochet-Escartin, O., Locke, T. T., Shi, W. H., Steele, R. E., and Collins, E.-M. S. (2017). Physical Mechanisms Driving Cell Sorting in Hydra. *Biophysical J.* 113 (12), 2827–2841. doi:10.1016/j.bpj.2017.10.045
- Coopman, P., and Djiane, A. (2016). Adherens Junction and E-Cadherin Complex Regulation by Epithelial Polarity. *Cell. Mol. Life Sci.* 73 (18), 3535–3553. doi:10.1007/s00018-016-2260-8
- den Hollander, A. I., ten Brink, J. B., de Kok, Y. J. M., van Soest, S., van den Born, L. I., van Driel, M. A., et al. (1999). Mutations in a Human Homologue of *Drosophila* Crumbs Cause Retinitis Pigmentosa (RP12). *Nat. Genet.* 23 (2), 217–221. doi:10.1038/13848
- Desai, B. V., Harmon, R. M., and Green, K. J. (2009). Desmosomes at a Glance. *J. Cell Sci.* 122 (Pt 24), 4401–4407. doi:10.1242/jcs.037457
- Devenport, D. (2014). The Cell Biology of Planar Cell Polarity. *J. Cell Biol.* 207 (2), 171–179. doi:10.1083/jcb.201408039
- Doerr, S., and Ragkousi, K. (2019). Cell Polarity Oscillations in Mitotic Epithelia. *Curr. Opin. Genet. Dev.* 57, 47–53. doi:10.1016/j.gde.2019.07.007
- Dohrmann, M., and Worheide, G. (2013). Novel Scenarios of Early Animal Evolution—Is it Time to Rewrite Textbooks? *Integr. Comp. Biol.* 53 (3), 503–511. doi:10.1093/icb/ict008
- Epp, L., Smid, I., and Tardent, P. (1986). Synthesis of the Mesoglea by Ectoderm and Endoderm in Reassembled hydra. *J. Morphol.* 189 (3), 271–279. doi:10.1002/jmor.1051890306
- Estephane, D., and Anttil, M. (2010). Retinoic Acid and Nitric Oxide Promote Cell Proliferation and Differentially Induce Neuronal Differentiation *In Vitro* in the Cnidarian *Renilla koellikeri*. *Dev. Neurobiol.* 70 (12), 842–852. doi:10.1002/dneu.20824
- Etemad-Moghadam, B., Guo, S., and Kempthues, K. J. (1995). Asymmetrically Distributed PAR-3 Protein Contributes to Cell Polarity and Spindle Alignment in Early *C. elegans* Embryos. *Cell* 83 (5), 743–752. doi:10.1016/0092-8674(95)90187-6
- Feng, S., Cokus, S. J., Zhang, X., Chen, P. Y., Bostick, M., Goll, M. G., et al. (2010). Conservation and Divergence of Methylation Patterning in Plants and Animals. *Proc. Natl. Acad. Sci. U S A.* 107 (19), 8689–8694. doi:10.1073/pnas.1002720107
- Ganot, P., Zoccola, D., Tambutte, E., Voolstra, C. R., Aranda, M., Allemand, D., et al. (2015). Structural Molecular Components of Septate Junctions in Cnidarians point to the Origin of Epithelial Junctions in Eukaryotes. *Mol. Biol. Evol.* 32 (1), 44–62. doi:10.1093/molbev/msu265
- Gul, I. S., Hulpiau, P., Saeys, Y., and van Roy, F. (2017). Evolution and Diversity of Cadherins and Catenins. *Exp. Cell Res.* 358 (1), 3–9. doi:10.1016/j.yexcr.2017.03.001
- Hendriks, D., Artegiani, B., Hu, H., Chuva de Sousa Lopes, S., and Clevers, H. (2021). Establishment of Human Fetal Hepatocyte Organoids and CRISPR-Cas9-Based Gene Knockin and Knockout in Organoid Cultures from Human Liver. *Nat. Protoc.* 16 (1), 182–217. doi:10.1038/s41596-020-00411-2
- Hicklin, J., and Wolpert, L. (1973). Positional Information and Pattern Regulation in hydra: the Effect of Gamma-Radiation. *J. Embryol. Exp. Morphol.* 30 (3), 741–752. doi:10.1242/dev.30.3.741
- How, J. Y., Caria, S., Humbert, P. O., and Kvasnakul, M. (2019). Crystal Structure of the Human Scribble PDZ1 Domain Bound to the PDZ-Binding Motif of APC. *FEBS Lett.* 593 (5), 533–542. doi:10.1002/1873-3468.13329
- Hulpiau, P., and van Roy, F. (2011). New Insights into the Evolution of Metazoan Cadherins. *Mol. Biol. Evol.* 28 (1), 647–657. doi:10.1093/molbev/msq233
- Humbert, P. O., Grzeschik, N. A., Brumby, A. M., Galea, R., Elsum, I., and Richardson, H. E. (2008). Control of Tumorigenesis by the Scribble/Dlg/Lgl Polarity Module. *Oncogene* 27 (55), 6888–6907. doi:10.1038/nc.2008.341
- Ikmi, A., McKinney, S. A., Delventhal, K. M., and Gibson, M. C. (2014). TALEN and CRISPR/Cas9-mediated Genome Editing in the Early-Branching Metazoan *Nematostella vectensis*. *Nat. Commun.* 5, 5486. doi:10.1038/ncomms6486
- Johnston, C. A., Hirono, K., Prehoda, K. E., and Doe, C. Q. (2009). Identification of an Aurora-A/Pins/LINKER/Dlg Spindle Orientation Pathway Using Induced Cell Polarity in S2 Cells. *Cell* 138 (6), 1150–1163. doi:10.1016/j.cell.2009.07.041
- Johnston, C. A., Whitney, D. S., Volkman, B. F., Doe, C. Q., and Prehoda, K. E. (2011). Conversion of the Enzyme Guanylate Kinase into a Mitotic-Spindle Orienting Protein by a Single Mutation that Inhibits GMP-Induced Closing. *Proc. Natl. Acad. Sci. U S A.* 108 (44), E973–E978. doi:10.1073/pnas.1104365108
- Jung, H. Y., Fattet, L., Tsai, J. H., Kajimoto, T., Chang, Q., Newton, A. C., et al. (2019). Apical-basal Polarity Inhibits Epithelial-Mesenchymal Transition and Tumour Metastasis by PAR-Complex-Mediated SNAIL Degradation. *Nat. Cell Biol.* 21 (3), 359–371. doi:10.1038/s41556-019-0291-8
- Kallay, L. M., McNickle, A., Brennwald, P. J., Hubbard, A. L., and Braiterman, L. T. (2006). Scribble Associates with Two Polarity Proteins, Lgl2 and Vangl2, via Distinct Molecular Domains. *J. Cell Biochem.* 99 (2), 647–664. doi:10.1002/jcb.20992
- Kamran, Z., Zellner, K., Kyriazis, H., Kraus, C. M., Reynier, J. B., and Malamy, J. E. (2017). *In Vivo* imaging of Epithelial Wound Healing in the Cnidarian *Clytia hemisphaerica* Demonstrates Early Evolution of Purse String and Cell Crawling Closure Mechanisms. *BMC Dev. Biol.* 17 (1), 17. doi:10.1186/s12861-017-0160-2
- Khoury, M. J., and Bilder, D. (2020). Distinct Activities of Scrib Module Proteins Organize Epithelial Polarity. *Proc. Natl. Acad. Sci. U S A.* 117 (21), 11531–11540. doi:10.1073/pnas.1918462117
- Kishimoto, Y., Murate, M., and Sugiyama, T. (1996). Hydra Regeneration from Recombined Ectodermal and Endodermal Tissue. I. Epibolic Ectodermal Spreading Is Driven by Cell Intercalation. *J. Cell Sci.* 109 (Pt 4), 763–772. doi:10.1242/jcs.109.4.763
- Knust, E., Tepass, U., and Wodarz, A. (1993). Crumbs and Stardust, Two Genes of *Drosophila* Required for the Development of Epithelial Cell Polarity. *Dev. Suppl.*, 261–268. doi:10.1242/dev.119.supplement.261
- Kraus, Y., Chevalier, S., and Houliston, E. (2020). Cell Shape Changes during Larval Body Plan Development in *Clytia hemisphaerica*. *Dev. Biol.* 468 (1–2), 59–79. doi:10.1016/j.ydbio.2020.09.013
- Kuchinke, U., Grawe, F., and Knust, E. (1998). Control of Spindle Orientation in *Drosophila* by the Par-3-Related PDZ-Domain Protein Bazooka. *Curr. Biol.* 8 (25), 1357–1365. doi:10.1016/s0960-9822(98)00016-5
- Kumburegama, S., Wijesena, N., and Wikramanayake, A. H. (2008). Detecting Expression Patterns of Wnt Pathway Components in *Nematostella vectensis* Embryos. *Methods Mol. Biol.* 469, 55–67. doi:10.1007/978-1-60327-469-2\_6

- Kumburegama, S., Wijesena, N., Xu, R., and Wikramanayake, A. H. (2011). Strabismus-mediated Primary Archenteron Invagination Is Uncoupled from Wnt/beta-catenin-dependent Endoderm Cell Fate Specification in *Nematostella vectensis* (Anthozoa, Cnidaria): Implications for the Evolution of Gastrulation. *Evodevo* 2 (1), 2. doi:10.1186/2041-9139-2-2
- Lapebie, P., Ruggiero, A., Barreau, C., Chevalier, S., Chang, P., Dru, P., et al. (2014). Differential Responses to Wnt and PCP Disruption Predict Expression and Developmental Function of Conserved and Novel Genes in a Cnidarian. *Plos Genet.* 10 (9), e1004590. doi:10.1371/journal.pgen.1004590
- Laprise, P., Beronja, S., Silva-Gagliardi, N. F., Pellicka, M., Jensen, A. M., McGlade, C. J., et al. (2006). The FERM Protein Yurt Is a Negative Regulatory Component of the Crumbs Complex that Controls Epithelial Polarity and Apical Membrane Size. *Dev. Biol.* 11 (3), 363–374. doi:10.1016/j.devcel.2006.06.001
- Laprise, P., Lau, K. M., Harris, K. P., Silva-Gagliardi, N. F., Paul, S. M., Beronja, S., et al. (2009). Yurt, Coracle, Neurexin IV and the Na(+),K(+)-ATPase Form a Novel Group of Epithelial Polarity Proteins. *Nature* 459 (7250), 1141–1145. doi:10.1038/nature08067
- Leclerc, L., Horin, C., Chevalier, S., Lapebie, P., Dru, P., Peron, S., et al. (2019). The Genome of the Jellyfish Clytia Hemisphaerica and the Evolution of the Cnidarian Life-Cycle. *Nat. Ecol. Evol.* 3 (5), 801–810. doi:10.1038/s41559-019-0833-2
- Lee, C. Y., Robinson, K. J., and Doe, C. Q. (2006). Lgl, Pins and aPKC Regulate Neuroblast Self-Renewal versus Differentiation. *Nature* 439 (7076), 594–598. doi:10.1038/nature04299
- Leys, S. P., and Riesgo, A. (2012). Epithelia, an Evolutionary novelty of Metazoans. *J. Exp. Zool. B Mol. Dev. Evol.* 318 (6), 438–447. doi:10.1002/jez.b.21442
- Li, W., Yu, J. C., Shin, D. Y., and Pierce, J. H. (1995). Characterization of a Protein Kinase C-delta (PKC-delta) ATP Binding Mutant. An Inactive Enzyme that Competitively Inhibits Wild Type PKC-delta Enzymatic Activity. *J. Biol. Chem.* 270 (14), 8311–8318. doi:10.1074/jbc.270.14.8311
- Li, X., Francies, H. E., Secrier, M., Perner, J., Miremadi, A., Galeano-Dalmau, N., et al. (2018). Organoid Cultures Recapitulate Esophageal Adenocarcinoma Heterogeneity Providing a Model for Clonality Studies and Precision Therapeutics. *Nat. Commun.* 9 (1), 2983. doi:10.1038/s41467-018-05190-9
- Lim, J., and Thiery, J. P. (2012). Epithelial-mesenchymal Transitions: Insights from Development. *Development* 139 (19), 3471–3486. doi:10.1242/dev.071209
- Lin, Y. C., Grigoriev, N. G., and Spencer, A. N. (2000). Wound Healing in Jellyfish Striated Muscle Involves Rapid Switching between Two Modes of Cell Motility and a Change in the Source of Regulatory Calcium. *Dev. Biol.* 225 (1), 87–100. doi:10.1006/dbio.2000.9807
- Lommel, M., Tursch, A., Rustarazo-Calvo, L., Trageser, B., and Holstein, T. W. (2017). Genetic Knockdown and Knockout Approaches in Hydra. *bioRxiv*. doi:10.1101/230300
- Lukonin, I., Serra, D., Challet Meylan, L., Volkmann, K., Baaten, J., Zhao, R., et al. (2020). Phenotypic Landscape of Intestinal Organoid Regeneration. *Nature* 586 (7828), 275–280. doi:10.1038/s41586-020-2776-9
- MacWilliams, H. K. (1982). Numerical Simulations of hydra Head Regeneration Using a Proportion-Regulating Version of the Gierer-Meinhardt Model. *J. Theor. Biol.* 99 (4), 681–703. doi:10.1016/0022-5193(82)90194-1
- Magie, C. R., and Martindale, M. Q. (2008). Cell-cell Adhesion in the Cnidaria: Insights into the Evolution of Tissue Morphogenesis. *Biol. Bull.* 214 (3), 218–232. doi:10.2307/25470665
- Makino, K., Kuwahara, H., Masuko, N., Nishiyama, Y., Morisaki, T., Sasaki, J., et al. (1997). Cloning and Characterization of NE-dlg: a Novel Human Homolog of the Drosophila Discs Large (Dlg) Tumor Suppressor Protein Interacts with the APC Protein. *Oncogene* 14 (20), 2425–2433. doi:10.1038/sj.onc.1201087
- Malamy, J. E., and Shribak, M. (2018). An Orientation-independent DIC Microscope Allows High Resolution Imaging of Epithelial Cell Migration and Wound Healing in a Cnidarian Model. *J. Microsc.* 270 (3), 290–301. doi:10.1111/jmi.12682
- Manninen, A. (2015). Epithelial Polarity-Generating and Integrating Signals from the ECM with Integrins. *Exp. Cell Res* 334 (2), 337–349. doi:10.1016/j.yexcr.2015.01.003
- Maroudas-Sacks, Y., Garion, L., Shani-Zerbib, L., Livshits, A., Braun, E., and Keren, K. 2021. "Topological Defects in the Nematic Order of Actin Fibres as Organization Centres of Hydra Morphogenesis." *Nat. Phys.* 17 (2):251. doi:10.1038/s41567-020-01083-1
- Martin-Belmonte, F., Gassama, A., Datta, A., Yu, W., Rescher, U., Gerke, V., et al. (2007). PTEN-mediated Apical Segregation of Phosphoinositides Controls Epithelial Morphogenesis through Cdc42. *Cell* 128 (2), 383–397. doi:10.1016/j.cell.2006.11.051
- Matsumine, A., Ogai, A., Senda, T., Okumura, N., Satoh, K., Baeg, G. H., et al. (1996). Binding of APC to the Human Homolog of the Drosophila Discs Large Tumor Suppressor Protein. *Science* 272 (5264), 1020–1023. doi:10.1126/science.272.5264.1020
- Meinhardt, H. (1993). A Model for Pattern Formation of Hypostome, Tentacles, and Foot in hydra: How to Form Structures Close to Each Other, How to Form Them at a Distance. *Dev. Biol.* 157 (2), 321–333. doi:10.1006/dbio.1993.1138
- Mellman, I., and Nelson, W. J. (2008). Coordinated Protein Sorting, Targeting and Distribution in Polarized Cells. *Nat. Rev. Mol. Cell Biol* 9 (11), 833–845. doi:10.1038/nrm2525
- Momose, T., De Cian, A., Shiba, K., Inaba, K., Giovannangeli, C., and Concordet, J. P. (2018). High Doses of CRISPR/Cas9 Ribonucleoprotein Efficiently Induce Gene Knockout with Low Mosaicism in the Hydrozoan Clytia Hemisphaerica through Microhomology-Mediated Deletion. *Sci. Rep.* 8 (1), 11734. doi:10.1038/s41598-018-30188-0
- Momose, T., Derelle, R., and Houliston, E. (2008). A Maternally Localised Wnt Ligand Required for Axial Patterning in the Cnidarian Clytia Hemisphaerica. *Development* 135 (12), 2105–2113. doi:10.1242/dev.021543
- Momose, T., and Houliston, E. (2007). Two Oppositely Localised Frizzled RNAs as axis Determinants in a Cnidarian Embryo. *Plos Biol.* 5 (4), e70. doi:10.1371/journal.pbio.0050070
- Momose, T., Kraus, Y., and Houliston, E. (2012). A Conserved Function for Strabismus in Establishing Planar Cell Polarity in the Ciliated Ectoderm during Cnidarian Larval Development. *Development* 139 (23), 4374–4382. doi:10.1242/dev.084251
- Morais-de-Sa, E., Mirouse, V., and St Johnston, D. (2010). aPKC Phosphorylation of Bazooka Defines the Apical/lateral Border in Drosophila Epithelial Cells. *Cell* 141 (3), 509–523. doi:10.1016/j.cell.2010.02.040
- Nagai-Tamai, Y., Mizuno, K., Hirose, T., Suzuki, A., and Ohno, S. (2002). Regulated Protein-Protein Interaction between aPKC and PAR-3 Plays an Essential Role in the Polarization of Epithelial Cells. *Genes Cells* 7 (11), 1161–1171. doi:10.1046/j.1365-2443.2002.00590.x
- Nathaniel Clarke, D., Lowe, C. J., and James Nelson, W. (2019). The Cadherin-Catenin Complex Is Necessary for Cell Adhesion and Embryogenesis in *Nematostella vectensis*. *Dev. Biol.* 447 (2), 170–181. doi:10.1016/j.ydbio.2019.01.007
- Nejsum, L. N., and Nelson, W. J. (2007). A Molecular Mechanism Directly Linking E-Cadherin Adhesion to Initiation of Epithelial Cell Surface Polarity. *J. Cell Biol* 178 (2), 323–335. doi:10.1083/jcb.200705094
- Omori, Y., and Malicki, J. (2006). Oko Meduzy and Related Crumbs Genes Are Determinants of Apical Cell Features in the Vertebrate Embryo. *Curr. Biol.* 16 (10), 945–957. doi:10.1016/j.cub.2006.03.058
- Otto, J. J. (1977). Orientation and Behavior of Epithelial Cell Muscle Processes during Hydra Budding. *J. Exp. Zool* 202 (3), 307–322. doi:10.1002/jez.1402020303
- Petronczki, M., and Knoblich, J. A. (2001). DmPAR-6 Directs Epithelial Polarity and Asymmetric Cell Division of Neuroblasts in Drosophila. *Nat. Cell Biol* 3 (1), 43–49. doi:10.1038/35050550
- Philipp, I., Aufschnaiter, R., Ozbek, S., Pontasch, S., Jenewein, M., Watanabe, H., et al. (2009). Wnt/beta-catenin and Noncanonical Wnt Signaling Interact in Tissue Evagination in the Simple Eumetazoan Hydra. *Proc. Natl. Acad. Sci. U S A.* 106 (11), 4290–4295. doi:10.1073/pnas.0812847106
- Piccolo, S. (2013). Developmental Biology: Mechanics in the Embryo. *Nature* 504 (7479), 223–225. doi:10.1038/504223a
- Plickert, G., and Krohner, M. (1988). Proliferation Kinetics and Cell Lineages Can Be Studied in Whole Mounts and Macerates by Means of BrdU/anti-BrdU Technique. *Development* 103 (4), 791–794. doi:10.1242/dev.103.4.791
- Pukhlyakova, E. A., Kirillova, A. O., Kraus, Y. A., Zimmermann, B., and Technau, U. (2019). A Cadherin Switch marks Germ Layer Formation in the Diploblastic Sea Anemone *Nematostella vectensis*. *Development* 146 (20). doi:10.1242/dev.174623
- Putnam, N. H., Srivastava, M., Hellsten, U., Dirks, B., Chapman, J., Salamov, A., et al. (2007). Sea Anemone Genome Reveals Ancestral Eumetazoan Gene

- Repertoire and Genomic Organization. *Science* 317 (5834), 86–94. doi:10.1126/science.1139158
- Qin, Y., Capaldo, C., Gumbiner, B. M., and Macara, I. G. (2005). The Mammalian Scribble Polarity Protein Regulates Epithelial Cell Adhesion and Migration through E-Cadherin. *J. Cell Biol* 171 (6), 1061–1071. doi:10.1083/jcb.200506094
- Ragkousi, K., Marr, K., McKinney, S., Ellington, L., and Gibson, M. C. (2017). Cell-Cycle-Coupled Oscillations in Apical Polarity and Intercellular Contact Maintain Order in Embryonic Epithelia. *Curr. Biol.* 27 (9), 1381–1386. doi:10.1016/j.cub.2017.03.064
- Rodriguez-Boulán, E., Kreitzer, G., and Musch, A. (2005). Organization of Vesicular Trafficking in Epithelia. *Nat. Rev. Mol. Cell Biol* 6 (3), 233–247. doi:10.1038/nrm1593
- Rodriguez-Boulán, E., and Macara, I. G. (2014). Organization and Execution of the Epithelial Polarity Programme. *Nat. Rev. Mol. Cell Biol* 15 (4), 225–242. doi:10.1038/nrm3775
- Rosenbluth, J. M., Schackmann, R. C. J., Gray, G. K., Selfors, L. M., Li, C. M., Boedicker, M., et al. (2020). Organoid Cultures from normal and Cancer-Prone Human Breast Tissues Preserve Complex Epithelial Lineages. *Nat. Commun.* 11 (1), 1711. doi:10.1038/s41467-020-15548-7
- Rothberg, J. M., Hartley, D. A., Walther, Z., and Artavanis-Tsakonas, S. (1988). Slit: an EGF-Homologous Locus of *D. melanogaster* Involved in the Development of the Embryonic central Nervous System. *Cell* 55 (6), 1047–1059. doi:10.1016/0092-8674(88)90249-8
- Salinas-Saavedra, M., and Martindale, M. Q. (2020). Par Protein Localization during the Early Development of *Mnemiopsis leidyi* Suggests Different Modes of Epithelial Organization in the Metazoa. *Elife* 9. doi:10.7554/eLife.54927
- Salinas-Saavedra, M., Rock, A. Q., and Martindale, M. Q. (2018). Germ Layer-specific Regulation of Cell Polarity and Adhesion Gives Insight into the Evolution of Mesoderm. *Elife* 7. doi:10.7554/eLife.36740
- Salinas-Saavedra, M., Stephenson, T. Q., Dunn, C. W., and Martindale, M. Q. (2015). Par System Components Are Asymmetrically Localized in Ectodermal Epithelia, but Not during Early Development in the Sea Anemone *Nematostella vectensis*. *Evodevo* 6, 20. doi:10.1186/s13227-015-0014-6
- Sarras, M. P., Jr., Zhang, X., Huff, J. K., Accavitti, M. A., St John, P. L., and Abrahamson, D. R. (1993). Extracellular Matrix (Mesoglea) of *Hydra vulgaris* III. Formation and Function during Morphogenesis of hydra Cell Aggregates. *Dev. Biol.* 157 (2), 383–398. doi:10.1006/dbio.1993.1143
- Sasaki, M., Kleinman, H. K., Huber, H., Deutzmann, R., and Yamada, Y. (1988). Laminin, a Multidomain Protein. The A Chain Has a Unique Globular Domain and Homology with the Basement Membrane Proteoglycan and the Laminin B Chains. *J. Biol. Chem.* 263 (32), 16536–16544. doi:10.1016/s0021-9258(18)37424-6
- Schiller, E. A., and Bergstralh, D. T. (2021). Interaction between Discs Large and Pins/LGN/GPSM2: a Comparison across Species. *Biol. Open* 10 (11). doi:10.1242/bio.058982
- Schuster, B., Junkin, M., Kashaf, S. S., Romero-Calvo, I., Kirby, K., Matthews, J., et al. (2020). Automated Microfluidic Platform for Dynamic and Combinatorial Drug Screening of Tumor Organoids. *Nat. Commun.* 11 (1), 5271. doi:10.1038/s41467-020-19058-4
- Schwaiger, M., Schonauer, A., Rendeiro, A. F., Pribitzer, C., Schauer, A., Gilles, A. F., et al. (2014). Evolutionary Conservation of the Eumetazoan Gene Regulatory Landscape. *Genome Res.* 24 (4), 639–650. doi:10.1101/gr.162529.113
- Sebe-Pedros, A., Saudemont, B., Chomsky, E., Plessier, F., Mailhe, M. P., Renno, J., et al. (2018). Cnidarian Cell Type Diversity and Regulation Revealed by Whole-Organism Single-Cell RNA-Seq. *Cell* 173 (6), 1520–1534. doi:10.1016/j.cell.2018.05.019
- Serra, D., Mayr, U., Boni, A., Lukonin, I., Rempfler, M., Challet Meylan, L., et al. (2019). Self-organization and Symmetry Breaking in Intestinal Organoid Development. *Nature* 569 (7754), 66–72. doi:10.1038/s41586-019-1146-y
- Seybold, A., Salvenmoser, W., and Hobmayer, B. (2016). Sequential Development of Apical-Basal and Planar Polarities in Aggregating Epitheliomuscular Cells of *Hydra*. *Dev. Biol.* 412 (1), 148–159. doi:10.1016/j.ydbio.2016.02.022
- Siebert, S., Farrell, J. A., Cazet, J. F., Abeykoon, Y., Primack, A. S., Schnitzler, C. E., et al. (2019). Stem Cell Differentiation Trajectories in *Hydra* Resolved at Single-Cell Resolution. *Science* 365 (6451). doi:10.1126/science.aav9314
- Sinigaglia, C., Peron, S., Eichelbrenner, J., Chevalier, S., Steger, J., Barreau, C., et al. (2020). Pattern Regulation in a Regenerating Jellyfish. *Elife* 9. doi:10.7554/eLife.54868
- Skokan, T. D., Vale, R. D., and McKinley, K. L. (2020). Cell Sorting in *Hydra vulgaris* Arises from Differing Capacities for Epithelialization between Cell Types. *Curr. Biol.* 30 (19), 3713–3723. doi:10.1016/j.cub.2020.07.035
- Soriano, E. V., Ivanova, M. E., Fletcher, G., Riou, P., Knowles, P. P., Barnouin, K., et al. (2016). aPKC Inhibition by Par3 CR3 Flanking Regions Controls Substrate Access and Underpins Apical-Junctional Polarization. *Dev. Cell* 38 (4), 384–398. doi:10.1016/j.devcel.2016.07.018
- Sotelo, N. S., Valiente, M., Gil, A., and Pulido, R. (2012). A Functional Network of the Tumor Suppressors APC, hDlg, and PTEN, that Relies on Recognition of Specific PDZ-Domains. *J. Cell Biochem* 113 (8), 2661–2670. doi:10.1002/jcb.24141
- Sperling, E. A., Peterson, K. J., and Pisani, D. (2009). Phylogenetic-signal Dissection of Nuclear Housekeeping Genes Supports the Paraphyly of Sponges and the Monophyly of Eumetazoa. *Mol. Biol. Evol.* 26 (10), 2261–2274. doi:10.1093/molbev/msp148
- St Johnston, D., and Ahringer, J. (2010). Cell Polarity in Eggs and Epithelia: Parallels and Diversity. *Cell* 141 (5), 757–774. doi:10.1016/j.cell.2010.05.011
- Subbiah, V. K., Narayan, N., Massimi, P., and Banks, L. (2012). Regulation of the DLG Tumor Suppressor by Beta-Catenin. *Int. J. Cancer* 131 (10), 2223–2233. doi:10.1002/ijc.27519
- Tabuse, Y., Izumi, Y., Piano, F., Kemphues, K. J., Miwa, J., and Ohno, S. (1998). Atypical Protein Kinase C Cooperates with PAR-3 to Establish Embryonic Polarity in *Caenorhabditis elegans*. *Development* 125 (18), 3607–3614. doi:10.1242/dev.125.18.3607
- Takashima, S., Gold, D., and Hartenstein, V. (2013). Stem Cells and Lineages of the Intestine: a Developmental and Evolutionary Perspective. *Dev. Genes Evol.* 223 (1–2), 85–102. doi:10.1007/s00427-012-0422-8
- Takizawa, S., Nagasaka, K., Nakagawa, S., Yano, T., Nakagawa, K., Yasugi, T., et al. (2006). Human Scribble, a Novel Tumor Suppressor Identified as a Target of High-Risk HPV E6 for Ubiquitin-Mediated Degradation, Interacts with Adenomatous Polyposis Coli. *Genes Cells* 11 (4), 453–464. doi:10.1111/j.1365-2443.2006.00954.x
- Tan, B., Yatim, Smjm., Peng, S. J., Gunaratne, W., Hunziker, A., and Ludwig, A. (2020). The Mammalian Crumbs Complex Defines a Distinct Polarity Domain Apical of Epithelial Tight Junctions. *Curr. Biol.* 30 (14), 2791–2804. e6. doi:10.1016/j.cub.2020.05.032
- Technau, U., Cramer von Laue, C., Rentzsch, F., Luft, S., Hobmayer, B., Bode, H. R., et al. (2000). Parameters of Self-Organization in *Hydra* Aggregates. *Proc. Natl. Acad. Sci. U S A* 97 (22), 12127–12131. doi:10.1073/pnas.97.22.12127
- Technau, U. (2020). Gastrulation and Germ Layer Formation in the Sea Anemone *Nematostella vectensis* and Other Cnidarians. *Mech. Dev.* 163, 103628. doi:10.1016/j.mod.2020.103628
- Technau, U., and Holstein, T. W. (1992). Cell Sorting during the Regeneration of *Hydra* from Reaggregated Cells. *Dev. Biol.* 151 (1), 117–127. doi:10.1016/0012-1606(92)90219-7
- Technau, U., and Steele, R. E. (2011). Evolutionary Crossroads in Developmental Biology: Cnidaria. *Development* 138 (8), 1447–1458. doi:10.1242/dev.048959
- Tennooren, I., Jenks, M. Z., Rashid, H., Cook, K. L., Muhlemann, J. K., Sistrunk, C., et al. (2019). Elevated Leptin Disrupts Epithelial Polarity and Promotes Premalignant Alterations in the Mammary Gland. *Oncogene* 38 (20), 3855–3870. doi:10.1038/s41388-019-0687-8
- Tepass, U., Tanentzapf, G., Ward, R., and Fehon, R. (2001). Epithelial Cell Polarity and Cell Junctions in *Drosophila*. *Annu. Rev. Genet.* 35, 747–784. doi:10.1146/annurev.genet.35.102401.091415
- Tepass, U., Theres, C., and Knust, E. (1990). Crumbs Encodes an EGF-like Protein Expressed on Apical Membranes of *Drosophila* Epithelial Cells and Required for Organization of Epithelia. *Cell* 61 (5), 787–799. doi:10.1016/0092-8674(90)90189-1
- Thompson, B. J., Pichaud, F., and Roper, K. (2013). Sticking Together the Crumbs - an Unexpected Function for an Old Friend. *Nat. Rev. Mol. Cell Biol* 14 (5), 307–314. doi:10.1038/nrm3568
- Tilston-Lunel, A., Mazzilli, S., Kingston, N. M., Szymaniak, A. D., Hicks-Berthet, J., Kern, J. G., et al. (2021). Aberrant Epithelial Polarity Cues Drive the Development of Precancerous Airway Lesions. *Proc. Natl. Acad. Sci. U S A* 118 (18). doi:10.1073/pnas.2019282118
- Trembley, A. (1744). *Mémoires pour servir à l'histoire d'un genre de ployes d'eau douce, à bras en forme de cornes*, 2. Paris: Chez Durand. doi:10.5962/bhl.title.64073

- Tucker, R. P., and Adams, J. C. (2014). Adhesion Networks of Cnidarians: a Postgenomic View. *Int. Rev. Cel Mol Biol* 308, 323–377. doi:10.1016/B978-0-12-800097-7.00008-7
- Ventura, G., Moreira, S., Barros-Carvalho, A., Osswald, M., and Morais-de-Sa, E. (2020). Lgl Cortical Dynamics Are Independent of Binding to the Scrib-Dlg Complex but Require Dlg-dependent Restriction of aPKC. *Development* 147 (15). doi:10.1242/dev.186593
- Ventura, P., Toullec, G., Fricano, C., Chapron, L., Meunier, V., Rottinger, E., et al. (2018). Cnidarian Primary Cell Culture as a Tool to Investigate the Effect of Thermal Stress at Cellular Level. *Mar. Biotechnol. (Ny)* 20 (2), 144–154. doi:10.1007/s10126-017-9791-3
- Vogg, M. C., Galliot, B., and Tsiaris, C. D. (2019). Model Systems for Regeneration: Hydra. *Development* 146 (21). doi:10.1242/dev.177212
- Webster, G., and Hamilton, S. (1972). Budding in hydra: the Role of Cell Multiplication and Cell Movement in Bud Initiation. *J. Embryol. Exp. Morphol.* 27 (2), 301–316. doi:10.1242/dev.27.2.301
- Whiteman, E. L., Liu, C. J., Fearon, E. R., and Margolis, B. (2008). The Transcription Factor Snail Represses Crumbs3 Expression and Disrupts Apico-Basal Polarity Complexes. *Oncogene* 27 (27), 3875–3879. doi:10.1038/onc.2008.9
- Wijesena, N., and Martindale, M. Q. (2018). Reengineering the Primary Body axis by Ectopic cWnt Signaling. *Curr. Biol.* 28 (5), R206–R207. doi:10.1016/j.cub.2018.01.042
- Wijesena, N., Sun, H., Kumburegama, S., and Wikramanayake, A. H. (2022). Distinct Frizzled Receptors Independently Mediate Endomesoderm Specification and Primary Archenteron Invagination during Gastrulation in Nematostella. *Dev. Biol.* 481, 215–225. doi:10.1016/j.ydbio.2021.11.002
- Williams, E., Villar-Prados, A., Bowser, J., Broaddus, R., and Gladden, A. B. (2017). Loss of Polarity Alters Proliferation and Differentiation in Low-Grade Endometrial Cancers by Disrupting Notch Signaling. *PLoS One* 12 (12), e0189081. doi:10.1371/journal.pone.0189081
- Wodarz, A., Hinz, U., Engelbert, M., and Knust, E. (1995). Expression of Crumbs Confers Apical Character on Plasma Membrane Domains of Ectodermal Epithelia of *Drosophila*. *Cell* 82 (1), 67–76. doi:10.1016/0092-8674(95)90053-5
- Wodarz, A., Ramrath, A., Grimm, A., and Knust, E. (2000). *Drosophila* Atypical Protein Kinase C Associates with Bazooka and Controls Polarity of Epithelia and Neuroblasts. *J. Cel Biol* 150 (6), 1361–1374. doi:10.1083/jcb.150.6.1361
- Zemach, A., McDaniel, I. E., Silva, P., and Zilberman, D. (2010). Genome-wide Evolutionary Analysis of Eukaryotic DNA Methylation. *Science* 328 (5980), 916–919. doi:10.1126/science.1186366
- Zemach, A., and Zilberman, D. (2010). Evolution of Eukaryotic DNA Methylation and the Pursuit of Safer Sex. *Curr. Biol.* 20 (17), R780–R785. doi:10.1016/j.cub.2010.07.007
- Zrzavy, J., Mihulka, S., Kepka, P., Bezdek, A., and Tietz, D. (1998). Phylogeny of the Metazoa Based on Morphological and 18S Ribosomal DNA Evidence. *Cladistics* 14 (3), 249–285. doi:10.1111/j.1096-0031.1998.tb00338.x

**Conflict of Interest:** The authors declare that the research was conducted in the absence of any commercial or financial relationships that could be construed as a potential conflict of interest.

**Publisher's Note:** All claims expressed in this article are solely those of the authors and do not necessarily represent those of their affiliated organizations, or those of the publisher, the editors, and the reviewers. Any product that may be evaluated in this article, or claim that may be made by its manufacturer, is not guaranteed or endorsed by the publisher.

Copyright © 2022 Rathbun, Everett and Bergstrahl. This is an open-access article distributed under the terms of the Creative Commons Attribution License (CC BY). The use, distribution or reproduction in other forums is permitted, provided the original author(s) and the copyright owner(s) are credited and that the original publication in this journal is cited, in accordance with accepted academic practice. No use, distribution or reproduction is permitted which does not comply with these terms.





# Polarity Events in the *Drosophila melanogaster* Oocyte

Ana Milas\* and Ivo A. Telley\*

Instituto Gulbenkian de Ciência, Oeiras, Portugal

## OPEN ACCESS

### Edited by:

Eurico Morais-de-Sá,  
Universidade do Porto, Portugal

### Reviewed by:

Dmitry Nashchekin,  
University of Cambridge,  
United Kingdom  
Acaimo González-Reyes,  
Andalusian Centre for Developmental  
Biology (CABD) (CSIC), Spain

### \*Correspondence:

Ana Milas  
amilas@igc.gulbenkian.pt  
Ivo A. Telley  
itelley@igc.gulbenkian.pt

### Specialty section:

This article was submitted to  
Morphogenesis and Patterning,  
a section of the journal  
Frontiers in Cell and Developmental  
Biology

**Received:** 14 March 2022

**Accepted:** 19 April 2022

**Published:** 05 May 2022

### Citation:

Milas A and Telley IA (2022) Polarity  
Events in the *Drosophila*  
*melanogaster* Oocyte.  
Front. Cell Dev. Biol. 10:895876.  
doi: 10.3389/fcell.2022.895876

Cell polarity is a pre-requirement for many fundamental processes in animal cells, such as asymmetric cell division, axon specification, morphogenesis and epithelial tissue formation. For all these different processes, polarization is established by the same set of proteins, called partitioning defective (Par) proteins. During development in *Drosophila melanogaster*, decision making on the cellular and organism level is achieved with temporally controlled cell polarization events. The initial polarization of Par proteins occurs as early as in the germline cyst, when one of the 16 cells becomes the oocyte. Another marked event occurs when the anterior–posterior axis of the future organism is defined by Par redistribution in the oocyte, requiring external signaling from somatic cells. Here, we review the current literature on cell polarity events that constitute the oogenesis from the stem cell to the mature egg.

**Keywords:** par polarity, body axis, mRNA localization, cytoskeletal polarization, follicle cells

## INTRODUCTION

Cell polarization is the canonical process of distributing cellular components—from molecules to organelles—unevenly, leading to intracellular and morphological asymmetry. The acquisition and definition of cell functions are often linked to this asymmetry. In broader terms, cell polarization can be viewed as cellular decision-making process generating spatial information. A well-studied example is apicobasal axis formation in epithelial cells. The apical membrane faces the outside of the cell, while the basal membrane contacts the inside. This polarization is the foundation for compartmentalization, organ formation and physical separation of the vertebrate body from the environment (Cereijido et al., 2004; Roignot et al., 2013; Rodriguez-Boulant and Macara, 2014). Another example is the distinction of the differentiating cell from the stemness maintaining cell during asymmetric stem cell division (Knoblich, 2008; Venkei and Yamashita, 2018).

A subclass of metazoans, called bilaterians, define two body axes during embryonic development, the anterior–posterior (AP) axis being the first and the dorsal–ventral (DV) axis following as second symmetry break (Kimelman and Martin, 2012; Anlas and Trivedi, 2021). For most species the AP axis defines head and tail. Some bilaterians, including humans, define a third (left–right) body axis and show, for example, asymmetric organ position (Capdevila et al., 2000). Different animals utilize a range of mechanisms to achieve the symmetry breaks. Vertebrates define these main body axes during embryogenesis (Meinhardt, 2006; Kimelman and Martin, 2012; Bénazéraf and Pourquie, 2013) while invertebrate body axis formation occurs prior or at fertilization (Kimelman and Martin, 2012). Dipterans define the first two body axes prior to fertilization, during late oogenesis.

In the fruit fly *Drosophila melanogaster* oogenesis occurs inside ovarioles, structures composed of the germarium at the anterior tip, and sequentially more mature egg chambers towards the posterior (Figure 1). The germarium hosts germline and somatic stem cells, which divide to give rise to a variety of cell types composing the egg chamber. Germline stem cells derive nurse cells and the oocyte,

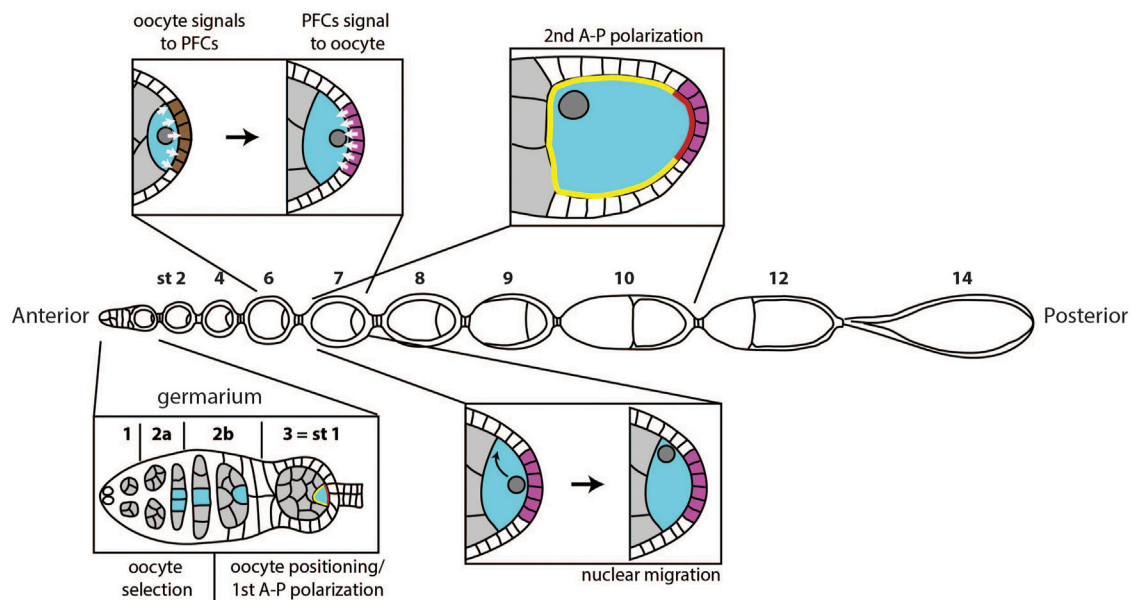


**FIGURE 1** | Overview of polarity events during oogenesis. A first polarity event happens in the germarium, when one of the cells in the germline cyst (grey) is selected to become the oocyte (blue). Next, the oocyte moves to the posterior of the germline cyst, and the egg chamber buds from the germarium, marking stage 1 of oogenesis. Around the same time, the oocyte cytoplasm becomes temporarily polarized, with defined anterior (yellow) and posterior (red) domain. At stage 6, the oocyte signals to the follicle cells at the posterior (brown), which causes them to adopt posterior follicle cell fate (magenta). At stage 7, posterior follicle cells (PFCs) signal back to the oocyte. This signal causes migration of the oocyte nucleus to the anterior of the oocyte at stage 7 and triggers a sequence of events that define anterior-posterior polarization of the oocyte between stages 7 and 10.

while follicle stem cells produce somatic follicle cells. Each egg chamber contains one oocyte and 15 nurse cells, surrounded by a layer of follicle cells.

Several polarization events occur during oogenesis for a mature egg to have properly specified axes (**Figure 1**). If one of these events fails, the system loses one or both axes of asymmetry (Roth and Lynch, 2009). The first symmetry breaking step of oogenesis happens in the germarium, when one of the cells in the germline cyst becomes the oocyte, while others become nurse cells. In the more anterior region of the germarium, follicle cells start surrounding the cyst and play an important role in the subsequent polarization event: the positioning of the oocyte to the posterior of the egg chamber. Positioning of the oocyte is accompanied by budding of the egg chamber from the germarium and the first anterior-posterior polarization of the oocyte. The following two polarization events happen during mid-oogenesis and require communication between the oocyte and follicle cells. First, the oocyte sends a signal to follicle cells at the posterior to induce posterior fate. Next, these cells send a signal back to the oocyte to induce the establishment of the two body axes. Establishment of the anterior-posterior body axis is achieved through polarization of the Par protein network. Par network asymmetry will repolarize the microtubule cytoskeleton, which will enable proper localization of *oskar* and *bicoid* mRNAs. Additionally, the signal from posterior follicle cells leads to the migration of the oocyte nucleus, which defines dorsal-ventral axis of the future embryo.

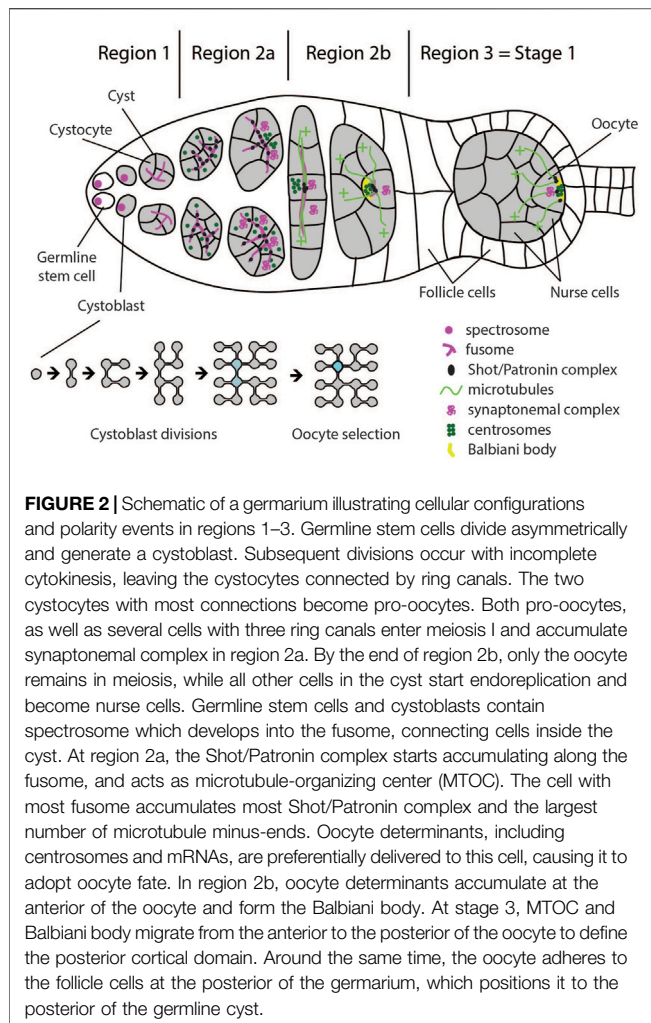
In this review, we highlight and discuss the current body of knowledge of oocyte polarization in the fruit fly, the molecular

players defining events of asymmetry, and we outline the most critical open questions on this topic.

## THE FIRST SYMMETRY BREAKING EVENT AND OOCYTE SELECTION

The most anterior tip of the germarium (region 1) hosts a number of germline stem cells (GSC). These cells divide asymmetrically to produce another stem cell and a differentiating daughter cell called cystoblast. This cystoblast undergoes four rounds of incomplete cell divisions giving rise to a cyst of 16 cells, which are called cystocytes. Due to these cell divisions being incomplete, the cystocytes remain connected through cytoplasmic bridges called ring canals. The cystoblast divides into two cystocytes, which go through three more rounds of division and, thus, have four ring canals. Due to the history of divisions, two of the sixteen cystocytes have three, four have two, and eight have only one ring canal (**Figure 2**, bottom). The two cells with four ring canals are called pro-oocytes, and one of them will differentiate into the oocyte. The other 15 cells in the cyst become nurse cells, which transport mRNAs, proteins, and nutrients to the oocyte through the ring canals (**Figure 2**) (De Cuevas et al., 1997).

The identity of the oocyte is established following two distinct events. In the nucleus, the oocyte arrests in the prophase of meiosis I, while the other cystocytes exit meiosis I and start the endoreplication cycle. In the cytoplasm, the microtubule network is organized such that, while passing the ring canals, the microtubule minus-ends predominantly accumulate in one of



the two pro-oocytes and form a non-centrosomal microtubule organizing centre (ncMTOC) (Theurkauf et al., 1993; Huynh and St Johnston, 2004). This leads to the accumulation of oocyte specific components in this pro-oocyte by means of dynein dependent transport from the other cystocytes (Suter and Steward, 1991; Mach and Lehmann, 1997; McGrail and Hays, 1997; Bolívar et al., 2001; Navarro et al., 2004; Nashchekin et al., 2021). Since all subsequent steps of oocyte polarization can be traced back to cytoskeletal polarization, the selection of one of the two pro-oocytes to become the oocyte is considered the symmetry breaking step of oogenesis (Roth and Lynch, 2009).

It has long been assumed that both pro-oocytes are equally competent to become the oocyte. This assumption was based on the naïve observation that the early transitions of the cell cycle in the two pro-oocytes are indistinguishable. Both pro-oocytes, as well as several cells with three ring canals, enter meiosis I and form synaptonemal complexes between homologous chromosomes (Figure 2). Only as the cyst develops, further progression through meiosis is first restricted to the two pro-oocytes in region 2b, and finally to the oocyte in region 3 of the germarium. All other cells start endocycling, thus becoming nurse cells (Carpenter, 1975; Carpenter, 1994; Röper and Brown, 2004;

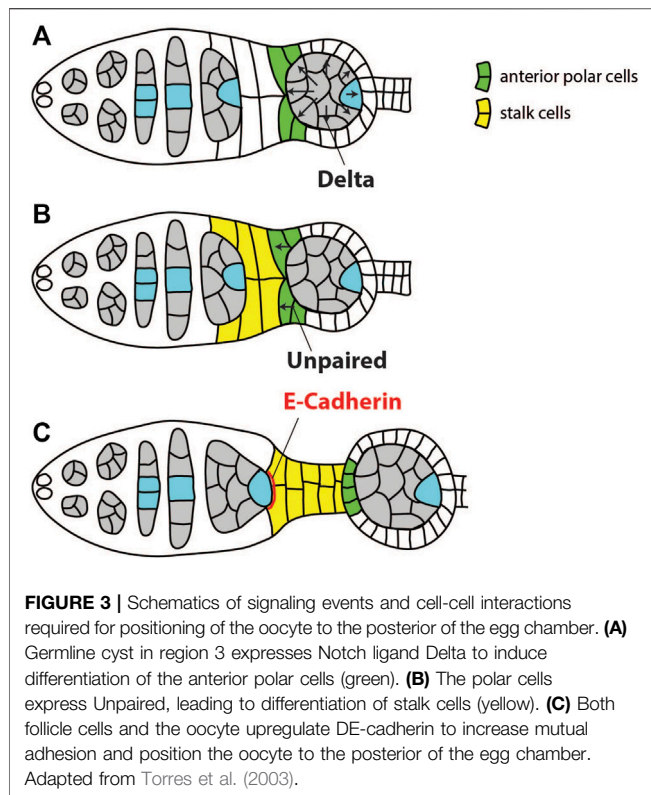
Nashchekin et al., 2021). However, increasing evidence suggests that the symmetry breaking event of oogenesis occurs already during the first mitotic division of the cystoblast in region 1 of the germarium. The evidence supporting this notion comes from the analysis of assembly and distribution of the “fusome” (de Cuevas and Spradling 1998). The fusome is a germline specific, membranous, branched intracellular structure that runs through the ring canals and connects all cystocytes (Lin et al., 1994). The cystoblast inherits the fusome from the germline stem cell. The inherited fusome then serves to orient the cell division of the cystoblast by anchoring one pole of the spindle. After division, only one cell inherits the fusome while the other cell initially lacks it. During interphase, a new fusome forms in the ring canal. The fusomes from both daughter cells migrate to each other and fuse, which ultimately results in an asymmetric distribution with one cell having the original fusome inherited from the germline stem cell plus half of the newly formed fusome, while the other cell has only half of the newly formed fusome. This asymmetric distribution continues to occur during the next three divisions. As a result, the cell that inherited the original fusome in the first division will end up having the largest amount of fusome (Lin and Spradling, 1995; Deng and Lin, 1997; De Cuevas and Spradling, 1998; Villa-Fombuena et al., 2021).

Following the observation that microtubules form along the fusome, the hypothesis was put forward that polarization of the microtubule network is a direct consequence of fusome polarity (Grieder et al., 2000). In agreement with this idea was the observation that the *Drosophila* homologue of Spectraplakins, Short Stop (Shot), a component of the fusome, is necessary for oocyte specification, and appears to stabilize microtubules and link them to the fusome (Röper and Brown, 2004). Recent data further supported this model by showing that Shot stabilizes microtubules by recruiting microtubule minus end stabilizing protein Patronin to the fusome, and that Patronin is necessary for oocyte specification (Nashchekin et al., 2021). Patronin stabilizes microtubule minus-ends in the cell with the largest portion of fusome, thereby establishing a weakly polarized microtubule network. This initial asymmetry is reinforced through positive feedback since dynein transports Patronin bound microtubules from neighboring cells to the cell that already contains most Patronin. Finally, a now highly polarized microtubule network is utilized by dynein to transport oocyte determinants into this cell (Figure 2) (Nashchekin et al., 2021).

If this model of oocyte specification is correct, then the cell that inherits the original fusome in the cystoblast division also accumulates most of the expressed Patronin and eventually becomes the oocyte. Indeed, two studies showed that centrosomes, *oskar* and *orb* mRNAs preferentially accumulate in the cell with the most fusome (Grieder et al., 2000; Cox and Spradling, 2003).

## POSITIONING OF THE OOCYTE TO THE POSTERIOR OF THE EGG CHAMBER

As the cyst moves through region 2 of the germarium, it is surrounded by a layer of somatic follicle cells. These cells arise



from asymmetric divisions of follicle stem cells that reside in the middle of the germarium. Follicle cells further differentiate into either main body follicle cells, or the precursors of stalk or polar cells (reviewed in Rust and Nystul, 2020). Oocyte determination and initial steps of follicle cell differentiation seem to be independent. However, many subsequent steps of polarization of both the oocyte and the layer of follicle cells depend on their mutual communication (see Merkle et al., 2020 for a recent review on signaling between soma and germline throughout oogenesis).

The first round of signaling from the germline cyst to the soma activates Notch and JAK/STAT pathways to induce differentiation of polar and stalk follicle cells (Figure 3). These cells are in turn required to position the oocyte to the posterior of the egg chamber. Before this round of signaling, undifferentiated precursors of stalk/polar follicle cells separate the younger cyst in region 2b from the older cyst in region 3 (Tworoger et al., 1999). The older cyst expresses Notch ligand Delta, which activates Notch in the surrounding follicle cells. This causes precursors of stalk/polar cells that are in direct contact with the anterior of the older cyst to differentiate into polar cells (Figure 3A) (Grammont and Irvine, 2001; López-Schier and St Johnston, 2001). These polar cells will then express Unpaired which will activate JAK-STAT signaling in more anterior stalk/polar precursors, leading to their differentiation into stalk cells (Figure 3B) (McGregor et al., 2002; Torres et al., 2003). Unpaired is unable to activate JAK-STAT in cells which previously underwent high activation of Notch. Thus, it will not act on polar cells themselves, or on follicle cells surrounding older cyst (Assa-Kunik et al., 2007). Newly

differentiated stalk cells form a stalk which directly contacts the younger germline cyst in region 2b. Both stalk cells and the oocyte express high levels of DE-cadherin, which causes the oocyte to adhere to follicle cells at the posterior, thereby positioning the oocyte to the posterior of the egg chamber (Figure 3C) (Godt and Tepass, 1998; González-Reyes and St Johnston, 1998a). Thus, in this round of signaling information is transferred from the older to the younger cyst through a relay mechanism to correctly differentiate polar and stalk cells, and to position the oocyte at the posterior of the egg chamber (Torres et al., 2003). It is not known how the oocyte in the first cyst, which does not have a leading older cyst, is positioned to the posterior. Stalk cells will also contribute to the establishment of the polar cells at the posterior pole of the oocyte (Torres et al., 2003; Assa-Kunik et al., 2007). These posterior polar cells, as well as the correct positioning of the oocyte, will be crucial in later stages of oogenesis when the new round of signaling between the oocyte and posterior follicle cells (PFCs) takes place to establish both AP and DV axis (González-Reyes and St Johnston, 1994; Grammont and Irvine, 2002).

## FIRST ROUND OF OOCYTE ANTERIOR-POSTERIOR POLARIZATION

Positioning of the oocyte to the posterior of the egg chamber is accompanied by changes in the oocyte cytoplasm. Components that were transported to the oocyte during the selection phase, such as centrosomes, Orb, BicD and Egl protein, *oskar* and *orb* mRNAs, are initially located at the anterior of the oocyte and form a structure called Balbiani body (Cox and Spradling, 2003). Minus-ends of microtubules, which facilitated the transport of Balbiani body components to the oocyte, are also accumulated at the anterior. When the oocyte moves through region 3, the microtubule network is reorganized so that minus-ends are more frequently found at the posterior (Grieder et al., 2000). This is followed by relocation of Balbiani body components to the posterior of the oocyte where they form a tight crescent to define the posterior oocyte cortex (Figure 4). If this step fails, the oocyte loses its fate and becomes a nurse cell by exiting meiosis and becoming polyploid (Huynh et al., 2001a). Mechanisms involved in early oocyte polarization are not well understood. However, a collection of experimental evidence suggests that it depends on all *Drosophila* homologues of *par* genes, as well as polarity proteins aPKC and Cdc42. When any of these genes are lacking, the oocyte de-differentiates into a nurse cell (Cox et al., 2001a; Cox et al., 2001b; Huynh et al., 2001a; Huynh et al., 2001b; Benton et al., 2002; Vaccari and Ephrussi, 2002; Martin and St Johnston, 2003; Leibfried et al., 2013). Par proteins are a highly conserved group of polarity proteins originally identified in *Caenorhabditis elegans*. In the *C. elegans* zygote, Par-1 and Par-2 localize to the posterior membrane, while Par-3 and Par-6 form a complex with aPKC and localize to the anterior. Polarity is maintained through mutual phosphorylation of Par proteins. Par-1 excludes Par-3 from the posterior, while aPKC excludes Par-1 from the anterior. Another highly conserved polarity protein, small GTPase Cdc-42, is also required at the



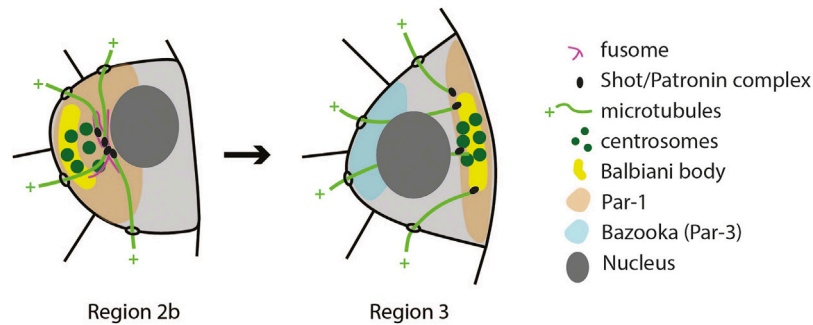


**FIGURE 4 |** Schematics of the first polarity event in the oocyte. The microtubule cytoskeleton reorganizes in the transition from Region 2b to Region 3 so that their nucleation sites (Shot/Patronin) are now at the posterior end. This causes the Balbiani body to reposition from the anterior to the posterior. Similarly, Par-1 localization changes from anterior to posterior, while Bazooka (Par-3) shows antagonistic localization in Region 3 (Vaccari and Ephrussi, 2002).

anterior where it activates aPKC (reviewed in Lang and Munro, 2017; St Johnston, 2018).

Initial efforts to determine the localization of Par proteins during early oogenesis showed that Bazooka (the *Drosophila* homologue of Par-3) and aPKC localize to adherens junctions that form around the ring canals (Cox et al., 2001b), while Par-1 localizes to the fusome (Cox et al., 2001a; Huynh et al., 2001a; Shulman et al., 2000). This work also suggested that Bazooka, aPKC and Par-1 do not depend on each other for their localization (Cox et al., 2001b; Huynh et al., 2001b). However, using isoform specific antibodies, Vaccari and Ephrussi (2002) detected Bazooka at the anterior, and Par-1 at the posterior pole of the oocyte (Figure 4). They also showed that Bazooka extends to the posterior in *par-1* mutants, while Par-1 remains anterior in *baz* mutants. This suggests that Par polarity in the early oocyte could be maintained by mutual antagonism between the Baz/Par6/aPKC complex and Par-1. Cdc42 localizes to the anterior of early oocytes, and in *cdc42* mutant egg chambers Bazooka localization is lost. Inversely, anterior localization of Cdc42 is lost in *baz* and *apkc* mutants (Leibfried et al., 2013).

It is unclear what triggers the polarization of the Par network in early oogenesis. But, since this event coincides with cadherin-mediated interactions between follicle cells and the oocyte, it has been suggested that a signal from follicle cells might play a role (Huynh and St Johnston, 2004; Roth and Lynch, 2009). This view has been supported by the finding that extracellular matrix receptor dystroglycan is required in the germline to polarize the oocyte at this stage (Deng et al., 2003). In addition, signaling between follicle cells and the oocyte is required for polarization of the Par network in later stages of oogenesis (Doerflinger et al., 2006).

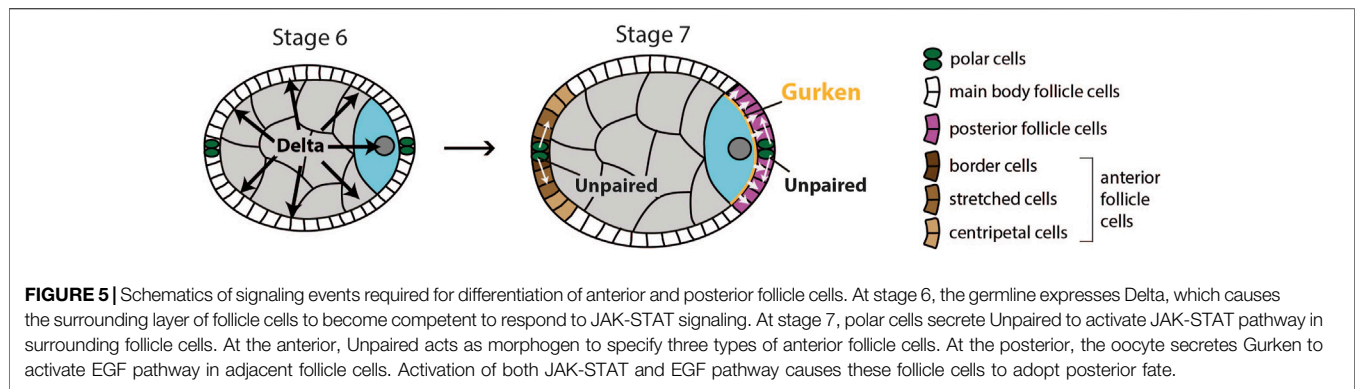
At this stage of oogenesis, a number of open questions are eminent. It is not clear how *par* genes maintain oocyte fate, or how they are involved in relocation of the Balbiani body. It is also not clear if the Par network needs to be polarized at this stage to maintain oocyte fate. The microtubule network is likely a downstream target of Par polarity. This is based on the finding that microtubule minus-ends do not relocate to the posterior cortex in any of the *par* mutants (Cox et al., 2001b; Huynh et al., 2001a; Benton et al., 2002; Vaccari and Ephrussi, 2002; Martin

and St Johnston, 2003; Leibfried et al., 2013). However, Par-1 was later shown to inhibit microtubule nucleation at the posterior in later stages of oogenesis (Parton et al., 2011; Nashchekin et al., 2016). Therefore, it is not clear how Par-1 localization at the posterior could induce localization of minus ends at the posterior in earlier stages. In addition, posterior localization of Par-1 at this stage requires an intact microtubule network, suggesting that microtubule polarity and Par protein localization are interdependent (Vaccari and Ephrussi, 2002).

Another possible target of the Par network is the actin cytoskeleton; *cdc42*, *apkc* and *baz* mutants show disrupted actin cytoskeleton, while treatment with Latrunculin A abolishes translocation of Orb from anterior to posterior of the oocyte (Leibfried et al., 2013). Additionally, components of the dynein/dynactin complex could also be targets of Par proteins (Huynh and St Johnston, 2004). This idea grew from the observation that translocation of proteins and centrosomes does not occur correctly in *Dhc*, *BicD* or *egl* mutants (Huynh and St Johnston, 2000; Bolívar et al., 2001; Vaccari and Ephrussi, 2002).

## SIGNAL FROM THE OOCYTE SPECIFIES POSTERIOR FOLLICLE CELLS

A second round of signaling between the oocyte and follicle cells involves Notch, JAK-STAT and EGF pathways, and occurs during stages 6 and 7 of oogenesis. At this point, Delta is once again upregulated in the germline and activates Notch signaling in the surrounding follicle cells (López-Schier and St Johnston, 2001). The activation of Notch signaling has two main effects on follicle cells. First, it initiates a switch from the mitotic cycle to the endoreplication cycle, which inhibits the proliferation of follicle cells (Deng et al., 2001; López-Schier and St Johnston, 2001). Second, it provides competency to respond to JAK-STAT signaling, which is activated by secretion of Unpaired from polar cells at the anterior and posterior ends of the egg chamber (Figure 5). This leads to specification of terminal cell fate in surrounding epithelial cells at both the anterior and the posterior end of the egg chamber. At the anterior, Unpaired



functions as a morphogen to specify three types of anterior follicle cells as a function of distance from the polar cells: 1) border cells, 2) stretched cells, and 3) centripetal cells. Border cells receive the highest, and centripetal cells the lowest levels of Unpaired (Xi et al., 2003). Proper differentiation of anterior follicle cells is not necessary for establishment of the anterior-posterior (AP) axis but is important for other aspects of egg chamber development (Wu et al., 2008).

For posterior follicle cells to differentiate correctly, the EGF signaling pathway needs to be activated. If that does not happen, follicle cells at the posterior pole of the egg chamber will differentiate into the three types of anterior follicle cells mentioned earlier (González-Reyes et al., 1995; Roth et al., 1995; González-Reyes and St Johnston, 1998b). EGFR in the follicle cells is activated by TGF $\alpha$ -like ligand Gurken (Neuman-Silberberg and Schüpbach, 1993). Gurken is secreted by the adjacent oocyte and activates EGFR in around 200 follicle cells (Neuman-Silberberg and Schüpbach, 1993; González-Reyes and St Johnston, 1998b). This leads to transcription of several target genes of EGF signaling such as *pointed* (Morimoto et al., 1996), *midline* and *H15* (Fregoso Lomas et al., 2013), determinants of posterior follicle cell fate. Importantly, Gurken can activate EGFR only in follicle cells that have previously received Notch and JAK-STAT signaling (Xi et al., 2003). Thus, all three pathways are needed for posterior follicle cells (PFCs) to correctly differentiate and to signal back to the oocyte, which establishes the AP and DV body axes.

## POSTERIOR FOLLICLE CELLS SIGNAL BACK TO THE OOCYTE

The role of the follicle cells in establishing anterior-posterior polarity of the oocyte has first been proposed in the early 1990s, based on the finding that Notch and Delta genes are required in follicle cells for proper localization of *bicoid* mRNA in the oocyte (Ruohola et al., 1991; Ruohola-Baker et al., 1994). González-Reyes and St Johnston (1994) showed that in a mutant in which the oocyte is mispositioned to the centre of the egg chamber, posterior follicle cells adopt anterior fate. This led them to propose a model according to which the oocyte signals to the follicle cells at the posterior to induce posterior fate, which in turn

signal back to the oocyte to promote reorganization of the microtubule cytoskeleton. Soon after this finding, it was determined that the signal coming from the oocyte is Gurken, which activates the EGF signaling pathway in the PFCs. This work also confirmed the need for a signal coming from the posterior follicle cells, by showing that components of the EGFR network in follicle cells were necessary for proper localization of *oskar* and *bicoid* mRNA, organization of the microtubule cytoskeleton, and positioning of the nucleus (González-Reyes et al., 1995; Roth et al., 1995). However, more than 25 years after the signal coming from the oocyte has been elucidated, the molecular nature of the returning signal from the follicle cells that polarizes the oocyte remains unknown.

In order to identify the returning signal, several forward genetic screens for downstream targets of Notch, JAK/STAT and EGFR in follicle cells have been performed. However, they have not been successful in identifying the gene that encodes the signal molecule (Pai et al., 2000; Chen and Schüpbach, 2006; Sun et al., 2011; Wittes and Schüpbach, 2019). Evidence coming from mosaic analysis of mutants in EGF and JAK-STAT signaling components suggests that the signal is transmitted in a local fashion. These studies looked at localization of *oskar* mRNA and Staufen protein [an RNA-binding protein that can be used as a proxy for *oskar* mRNA localization (St Johnston et al., 1991)] in egg chambers in which mutant cell clones encompass only a subset of the PFCs. Both *oskar* mRNA and Staufen protein localize normally at the regions of the oocyte cortex that face wildtype PFCs, while mislocalisation is observed only in regions facing mutant follicle cells (Frydman and Spradling, 2001; Xi et al., 2003).

It is also unknown what the immediate target of the PFC signal is once it reaches the oocyte. The first sign of AP polarity identified to date is activation of non-muscle Myosin II at the posterior of the oocyte, and this does not happen in *grk* mutants, in which PFCs do not differentiate correctly (Doerflinger et al., 2022). However, it is unclear if this change is the direct target of the signal. On the other hand, the oocyte nucleus has to migrate from the posterior to the anterior of the oocyte to define the dorsal side of the egg chamber. In *grk* mutants, the oocyte is not released from the posterior anchor and cannot migrate (Zhao et al., 2012). All the evidence suggests that a PFC signal is necessary to establish both the AP and DV axis of the oocyte.

However, the establishment of the two axes seems to be independent since the nucleus migrates normally in *par-1* mutants, which do not properly establish the AP axis (Zhao et al., 2012). This also raises the possibility that the PFCs send two different signals to polarize the two main body axes.

## MIGRATION OF THE OOCYTE NUCLEUS AND DORSAL-VENTRAL AXIS FORMATION

One of the downstream targets of the unidentified PFC signal is the movement of the nucleus from the posterior pole to the anterior at stage 7. Once it reaches the anterior, the nucleus is anchored to the oocyte membrane in contact with follicle cells. When the migration is completed, the nucleus accumulates high levels of *grk* mRNA and protein, and one more round of EGF signaling follows inducing dorsal fate in adjacent follicle cells (Neuman-Silberberg and Schüpbach, 1993; Roth et al., 1995; Schüpbach, 1987, see Merkle et al., 2020 for recent review on downstream targets of EGFR activation in dorsal follicle cells).

In the mutants producing bi-nucleated oocytes due to a defect in cystoblast cytokinesis, both nuclei move to the anterior and induce dorsal fate in adjacent follicle cells. Additionally, both nuclei choose the position randomly with regard to each other (Roth et al., 1999). Thus, the nucleus can be localized at any position of the oocyte anterior margin, meaning that, prior to nuclear movement, the oocyte lacks any dorsal-ventral asymmetry. This attributes the migration of the nucleus to the specific point of the margin a symmetry breaking event.

The movement of the nucleus across the oocyte has been well characterized using live imaging (Zhao et al., 2012; Tissot et al., 2017, reviewed in; Bernard et al., 2018). Studies have shown that microtubules nucleating at the posterior pole of the oocyte push the nucleus to the anterior. First, Zhao et al. (2012) showed that centrosomes, which are transported to the posterior at stage 1 of oogenesis, are the main nucleators of microtubules. However, detailed 3D analysis of migratory paths revealed that there are complementary mechanisms driving nuclear movement. While centrosomes control one migratory path, microtubule-associated protein Mud/NuMA, promotes a separate route (Tissot et al., 2017). This mechanistic redundancy provides robustness to the process of nuclear migration. In addition, it explains why centrosomes are not necessary for the correct positioning of the nucleus (Stevens et al., 2007). In the absence of centrosomes, nucleus movement is mediated either by the Mud/NuMA pathway (Tissot et al., 2017), or by acentrosomal microtubule organizing centers that form behind the nucleus and provide the pushing force for nuclear migration (Zhao et al., 2012).

Although migration of the nucleus has been well described, it is not clear how the PFC signal triggers the movement of the nucleus. It has been suggested that the signal releases the nucleus from the posterior anchor (Zhao et al., 2012). This is based on the observation that active centrosomes are localized behind the nucleus already at the stage 5 of oogenesis. These centrosomes nucleate microtubules, inducing indentation of the nucleus at the posterior. However, the nucleus is set in motion only following

the PFC signal at stage 7. In *grk* mutants, the nucleus still maintains posterior indentation, but fails to migrate since the pushing force remains countered by an anchor that keeps the nucleus in place (Zhao et al., 2012). Once the nucleus has reached its final position, it needs to be anchored (Guichet et al., 2001). If anchoring is omitted, the nucleus is found in the middle of the oocyte, which has been referred to as a floating phenotype (Bernard et al., 2018). Not much is known about the mechanisms of the nucleus anchoring. However, microtubules play a role since a floating phenotype is observed when microtubules are depolymerized after the migration is completed (Januschke et al., 2006).

## SECOND ROUND OF OOCYTE ANTERIOR-POSTERIOR POLARIZATION

The final goal of establishing anterior-posterior polarity of the oocyte is the robust and precise delivery of anterior and posterior determinants, which will specify the poles of the future embryo. The anterior region will develop into the head while the posterior region will become the abdomen of the fly. The main posterior determinant is *oskar* mRNA (Lehmann and Nüsslein-Volhard, 1986), and the anterior determinant is *bicoid* mRNA (Frohnhofer and Nüsslein-Volhard, 1986). The process of anterior-posterior polarization of the oocyte occurs from stage 7 to stage 10 and can be divided into three steps (Figure 6). First, an asymmetry of the Par network is established, with Par-1 at the posterior and Bazooka/Par6/aPKC complex at the anterior cortex. Next, Par-1 inhibits microtubule nucleation at the posterior, which polarizes the microtubule cytoskeleton. Finally, motor protein-based transport of mRNAs on a polarized microtubule network leads to asymmetric mRNA localization.

### Polarization of the Par Protein Network

The first sign of Par polarity is the appearance of a Par-1 crescent at the posterior of the oocyte at stage 7 of oogenesis (Shulman et al., 2000; Tomancak et al., 2000). Interestingly, at this stage Bazooka and Par-6 are also detected at the posterior, where they colocalize with Par-1. During stages 8 and 9, the Par-1 crescent intensifies and expands, while Bazooka and Par-6 gradually disappear from the posterior, and re-localize to the anterolateral cortex during stage 9 (Doerflinger et al., 2010; Jouette et al., 2019). Two other Par proteins, Par-4/LKB1 and Par-5/14-3-3, do not show any polarized distribution. Par-4 is uniformly distributed around the cortex (Martin and St Johnston, 2003), while Par-5 is detected in the cytoplasm (Benton et al., 2002). In addition to Par proteins, tumor suppressor Lethal (2) giant larvae (Lgl) is required for the polarization of the oocyte. Lgl also shows a polarized distribution and localizes to the posterior of the oocyte (Figure 6) (Tian and Deng, 2008; Doerflinger et al., 2010).

According to the current model, the Par polarity in the oocyte is maintained by mutual phosphorylation of posterior and anterior Par proteins. At the posterior, the main kinase is Par-1, which phosphorylates Bazooka to reduce its affinity for, and to exclude it from, the membrane. Since Bazooka is a scaffold

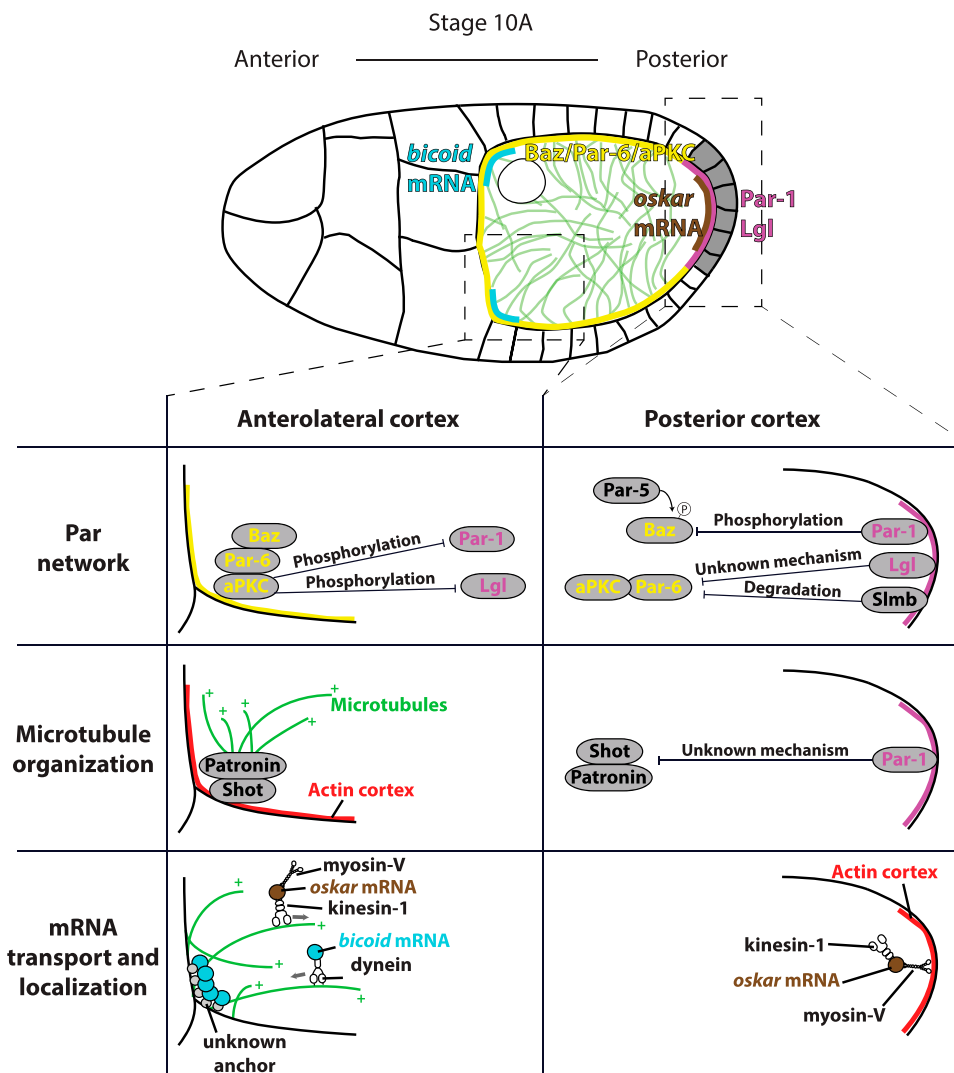


**FIGURE 6 |** Top: overview of anterior-posterior polarization of the oocyte in mid-oogenesis. Signal from PFCs (grey) induces establishment of posterior (magenta) and anterolateral (yellow) Par domains. Par polarity induces polarization of microtubule cytoskeleton (green) by inhibiting microtubule nucleation at the posterior. Polarized microtubule cytoskeleton directs delivery of *bicoid* mRNAs (blue) to the anterior and *oskar* mRNA (brown) to the posterior. Bottom: Detailed schematics showing three processes necessary for the oocyte polarization. Par network polarity: at the anterior, Bazooka/Par-6/aPKC complex binds to the membrane through interaction between Bazooka and membrane lipids. aPKC phosphorylates both Par-1 and Lgl to exclude them from the anterolateral membrane. At the posterior, Par-1 phosphorylates Bazooka, which is excluded from the posterior membrane following the binding by Par-5. In addition, Lgl and Slimb exclude aPKC/Par-6 complex from the posterior through not well defined mechanisms. Microtubule organization: at the anterior, Shot binds to actin and recruits Patronin. Patronin binds minus ends of existing microtubules, which template growth of new microtubules. At the posterior, Par-1 excludes Shot/Patronin through unknown mechanism to inhibit posterior nucleation of microtubules. mRNA transport and localization: at the anterior, dynein delivers *bicoid* mRNA to the cortex by moving towards the minus ends of the microtubules. *bicoid* is anchored only at the anterior of the oocyte by an unidentified linker. Kinesin-1 removes *oskar* mRNA from the anterolateral cortex by moving towards the plus ends of the microtubules. At the posterior, myosin-V anchors *oskar* mRNA to the cortical actin at the posterior of the oocyte, where the microtubule nucleation is inhibited.

protein that recruits Par-6 and aPKC to the membrane, exclusion of Bazooka also removes Par-6 and aPKC from the posterior. Additionally, Lgl binds to aPKC/Par-6 complex and inhibits aPKC activity. At the anterolateral cortex, aPKC phosphorylates both Par-1 and Lgl to exclude them from this domain (St Johnston and Ahringer, 2010). However, while evidence for some parts of this mechanism is strong, some

have been inferred from other organisms and lack strong support in experiments using the *Drosophila* oocyte.

Evidence that Par-1 is required for Bazooka exclusion from the posterior is convincing. Phosphorylation of Bazooka by Par-1 has been shown both *in vitro*, by using biochemical assays; as well as *in vivo*, in both epithelia and the oocyte. Par-1 phosphorylates Bazooka on two conserved serines to generate a 14-3-3 binding



site. Binding of 14-3-3/Par-5 to Bazooka disrupts its oligomerization and interaction with aPKC (Benton and St Johnston, 2003). In addition, in *par-1* mutants Bazooka is localized all around the oocyte cortex; and a non-phosphorylatable form of Bazooka also shows uniform localization (Benton and St Johnston, 2003; Doerflinger et al., 2010). However, while phosphorylation of Bazooka by Par-1 is essential for its exclusion, it might not be sufficient. At stages 7 and 8, Par-1 and Bazooka co-localize at the posterior, and Bazooka exclusion is only observed at late stage 9 (Doerflinger et al., 2010; Jouette et al., 2019). Recent work has suggested the role of membrane trafficking and dynein-mediated transport in maintenance of Bazooka asymmetry (Jouette et al., 2019).

While the requirement of Par-1 for Bazooka localization is clear, contradicting observations concerning how Bazooka influences Par-1 cortical recruitment have been made. One study reported a *baz* mutant in which Par-1 cortical localization is lost (Becalska and Gavis, 2010). Another study reported that Par-1 localizes all around the cortex in *baz* mutant (Doerflinger et al., 2010). When the conserved aPKC phosphorylation site is mutated, Par-1 localizes all around the cortex (Doerflinger et al., 2006; Doerflinger et al., 2010). Additionally, aPKC, as well as its binding partner Par-6, is excluded from posterior in mid-oogenesis (Doerflinger et al., 2010; Morais-de-Sá et al., 2014). From this, it has been inferred that aPKC phosphorylates Par-1 to exclude it from the anterolateral cortex (Doerflinger et al., 2010). However, direct evidence for the requirement of aPKC and Par-6 in oocyte polarization is still missing. The reasoning behind is that most of the oocytes which are mutant for *apkc* and *par-6* lose their fate and revert to that of nurse cells. This problem has been partially circumvented by studying escapers—egg chambers that overcome the early defects and develop to stage 9–10. By analysing escapers of a strong *apkc* mutant, Tian and Deng (2008) found mislocalization of Stauf in half of the oocytes. Conversely, Doerflinger et al. (2006) reported that these escapers develop normal anterior-posterior axis at stage 9. Similarly, hypomorphic aPKC alleles, which lack either kinase activity or Par-6 binding site, do not cause polarity defects (Kim et al., 2009). Additionally, Huynh et al. (2001b) reported that *par-6* escapers produce normal eggs. More recently, it has been reported that Slmb, the substrate specificity subunit of the SCF E3 ubiquitin ligase, excludes Par-6 and aPKC from the posterior by targeting them for degradation (Morais-de-Sá et al., 2014).

## Polarization of Microtubule Cytoskeleton

While exact mechanisms of Par asymmetry establishment in mid-oogenesis remain unclear, much more is known about the downstream polarity event: the organization of the microtubule cytoskeleton. Initially, microtubule organization in the oocyte was inferred from final distributions of cargoes and motor proteins. This has led to a view that microtubules are highly polarized along the anterior-posterior axis, with minus ends at the anterior, and plus ends at the posterior (Clark et al., 1994; Clark et al., 1997). Immunostaining of microtubules has led to the model of microtubules being nucleated at the anterior and lateral cortex of the oocyte, but not at the posterior (Theurkauf

et al., 1992; Cha et al., 2002; Serbus et al., 2005), while Januschke et al. (2006) proposed that nucleation occurs predominantly from the oocyte nucleus.

Our current understanding of microtubule organization greatly benefited from the use of high-resolution live imaging. Visualization of *oskar* mRNA particles showed that they are transported in all directions, with only a small bias towards the posterior (Zimyanin et al., 2008). This suggested that the microtubule network is only marginally polarized. Parton et al. used live imaging of microtubule plus end marker EB1-GFP to show that the microtubule network is highly dynamic, and only subtly polarized; around 60% of the microtubules grow towards the posterior, and 40% towards the anterior (Parton et al., 2011). At the anterolateral cortex of the oocyte, microtubules are organized by non-centrosomal microtubule organizing centers (ncMTOCs). These ncMTOCs are composed of spectraplakins, Shot and a microtubule minus end-binding protein, Patronin. Shot binds to the cortical f-actin, and recruits Patronin to form cortical ncMTOC (Figure 6). The Shot/Patronin complex does not nucleate microtubules but captures existing microtubule minus ends, which template growth of new microtubules (Nashchekin et al., 2016). A line of studies showed that Par-1 is a major effector of microtubule organization in the oocyte. In *par-1* mutants, the exclusion of Shot and Patronin from the posterior cortex is lost (Nashchekin et al., 2016), as is the suppression of microtubule nucleation at the posterior (Shulman et al., 2000; Parton et al., 2011). In contrast, expression of the non-phosphorylatable form of Par-1, which localizes all around the cortex, causes loss of all cortex-associated microtubules (Doerflinger et al., 2010). Whether Par-1 interacts directly with the Shot/Patronin complex to exclude it from the membrane, or whether it blocks its cortical recruitment through indirect mechanism, remains to be determined.

## Localization of mRNAs

The final step of anterior-posterior polarization of the oocyte is the delivery of *oskar* mRNA to the posterior, and of *bicoid* mRNA to the anterior of the oocyte. It has been known for a long time that the localization of both mRNAs depends on microtubules (Pokrywka and Stephenson, 1991; Clark et al., 1994). These early results led to the model of mRNAs being transported towards the opposite poles by motor proteins moving in opposite directions on a highly polarized microtubule cytoskeleton (Figure 6, bottom). This idea was corroborated with the finding that correct *oskar* mRNA localization requires plus-end directed motor protein kinesin-1 (Brendza et al., 2000), while localization of *bicoid* mRNA is affected when the Dynein/Dynactin complex is disrupted (Duncan and Warrior, 2002; Januschke et al., 2002). However, as it became clear that the microtubule cytoskeleton is not as polarized as was initially assumed, novel mechanisms of mRNA transport and localization have been considered.

Once again, live imaging was essential for our current understanding of this process. As mentioned previously, high-resolution time-lapse imaging and image analysis revealed that *oskar* mRNA localizes by biased random walk along a weakly polarized microtubule cytoskeleton (Zimyanin et al., 2008).

Similarly, Trovisco et al. (2016) found that *bicoid* is randomly transported by dynein walking toward the minus-ends of the microtubules. Computer simulations suggested that the existence of an anterior-posterior gradient of cortical microtubule nucleation is already sufficient to account for the localization of mRNAs (Khuc Trong et al., 2015). However, recent experiments suggested that dynactin is necessary to protect growing plus-ends of MTs from depolymerization, making them long enough for *oskar* to be delivered to the posterior (Nieuwburg et al., 2017). In addition, both *bicoid* and *oskar* mRNAs seem to require anchoring for stable localization. FRAP and photo-conversion experiments of fluorescently labelled *bicoid* mRNA showed slow turnover kinetics of these particles suggesting that they are stably anchored (Trovisco et al., 2016). These observations led the authors to propose that dynein delivers *bicoid* mRNA to a broader anterolateral region by walking towards the minus end of the microtubules. *bicoid* is anchored by an unknown mechanism, which is active only at the anterior, but not at the lateral cortex. The molecular nature of this mechanism is unknown, but it is independent of microtubule dynamics and polarization (Trovisco et al., 2016). Interestingly, *bicoid* mRNA that is injected into the oocyte localizes to the nearest region of anterolateral cortex. When treated with the nurse cell cytoplasm prior to the injection, it properly localizes only at the anterior (Cha et al., 2001). A nurse cell specific factor could bind to mRNA-protein complexes rendering it competent for anterior anchoring (Trovisco et al., 2016). A model that includes anchoring specifically at the anterior can explain why *bicoid* is not found at the lateral cortex. This model also predicts that the microtubule cytoskeleton does not need to be polarized for correct *bicoid* localization. Indeed, *bicoid* localizes correctly in the *shot* mutants, in which the microtubule cytoskeleton is not polarized (Trovisco et al., 2016). However, defects in *bicoid* mRNA localization occur in other mutants in which cytoskeleton polarization is compromised, such as *par-1*, *baz* and *grk* (González-Reyes et al., 1995; Benton et al., 2002; Doerflinger et al., 2010).

The mechanism of *oskar* mRNA anchoring is far better understood. First, cortical localization of *oskar* is reduced upon F-actin fragmentation (Cha et al., 2002) and depends on the actin-based motor, myosin-V (*didum* in *Drosophila*) (Krauss et al., 2009). This suggested that myosin-V could be part of an anchoring machinery. However, since both myosin-V and actin are uniformly distributed throughout the oocyte cortex, it was unclear how they can anchor *oskar* mRNA specifically at the posterior. To elucidate the mechanism of *oskar* mRNA transport and anchoring, Lu et al. (2020) analysed the localization of Staufen in different kinesin-1 and myosin-V mutants. According to the model proposed by Lu et al. (2020) (Figure 6, bottom), *oskar* mRNA is transported by kinesin-1 towards the plus-ends of microtubules, followed by anchoring at the posterior by myosin-V. A stochastic competition between kinesin dependent removal of *oskar* mRNA from the cortex along microtubules and myosin-V anchoring leads to differential

steady-states along the oocyte cortex. While the density of microtubules is high at the anterolateral cortex, kinesin removal wins in that region. At the posterior, where nucleation of microtubules is suppressed, anchoring by myosin-V is predominant (Lu et al., 2020). This model explains why posterior localization of *oskar* can be achieved by myosin dependent anchoring, although myosin localization is not polarized. Furthermore, it explains why *oskar* localization critically depends on the polarization of the microtubule cytoskeleton.

## FUTURE PERSPECTIVES AND FOCUS POINTS

In *Drosophila*, the development from stem cell to mature oocyte is critically determined by a series of spatial decision-making processes. These processes go back to canonical cell polarity events governed by the Par protein network. Despite recent advances in our understanding of cell polarity and the downstream processes leading to cell selection and differentiation, intracellular reorganisation of the oocyte, and body axes formation, several major gaps of knowledge persist. In our view the most critical open questions relate to the interplay between follicle cells and the oocyte. Unlike in other species, for example in *C. elegans*, where polarization of the zygote and first body axis determination occurs cell autonomously, an intimate mechanistic relationship between soma and germline has been retained in *Drosophila*. Most importantly, the identification of the follicle cell signal that determines the second polarity event and body axis formation is long overdue, but all the past studies so far suggest that this would require analyses beyond genetic screens and knockout studies. Biophysical approaches that test the cell-cell interface between oocyte and posterior follicle cells could give new insight.

## AUTHOR CONTRIBUTIONS

AM and IAT created the figures and wrote the manuscript.

## FUNDING

Fundação para a Ciência e Tecnologia (FCT) awarded an individual PhD fellowship 2020.04666.BD to AM, Human Frontiers Science Program (HFSP) awarded grant RGY0083/2016 to IAT supporting AM, and Fundação Calouste Gulbenkian provided core funding support.

## ACKNOWLEDGMENTS

We thank Funding agencies and the host institute (IGC) for their financial support.

## REFERENCES

- Anlas, K., and Trivedi, V. (2021). Studying Evolution of the Primary Body axis *In Vivo* and *In Vitro*. *Elife* 10, e69066. doi:10.7554/elifesciences.69066
- Assa-Kunik, E., Torres, I. L., Schejter, E. D., Johnston, D. S., and Shilo, B.-Z. (2007). *Drosophila* follicle Cells are Patterned by Multiple Levels of Notch Signaling and Antagonism Between the Notch and JAK/STAT Pathways. *Development* 134, 1161–1169. doi:10.1242/dev.02800
- Becalska, A. N., and Gavis, E. R. (2010). Bazooka Regulates Microtubule Organization and Spatial Restriction of Germ Plasm Assembly in the *Drosophila* Oocyte. *Development* 134, 528–538. doi:10.1016/j.ydbio.2010.02.006
- Bénazéraf, B., and Pourquié, O. (2013). Formation and Segmentation of the Vertebrate Body axis. *Annu. Rev. Cell Dev. Biol.* 29, 1–26. doi:10.1146/annurev-cellbio-101011-155703
- Benton, R., and Johnston, D. S. (2003). *Drosophila* PAR-1 and 14-3-3 Inhibit Bazooka/PAR-3 to Establish Complementary Cortical Domains in Polarized Cells. *Cell* 115, 691–704. doi:10.1016/s0092-8674(03)00938-3
- Benton, R., Palacios, I. M., and Johnston, D. S. (2002). *Drosophila* 14-3-3/PAR-5 Is an Essential Mediator of PAR-1 Function in Axis Formation. *Dev. Cell* 3, 659–671. doi:10.1016/s1534-5807(02)00320-9
- Bernard, F., Lepesant, J.-A., and Guichet, A. (2018). Nucleus Positioning within *Drosophila* Egg Chamber. *Semin. Cell Dev. Biol.* 82, 25–33. doi:10.1016/j.semcdb.2017.10.013
- Bolívar, J., Huynh, J. R., López-Schier, H., González, C., St Johnston, D., and González-Reyes, A. (2001). Centrosome Migration into the *Drosophila* Oocyte Is Independent of BicD and Egl, and of the Organisation of the Microtubule Cytoskeleton. *Development* 128, 1889–1897.
- Brendza, R. P., Serbus, L. R., Duffy, J. B., and Saxton, W. M. (2000). A Function for Kinesin I in the Posterior Transport of Oskar mRNA and Staufen Protein. *Science* 289, 2120–2122. doi:10.1126/science.289.5487.2120
- Capdevila, J., Vogan, K. J., Tabin, C. J., and Izpisua Belmonte, J. C. (2000). Mechanisms of Left-Right Determination in Vertebrates. *Cell* 101, 9–21. doi:10.1016/s0092-8674(00)80619-4
- Carpenter, A. T. (1994). Egalitarian and the Choice of Cell Fates in *Drosophila melanogaster* Oogenesis. *Ciba Found. Symp.* 182, 223–254.
- Carpenter, A. T. C. (1975). Electron Microscopy of Meiosis in *Drosophila melanogaster* Females. *Chromosoma* 51, 157–182. doi:10.1007/bf00319833
- Cereijido, M., Contreras, R. G., and Shoshani, L. (2004). Cell Adhesion, Polarity, and Epithelia in the Dawn of Metazoans. *Physiol. Rev.* 84, 1229–1262. doi:10.1152/physrev.00001.2004
- Cha, B.-J., Koppetsch, B. S., and Theurkauf, W. E. (2001). *In Vivo* analysis of *Drosophila* Bicoid mRNA Localization Reveals a Novel Microtubule-dependent axis Specification Pathway. *Cell* 106, 35–46. doi:10.1016/s0092-8674(01)00419-6
- Cha, B.-J., Serbus, L. R., Koppetsch, B. S., and Theurkauf, W. E. (2002). Kinesin I-dependent Cortical Exclusion Restricts Pole Plasm to the Oocyte Posterior. *Nat. Cell Biol.* 4, 592–598. doi:10.1038/ncb832
- Chen, Y., and Schüpbach, T. (2006). The Role of Brinker in Eggshell Patterning. *Mech. Dev.* 123, 395–406. doi:10.1016/j.mod.2006.03.007
- Clark, I. E., Jan, L. Y., and Jan, Y. N. (1997). Reciprocal Localization of Nod and Kinesin Fusion Proteins Indicates Microtubule Polarity in the *Drosophila* Oocyte, Epithelium, Neuron and Muscle. *Development* 124, 461–470. doi:10.1242/dev.124.2.461
- Clark, I., Giniger, E., Ruohola-Baker, H., Jan, L. Y., and Jan, Y. N. (1994). Transient Posterior Localization of a Kinesin Fusion Protein Reflects Anteroposterior Polarity of the *Drosophila* Oocyte. *Curr. Biol.* 4, 289–300. doi:10.1016/s0960-9822(00)00068-3
- Cox, D. N., Lu, B., Sun, T.-Q., Williams, L. T., and Jan, Y. N. (2001a). *Drosophila* Par-1 Is Required for Oocyte Differentiation and Microtubule Organization. *Curr. Biol.* 11, 75–87. doi:10.1016/s0960-9822(01)00027-6
- Cox, D. N., Seyfried, S. A., Jan, L. Y., and Jan, Y. N. (2001b). Bazooka and Atypical Protein Kinase C Are Required to Regulate Oocyte Differentiation in the *Drosophila* Ovary. *Proc. Natl. Acad. Sci. U.S.A.* 98, 14475–14480. doi:10.1073/pnas.261565198
- Cox, R. T., and Spradling, A. C. (2003). A Balbiani Body and the Fusome Mediate Mitochondrial Inheritance during *Drosophila* oogenesis. *Development* 130, 1579–1590. doi:10.1242/dev.00365
- De Cuevas, M., Lilly, M., and Spradling, A. (1997). Germline Cyst Formation in *Drosophila*. *Annu. Rev. Genet.* 31, 405–428. doi:10.1146/annurev.genet.31.1.405
- De Cuevas, M., and Spradling, A. C. (1998). Morphogenesis of the *Drosophila* Fusome and its Implications for Oocyte Specification. *Development* 125, 2781–2789. doi:10.1242/dev.125.15.2781
- Deng, W.-M., Althaus, C., and Ruohola-Baker, H. (2001). Notch-Delta Signaling Induces a Transition from Mitotic Cell Cycle to Endocycle in *Drosophila* follicle Cells. *Development* 128, 4737–4746. doi:10.1242/dev.128.23.4737
- Deng, W.-M., Schneider, M., Frock, R., Castillejo-Lopez, C., Gaman, E. A., Baumgartner, S., et al. (2003). Dystroglycan Is Required for Polarizing the Epithelial Cells and the Oocyte in *Drosophila*. *Development* 130, 173–184. doi:10.1242/dev.00199
- Deng, W., and Lin, H. (1997). Spectrosomes and Fusomes Anchor Mitotic Spindles During Asymmetric Germ Cell Divisions and Facilitate the Formation of a Polarized Microtubule Array for Oocyte Specification in *Drosophila*. *Development* 125, 79–94. doi:10.1006/dbio.1997.8669
- Doerflinger, H., Benton, R., Torres, I. L., Zwart, M. F., and St Johnston, D. (2006). *Drosophila* Anterior-Posterior Polarity Requires Actin-dependent PAR-1 Recruitment to the Oocyte Posterior. *Curr. Biol.* 16, 1090–1095. doi:10.1016/j.cub.2006.04.001
- Doerflinger, H., Vogt, N., Torres, I. L., Mirouse, V., Koch, I., Nüsslein-Volhard, C., et al. (2010). Bazooka Is Required for Polarisation of the *Drosophila* Anterior-Posterior axis. *Development* 137, 1765–1773. doi:10.1242/dev.045807
- Doerflinger, H., Zimyanin, V., and St Johnston, D. (2022). The *Drosophila* Anterior-Posterior axis Is Polarized by Asymmetric Myosin Activation. *Curr. Biol.* 32, 374–385.e4. doi:10.1016/j.cub.2021.11.024
- Duncan, J. E., and Warrior, R. (2002). The Cytoplasmic Dynein and Kinesin Motors Have Interdependent Roles in Patterning the *Drosophila* Oocyte. *Curr. Biol.* 12, 1982–1991. doi:10.1016/s0960-9822(02)01303-9
- Fregoso Lomas, M., Hails, F., Lachance, J. F., and Nilsson, L. A. (2013). Response to the Dorsal Anterior Gradient of EGFR Signaling in *Drosophila* Oogenesis is Prepatterned by Earlier Posterior EGFR Activation. *Cell Rep* 4, 791–802. doi:10.1016/j.celrep.2013.07.038
- Frohnhofer, H. G., and Nüsslein-Volhard, C. (1986). Organization of Anterior Pattern in the *Drosophila* Embryo by the Maternal Gene Bicoid. *Nature* 324, 120–125. doi:10.1038/324120a0
- Frydman, H. M., and Spradling, A. C. (2001). The Receptor-Like Tyrosine Phosphatase Lar Is Required for Epithelial Planar Polarity and for Axis Determination with *Drosophila* Ovarian Follicles. *Development* 128, 3209–3220. doi:10.1242/dev.128.16.3209
- Godt, D., and Tepass, U. (1998). *Drosophila* Oocyte Localization is Mediated by Differential Cadherin-Based Adhesion. *Nature* 395, 387–391. doi:10.1038/26493
- González-Reyes, A., Elliott, H., and St Johnston, D. (1995). Polarization of Both Major Body Axes in *Drosophila* by Gurken-torpedo Signalling. *Nature* 375, 654–658. doi:10.1038/375654a0
- González-Reyes, A., and St Johnston, D. (1998b). Patterning of the Follicle Cell Epithelium along the Anterior-Posterior axis during *Drosophila* Oogenesis. *Development* 125, 2837–2846. doi:10.1242/dev.125.15.2837
- González-Reyes, A., and St Johnston, D. (1994). Role of Oocyte Position in Establishment of Anterior-Posterior Polarity in *Drosophila*. *Science* 266, 639–642. doi:10.1126/science.7939717
- González-Reyes, A., and St Johnston, D. (1998a). The *Drosophila* AP axis Is Polarised by the Cadherin-Mediated Positioning of the Oocyte. *Development* 125, 3635–3644. doi:10.1242/dev.125.18.3635
- Grammont, M., and Irvine, K. D. (2001). fringe and Notch Specify Polar Cell Fate During *Drosophila* oogenesis. *Development* 128, 2243–2253. doi:10.1242/dev.128.12.2243
- Grammont, M., and Irvine, K. D. (2002). Organizer Activity of the Polar Cells During *Drosophila* oogenesis. *Development* 129, 5131–5140. doi:10.1242/dev.129.22.5131
- Grieder, N. C., de Cuevas, M., and Spradling, A. C. (2000). The Fusome Organizes the Microtubule Network During Oocyte Differentiation in *Drosophila*. *Development* 127, 4253–4264. doi:10.1242/dev.127.19.4253

- Guichet, A., Peri, F., and Roth, S. (2001). Stable Anterior Anchoring of the Oocyte Nucleus Is Required to Establish Dorsoventral Polarity of the *Drosophila* Egg. *Develop. Biol.* 237, 93–106. doi:10.1006/dbio.2001.0354
- Huynh, J.-R., Petronczki, M., Knoblich, J. A., and Johnston, D. S. (2001b). Bazooka and PAR-6 Are Required with PAR-1 for the Maintenance of Oocyte Fate in *Drosophila*. *Curr. Biol.* 11, 901–906. doi:10.1016/s0960-9822(01)00244-5
- Huynh, J.-R., and St Johnston, D. (2004). The Origin of Asymmetry : Early Polarisation of the *Drosophila* Germline Cyst and Oocyte. *Curr. Biol.* 14, 438–449. doi:10.1016/j.cub.2004.05.040
- Huynh, J. R., Shulman, J. M., Benton, R., and St Johnston, D. (2001a). PAR-1 Is Required for the Maintenance of Oocyte Fate in *Drosophila*. *Development* 128, 1201–1209. doi:10.1242/dev.128.7.1201
- Huynh, J., and St Johnston, D. (2000). The Role of BicD, Egl, Orb and the Microtubules in the Restriction of Meiosis to the *Drosophila* Oocyte. *Development* 127, 2785–2794. doi:10.1242/dev.127.13.2785
- Januschke, J., Gervais, L., Dass, S., Kaltschmidt, J. A., Lopez-Schier, H., Johnston, D. S., et al. (2002). Polar Transport in the *Drosophila* Oocyte Requires Dynein and Kinesin I Cooperation. *Curr. Biol.* 12, 1971–1981. doi:10.1016/s0960-9822(02)01302-7
- Januschke, J., Gervais, L., Gillet, L., Keryer, G., Bornens, M., and Guichet, A. (2006). The Centrosome-Nucleus Complex and Microtubule Organization in the *Drosophila* Oocyte. *Development* 133, 129–139. doi:10.1242/dev.02179
- Jouette, J., Guichet, A., and Claret, S. B. (2019). Dynein-mediated Transport and Membrane Trafficking Control PAR3 Polarised Distribution. *Elife* 8, e402128. doi:10.7554/eLife.40212
- Khuc Trong, P., Doerflinger, H., Dunkel, J., St Johnston, D., and Goldstein, R. E. (2015). Cortical Microtubule Nucleation Can Organise the Cytoskeleton of *Drosophila* Oocytes to Define the Anteroposterior Axis. *Elife* 4, e06088. doi:10.7554/eLife.06088
- Kim, S., Gailite, I., Moussian, B., Luschnig, S., Goette, M., Fricke, K., et al. (2009). Kinase-activity-independent Functions of Atypical Protein Kinase C in *Drosophila*. *J. Cell Sci.* 122, 3759–3771. doi:10.1242/jcs.052514
- Kimelman, D., and Martin, B. L. (2012). Anterior-posterior Patterning in Early Development: Three Strategies. *Wiley Interdiscip. Rev. Dev. Biol.* 1 (253–266), 253–266. doi:10.1002/wdev.25
- Knoblich, J. A. (2008). Mechanisms of Asymmetric Stem Cell Division. *Cell* 132, 583–597. doi:10.1016/j.cell.2008.02.007
- Krauss, J., López de Quinto, S., Nüsslein-Volhard, C., and Ephrussi, A. (2009). Myosin-V Regulates Oskar mRNA Localization in the *Drosophila* Oocyte. *Curr. Biol.* 19, 1058–1063. doi:10.1016/j.cub.2009.04.062
- Lang, C. F., and Munro, E. (2017). The PAR Proteins: from Molecular Circuits to Dynamic Self-Stabilizing Cell Polarity. *Development* 144, 3405–3416. doi:10.1242/dev.139063
- Lehmann, R., and Nüsslein-Volhard, C. (1986). Abdominal Segmentation, Pole Cell Formation, and Embryonic Polarity Require the Localized Activity of Oskar, a Maternal Gene in *Drosophila*. *Cell* 47, 141–152. doi:10.1016/0092-8674(86)90375-2
- Leibfried, A., Müller, S., and Ephrussi, A. (2013). A Cdc42-Regulated Actin Cytoskeleton Mediates *Drosophila* Oocyte Polarization. *Development* 140, 362–371. doi:10.1242/dev.089250
- Lin, H., and Spradling, A. C. (1995). Fusome Asymmetry and Oocyte Determination in *Drosophila*. *Dev. Genet.* 16, 6–12. doi:10.1002/dvg.1020160104
- Lin, H., Yue, L., and Spradling, A. C. (1994). The *Drosophila* Fusome, a Germline-specific Organelle, Contains Membrane Skeletal Proteins and Functions in Cyst Formation. *Development* 120, 947–956. doi:10.1242/dev.120.4.947
- López-Schier, H., and St Johnston, D. (2001). Delta Signaling from the Germ Line *Drosophila* Oogenesis of the Somatic Follicle Cells during Controls the Proliferation and Differentiation. *Genes Dev.* 15, 1393–1405.
- Lu, W., Lakonishok, M., Liu, R., Billington, N., Rich, A., Glotzer, M., et al. (2020). Competition between Kinesin-1 and Myosin-V Defines *Drosophila* Posterior Determination. *Elife* 9, e54216. doi:10.7554/eLife.54216
- Mach, J. M., and Lehmann, R. (1997). An Egalitarian-BicaudalD Complex Is Essential for Oocyte Specification and axis Determination in *Drosophila*. *Genes Dev.* 11, 423–435. doi:10.1101/gad.11.4.423
- Martin, S. G., and St Johnston, D. (2003). A Role for *Drosophila* LKB1 in Anterior-Posterior axis Formation and Epithelial Polarity. *Nature* 421, 379–384. doi:10.1038/nature01296
- McGrail, M., and Hays, T. S. (1997). The Microtubule Motor Cytoplasmic Dynein Is Required for Spindle Orientation during Germline Cell Divisions and Oocyte Differentiation in *Drosophila*. *Development* 124, 2409–2419. doi:10.1242/dev.124.12.2409
- McGregor, J. R., Xi, R., and Harrison, D. A. (2002). JAK Signaling is Somatically Required for Follicle Cell Differentiation in *Drosophila*. *Development* 129, 705–717. doi:10.1242/dev.129.3.705
- Meinhardt, H. (2006). Primary Body Axes of Vertebrates: Generation of a Near-Cartesian Coordinate System and the Role of Spemann-Type Organizer. *Dev. Dyn.* 235, 2907–2919. doi:10.1002/dvdy.20952
- Merkle, J. A., Wittes, J., and Schüpbach, T. (2020). Signaling Between Somatic Follicle Cells and the Germline Patterns the Egg and Embryo of *Drosophila*. *Curr. Top. Develop. Biol.* 140, 55–86. doi:10.1016/bs.ctdb.2019.10.004
- Morais-de-Sá, E., Mukherjee, A., Lowe, N., and St Johnston, D. (2014). Slmb Antagonises the aPKC/Par-6 Complex to Control Oocyte and Epithelial Polarity. *Development* 141, 2984–2992. doi:10.1242/dev.109827
- Morimoto, A. M., Jordan, K. C., Tietze, K., Britton, J. S., O'Neill, E. M., and Ruohola-Baker, H. (1996). Pointed, an ETS Domain Transcription Factor, Negatively Regulates the EGF Receptor Pathway in *Drosophila* Oogenesis. *Development* 122, 3745–3754. doi:10.1242/dev.122.12.3745
- Nashchekin, D., Busby, L., Jakobs, M., Squires, I., and St Johnston, D. (2021). Symmetry Breaking in the Female Germline Cyst. *Science* 374, 874–879. doi:10.1126/science.abj3125
- Nashchekin, D., Fernandes, A. R., and St Johnston, D. (2016). Patronin/Shot Cortical Foci Assemble the Noncentrosomal Microtubule Array that Specifies the *Drosophila* Anterior-Posterior Axis. *Dev. Cell* 38, 61–72. doi:10.1016/j.devcel.2016.06.010
- Navarro, C., Puthalakath, H., Adams, J. M., Strasser, A., and Lehmann, R. (2004). Egalitarian Binds Dynein Light Chain to Establish Oocyte Polarity and Maintain Oocyte Fate. *Nat. Cell Biol.* 6, 427–435. doi:10.1038/ncb1122
- Neuman-Silberberg, F. S., and Schüpbach, T. (1993). The *drosophila* Dorsoventral Patterning Gene Gurken Produces a Dorsally Localized RNA and Encodes a TGF $\alpha$ -Like Protein. *Cell* 75, 165–174. doi:10.1016/s0092-8674(05)80093-5
- Nieuwburg, R., Nashchekin, D., Jakobs, M., Carter, A. P., Khuc Trong, P., Goldstein, R. E., et al. (2017). Localised Dynactin Protects Growing Microtubules to Deliver Oskar mRNA to the Posterior Cortex of the *Drosophila* Oocyte. *Elife* 6, e27237. doi:10.7554/eLife.27237
- Pai, L.-M., Barcelo, G., and Schüpbach, T. (2000). D-cbl, a Negative Regulator of the Egfr Pathway, is Required for Dorsoventral Patterning in *Drosophila* Oogenesis. *Cell* 103, 51–61. doi:10.1016/s0092-8674(00)00104-5
- Parton, R. M., Hamilton, R. S., Ball, G., Yang, L., Cullen, C. F., Lu, W., et al. (2011). A PAR-1-dependent Orientation Gradient of Dynamic Microtubules Directs Posterior Cargo Transport in the *Drosophila* Oocyte. *J. Cell Biol.* 194, 121–135. doi:10.1083/jcb.201103160
- Pokrywka, N. J., and Stephenson, E. C. (1991). Microtubules Mediate the Localization of Bicoid RNA during *Drosophila* Oogenesis. *Development* 113, 55–66. doi:10.1242/dev.113.1.55
- Rodriguez-Boulán, E., and Macara, I. G. (2014). Organization and Execution of the Epithelial Polarity Programme. *Nat. Rev. Mol. Cell Biol.* 15, 225–242. doi:10.1038/nrm3775
- Roignot, J., Peng, X., and Mostov, K. (2013). Polarity in Mammalian Epithelial Morphogenesis. *Cold Spring Harb. Perspect. Biol.* 5, 1–16. doi:10.1101/cshperspect.a013789
- Röper, K., and Brown, N. H. (2004). A Spectraplakins is Enriched on the Fusome and Organizes Microtubules during Oocyte Specification in *Drosophila*. *Curr. Biol.* 14, 99–110. doi:10.1016/j.cub.2003.12.056
- Roth, S., Jordan, P., and Karess, R. (1999). Binuclear *Drosophila* Oocytes: Consequences and Implications for Dorsal-Ventral Patterning in Oogenesis and Embryogenesis. *Development* 126, 927–934. doi:10.1242/dev.126.5.927
- Roth, S., and Lynch, J. A. (2009). Symmetry Breaking during *Drosophila* Oogenesis. *Cold Spring Harbor Perspect. Biol.* 1, a001891. doi:10.1101/cshperspect.a001891
- Roth, S., Shira Neuman-Silberberg, F., Barcelo, G., and Schüpbach, T. (1995). Cornichon and the EGF Receptor Signaling Process Are Necessary for Both Anterior-Posterior and Dorsal-Ventral Pattern Formation in *Drosophila*. *Cell* 81, 967–978. doi:10.1016/0092-8674(95)90016-0
- Ruohola, H., Bremer, K. A., Baker, D., Swedlow, J. R., Jan, L. Y., and Jan, Y. N. (1991). Role of Neurogenic Genes in Establishment of Follicle Cell Fate and



- Oocyte Polarity during Oogenesis in *Drosophila*. *Cell* 66, 433–449. doi:10.1016/0092-8674(81)90008-8
- Ruohola-Baker, H., Jan, L. Y., and Jan, Y. N. (1994). The Role of Gene Cassettes in axis Formation during *Drosophila* Oogenesis. *Trends Genet.* 10, 89–94. doi:10.1016/0168-9525(94)90231-3
- Rust, K., and Nystul, T. (2020). Signal Transduction in the Early *Drosophila* Follicle Stem Cell Lineage. *Curr. Opin. Insect Sci.* 37, 39–48. doi:10.1016/j.cois.2019.11.005
- Schüpbach, T. (1987). Germ Line and Soma Cooperate during Oogenesis to Establish the Dorsoventral Pattern of Egg Shell and Embryo in *Drosophila melanogaster*. *Cell* 49, 699–707. doi:10.1016/0092-8674(87)90546-0
- Serbus, L. R., Cha, B.-J., Theurkauf, W. E., and Saxton, W. M. (2005). Dynein and the Actin Cytoskeleton Control Kinesin-Driven Cytoplasmic Streaming in *Drosophila* oocytes. *Development* 132, 3743–3752. doi:10.1242/dev.01956
- Shulman, J. M., Benton, R., and St Johnston, D. (2000). The *Drosophila* Homolog of *C. elegans* PAR-1 Organizes the Oocyte Cytoskeleton and Directs Oskar mRNA Localization to the Posterior Pole. *Cell* 101, 377–388. doi:10.1016/S0092-8674(00)80848-X
- St Johnston, D., and Ahringer, J. (2010). Cell Polarity in Eggs and Epithelia: Parallels and Diversity. *Cell* 141, 757–774. doi:10.1016/j.cell.2010.05.011
- St Johnston, D., Beuchle, D., and Nüsslein-Volhard, C. (1991). Staufén, a Gene Required to Localize Maternal RNAs in the *Drosophila* Egg. *Cell* 66, 51–63. doi:10.1016/0092-8674(91)90138-0
- St Johnston, D. (2018). Establishing and Transducing Cell Polarity: Common Themes and Variations. *Curr. Opin. Cell Biol.* 51, 33–41. doi:10.1016/j.celb.2017.10.007
- Stevens, N. R., Raposo, A. A. S. F., Basto, R., St Johnston, D., and Raff, J. W. (2007). From Stem Cell to Embryo without Centrioles. *Curr. Biol.* 17, 1498–1503. doi:10.1016/j.cub.2007.07.060
- Sun, Y., Yan, Y., Deneff, N., and Schüpbach, T. (2011). Regulation of Somatic Myosin Activity by Protein Phosphatase 1 $\beta$  Controls *Drosophila* Oocyte Polarization. *Development* 138, 1991–2001. doi:10.1242/dev.062190
- Suter, B., and Steward, R. (1991). Requirement for Phosphorylation and Localization of the Bicaudal-D Protein in *Drosophila* Oocyte Differentiation. *Cell* 67, 917–926. doi:10.1016/0092-8674(91)90365-6
- Theurkauf, W. E., Alberts, B. M., Jan, Y. N., and Jongens, T. A. (1993). A central Role for Microtubules in the Differentiation of *Drosophila* Oocytes. *Development* 118, 1169–1180. doi:10.1242/dev.118.4.1169
- Theurkauf, W. E., Smiley, S., Wong, M. L., and Alberts, B. M. (1992). Reorganization of the Cytoskeleton during *Drosophila* Oogenesis: Implications for axis Specification and Intercellular Transport. *Development* 115, 923–936. doi:10.1242/dev.115.4.923
- Tian, A.-G., and Deng, W.-M. (2008). Lgl and its Phosphorylation by aPKC Regulate Oocyte Polarity Formation in *Drosophila*. *Development* 135, 463–471. doi:10.1242/dev.016253
- Tissot, N., Lepesant, J.-A., Bernard, F., Legent, K., Bosveld, F., Martin, C., et al. (2017). Distinct Molecular Cues Ensure a Robust Microtubule-dependent Nuclear Positioning in the *Drosophila* Oocyte. *Nat. Commun.* 8, 15168. doi:10.1038/ncomms15168
- Tomancak, P., Piano, F., Riechmann, V., Gunsalus, K. C., Kempthues, K. J., and Ephrussi, A. (2000). A *Drosophila melanogaster* Homologue of *Caenorhabditis elegans* Par-1 Acts at an Early Step in Embryonic-axis Formation. *Nat. Cell Biol.* 2, 458–460. doi:10.1038/35017101
- Torres, I. L., López-Schier, H., and Johnston, D. S. (2003). A notch/delta-dependent Relay Mechanism Establishes Anterior-Posterior Polarity in *Drosophila*. *Dev. Cell* 5, 547–558. doi:10.1016/S1534-5807(03)00272-7
- Trovisco, V., Belaya, K., Nashchekin, D., Irion, U., Sirinakakis, G., Butler, R., et al. (2016). Bicoid mRNA Localises to the *Drosophila* Oocyte Anterior by Random Dynein-Mediated Transport and Anchoring. *Elife* 5, e17537. doi:10.7554/eLife.17537
- TwoRoger, M., Larkin, M. K., Bryant, Z., and Ruohola-Baker, H. (1999). Mosaic Analysis in the *Drosophila* Ovary Reveals a Common Hedgehog-Inducible Precursor Stage for Stalk and Polar Cells. *Genetics* 151, 739–748. doi:10.1093/genetics/151.2.739
- Vaccari, T., and Ephrussi, A. (2002). The Fusome and Microtubules Enrich Par-1 in the Oocyte, where it Effects Polarization in Conjunction with Par-3, BicD, Egl, and Dynein. *Curr. Biol.* 12, 1524–1528. doi:10.1016/S0960-9822(02)01079-5
- Venkei, Z. G., and Yamashita, Y. M. (2018). Emerging Mechanisms of Asymmetric Stem Cell Division. *J. Cell Biol.* 217, 3785–3795. doi:10.1083/jcb.201807037
- Villa-Fombuena, G., Lobo-Pecellín, M., Mariñ-Menguiano, M., Rojas-Ríos, P., and González-Reyes, A. (2021). Live Imaging of the *Drosophila* Ovarian Niche Shows Spectrosome and Centrosome Dynamics during Asymmetric Germline Stem Cell Division. *Development* 148, 18. doi:10.1242/dev.199716
- Wittes, J., and Schüpbach, T. (2019). A Gene Expression Screen in *Drosophila melanogaster* Identifies Novel JAK/STAT and EGFR Targets during Oogenesis. *G3* 9, 47–60. doi:10.1534/g3.118.200786
- Wu, X., Tanwar, P. S., and Raftery, L. A. (2008). *Drosophila* Follicle Cells: Morphogenesis in an Eggshell. *Semin. Cell Develop. Biol.* 19, 271–282. doi:10.1016/j.semcdb.2008.01.004
- Xi, R., McGregor, J. R., and Harrison, D. A. (2003). A Gradient of JAK Pathway Activity Patterns the Anterior-Posterior axis of the Follicular Epithelium. *Dev. Cell* 4, 167–177. doi:10.1016/S1534-5807(02)00412-4
- Zhao, T., Graham, O. S., Raposo, A., and St Johnston, D. (2012). Growing Microtubules Push the Oocyte Nucleus to Polarize the *Drosophila* Dorsal-Ventral Axis. *Science* 336, 999–1003. doi:10.1126/science.1219147
- Zimyanin, V. L., Belaya, K., Pecreaux, J., Gilchrist, M. J., Clark, A., Davis, I., et al. (2008). *In Vivo* Imaging of Oskar mRNA Transport Reveals the Mechanism of Posterior Localization. *Cell* 134, 843–853. doi:10.1016/j.cell.2008.06.053

**Conflict of Interest:** The authors declare that the research was conducted in the absence of any commercial or financial relationships that could be construed as a potential conflict of interest.

**Publisher's Note:** All claims expressed in this article are solely those of the authors and do not necessarily represent those of their affiliated organizations, or those of the publisher, the editors and the reviewers. Any product that may be evaluated in this article, or claim that may be made by its manufacturer, is not guaranteed or endorsed by the publisher.

Copyright © 2022 Milas and Telley. This is an open-access article distributed under the terms of the Creative Commons Attribution License (CC BY). The use, distribution or reproduction in other forums is permitted, provided the original author(s) and the copyright owner(s) are credited and that the original publication in this journal is cited, in accordance with accepted academic practice. No use, distribution or reproduction is permitted which does not comply with these terms.



# Won't You be My Neighbor: How Epithelial Cells Connect Together to Build Global Tissue Polarity

Lauren E. Cote and Jessica L. Feldman\*

Department of Biology, Stanford University, Stanford, CA, United States

## OPEN ACCESS

### Edited by:

Josana Rodriguez,  
Newcastle University, United Kingdom

### Reviewed by:

Clare Buckley,  
University of Cambridge,  
United Kingdom  
Jeff Hardin,  
University of Wisconsin-Madison,  
United States

### \*Correspondence:

Jessica L. Feldman  
feldmanj@stanford.edu

### Specialty section:

This article was submitted to  
Morphogenesis and Patterning,  
a section of the journal  
Frontiers in Cell and Developmental  
Biology

**Received:** 01 March 2022

**Accepted:** 30 May 2022

**Published:** 21 June 2022

### Citation:

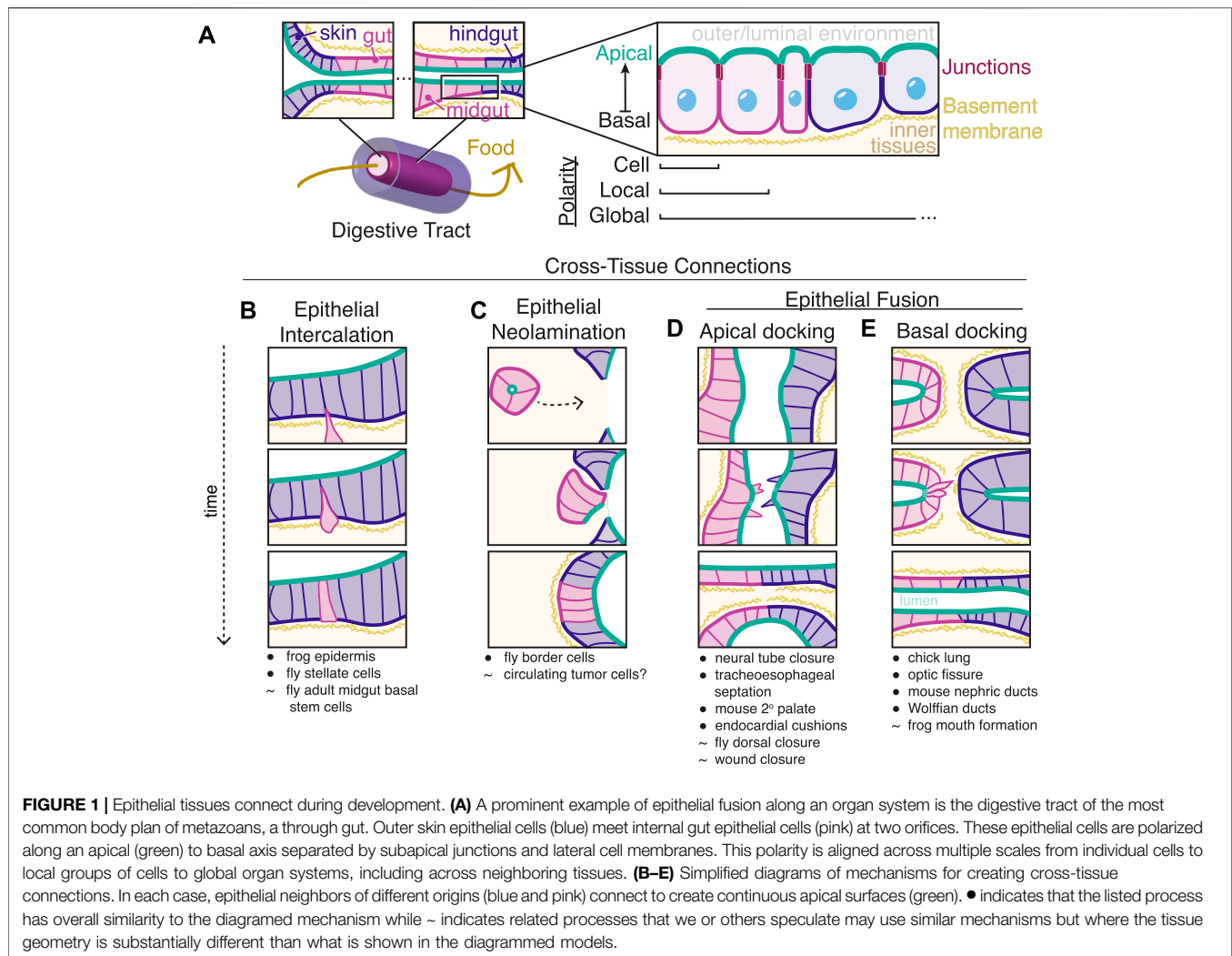
Cote LE and Feldman JL (2022) Won't  
You be My Neighbor: How Epithelial  
Cells Connect Together to Build Global  
Tissue Polarity.  
Front. Cell Dev. Biol. 10:887107.  
doi: 10.3389/fcell.2022.887107

Epithelial tissues form continuous barriers to protect against external environments. Within these tissues, epithelial cells build environment-facing apical membranes, junction complexes that anchor neighbors together, and basolateral surfaces that face other cells. Critically, to form a continuous apical barrier, neighboring epithelial cells must align their apico-basolateral axes to create global polarity along the entire tissue. Here, we will review mechanisms of global tissue-level polarity establishment, with a focus on how neighboring epithelial cells of different origins align their apical surfaces. Epithelial cells with different developmental origins and/or that polarize at different times and places must align their respective apico-basolateral axes. Connecting different epithelial tissues into continuous sheets or tubes, termed epithelial fusion, has been most extensively studied in cases where neighboring cells initially dock at an apical-to-apical interface. However, epithelial cells can also meet basal-to-basal, posing several challenges for apical continuity. Pre-existing basement membrane between the tissues must be remodeled and/or removed, the cells involved in docking are specialized, and new cell-cell adhesions are formed. Each of these challenges can involve changes to apico-basolateral polarity of epithelial cells. This minireview highlights several *in vivo* examples of basal docking and how apico-basolateral polarity changes during epithelial fusion. Understanding the specific molecular mechanisms of basal docking is an area ripe for further exploration that will shed light on complex morphogenetic events that sculpt developing organisms and on the cellular mechanisms that can go awry during diseases involving the formation of cysts, fistulas, atresias, and metastases.

**Keywords:** epithelial fusion, tissue polarity, apical polarity, basal docking, *in vivo*, cell-cell adhesion, lumenogenesis

## INTRODUCTION

The fundamental function of epithelial cells is to encase internal tissues to protect them from external challenges while allowing for regulated interactions with the environment. A defining feature of metazoan epithelial tissues is the polarization of cells so that the plasma membrane is divided into an apical surface that faces the “external” environment (e.g., the lumen of an epithelial tube or outside of an epithelial sheet) and a basolateral surface that faces internal tissues [reviewed in (Pickett et al., 2019; Buckley and St Johnston, 2022)]. Cell-cell junctions that reside just below the apical surface tightly link epithelial cells together and provide a selectively permeable barrier [reviewed in (Vasquez et al., 2021)]. Thus, to achieve epithelial integrity, epithelial cells must coordinate apico-basolateral polarity with their cellular neighbors during development, often requiring the coordination of cells



from different developmental origins to form functional, continuous epithelial tissues that sustain multicellular life.

As an example, consider the formation of the most common basic body plan present in bilaterian animals (Dunn et al., 2014), a “through gut” with two orifices opening to the external environment at either end (**Figure 1A**). At the ends of a through gut, the internal endoderm-derived digestive tissues must connect with external ectoderm-derived epithelial tissues and throughout the digestive tract different tissues (foregut, midgut, hindgut) must connect to create a continuous apical surface. At each of these tissue-tissue interfaces, neighboring cells must align along a common apico-basolateral axis. The ability to form and align such cross-tissue connections correctly is a common requirement in development and defects in these processes can lead to a wide variety of developmental diseases such as oesophageal atresia (van Lennep et al., 2019), spina bifida (Copp et al., 2015), ocular coloboma (Gregory-Evans et al., 2004), congenital abnormalities of the kidney and urinary tract (Murugapopathy and Gupta, 2020), and persistent cloaca (Escobar et al., 2007). Crohn’s disease patients often develop improper cross-tissue connections (fistulas) between rectal and nearby epithelia

(Scharl and Rogler, 2014). The integration of epithelial metastases into foreign tissue (Tsai et al., 2012; Somarelli et al., 2016; Lambert et al., 2017) could also be a type of improper cross-tissue connection.

Connecting different epithelial tissues together requires the coordination of apico-basolateral polarity across multiple scales (**Figure 1A**). At the scale of the individual cell in an epithelial tissue, an epithelial cell is polarized along its own apico-basolateral axis. A nonadherent apical membrane interacts with the outside or luminal environment and is marked by proteins of the conserved PAR and Crumbs complexes, while the basal surface faces internal tissues and interacts with a specialized extracellular matrix called the basement membrane, primarily made of laminin and type IV collagen. Cell-cell junctions link cells just below the apical surface and include adherens junctions, which contain many transmembrane proteins, most notably E-cadherin, that link actin cytoskeletons across neighboring cells, and occluding (septate or tight) junctions, which form selectively permeable extracellular barriers between adjacent cells (Garcia et al., 2018). While the components of apical, junctional, lateral, and basal complexes are

broadly conserved, the initial establishment of apico-basolateral polarity is context dependent (Pickett et al., 2019): for instance, the polarization of the *C. elegans* intestine depends upon the presence of the conserved protein scaffold PAR-3, while the *C. elegans* epidermis can polarize in the absence of PAR-3 (Achilleos et al., 2010). During fly gut development, ectodermally-derived epithelial tissues such as the hindgut, require the apical polarity determinant Crumbs while endodermally-derived midgut cells lose Crumbs expression (Tepass et al., 1990; Campbell et al., 2011) and instead rely on interactions with underlying laminin to correctly polarize (Tepass and Hartenstein, 1994; Yarnitzky and Volk, 1995; Pitsidianaki et al., 2021). Regardless of the mechanism for apico-basolateral polarity establishment within cells, molecular circuits maintain polarity through positive feedback and mutual antagonism of apical, junctional, lateral, and basal protein complexes (Pickett et al., 2019; Buckley and St Johnston, 2022).

Apico-basolateral polarization of an epithelial tissue is only functional if neighboring epithelial cells all orient uniformly to form a continuous barrier. At a local scale within a tissue, epithelial cells coordinate with immediate neighbors to align apico-basolateral axes. At a global scale across a tissue and even across entire organ systems such as a through gut digestive tract, this local polarity must be coordinated into a global apico-basolateral polarity that is consistent across all connected epithelial cells, regardless of their origin or their polarity establishment mechanisms (Figure 1A). Recent *in vivo* work has found that local and global polarity establishment are temporally and genetically separable during the development of the *C. elegans* intestine (Pickett et al., 2021). In the absence of PAR-3, local pockets of apical proteins align between neighboring cells in a HMR-1/E-cadherin-dependent manner, leading to a cystic, non-functional intestine that lacks global polarity (Pickett et al., 2021). Global coordination of apical membrane initiation sites to one common lumen involves the location of the midbody after oriented cell divisions and cadherin-mediated mechanisms that are independent of cell division (Jewett and Prekeris, 2018; Buckley and St Johnston, 2022), as shown in cultured cells (Schluter et al., 2009; Li et al., 2014; Lujan et al., 2016; Liang et al., 2022) and zebrafish development (Tawk et al., 2007; Zigman et al., 2011; Rathbun et al., 2020). The existence of mechanisms to align global polarity that involve cell-cell contact between neighboring cells within one tissue raises the question of how neighboring cells of different tissue types or of different origins ensure alignment of apico-basolateral axes across multiple tissues at a global scale.

## New Neighbors Need Polarity Orientation Information

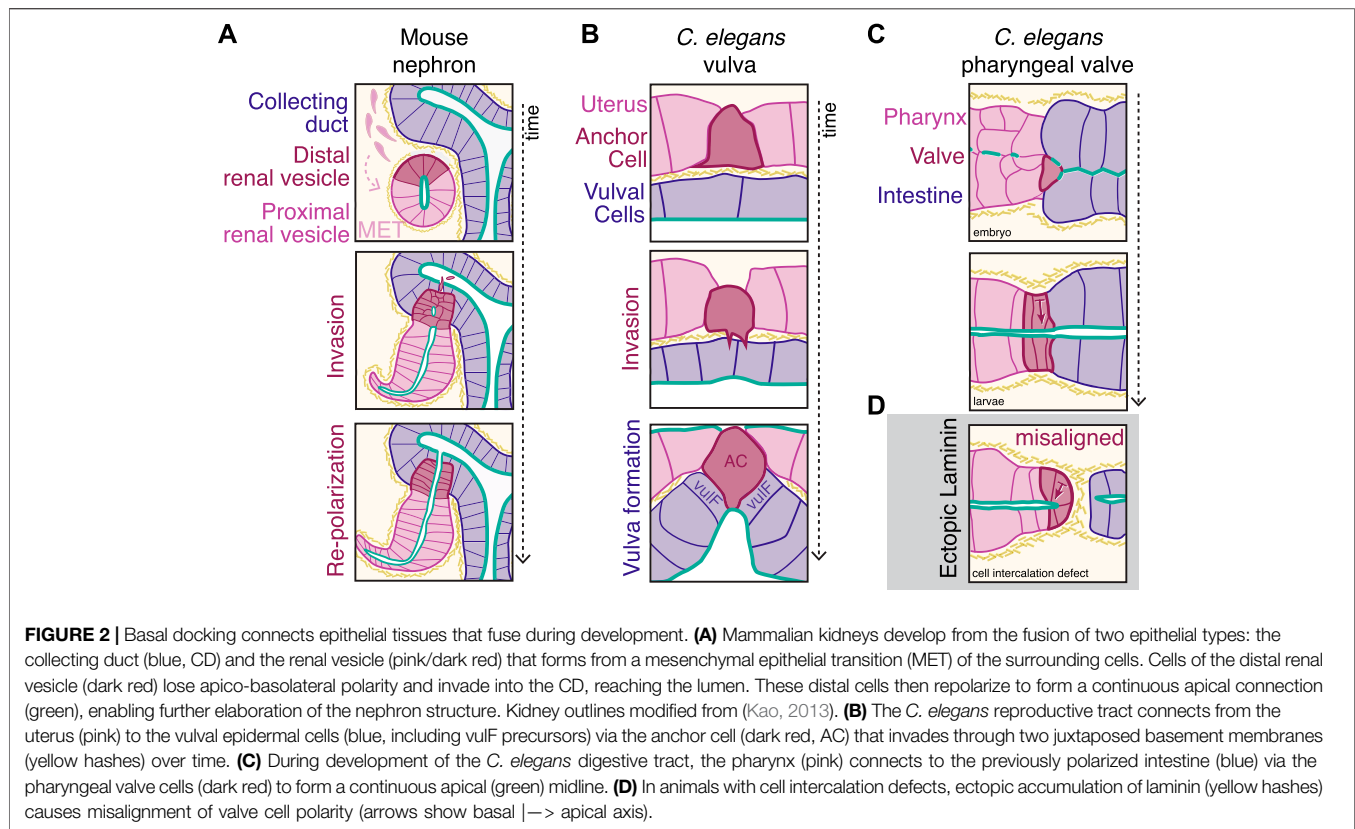
Complex organ formation requires the connection of cells of different types and origins. While the processes of cell division, cell death, cell extrusion, and lateral intercalation *via* neighbor exchange can bring formerly separated epithelial cells next to one another, these processes typically occur within a field of similar cell types with a common developmental origin. Cells of different types and/or origins become new neighbors by various different

ways, some of which are diagrammed in Figures 1B–E and detailed below.

Cells can radially intercalate into an existing epithelium (Figure 1B) to diversify the kinds of cells within the epithelium and to replace old cells (Walck-Shannon and Hardin, 2014). Cells newly joining an epithelium need cues for polarity orientation and/or establishment and these cues can be provided externally by neighboring cells or can arise from within the intercalating cell. In the case of *Drosophila* renal tubes, principal cells (Figure 1B, blue) form an epithelial tube into which secretory stellate cells (Figure 1B, pink) intercalate (Denholm et al., 2003). During this intercalation event, the mesenchymal stellate cells express and localize basal and apical markers only once the cells physically contact the basal and apical domains of the principal cells, respectively (Campbell et al., 2010). In addition to existing epithelia polarizing incoming intercalating cells, existing external structures like the basement membrane can polarize intercalating cells (Chen et al., 2018). In other examples of intercalation, such as in the multiciliated cells of the developing *Xenopus* epidermis, the nascent apical surface is constrained by the geometry of overlying cells and forms an apical surface only at vertices (Stubbs et al., 2006) through directional trafficking of Rab11<sup>+</sup> vesicles (Kim et al., 2012) and through PAR polarity proteins that promote the formation of apical stabilized microtubules (Werner et al., 2014).

Instead of joining tissue types through the intercalation of individual cells, a migrating cluster of cells can join an epithelium *via* a process recently termed neolamination (Miao et al., 2020) (Figure 1C). Neolamination involves the creation of new, specific, and stable cell-cell contacts, in contrast to delamination or the process of cells losing attachment and leaving an epithelium (Miao et al., 2020). Both cell intercalation and neolamination are closely related to mesenchymal-epithelial transitions (MET) (Pei et al., 2019), during which cells lose mobility and gain clear apico-basolateral polarity. Neolamination refers to one specific step at the very end of a migration event and can describe cells undergoing a MET or cells collectively migrating that never lose apicobasal polarity. In the *Drosophila* egg chamber, border cells (Figure 1C, pink) delaminate from the epithelium at one end of the egg chamber, migrate through the egg chamber as a cluster polarized towards a central apical domain, and finally reorient to an open apical domain that integrates with follicular epithelial cells (Figure 1C, blue) to form a continuous epithelium around the oocyte (Mishra et al., 2019). While the signals that promote the initial rearrangement of polarity in this neolamination process are yet to be determined, the border cells stably attach to the oocyte and follicular cells through noncanonical adhesion by innexins, invertebrate gap junctions (Miao et al., 2020). Speculatively, circulating tumor cell clusters (Aceto et al., 2014; Cheung et al., 2016) may undergo a similar neolamination process upon extravasion out of the blood stream and into new tissues. Supporting this hypothesis, the metastatic potential and survival of circulating cells increases with maintenance of E-cadherin (Padmanaban et al., 2019; Na et al., 2020) and only partial but not full loss of epithelial character (Lüönd et al., 2021), which may correspond to the ability of these cells to create more stable cell-cell attachments than more mesenchymal-like metastatic cells in novel environments.





Epithelial tissues can also join on much larger scales when large sheets of cells fuse, fold, and sort to correctly shape organs. Many classical models of epithelial-to-epithelial connection involve epithelial sheets folding to create internal tubes or are cases of epithelial fusion and sorting (Jacinto et al., 2001; Ray and Niswander, 2012; Fagotto, 2015). In these cases, different epithelial cells initially contact each other at their respective apical or sub-apical/junctional surfaces (Figure 1D): examples include murine secondary palate fusion (Farbman, 1968), endocardial cushion formation (Ghyselinck et al., 1998; Ray and Niswander, 2012), neural tube closure (Pai et al., 2012), and tracheoesophageal separation (Billmyre et al., 2015; Kim et al., 2019; Nasr et al., 2019). Many of these processes may mimic aspects of wound closure or *Drosophila* dorsal closure (Kiehart et al., 2017) in which cells connect while maintaining an outward-facing apical surface that requires minor adjustments within cells to reorient towards a new apical surface. Additionally, actin-rich protrusions are often present at the site of apical fusion (Taya et al., 1999; Jacinto et al., 2000; Rolo et al., 2016). Neighboring tissues fusing at the apical surfaces of contacting cells can bring subapical cell-cell junctions into close proximity to promote correct neighbor-neighbor associations (Nikolopoulou et al., 2017). In the case of neural tube closure, neural-epidermal junctions at the point of fusion are rearranged to neural-neural and epidermal-epidermal junctions to separate the epidermis and neural tube. This junctional exchange at heterotypic neural-epidermal contacts is promoted by localized

intracellular Myosin-II contractility in ascidians (Hashimoto and Munro, 2019) or by integrin based adhesions in mice (Escuin et al., 2015; Molè et al., 2020).

While apical-to-apical epithelial fusion events are well-studied, recent investigations of development have revealed instances of basal-to-basal epithelial fusion (Figure 1E), including parabronchial fusion in chick lungs (Palmer and Nelson, 2020), vertebrate optic fissure closure (Chan et al., 2020), urogenital development (Pyati et al., 2006; Chia et al., 2011; Slanchev et al., 2011; Weiss et al., 2014; Hoshi et al., 2018; Mello Santos and Hinton, 2019), and vertebrate mouth formation (Soukup et al., 2013; Chen et al., 2017). This arrangement presents unique challenges including the barrier of the basement membrane between tissues and necessary polarity rearrangements upon fusion. Specific dedicated subsets of cells mediate physical tissue fusion from this end-to-end configuration to promote the formation of continuous epithelial surfaces (Figure 2, dark red specialized cells). The remainder of this minireview will focus on examples of these so-called basal docking events and the strategies cells and tissues use to overcome these challenges to maintain global polarity.

## Basement Membrane Is a Barrier to Docking

A key challenge in connecting epithelial tissues that initially meet basal-to-basal and reorient into a continuous epithelium is that

joining cells must often contend with at least one layer of basement membrane that separates the tissues. During basal docking, the basement membrane presents a physical barrier between the tissues, and regulated basement membrane breakdown is a key general feature of basal docking between epithelial tissues. In mouse kidney development, loss of the basement membrane between the distal renal vesicle cells and the collecting duct is an early step in connecting these two epithelial tissues (Georgas et al., 2009) (**Figure 2A**). In the chicken lung, anterior and posterior parabronchial tubules grow towards one another and fuse to form the continuous bronchial tubes required for respiration (Palmer and Nelson, 2020), which involves basement membrane breakdown. Protrusive Wolffian Duct cells contact the cloacal lumen after basement membrane breakdown and then promote localized apoptosis to create the initial plumbing of the murine urogenital tract (Hoshi et al., 2018). During vertebrate eye development, the process of optic fissure closure to create the optic cup involves basement membrane breakdown (Chan et al., 2020). Ocular coloboma, the failure to fuse the retinal epithelium at the optic fissure, is a significant source of human childhood visual impairment, and a zebrafish model of ocular coloboma showed that matrix metalloprotease secretion from the nearby vasculature is required for fusion (Weaver et al., 2020). During *Xenopus* mouth formation, Hedgehog signaling and Wnt antagonists induce basement membrane breakdown between the ectoderm and endoderm (Dickinson and Sive, 2009; Chen et al., 2017). When basement membrane breakdown is blocked during mouth formation, the tissues that would normally connect no longer have a continuous luminal connection, and the resulting tadpoles are unable to feed (Tabler et al., 2014).

The molecular mechanisms that underlie physical basement membrane breakdown, cellular protrusions, and apico-basolateral polarity orientation to promote tissue fusion are best characterized in the *C. elegans* uterine anchor cell, which invades from the uterus into the vulval epithelium during larval development [reviewed in (Hagedorn and Sherwood, 2011; Sherwood and Plastino, 2018)] (**Figure 2B**). Netrin secretion by the ventral nerve chord (Ziel et al., 2009) polarizes the anchor cell due to clustering of the netrin receptor on the future invasive membrane of the anchor cell at the basement membrane surface (Hagedorn et al., 2009). The polarized anchor cell then invades the underlying vulval epithelium (Sherwood and Sternberg, 2003). The process of invasion involves stabilizing the two juxtaposing uterine and vulval basement membranes (Morrissey et al., 2014), removing basement membrane *via* proteolysis and increasing collagen solubility (Morrissey et al., 2016; Kelley et al., 2019), and forming actin-rich cellular protrusions that are necessary to break through the basement membrane (Caceres et al., 2018). In fact, these cellular protrusions are even strong enough to promote uterus-vulval fusion in the absence of matrix metalloproteases (Kelley et al., 2019).

Although the anchor cell is the major specialized cell that promotes tissue fusion *via* basement membrane breakdown and protrusion formation in this system, the surrounding uterine cells and invaginating vulval cells also play key roles in completing this

morphogenetic event. Surrounding cells help enlarge and then stabilize the breach in the basement membrane created by the invasion process. Uterine cells limit trafficking of a basement membrane receptor to the cell surface to promote basement membrane sliding away from the breach, and the underlying invaginating vulval cells stabilize the edge of the breach *via* integrin-based adhesions (Ihara et al., 2011; McClatchey et al., 2016). As the anchor cell invades, it physically deforms the cell membrane of its newly-contacted neighboring vulval cells (vulF cells) to induce lateral membrane constriction (Yang et al., 2017) to promote the reorientation of their apical surface to form a pointed invagination that will become the vulval lumen (Estes and Hanna-Rose, 2009). How adhesion molecules actually mediate the formation of adherens junctions between the anchor cell and the underlying vulval vulF cells after invasion remain unknown, although recent advances in long-term *in vivo* imaging techniques combined with a tissue-specific conditional allele have shown that EGFR signaling within the anchor cell is required to stabilize and align the nascent adherens junctions that connect the anchor cell to the vulF cells (Spiri et al., 2022). Once the anchor cell-vulval connection is complete, the anchor cell fuses with the neighboring uterine cell syncytium (Sapir et al., 2007) to form a thin hymen that is ruptured upon the worm laying its first egg from the internal reproductive tract into the external environment.

## Basement Membrane can Provide Polarity Information

In addition to presenting a physical challenge to basal docking, laminin-rich basement membranes can function in some systems and cell types as a cue to orient, maintain, and even establish apico-basolateral polarity (Lee and Streuli, 2014; Overeem et al., 2015; Matlin et al., 2017). For example, cysts of cultured MDCK cells grown in the absence of basement-membrane components or which lack integrin-mediated signaling have inverted polarity such that apical surfaces face the substrate instead of the lumen, and this defect in polarity orientation can be rescued by the addition of high levels of exogenous laminin (O'Brien et al., 2001; Yu et al., 2005). In the developing murine mammary gland, apical orientation towards a central lumen is actively maintained by  $\beta$ -integrin after it engages with the basement membrane through endocytic removal and polarized trafficking of apical proteins away from the basal surface (Akhtar and Streuli, 2013). In the absence of laminin, but not other basement membrane components, *C. elegans* pharyngeal cells no longer polarize towards a central common midline to form one lumen but rather invert their apico-basolateral polarity, leading to the formation of two lumens (Rasmussen et al., 2012). In developing *Drosophila* midgut, a specific laminin subunit secreted by the underlying mesoderm is required for the repolarization of migrating endodermal cells (Pitsidianaki et al., 2021). In the adult *Drosophila* midgut, intercalating intestinal stem cells do not require any of the known canonical apical, junctional, or basolateral polarity complexes to establish apico-basolateral polarity, but do rely upon basal integrin signaling to polarize as these cells differentiate into enterocytes and join the intestinal epithelium (Chen et al., 2018).

While these examples show evidence for the role of basement membrane in establishing and maintaining apico-basolateral polarity within individual developing epithelia, other examples show that controlling the initial presence or absence of the basement membrane is crucial for globally aligning fusing epithelial tissues. During *C. elegans* digestive tract development, placement of the basement membrane is important in the connection of the polarized intestine to the polarizing pharyngeal valve cells (**Figure 2C**). At the connection between the pharynx and intestine, the pharyngeal valve cells normally orient towards a central midline, creating a continuous digestive tract. However, when cell-cell contacts between valve cells and the intestine are abnormal (**Figure 2D**), ectopic laminin inappropriately surrounds the entire pharynx, and valve cells misorient to close off the lumen and block the remainder of the digestive tract (Rasmussen et al., 2013). Mutations that disrupt normal cell-cell intercalation patterns and gut ablation experiments indicate that E-cadherin-positive contacts between the valve and intestinal cells normally prevent laminin from accumulating at the interface between these two tissues, thereby promoting the correct connection and alignment between the valve and intestine (Rasmussen et al., 2013). Finally, cells of the pharyngeal valve that self-fuse to create a single-celled tube [pm8, vpi1 (Rasmussen et al., 2008)] follow laminin tracts to spread around the midline (Rasmussen et al., 2013), indicating that spatiotemporal patterning of the basement membrane guides the formation of the digestive tract. The use of cell-cell contacts to prevent or promote basement membrane accumulation may be more broadly used to correctly orient cells during cross-tissue connections in multiple contexts and organisms.

## Specialized Cells Guide Basal-to-Basal Docking

The specialized cells that contact tissue ends and connect at basal surfaces during epithelial fusion are different from the rest of the cells within a tissue (dark red cells, **Figure 2**). A key feature often observed of these specialized cells is the presence of actin-rich protrusions that extend from the basolateral surface and may promote the initial connection between tissues. Some specialized cells maintain aspects of apico-basolateral polarity, such as the preservation of E-cadherin throughout the process of parabronchial tube fusion in the developing chick lung (Palmer and Nelson, 2020). Conversely, in other contexts such as kidney morphogenesis, apico-basolateral polarity is temporarily lost during fusion (Kao et al., 2012; Yang et al., 2013). During basal-to-basal docking of developing chick parabronchial tubes, the cells that mediate epithelial fusion have been identified only by the formation of actin-rich protrusions at the site of basement membrane breakdown (Palmer and Nelson, 2020). How these specific cells send out protrusions while maintaining adherens junctions is unknown, although epithelial cells can send out basolateral protrusions while remodeling junctional contacts (Williams et al., 2014; Walck-Shannon et al., 2015; Sun et al., 2017). Whether the kinds of cellular behaviors present during lateral cell-cell

intercalation within tissues (Huebner and Wallingford, 2018) also function during basal docking will be key areas of future exploration.

Kidney morphogenesis is a particularly well-studied example in which a specialized subset of cells facilitates epithelial fusion. Kidney morphogenesis requires the fusion between two tissues, the ureteric collecting duct epithelium and the renal vesicle, a cyst which coalesces as cells undergo an MET (McMahon, 2016). The distal cells of the renal vesicle nearest to the ureteric duct initiate basal docking in a Notch-dependent manner (dark red cells, **Figure 2A**). Distal cells show a distinct transcriptional profile even from early renal vesicle establishment (Georgas et al., 2009), and lack of distal cells arrests further nephron development after the renal vesicle stage (Kobayashi et al., 2005). Surprisingly, during epithelial fusion with the collecting duct, the distal cells that invade the collecting duct lack apical markers (Kao et al., 2012). After the distal-most cells reach the lumen of the collecting duct, the invading cells repolarize, as seen through the re-expression of E-cadherin, to form local microlumens that eventually combine to form a fully continuous lumen (Georgas et al., 2009; Kao et al., 2012).

Although the identity of these specialized, invasive cells in normal renal development is clear, the cells and/or cues that promote invasive and then repolarization behavior of the distal renal vesicle cells remain unknown (Kao, 2013; Marciano, 2017). Several proteins that influence apico-basolateral polarity in the kidney seem dispensable for parts of the fusion process. Apical continuity and lumen formation in the renal vesicle requires intracellular adherens-junction-associated molecules Afadin (Yang et al., 2013) and p120 catenin (Marciano et al., 2011), however in both cases, removal of either gene in renal vesicle progenitors did not fully inhibit invasion into collecting duct. Cadherin-6 is required globally for robust fusion of the renal vesicle to the ureteric bud (Mah et al., 2000), despite being a canonical marker of later proximal cell fate (Cho et al., 1998), and its specific requirement within the distal cells remains untested. Similar to the kidney, investigations of other basal-to-basal docking events have identified putative specific cells that mediate fusion (optic fissure fusion (Bernstein et al., 2018; Eckert et al., 2020), Wolffian duct (Hoshi et al., 2018), nephric duct (Weiss et al., 2014)), however further work is required to understand the specific roles that polarity and adhesion proteins play within these cells during apico-basolateral polarity maintenance, (re)establishment, and alignment.

## CONCLUDING REMARKS

To form continuous epithelia of the complicated organs found in metazoans, sheets and tubes must fuse and connect. As mesenchymal or other surrounding tissues are likely crucial to promoting correct epithelial connections (Leung et al., 1999; Weiss et al., 2014; Gestri et al., 2018), these processes must be studied within an *in vivo* context with tissue-specific approaches. Consequently, remarkably little is known about the specific adhesion molecules that mediate different *in vivo* docking interactions. Stable, specific adhesion between two different

epithelial tissues is a necessary step in establishing a continuous epithelium with aligned apico-basolateral polarity (Vasquez et al., 2021). One intriguing possibility is that specific adhesive complexes between docking epithelia could provide a mechanism for ensuring that the correct epithelial types find one another. Similar to the neural adhesion code hypothesis that postulates that specific combinations of cell surface receptors specify synaptic connections (Shapiro and Colman, 1999), particular epithelial cells that must dock and undergo tissue fusion could display specific combinations of receptors. The use of different innexins for different steps in neolaminating border cells (Miao et al., 2020) and the Toll receptor code for specifying different boundaries within the *Drosophila* germband epithelium (Paré et al., 2014) are both consistent with the idea that epithelial cell-cell connections are more unique and varied than previously thought.

In returning to the example of the through gut digestive tract, foregut cells must correctly adhere and align with midgut cells on one side and with epidermal cells on the other side. These correct connections across neighbors of different tissues are crucial for organ function and organism survival. Specific epithelial fusion events between different tissues may arise through preferential stabilization of certain cell-cell contacts, just as specific cells sort into separate tissues *via* differential cadherin-based adhesion (Takeichi, 1991; Godt and Tepass, 1998; Price et al., 2002; Tsai et al., 2020), Ephrin-receptor adhesion (Cooke et al., 2005), and

capacity to establish stable cell-cell contacts (Skokan et al., 2020). Determining how docking epithelial cells initiate and stabilize adhesions with their neighbors will be critical in the future to determine how epithelial tissues properly align global apico-basolateral polarity and thereby protect organismal integrity.

## AUTHOR CONTRIBUTIONS

LEC wrote the manuscript with input from JLF.

## FUNDING

LEC is a Damon Runyon Fellow supported by the Damon Runyon Cancer Research Foundation (DRG-2428-21). JLF is supported by R01GM136902 and R01GM133950.

## ACKNOWLEDGMENTS

The authors apologize to those whose related publications were not cited due to space limitations. The authors acknowledge the many helpful comments from members of the Feldman Lab and from the reviewers.

## REFERENCES

- Aceto, N., Bardia, A., Miyamoto, D. T., Donaldson, M. C., Wittner, B. S., Spencer, J. A., et al. (2014). Circulating Tumor Cell Clusters Are Oligoclonal Precursors of Breast Cancer Metastasis. *Cell* 158 (5), 1110–1122. doi:10.1016/j.cell.2014.07.013
- Achilleos, A., Wehman, A. M., and Nance, J. (2010). PAR-3 Mediates the Initial Clustering and Apical Localization of Junction and Polarity Proteins during *C. elegans* Intestinal Epithelial Cell Polarization. *Development* 137 (11), 1833–1842. doi:10.1242/dev.047647
- Akhtar, N., and Streuli, C. H. (2013). An Integrin-ILK-Microtubule Network Orients Cell Polarity and Lumen Formation in Glandular Epithelium. *Nat. Cell Biol.* 15 (1), 17–27. doi:10.1038/ncb2646
- Bernstein, C. S., Anderson, M. T., Gohel, C., Slater, K., Gross, J. M., and Agarwala, S. (2018). The Cellular Bases of Choroid Fissure Formation and Closure. *Dev. Biol.* 440 (2), 137–151. doi:10.1016/j.ydbio.2018.05.010
- Billmyre, K. K., Hutson, M., and Klingensmith, J. (2015). One Shall Become Two: Separation of the Esophagus and Trachea from the Common Foregut Tube. *Dev. Dyn.* 244 (3), 277–288. doi:10.1002/dvdy.24219
- Buckley, C. E., and St Johnston, D. (2022). Apical-basal Polarity and the Control of Epithelial Form and Function. *Nat. Rev. Mol. Cell Biol.* doi:10.1038/s41580-022-00465-y
- Cáceres, R., Bojanala, N., Kelley, L. C., Dreier, J., Manzi, J., Di Federico, F., et al. (2018). Forces Drive Basement Membrane Invasion in *Caenorhabditis elegans*. *Proc. Natl. Acad. Sci. U.S.A.* 115 (45), 11537–11542. doi:10.1073/pnas.1808760115
- Campbell, K., Casanova, J., and Skaer, H. (2010). Mesenchymal-to-epithelial Transition of Intercalating Cells in *Drosophila* Renal Tubules Depends on Polarity Cues from Epithelial Neighbours. *Mech. Dev.* 127 (7–8), 345–357. doi:10.1016/j.mod.2010.04.002
- Campbell, K., Whissell, G., Franch-Marro, X., Batlle, E., and Casanova, J. (2011). Specific GATA Factors Act as Conserved Inducers of an Endodermal-EMT. *Dev. Cell* 21 (6), 1051–1061. doi:10.1016/j.devcel.2011.10.005
- Chan, B. H. C., Moosajee, M., and Rainger, J. (2020). Closing the Gap: Mechanisms of Epithelial Fusion during Optic Fissure Closure. *Front. Cell Dev. Biol.* 8, 620774. doi:10.3389/fcell.2020.620774
- Chen, J., Jacox, L. A., Saldanha, F., and Sive, H. (2017). Mouth Development. *Wiley Interdiscip. Rev. Dev. Biol.* 6 (5), e275. doi:10.1002/wdev.275
- Chen, J., Sayadian, A.-C., Lowe, N., Lovegrove, H. E., and St Johnston, D. (2018). An Alternative Mode of Epithelial Polarity in the *Drosophila* Midgut. *PLoS Biol.* 16 (10), e3000041. doi:10.1371/journal.pbio.3000041
- Cheung, K. J., Padmanaban, V., Silvestri, V., Schipper, K., Cohen, J. D., Fairchild, A. N., et al. (2016). Polyclonal Breast Cancer Metastases Arise from Collective Dissemination of Keratin 14-expressing Tumor Cell Clusters. *Proc. Natl. Acad. Sci. U.S.A.* 113 (7), E854–E863. doi:10.1073/pnas.1508541113
- Chia, I., Grote, D., Marcotte, M., Batourina, E., Mendelsohn, C., and Bouchard, M. (2011). Nephric Duct Insertion Is a Crucial Step in Urinary Tract Maturation that Is Regulated by a Gata3-Raldh2-Retmolecular Network in Mice. *Development* 138 (10), 2089–2097. doi:10.1242/dev.056838
- Cho, E. A., Patterson, L. T., Brookhiser, W. T., Mah, S., Kintner, C., and Dressler, G. R. (1998). Differential Expression and Function of Cadherin-6 during Renal Epithelium Development. *Development* 125 (5), 803–812. doi:10.1242/dev.125.5.803
- Cooke, J. E., Kemp, H. A., and Moens, C. B. (2005). EphA4 Is Required for Cell Adhesion and Rhombomere-Boundary Formation in the Zebrafish. *Curr. Biol.* 15 (6), 536–542. doi:10.1016/j.cub.2005.02.019
- Copp, A. J., Adzick, N. S., Chitty, L. S., Fletcher, J. M., Holmbeck, G. N., and Shaw, G. M. (2015). Spina Bifida. *Nat. Rev. Dis. Prim.* 1, 15007. doi:10.1038/nrdp.2015.7
- Denholm, B., Sudarsan, V., Pasalodos-Sanchez, S., Artero, R., Lawrence, P., Maddrell, S., et al. (2003). Dual Origin of the Renal Tubules in *Drosophila* Mesodermal Cells Integrate and Polarize to Establish Secretory Function. *Curr. Biol.* 13 (12), 1052–1057. doi:10.1016/s0960-9822(03)00375-0
- Dickinson, A. J. G., and Sive, H. L. (2009). The Wnt Antagonists Frzb-1 and Crescent Locally Regulate Basement Membrane Dissolution in the Developing Primary Mouth. *Development* 136 (7), 1071–1081. doi:10.1242/dev.032912



- Dunn, C. W., Giribet, G., Edgecombe, G. D., and Hejnol, A. (2014). Animal Phylogeny and its Evolutionary Implications. *Annu. Rev. Ecol. Evol. Syst.* 45, 371–395. doi:10.1146/annurev-ecolsys-120213-091627
- Eckert, P., Knickmeyer, M. D., and Heermann, S. (2020). *In Vivo* Analysis of Optic Fissure Fusion in Zebrafish: Pioneer Cells, Basal Lamina, Hyaloid Vessels, and How Fissure Fusion Is Affected by BMP. *Int. J. Mol. Sci.* 21 (8), 2760. doi:10.3390/ijms21082760
- Escobar, L. F., Heiman, M., Zimmer, D., and Careskey, H. (2007). Urorectal Septum Malformation Sequence: Prenatal Progression, Clinical Report, and Embryology Review. *Am. J. Med. Genet.* 143A (22), 2722–2726. doi:10.1002/ajmg.a.31925
- Escuin, S., Vernay, B., Savery, D., Gurniak, C. B., Witke, W., Greene, N. D. E., et al. (2015). Rho Kinase-dependent Actin Turnover and Actomyosin Disassembly Are Necessary for Mouse Spinal Neural Tube Closure. *J. Cell Sci.* 128 (14), 2468–2481. doi:10.1242/jcs.164574
- Estes, K. A., and Hanna-Rose, W. (2009). The Anchor Cell Initiates Dorsal Lumen Formation during *C. elegans* Vulval Tubulogenesis. *Dev. Biol.* 328 (2), 297–304. doi:10.1016/j.ydbio.2009.01.034
- Fagotto, F. (2015). Regulation of Cell Adhesion and Cell Sorting at Embryonic Boundaries. *Curr. Top. Dev. Biol.* 112, 19–64. doi:10.1016/bs.ctdb.2014.11.026
- Farbman, A. I. (1968). Electron Microscope Study of Palate Fusion in Mouse Embryos. *Dev. Biol.* 18 (2), 93–116. doi:10.1016/0012-1606(68)90038-9
- Garcia, M. A., Nelson, W. J., and Chavez, N. (2018). Cell-Cell Junctions Organize Structural and Signaling Networks. *Cold Spring Harb. Perspect. Biol.* 10 (4), a029181. doi:10.1101/cshperspect.a029181
- Georgas, K., Rumballe, B., Valerius, M. T., Chiu, H. S., Thiagarajan, R. D., Lesieur, E., et al. (2009). Analysis of Early Nephron Patterning Reveals a Role for Distal RV Proliferation in Fusion to the Ureteric Tip via a Cap Mesenchyme-Derived Connecting Segment. *Dev. Biol.* 332 (2), 273–286. doi:10.1016/j.ydbio.2009.05.578
- Gestri, G., Bazin-Lopez, N., Scholes, C., and Wilson, S. W. (2018). Cell Behaviors during Closure of the Choroid Fissure in the Developing Eye. *Front. Cell. Neurosci.* 12, 42. doi:10.3389/fncel.2018.00042
- Ghyselinck, N. B., Wendling, O., Messaddeq, N., Dierich, A., Lampron, C., Décimo, D., et al. (1998). Contribution of Retinoic Acid Receptor  $\beta$  Isoforms to the Formation of the Conotruncal Septum of the Embryonic Heart. *Dev. Biol.* 198 (2), 303–318. doi:10.1016/s0012-1606(98)80007-9
- Godt, D., and Tepass, U. (1998). *Drosophila* Oocyte Localization Is Mediated by Differential Cadherin-Based Adhesion. *Nature* 395 (6700), 387–391. doi:10.1038/26493
- Gregory-Evans, C. Y., Williams, M. J., Halford, S., and Gregory-Evans, K. (2004). Ocular Coloboma: a Reassessment in the Age of Molecular Neuroscience. *J. Med. Genet.* 41 (12), 881–891. doi:10.1136/jmg.2004.025494
- Hagedorn, E. J., and Sherwood, D. R. (2011). Cell Invasion through Basement Membrane: the Anchor Cell Breaches the Barrier. *Curr. Opin. Cell Biol.* 23 (5), 589–596. doi:10.1016/j.ccb.2011.05.002
- Hagedorn, E. J., Yashiro, H., Ziel, J. W., Ihara, S., Wang, Z., and Sherwood, D. R. (2009). Integrin Acts Upstream of Netrin Signaling to Regulate Formation of the Anchor Cell's Invasive Membrane in *C. elegans*. *Dev. Cell* 17 (2), 187–198. doi:10.1016/j.devcel.2009.06.006
- Hashimoto, H., and Munro, E. (2019). Differential Expression of a Classic Cadherin Directs Tissue-Level Contractile Asymmetry during Neural Tube Closure. *Dev. Cell* 51 (2), 158. doi:10.1016/j.devcel.2019.10.001
- Hoshi, M., Reginensi, A., Joens, M. S., Fitzpatrick, J. A. J., McNeill, H., and Jain, S. (2018). Reciprocal Spatiotemporally Controlled Apoptosis Regulates Wolffian Duct Cloaca Fusion. *J. Am. Soc. Nephrol.* 29 (3), 775–783. doi:10.1681/ASN.2017040380
- Huebner, R. J., and Wallingford, J. B. (2018). Coming to Consensus: A Unifying Model Emerges for Convergent Extension. *Dev. Cell* 46 (4), 389–396. doi:10.1016/j.devcel.2018.08.003
- Ihara, S., Hagedorn, E. J., Morrissey, M. A., Chi, Q., Motegi, F., Kramer, J. M., et al. (2011). Basement Membrane Sliding and Targeted Adhesion Remodels Tissue Boundaries during Uterine-Vulval Attachment in *Caenorhabditis elegans*. *Nat. Cell Biol.* 13 (6), 641–651. doi:10.1038/ncb2233
- Jacinto, A., Martinez-Arias, A., and Martin, P. (2001). Mechanisms of Epithelial Fusion and Repair. *Nat. Cell Biol.* 3 (5), E117–E123. doi:10.1038/35074643
- Jacinto, A., Wood, W., Balayo, T., Turmaine, M., Martinez-Arias, A., and Martin, P. (2000). Dynamic Actin-Based Epithelial Adhesion and Cell Matching during *Drosophila* Dorsal Closure. *Curr. Biol.* 10 (22), 1420–1426. doi:10.1016/s0960-9822(00)00796-x
- Jewett, C. E., and Prekeris, R. (2018). Insane in the Apical Membrane: Trafficking Events Mediating Apicobasal Epithelial Polarity during Tube Morphogenesis. *Traffic* 19, 666–678. doi:10.1111/tra.12579
- Kao, R. M. (2013). The Luminal Connection: From Animal Development to Lumopathies. *Organogenesis* 9 (2), 111–117. doi:10.4161/org.25225
- Kao, R. M., Vasilyev, A., Miyawaki, A., Drummond, I. A., and McMahon, A. P. (2012). Invasion of Distal Nephron Precursors Associates with Tubular Interconnection during Nephrogenesis. *J. Am. Soc. Nephrol.* 23 (10), 1682–1690. doi:10.1681/ASN.2012030283
- Kelley, L. C., Chi, Q., Cáceres, R., Hastie, E., Schindler, A. J., Jiang, Y., et al. (2019). Adaptive F-Actin Polymerization and Localized ATP Production Drive Basement Membrane Invasion in the Absence of MMPs. *Dev. Cell* 48 (3), 313. doi:10.1016/j.devcel.2018.12.018
- Kiehart, D. P., Crawford, J. M., Aristotelous, A., Venakides, S., and Edwards, G. S. (2017). Cell Sheet Morphogenesis: Dorsal Closure in *Drosophila melanogaster* as a Model System. *Annu. Rev. Cell Dev. Biol.* 33 (1), 169–202. doi:10.1146/annurev-cellbio-111315-125357
- Kim, E., Jiang, M., Huang, H., Zhang, Y., Tjota, N., Gao, X., et al. (2019). Isl1 Regulation of Nkx2.1 in the Early Foregut Epithelium Is Required for Trachea-Esophageal Separation and Lung Lobation. *Dev. Cell* 51 (6), 675–683. doi:10.1016/j.devcel.2019.11.002
- Kim, K., Lake, B. B., Haremak, T., Weinstein, D. C., and Sokol, S. Y. (2012). Rab11 Regulates Planar Polarity and Migratory Behavior of Multiciliated Cells in *Xenopus* Embryonic Epidermis. *Dev. Dyn.* 241 (9), 1385–1395. doi:10.1002/dvdy.23826
- Kobayashi, A., Kwan, K.-M., Carroll, T. J., McMahon, A. P., Mendelsohn, C. L., and Behringer, R. R. (2005). Distinct and Sequential Tissue-specific Activities of the LIM-Class Homeobox Gene *Lim1* for Tubular Morphogenesis during Kidney Development. *Development* 132 (12), 2809–2823. doi:10.1242/dev.01858
- Lambert, A. W., Pattabiraman, D. R., and Weinberg, R. A. (2017). Emerging Biological Principles of Metastasis. *Cell* 168 (4), 670–691. doi:10.1016/j.cell.2016.11.037
- Lee, J. L., and Streuli, C. H. (2014). Integrins and Epithelial Cell Polarity. *J. Cell Sci.* 127 (Pt 15), 3217–3225. doi:10.1242/jcs.146142
- Leung, B., Hermann, G. J., and Priess, J. R. (1999). Organogenesis of the *Caenorhabditis elegans* Intestine. *Dev. Biol.* 216 (1), 114–134. doi:10.1006/dbio.1999.9471
- Li, D., Mangan, A., Cicchini, L., Margolis, B., and Prekeris, R. (2014). FIP 5 Phosphorylation during Mitosis Regulates Apical Trafficking and Lumenogenesis. *EMBO Rep.* 15 (4), 428–437. doi:10.1002/embr.201338128
- Liang, X., Weberling, A., Hii, C. Y., Zernicka-Goetz, M., and Buckley, C. (2022). E-cadherin Mediated AMIS Localisation. *bioRxiv*, [Preprint], 2021.2030.470571. doi:10.1101/2021.11.30.470571
- Luján, P., Varsano, G., Rubio, T., Hennrich, M. L., Sachsenheimer, T., Gálvez-Santisteban, M., et al. (2016). Phosphatase of Regenerating Liver (PRL)-3 Disrupts Epithelial Architecture by Altering the Post-mitotic Midbody Position. *J. Cell Sci.* 129 (21), 4130–4142. doi:10.1242/jcs.190215
- Lüönd, F., Sugiyama, N., Bill, R., Bornes, L., Hager, C., Tang, F., et al. (2021). Distinct Contributions of Partial and Full EMT to Breast Cancer Malignancy. *Dev. Cell* 56, 3203–3221. doi:10.1016/j.devcel.2021.11.006
- Mah, S. P., Saueressig, H., Goulding, M., Kintner, C., and Dressler, G. R. (2000). Kidney Development in Cadherin-6 Mutants: Delayed Mesenchyme-To-Epithelial Conversion and Loss of Nephrons. *Dev. Biol.* 223 (1), 38–53. doi:10.1006/dbio.2000.9738
- Marciano, D. K. (2017). A Holey Pursuit: Lumen Formation in the Developing Kidney. *Pediatr. Nephrol.* 32 (1), 7–20. doi:10.1007/s00467-016-3326-4
- Marciano, D. K., Brakeman, P. R., Lee, C.-Z., Spivak, N., Eastburn, D. J., Bryant, D. M., et al. (2011). p120 Catenin Is Required for Normal Renal Tubulogenesis and Glomerulogenesis. *Development* 138 (10), 2099–2109. doi:10.1242/dev.056564
- Matlin, K. S., Myllymäki, S.-M., and Manninen, A. (2017). Laminins in Epithelial Cell Polarization: Old Questions in Search of New Answers. *Cold Spring Harb. Perspect. Biol.* 9 (10), a027920. doi:10.1101/cshperspect.a027920
- McClatchey, S. T., Wang, Z., Linden, L. M., Hastie, E. L., Wang, L., Shen, W., et al. (2016). Boundary Cells Restrict Dystroglycan Trafficking to Control Basement Membrane Sliding during Tissue Remodeling. *Elife* 5, e17218. doi:10.7554/eLife.17218

- McMahon, A. P. (2016). Development of the Mammalian Kidney. *Curr. Top. Dev. Biol.* 117, 31–64. doi:10.1016/bs.ctdb.2015.10.010
- Mello Santos, T., and Hinton, B. T. (2019). We, the Developing Rete Testis, Efferent Ducts, and Wolffian Duct, All Hereby Agree that We Need to Connect. *Andrology* 7 (5), 581–587. doi:10.1111/andr.12631
- Miao, G., Godt, D., and Montell, D. J. (2020). Integration of Migratory Cells into a New Site *In Vivo* Requires Channel-independent Functions of Innexins on Microtubules. *Dev. Cell* 54 (4), 501. doi:10.1016/j.devcel.2020.06.024
- Mishra, A. K., Campanale, J. P., Mondo, J. A., and Montell, D. J. (2019). Cell Interactions in Collective Cell Migration. *Development* 146 (23), dev172056. doi:10.1242/dev.172056
- Molè, M. A., Galea, G. L., Rolo, A., Weberling, A., Nychyk, O., De Castro, S. C., et al. (2020). Integrin-Mediated Focal Anchorage Drives Epithelial Zippering during Mouse Neural Tube Closure. *Dev. Cell* 52 (3), 321–334. doi:10.1016/j.devcel.2020.01.012
- Morrissey, M. A., Jayadev, R., Miley, G. R., Blebea, C. A., Chi, Q., Ihara, S., et al. (2016). SPARC Promotes Cell Invasion *In Vivo* by Decreasing Type IV Collagen Levels in the Basement Membrane. *PLoS Genet.* 12 (2), e1005905. doi:10.1371/journal.pgen.1005905
- Morrissey, M. A., Keeley, D. P., Hagedorn, E. J., McClatchey, S. T. H., Chi, Q., Hall, D. H., et al. (2014). B-LINK: a Hemicentin, Plakin, and Integrin-dependent Adhesion System that Links Tissues by Connecting Adjacent Basement Membranes. *Dev. Cell* 31 (3), 319–331. doi:10.1016/j.devcel.2014.08.024
- Murugapoopathy, V., and Gupta, I. R. (2020). A Primer on Congenital Anomalies of the Kidneys and Urinary Tracts (CAKUT). *Clin. J. Am. Soc. Nephrol.* 15 (5), 723–731. doi:10.2215/CJN.12581019
- Na, T.-Y., Schecterson, L., Mendonsa, A. M., and Gumbiner, B. M. (2020). The Functional Activity of E-Cadherin Controls Tumor Cell Metastasis at Multiple Steps. *Proc. Natl. Acad. Sci. U.S.A.* 117 (11), 5931–5937. doi:10.1073/pnas.1918167117
- Nasr, T., Mancini, P., Rankin, S. A., Edwards, N. A., Agricola, Z. N., Kenny, A. P., et al. (2019). Endosome-Mediated Epithelial Remodeling Downstream of Hedgehog-Gli Is Required for Tracheoesophageal Separation. *Dev. Cell* 51 (6), 665. doi:10.1016/j.devcel.2019.11.003
- Nikolopoulou, E., Galea, G. L., Rolo, A., Greene, N. D. E., and Copp, A. J. (2017). Neural Tube Closure: Cellular, Molecular and Biomechanical Mechanisms. *Development* 144 (4), 552–566. doi:10.1242/dev.145904
- O'Brien, L. E., Jou, T.-S., Pollack, A. L., Zhang, Q., Hansen, S. H., Yurchenco, P., et al. (2001). Rac1 Orientates Epithelial Apical Polarity through Effects on Basolateral Laminin Assembly. *Nat. Cell Biol.* 3 (9), 831–838. doi:10.1038/ncb0901-831
- Overeem, A. W., Bryant, D. M., and van IJzendoorn, S. C. D. (2015). Mechanisms of Apical-Basal axis Orientation and Epithelial Lumen Positioning. *Trends Cell Biol.* 25 (8), 476–485. doi:10.1016/j.tcb.2015.04.002
- Padmanaban, V., Krol, I., Suhail, Y., Szczepa, B. M., Aceto, N., Bader, J. S., et al. (2019). E-cadherin Is Required for Metastasis in Multiple Models of Breast Cancer. *Nature* 573 (7774), 439–444. doi:10.1038/s41586-019-1526-3
- Pai, Y. J., Abdullah, N. L., Mohd-Zin, S. W., Mohammed, R. S., Rolo, A., Greene, N. D., et al. (2012). Epithelial Fusion during Neural Tube Morphogenesis. *Birth Defects Res. A Clin. Mol. Teratol.* 94 (10), 817–823. doi:10.1002/bdra.23072
- Palmer, M. A., and Nelson, C. M. (2020). Fusion of Airways during Avian Lung Development Constitutes a Novel Mechanism for the Formation of Continuous Lumina in Multicellular Epithelia. *Dev. Dyn.* 249 (11), 1318–1333. doi:10.1002/dvdy.215
- Paré, A. C., Vichas, A., Fincher, C. T., Mirman, Z., Farrell, D. L., Mainieri, A., et al. (2014). A Positional Toll Receptor Code Directs Convergent Extension in *Drosophila*. *Nature* 515 (7528), 523–527. doi:10.1038/nature13953
- Pei, D., Shu, X., Gassama-Diagne, A., and Thiery, J. P. (2019). Mesenchymal-epithelial Transition in Development and Reprogramming. *Nat. Cell Biol.* 21 (1), 44–53. doi:10.1038/s41556-018-0195-z
- Pickett, M. A., Nature, V. F., and Feldman, J. L. (2019). A Polarizing Issue: Diversity in the Mechanisms Underlying Apico-Basolateral Polarization *In Vivo*. *Annu. Rev. Cell Dev. Biol.* 35 (1), 285–308. doi:10.1146/annurev-cellbio-100818-125134
- Pickett, M. A., Sallee, M. D., Nature, V. F., Akpinaroglu, D., Lee, J., Shen, K., et al. (2021). Separable Mechanisms Drive Local and Global Polarity Establishment in the *C. elegans* Intestinal Epithelium. *bioRxiv*, [Preprint], 2021.2011.2001.466827. doi:10.1101/2021.11.01.466827
- Pitsidianaki, I., Morgan, J., Adams, J., and Campbell, K. (2021). Mesenchymal-to-epithelial Transitions Require Tissue-specific Interactions with Distinct Laminins. *J. Cell Biol.* 220 (8), e202010154. doi:10.1083/jcb.202010154
- Price, S. R., De Marco Garcia, N. V., Ranscht, B., and Jessell, T. M. (2002). Regulation of Motor Neuron Pool Sorting by Differential Expression of Type II Cadherins. *Cell* 109 (2), 205–216. doi:10.1016/s0092-8674(02)00695-5
- Pyati, U. J., Cooper, M. S., Davidson, A. J., Nechiporuk, A., and Kimelman, D. (2006). Sustained Bmp Signaling Is Essential for Cloaca Development in Zebrafish. *Development* 133 (11), 2275–2284. doi:10.1242/dev.02388
- Rasmussen, J. P., English, K., Tenlen, J. R., and Priess, J. R. (2008). Notch Signaling and Morphogenesis of Single-Cell Tubes in the *C. elegans* Digestive Tract. *Dev. Cell* 14 (4), 559–569. doi:10.1016/j.devcel.2008.01.019
- Rasmussen, J. P., Feldman, J. L., Reddy, S. S., and Priess, J. R. (2013). Cell Interactions and Patterned Intercalations Shape and Link Epithelial Tubes in *C. elegans*. *PLoS Genet.* 9 (9), e1003772. doi:10.1371/journal.pgen.1003772
- Rasmussen, J. P., Reddy, S. S., and Priess, J. R. (2012). Laminin Is Required to Orient Epithelial Polarity in the *C. elegans* Pharynx. *Development* 139 (11), 2050–2060. doi:10.1242/dev.078360
- Rathbun, L. I., Colicino, E. G., Manikas, J., O'Connell, J., Krishnan, N., Reilly, N. S., et al. (2020). Cytokinetic Bridge Triggers De Novo Lumen Formation *In Vivo*. *Nat. Commun.* 11 (1), 1269. doi:10.1038/s41467-020-15002-8
- Ray, H. J., and Niswander, L. (2012). Mechanisms of Tissue Fusion during Development. *Development* 139 (10), 1701–1711. doi:10.1242/dev.068338
- Rolo, A., Savery, D., Escuin, S., de Castro, S. C., Armer, H. E., Munro, P. M., et al. (2016). Regulation of Cell Protrusions by Small GTPases during Fusion of the Neural Folds. *Elife* 5, e13273. doi:10.7554/eLife.13273
- Sapir, A., Choi, J., Leikina, E., Avinoam, O., Valansi, C., Chernomordik, L. V., et al. (2007). AFF-1, a FOS-1-Regulated Fusogen, Mediates Fusion of the Anchor Cell in *C. elegans*. *Dev. Cell* 12 (5), 683–698. doi:10.1016/j.devcel.2007.03.003
- Scharl, M., and Rogler, G. (2014). Pathophysiology of Fistula Formation in Crohn's Disease. *World J. Gastrointest. Pathophysiol.* 5 (3), 205–212. doi:10.4291/wjgp.v5.i3.205
- Schlüter, M. A., Pfarr, C. S., Pieczynski, J., Whiteman, E. L., Hurd, T. W., Fan, S., et al. (2009). Trafficking of Crumbs3 during Cytokinesis Is Crucial for Lumen Formation. *Mol. Biol. Cell* 20 (22), 4652–4663. doi:10.1091/mbc.E09-02-0137
- Shapiro, L., and Colman, D. R. (1999). The Diversity of Cadherins and Implications for a Synaptic Adhesive Code in the CNS. *Neuron* 23 (3), 427–430. doi:10.1016/s0896-6273(00)80796-5
- Sherwood, D. R., and Plastino, J. (2018). Invading, Leading and Navigating Cells in *Caenorhabditis elegans*: Insights into Cell Movement *In Vivo*. *Genetics* 208 (1), 53–78. doi:10.1534/genetics.117.300082
- Sherwood, D. R., and Sternberg, P. W. (2003). Anchor Cell Invasion into the Vulval Epithelium in *C. elegans*. *Dev. Cell* 5 (1), 21–31. doi:10.1016/s1534-5807(03)00168-0
- Skokan, T. D., Vale, R. D., and McKinley, K. L. (2020). Cell Sorting in *Hydra vulgaris* Arises from Differing Capacities for Epithelialization between Cell Types. *Curr. Biol.* 30 (19), 3713. doi:10.1016/j.cub.2020.07.035
- Slanchev, K., Pütz, M., Schmitt, A., Kramer-Zucker, A., and Walz, G. (2011). Nephrocystin-4 Is Required for Pronephric Duct-dependent Cloaca Formation in Zebrafish. *Hum. Mol. Genet.* 20 (16), 3119–3128. doi:10.1093/hmg/ddr214
- Somarelli, J. A., Schaeffer, D., Marengo, M. S., Bepler, T., Rouse, D., Ware, K. E., et al. (2016). Distinct Routes to Metastasis: Plasticity-dependent and Plasticity-independent Pathways. *Oncogene* 35 (33), 4302–4311. doi:10.1038/nc.2015.497
- Soukup, V., Horáček, I., and Cerny, R. (2013). Development and Evolution of the Vertebrate Primary Mouth. *J. Anat.* 222 (1), 79–99. doi:10.1111/j.1469-7580.2012.01540.x
- Spiri, S., Berger, S., Mereu, L., DeMello, A., and Hajnal, A. (2022). Reciprocal EGFR Signaling in the Anchor Cell Ensures Precise Inter-organ Connection during *Caenorhabditis elegans* Vulval Morphogenesis. *Development* 149 (1), dev199900. doi:10.1242/dev.199900
- Stubbs, J. L., Davidson, L., Keller, R., and Kintner, C. (2006). Radial Intercalation of Ciliated Cells during *Xenopus* Skin Development. *Development* 133 (13), 2507–2515. doi:10.1242/dev.02417
- Sun, Z., Amourda, C., Shagirov, M., Hara, Y., Saunders, T. E., and Toyama, Y. (2017). Basolateral Protrusion and Apical Contraction Cooperatively Drive *Drosophila* Germ-Band Extension. *Nat. Cell Biol.* 19 (4), 375–383. doi:10.1038/ncb3497

- Tabler, J. M., Bolger, T. G., Wallingford, J., and Liu, K. J. (2014). Hedgehog Activity Controls Opening of the Primary Mouth. *Dev. Biol.* 396 (1), 1–7. doi:10.1016/j.ydbio.2014.09.029
- Takeichi, M. (1991). Cadherin Cell Adhesion Receptors as a Morphogenetic Regulator. *Science* 251 (5000), 1451–1455. doi:10.1126/science.2006419
- Tawk, M., Araya, C., Lyons, D. A., Reugels, A. M., Girdler, G. C., Bayley, P. R., et al. (2007). A Mirror-Symmetric Cell Division that Orchestrates Neuroepithelial Morphogenesis. *Nature* 446 (7137), 797–800. doi:10.1038/nature05722
- Taya, Y., O'Kane, S., and Ferguson, M. W. (1999). Pathogenesis of Cleft Palate in TGF- $\beta$ 3 Knockout Mice. *Development* 126 (17), 3869–3879. doi:10.1242/dev.126.17.3869
- Tepass, U., and Hartenstein, V. (1994). Epithelium Formation in the *Drosophila* Midgut Depends on the Interaction of Endoderm and Mesoderm. *Development* 120 (3), 579–590. doi:10.1242/dev.120.3.579
- Tepass, U., Theres, C., and Knust, E. (1990). Crumbs Encodes an EGF-like Protein Expressed on Apical Membranes of *Drosophila* Epithelial Cells and Required for Organization of Epithelia. *Cell* 61 (5), 787–799. doi:10.1016/0092-8674(90)90189-1
- Tsai, J. H., Donaher, J. L., Murphy, D. A., Chau, S., and Yang, J. (2012). Spatiotemporal Regulation of Epithelial-Mesenchymal Transition Is Essential for Squamous Cell Carcinoma Metastasis. *Cancer Cell* 22 (6), 725–736. doi:10.1016/j.ccr.2012.09.022
- Tsai, T. Y.-C., Sikora, M., Xia, P., Colak-Champollion, T., Knaut, H., Heisenberg, C.-P., et al. (2020). An Adhesion Code Ensures Robust Pattern Formation during Tissue Morphogenesis. *Science* 370 (6512), 113–116. doi:10.1126/science.aba6637
- van Lennep, M., Singendonk, M. M. J., Dall'Oglio, L., Gottrand, F., Krishnan, U., Terheggen-Lagro, S. W. J., et al. (2019). Oesophageal Atresia. *Nat. Rev. Dis. Prim.* 5 (1), 26. doi:10.1038/s41572-019-0077-0
- Vasquez, C. G., de la Serna, E. L., and Dunn, A. R. (2021). How Cells Tell up from Down and Stick Together to Construct Multicellular Tissues - Interplay between Apicobasal Polarity and Cell-Cell Adhesion. *J. Cell Sci.* 134 (21), jcs248757. doi:10.1242/jcs.248757
- Walck-Shannon, E., and Hardin, J. (2014). Cell Intercalation from Top to Bottom. *Nat. Rev. Mol. Cell Biol.* 15 (1), 34–48. doi:10.1038/nrm3723
- Walck-Shannon, E., Reiner, D., and Hardin, J. (2015). Polarized Rac-dependent Protrusions Drive Epithelial Intercalation in the Embryonic Epidermis of *C. elegans*. *Development* 142 (20), 3549–3560. doi:10.1242/dev.127597
- Weaver, M. L., Piedade, W. P., Meshram, N. N., and Famulski, J. K. (2020). Hyaloid Vasculature and Mmp2 Activity Play a Role during Optic Fissure Fusion in Zebrafish. *Sci. Rep.* 10 (1), 10136. doi:10.1038/s41598-020-66451-6
- Weiss, A.-C., Airik, R., Bohnenpoll, T., Greulich, F., Foik, A., Trowe, M.-O., et al. (2014). Nephric Duct Insertion Requires EphA4/EphA7 Signaling from the Pericloacal Mesenchyme. *Development* 141 (17), 3420–3430. doi:10.1242/dev.113928
- Werner, M. E., Mitchell, J. W., Putzbach, W., Bacon, E., Kim, S. K., and Mitchell, B. J. (2014). Radial Intercalation Is Regulated by the Par Complex and the Microtubule-Stabilizing Protein CLAMP/Spel. *J. Cell Biol.* 206 (3), 367–376. doi:10.1083/jcb.201312045
- Williams, M., Yen, W., Lu, X., and Sutherland, A. (2014). Distinct Apical and Basolateral Mechanisms Drive Planar Cell Polarity-dependent Convergent Extension of the Mouse Neural Plate. *Dev. Cell* 29 (1), 34–46. doi:10.1016/j.devcel.2014.02.007
- Yang, Q., Roiz, D., Mereu, L., Daube, M., and Hajnal, A. (2017). The Invading Anchor Cell Induces Lateral Membrane Constriction during Vulval Lumen Morphogenesis in *C. elegans*. *Dev. Cell* 42 (3), 271–285. doi:10.1016/j.devcel.2017.07.008
- Yang, Z., Zimmerman, S., Brakeman, P. R., Beaudoin, G. M., 3rd, Reichardt, L. F., and Marciano, D. K. (2013). De Novo lumen Formation and Elongation in the Developing Nephron: a Central Role for Afadin in Apical Polarity. *Development* 140 (8), 1774–1784. doi:10.1242/dev.087957
- Yarnitzky, T., and Volk, T. (1995). Laminin Is Required for Heart, Somatic Muscles, and Gut Development in the *Drosophila* Embryo. *Dev. Biol.* 169 (2), 609–618. doi:10.1006/dbio.1995.1173
- Yu, W., Datta, A., Leroy, P., O'Brien, L. E., Mak, G., Jou, T.-S., et al. (2005).  $\beta$ 1-Integrin Orients Epithelial Polarity via Rac1 and Laminin. *Mol. Biol. Cell* 16 (2), 433–445. doi:10.1091/mbc.e04-05-0435
- Ziel, J. W., Hagedorn, E. J., Audhya, A., and Sherwood, D. R. (2009). UNC-6 (Netrin) Orients the Invasive Membrane of the Anchor Cell in *C. elegans*. *Nat. Cell Biol.* 11 (2), 183–189. doi:10.1038/ncb1825
- Žigman, M., Trinh, L. A., Fraser, S. E., and Moens, C. B. (2011). Zebrafish Neural Tube Morphogenesis Requires Scribble-dependent Oriented Cell Divisions. *Curr. Biol.* 21 (1), 79–86. doi:10.1016/j.cub.2010.12.005

**Conflict of Interest:** The authors declare that the research was conducted in the absence of any commercial or financial relationships that could be construed as a potential conflict of interest.

**Publisher's Note:** All claims expressed in this article are solely those of the authors and do not necessarily represent those of their affiliated organizations, or those of the publisher, the editors and the reviewers. Any product that may be evaluated in this article, or claim that may be made by its manufacturer, is not guaranteed or endorsed by the publisher.

Copyright © 2022 Cote and Feldman. This is an open-access article distributed under the terms of the Creative Commons Attribution License (CC BY). The use, distribution or reproduction in other forums is permitted, provided the original author(s) and the copyright owner(s) are credited and that the original publication in this journal is cited, in accordance with accepted academic practice. No use, distribution or reproduction is permitted which does not comply with these terms.



# Epithelial Cell Polarity During *Drosophila* Midgut Development

Jia Chen and Daniel St Johnston\*

Gurdon Institute and the Department of Genetics, University of Cambridge, Cambridge, United Kingdom

The adult *Drosophila* midgut epithelium is derived from a group of stem cells called adult midgut precursors (AMPs) that are specified during the migration of the endoderm in early embryogenesis. AMPs are maintained and expanded in AMP nests that lie on the basal side of the larval midgut throughout the larval development. During metamorphosis, the larval midgut undergoes histolysis and programmed cell death, while the central cells in the AMP nests form the future adult midgut and the peripheral cells form the transient pupal midgut. Here we review what is known about how cells polarise in the embryonic, larval, pupal and adult midgut, and discuss the open questions about the mechanisms that control the changes in cell arrangements, cell shape and cell polarity during midgut development.

**Keywords:** *Drosophila*, midgut, polarity, apical, basal, junction

## OPEN ACCESS

### Edited by:

Josana Rodriguez,  
Newcastle University, United Kingdom

### Reviewed by:

Marc Amoyel,  
University College London,  
United Kingdom  
José Carlos Pastor-Pareja,  
Tsinghua University, China

### \*Correspondence:

Daniel St Johnston  
d.stjohnston@gurdon.cam.ac.uk

### Specialty section:

This article was submitted to  
Morphogenesis and Patterning,  
a section of the journal  
Frontiers in Cell and Developmental  
Biology

**Received:** 28 February 2022

**Accepted:** 30 May 2022

**Published:** 30 June 2022

### Citation:

Chen J and St Johnston D (2022)  
Epithelial Cell Polarity During  
*Drosophila* Midgut Development.  
Front. Cell Dev. Biol. 10:886773.  
doi: 10.3389/fcell.2022.886773

## INTRODUCTION

The *Drosophila* intestine is composed of several different cell types, including epithelial cells, muscle cells, neurons, and trachea cells (Miguel-Aliaga et al., 2018). The gut tube is formed by single layer of polarised epithelial cells surrounded basally by the muscles, trachea and nerves. The fly intestine is anatomically organised into the foregut, midgut and hindgut regions with the crop and Malpighian tubules emanating at the foregut/midgut and hindgut/midgut boundaries. The midgut is the longest section of the intestine and forms the conduit between the foregut and hindgut. It can be further subdivided into the anterior, middle and posterior midgut, which are marked by tissue constrictions and differences in luminal pH (Shanbhag and Tripathi, 2005, 2009). The epithelium performs the major functions of the midgut: acting as a barrier between the gut lumen and the inside of the organism and absorbing nutrients. It is composed of two types of mature epithelial cells: enterocytes (EC) and enteroendocrine (ee) cells. Based on cell morphology, physiology and gene expression profiles, epithelial cells in the midgut can be further classified into at least 10 different subregions and 22 clusters (Buchon et al., 2013; Marianes and Spradling, 2013; Dutta et al., 2015; Hung et al., 2020).

Despite their diverse shapes and gene expression profiles, all epithelial cells share the same features of apical-basal polarity along the whole midgut (Figure 1). The major type of epithelial cells in midgut, the ECs, are absorptive and are usually of cuboidal/columnar shape, but in the middle midgut, specialised acid secreting ECs called the copper cells adopt a cup shape (Hoppler and Bienz, 1994; Strand and Micchelli, 2011). The apical membrane of ECs is covered in a brush border of

**Abbreviations:** AJ, adherens junction; AMG, presumptive adult midgut; AMIS, apical membrane initiation site; AMP, adult midgut precursor; APF, after puparium formation; BM, basement membrane; EB, enteroblast; EC, enterocyte; ee, enteroendocrine cell; ECM, extracellular matrix; EMT, epithelial to mesenchymal transition; ICP, interstitial cell precursor; ISC, intestinal stem cell; MET, mesenchymal to epithelial transition; PAC, preformed apical compartment; pISC, presumptive intestinal stem cell; pLee, progenitor cell for larval enteroendocrine cell; PM, peritrophic membrane; P MEC, principal midgut epithelial cell; PMG, posterior midgut primordium; SJ, septate junction; tPMG, transient pupal midgut; VM, visceral mesoderm.



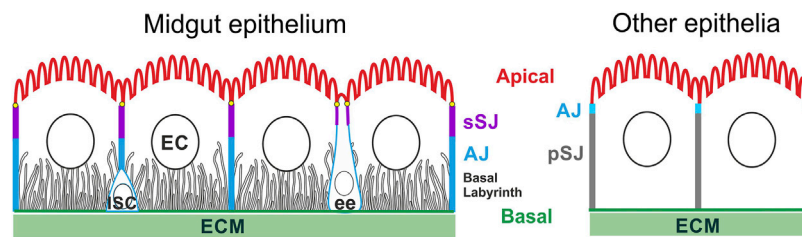


**FIGURE 1 |** The apical-basal organisation of the *Drosophila* adult midgut epithelium in comparison with other epithelia. Intestinal stem cells (ISC) can differentiate into enterocytes (EC) and enteroendocrine cells (ee). The apical domain forms a brush border facing the gut lumen; the basal membrane contacts the ECM and develops long invaginations that form the basal labyrinth. The lateral domain contains apical smooth septate junctions (sSJ), above lateral adherens junctions (AJ). By contrast, the AJs form apical to the pleated SJs in the other *Drosophila* epithelia. The ee cells typically adopt a bottle shape with the cell body shifted basally, and a narrow neck ending with a bulbous apical domain facing the gut lumen.

microvilli, while infoldings of the basal membrane generate the basal labyrinth. Each structure serves to maximize surface area, which is thought to facilitate nutrient absorption, although how the basal labyrinth forms and functions is not well studied (Shanbhag and Tripathi, 2009; Sauvanet et al., 2015). The ee cells are secretory cells that release neuropeptide hormones in response to gut contents (Beehler-Evans and Micchelli, 2015; Hung et al., 2020). They exist as isolated diploid cells throughout the midgut epithelium, often have a bottle or fusiform shape and have little or no basal labyrinth. Recent work has shown that ee cells lack an apical brush border (Xu et al., 2018), as observed in midgut endocrine cells in other insect species (Billingsley and Lehan, 1996).

The brush border is enriched in actin and contains MyoIA, MyoIB and other actin crosslinking proteins (Table 1) (Morgan et al., 1995; Crawley et al., 2014). The region of the cortex at the base of the microvilli, which is called the “terminal web” in mammalian cells, contains MyoIA, Myo7a, aPKC and Par-6 (Table 1) (Morgan et al., 1995; Chen et al., 2018). The apical domain is supported by a submembrane spectrin scaffold composed of  $\beta_H$ -spectrin/ $\alpha$ -spectrin heterotetramers that links the membrane to the actin cytoskeleton (Table 1) (Baumann, 2001; Chen and St Johnston, 2022). The apical surface of the epithelial layer in the adult is closely associated with, but does not necessarily contact, the peritrophic membrane (PM), which is composed of Type I PM produced by the entire midgut and type II PM that is secreted by the cardia/proventriculus at the most anterior region in midgut (Lehan, 1997). The PM serves a similar function to the mucous lining in mammalian gut as the outmost protective barrier (Zhang et al., 2017).

As mentioned above, the basal sides of the epithelial cells contact the extracellular matrix (ECM), except for the invaginations of the basal labyrinth, which do not appear to have any ECM in their lumens (Baumann, 2001; Shanbhag and Tripathi, 2009). Integrin associated proteins, such as Integrin linked kinase (Ilk), Rhea and Fit localise to the basal cortex (Table 1) (Chen et al., 2018). The ECM is assembled into a sheet-like basement membrane (BM) between the epithelium and the visceral muscle layers (Shanbhag and Tripathi, 2009). All four main types of the basement membrane components are present: type IV collagen ( $\alpha_1\alpha_2$  heterotrimers with Col4a1 as the  $\alpha_1$  subunit and Vkg as the  $\alpha_2$  subunit), Laminins ( $\alpha\beta\gamma$ -heterotrimers

with LanA and Wb as  $\alpha$  subunits, LanB1 as the  $\beta$  subunit and LanB2 as the  $\gamma$  subunit), Nidogen and Perlecan (Table 1) (Broadie et al., 2011; Davis et al., 2019; Töpfer and Holz, 2020). Laminins and Type IV collagen form independent mesh-like structures with the Laminins closer to the epithelial cells. In addition, the gut BM contains Netrins (Pert et al., 2015), Secreted protein, acidic, cysteine-rich (SPARC) (Martinek et al., 2002, 2008), Macrophage derived proteoglycan-1 (MDP-1) (Kramerova et al., 2003), Glutactin (Olson et al., 1990) and Peroxidase (Table 1) (Nelson et al., 1994).

Unlike most other fly epithelia, the *Drosophila* midgut epithelium is derived from the endoderm and the intercellular junctions in both the EC and ee cells have a different morphology and arrangement from the junctions in non-endodermal epithelia (Figure 1). Endodermal epithelia form smooth septate junctions (sSJs), analogous to tight junction in mammals, which lie apical to the adherens junctions (AJs), whereas in other epithelial cells, the electron-dense AJs lie above the septate junctions, which are pleated not smooth (Figure 1) (Lane and Skaer, 1980; Tepass and Hartenstein, 1994b; Baumann, 2001). Recent studies reveal that the smooth SJs are organized by the endoderm-specific proteins, Mesh, Snakeskin, Tsp2a and Hoka, which form a transmembrane protein complex (Table 1) (Izumi et al., 2012, 2016, 2021; Furuse and Izumi, 2017). The SJs at the vertices where three cells meet contain additional components, including Bark, Gli and M6, which are also found in the tri-cellular junctions in epithelia with pleated SJs (Table 1) (Schulte et al., 2003; Byri et al., 2015; Hildebrandt et al., 2015; Bosveld et al., 2018; Esmangart de Bournonville and le Borgne, 2020; Wittek et al., 2020). Loss of these tri-cellular SJ proteins during ageing leads to defects in the function of the intestinal barrier in older flies (Resnik-Docampo et al., 2017). In ectodermally-derived epithelia, Sidekick localises to the tri-cellular AJs and modulates apical adhesion and tension during the active junctional remodelling during embryo morphogenesis (Finegan et al., 2019; Letizia et al., 2019; Uechi and Kuranaga, 2019). It is not known whether bi- or tri-cellular AJ in the midgut also contain specific components since ECad, Arm and  $\alpha$ -Cat are the only known components of AJs in the midgut (Choi et al., 2011; Campbell and Casanova, 2015; Liang et al., 2017).

During the past 20 years, *Drosophila* midgut has proven an exciting model system to study epithelial homeostasis, since

**TABLE 1 |** *Drosophila* genes and their encoded protein's localization during midgut development.

<b>Drosophila gene (Abbreviation)/Alias</b>	<b>Human ortholog</b>	<b>Protein type</b>	<b>Protein localisation in the <i>Drosophila</i> midgut epithelial cell</b>	<b>References</b>
Myosin 31DF (Myo31DF)/MyoIA	<i>MYO1D</i>	Myosin	Apical brush border and terminal web in stage 17 E <sup>#1</sup> , L <sup>#2</sup> and A <sup>#3</sup>	Morgan et al. (1995); Crawley et al. (2014)
Myosin 61F (Myo61F)/MyoIB	<i>MYOIC</i>		Relocates from basolateral domain to apical brush border in stage 17 E; apical brush border in L and A	
Crinkled (ck)/myosin VIIA (myo7a)	<i>MYO7A</i>		Apical in A	Chen et al. (2018)
Atypical protein kinase C (aPKC)	<i>PRKCI/PRKCZ</i>	Kinase		
Par-6	<i>PARD6</i>	PDZ <sup>#4</sup>		
Bazooka (baz)/par-3	<i>PARD3</i>		Apical side of the lateral junction in stage 9 E	Campbell et al. (2011)
Karst (kst)/ $\beta$ -Heavy-spectrin	<i>SPTBN5</i>	Spectrin	Apical domain in L and A	Baumann, (2001); Chen et al. (2018)
$\beta$ Spectrin ( $\beta$ -Spec)	<i>SPTBN1</i>		Basolateral domain in L and A	
$\alpha$ Spectrin ( $\alpha$ Spec)	<i>SPTAN1</i>		Cell cortex in L and A	
Cheerio (cher)	<i>FLNA</i>	Actin cross linker, filamin	Apical in A; basal in stage 12/13 E	Chen and St Johnston, (2022); Devenport and Brown, (2004)
Crumbs (crb)	<i>CRB1</i>	TM <sup>#5</sup>	Apical in stage 9 E	Campbell et al. (2011)
Stardust (sdt)/pals1	<i>MPP5</i>	PDZ		
Stranded at second (sas)	-	TM		
Rhea/talin	<i>TLN</i>	FERM <sup>#6</sup>		
Fermitin 1 (Fit1)	<i>FERMT</i>		Basal domain in stage 12 E and A	Devenport and Brown, (2004); Chen et al. (2018)
Fermitin 2 (Fit2)	<i>/KINDLIN</i>		Basal domain in A	
Integrin linked kinase (Ilk)	<i>ILK</i>	Kinase		
Multiple edematous wings (mew)/ $\alpha$ PS1	<i>ITGA6/7</i>	TM, ECM receptor	Mainly basal in stage 12–15 E; basal in A	(Yee and Hynes, 1993; Martin-Bermudo et al., 1999; Lin et al., 2013; Okumura et al., 2014; Pitsidianaki et al., 2021)
Inflated (if)/ $\alpha$ PS2	<i>ITGA8</i>		Muscle layer	
Scab (scb)/ $\alpha$ PS3	<i>ITGA4</i>		Mainly apical in stage 12–15 E; basal in A	
Myospheroid (mys)/ $\beta$ PS	<i>ITGB1</i>		Mainly basal in E; basal in A	
Integrin betan subunit (Itgbn)/ $\beta$ v	-		Mainly apical in E; basal in A	
Frazzled (fra)/DCC	<i>NEO1</i>		Basal domain in from stage 12 E	Pert et al. (2015)
Dystroglycan (Dg)	<i>DAG1</i>		Tissue constriction region in stage 16 E	Schneider and Baumgartner, (2008)
Division abnormally delayed (dally)	<i>GPC5</i>	Glypican TM	-	-
Dally-like (dlp)	<i>GPC4</i>		-	-
Syndecan (Sdc)	<i>SDC</i>	Proteo-glycan TM	-	-
Laminin A (LanA)	<i>LAMA5</i>	ECM	LanA heterotrimer is mainly basal between the endoderm and mesoderm, also surrounding ICP cells and weakly at apical side in E; basal in L and A	(Wolfstetter and Holz, 2012; Lin et al., 2013; You et al., 2014; Pert et al., 2015; Töpfer and Holz, 2020; Pitsidianaki et al., 2021)
Wing blister (wb)	<i>LAMA1</i>		Basal ECM in E, L and A	
LanB1/LamininB1	<i>LAMB2</i>			
Laminin B2 (LanB2)	<i>LAMB2</i>			
Collagen type IV alpha 1 (Col4 $\alpha$ 1)/Cg25C	<i>COL4A1</i>		Basal ECM from stage 16 E, L and A	
Viking (Vkg)	<i>COL4A1</i>			
Terribly reduced optic lobes (trol)/Perlecan	<i>HSPG</i>			
Nidogen (Ndg)	<i>NID1</i>		Basal ECM from stage 16 E and L	
Netrin-A (NetA)	<i>NTN1</i>		Basal ECM from stage 12 E	
Netrin-B (NetB)				
Secreted protein, acidic, cysteine-rich (SPARC)	<i>SPARC</i>		Basal ECM from stage 16 E and L	
Macrophage derived proteoglycan-1 (Mdp-1)/papilin (ppn)	-			
Glutactin (Glt)	-		Basal ECM in E	Olson et al. (1990)
Peroxidasin (Pxn)	<i>PXDN</i>			Nelson et al. (1994)
Mesh	<i>SUSD2</i>	TM	SJs from stage 16 E, L and A	(Izumi et al., 2012, 2016, 2021)
Snakeskin (Ssk)	-			
Tetraspanin 2A (Tsp2A)	<i>TSPAN8</i>			
Hoka	-			

(Continued on following page)

**TABLE 1 |** (Continued) *Drosophila* genes and their encoded protein's localization during midgut development.

<b>Drosophila gene (Abbreviation)/Alias</b>	<b>Human ortholog</b>	<b>Protein type</b>	<b>Protein localisation in the <i>Drosophila</i> midgut epithelial cell</b>	<b>References</b>
Bark beetle (bark)/anakonda (aka)	-	TM	Tri-cellular junctions in E	Byri et al. (2015); Wittek et al. (2020)
Gliotactin (Gli)	-			
M6	<i>GPM6A</i>			
Shotgun (shg)/DECad	<i>CDH20</i>	TM Cadherin	Apical side of the lateral junction in stage 9 E; AJ in A	Campbell et al. (2011); Chen et al. (2018)
armadillo (arm)/ $\beta$ -catenin	<i>CTNNB1</i>	Armadillo repeat	AJ in A	Chen et al. (2018)
$\alpha$ Catenin ( $\alpha$ -Cat)	<i>CTNNA</i>	Catenin		
Discs large 1 (dlg1)	<i>DLG1</i>	PDZ	Apical side of the lateral domain in the developing adult midgut	Takashima et al. (2011b)
Fasciclin 3 (Fas3)	<i>NECTIN3</i>	TM	at pupal stage	

-, Not found.

#1,2,3 E, L and A denote the embryonic, larval and adult midgut epithelium separately.

#4, PDZ domain containing scaffolding protein.

#5, TM denotes transmembrane protein.

#6, FERM domain containing protein.

basally-localised intestinal stem cells (ISC) can divide and differentiate into both ECs and ee cells in the adult midgut. The signals and mechanical cues that regulate ISC division and differentiation have been extensively characterised and have been summarised in many excellent reviews of this topic (Micchelli and Perrimon, 2006; Ohlstein and Spradling, 2006; Jiang and Edgar, 2011; Lucchetta and Ohlstein, 2012; Zeng et al., 2013; Antonello et al., 2015; He et al., 2018; Miguel-Aliaga et al., 2018; Reiff and Antonello, 2019; Rojas Villa et al., 2019; Jasper, 2020). The ISCs reside beneath the tri-cellular SJs between ECs, and do not contact the gut lumen or have an apical brush border, forming only AJs with their neighbours (Shanbhag and Tripathi, 2009; Xu et al., 2018; Chen and St Johnston, 2022). ISCs divisions give rise to new ISCs and to enteroblasts (EBs), which are the post-mitotic precursor of the ECs. EBs remain quiescent until new ECs are required, either through damage or normal cellular turnover. They are activated to differentiate into ECs by a network of transcription factors, including Zfh2, Sox100B and Sox21a (Meng and Biteau, 2015; Zhai et al., 2015, 2017; Chen et al., 2016; Doupé et al., 2018; Rojas Villa et al., 2019). Once activated, differentiating EBs polarise as they integrate into the epithelium (Chen and St Johnston, 2022; Moreno-Roman et al., 2022) (note #1). When the EB reaches the SJ between the overlying ECs, ECad containing AJs are cleared from its apical surface. The margins of the apical surface form new SJs with the neighbouring ECs and the centre becomes an apical membrane initiation site (AMIS). Secretion of apical components at the AMIS then leads to the formation of a preformed apical compartment (PAC) with a brush border beneath an intra-epithelial lumen that forms below the overlying EC-EC septate junction. As the differentiating EB/pre-EC expands further apically, the EC-EC SJ disassembles from its basal side and it eventually disappears when the EB/pre-EC reaches the gut lumen. It is not known how the ee precursor cells differentiate and integrate into the epithelia layer, although early work described a “closed” type of ee cell identified by the electron dense secretory granules in midguts of other insect species. These cells do not contact the apical lumen,

have minimal basal contacts with the basement membrane and may represent an intermediate stage in ee cell differentiation (Billingsley and Lehane, 1996; Caccia et al., 2019).

The exact mechanism that polarises ECs and ee cells in the adult midgut is not understood, but this does not require any of the canonical epithelial polarity factors that polarise non-endodermal epithelia, including Bazooka (Par-3), Par-6, atypical protein kinase C (aPKC), Crumbs (Crb), Stardust (Sdt), Discs large (Dlg), Lethal (2) giant larvae (Lgl) or Scribble (Chen et al., 2018). Instead, the basally localised integrin associated proteins, Rhea and Fit1 are required for all steps in EC polarisation and sSJ components are required for the formation of the PAC during EB integration (Chen et al., 2018; Chen and St Johnston, 2022). The progenitor and precursor cells, ISCs and EBs, lie at the basal side of the epithelium without any access to the apical lumen and do not form SJs with neighbouring cells. This indicates that the midgut epithelial cells require sustained basal signalling from the contact with the ECM to polarise in a basal to apical fashion. Their further polarisation, including the formation of sSJ and the apical brush border, requires positional cues from the SJs and the gradual growth of the apical domain via polarised membrane trafficking. The *Drosophila* midgut epithelium provides an excellent model for mammalian epithelia, which have a similar junctional arrangement and also require ECM contacts for polarity (Yu et al., 2005).

The adult *Drosophila* midgut epithelium is derived from AMPs, which are specified during early embryogenesis and segregated from the cells of the larval and pupal midgut during development (Campos-Ortega and Hartenstein, 1985; Tepass and Hartenstein, 1994a, 1995; Takashima et al., 2011b, 2011a, 2016a). Developmentally, the midgut epithelium is categorised as “a secondary epithelium”, since it goes through an epithelial-to-mesenchymal-transition (EMT) during early endoderm formation and later undergoes a mesenchymal-to-epithelial-transition (MET) to repolarise. In embryos, both the migration of the midgut primordia and repolarisation require

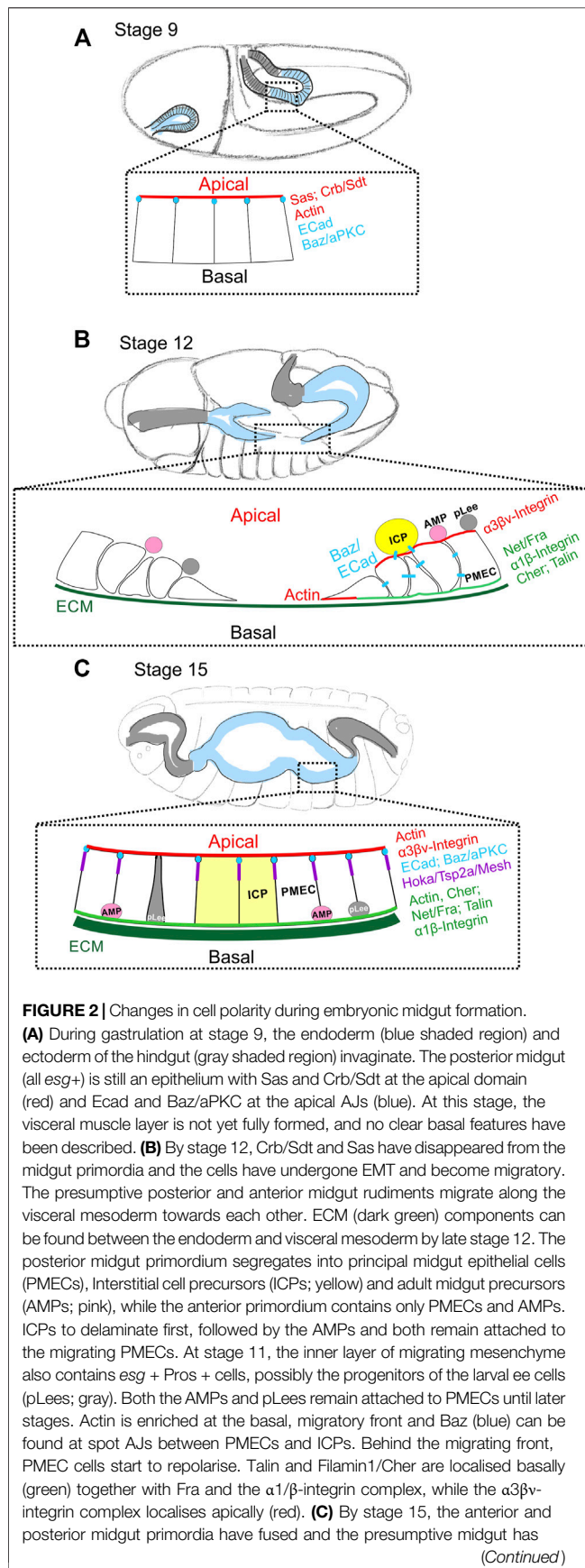


**FIGURE 2 |** Changes in cell polarity during embryonic midgut formation. **(A)** During gastrulation at stage 9, the endoderm (blue shaded region) and ectoderm of the hindgut (gray shaded region) invaginate. The posterior midgut (all *esg*+) is still an epithelium with Sas and Crb/Sdt at the apical domain (red) and Ecad and Baz/aPKC at the apical AJs (blue). At this stage, the visceral muscle layer is not yet fully formed, and no clear basal features have been described. **(B)** By stage 12, Crb/Sdt and Sas have disappeared from the midgut primordia and the cells have undergone EMT and become migratory. The presumptive posterior and anterior midgut rudiments migrate along the visceral mesoderm towards each other. ECM (dark green) components can be found between the endoderm and visceral mesoderm by late stage 12. The posterior midgut primordium segregates into principal midgut epithelial cells (PMECs), Interstitial cell precursors (ICPs; yellow) and adult midgut precursors (AMPs; pink), while the anterior primordium contains only PMECs and AMPs. ICPs to delaminate first, followed by the AMPs and both remain attached to the migrating PMECs. At stage 11, the inner layer of migrating mesenchyme also contains *esg* + Pros + cells, possibly the progenitors of the larval ee cells (pLees; gray). Both the AMPs and pLees remain attached to PMECs until later stages. Actin is enriched at the basal, migratory front and Baz (blue) can be found at spot AJs between PMECs and ICPs. Behind the migrating front, PMEC cells start to repolarise. Talin and Filamin1/Cher are localised basally (green) together with Fra and the  $\alpha1\beta$ -integrin complex, while the  $\alpha3\beta$ -integrin complex localises apically (red). **(C)** By stage 15, the anterior and posterior midgut primordia have fused and the presumptive midgut has

(Continued)

**FIGURE 2 |** closed ventrally and dorsally to form a continuous tube. ECM (dark green) forms a more complex network at this stage. The repolarised PMECs start to form smooth SJs (purple). Ecad and Baz localise to the apical junctions (blue), Actin to both the apical and basal sides and Filamin-1/Cher to the basal domain. Fra and the  $\alpha1\beta$ -integrin complex remain at the basal domain (green), while the  $\alpha3\beta$ -integrin complex localises mainly apically (red). By the end of embryonic development, ICPs (yellow) have integrated into larval midgut epithelium and AMPs (pink), which are the only remaining *esg* + cells, have translocated to the basal side of the epithelium. It is not known when the pLee cells (gray) integrate into the epithelium.

basal contact with the mesoderm and ECM components surrounding the endoderm layer (Tepass and Hartenstein, 1994a; Yarnitzky and Volk, 1995). It has been suggested that a similar mechanism is deployed during EB polarisation and differentiation, when EBs acquire a migratory potential before repolarising and integrating into the epithelial layer (Micchelli, 2012; Antonello et al., 2015). In this review, we will describe what is known about cell polarity changes during embryonic, larval and pupal midgut development and discuss what this suggests about the mechanisms of apical-basal polarisation in endodermal tissues.

## Cell Polarity During Embryonic Midgut Development

The *Drosophila* midgut primordium forms from the endoderm during gastrulation (Campos-Ortega and Hartenstein, 1985). Under the coordinated action of the GATA transcription factor Serpent and the winged-helix transcription factor Forkhead, the posterior midgut primordium (PMG) together with the ectodermally-derived hindgut primordium are internalised into the embryo (Weigel et al., 1989; Reuter, 1994; Nakagoshi, 2005). The PMG cells initially have the same apical-basal polarity as all ectodermal cells, which is established during the process of cellularisation (Tepass and Hartenstein, 1994b). Stranded-at-second (Sas), and the canonical apical polarity factors, Crb and Sdt, localise to the apical surface and Baz and Ecad are localised to the apical AJs (Table 1) (Figure 2A) (Campbell et al., 2011). During stage 10 of embryogenesis, Serpent induces the PMG to undergo an EMT and become migratory by repressing the expression of Crb, Sdt, Sas, and pleated SJ genes (Tepass and Hartenstein, 1994b; Campbell et al., 2011). As a result, the apical AJs dissolve and Ecad and Baz relocate from the AJs to dynamic puncta at cell-cell contacts, which are presumably scattered spot AJs. At stage 11, the PMG has established contact with the visceral muscle primordium and uses it as a substrate for its migration (Tepass and Hartenstein, 1994a). Three different cell types can be distinguished transcriptionally and morphologically among the migrating midgut mass. Most cells are principal midgut epithelial cells (PMECs), which will give rise to the larval midgut ECs and always contact the muscle primordium. The other two populations of mesenchymal cells, interstitial cell precursors (ICPs) and AMPs, are attached to the apical surface of PMECs and are carried along by the latter. ICPs express *Inscuteable* and *Asense* from late stage 10 to mid-stage 11, and AMPs, which will



give rise to the future adult midgut, are Asense-positive from early stage 11 to late stage 12 (**Figure 2B**) (Tepass and Hartenstein, 1994a, 1995; Campbell and Casanova, 2015). ICPs and AMPs delaminate sequentially from the outer layer of PMECs between stage 10–11 during their posterior migration (Tepass and Hartenstein, 1995). Some AMPs at this stage can also be marked with anti-Pros antibody staining, suggesting that they may be progenitor cells for future larval ee cells (pLee), although there is no lineage tracing data to support this. Like AMPs, pLees remain in the mesenchymal inner mass during migration, but become *esg*- and segregate from the AMPs by stage 14 (Jiang and Edgar, 2009; Takashima et al., 2011a). The cohesive and ordered migration of these three/four types of cells along the visceral mesoderm is coordinated through ECad-mediated cell adhesion and relies on the Integrin/Laminin and Frazzled/Netrin signalling pathways (Martin-Bermudo et al., 1999; Devenport and Brown, 2004; Campbell and Casanova, 2015; Pert et al., 2015; Pitsidianaki et al., 2021). Between late stage 11 and stage 12, shortly before and during germ band retraction, the PMECs reorganize and go through MET to form the midgut epithelium. By the end of germ band retraction at stage 13, the anterior and posterior midgut rudiments approach each other and finally fuse, the PMECs assume a columnar shape and the ICPs form two clusters in the middle of the developing midgut (Tepass and Hartenstein, 1994a). MET coincides with the downregulation of Fkh and Srp (Weigel et al., 1989; Campbell et al., 2011). However, Srp down-regulation is not sufficient to trigger MET, which instead depends on basal cues from Laminin and Netrins produced by the visceral mesoderm acting through Integrins and Fra respectively (Pert et al., 2015; Pitsidianaki et al., 2021) (**Figure 2B** and discussed later).

During endoderm migration, the ECM between the endoderm and the mesoderm is not yet fully organised, since early electron microscopy studies demonstrated that PMEC migration is mediated through direct mesoderm/endoderm contact without any detectable ECM or junctional specialisations (Tepass and Hartenstein, 1994a). However, Srp activates *LanB1* and *LanB2* RNA expression in stage 11 midgut primordium cells (Wolfstetter and Holz, 2012; Töpfer et al., 2019). Moreover, the laminin matrix secreted by the visceral muscle primordium contains Wb, which is thought to induce MET, whereas that secreted by endodermal cells contain LanA, and both LanA and Wb play crucial roles in controlling the speed of migration (Urbano et al., 2009; Wolfstetter and Holz, 2012; Pitsidianaki et al., 2021). At this stage, haemocytes (migrating macrophages) are the only source of secreted type IV collagen and Perlecan (Matsubayashi et al., 2017) and they do not reach the endoderm until after the migration is complete (Urbano et al., 2011; Pitsidianaki et al., 2021). Nidogen is reported to have similar expression pattern to LanB1 during embryogenesis but is not required for endoderm migration or formation (Urbano et al., 2009; Dai et al., 2018; Töpfer and Holz, 2020). At stage 16, Laminins, Collagens, Nidogen, and Perlecan, as well as other mature ECM components, such as MDP-1 and SPARC are all found in between the endoderm and mesoderm, forming a more complex ECM network (Wolfstetter and Holz, 2012).

Cells rely on ECM receptors to receive migratory/adhesive cues from the ECM, including Integrins, Fra, Dystroglycan (Dg),

the Glycicans Dally and Dally-like and Syndecan (Sdc) (**Table 1**). Integrins function as heterodimers of  $\alpha$  and  $\beta$  subunits and are required for both midgut migration and visceral muscle formation (Devenport and Brown, 2004). Flies have five  $\alpha$  integrin subunits,  $\alpha$ PS1–5 and two  $\beta$  subunits, Mys and  $\beta$ v (**Table 1**). Embryonic midgut migration requires the expression of both  $\alpha$ PS1 in the endoderm and  $\alpha$ PS2 in the visceral muscle, while  $\alpha$ PS3 cooperates with  $\alpha$ PS1 in the endoderm layer but is not required (Brown, 1994; Stark et al., 1997; Martin-Bermudo and Brown, 1999; Martin-Bermudo et al., 1999). Phylogenetic studies show that the  $\alpha$ PS3–5 subunits are closely related and the result of gene duplication events (Hughes, 2001).  $\alpha$ PS3 and  $\alpha$ PS4 are expressed in adult midgut ECs, whereas  $\alpha$ PS5 is not (Lin et al., 2013; Patel et al., 2015). Mys is widely expressed and is essential for viability, whereas  $\beta$ v is specifically expressed in the developing endoderm and the larval and adult midgut, but is not required for viability or fertility (Yee and Hynes, 1993). Integrins must form heterodimers in the endoplasmic reticulum to be trafficked to the cell surface and flies without both  $\beta$  subunits have no integrin function at all (Leptin et al., 1989; Devenport and Brown, 2004). Both  $\alpha$ PS1/Mys and  $\alpha$ PS3/ $\beta$ v pairs of integrins can be found in the migrating endoderm at late stage 11, with  $\alpha$ PS1/Mys localising to basal side and  $\alpha$ PS3/ $\beta$ v localising mainly apically at the end of migration (**Figure 2B**) (Devenport and Brown, 2004; Pitsidianaki et al., 2021). Two of the three Dystroglycan splicing isoforms are expressed in the midgut at stage 16, but their functions have not yet been characterised (Schneider and Baumgartner, 2008). Fra localises to the basal side of the PMECs at stage 12 and to the basal and junctional domain of the migrating midgut cells at stage 13 (**Figures 2B,C**). Interestingly, AMPs, which normally remain apical to the migrating PMECs at stage 12, are mis-localised and contact the visceral muscle in *netrin* mutant embryos. This phenotype has been attributed to the dis-organisation and loose adhesion of the PMG epithelium, rather than loss of direct signalling to AMPs, (Pert et al., 2015).

The PMECs are the first cell-type in the midgut primordia to go through MET, with AMPs, pLees, and ICPs remaining mesenchymal in the apical lumen until later. Although the exact time at which AMPs invade and translocate across the epithelium is not defined, they are located at the basal side of the gut in newly hatched larvae while the pLees have polarised and integrated into the epithelium (Hartenstein and Nung Jan 1992; Micchelli, 2012). This raises the question of how AMPs translocate to the basal side of the epithelium, since the apical junctions between the PMECs, which are marked by ECad, start to develop during migration in the outermost trailing region of the posterior midgut and sSJs start to develop in midgut from stage 15. Moreover, it is not clear whether the pLees become polarised and integrate into the epithelium during translocation or repolarise/integrate after translocating to the basal side (Takashima et al., 2011a). It has been hypothesized that the early delamination and late segregation and translocation of the AMPs and ICPs are due to differences in cell-cell affinity (Tepass and Hartenstein, 1995). However, there are no defects in the apical location of AMPs in *Ecad/shg* mutant embryos, it is therefore unclear whether their delamination and translocation is

a passive cell-sorting event or an active migration process (Tepass and Hartenstein, 1994a). Furthermore, it will be important to determine the relationship between cell fate determination and the corresponding EMT-MET processes.

By stage 15, the visceral mesoderm (VM) expands ventrally and dorsally to form the circular muscle fibres and the endodermal layer follows this movement to form a closed chamber. Although the early specification of the endoderm into distinct PMEC, ICP, pLee and AMP cell types does not depend on interaction with the mesoderm, VM induces the further specification and development of future larval midgut epithelium after the midgut rudiments fuse, including the formation of the three midgut constrictions during stages 14–16 and the specification of the middle midgut region and proventriculus (Nakagoshi, 2005).

Between stage 16 and 17, the future larval ECs change their morphology from short cuboidal cells to tall columnar cells and develop elaborate cellular junctions and an apical brush border (Morgan et al., 1995). Smooth SJ components start to express during stage 12 and become localised at stage 16, but mature sSJs only become visible at late stage 17 (Tepass and Hartenstein, 1994a; Izumi et al., 2012). Myo61F relocates from the basal-lateral region to the apical microvilli, coincident with the disappearance of the yolk mass which indicates the start of digestive function (Morgan et al., 1995).

*Drosophila* embryonic midgut formation takes less than 9 h, between stage 10 when PMG starts EMT and stage 15 when the midgut migration finishes. Both EMT and MET happen gradually, whereas cell polarity changes dramatically and rapidly during this process. The apical polarity factor Crb disappears early on, the original apical-lateral junctions dissolve, giving rise to a group of mesenchymal migratory cells connected by limited spot AJs. These cells later re-polarise forming smooth SJs rather than pleated SJs at the apical/lateral side of the cell-cell junctions. Embryonic midgut development also demonstrates the importance of the sustained basal signalling from the mesoderm much like the polarisation of the EBs in the adult midgut epithelium. It is still unclear, however, what lies downstream of basal ECM and their receptors to induce epithelial polarisation, and whether apical extracellular LanA and apically localised  $\alpha$ PS3/ $\beta$ v integrins plays any role in polarising the embryonic midgut epithelium. Past work has focused on the morphological development of the midgut and the genetic control of endoderm formation and differentiation (Bilder and Scott, 1995; Harbecke and Lengyel, 1995). Much less is known about the genetic control of AMP and ICP delamination and translocation, which also involves the loss and gain of cell polarity. These processes are challenging to study, however, because they occur over short time periods in the centre of the embryo.

## Larval Midgut Epithelial Cells

The larval midgut is composed of anterior, middle and posterior regions, each maintaining a different pH, and is anatomically similar to the adult midgut, although the constriction around the middle midgut is less obvious (Shanbhag and Tripathi, 2005; Overend et al., 2016). The larval midgut contains four gastric caeca, which are blind

sacs that emerge from the anterior midgut just posterior to the proventriculus. They persist in the larva but are lost during pupation and are not present in the adult fly (Skaer, 1993). Larval ECs are polyploid and derive from PMECs, whereas larval ee (lee) cells are diploid and derive from pLees (Takashima et al., 2011a). Cell specification has been well-studied in the larval middle midgut (Hoppler and Bienz, 1994, 1995). Large cells in this region were first called calycocytes, and were later named cuprophilic or copper cells, since they accumulate copper and display orange fluorescence when the larvae are fed with copper-enriched food. This property is attributed to the binding of copper ions to metallothionein, which is constitutively expressed in the cytoplasm in the middle midgut region (Skaer, 1993; Durlat et al., 1995; McNulty et al., 2001). It has been proposed that copper cells derive from the ICPs, although this is at odds with the observation that the ICPs disseminate over the whole embryonic midgut after stage 15 (Poulson and Waterhouse, 1960; Skaer, 1993). The copper cells are cup-shaped, with an invaginated apical domain containing long microvilli. They are surrounded by columnar interstitial cells with a normal apical domain, short microvilli and a more extensive basal labyrinth (Filshie et al., 1971). It is thought that the copper cells are the acid secreting cells, based on the correlation between the number of residual copper cells in *labial* mutant larvae and the number of remaining acid-retaining cells (Hoppler and Bienz, 1994; Dubreuil et al., 1998; Dubreuil, 2004). Several V-ATPase and other ion transporters are required for the acidic pH generation (Overend et al., 2016; Tian et al., 2022). Interestingly, copper absorption from the food can inhibit acid secretion and the acid secretion defective  *$\alpha$ -spec* mutant copper cells are not able to accumulate copper, which raises the question of how copper absorption and acid secretion are linked (Dubreuil et al., 1998; McNulty et al., 2001). Furthermore, we still do not know how and why the apical domain in the copper cells invaginates nor how the interdigitated arrangement of copper cells and interstitial cells arises. One clue comes from the stage 15 embryonic midgut, when the inner ICPs interdigitate between the outer *labial*-positive ICPs (Skaer, 1993), which means that the arrangement of copper cells and interstitial cells are probably also under the control of *labial*.

The larval midgut is remarkably similar to the adult midgut at the level of cellular structure, with an apical brush border facing the gut lumen, a basal side in contact with the visceral muscle and a basal labyrinth of invaginations from the basal membrane (**Figure 3**) (Shanbhag and Tripathi, 2005, 2009). The larval midgut also forms sSJs (Izumi et al., 2012, 2016, 2021) and the apical domain is enriched for actin and  $\beta_{\text{H}}$ -spectrin/ $\alpha$ -spectrin, while  $\beta$ -spectrin/ $\alpha$ -spectrin heterotetramers label the basolateral domain (Dubreuil et al., 1998). Spectrins are not required for copper cell polarity, but loss of  $\beta_{\text{H}}$ -spectrin leads to loss of the apical proton pump, the  $\text{H}^{+}$ V-ATPase which probably causes the defect in acid secretion seen in  *$\alpha$ -spec* mutant larvae (Phillips and Thomas, 2006). The two class I myosin family proteins, Myo31DF and Myo61DF can also be found in the apical terminal web and brush border microvilli in the larval ECs, but neither is required for cell polarity or brush border organisation (Morgan et al., 1995; Okumura et al., 2015). Interestingly, the AJs marked by ECad and Baz localise apical to the sSJ before the embryo hatches, whereas, AJs localise to the basal side of the sSJ in the first instar larva and adult ECs (Tepass

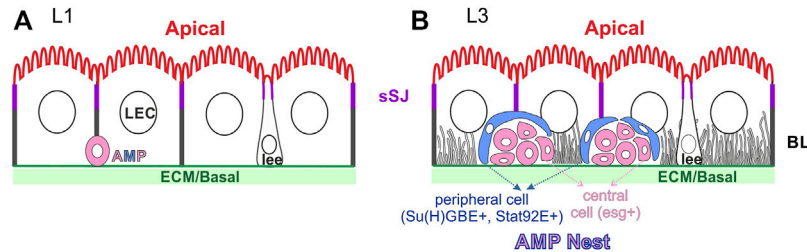


**FIGURE 3 |** The organisation of the larval midgut. The larval enterocytes (LEC) have a similar polarity to the adult ECs, with an apical brush border, sSJs and a basal labyrinth (BL) (possibly only at later stages). The larval ee cells (lee) have inserted into the larval midgut epithelium and are bottle-shaped, like adult ee cells. **(A)** The *esg* + AMPs keep dividing during the first larval instar and the daughter cells migrate and distribute along the basal surface of the epithelium. **(B)** 1-3 *10xSTAT92E-GFP* + peripheral cells (blue) ensheath the diploid central, *esg* + cells (pink) to form the AMP nests in the late third instar larval midgut. Some cells in each nest become Pros + at this stage and will contribute to the future tPMG.

and Hartenstein, 1994b; Chen et al., 2018). It is not clear how and when apical AJs disappear and basal AJs form during larval midgut formation.

One important feature of the larval midgut is the presence of AMPs. They first appear as single cells residing at the basal side of the larval midgut epithelium (L1, **Figure 3A**). They divide 7-10 times during the larval midgut development. The daughter cells of the first three divisions migrate and spread along the basal surface of the epithelium. The AMPs continue to divide during the third instar stage, but the daughter cells stay attached to each other to form AMP nests, which contain 8-30 cells by the onset of metamorphosis (**Figure 3B**) (Mathur et al., 2010; Takashima et al., 2011a; Jiang et al., 2011). 1-3 of the cells in an AMP nest differentiate into *STAT92E* > *GFP* (JAK-STAT pathway reporter) and *Su(H)GBE* > *GFP/lacZ* (Notch signalling reporter)-positive peripheral cells, which elongate and surround the inner mass of small, round central cells. Peripheral cells are post-mitotic with bigger nuclei than the central cells. They function as a niche to maintain the stem-cell state of the central AMP cells until metamorphosis (Mathur et al., 2010). However, the central cells can differentiate and become partially regenerative when the larval midgut is challenged with infection (Houtz et al., 2019). Some AMP cells also differentiate into Pros + cells and become an integral part of the future transient pupal midgut (Takashima et al., 2011b). The AMP nests can reach 2/3 of the height of the larval ECs, but do not reach the apical lumen, presumably because they cannot pass the sSJs between the larval ECs (**Figure 3B**). Both peripheral cells and central cells appear to maintain the contact with ECM and the peripheral cells contact the larval ECs. It is not known how the peripheral cells adopt a sheath-like shape and encase the central cells, nor how they provide a niche for the central AMP cells, except that the Dpp signalling is required (Mathur et al., 2010).

## Pupal Midgut Epithelial Layer and the Formation of Adult Midgut Epithelium

Shortly after puparium formation (APF), the larval midgut shortens, bringing the scattered AMP nests together. The outer peripheral cells contact each other first and by 6h APF become squamous and join together to form a multi-layered sheet called the transient pupal midgut (tPMG). Central cells

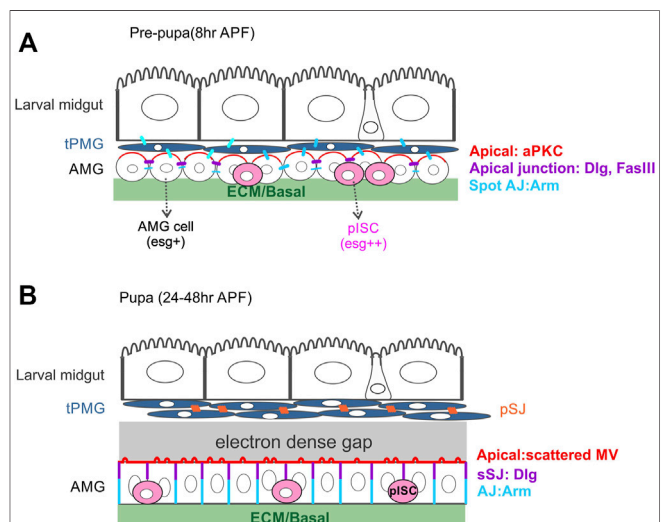


**FIGURE 4 |** The organisation of the midgut during pupal development.

**(A)** During the first hours after puparium formation, the peripheral cells of late larval midgut AMP nests re-arrange to form the tPMG (dark blue) around the degenerating larval midgut cells. At the onset of metamorphosis, the central cells of late larval midgut AMP nests spread out to surround the tPMG. This layer of AMP cells initially express *esg* homogeneously, but most AMG cells downregulate *esg* as they differentiate into ECs. A subset of AMPs maintain *esg* expression and become the presumptive intestinal stem cells (pISCs, pink), the precursors of the adult intestinal stem cells. At this stage, aPKC (red) localises to the apical domain of the AMG cells and Dlg and FasIII to the apical side of the lateral domain (purple). Spot AJs (blue) connect the larval ECs, the tPMG and the AMG cells. **(B)** From 20 h APF onwards, the tPMG appears as a tightly packed multi-layered structure with pleated SJs (orange) connecting the cells. By this stage, the tPMG has separated from the surrounding AMG and an electron dense liquid can be found between the two tissues. The AMG starts to develop irregularly spaced apical microvilli and smooth SJs at the apical side of the lateral membrane. AJs connect the more basal regions of the lateral membrane. pISCs remain basally localised.

also change their shape, flattening longitudinally and expanding laterally, to form a continuous layer of presumptive adult midgut (AMG) in a process that is thought to be MET (Takashima et al., 2011b). At this stage, the larval midgut, tPMG and AMG are all connected via spot AJs. At 8 h APF,



the AMG starts to show polarised features, with aPKC localising apically, Fas3 at the apical and lateral domains and Arm along the lateral and basal domains. Precursors of the adult ISCs, the presumptive intestinal stem cells (pISCs), remain at the basal side of the AMG layer (**Figure 4A**). At the same time, the tPMG also differentiates to a certain degree, forming microvilli and containing ee cells that have a spindle shape and remain detectable until 24 h APF (**Figure 4A, 3B**) (Takashima et al., 2011b; Takashima et al., 2016b). At 6 h APF, the ECM layer surrounding the midgut and visceral muscle starts to break down and disappears by 24 h APF. By 36 h APF, myofibrils disappear since the visceral muscle fibres surrounding midgut de-differentiate into secondary myoblasts (Aghajanian et al., 2016). During this time, both the tPMG and the AMG keep differentiating. The tPMG develops pleated SJs, whereas the AMG develops apical microvilli and smooth SJs at the apical side of the lateral domain. The AMG is in direct contact with the myoblasts since no ECM is observed in between (Aghajanian et al., 2016). Interestingly, an electron dense liquid has been observed separating the larval and tPMG from the AMG at this stage (**Figure 4B**) (Takashima et al., 2011b). Both the myofibrils and ECM reorganise and reappear by 48 h APF (Aghajanian et al., 2016). Between 48 and 72 h APF, some esg-positive pISCs express Pros and divide asymmetrically to give rise to the adult ee cells (Guo and Ohlstein, 2015). The re-emergence of ECM is thought to be important for the pISC division and specification at this stage (Aghajanian et al., 2016). During later stages of metamorphosis, the larval and transient pupal midguts remain closely associated and further contract and become the “yellow body” in the lumen of the developing adult midgut. They are eventually discharged from the intestinal tract after eclosion.

The separation between larval midgut/tPMG and the AMG is essentially the delamination of larval midgut epithelial cells and the detachment between peripheral cells and central cells of the AMP nests. This results in the reorganisation of the tissue into three layers with spot AJ still present among them (Takashima et al., 2011b). The reorganisation happens within the first 12 h during pupal development, while the visceral muscle and ECM are still present. Both the tPMG and AMG keep differentiating, but only the AMG remains attached to the ECM, which means the separation cannot be simply explained by apoptosis-induced cell extrusion. It would be interesting to find out whether basal integrin adhesion is weakened in the larval epithelium and tPMG but retained in the AMG. Many other questions still remain about the adult midgut formation during pupal metamorphosis. First of all, before metamorphosis begins, there is direct signalling between the peripheral cells and central cells in the seemingly compact AMP nests, but almost nothing is known about the molecules that mediate adhesion between them or the molecular mechanisms that control the separation and reorganisation of the tPMG and AMG. Secondly, although the tPMG loses contact with the ECM and muscle layer, it still manages to differentiate to form pleated SJ. The functional significance of this junction and how it is formed are unclear. Thirdly, the AMG cells are believed to go through MET as they polarise, while the pISCs remain basal and in contact

with the re-formed ECM and muscle layer. Based on what we know about the formation of the embryonic and adult midgut, it will be interesting to determine whether pISC specification requires a similar translocation process to AMPs in the embryo and if the AMG cells polarise in the same way as adult EBs and form a PAC as they integrate into the epithelium, and if their polarisation requires basal integrin signalling and SJ components.

## CONCLUDING REMARKS

AMPs are specified at an early embryonic stage, delaminate apically but remain attached to the PMECs via spot AJs and stay in the apical lumen of the migrating midgut primordium. They then translocate across the newly formed epithelium at the end of midgut development and remain basally after the embryo hatches. The mesoderm is not involved in the AMP specification and delamination, whereas cell-cell adhesion is proposed to play an important role in both the delamination and translocation. These processes are accompanied by the migration and repolarisation of the midgut primordium to form the future larval midgut epithelium. The migration and repolarisation require secreted Laminins from both germ layers, LanW at the basal side from the mesoderm and LanA at the apical side from the endoderm. The LanW from the basal side interacts with integrins receptors to activate downstream signaling pathways that are proposed to provide the cue that polarises the midgut epithelium and induce further polarised trafficking. The smooth SJs and the apical brush border microvilli form as the last step of polarisation in the epithelium. The polarised membrane features in the embryonic midgut epithelium are different from the steady state adult midgut epithelium, where integrin signalling components are only found basally and the lateral cell-cell junctions are clearly separated into apical-lateral sSJs and basal-lateral AJs. However, similar transcription factors control adult ISC maintenance and differentiation and embryonic midgut morphogenesis (Okumura et al., 2016). Moreover, EBs also go through a migratory stage before repolarising into ECs (Antonello et al., 2015). This means that the molecular mechanisms governing cell migration, cell translocation and MET-EMT could be the same in the embryo and adult.

During larval development, the AMPs expand, differentiate and form a nest containing peripheral cells and central cells. The peripheral cells are polarised to form sheath that surrounds and presumably isolates the central cells from the larval epithelial cells. It is not clear what type of cell-cell junctions form in the AMP nest and between the nest and larval epithelial cells. The peripheral cells later separate from the central cells to form the tPMG and delaminate with the larval epithelium at the start of pupation. By contrast, the central cells remain in contact with the basement membrane while adhering with each other to form the future AMG. Although both peripheral cells and central cells originate from AMPs, the peripheral cell-derived tPMG will develop pleated



SJs instead of smooth SJs. During the separation and reorganisation, spot AJs are found connecting the larval midgut, tPMG and AMG. This raises the possibility that cell-cell adhesion dynamics regulate the separation. After the visceral muscle and ECM layer reform at the basal side, the central cells start to polarise. Little is known about how polarised domains form in the AMG, except that aPKC localises to the apical domain, Dlg and FasIII occupy the apical-lateral junction and Arm/Ecad are localised at the basal-lateral domain (Takashima et al., 2011b). Since both embryonic midgut formation and EB polarisation in the adult midgut require sustained basal signalling, it seems likely that the AMG requires basal signalling from the newly-formed ECM to polarise, but the molecular mechanisms remain to be discovered.

In summary, studies on the behaviour of stem cells and the stem cell niche in the *Drosophila* midgut during embryonic, larval, pupal and adult development have paved the way for investigations into how cells are specified at each stage and how their polarity is controlled. Elucidating the roles of cell-cell interactions and signals from the ECM in the control of cell fate, cell shape and cell polarisation, will advance our understanding of how the gut epithelium develops and functions under healthy conditions, and how this is perturbed in diseased states such as cancer.

## REFERENCES

- Aghajanian, P., Takashima, S., Paul, M., Younossi-Hartenstein, A., and Hartenstein, V. (2016). Metamorphosis of the *Drosophila* Visceral Musculature and its Role in Intestinal Morphogenesis and Stem Cell Formation. *Dev. Biol.* 420, 43–59. doi:10.1016/j.ydbio.2016.10.011
- Antonello, Z. A., Reiff, T., Ballesta-Illan, E., and Dominguez, M. (2015). Robust Intestinal Homeostasis Relies on Cellular Plasticity in Enteroblasts Mediated by miR-8-Escargot Switch. *Embo J.* 34, 2025–2041. doi:10.15252/embj.201591517
- Baumann, O. (2001). Posterior Midgut Epithelial Cells Differ in Their Organization of the Membrane Skeleton from Other *drosophila* Epithelia. *Exp. Cell. Res.* 270, 176–187. doi:10.1006/excr.2001.5343
- Beehler-Evans, R., and Micchelli, C. A. (2015). Generation of Enteroendocrine Cell Diversity in Midgut Stem Cell Lineages. *Dev. Camb.* 142, 654–664. doi:10.1242/dev.114959
- Bilder, D., and Scott, M. P. (1995). Genomic Regions Required for Morphogenesis of the *Drosophila* Embryonic Midgut. *Genetics* 141, 1087–1100. doi:10.1093/genetics/141.3.1087
- Billingsley, P. F., and Lehane, M. J. (1996). “Structure and Ultrastructure of the Insect Midgut,” in *Biology of the Insect Midgut* (Dordrecht: Springer Netherlands), 3–30. doi:10.1007/978-94-009-1519-0\_1
- Bosveld, F., Wang, Z., and Bellaïche, Y. (2018). Tricellular Junctions: a Hot Corner of Epithelial Biology. *Curr. Opin. Cell. Biol.* 54, 80–88. doi:10.1016/j.ccb.2018.05.002
- Broadie, K., Baumgartner, S., and Prokop, A. (2011). Extracellular Matrix and its Receptors in *drosophila* Neural Development. *Devel Neurobio* 71, 1102–1130. doi:10.1002/dneu.20935
- Brown, N. H. (1994). Null Mutations in the Alpha PS2 and Beta PS Integrin Subunit Genes Have Distinct Phenotypes. *Development* 120, 1221–1231. doi:10.1242/dev.120.5.1221
- Buchon, N., Osman, D., David, F. P. A., Yu Fang, H., Boquete, J.-P., Deplancke, B., et al. (2013). Morphological and Molecular Characterization of Adult Midgut Compartmentalization in *Drosophila*. *Cell. Rep.* 3, 1725–1738. doi:10.1016/j.celrep.2013.04.001

## NOTE#1

By the time of submitting this review paper, these two research papers (Chen and St Johnston, 2022; Moreno-Roman et al., 2022) are still in the peer-reviewed stage for publishing. The citations are referring to the versions published on bioRxiv.org.

## AUTHOR CONTRIBUTIONS

JC made the figures, JC and DStJ wrote the manuscript.

## FUNDING

This work was supported by a Wellcome Principal Fellowship (207496) to DStJ and core funding from the Wellcome Trust (203144) and Cancer Research United Kingdom (A24843). JC was supported by a Royal Society K.C. Wong Postdoctoral Fellowship.

## ACKNOWLEDGMENTS

We would like to thank all past and present members of the St Johnston laboratory for their advice and support.

- Byri, S., Misra, T., Syed, Z. A., Bätz, T., Shah, J., Boril, L., et al. (2015). The Triple-Repeat Protein Anakonda Controls Epithelial Tricellular Junction Formation in *Drosophila*. *Dev. Cell.* 33, 535–548. doi:10.1016/j.devcel.2015.03.023
- Caccia, S., Casartelli, M., and Tettamanti, G. (2019). The Amazing Complexity of Insect Midgut Cells: Types, Peculiarities, and Functions. *Cell. Tissue Res.* 377, 505–525. doi:10.1007/s00441-019-03076-w
- Campbell, K., and Casanova, J. (2015). A Role for E-Cadherin in Ensuring Cohesive Migration of a Heterogeneous Population of Non-epithelial Cells. *Nat. Commun.* 6. doi:10.1038/ncomms8998
- Campbell, K., Whissell, G., Franch-Marro, X., Batlle, E., and Casanova, J. (2011). Specific GATA Factors Act as Conserved Inducers of an Endodermal-EMT. *Dev. Cell.* 21, 1051–1061. doi:10.1016/j.devcel.2011.10.005
- Campos-Ortega, J. A., and Hartenstein, V. (1985). *The Embryonic Development of Drosophila melanogaster*. Berlin, Heidelberg: Springer Berlin Heidelberg. doi:10.1007/978-3-662-02454-6
- Chen, J., Sayadian, A.-C., Lowe, N., Lovegrove, H. E., and St Johnston, D. (2018). An Alternative Mode of Epithelial Polarity in the *Drosophila* Midgut. *PLoS Biol.* 16, e3000041. doi:10.1371/journal.pbio.3000041
- Chen, J., and St Johnston, D. (2022). De Novo apical Domain Formation inside the *Drosophila* Adult Midgut Epithelium. doi:10.1101/2021.12.10.472136
- Chen, J., Xu, N., Huang, H., Cai, T., and Xi, R. (2016). A Feedback Amplification Loop between Stem Cells and Their Progeny Promotes Tissue Regeneration and Tumorigenesis. *Elife*. doi:10.7554/eLife.14330.001
- Choi, N. H., Lucchetta, E., and Ohlstein, B. (2011). Nonautonomous Regulation of *Drosophila* Midgut Stem Cell Proliferation by the Insulin-Signaling Pathway. *Proc. Natl. Acad. Sci. U.S.A.* 108, 18702–18707. doi:10.1073/pnas.1109348108
- Crawley, S. W., Mooseker, M. S., and Tyska, M. J. (2014). Shaping the Intestinal Brush Border. *J. Cell. Biol.* 207, 441–451. doi:10.1083/jcb.201407015
- Dai, J., Estrada, B., Jacobs, S., Sánchez-Sánchez, B. J., Tang, J., Ma, M., et al. (2018). Dissection of Nidogen Function in *Drosophila* Reveals Tissue-specific Mechanisms of Basement Membrane Assembly. *PLoS Genet.* 14, e1007483. doi:10.1371/journal.pgen.1007483
- Davis, M. N., Horne-Badovinac, S., and Naba, A. (2019). In-silico Definition of the *Drosophila melanogaster* Matrisome. *Matrix Biol. Plus* 4, 100015. doi:10.1016/j.mbpplus.2019.100015

- Devenport, D., and Brown, N. H. (2004). Morphogenesis in the Absence of Integrins: Mutation of both *Drosophila*  $\beta$  Subunits Prevents Midgut Migration. *Development* 131, 5405–5415. doi:10.1242/dev.01427
- Doupé, D. P., Marshall, O. J., Dayton, H., Brand, A. H., and Perrimon, N. (2018). *Drosophila* Intestinal Stem and Progenitor Cells Are Major Sources and Regulators of Homeostatic Niche Signals. *Proc. Natl. Acad. Sci. U.S.A.* 115, 12218–12223. doi:10.1073/pnas.1719169115
- Dubreuil, R. R. (2004). Copper Cells and Stomach Acid Secretion in the *Drosophila* Midgut. *Int. J. Biochem. Cell. Biol.* 36, 742–752. doi:10.1016/j.biocel.2003.07.004
- Dubreuil, R. R., Frankel, J., Wang, P., Howrylak, J., Kappil, M., and Grushko, T. A. (1998). Mutations of a Spectrin and labial Block Cuprophilic Cell Differentiation and Acid Secretion in the Middle Midgut of *Drosophila* Larvae. *Dev. Biol.* 194, 1–11. doi:10.1006/dbio.1997.8821
- Durliat, M. I., Bonneton, F. O., Boissonneau, E., André, M. I., and Wegnez, M. (1995). Expression of Metallothionein Genes during the Post-embryonic Development of *Drosophila melanogaster*. *Biomaterials* 8. doi:10.1007/BF00141608
- Dutta, D., Dobson, A. J., Houtz, P. L., Gläßer, C., Revah, J., Korzeliuss, J., et al. (2015). Regional Cell-specific Transcriptome Mapping Reveals Regulatory Complexity in the Adult *Drosophila* Midgut. *Cell. Rep.* 12, 346–358. doi:10.1016/j.celrep.2015.06.009
- Esmangart de Bournonville, T., and le Borgne, R. (2020). Interplay between Anakonda, Gliotactin, and M6 for Tricellular Junction Assembly and Anchoring of Septate Junctions in *Drosophila* Epithelium. *Curr. Biol.* 30, 4245–4253.e4. doi:10.1016/j.cub.2020.07.090
- Filshie, B. K., Poulson, D. F., and Waterhouse, D. F. (1971). Ultrastructure of the Copper-Accumulating Region of the *Drosophila* Larval Midgut. *Tissue Cell* 3, 77–102. doi:10.1016/S0040-8166(71)80033-2
- Finegan, T. M., Hervieux, N., Nestor-Bergmann, A., Fletcher, A. G., Blanchard, G. B., and Sanson, B. (2019). The Tricellular Vertex-specific Adhesion Molecule Sidekick Facilitates Polarised Cell Intercalation during *Drosophila* axis Extension. *PLoS Biol.* 17, e3000522. doi:10.1371/journal.pbio.3000522
- Furuse, M., and Izumi, Y. (2017). Molecular Dissection of Smooth Septate Junctions: Understanding Their Roles in Arthropod Physiology. *Ann. N.Y. Acad. Sci.* 1397, 17–24. doi:10.1111/nyas.13366
- Guo, Z., and Ohlstein, B. (2015/1979). Bidirectional Notch Signaling Regulates *Drosophila* Intestinal Stem Cell Multipotency. *Science* 350, 927. doi:10.1126/science.aab0988
- Harbecke, R., and Lengyel, J. A. (1995). Genes Controlling Posterior Gut Development in the *Drosophila* Embryo. *Roux's Arch. Dev. Biol.* 204, 308–329. doi:10.1007/BF02179500
- Hartenstein, V., and Nung Jan, Y. (1992). Studying *Drosophila* Embryogenesis with P-lacZ Enhancer Trap Lines. *Roux's Arch. Dev. Biol.* 201 (4), 194–220. doi:10.1007/BF00188752
- He, L., Si, G., Huang, J., Samuel, A. D. T., and Perrimon, N. (2018). Mechanical Regulation of Stem-Cell Differentiation by the Stretch-Activated Piezo Channel. *Nature* 555, 103–106. doi:10.1038/nature25744
- Hildebrandt, A., Pflanz, R., Behr, M., Tarp, T., Riedel, D., and Schuh, R. (2015). Bark Beetle Controls Epithelial Morphogenesis by Septate Junction Maturation in *Drosophila*. *Dev. Biol.* 400, 237–247. doi:10.1016/j.ydbio.2015.02.008
- Hoppler, S., and Bienz, M. (1994). Specification of a Single Cell Type by a *Drosophila* Homeotic Gene. *Cell* 76, 689–702. doi:10.1016/0092-8674(94)90508-8
- Hoppler, S., and Bienz, M. (1995). Two Different Thresholds of Wingless Signalling with Distinct Developmental Consequences in the *Drosophila* Midgut. *EMBO J.* 14, 5016–5026. doi:10.1002/j.1460-2075.1995.tb00184.x
- Houtz, P., Bonfini, A., Bing, X., and Buchon, N. (2019). Recruitment of Adult Precursor Cells Underlies Limited Repair of the Infected Larval Midgut in *Drosophila*. *Cell. Host Microbe* 26, 412–425.e5. doi:10.1016/j.chom.2019.08.006
- Hughes, A. L. (2001). Evolution of the Integrin  $\alpha$  and  $\beta$  Protein Families. *J. Mol. Evol.* 52, 63–72. doi:10.1007/s002390010134
- Hung, R.-J., Hu, Y., Kirchner, R., Liu, Y., Xu, C., Comjean, A., et al. (2020). A Cell Atlas of the Adult *Drosophila* Midgut. *Proc. Natl. Acad. Sci. U.S.A.* 117, 1514–1523. doi:10.1073/pnas.1916820117
- Izumi, Y., Furuse, K., and Furuse, M. (2021). The Novel Membrane Protein Hoka Regulates Septate Junction Organization and Stem Cell Homeostasis in the *Drosophila* Gut. *J. Cell. Sci.* 134. doi:10.1242/jcs.257022
- Izumi, Y., Motoishi, M., Furuse, K., and Furuse, M. (2016). A Tetraspanin Regulates Septate Junction Formation in *Drosophila* Midgut. *J. Cell. Sci.* 129, 1155–1164. doi:10.1242/jcs.180448
- Izumi, Y., Yanagihashi, Y., and Furuse, M. (2012). A Novel Protein Complex, Mesh-Ssk, Is Required for Septate Junction Formation in *Drosophila* Midgut. *J. Cell. Sci.* 125, 4923–4933. doi:10.1242/jcs.112243
- Jasper, H. (2020). Intestinal Stem Cell Aging: Origins and Interventions. *Annu. Rev. Physiol.* 82, 203–226. doi:10.1146/annurev-physiol-021119-034359
- Jiang, H., and Edgar, B. A. (2009). EGFR Signaling Regulates the Proliferation of *Drosophila* Adult Midgut Progenitors. *Development* 136, 483–493. doi:10.1242/dev.026955
- Jiang, H., and Edgar, B. A. (2011). Intestinal Stem Cells in the Adult *Drosophila* Midgut. *Exp. Cell. Res.* 317, 2780–2788. doi:10.1016/j.yexcr.2011.07.020
- Jiang, H., Grenley, M. O., Bravo, M.-J., Blumhagen, R. Z., and Edgar, B. A. (2011). EGFR/Ras/MAPK Signaling Mediates Adult Midgut Epithelial Homeostasis and Regeneration in *Drosophila*. *Cell. Stem Cell* 8, 84–95. doi:10.1016/j.stem.2010.11.026
- Kramerova, I. A., Kramerov, A. A., and Fessler, J. H. (2003). Alternative Splicing of Papilin and the Diversity of *Drosophila* Extracellular Matrix during Embryonic Morphogenesis. *Dev. Dyn.* 226, 634–642. doi:10.1002/dvdy.10265
- Lane, N. J., and Skaer, H. I. (1980). Intercellular Junctions in Insect Tissues. *Adv. Insect Phys.* 15, 35–213. doi:10.1016/S0065-2806(08)60141-1
- Lehane, M. J. (1997). Peritrophic Matrix Structure and Function. Available at: www.annualreviews.org. doi:10.1146/annurev.ento.42.1.525
- Leptin, M., Bogaert, T., Lehmann, R., and Wilcox, M. (1989). The Function of PS Integrins during *Drosophila* Embryogenesis. *Cell* 56, 401–408. doi:10.1016/0092-8674(89)90243-2
- Letizia, A., He, D., Astigarraga, S., Colombelli, J., Hatini, V., Llimargas, M., et al. (2019). Sidekick Is a Key Component of Tricellular Adherens Junctions that Acts to Resolve Cell Rearrangements. *Dev. Cell* 50, 313–326.e5. doi:10.1016/j.devcel.2019.07.007
- Liang, J., Balachandra, S., Ngo, S., and O'Brien, L. E. (2017). Feedback Regulation of Steady-State Epithelial Turnover and Organ Size. *Nature* 548, 588–591. doi:10.1038/nature23678
- Lin, G., Zhang, X., Ren, J., Pang, Z., Wang, C., Xu, N., et al. (2013). Integrin Signaling Is Required for Maintenance and Proliferation of Intestinal Stem Cells in *Drosophila*. *Dev. Biol.* 377, 177–187. doi:10.1016/j.ydbio.2013.01.032
- Lucchetta, E. M., and Ohlstein, B. (2012). The *Drosophila* Midgut: a Model for Stem Cell Driven Tissue Regeneration. *WIREs Dev. Biol.* 1, 781–788. doi:10.1002/wdev.51
- Marianes, A., and Spradling, A. C. (2013/2013). Physiological and Stem Cell Compartmentalization within the *Drosophila* Midgut. *Elife* 2, e00886. doi:10.7554/eLife.00886
- Martin-Bermudo, M. D., Alvarez-Garcia, I., and Brown, N. H. (1999). Migration of the *Drosophila* Primordial Midgut Cells Requires Coordination of Diverse PS Integrin Functions. *Development* 126, 5161–5169. doi:10.1242/dev.126.22.5161
- Martin-Bermudo, M. D., and Brown, N. H. (1999). Uncoupling Integrin Adhesion and Signaling: the PS Cytoplasmic Domain Is Sufficient to Regulate Gene Expression in the *Drosophila* Embryo. Available at: www.genesdev.org.
- Martinek, N., Shahab, J., Saathoff, M., and Ringuette, M. (2008). Haemocyte-derived SPARC Is Required for Collagen-IV-dependent Stability of Basal Laminae in *Drosophila* Embryos. *J. Cell. Sci.* 121, 1671–1680. doi:10.1242/jcs.021931
- Martinek, N., Zou, R., Berg, M., Sodek, J., and Ringuette, M. (2002). Evolutionary Conservation and Association of SPARC with the Basal Lamina in *Drosophila*. *Dev. Genes. Evol.* 212, 124–133. doi:10.1007/s00427-002-0220-9
- Mathur, D., Bost, A., Driver, I., and Ohlstein, B. (2010/1979). A Transient Niche Regulates the Specification of *Drosophila* Intestinal Stem Cells. *Science* 327, 210–213. doi:10.1126/science.1181958
- Matsubayashi, Y., Louani, A., Dragu, A., Sánchez-Sánchez, B. J., Serna-Morales, E., Yolland, L., et al. (2017). A Moving Source of Matrix Components Is Essential for De Novo Basement Membrane Formation. *Curr. Biol.* 27, 3526–3534.e4. doi:10.1016/j.cub.2017.10.001
- McNulty, M., Puljung, M., Jefford, G., and Dubreuil, R. (2001). Evidence that a Copper-Metallothionein Complex Is Responsible for Fluorescence in Acid-Secreting Cells of the *Drosophila* Stomach. *Cell. Tissue Res.* 304, 383–389. doi:10.1007/s004410100371

- Meng, F. W., and Biteau, B. (2015). A Sox Transcription Factor Is a Critical Regulator of Adult Stem Cell Proliferation in the Drosophila Intestine. *Cell. Rep.* 13, 906–914. doi:10.1016/j.celrep.2015.09.061
- Micchelli, C. A., and Perrimon, N. (2006). Evidence that Stem Cells Reside in the Adult Drosophila Midgut Epithelium. *Nature* 439, 475–479. doi:10.1038/nature04371
- Micchelli, C. A. (2012). The Origin of Intestinal Stem Cells in Drosophila. *Dev. Dyn.* 241, 85–91. doi:10.1002/dvdy.22759
- Miguel-Aliaga, I., Jasper, H., and Lemaitre, B. (2018). Anatomy and Physiology of the Digestive Tract of drosophila Melanogaster. *Genetics* 210, 357–396. doi:10.1534/genetics.118.300224
- Moreno-Roman, P., Su, Y.-H., Galenza, A., Acosta-Alvarez, L., Debec, A., Guichet, A., et al. (2022). Progenitor Cell Integration into a Barrier Epithelium during Adult Organ Turnover. doi:10.1101/2021.09.19.457819
- Morgan, N. S., Heintzelman, M. B., and Mooseker, M. S. (1995). Characterization of Myosin-IA and Myosin-IB, Two Unconventional Myosins Associated with the Drosophila Brush Border Cytoskeleton. *Dev. Biol.* 172, 51–71. doi:10.1006/dbio.1995.0005
- Nakagoshi, H. (2005). Functional Specification in the Drosophila Endoderm. *Dev. Growth Differ.* 47 (6), 383–392. doi:10.1111/j.1440-169x.2005.00811.x
- Nelson, R. E., Fessler, L. I., Takagi, Y., Blumberg, B., Keene, D. R., Olson, P. F., et al. (1994). Peroxidase: a Novel Enzyme-Matrix Protein of Drosophila Development. *EMBO J.* 13, 3438–3447. doi:10.1002/j.1460-2075.1994.tb06649.x
- Ohlstein, B., and Spradling, A. (2006). The Adult Drosophila Posterior Midgut Is Maintained by Pluripotent Stem Cells. *Nature* 439, 470–474. doi:10.1038/nature04333
- Okumura, T., Sasamura, T., Inatomi, M., Hozumi, S., Nakamura, M., Hatori, R., et al. (2015). Class I Myosins Have Overlapping and Specialized Functions in Left-Right Asymmetric Development in Drosophila. *Genetics* 199, 1183–1199. doi:10.1534/genetics.115.174698
- Okumura, T., Takeda, K., Kuchiki, M., Akaishi, M., Taniguchi, K., and Adachi-Yamada, T. (2016). GATAe Regulates Intestinal Stem Cell Maintenance and Differentiation in Drosophila Adult Midgut. *Dev. Biol.* 410, 24–35. doi:10.1016/j.ydbio.2015.12.017
- Okumura, T., Takeda, K., Taniguchi, K., and Adachi-Yamada, T. (2014). Bv Integrin Inhibits Chronic and High Level Activation of JNK to Repress Senescence Phenotypes in Drosophila Adult Midgut. *PLoS ONE* 9, e89387. doi:10.1371/journal.pone.0089387
- Olson, P. F., Fessler, L. I., Nelson, R. E., Sterne, R. E., Campbell, A. G., and Fessler, J. H. (1990). Glutactin, a Novel Drosophila Basement Membrane-Related Glycoprotein with Sequence Similarity to Serine Esterases. *EMBO J.* 9, 1219–1227. doi:10.1002/j.1460-2075.1990.tb08229.x
- Overend, G., Luo, Y., Henderson, L., Douglas, A. E., Davies, S. A., and Dow, J. A. T. (2016). Molecular Mechanism and Functional Significance of Acid Generation in the Drosophila Midgut. *Sci. Rep.* 6. doi:10.1038/srep27242
- Patel, P. H., Dutta, D., and Edgar, B. A. (2015). Niche Appropriation by Drosophila Intestinal Stem Cell Tumours. *Nat. Cell. Biol.* 17, 1182–1192. doi:10.1038/ncb3214
- Pert, M., Gan, M., Saint, R., and Murray, M. J. (2015). Netrins and Frazzled/DCC Promote the Migration and Mesenchymal to Epithelial Transition of Drosophila Midgut Cells. *Biol. Open* 4, 233–243. doi:10.1242/bio.201410827
- Phillips, M. D., and Thomas, G. H. (2006). Brush Border Spectrin Is Required for Early Endosome Recycling in Drosophila. *J. Cell. Sci.* 119, 1361–1370. doi:10.1242/jcs.02839
- Pitsidianaki, I., Morgan, J., Adams, J., and Campbell, K. (2021). Mesenchymal-to-epithelial Transitions Require Tissue-specific Interactions with Distinct Laminins. *J. Cell. Biol.* 220. doi:10.1083/jcb.202010154
- Poulson, D., and Waterhouse, D. (1960). Experimental Studies on Pole Cells and Midgut Differentiation in Diptera. *Aust. Jnl. Bio. Sci.* 13, 541. doi:10.1071/B19600541
- Reiff, T., Antonello, Z. A., Ballesta-Illán, E., Mira, L., Sala, S., Navarro, M., et al. (2019). Notch and EGFR Regulate Apoptosis in Progenitor Cells to Ensure Gut Homeostasis in Drosophila. *EMBO J.* 38, e101346. doi:10.15252/embj.2018101346
- Resnik-Docampo, M., Koehler, C. L., Clark, R. I., Schinaman, J. M., Sauer, V., Wong, D. M., et al. (2017). Tricellular Junctions Regulate Intestinal Stem Cell Behaviour to Maintain Homeostasis. *Nat. Cell. Biol.* 19, 52–59. doi:10.1038/ncb3454
- Reuter, R. (1994). The Gene Serpent Has Homeotic Properties and Specifies Endoderm versus Ectoderm within the Drosophila Gut. *Development* 120, 1123–1135. doi:10.1242/dev.120.5.1123
- Rojas Villa, S. E., Meng, F. W., and Biteau, B. (2019). zfh2 Controls Progenitor Cell Activation and Differentiation in the Adult Drosophila Intestinal Absorptive Lineage. *PLoS Genet.* 15, e1008553. doi:10.1371/journal.pgen.1008553
- Sauvanet, C., Wayt, J., Pelaseyed, T., and Bretscher, A. (2015). Structure, Regulation, and Functional Diversity of Microvilli on the Apical Domain of Epithelial Cells. *Annu. Rev. Cell. Dev. Biol.* 31, 593–621. doi:10.1146/annurev-cellbio-100814-125234
- Schneider, M., and Baumgartner, S. (2008). Differential Expression of Dystroglycan-Spliceforms with and without the Mucin-like Domain during Drosophila Embryogenesis. *Fly* 2, 29–35. doi:10.4161/fly.5726
- Schulte, J., Tepass, U., and Auld, V. J. (2003). Gliotactin, a Novel Marker of Tricellular Junctions, Is Necessary for Septate Junction Development in Drosophila. *J. Cell. Biol.* 161, 991–1000. doi:10.1083/jcb.200303192
- Shanbhag, S., and Tripathi, S. (2005). Electrogenic H<sup>+</sup> Transport and pH Gradients Generated by a V-H<sup>+</sup>-ATPase in the Isolated Perfused Larval Drosophila Midgut. *J. Membr. Biol.* 206, 61–72. doi:10.1007/s00232-005-0774-1
- Shanbhag, S., and Tripathi, S. (2009). Epithelial Ultrastructure and Cellular Mechanisms of Acid and Base Transport in the Drosophilamidgut. *J. Exp. Biol.* 212, 1731–1744. doi:10.1242/jeb.029306
- Skaer, H. (1993). “The Alimentary Canal,” in *The Development of Drosophila melanogaster*. Editors M. Bate, A. Martinez-Arias, and N. Y. Woodbury (New York, NY: Cold Spring Harbor Laboratory Press), 941–1012.
- Stark, K. A., Yee, G. H., Roote, C. E., Williams, E. L., Zusman, S., and Hynes, R. O. (1997). A Novel Alpha Integrin Subunit Associates with betaPS and Functions in Tissue Morphogenesis and Movement during Drosophila Development. *Development* 124, 4583–4594. doi:10.1242/dev.124.22.4583
- Strand, M., and Micchelli, C. A. (2011). Quiescent Gastric Stem Cells Maintain the Adult Drosophila Stomach. *Proc. Natl. Acad. Sci. U.S.A.* 108, 17696–17701. doi:10.1073/pnas.1109794108
- Takashima, S., Adams, K. L., Ortiz, P. A., Ying, C. T., Moridzadeh, R., Younossi-Hartenstein, A., et al. (2011a). Development of the Drosophila Entero-Endocrine Lineage and its Specification by the Notch Signaling Pathway. *Dev. Biol.* 353, 161–172. doi:10.1016/j.ydbio.2011.01.039
- Takashima, S., Aghajanian, P., Younossi-Hartenstein, A., and Hartenstein, V. (2016a). Origin and Dynamic Lineage Characteristics of the Developing Drosophila Midgut Stem Cells. *Dev. Biol.* 416, 347–360. doi:10.1016/j.ydbio.2016.06.018
- Takashima, S., Aghajanian, P., Younossi-Hartenstein, A., and Hartenstein, V. (2016b). Origin and Dynamic Lineage Characteristics of the Developing Drosophila Midgut Stem Cells. *Dev. Biol.* 416, 347–360. doi:10.1016/j.ydbio.2016.06.018
- Takashima, S., Younossi-Hartenstein, A., Ortiz, P. A., and Hartenstein, V. (2011b). A Novel Tissue in an Established Model System: The Drosophila Pupal Midgut. *Dev. Genes. Evol.* 221, 69–81. doi:10.1007/s00427-011-0360-x
- Tepass, U., and Hartenstein, V. (1994a). Epithelium Formation in the Drosophila Midgut Depends on the Interaction of Endoderm and Mesoderm. *Development* 120, 579–590. doi:10.1242/dev.120.3.579
- Tepass, U., and Hartenstein, V. (1995). Neurogenic and Proneural Genes Control Cell Fate Specification in the Drosophila Endoderm. *Development* 121, 393–405. doi:10.1242/dev.121.2.393
- Tepass, U., and Hartenstein, V. (1994b). The Development of Cellular Junctions in the Drosophila Embryo. *Dev. Biol.* 161, 563–596. doi:10.1006/dbio.1994.1054
- Tian, Y., Tian, Y., Yu, G., Li, K., Du, Y., Yuan, Z., et al. (2022). VhaAC39-1 Regulates Gut Homeostasis and Affects the Health Span in Drosophila. *Mech. Ageing Dev.* 204, 111673. doi:10.1016/j.mad.2022.111673
- Töpfer, U., Bischoff, M. C., Bartkuhn, M., and Holz, A. (2019). Serpent/dGATAb Regulates Laminin B1 and Laminin B2 Expression during Drosophila Embryogenesis. *Sci. Rep.* 9. doi:10.1038/s41598-019-52210-9
- Töpfer, U., and Holz, A. (2020). Analysis of Extracellular Matrix Composition in the Visceral Muscles of Nidogen Mutant Larvae in Drosophila. *Micropubl. Biol.* doi:10.17912/micropub.biology.000251
- Uechi, H., and Kuranaga, E. (2019). The Tricellular Junction Protein Sidekick Regulates Vertex Dynamics to Promote Bicellular Junction Extension. *Dev. Cell.* 50, 327–338.e5. doi:10.1016/j.devcel.2019.06.017

- Urbano, J. M., Domínguez-Giménez, P., Estrada, B., and Martín-Bermudo, M. D. (2011). PS Integrins and Laminins: Key Regulators of Cell Migration during Drosophila Embryogenesis. *PLoS ONE* 6, e23893. doi:10.1371/journal.pone.0023893
- Urbano, J. M., Torgler, C. N., Molnar, C., Tepass, U., López-Varea, A., Brown, N. H., et al. (2009). Drosophilalaminins Act as Key Regulators of Basement Membrane Assembly and Morphogenesis. *Development* 136, 4165–4176. doi:10.1242/dev.044263
- Weigel, D., Bellen, H. J., Jürgens, G., and Jäckle, H. (1989). Primordium Specific Requirement of the Homeotic Gene Fork Head in the Developing Gut of the Drosophila Embryo. *Roux's Arch. Dev. Biol.* 198, 201–210. doi:10.1007/BF00375906
- Witteck, A., Hollmann, M., Schleutker, R., and Luschnig, S. (2020). The Transmembrane Proteins M6 and Anakonda Cooperate to Initiate Tricellular Junction Assembly in Epithelia of Drosophila. *Curr. Biol.* 30, 4254–4262.e5. doi:10.1016/j.cub.2020.08.003
- Wolfstetter, G., and Holz, A. (2012). The Role of LamininB2 (LanB2) during Mesoderm Differentiation in Drosophila. *Cell. Mol. Life Sci.* 69, 267–282. doi:10.1007/s00018-011-0652-3
- Xu, C., Ericsson, M., and Perrimon, N. (2018). Understanding Cellular Signaling and Systems Biology with Precision: A Perspective from Ultrastructure and Organelle Studies in the Drosophila Midgut. *Curr. Opin. Syst. Biol.* 11, 24–31. doi:10.1016/j.coisb.2018.07.003
- Yarnitzky, T., and Volk, T. (1995). Laminin Is Required for Heart, Somatic Muscles, and Gut Development in the Drosophila Embryo. *Dev. Biol.* 169, 609–618. doi:10.1006/dbio.1995.1173
- Yee, G. H., and Hynes, R. O. (1993). A Novel, Tissue-specific Integrin Subunit, Beta Nu, Expressed in the Midgut of *Drosophila melanogaster*. *Development* 118, 845–858. doi:10.1242/dev.118.3.845
- You, J., Zhang, Y., Li, Z., Lou, Z., Jin, L., and Lin, X. Drosophila perlecan regulates intestinal stem cell activity via cell-matrix attachment. *Stem Cell Reports*. 2014 May 9; 2(6):761–769. doi:10.1016/j.stemcr.2014.04.007
- Yu, W., Datta, A., Leroy, P., O'Brien, L. E., Mak, G., Jou, T.-S., et al. (2005).  $\beta$ 1-Integrin Orients Epithelial Polarity via Rac1 and Laminin. *MBoC* 16, 433–445. doi:10.1091/mbc.E04-05-0435
- Zeng, X., Chauhan, C., and Hou, S. X. (2013). Stem Cells in the Drosophila Digestive System. *Adv. Exp. Med. Biol.*, 63–78. doi:10.1007/978-94-007-6621-1\_5
- Zhai, Z., Boquete, J.-P., and Lemaitre, B. (2017). A Genetic Framework Controlling the Differentiation of Intestinal Stem Cells during Regeneration in Drosophila. *PLoS Genet.* 13, e1006854. doi:10.1371/journal.pgen.1006854
- Zhai, Z., Kondo, S., Ha, N., Boquete, J.-P., Brunner, M., Ueda, R., et al. (2015). Accumulation of Differentiating Intestinal Stem Cell Progenies Drives Tumorigenesis. *Nat. Commun.* 6, 10219. doi:10.1038/ncomms10219
- Zhang, L., Turner, B., Ribbeck, K., and ten Hagen, K. G. (2017). Loss of the Mucosal Barrier Alters the Progenitor Cell Niche via Janus Kinase/signal Transducer and Activator of Transcription (JAK/STAT) Signaling. *J. Biol. Chem.* 292, 21231–21242. doi:10.1074/jbc.M117.809848

**Conflict of Interest:** The authors declare that the research was conducted in the absence of any commercial or financial relationships that could be construed as a potential conflict of interest.

**Publisher's Note:** All claims expressed in this article are solely those of the authors and do not necessarily represent those of their affiliated organizations, or those of the publisher, the editors and the reviewers. Any product that may be evaluated in this article, or claim that may be made by its manufacturer, is not guaranteed or endorsed by the publisher.

Copyright © 2022 Chen and St Johnston. This is an open-access article distributed under the terms of the Creative Commons Attribution License (CC BY). The use, distribution or reproduction in other forums is permitted, provided the original author(s) and the copyright owner(s) are credited and that the original publication in this journal is cited, in accordance with accepted academic practice. No use, distribution or reproduction is permitted which does not comply with these terms.





# Rho and Rab Family Small GTPases in the Regulation of Membrane Polarity in Epithelial Cells

Klaus Ebnet<sup>1,2,3†\*</sup> and Volker Gerke<sup>1,2,3†\*</sup>

<sup>1</sup>Institute-Associated Research Group: Cell Adhesion and Cell Polarity, Institute of Medical Biochemistry, ZMBE, University of Münster, Münster, Germany, <sup>2</sup>Interdisciplinary Clinical Research Center (IZKF), University of Münster, Münster, Germany, <sup>3</sup>Cells-In-Motion Cluster of Excellence (EXC1003-CIM), University of Münster, Münster, Germany

## OPEN ACCESS

### Edited by:

Alexander Ludwig,  
Nanyang Technological University,  
Singapore

### Reviewed by:

Ceniz Zihni,  
University College London,  
United Kingdom  
Rytis Prekeris,  
University of Colorado Denver,  
United States

### \*Correspondence:

Klaus Ebnet  
ebnetk@uni-muenster.de  
Volker Gerke  
gerke@uni-muenster.de

### †ORCID:

Klaus Ebnet  
orcid.org/0000-0002-0417-7888  
Volker Gerke  
orcid.org/0000-0001-7208-8206

### Specialty section:

This article was submitted to  
Morphogenesis and Patterning,  
a section of the journal  
Frontiers in Cell and Developmental  
Biology

**Received:** 19 May 2022

**Accepted:** 14 June 2022

**Published:** 04 July 2022

### Citation:

Ebnet K and Gerke V (2022) Rho and  
Rab Family Small GTPases in the  
Regulation of Membrane Polarity in  
Epithelial Cells.  
Front. Cell Dev. Biol. 10:948013.  
doi: 10.3389/fcell.2022.948013

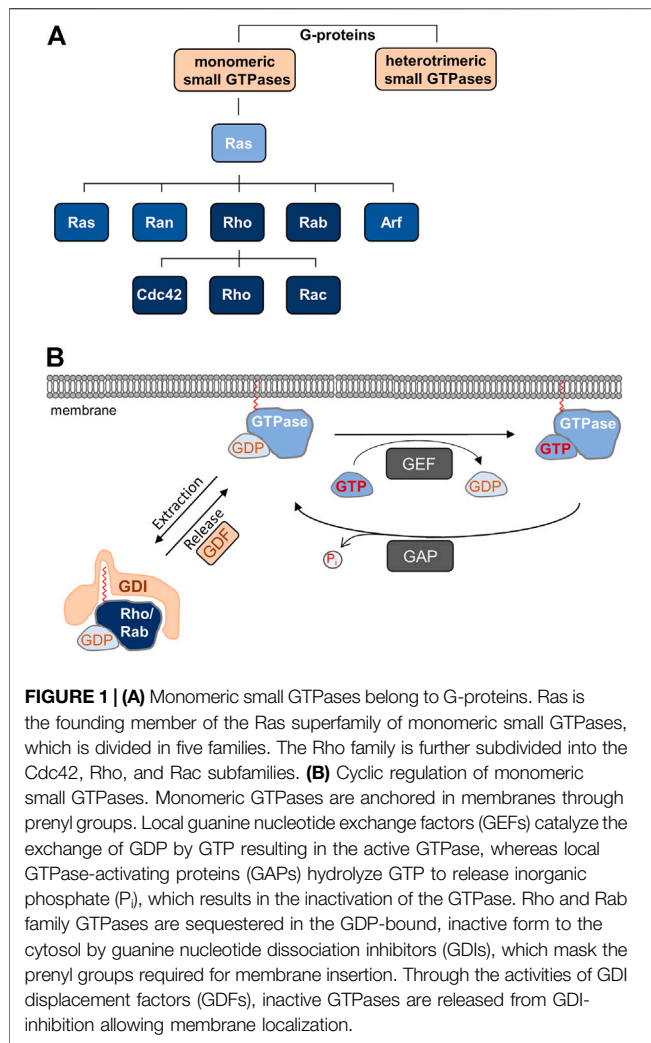
Membrane polarity, defined as the asymmetric distribution of lipids and proteins in the plasma membrane, is a critical prerequisite for the development of multicellular tissues, such as epithelia and endothelia. Membrane polarity is regulated by polarized trafficking of membrane components to specific membrane domains and requires the presence of intramembrane diffusion barriers that prevent the intermixing of asymmetrically distributed membrane components. This intramembrane diffusion barrier is localized at the tight junctions (TJs) in these cells. Both the formation of cell-cell junctions and the polarized traffic of membrane proteins and lipids are regulated by Rho and Rab family small GTPases. In this review article, we will summarize the recent developments in the regulation of apico-basal membrane polarity by polarized membrane traffic and the formation of the intramembrane diffusion barrier in epithelial cells with a particular focus on the role of Rho and Rab family small GTPases.

**Keywords:** apico-basal membrane polarity, Rab small GTPase, Rho small GTPase, tight junctions, vesicle transport

## 1 INTRODUCTION

Epithelia and endothelia form sheets of cells which separate different tissue compartments and which segregate the organism's interior from the external environment. Individual cells embedded in these sheets are connected to each other by cell-cell junctions. Cell-cell junctions not only integrate individual cells in the cellular sheet but also separate the plasma membrane of each cell into separate domains, a membrane domain that faces the free space (typically the lumen of an organ) and that is defined as the apical membrane domain, and a bounded membrane domain that is in contact with either another cell or the extracellular matrix and that is defined as the basolateral membrane domain. Apical membrane domains regulate the absorption of materials and, in case of endothelial cells, the transient interaction with cells of the immune system, whereas basolateral membrane domains regulate the integrity of the cellular sheet, the response to mechanical forces during morphogenetic processes or during collective cell migration, and the resistance of the sheets towards physical impact. Consequently, apical and basolateral membrane domains differ in their composition of integral membrane proteins and lipids, a phenomenon which is commonly referred to as apico-basal membrane polarity.

Apico-basal polarization requires the presence of an intramembrane diffusion barrier which prevents the intermixing of freely diffusible membrane components between the two membrane compartments. This is particularly important for lipids, which in contrast to integral membrane proteins are mostly not embedded in larger complexes or clusters connected to the actin cytoskeleton, and are thus more mobile. In vertebrates, the diffusion barrier is localized at the



tight junctions (TJ), a structure at the most apical region of cell-cell junctions (Tsukita et al., 2001). TJs are characterized by close appositions of the membranes of two adjacent cells, which on freeze-fracture electron micrographs appear as anastomosing intramembrane particle strands (Farquhar and Palade, 1963; Claude and Goodenough, 1973). The particle strands are generated by proteins of the claudin family, which multimerize in cis and trans to form a mesh-like structure (Gunzel and Yu, 2013).

TJs contain a large number of proteins including integral membrane proteins like claudins, Marvel proteins and junctional adhesion molecules (JAMs), peripheral membrane proteins like zonula occludens (ZO) proteins, partitioning-defective (PAR) proteins, Protein associated with Lin-7 1 (Pals1) and Pals-1-associated tight junction protein (PATJ), but also adapter proteins, heterotrimeric G-proteins and small GTPases and their regulators, and kinases and phosphatases (Zihni et al., 2016; Tan et al., 2020). Many of these proteins are assembled in specific proteins complexes, like the Crumbs (CRB) complex or the partitioning-defective (PAR)—aPKC complex. The abundance of PDZ domain-containing

scaffolding proteins indicates that TJs are sites of intensive signalling activities, and that their function in regulating the permeability of cellular sheets is subject to dynamic and sophisticated regulation.

Early studies suggested that the TJs act both as a barrier to the diffusion of small solutes across the paracellular pathway (paracellular gate function) (Goodenough and Revel, 1970) and as a barrier to the diffusion of intramembrane proteins and lipids (molecular fence function) (Dragsten et al., 1981). These two functions seem to be regulated by different molecular mechanisms. While in the absence of claudins or in the absence of the claudin-scaffolding zonula occludens (ZO) proteins the barrier function is lost, the fence function is retained under these conditions (Umeda et al., 2006; Otani et al., 2019). Thus, the gate and the fence functions of TJs reside in the same subcellular structure but differ in their molecular nature.

After the establishment of a diffusion barrier at the TJs, targeted vesicle transport to the apical and basolateral membrane domains is required to generate and maintain membrane identity. This is achieved by selective anterograde transport to the two principal membrane domains and by unique recycling pathways (Nelson and Yeaman, 2001; Ang and Folsch, 2012).

TJs are subject to dynamic regulation in physiological and pathological situations. Dynamic cellular processes are frequently regulated by monomeric small GTPases, a superfamily of proteins which bind and hydrolyze GTP, and which switch between inactive and active states by binding GDP or GTP, respectively (Bourne et al., 1990) (Figure 1). Based on sequence homology and functional similarity the GTPase superfamily, which contains more than 150 members, is subdivided in five families, the Ras, Rho, Rab, Ran, and Arf families (Kahn et al., 1992) (Figure 1A). While the functions of these families do overlap to some extent, the Rho family GTPases regulate cell morphology through their activities on the actin cytoskeleton, whereas the Rab and Arf families are important regulators of vesicle trafficking (Jaffe and Hall, 2005; Goitre et al., 2014). In this review article, we describe the role of Rho and Rab family small GTPases in the regulation of apico-basal membrane polarity through their functions during cell-cell contact formation and in directed vesicle transport. We will focus on the role of these small GTPases during key processes regulating apico-basal membrane polarity in vertebrate epithelial cells. For the role of Ras and Arf family monomeric small GTPases in polarity, we refer the reader to recent reviews (Young and Rodriguez-Viciana, 2018; Mima, 2021).

## 2 RHO AND RAB FAMILY SMALL GTPASES

All GTPases have in common that their activity is regulated by guanine nucleotide exchange factors (GEFs) and GTPase-activating proteins (GAPs) (Mosaddeghzadeh and Ahmadian, 2021) (Figure 1). GEFs catalyze the dissociation of GDP thus allowing the binding of GTP, which results in the active form of the GTPase and binding to its effector proteins. GAPs stimulate the intrinsic activity of the proteins to hydrolyze GTP to GDP, leading to the inactive form of the GTPase (Cherfils and Zeghouf,

2013). A second commonality of GTPases is the posttranslational addition of lipid moieties consisting of either three (farnesyl) or four (geranylgeranyl) isoprene units, a process referred to as prenylation. In Rho GTPases, the prenyl groups are attached to the cysteine residue present in the CAAX motif, whereas in Rab GTPases, the prenyl groups are attached to C-terminal Cys residues (Muller and Goody, 2018; Brandt et al., 2021). The prenyl groups anchor the GTPases in lipid bilayers, for example in the plasma membrane or in endomembranes, where they are activated by locally resident GEFs (Hodge and Ridley, 2016). Most GTPases depend on prenylation and membrane localization for function. Membrane targeting of Rho and Rab GTPases is antagonized by a third family of GTPase regulators, guanine nucleotide dissociation inhibitors (GDIs). GDIs binding to inactive (GDP-bound) Rho and Rab GTPases masks the prenyl group, thus blocking membrane insertion and promoting their sequestration to the cytosol. GDI binding also protects GTPases from degradation (Garcia-Mata et al., 2011; Muller and Goody, 2018) (**Figure 1**). At any given time, only a small fraction of all Rho GTPases is associated with membranes. The vast majority is maintained in the cytosol through GDIs (Garcia-Mata et al., 2011). As opposed to GEFs and GAPs, GDIs exist in a limited number with only three members (RhoGDI-1, -2, -3, RabGDI $\alpha$ , - $\beta$ , -3) identified so far (Nazlamova et al., 2017; Muller and Goody, 2018; Ahmad Mokhtar et al., 2021).

### 3 RHO FAMILY SMALL GTPASES IN MEMBRANE POLARITY

#### 3.1 Rho Small GTPases During Early Cell-Cell Contact Formation

Given the critical role of TJs in membrane polarity, it is important to understand the process of cell-cell contact and TJ formation. When migrating epithelial cells encounter other cells through cellular protrusions, they first engage in initial cell-cell contacts called “puncta” or “primordial, spot-like adherens junctions” (pAJs) (Yonemura et al., 1995). These puncta localize at the tips of F-actin-rich protrusions and are positive for several cell-cell adhesion receptors including E-cadherin, Nectin-2, and Junctional Adhesion Molecule (JAM)-A, as well as for cytoplasmic scaffolding proteins associated with cell adhesion receptors, including  $\alpha$ -catenin,  $\beta$ -catenin, ZO-1 and Afadin (Yonemura et al., 1995; Ando-Akatsuka et al., 1999; Asakura et al., 1999; Ebnet et al., 2001; Suzuki et al., 2002). Molecules that are localized separated from each other at TJs and AJs in fully polarized epithelial cells, co-localize at pAJs at this early stage of junction formation. The next step in the maturation process involves the activation of Rho GTPases as a direct consequence of cell-cell adhesion. Several adhesion receptors that are localized at pAJs can activate Rho family small GTPases, including E-cadherin (Ehrlich et al., 2002; Yamada and Nelson, 2007), Nectins (Kawakatsu et al., 2002), and JAM-A (Tuncay et al., 2015), and the importance of Rho family GTPases in the regulation of cell-cell contact formation is widely documented (Arnold et al., 2017; Cerutti and Ridley, 2017; Braga, 2018). A critical step in the generation of membrane polarity, however, is

the maturation of immature cell-cell junctions to mature cell-cell junctions with TJs being separated from AJs. This step requires the activation of atypical protein kinase C (aPKC) mediated by Rac1 and/or Cdc42.

Atypical PKC is part of a highly conserved polarity protein complex, the partitioning-defective (PAR)—aPKC complex (Suzuki and Ohno, 2006). The PAR—aPKC complex regulates various aspects of cell polarity including apico-basal membrane polarity in epithelial cells, anterior-posterior polarity in the *C.elegans* zygote, or the specification of the axon in neurons (Suzuki and Ohno, 2006; Iden and Collard, 2008). In epithelial cells, aPKC exists in a ternary complex with the polarity proteins PAR-3 and PAR-6, which both directly interact with aPKC (Ohno, 2001). In this complex, aPKC is maintained in an inactive conformation. The binding of active Cdc42 or active Rac1 to PAR-6 induces a conformational change of PAR-6 that releases aPKC from PAR-6 inhibition (Yamanaka et al., 2001). Active aPKC then phosphorylates a number of substrates including PAR-3 and PAR1 (Nagai-Tamai et al., 2002; Suzuki et al., 2004), which results in their separate localization at TJs and at the basolateral membrane domain, respectively. Of note, in the absence of aPKC kinase activity, cells are able to form pAJs but fail to develop belt-like AJs and TJs (Suzuki et al., 2001; Suzuki et al., 2002). The activation of aPKC by Rho GTPases Cdc42 and/or Rac1 is thus a key step in the development of membrane asymmetry in polarized epithelial cells.

Many studies that address the role of RhoGTPase regulation in TJ formation and maintenance focus on actomyosin-driven contractility and the paracellular permeability of TJs. However, since the two principal functions of TJs, i.e., gate and fence function are regulated through distinct molecular mechanisms (Umeda et al., 2006), it is well possible that Rho family regulators involved in the regulation of TJ formation or maintenance may selectively affect one of the two principal functions of TJs.

#### 3.2 Rho Small GTPases in the Maintenance of Membrane Asymmetry

After the formation of TJs which separate apical and basolateral membrane domains, the activity of Rho GTPases is continuously required for the maintenance of membrane identity. After the activation of aPKC and the subsequent phosphorylation of PAR-3, the PAR-6—aPKC complex remains as a unit whereas PAR-3 separates from PAR-6—aPKC (Nagai-Tamai et al., 2002). In fully polarized epithelial cells, PAR-6—aPKC segregates into the apical domain whereas PAR-3 localizes to the TJs. Apical membrane localization is particularly evident when cells are grown under three-dimensional culture conditions embedded in extracellular matrix (Durgan et al., 2011). Under these conditions, polarized epithelial cells form cysts, hollow spheres consisting of a single layer of epithelial cells which surround a single lumen (O’Brien et al., 2002). In cells grown to cysts, PAR-6 and aPKC are highly enriched in the lumen-facing apical membrane domain whereas PAR-3 is excluded from the apical membrane (Durgan et al., 2011). Although the formation of a ternary PAR-3—aPKC—PAR-6 complex is required for the development of apico-basal membrane polarity (Horikoshi et al., 2009), it has

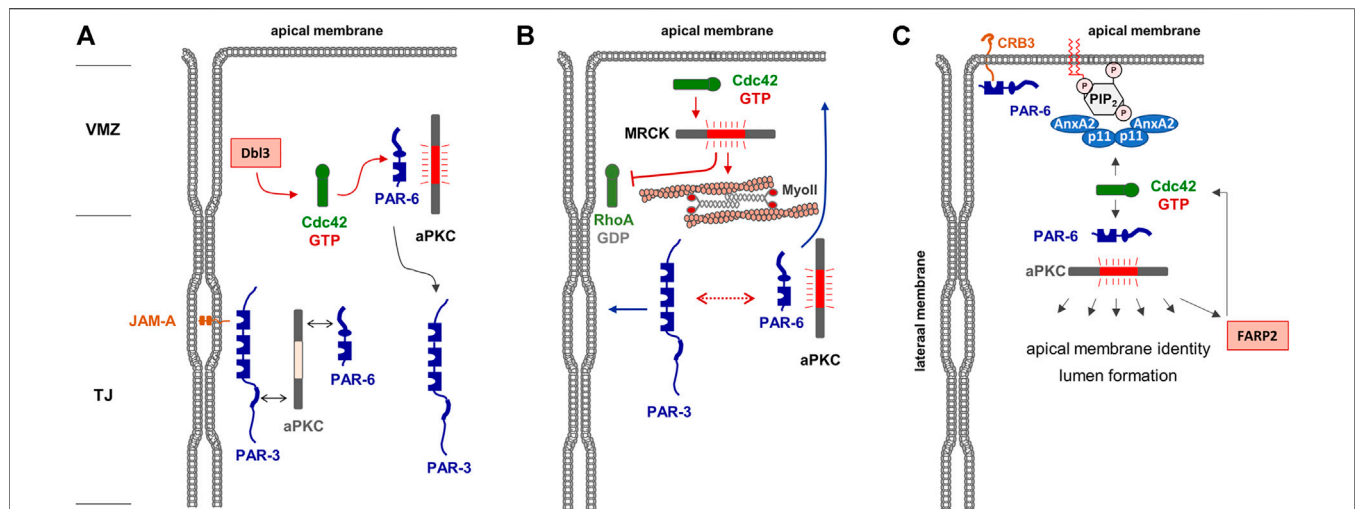


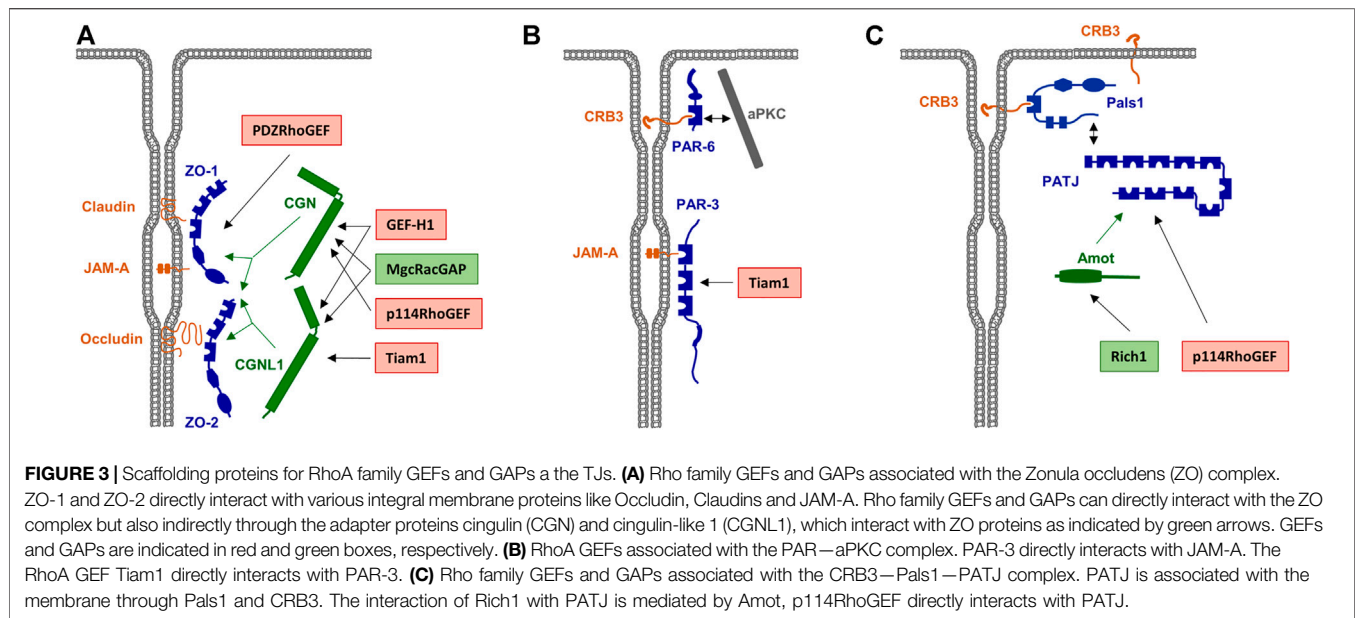
**FIGURE 2 |** Regulation of apical membrane identity in polarized epithelial cells. **(A)** The Par-aPKC complex is localized at the TJs, most likely through PAR-3 interacting with JAM-A. The Cdc42 GEF Dbp3 is localized at the vertebrate marginal zone (VMZ) and activates Cdc42, which in turn interacts with PAR-6 and induces a conformational change of PAR-6 that allows activation of aPKC. Phosphorylation of PAR-3 results in the dissociation of PAR-3. Note that this is a dynamic cycle, and that the stable association of the heterotrimeric PAR-3-aPKC-PAR-6 complex may be short-lived. **(B)** Active Cdc42 activates MRCK which stimulates actomyosin contractility-mediated segregation of PAR-3 and PAR-6-aPKC (dotted line with double arrows) to lateral and apical membrane domains, respectively (blue arrows). In addition, MRCK inhibits RhoA at the lateral membrane domain. **(C)** A tetrameric complex of Annexin A2 (AnxA2) and p11 is localized in the apical membrane by interacting with phosphatidylinositol-4,5-bisphosphate (PIP<sub>2</sub>). This complex recruits and activates the PAR-6-aPKC complex which phosphorylates various substrates involved in apical membrane identity and lumen formation. Among its substrates is the Cdc42 GEF FARP2, which catalyzes GDP-exchange of Cdc42, providing a possible positive feedback loop of Cdc42 activation in the apical membrane. Note that CRB3 present in the apical membrane may provide an additional anchor for PAR-6 and possibly the PAR-6-aPKC complex.

long been unclear by which mechanisms the separation of PAR-6-aPKC from PAR-3 is regulated, and how this separation into different membrane domains is maintained. Studies in *Drosophila* follicle epithelial cells already indicated that PAR-6-aPKC localize above PAR-3/Bazooka in the so-called marginal zone, and that the phosphorylation of PAR-3 by aPKC excludes PAR-3 from the apical domains (Morais-de-Sa et al., 2010). More recent studies in vertebrate epithelial cells showed that a similar mechanism operates in vertebrate epithelial cells and that Cdc42 is a central component of this mechanism. Cdc42 is activated at the border between the cell-cell contacts and the contact-free apical membrane domain, the vertebrate marginal zone (VMZ), through the activity of the Cdc42 GEF Dbp3 (Zihni et al., 2014). Locally active Cdc42 can bind to PAR-6 triggering the activation of PAR-6/PAR-3-associated aPKC resulting in PAR-3 phosphorylation and its segregation to the lateral membrane domain (Zihni et al., 2014) (Figure 2A). Through an additional pathway that involves the Cdc42-mediated activation of the Rho kinase (ROCK)-related myotonic dystrophy kinase-related Cdc42-binding kinase (MRCK), apical Cdc42 stimulates apical myosin II activation and junctional RhoA inhibition, thereby mediating actomyosin contractility-mediated PAR protein segregation (Zihni et al., 2017), a mechanism that has also been described in the regulation of PAR protein asymmetry in the *C. elegans* zygote (Munro et al., 2004) (Figure 2B). MRCK-regulated actomyosin contractility appears to emerge as a more general regulator of membrane specification (Zihni, 2021). By activating aPKC at the marginal zone, Cdc42 thus triggers a biochemical and a

mechanical mechanism of PAR protein segregation to regulate the positioning of the apical-lateral border and the specification of the apical and basolateral membranes, which defines Cdc42 as a central regulator of apico-basal membrane polarity in epithelial cells. Interestingly, recent findings in the *Drosophila* follicular epithelium identified the Cdc42 GAP RhoGAP19D at the lateral membrane domain of follicular epithelial cells (Fic et al., 2021). RhoGAP19D mutants lead to Cdc42 activity at the lateral membrane, which results in lateral contractility through the activity of the MRCK orthologue Genghis Khan (Gek), and expansion of the apical domain through increased PAR-6-aPKC activity (Fic et al., 2021). These observations provide a mechanism to inhibit the activity of Cdc42 at the lateral membrane domain and further underline the role of MRCK in apical membrane specification.

Studies with 3D-cultured MDCK cells further supported that Cdc42 activity is continuously needed at the apical membrane domain. Cdc42 interacts with annexin A2 (AnxA2) localized in the apical membrane in a GTP-dependent manner (Martin-Belmonte et al., 2007). Apical membrane specification is regulated by the lipid phosphatase PTEN present in the apical membrane, which mediates enrichment of PtdIns(4,5)P<sub>2</sub> at this membrane compartment. AnxA2 binding to PtdIns(4,5)P<sub>2</sub> mediates the specific enrichment of active Cdc42 in the apical membrane domain. Active Cdc42 then binds and recruits the PAR-6-aPKC module to the apical membrane, which is necessary for lumen formation. More recent findings indicate that aPKC interacts with and phosphorylates the Cdc42 GEF FARP2, and that FARP2 activity is required for apico-basal





polarity and a functional barrier in polarized Caco2 cells (Elbediwy et al., 2019) suggesting that Cdc42 may also act downstream of aPKC, which would represent a positive feedback loop in the regulation of apical membrane identity and TJ formation (Figure 2C).

The activity of Rac1 is regulated in a different way. During the process of MDCK cyst formation, Rac1 activity is downregulated at the apical membrane domain relative to the basolateral membrane domain (Yagi et al., 2012b). Ectopic activation of Rac1 at the apical membrane in mature cysts disturbs TJs and mislocalizes polarity proteins such as syntaxin-4, which localizes to the basolateral domain in unperturbed cells (Yagi et al., 2012b). Inactivation of Rac1 is most likely mediated by the Rac1-specific GAPs chimaerin (CHN)-1 (ARHGAP2) and CHN-2 (ARHGAP3), which localize to the apical membrane domain through their interaction with diacylglycerol (Yagi et al., 2012a). The enrichment of chimaerins CHN-1 and CHN-2 at the apical membrane thus suppresses Rac1 activity at the apical membrane to maintain apico-basal membrane polarity.

### 3.3 The Apical Junctional Complex in Vertebrate Epithelial Cells and the Localization of Rho GTPases and Their Regulators

TJs contain two conserved polarity protein complexes, the PAR—aPKC complex and the Crumbs (CRB)—Pals1—PATJ complex (shortly Crumbs complex) (Wang and Margolis, 2007) (Figure 3). As outlined in the previous section, PAR-6 and aPKC segregate from PAR-3 to occupy a region that is apical to PAR-3 in polarized epithelial cells. The Crumbs polarity complex—similar to PAR-6 and aPKC—is also part of the most apical region of interepithelial cell junctions and reaches partially into the free apical membrane domain of the epithelial cells (Lemmers et al., 2004) (Figure 3). The Crumbs complex can

directly interact with PAR-6 through both CRB3 and Pals1 (Hurd et al., 2003; Lemmers et al., 2004). The interaction of PAR-6—aPKC with CRB3 is promoted by the WD40 repeat domain-containing protein Morgl and by apically localized Cdc42 (Hayase et al., 2013). The Crumbs complex thus defines a region apically to the TJs, which in analogy to a region at cell-cell contacts of invertebrates has been named vertebrate marginal zone (Tan et al., 2020). Based on the proteomes identified at the VMZ and at the TJ area of vertebrate epithelial cells, it is likely that small GTPase signalling is involved in the formation and/or maintenance of both subregions of vertebrate TJs.

Since Rho GTPases are sequestered to the cytosol immediately after their inactivation, it has been difficult to directly demonstrate their localization at specific membranous sites. However, the identification of RhoGEFs or RhoGAPs at the TJs provides strong evidence for GTPase signalling at TJs. For example, the RhoGEFs ARHGEF2/GEF-H1 (Benais-Pont et al., 2003; Aijaz et al., 2005), ARHGEF18/p114RhoGEF (Terry et al., 2011), ARHGEF11/PDZ-RhoGEF (Itoh et al., 2012), and Tiam1 (Mack et al., 2012) have been identified at the TJ area. Also, the RhoGAPs MgcRacGAP (Guillemot et al., 2014), Rich1 (Wells et al., 2006) and ARHGAP29 (Tan et al., 2020) have been identified at the TJs and at the VMZ. As additional evidence for a TJ-specific regulation of RhoGTPase activities, several TJ-localized peripheral membrane proteins serve as scaffolds for RhoGTPase regulators. These include ZO-1 (Itoh et al., 2012), ZO-2 (Raya-Sandino et al., 2017), cingulin (CGN) and cingulin-like 1 (CGNL1/paracingulin/JACOP) (Aijaz et al., 2005; Guillemot et al., 2008; Terry et al., 2011; Guillemot et al., 2014), and the polarity proteins PAR-3 (Mack et al., 2012) and PATJ (Nakajima and Tanoue, 2011). The presence of both regulators of GTPase activity as well as of scaffolds for these regulators thus makes a strong point for a highly complex and dynamic regulation of Rho GTPase signaling at the TJs (Figure 3).

### 3.4 Regulation of Rac1/Cdc42 Activities at the Tight Junctions and at the Apical Membrane Domain

As outline before, the activity of Rho family GTPases is critical for the maturation of pAJs to polarized, mature cell-cell contacts with AJs and TJs, and this activity is most likely required for the activation of aPKC as part of the PAR—aPKC complex. A potential regulator of Rac1 activity is PAR-3, which directly interacts with the Rac1 GEF Tiam1 (Nishimura et al., 2005). Studies in both cultured primary keratinocytes and in MDCK cells showed that the binding of Tiam1 to PAR-3 regulates TJ biogenesis. In the absence of Tiam1, keratinocytes are able to form pAJs but fail to develop these immature contacts into mature cell-cell junctions, which is highly reminiscent to epithelial cells lacking aPKC (Suzuki et al., 2001). These finding strongly suggest that PAR-3-bound Tiam1 activates aPKC after initial junctions have been formed in keratinocytes. In MDCK cells, the absence of PAR-3 was found to disrupt TJ assembly with a concomitant constitutive activation of Rac1 (Chen and Macara, 2005), which can be interpreted as a negative regulatory function of PAR-3 in sequestering Tiam1 away from Rac1 at cell-cell contacts. Since the subcellular localization of active Rac1, for example by Förster resonance energy transfer (FRET) experiments, has not been analyzed in these studies it could as well be that PAR-3 deletion results in enhanced recruitment of Tiam1 to other subcellular locations, which could also result in constitutive Rac1 activation at such sites, a scenario that would be compatible with a positive regulatory function of the PAR-3—Tiam1 complex at cell-cell junctions. Interestingly, in MDCK cells it has also been observed that a Rac1 activity gradient exists along the apical—basal polarity axis that is generated by a negative regulatory role of PAR-3 on Rac1 *via* Tiam1 at the apical region of cell-cell junctions, and a positive regulatory role of  $\beta$ 2-syntrophin *via* Tiam1 at the subapical region of cell-cell junctions (Mack et al., 2012). Thus, it is likely that PAR-3 localized at TJs sequesters Tiam1 thereby preventing high Rac1 activity levels to facilitate the generation of a Rac1 activity gradient along cell-cell junctions (Yagi et al., 2012b; Mack et al., 2012) (Figure 3).

Rich1/ARHGAP17 is a RhoGAP for Rac1 and Cdc42 with a strong selectivity for Cdc42 in epithelial cells (Richnau and Aspenstrom, 2001). Rich1 is targeted to TJs through its association with the scaffold protein Angiomotin (Amot), which interacts with the Crumbs complex component PATJ (Wells et al., 2006). Downregulation of Rich1 accelerates the loss of the barrier functions induced by  $\text{Ca}^{2+}$  removal (Wells et al., 2006), which suggests that the maintenance of functional TJs requires that the levels of active Cdc42 at TJs are kept low. Interestingly, observations in HEK293 cells and MDCK cells also indicate that Merlin, the protein encoded by the neurofibromatosis type 2 (NF2) tumor suppressor gene and a regulator of Hippo signalling (Zheng and Pan, 2019), is part of the Amot—PATJ—Pals1 complex and directly interacts with Amot in a competitive manner with Rich1 to regulate Rac1 activity (Yi et al., 2011). These findings suggested that also the activity of Rac1 at the TJs may be subject to regulation by Rich1.

MgcRacGAP/RacGAP1 is a RhoGAP with strong activity towards Cdc42 and Rac1 and weak activity towards RhoA (Touret et al., 1998). MgcRacGAP is enriched at the apical junctional complex of *Xenopus* epithelial cells (Brenzau et al., 2015) and of MDCK cells (Guillemot et al., 2014). Its recruitment to TJ can be mediated by both CGN and CGNL1, which both directly interact with MgcRacGAP (Guillemot et al., 2014) (Figure 3). The localization of MgcRacGAP at the TJ further indicates that Cdc42 and Rac1 activities must be kept at low levels there to maintain the epithelial barrier function.

### 3.5 Regulation of RhoA Activity at the Tight Junctions

GEF-H1/ARHGEF2 is a GEF for RhoA which localizes to the TJs (Benaï-Pont et al., 2003). Its localization at the TJs is most likely regulated by its interaction with CGN and CGNL1 (Rouaud et al., 2020) (Figure 3). Importantly, depletion of either CGN or CGNL1 increases RhoA activity in both epithelial and endothelial cells (Aijaz et al., 2005; Guillemot et al., 2008; Tian et al., 2016; Holzner et al., 2021), suggesting that CGN and CGNL1 sequester GEF-H1 from RhoA within the TJ area or maintain GEF-H1 functionally inactive. In line with an inhibitory function of CGN and CGNL1 on RhoA activation, depletion of CGN in endothelial cells enhances the permeability of endothelial cells induced by agonists such as thrombin or histamine concomitant with increased association of GEF-H1 with RhoA and increased RhoA-GTP levels, whereas ectopic expression of CGN protects endothelial cells from the effects of these agonists (Tian et al., 2016; Holzner et al., 2021). These observations are, thus, in line with a model that the binding of GEF-H1 to CGN or CGNL1 is required to inhibit RhoA activation at the TJs and prevent a loss of the barrier function. Interestingly, CGN and CGNL1 negatively regulate the expression levels of claudin-2 (Guillemot et al., 2013), and, similar to CGN and CGNL1, depletion of claudin-2 activates GEF-H1 and increases RhoA activity (Dan et al., 2019).

p114RhoGEF/ARHGEF18 is a GEF with high specificity for RhoA (Blomquist et al., 2000). It is also localized at the TJs and interacts with both cingulin (Terry et al., 2011) and PATJ (Nakajima and Tanoue, 2011) (Figure 3). Its depletion leads to a disorganized circumferential actomyosin belt as a result of reduced F-actin and myosin IIA accumulation along apical cell-cell junctions (Nakajima and Tanoue, 2011). Ectopic expression of CRB3 induces an epithelial phenotype in HeLa cells which is associated with recruitment of Pals1 and p114RhoGEF to cell-cell junctions, formation of a cortical F-actin belt, and increased activities of RhoA and ROCK1/2 (Loie et al., 2015). These findings strongly suggest that p114RhoGEF activity is required to maintain the apical actomyosin organization. p114RhoGEF depletion also results in an impaired barrier function after  $\text{Ca}^{2+}$ -switch-triggered junction formation (Terry et al., 2011). This observation indicates that p114RhoGEF is required during cell-cell contact and TJ formation (Terry et al., 2011). Of note, despite defects in lumen formation when cells are grown in a three-dimensional matrix after p114RhoGEF depletion, as indicated by multiple lumen formation, apico-basal membrane polarity is not

grossly altered in these cells (Terry et al., 2011), suggesting that p114RhoGEF specifically regulates the gate function of TJs.

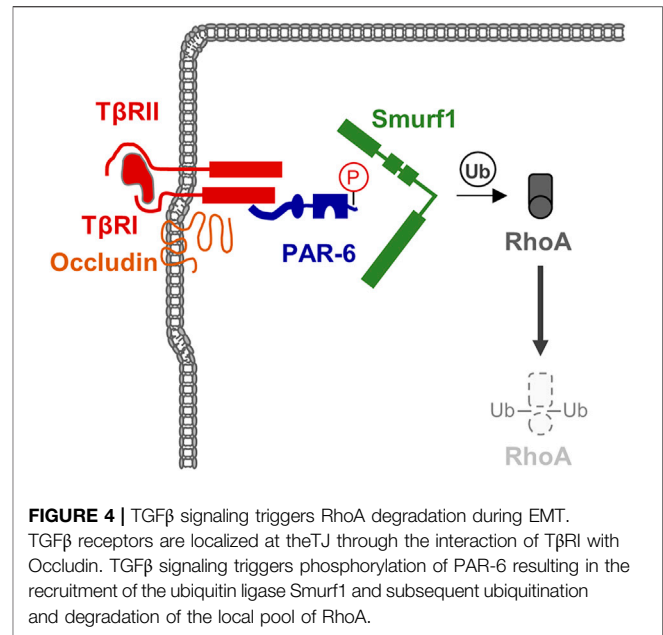
PDZ-RhoGEF/ARHGEF11 is a RhoA-specific GEF which has been found to localize at the TJs in polarized epithelial cells *in vitro* as well as *in vivo* (Itoh et al., 2012). PDZ-RhoGEF directly interacts with ZO-1 (Itoh et al., 2012) (Figure 3), and its localization at the TJs depends on ZO-1, strongly suggesting that ZO-1 serves as a scaffold for PDZ-RhoGEF at the TJs. PDZ-RhoGEF is required for the timely maturation of TJs and development of the barrier function after  $\text{Ca}^{2+}$  switch-triggered junction formation but its activity seems not to be required once mature TJs have been formed (Itoh et al., 2012). This suggests that PDZ-RhoGEF is primarily necessary during junction maturation and TJ formation. Its constitutive association with ZO-1 (Itoh et al., 2012) also suggests that it serves to regulate RhoA and myosin light chain (MLC) kinase activity in close spatial proximity of ZO-1, which is in agreement with the localization of ZO-1 at cell-cell junctions early on from the formation of pAJs to fully matured cell-cell junctions (Yonemura et al., 1995; Ando-Akatsuka et al., 1999). Its association with ZO-1 at the TJs, however, could also mean that PDZ-RhoGEF activity is necessary when TJ need to be repaired, for example after mechanical injury (see below). Studies in keratinocytes further indicated a role of an epithelial-specific splicing variant of PDZ-RhoGEF in the maintenance of TJs *via* RhoA activation and MLC phosphorylation (Lee et al., 2018).

### 3.6 Rho Small GTPases During Tight Junctions Remodeling

As opposed to the intuitive view of the TJs as a stable and rather unchanging barrier at the apical region of cell-cell contacts, individual molecular components of the TJs are remarkably dynamic (Shen et al., 2011). This is probably necessary to maintain the TJs in a regulatable condition and allows the tissue to adapt to changes in the environment, for example after physical damage, or in physiological situations that impose challenges to the maintenance of the barrier function and tissue integrity, such as cell division or cell extrusion. At the same time, however, an intrinsic dynamics bears the risk of interference by exogenous factors that might contribute to a loss of the barrier, cell-cell adhesion and eventually tissue integrity. Given that several regulators of Rho GTPase activity are localized at the TJs at steady state, it is conceivable that Rho GTPases are targeted during processes requiring TJ remodeling. RhoA seems to be particularly important for the maintenance of TJ integrity.

#### 3.6.1 RhoGTPases and Epithelial-Mesenchymal Transition

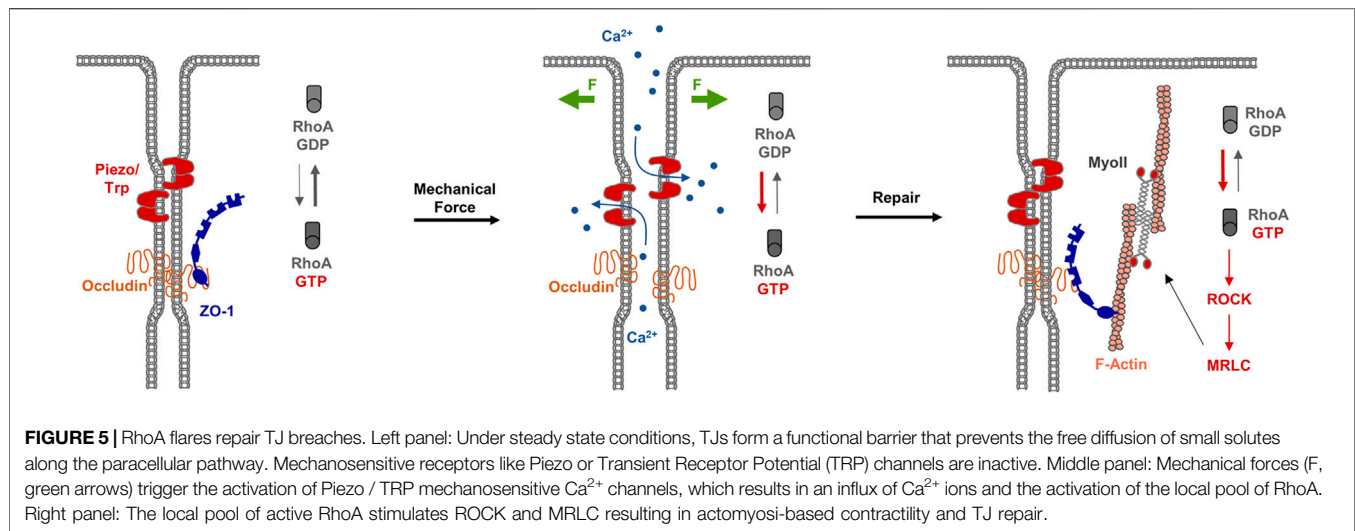
Epithelial-mesenchymal transition (EMT) is a cellular programme that allows epithelial cells embedded in an epithelial tissue to transdifferentiate into motile mesenchymal cells (Yang and Weinberg, 2008; Lamouille et al., 2014). A key event during EMT is the suppression of E-cadherin by a number of transcription factors, which supports the disassembly of cell-



cell contacts and a loss of apico-basal polarity (Lamouille et al., 2014). Among the various signaling pathways identified to operate during EMT, TGFβ signaling has turned out as a key signaling pathway during EMT (Yang and Weinberg, 2008). TGFβ signaling targets RhoA at the TJs. By inducing TGFβ receptor I (TβRI) and TβRII dimerization at the TJs, TGFβ triggers PAR-6 phosphorylation, followed by recruitment of the ubiquitin ligase Smurf1, which ubiquitinates RhoA and thus targets RhoA for proteasomal degradation (Barrios-Rodiles et al., 2005; Ozdamar et al., 2005) (Figure 4). The TJ-specific targeting of RhoA activity by TGFβ further underlines the necessity of active RhoA at TJs to maintain TJ integrity. Importantly, TGFβ-activated transcription factors such as Snail repress the expression of a number of TJ-localized integral membrane and peripheral membrane proteins, including claudins, occludin and CRB3, and Pals1, PATJ, and PAR-3 (Lamouille et al., 2014), many of which are involved in Rho GTPase regulation (see above).

#### 3.6.2 RhoGTPases and Tight Junctions Repair—Rho Flares

During development, epithelial tissues frequently face challenges to the barrier function, for example during morphogenetic changes as they occur during gastrulation (Wallingford et al., 2001), or during cellular events like cell division (Fink et al., 2011) or cell extrusion (Kocgozlu et al., 2016). As recent observations during *X.laevis* gastrulation indicate, breaches at the TJs sporadically occur, which are shortlived and are rapidly repaired (Stephenson et al., 2019). A detailed investigation of the underlying mechanisms indicated that at sites of local TJ breaches, visualized with a sensitive tracer detection system, GTP-loaded RhoA rapidly accumulates and triggers local actin polymerization and acto-myosin-based contraction. At sites of TJ breaches markers like ZO-1 disappear, and they reappear shortly



after the recruitment of active RhoA (Stephenson et al., 2019). This repair process is preceded by a local increase in the intracellular  $\text{Ca}^{2+}$  concentration, suggesting that mechanosensitive  $\text{Ca}^{2+}$  channels act as sensors of TJ breaches, and that a local increase in intracellular  $\text{Ca}^{2+}$  activates RhoA at the TJs (Varadarajan et al., 2022) (Figure 5). These findings thus provide strong evidence that in response to local perturbations of TJ integrity, RhoA is recruited and/or activated locally to induce contractility of the actin cytoskeleton to support the repair of TJs and to re-establish the epithelial barrier function.

## 4 RAB FAMILY SMALL GTPASES IN MEMBRANE POLARITY

### 4.1 Rab Family GTPases in Polarized Vesicle Transport

Rab GTPases are central regulators of intracellular membrane trafficking involved in the biogenesis, transport and fusion of organelles and vesicles (for reviews see (Zerial and McBride, 2001; Novick, 2016; Pfeffer, 2017). Typically, they bind to specific organelle/vesicle membranes in their active, GTP-loaded conformation with specificity mediated by membrane-resident GEFs but also the Rab protein itself. The membrane-associated Rabs then serve as a platform for a large group of effector proteins that transmit functional specificity, e.g., by initiating vesicle budding at a donor organelle, mediating transport through direct or indirect interactions with microtubule or actin tracks, establishing tethers between membrane surfaces in the course of fusion events and links to the actual fusion machinery (for reviews see (Langemeyer et al., 2018; Lamber et al., 2019). Interestingly, Rab proteins can also provide directionality to membrane transport pathways by recruiting specific GEFs or GAPs for a downstream activation or an upstream inactivation of another family member. This Rab cascade has been well established for endosomal membrane trafficking where the progression from early to late endosomes is catalyzed by a conversion from Rab5 to Rab7, which itself is mediated by the

recruitment of a Rab7 GEF through endosome-bound Rab5 (Rink et al., 2005; Poteryaev et al., 2010). Rab-mediated directional movement of vesicles that transport cargo from and to the plasma membrane is of particular relevance in polarized epithelial and endothelial cells where selective exocytotic transport and unique recycling pathways help establish and maintain the apical and basolateral plasma membrane compartments with their unique protein and lipid compositions.

### 4.2 Rab11 as a Central Regulator of Apical Delivery Pathways

Once a polarized state of an epithelium or endothelium characterized by the two principal membrane domains is established, it has to be maintained, among other things by directed transport of vesicular carriers from the post-trans-Golgi network (TGN) to these domains. Sorting motifs that define the transport of such carriers to either the apical or basolateral domain had been identified already early on. They include tyrosine-based motifs, e.g. found in the LDL receptor, directing a protein to the basolateral membrane, and glycosylations and GPI anchors routing the protein to the apical surface (for review see (Nelson and Yeaman, 2001). The cellular machinery mediating this selective transport involves coat proteins as well as membrane segregation and the formation of raft-like microdomains but is yet far from being fully understood.

Several Rab proteins function in the post-TGN transport to the different membrane domains in polarized epithelial and endothelial cells. A central role has been described for Rab11, which has been linked to the transport of apically destined proteins and vesicles in polarized cells. Examples are the apical delivery of the sodium/hydrogen exchanger 3 (NHE3) and the cystic fibrosis conductance regulator (CFTR) in human intestinal epithelial cells, and the apical exocytosis of discoidal/fusiform-shaped vesicles (DFVs) in bladder umbrella cells (Khandelwal et al., 2008; Vogel et al., 2015). These observations analyzing apical trafficking in fully polarized cells are in line with the role of



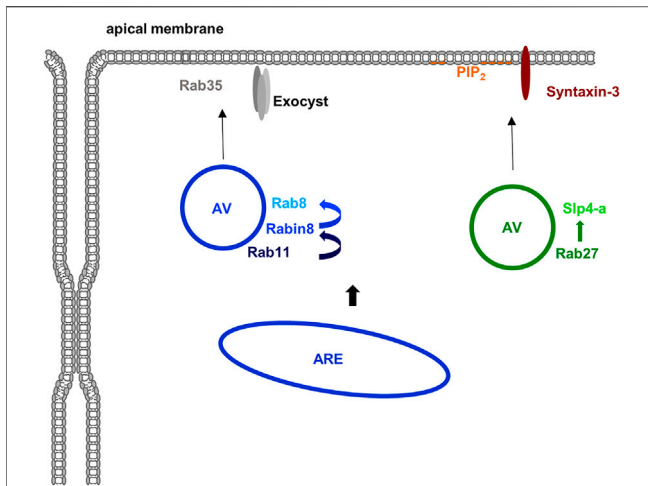


**FIGURE 6 | Rab proteins in apical membrane traffic.** Several Rab proteins are known to participate in the delivery of material to the apical membrane domain in polarized epithelial cells. Apically destined vesicles (AV) contain Rab11 which recruits the Rab8 GEF Rabin8 thereby activating Rab8. Rab35 and the exocyst complex are most likely involved in the apical membrane targeting of these vesicles. Another class of apically destined vesicles operating in the formation of an apical lumen in 3D are positive for Rab27 (and most likely also Rab3 isoforms). The Rab27 effector Slp4-a is targeted to these vesicles and most likely functions in conjunction with Slp2-a to tether the vesicles at PtdIns(4,5)P<sub>2</sub>-rich apical membrane domains with fusion eventually mediated by syntaxin-3. Most likely, both types of vesicles originate at the apical recycling endosome (ARE) although formation at the TGN is also feasible at least for the Rab27 positive vesicles.

Rab11 in the *de novo* specification of an apical membrane domain in the course of tubular morphogenesis. Often using MDCK cyst formation as a model for polarization in 3D, several studies have identified a crucial role for Rab11 (Bryant et al., 2010); for reviews see (Apodaca et al., 2012; Jewett and Prekeris, 2018). Here, early specification of an apical membrane domain already begins during cell division, when endosomal vesicles are recycled in a polarized manner. During cytokinesis, the vesicles are directed to the cleavage furrow which forms at the site of the midbody, a microtubule-rich structure that marks the location of future lumen formation and that is positive for several Rab proteins including Rab8, Rab11 and Rab35 (Bryant et al., 2010; Klinkert et al., 2016).

Rab11, a well known Rab of recycling endosomes, triggers a Rab cascade by recruiting a GEF for Rab8 (Rabin8) which in turn activates Rab8 (**Figure 6**). The Rabs, both known to interact with the plasma membrane-associated and fusion-promoting exocyst complex (Zhang et al., 2004; Wu et al., 2005), together with other components including the Cdc42 GEF Tuba then assemble at an apical membrane initiation site (AMIS) where lumen formation occurs (Bryant et al., 2010). In the order of these events, the Rab11/8 vesicles transition an apical (recycling) endosome which is also found in fully polarized cells where it organizes endosomal recycling pathways to the (established) apical membrane (see below). The exocyst complex likely has multiple additional functions in the establishment and maintenance of epithelial polarity. For instance, it is involved in the clustering of

E-cadherin and the proper formation of adherens (Yeaman et al., 2004; Xiong et al., 2012) and also localizes to tight junctions where it participates in TJ formation through interactions with RalGTPases (Hazelett et al., 2011), which also regulate basolateral protein traffic (Moskalenko et al., 2002), and is interacting with PAR-3 (Ahmed and Macara, 2017). Due to the focus of this review on Rho and Rab GTPases these exocyst functions are not discussed in detail and the interested reader is referred to other reviews on this topic (Wu and Guo, 2015; Polgar and Fogelgren, 2018).

### 4.3 Other Rab Proteins in Apical Exocytosis

In addition to Rab8 and Rab11, other Rab proteins have been described to participate in the delivery of material to the apical membrane of polarized epithelial and endothelial cells. They include Rab3 and Rab27 isoforms which have been implicated in the early specification of the apical membrane domain during lumen formation. Both have been identified on vesicles that deliver material to the apical membrane to initiate lumen formation. Their effectors, synaptotagmin-like protein (Slp) 2-a and Slp4-a are mediating this event by linking the vesicles to the PtdIns(4,5)P<sub>2</sub>-rich apical membrane and promoting tethering and fusion in conjunction with the t-SNARE syntaxin-3 (Galvez-Santisteban et al., 2012) (**Figure 6**). Further supporting a role of this Rab27/Slp2/4-centered network in establishing/maintaining epithelial polarity, mutations in syntaxin-3 have been identified in patients suffering from microvillus inclusion disease, a congenital enteropathy that is characterized by disturbed polarity of intestinal epithelial cells which show a loss of brush borders and a subapical accumulation of vesicles (Cutz et al., 1989). Interestingly, these vesicles are positive for Rab11 and Rab8 indicative of a perturbed apical recycling compartment. Together with the observation that the exocyst-binding Rab8 is also present on the apical Rab27 vesicles these findings suggest a connection between the Rab11 and Rab27 centered pathways of lumen initiation (for review see (Jewett and Prekeris, 2018; Polgar and Fogelgren, 2018). Yet another Rab implicated in the specification of the apical membrane and the initiation of lumen formation is Rab35. It localizes to apical vesicles and Rab35 depletion leads to multiple lumen formation in the MDCK cyst assay (Klinkert et al., 2016; Mrozowska and Fukuda, 2016).

Several components described to be involved in apical membrane transport and lumen formation in epithelial cells, in particular Rab3 isoforms, Rab27a and Rab35, have also been identified as regulators of the exocytotic delivery of specialized secretory granules in endothelial cells. In their mature form these lysosome-related organelles, the so-called Weibel-Palade bodies, are preferentially secreted at the apical membrane of the polarized endothelium in a process that is induced by endothelial cell activation and that involves Rab3b/d and Rab27a and their effectors MyRIP and Slp4-a (for review see (McCormack et al., 2017; Schillemans et al., 2019; Nass et al., 2021)). A related Rab27 isoform, Rab27b, was identified on subapical vesicles in lacrimal gland acinar cells, and by expression of dominant active and inactive mutant proteins as well as knock-out mouse studies was reported to participate, possibly in conjunction with Rab3D, in the formation and apical release of secretory vesicles in these cells

(Chiang et al., 2011). DFVs of umbrella bladder cells (see above) are another pool of subapical vesicles positive for Rab27b. The apical exocytosis of these vesicles is triggered by filling of the bladder and was shown to be inhibited by depletion of Rab27b, but not Rab27a. Interestingly, the Rab27b-dependent regulation of DFV exocytosis appears to operate in parallel to the Rab11-Rab8 pathway discussed above, as Rab27b depletion has no effect of the Rab11-positive parameters (Gallo et al., 2018). Although less well characterized, Rab17 also appears to regulate the apical delivery of exocytotic vesicles, as shown for transcytosis in polarized hepatic WIF-B cells (Striz et al., 2018).

#### 4.4 Rabs in Basolateral Transport

As compared to the apical delivery of transport vesicles in polarized epithelial and endothelial cells, much less is known about the involvement of Rab proteins in basolateral trafficking, also because this had long been considered the default route of post-TGN traffic. Indirect evidence based on localization suggests that Rab13 could be involved in basolateral membrane transport in polarized osteoclast (Hirvonen et al., 2012) and in polarized *Drosophila* follicle cells, Rab10 is required for the secretion of basement membrane at the basal surface (Lerner et al., 2013). Rab10 was also identified in polarized MDCK cells to support the biosynthetic transport of basolateral cargo (Schuck et al., 2007) and to affect basolateral endocytic sorting/recycling pathways (Babbey et al., 2006). Moreover, in the *C. elegans* intestinal epithelium Rab10 was shown to participate in the formation of an endosomal tubular network required for the efficient recycling of cargo that is subject to clathrin independent internalization (Chen et al., 2014). Together these observations suggest that Rab10 could regulate transport routes between basolateral sorting and recycling endosomes and thereby also exocytotic delivery of certain cargo to the basolateral membrane domain.

#### 4.5 Rabs in Endosomal Recycling in Polarized Cells

The above considerations indicate that biosynthetic post-TGN transport routes and endosomal recycling pathways are tightly interlinked also in polarized cells. Endocytic recycling is required both during establishment of the two distinct membrane domains of polarized cells but also when they have to be maintained in fully polarized tissues. For example, newly synthesized material (proteins, lipids) that is delivered to the basolateral domain either by default or mistake but is destined for and functions at the apical domain has to be re-internalized and then delivered to the correct membrane domain. A paradigm for the analysis of these trafficking routes has been the glycoprotein podocalyxin (PCX) initially identified in renal podocytes but present in the apical glycocalyx of many epithelia and endothelia. The transcytotic endosomal recycling of podocalyxin involves an internalization from the basolateral membrane, transport through basolateral early/sorting endosomes and delivery to the Rab11 positive apical recycling compartment (for review see (Roman-Fernandez and Bryant, 2016). A comprehensive analysis of Rab GTPases

involved in podocalyxin trafficking in epithelial cells was performed by Mrozowska and Fukuda (Mrozowska and Fukuda, 2016) who studied the transport in MDCK cells cultivated to polarize in 2D (epithelial sheet formation) and 3D (luminogenesis and cyst formation). Using a combination of colocalization and knockdown screenings they could show that the majority of Rabs are involved and function at different stages of the PCX transcytosis in both 2D and 3D conditions but that some of them appeared to be primarily engaged in either the 2D (Rab13 and Rab14) or 3D cultures (Rab4, Rab15, Rab19, Rab25). An interesting finding concerned Rab35 which participated in the polarized PCX transport both in 2D and 3D but engaged different effectors, the inositol polyphosphate 5-phosphatase OCRL in 2D monolayers, and the Arf GAP ACAP2 in 3D cysts. This supports the notion that transcytosis and endosomal recycling of apical membrane proteins in polarized epithelial cells is rather complex, is context dependent (2D vs 3D), and is intricately regulated by different Rab protein family members.

### 5 CONCLUSION

Epithelial cells and endothelial cells develop a highly pronounced apico-basal polarity to form membrane compartments with distinct functions. Rho family GTPases contribute to the development of membrane polarity by regulating the formation as well as the maintenance of TJs. Rab family GTPases contribute to membrane polarity by regulating the trafficking and delivery of vesicles and cargo to distinct membrane compartments. The involvement of Rho and Rab small GTPases and in particular the increasing number of Rho GEFs and GAPs at the TJs indicates that the generation of membrane polarity is a sophisticated and dynamically regulated process. Evidence accumulates suggesting that the gate function and the fence function of TJs are regulated through distinct Rho GTPase-based mechanisms. Given that the molecular mechanism underlying the fence function is still largely unknown, it will be important to understand in more detail the site-specific regulation of Rho small GTPases through their interaction with GEFs, GAPs and GDIs at the TJs.

### AUTHOR CONTRIBUTIONS

All authors listed have made a substantial, direct, and intellectual contribution to the work and approved it for publication.

### FUNDING

This work was supported by grants from the Deutsche Forschungsgemeinschaft (EB 160/5-1, EB 160/8-1, and EXC 1003-CiMIC to KE; GE514/6-3 and SFB1009/A06 to VG) and from the Medical Faculty of the University of Münster (IZKF Eb2/020/14 to KE).

## REFERENCES

- Ahmad Mokhtar, A. M. b., Ahmed, S. B. M., Darling, N. J., Harris, M., Mott, H. R., and Owen, D. (2021). A Complete Survey of RhoGDI Targets Reveals Novel Interactions with Atypical Small GTPases. *Biochemistry* 60, 1533–1551. doi:10.1021/acs.biochem.1c00120
- Ahmed, S. M., and Macara, I. G. (2017). The Par3 Polarity Protein Is an Exocyst Receptor Essential for Mammary Cell Survival. *Nat. Commun.* 8, 14867. doi:10.1038/ncomms14867
- Aijaz, S., D'Atri, F., Citi, S., Balda, M. S., and Matter, K. (2005). Binding of GEF-H1 to the Tight Junction-Associated Adaptor Cingulin Results in Inhibition of Rho Signaling and G1/S Phase Transition. *Dev. Cell.* 8, 777–786. doi:10.1016/j.devcel.2005.03.003
- Ando-Akatsuka, Y., Yonemura, S., Itoh, M., Furuse, M., and Tsukita, S. (1999). Differential Behavior of E-Cadherin and Occludin in Their Colocalization with ZO-1 during the Establishment of Epithelial Cell Polarity. *J. Cell. Physiol.* 179, 115–125. doi:10.1002/(sici)1097-4652(199905)179:2<115:aid-jcp1>3.0.co;2-t
- Ang, S. F., and Fölsch, H. (2012). The Role of Secretory and Endocytic Pathways in the Maintenance of Cell Polarity. *Essays Biochem.* 53, 29–39. doi:10.1042/bse0530029
- Apodaca, G., Gallo, L. I., and Bryant, D. M. (2012). Role of Membrane Traffic in the Generation of Epithelial Cell Asymmetry. *Nat. Cell. Biol.* 14, 1235–1243. doi:10.1038/ncb2635
- Arnold, T. R., Stephenson, R. E., and Miller, A. L. (2017). Rho GTPases and Actomyosin: Partners in Regulating Epithelial Cell-Cell Junction Structure and Function. *Exp. Cell. Res.* 358, 20–30. doi:10.1016/j.yexcr.2017.03.053
- Asakura, T., Nakanishi, H., Sakisaka, T., Takahashi, K., Mandai, K., Nishimura, M., et al. (1999). Similar and Differential Behaviour between the Nectin-Afadin-Ponsin and Cadherin-Catenin Systems during the Formation and Disruption of the Polarized Junctional Alignment in Epithelial Cells. *Genes. Cells* 4, 573–581. doi:10.1046/j.1365-2443.1999.00283.x
- Babbey, C. M., Ahktar, N., Wang, E., Chen, C. C.-H., Grant, B. D., and Dunn, K. W. (2006). Rab10 Regulates Membrane Transport through Early Endosomes of Polarized Madin-Darby Canine Kidney Cells. *MBoC* 17, 3156–3175. doi:10.1091/mbc.e05-08-0799
- Barrios-Rodiles, M., Brown, K. R., Ozdamar, B., Bose, R., Liu, Z., Donovan, R. S., et al. (2005). High-throughput Mapping of a Dynamic Signaling Network in Mammalian Cells. *Science* 307, 1621–1625. doi:10.1126/science.1105776
- Benaïs-Pont, G., Punna, A., Flores-Maldonado, C., Eckert, J., Raposo, G., Fleming, T. P., et al. (2003). Identification of a Tight Junction-Associated Guanine Nucleotide Exchange Factor that Activates Rho and Regulates Paracellular Permeability. *J. Cell. Biol.* 160, 729–740. doi:10.1083/jcb.200211047
- Blomquist, A., Schwörer, G., Schabowski, H., Psoma, A., Lehnen, M., Jakobs, K. H., et al. (2000). Identification and Characterization of a Novel Rho-specific Guanine Nucleotide Exchange Factor. *Biochem. J.* 352, 319–325. doi:10.1042/bj3520319
- Bourne, H. R., Sanders, D. A., and McCormick, F. (1990). The GTPase Superfamily: a Conserved Switch for Diverse Cell Functions. *Nature* 348, 125–132. doi:10.1038/348125a0
- Braga, V. (2018). Signaling by Small GTPases at Cell-Cell Junctions: Protein Interactions Building Control and Networks. *Cold Spring Harb. Perspect. Biol.* 10, a028746. doi:10.1101/cshperspect.a028746
- Brandt, A. C., Koehn, O. J., and Williams, C. L. (2021). SmgGDS: An Emerging Master Regulator of Prenylation and Trafficking by Small GTPases in the Ras and Rho Families. *Front. Mol. Biosci.* 8, 685135. doi:10.3389/fmolb.2021.685135
- Brezna, E. B., Semack, A. C., Higashi, T., and Miller, A. L. (2015). MgcRacGAP Restricts Active RhoA at the Cytokinetic Furrow and Both RhoA and Rac1 at Cell-Cell Junctions in Epithelial Cells. *MBoC* 26, 2439–2455. doi:10.1091/mbc.e14-11-1553
- Bryant, D. M., Datta, A., Rodríguez-Fraticelli, A. E., Peränen, J., Martín-Belmonte, F., and Mostov, K. E. (2010). A Molecular Network for De Novo Generation of the Apical Surface and Lumen. *Nat. Cell. Biol.* 12, 1035–1045. doi:10.1038/ncb2106
- Cerutti, C., and Ridley, A. J. (2017). Endothelial Cell-Cell Adhesion and Signaling. *Exp. Cell. Res.* 358, 31–38. doi:10.1016/j.yexcr.2017.06.003
- Chen, S., Li, L., Li, J., Liu, B., Zhu, X., Zheng, L., et al. (2014). SEC-10 and RAB-10 Coordinate Basolateral Recycling of Clathrin-independent Cargo through Endosomal Tubules in *Caenorhabditis elegans*. *Proc. Natl. Acad. Sci. U.S.A.* 111, 15432–15437. doi:10.1073/pnas.1408327111
- Chen, X., and Macara, I. G. (2005). Par-3 Controls Tight Junction Assembly through the Rac Exchange Factor Tiam1. *Nat. Cell. Biol.* 7, 262–269. doi:10.1038/ncb1226
- Cherfils, J., and Zeghouf, M. (2013). Regulation of Small GTPases by GEFs, GAPs, and GDIs. *Physiol. Rev.* 93, 269–309. doi:10.1152/physrev.00003.2012
- Chiang, L., Ngo, J., Schechter, J. E., Karvar, S., Tolmachova, T., Seabra, M. C., et al. (2011). Rab27b Regulates Exocytosis of Secretory Vesicles in Acinar Epithelial Cells from the Lacrimal Gland. *Am. J. Physiology-Cell Physiology* 301, C507–C521. doi:10.1152/ajpcell.00355.2010
- Claude, P., and Goodenough, D. A. (1973). Fracture Faces of Zonulae Occludentes from "tight" and "leaky" Epithelia. *J. Cell. Biol.* 58, 390–400. doi:10.1083/jcb.58.2.390
- Cutz, E., Rhoads, J. M., Drumm, B., Sherman, P. M., Durie, P. R., and Forstner, G. G. (1989). Microvillus Inclusion Disease: an Inherited Defect of Brush-Border Assembly and Differentiation. *N. Engl. J. Med.* 320, 646–651. doi:10.1056/nejm198903093201006
- Dan, Q., Shi, Y., Rabani, R., Venugopal, S., Xiao, J., Anwer, S., et al. (2019). Claudin-2 Suppresses GEF-H1, RHOA, and MRTF, Thereby Impacting Proliferation and Profibrotic Phenotype of Tubular Cells. *J. Biol. Chem.* 294, 15446–15465. doi:10.1074/jbc.ra118.006484
- Dragsten, P. R., Blumenthal, R., and Handler, J. S. (1981). Membrane Asymmetry in Epithelia: Is the Tight Junction a Barrier to Diffusion in the Plasma Membrane? *Nature* 294, 718–722. doi:10.1038/294718a0
- Durgan, J., Kaji, N., Jin, D., and Hall, A. (2011). Par6B and Atypical PKC Regulate Mitotic Spindle Orientation during Epithelial Morphogenesis. *J. Biol. Chem.* 286, 12461–12474. doi:10.1074/jbc.m110.174235
- Ebnet, K., Suzuki, A., Horikoshi, Y., Hirose, T., Meyer Zu Brickwedde, M. K., Ohno, S., et al. (2001). The Cell Polarity Protein ASIP/Par-3 Directly Associates with Junctional Adhesion Molecule (JAM). *Embo J.* 20, 3738–3748. doi:10.1093/emboj/20.14.3738
- Ehrlich, J. S., Hansen, M. D. H., and Nelson, W. J. (2002). Spatio-temporal Regulation of Rac1 Localization and Lamellipodia Dynamics during Epithelial Cell-Cell Adhesion. *Dev. Cell.* 3, 259–270. doi:10.1016/s1534-5807(02)00216-2
- Elbediwy, A., Zhang, Y., Cobbaut, M., Riou, P., Tan, R. S., Roberts, S. K., et al. (2019). The Rho Family GEF FARP2 Is Activated by aPKC $\alpha$  to Control Tight Junction Formation and Polarity. *J. Cell. Sci.* 132, jcs223743. doi:10.1242/jcs.223743
- Farquhar, M. G., and Palade, G. E. (1963). Junctional Complexes in Various Epithelia. *J. Cell. Biol.* 17, 375–412. doi:10.1083/jcb.17.2.375
- Fic, W., Bastock, R., Raimondi, F., Los, E., Inoue, Y., Gallop, J. L., et al. (2021). RhoGAP19D Inhibits Cdc42 Laterally to Control Epithelial Cell Shape and Prevent Invasion. *J. Cell. Biol.* 220, e202009116. doi:10.1083/jcb.202009116
- Fink, J., Carpi, N., Betz, T., Betard, A., Chebah, M., Azioune, A., et al. (2011). External Forces Control Mitotic Spindle Positioning. *Nat. Cell. Biol.* 13, 771. doi:10.1038/ncb2269
- Gallo, L. I., Dalghi, M. G., Clayton, D. R., Ruiz, W. G., Khandelwal, P., and Apodaca, G. (2018). RAB27B Requirement for Stretch-Induced Exocytosis in Bladder Umbrella Cells. *Am. J. Physiology-Cell Physiology* 314, C349–C365. doi:10.1152/ajpcell.00218.2017
- Gálvez-Santesteban, M., Rodríguez-Fraticelli, A. E., Bryant, D. M., Vergara-Jauregui, S., Yasuda, T., Bañón-Rodríguez, I., et al. (2012). Synaptotagmin-like Proteins Control the Formation of a Single Apical Membrane Domain in Epithelial Cells. *Nat. Cell. Biol.* 14, 838–849. doi:10.1038/ncb2541
- García-Mata, R., Boulter, E., and Burridge, K. (2011). The 'invisible Hand': Regulation of RHO GTPases by RHOGDIs. *Nat. Rev. Mol. Cell. Biol.* 12, 493–504. doi:10.1038/nrm3153
- Goitre, L., Trapani, E., Tralbalzini, L., and Retta, S. F. (2014). The Ras Superfamily of Small GTPases: the Unlocked Secrets. *Methods Mol. Biol.* 1120, 1–18. doi:10.1007/978-1-62703-791-4\_1
- Goodenough, D. A., and Revel, J. P. (1970). A Fine Structural Analysis of Intercellular Junctions in the Mouse Liver. *J. Cell. Biol.* 45, 272–290. doi:10.1083/jcb.45.2.272
- Guillemot, L., Guerrero, D., Spadaro, D., Tapia, R., Jond, L., and Citi, S. (2014). MgcRacGAP Interacts with Cingulin and Paracingulin to Regulate Rac1

- Activation and Development of the Tight Junction Barrier during Epithelial Junction Assembly. *MBoC* 25, 1995–2005. doi:10.1091/mbc.e13-11-0680
- Guillemot, L., Paschoud, S., Jond, L., Foglia, A., and Citi, S. (2008). Paracaulin Regulates the Activity of Rac1 and RhoA GTPases by Recruiting Tiam1 and GEF-H1 to Epithelial Junctions. *MBoC* 19, 4442–4453. doi:10.1091/mbc.e08-06-0558
- Guillemot, L., Spadaro, D., and Citi, S. (2013). The Junctional Proteins Cingulin and Paracaulin Modulate the Expression of Tight Junction Protein Genes through GATA-4. *PLoS One* 8, e55873. doi:10.1371/journal.pone.0055873
- Günzel, D., and Yu, A. S. L. (2013). Claudins and the Modulation of Tight Junction Permeability. *Physiol. Rev.* 93, 525–569. doi:10.1152/physrev.00019.2012
- Hayase, J., Kamakura, S., Iwakiri, Y., Yamaguchi, Y., Izaki, T., Ito, T., et al. (2013). The WD40 Protein Morg1 Facilitates Par6-aPKC Binding to Crb3 for Apical Identity in Epithelial Cells. *J. Cell. Biol.* 200, 635–650. doi:10.1083/jcb.201208150
- Hazelett, C. C., Sheff, D., and Yeaman, C. (2011). RalA and RalB Differentially Regulate Development of Epithelial Tight Junctions. *MBoC* 22, 4787–4800. doi:10.1091/mbc.e11-07-0657
- Hirvonen, M. J., Mulari, M. T. K., Büki, K. G., Vihko, P., Härkönen, P. L., and Väänänen, H. K. (2012). Rab13 Is Upregulated during Osteoclast Differentiation and Associates with Small Vesicles Revealing Polarized Distribution in Resorbing Cells. *J. Histochem Cytochem.* 60, 537–549. doi:10.1369/0022155412448069
- Hodge, R. G., and Ridley, A. J. (2016). Regulating Rho GTPases and Their Regulators. *Nat. Rev. Mol. Cell. Biol.* 17, 496–510. doi:10.1038/nrm.2016.67
- Holzner, S., Bromberger, S., Wenzina, J., Neumüller, K., Holper, T. M., Petzelbauer, P., et al. (2021). Phosphorylated Cingulin Localises GEF-H1 at Tight Junctions to Protect Vascular Barriers in Blood Endothelial Cells. *J. Cell. Sci.* 134, jcs258557. doi:10.1242/jcs.258557
- Horikoshi, Y., Suzuki, A., Yamanaka, T., Sasaki, K., Mizuno, K., Sawada, H., et al. (2009). Interaction between PAR-3 and the aPKC-PAR-6 Complex Is Indispensable for Apical Domain Development of Epithelial Cells. *J. Cell. Sci.* 122, 1595–1606. doi:10.1242/jcs.043174
- Hurd, T. W., Gao, L., Roh, M. H., Macara, I. G., and Margolis, B. (2003). Direct Interaction of Two Polarity Complexes Implicated in Epithelial Tight Junction Assembly. *Nat. Cell. Biol.* 5, 137–142. doi:10.1038/ncb923
- Iden, S., and Collard, J. G. (2008). Crosstalk between Small GTPases and Polarity Proteins in Cell Polarization. *Nat. Rev. Mol. Cell. Biol.* 9, 846–859. doi:10.1038/nrm2521
- Itoh, M., Tsukita, S., Yamazaki, Y., and Sugimoto, H. (2012). Rho GTP Exchange Factor ARHGEF11 Regulates the Integrity of Epithelial Junctions by Connecting ZO-1 and RhoA-Myosin II Signaling. *Proc. Natl. Acad. Sci. U.S.A.* 109, 9905–9910. doi:10.1073/pnas.1115063109
- Jaffe, A. B., and Hall, A. (2005). Rho GTPases: Biochemistry and Biology. *Annu. Rev. Cell. Dev. Biol.* 21, 247–269. doi:10.1146/annurev.cellbio.21.020604.150721
- Jewett, C. E., and Prekeris, R. (2018). Insane in the Apical Membrane: Trafficking Events Mediating Apical Basal Epithelial Polarity during Tube Morphogenesis. *Traffic* 19 (9), 666–678. doi:10.1111/tra.12579
- Kahn, R. A., Der, C. J., and Bokoch, G. M. (1992). The Ras Superfamily of GTP-binding Proteins: Guidelines on Nomenclature. *FASEB J.* 6, 2512–2513. doi:10.1096/fasebj.6.8.1592203
- Kawakatsu, T., Shimizu, K., Honda, T., Fukuhara, T., Hoshino, T., and Takai, Y. (2002). Trans-interactions of Nectins Induce Formation of Filopodia and Lamellipodia through the Respective Activation of Cdc42 and Rac Small G Proteins. *J. Biol. Chem.* 277, 50749–50755. doi:10.1074/jbc.m209846200
- Khandelwal, P., Ruiz, W. G., Balestreire-Hawryluk, E., Weisz, O. A., Goldenring, J. R., and Apodaca, G. (2008). Rab11a-dependent Exocytosis of Discoidal/fusiform Vesicles in Bladder Umbrella Cells. *Proc. Natl. Acad. Sci. U.S.A.* 105, 15773–15778. doi:10.1073/pnas.0805636105
- Klinkert, K., Rocancourt, M., Houdusse, A., and Echard, A. (2016). Rab35 GTPase Couples Cell Division with Initiation of Epithelial Apico-Basal Polarity and Lumen Opening. *Nat. Commun.* 7, 11166. doi:10.1038/ncomms11166
- Kocgozlu, L., Saw, T. B., Le, A. P., Yow, I., Shagirov, M., Wong, E., et al. (2016). Epithelial Cell Packing Induces Distinct Modes of Cell Extrusions. *Curr. Biol.* 26, 2942–2950. doi:10.1016/j.cub.2016.08.057
- Lamber, E. P., Siedenbueg, A.-C., and Barr, F. A. (2019). Rab Regulation by GEFs and GAPs during Membrane Traffic. *Curr. Opin. Cell. Biol.* 59, 34–39. doi:10.1016/j.cub.2019.03.004
- Lamouille, S., Xu, J., and Derynck, R. (2014). Molecular Mechanisms of Epithelial-Mesenchymal Transition. *Nat. Rev. Mol. Cell. Biol.* 15, 178–196. doi:10.1038/nrm3758
- Langemeyer, L., Fröhlich, F., and Ungermann, C. (2018). Rab GTPase Function in Endosome and Lysosome Biogenesis. *Trends Cell. Biol.* 28, 957–970. doi:10.1016/j.tcb.2018.06.007
- Lee, S., Cieply, B., Yang, Y., Peart, N., Glaser, C., Chan, P., et al. (2018). Esrp1-Regulated Splicing of Arhgef11 Isoforms Is Required for Epithelial Tight Junction Integrity. *Cell. Rep.* 25, 2417–2430. e2415. doi:10.1016/j.celrep.2018.10.097
- Lemmers, C., Michel, D., Lane-Guermonprez, L., Delgrossi, M.-H., Médina, E., Arsanto, J.-P., et al. (2004). CRB3 Binds Directly to Par6 and Regulates the Morphogenesis of the Tight Junctions in Mammalian Epithelial Cells. *MBoC* 15, 1324–1333. doi:10.1091/mbc.e03-04-0235
- Lerner, D. W., McCoy, D., Isabella, A. J., Mahowald, A. P., Gerlach, G. F., Chaudhry, T. A., et al. (2013). A Rab10-dependent Mechanism for Polarized Basement Membrane Secretion during Organ Morphogenesis. *Dev. Cell.* 24, 159–168. doi:10.1016/j.devcel.2012.12.005
- Loie, E., Charrier, L. E., Sollier, K., Masson, J.-Y., and Laprise, P. (2015). CRB3A Controls the Morphology and Cohesion of Cancer Cells through Ehm2/p114RhoGEF-dependent Signaling. *Mol. Cell. Biol.* 35, 3423–3435. doi:10.1128/mcb.00673-15
- Mack, N. A., Porter, A. P., Whalley, H. J., Schwarz, J. P., Jones, R. C., Khaja, A. S. S., et al. (2012).  $\beta$ 2-syntrophin and Par-3 Promote an Apical Basal Rac Activity Gradient at Cell-Cell Junctions by Differentially Regulating Tiam1 Activity. *Nat. Cell. Biol.* 14, 1169–1180. doi:10.1038/ncb2608
- Martin-Belmonte, F., Gassama, A., Datta, A., Yu, W., Rescher, U., Gerke, V., et al. (2007). PTEN-mediated Apical Segregation of Phosphoinositides Controls Epithelial Morphogenesis through Cdc42. *Cell* 128, 383–397. doi:10.1016/j.cell.2006.11.051
- Mccormack, J. J., Lopes Da Silva, M., Ferraro, F., Patella, F., and Cutler, D. F. (2017). Weibel-Palade Bodies at a Glance. *J. Cell. Sci.* 130, 3611–3617. doi:10.1242/jcs.208033
- Mima, J. (2021). Self-assemblies of Rab- and Arf-Family Small GTPases on Lipid Bilayers in Membrane Tethering. *Biophys. Rev.* 13, 531–539. doi:10.1007/s12551-021-00819-4
- Morais-de-Sá, E., Mirose, V., and St Johnston, D. (2010). aPKC Phosphorylation of Bazooka Defines the Apical/lateral Border in Drosophila Epithelial Cells. *Cell* 141, 509–523. doi:10.1016/j.cell.2010.02.040
- Mosaddeghzadeh, N., and Ahmadian, M. R. (2021). The RHO Family GTPases: Mechanisms of Regulation and Signaling. *Cells* 10, 1831. doi:10.3390/cells10071831
- Moskalenko, S., Henry, D. O., Rosse, C., Mirey, G., Camonis, J. H., and White, M. A. (2002). The Exocyst Is a Ral Effector Complex. *Nat. Cell. Biol.* 4, 66–72. doi:10.1038/ncb728
- Mrozowska, P. S., and Fukuda, M. (2016). Regulation of Podocalyxin Trafficking by Rab Small GTPases in 2D and 3D Epithelial Cell Cultures. *J. Cell. Biol.* 213, 355–369. doi:10.1083/jcb.201512024
- Müller, M. P., and Goody, R. S. (2018). Molecular Control of Rab Activity by GEFs, GAPs and GDI. *Small GTPases* 9, 5–21. doi:10.1080/21541248.2016.1276999
- Munro, E., Nance, J., and Priess, J. R. (2004). Cortical Flows Powered by Asymmetrical Contraction Transport PAR Proteins to Establish and Maintain Anterior-Posterior Polarity in the Early *C. elegans* Embryo. *Dev. Cell* 7, 413–424. doi:10.1016/j.devcel.2004.08.001
- Nagai-Tamai, Y., Mizuno, K., Hirose, T., Suzuki, A., and Ohno, S. (2002). Regulated Protein-Protein Interaction between aPKC and PAR-3 Plays an Essential Role in the Polarization of Epithelial Cells. *Genes. cells.* 7, 1161–1171. doi:10.1046/j.1365-2443.2002.00590.x
- Nakajima, H., and Tanoue, T. (2011). Lulu2 Regulates the Circumferential Actomyosin Tensile System in Epithelial Cells through p114RhoGEF. *J. Cell. Biol.* 195, 245–261. doi:10.1083/jcb.201104118
- Nass, J., Terplane, J., and Gerke, V. (2021). Weibel Palade Bodies: Unique Secretory Organelles of Endothelial Cells that Control Blood Vessel Homeostasis. *Front. Cell. Dev. Biol.* 9, 813995. doi:10.3389/fcell.2021.813995
- Nazlamova, L., Noble, A., Schubert, F. R., Mcgeehan, J., Myers, F., Guille, M., et al. (2017). A Newly Identified Rab-GDI Parologue Has a Role in Neural Development in Amphibia. *Gene* 599, 78–86. doi:10.1016/j.gene.2016.11.013



- Nelson, W. J., and Yeaman, C. (2001). Protein Trafficking in the Exocytic Pathway of Polarized Epithelial Cells. *Trends Cell. Biol.* 11, 483–486. doi:10.1016/s0962-8924(01)02145-6
- Nishimura, T., Yamaguchi, T., Kato, K., Yoshizawa, M., Nabeshima, Y.-i., Ohno, S., et al. (2005). PAR-6-PAR-3 Mediates Cdc42-Induced Rac Activation through the Rac GEFs STEF/Tiam1. *Nat. Cell. Biol.* 7, 270–277. doi:10.1038/ncb1227
- Novick, P. (2016). Regulation of Membrane Traffic by Rab GEF and GAP Cascades. *Small GTPases* 7, 252–256. doi:10.1080/21541248.2016.1213781
- O'Brien, L. E., Zegers, M. M. P., and Mostov, K. E. (2002). Building Epithelial Architecture: Insights from Three-Dimensional Culture Models. *Nat. Rev. Mol. Cell. Biol.* 3, 531–537. doi:10.1038/nrm859
- Ohno, S. (2001). Intercellular Junctions and Cellular Polarity: the PAR-aPKC Complex, a Conserved Core Cassette Playing Fundamental Roles in Cell Polarity. *Curr. Opin. Cell. Biol.* 13, 641–648. doi:10.1016/s0955-0674(00)00264-7
- Otani, T., Nguyen, T. P., Tokuda, S., Sugihara, K., Sugawara, T., Furuse, K., et al. (2019). Claudins and JAM-A Coordinately Regulate Tight Junction Formation and Epithelial Polarity. *J. Cell. Biol.* 218 (10), 3372–3396. doi:10.1083/jcb.201812157
- Ozdamar, B., Bose, R., Barrios-Rodiles, M., Wang, H.-R., Zhang, Y., and Wrana, J. L. (2005). Regulation of the Polarity Protein Par6 by TGF $\beta$  Receptors Controls Epithelial Cell Plasticity. *Science* 307, 1603–1609. doi:10.1126/science.1105718
- Pfeffer, S. R. (2017). Rab GTPases: Master Regulators that Establish the Secretory and Endocytic Pathways. *MBoC* 28, 712–715. doi:10.1091/mbc.e16-10-0737
- Polgar, N., and Fogelgren, B. (2018). Regulation of Cell Polarity by Exocyst-Mediated Trafficking. *Cold Spring Harb. Perspect. Biol.* 10, a031401. doi:10.1101/cshperspect.a031401
- Poteryaev, D., Datta, S., Ackema, K., Zerial, M., and Spang, A. (2010). Identification of the Switch in Early-To-Late Endosome Transition. *Cell* 141, 497–508. doi:10.1016/j.cell.2010.03.011
- Raya-Sandino, A., Castillo-Kauli, A., Domínguez-Calderón, A., Alarcón, L., Flores-Benitez, D., Cuellar-Perez, F., et al. (2017). Zonula Occludens-2 Regulates Rho Proteins Activity and the Development of Epithelial Cytoarchitecture and Barrier Function. *Biochimica Biophysica Acta (BBA) - Mol. Cell. Res.* 1864, 1714–1733. doi:10.1016/j.bbamer.2017.05.016
- Richna, N., and Aspenström, P. (2001). Rich, a Rho GTPase-Activating Protein Domain-Containing Protein Involved in Signaling by Cdc42 and Rac1. *J. Biol. Chem.* 276, 35060–35070. doi:10.1074/jbc.m103540200
- Rink, J., Ghigo, E., Kalaidzidis, Y., and Zerial, M. (2005). Rab Conversion as a Mechanism of Progression from Early to Late Endosomes. *Cell* 122, 735–749. doi:10.1016/j.cell.2005.06.043
- Román-Fernández, A., and Bryant, D. M. (2016). Complex Polarity: Building Multicellular Tissues through Apical Membrane Traffic. *Traffic* 17, 1244–1261. doi:10.1111/tra.12417
- Rouaud, F., Sluysmans, S., Flinois, A., Shah, J., Vasileva, E., and Citi, S. (2020). Scaffolding Proteins of Vertebrate Apical Junctions: Structure, Functions and Biophysics. *Biochimica Biophysica Acta (BBA) - Biomembr.* 1862, 183399. doi:10.1016/j.bbamem.2020.183399
- Schillemans, M., Karampini, E., Kat, M., and Bierings, R. (2019). Exocytosis of Weibel-Palade Bodies: How to Unpack a Vascular Emergency Kit. *J. Thromb. Haemost.* 17, 6–18. doi:10.1111/jth.14322
- Schuck, S., Gerl, M. J., Ang, A., Manninen, A., Keller, P., Mellman, I., et al. (2007). Rab10 Is Involved in Basolateral Transport in Polarized Madin-Darby Canine Kidney Cells. *Traffic* 8, 47–60. doi:10.1111/j.1600-0854.2006.00506.x
- Shen, L., Weber, C. R., Raleigh, D. R., Yu, D., and Turner, J. R. (2011). Tight Junction Pore and Leak Pathways: a Dynamic Duo. *Annu. Rev. Physiol.* 73, 283–309. doi:10.1146/annurev-physiol-012110-142150
- Stephenson, R. E., Higashi, T., Erofeev, I. S., Arnold, T. R., Leda, M., Goryachev, A. B., et al. (2019). Rho Flares Repair Local Tight Junction Leaks. *Dev. Cell* 48, 445–459. doi:10.1016/j.devcel.2019.01.016
- Striz, A. C., Stephan, A. P., López-Coral, A., and Tuma, P. L. (2018). Rab17 Regulates Apical Delivery of Hepatic Transcytotic Vesicles. *MBoC* 29, 2887–2897. doi:10.1091/mbc.e18-07-0433
- Suzuki, A., Hirata, M., Kamimura, K., Maniwa, R., Yamanaka, T., Mizuno, K., et al. (2004). aPKC Acts Upstream of PAR-1b in Both the Establishment and Maintenance of Mammalian Epithelial Polarity. *Curr. Biol.* 14, 1425–1435. doi:10.1016/j.cub.2004.08.021
- Suzuki, A., Ishiyama, C., Hashiba, K., Shimizu, M., Ebnet, K., and Ohno, S. (2002). aPKC Kinase Activity Is Required for the Asymmetric Differentiation of the Premature Junctional Complex during Epithelial Cell Polarization. *J. Cell. Sci.* 115, 3565–3573. doi:10.1242/jcs.00032
- Suzuki, A., and Ohno, S. (2006). The PAR-aPKC System: Lessons in Polarity. *J. Cell. Sci.* 119, 979–987. doi:10.1242/jcs.02898
- Suzuki, A., Yamanaka, T., Hirose, T., Manabe, N., Mizuno, K., Shimizu, M., et al. (2001). Atypical Protein Kinase C Is Involved in the Evolutionarily Conserved Par Protein Complex and Plays a Critical Role in Establishing Epithelia-specific Junctional Structures. *J. Cell. Biol.* 152, 1183–1196. doi:10.1083/jcb.152.6.1183
- Tan, B., Yatim, S. M. J. M., Peng, S., Gunaratne, J., Hunziker, W., and Ludwig, A. (2020). The Mammalian Crumbs Complex Defines a Distinct Polarity Domain Apical of Epithelial Tight Junctions. *Curr. Biol.* 30, 2791–2804. e2796. doi:10.1016/j.cub.2020.05.032
- Terry, S. J., Zihni, C., Elbediwy, A., Vitiello, E., Leefa Chong San, I. V., Balda, M. S., et al. (2011). Spatially Restricted Activation of RhoA Signalling at Epithelial Junctions by p115RhoGEF Drives Junction Formation and Morphogenesis. *Nat. Cell. Biol.* 13, 159–166. doi:10.1038/ncb2156
- Tian, Y., Gawlak, G., Tian, X., Shah, A. S., Sarich, N., Citi, S., et al. (2016). Role of Cingulin in Agonist-Induced Vascular Endothelial Permeability. *J. Biol. Chem.* 291, 23681–23692. doi:10.1074/jbc.m116.720763
- Touré, A., Dorseuil, O., Morin, L., Timmons, P., Jégou, B., Reibel, L., et al. (1998). MgcRacGAP, a New Human GTPase-Activating Protein for Rac and Cdc42 Similar to Drosophila rotundRacGAP Gene Product, Is Expressed in Male Germ Cells. *J. Biol. Chem.* 273, 6019–6023. doi:10.1074/jbc.273.11.6019
- Tsukita, S., Furuse, M., and Itoh, M. (2001). Multifunctional Strands in Tight Junctions. *Nat. Rev. Mol. Cell. Biol.* 2, 285–293. doi:10.1038/35067088
- Tuncay, H., Brinkmann, B. F., Steinbacher, T., Schürmann, A., Gerke, V., Iden, S., et al. (2015). JAM-A Regulates Cortical Dynein Localization through Cdc42 to Control Planar Spindle Orientation during Mitosis. *Nat. Commun.* 6, 8128. doi:10.1038/ncomms9128
- Umeda, K., Ikenouchi, J., Katahira-Tayama, S., Furuse, K., Sasaki, H., Nakayama, M., et al. (2006). ZO-1 and ZO-2 Independently Determine where Claudins Are Polymerized in Tight-Junction Strand Formation. *Cell* 126, 741–754. doi:10.1016/j.cell.2006.06.043
- Varadarajan, S., Chumki, S. A., Stephenson, R. E., Misterovich, E. R., Wu, J. L., Dudley, C. E., et al. (2022). Mechanosensitive Calcium Flashes Promote Sustained RhoA Activation during Tight Junction Remodeling. *J. Cell. Biol.* 221, e202105107. doi:10.1083/jcb.202105107
- Vogel, G. F., Klee, K. M. C., Janecke, A. R., Müller, T., Hess, M. W., and Huber, L. A. (2015). Cargo-selective Apical Exocytosis in Epithelial Cells Is Conducted by Myo5B, Slp4a, Vamp7, and Syntaxin 3. *J. Cell. Biol.* 211, 587–604. doi:10.1083/jcb.201506112
- Wallingford, J. B., Ewald, A. J., Harland, R. M., and Fraser, S. E. (2001). Calcium Signaling during Convergent Extension in *Xenopus*. *Curr. Biol.* 11, 652–661. doi:10.1016/s0960-9822(01)00201-9
- Wang, Q., and Margolis, B. (2007). Apical Junctional Complexes and Cell Polarity. *Kidney Int.* 72, 1448–1458. doi:10.1038/sj.ki.5002579
- Wells, C. D., Fawcett, J. P., Traweger, A., Yamanaka, Y., Goudreau, M., Elder, K., et al. (2006). A Rich1/Amot Complex Regulates the Cdc42 GTPase and Apical-Polarity Proteins in Epithelial Cells. *Cell* 125, 535–548. doi:10.1016/j.cell.2006.02.045
- Wu, S., Mehta, S. Q., Pichaud, F., Bellen, H. J., and Quiocho, F. A. (2005). Sec15 Interacts with Rab11 via a Novel Domain and Affects Rab11 Localization *In Vivo*. *Nat. Struct. Mol. Biol.* 12, 879–885. doi:10.1038/nsmb987
- Wu, X., and Guo, W. (2015). Mutagen Sensitivity. *J. Cell. Sci.* 128, 2957–2961. doi:10.1007/978-3-662-46875-3\_3908
- Xiong, X., Xu, Q., Huang, Y., Singh, R. D., Anderson, R., Leof, E., et al. (2012). An Association between Type Iy PI4P 5-kinase and Exo70 Directs E-Cadherin Clustering and Epithelial Polarization. *MBoC* 23, 87–98. doi:10.1091/mbc.e11-05-0449
- Yagi, S., Matsuda, M., and Kiyokawa, E. (2012a). Chimaerin Suppresses Rac1 Activation at the Apical Membrane to Maintain the Cyst Structure. *PLoS One* 7, e52258. doi:10.1371/journal.pone.0052258
- Yagi, S., Matsuda, M., and Kiyokawa, E. (2012b). Suppression of Rac1 Activity at the Apical Membrane of MDCK Cells Is Essential for Cyst Structure Maintenance. *EMBO Rep.* 13, 237–243. doi:10.1038/embor.2011.249
- Yamada, S., and Nelson, W. J. (2007). Localized Zones of Rho and Rac Activities Drive Initiation and Expansion of Epithelial Cell-Cell Adhesion. *J. Cell. Biol.* 178, 517–527. doi:10.1083/jcb.200701058

- Yamanaka, T., Horikoshi, Y., Suzuki, A., Sugiyama, Y., Kitamura, K., Maniwa, R., et al. (2001). PAR-6 Regulates aPKC Activity in a Novel Way and Mediates Cell-Cell Contact-Induced Formation of the Epithelial Junctional Complex. *Genes. cells.* 6, 721–731. doi:10.1046/j.1365-2443.2001.00453.x
- Yang, J., and Weinberg, R. A. (2008). Epithelial-mesenchymal Transition: at the Crossroads of Development and Tumor Metastasis. *Dev. Cell.* 14, 818–829. doi:10.1016/j.devcel.2008.05.009
- Yeaman, C., Grindstaff, K. K., and Nelson, W. J. (2004). Mechanism of Recruiting Sec6/8 (Exocyst) Complex to the Apical Junctional Complex during Polarization of Epithelial Cells. *J. Cell. Sci.* 117, 559–570. doi:10.1242/jcs.00893
- Yi, C., Troutman, S., Fera, D., Stemmer-Rachamimov, A., Avila, J. L., Christian, N., et al. (2011). A Tight Junction-Associated Merlin-angiomotin Complex Mediates Merlin's Regulation of Mitogenic Signaling and Tumor Suppressive Functions. *Cancer Cell.* 19, 527–540. doi:10.1016/j.ccr.2011.02.017
- Yonemura, S., Itoh, M., Nagafuchi, A., and Tsukita, S. (1995). Cell-to-cell Adherens Junction Formation and Actin Filament Organization: Similarities and Differences between Non-polarized Fibroblasts and Polarized Epithelial Cells. *J. Cell. Sci.* 108, 127–142. doi:10.1242/jcs.108.1.127
- Young, L. C., and Rodriguez-Viciana, P. (2018). MRAS: A Close but Understudied Member of the RAS Family. *Cold Spring Harb. Perspect. Med.* 8, a033621. doi:10.1101/cshperspect.a033621
- Zerial, M., and McBride, H. (2001). Rab Proteins as Membrane Organizers. *Nat. Rev. Mol. Cell. Biol.* 2, 107–117. doi:10.1038/35052055
- Zhang, X.-M., Ellis, S., Sriratanana, A., Mitchell, C. A., and Rowe, T. (2004). Sec15 Is an Effector for the Rab11 GTPase in Mammalian Cells. *J. Biol. Chem.* 279, 43027–43034. doi:10.1074/jbc.M402264200
- Zheng, Y., and Pan, D. (2019). The Hippo Signaling Pathway in Development and Disease. *Dev. Cell.* 50, 264–282. doi:10.1016/j.devcel.2019.06.003
- Zihni, C., Mills, C., Matter, K., and Balda, M. S. (2016). Tight Junctions: from Simple Barriers to Multifunctional Molecular Gates. *Nat. Rev. Mol. Cell. Biol.* 17, 564–580. doi:10.1038/nrm.2016.80
- Zihni, C. (2021). MRCK: a Master Regulator of Tissue Remodeling or Another 'ROCK' in the Epithelial Block? *Tissue Barriers* 9, 1916380. doi:10.1080/21688370.2021.1916380
- Zihni, C., Munro, P. M. G., Elbediwy, A., Keep, N. H., Terry, S. J., Harris, J., et al. (2014). Dbl3 Drives Cdc42 Signaling at the Apical Margin to Regulate Junction Position and Apical Differentiation. *J. Cell. Biol.* 204, 111–127. doi:10.1083/jcb.201304064
- Zihni, C., Vlassaks, E., Terry, S., Carlton, J., Leung, T. K. C., Olson, M., et al. (2017). An Apical MRCK-Driven Morphogenetic Pathway Controls Epithelial Polarity. *Nat. Cell. Biol.* 19, 1049–1060. doi:10.1038/ncb3592

**Conflict of Interest:** The authors declare that the research was conducted in the absence of any commercial or financial relationships that could be construed as a potential conflict of interest.

**Publisher's Note:** All claims expressed in this article are solely those of the authors and do not necessarily represent those of their affiliated organizations, or those of the publisher, the editors and the reviewers. Any product that may be evaluated in this article, or claim that may be made by its manufacturer, is not guaranteed or endorsed by the publisher.

Copyright © 2022 Ebnet and Gerke. This is an open-access article distributed under the terms of the Creative Commons Attribution License (CC BY). The use, distribution or reproduction in other forums is permitted, provided the original author(s) and the copyright owner(s) are credited and that the original publication in this journal is cited, in accordance with accepted academic practice. No use, distribution or reproduction is permitted which does not comply with these terms.



## OPEN ACCESS

EDITED BY  
Eurico Morais-de-Sá,  
Universidade do Porto, Portugal

REVIEWED BY  
Denise Montell,  
University of California, Santa Barbara,  
United States  
Elias H. Barriga,  
Gulbenkian Institute of Science (IGC),  
Portugal

\*CORRESPONDENCE  
Jakub Sedzinski,  
jakub.sedzinski@sund.ku.dk

SPECIALTY SECTION  
This article was submitted to  
Morphogenesis and Patterning,  
a section of the journal  
Frontiers in Cell and Developmental  
Biology

RECEIVED 04 June 2022  
ACCEPTED 08 August 2022  
PUBLISHED 27 September 2022

CITATION  
Ventura G and Sedzinski J (2022),  
Emerging concepts on the mechanical  
interplay between migrating cells and  
microenvironment *in vivo*.  
*Front. Cell Dev. Biol.* 10:961460.  
doi: 10.3389/fcell.2022.961460

COPYRIGHT  
© 2022 Ventura and Sedzinski. This is an  
open-access article distributed under  
the terms of the [Creative Commons  
Attribution License \(CC BY\)](https://creativecommons.org/licenses/by/4.0/). The use,  
distribution or reproduction in other  
forums is permitted, provided the  
original author(s) and the copyright  
owner(s) are credited and that the  
original publication in this journal is  
cited, in accordance with accepted  
academic practice. No use, distribution  
or reproduction is permitted which does  
not comply with these terms.

# Emerging concepts on the mechanical interplay between migrating cells and microenvironment *in vivo*

Guilherme Ventura and Jakub Sedzinski\*

The Novo Nordisk Foundation Center for Stem Cell Medicine (reNEW), University of Copenhagen, Copenhagen, Denmark

During embryogenesis, tissues develop into elaborate collectives through a myriad of active mechanisms, with cell migration being one of the most common. As cells migrate, they squeeze through crowded microenvironments to reach the positions where they ultimately execute their function. Much of our knowledge of cell migration has been based on cells' ability to navigate *in vitro* and how cells respond to the mechanical properties of the extracellular matrix (ECM). These simplified and largely passive surroundings contrast with the complexity of the tissue environments *in vivo*, where different cells and ECM make up the milieu cells migrate in. Due to this complexity, comparatively little is known about how the physical interactions between migrating cells and their tissue environment instruct cell movement *in vivo*. Work in different model organisms has been instrumental in addressing this question. Here, we explore various examples of cell migration *in vivo* and describe how the physical interplay between migrating cells and the neighboring microenvironment controls cell behavior. Understanding this mechanical cooperation *in vivo* will provide key insights into organ development, regeneration, and disease.

## KEYWORDS

*in vivo* cell migration, mechanotransduction, confinement, topography, durotaxis, microenvironment sensing

## Introduction

The formation of organs during morphogenesis is an intricate process that relies on cells assembling into tissues, forming orderly units with defined shape and function. The mechanisms generating such complex collectives have long intrigued biologists. It is now clear that cell migration is essential for establishing and maintaining these diverse cellular architectures (Yamada and Sixt 2019). In its most simplified view, cell migration is initiated by the polarization of an individual cell (or group of cells) along a specific axis, propelled by actomyosin contraction and traction-generating actin-based protrusions that engage with the substrate, and directed by a gradient of biochemical cues (Figure 1A) (SenGupta, Parent, and Bear 2021). Recently, however, the

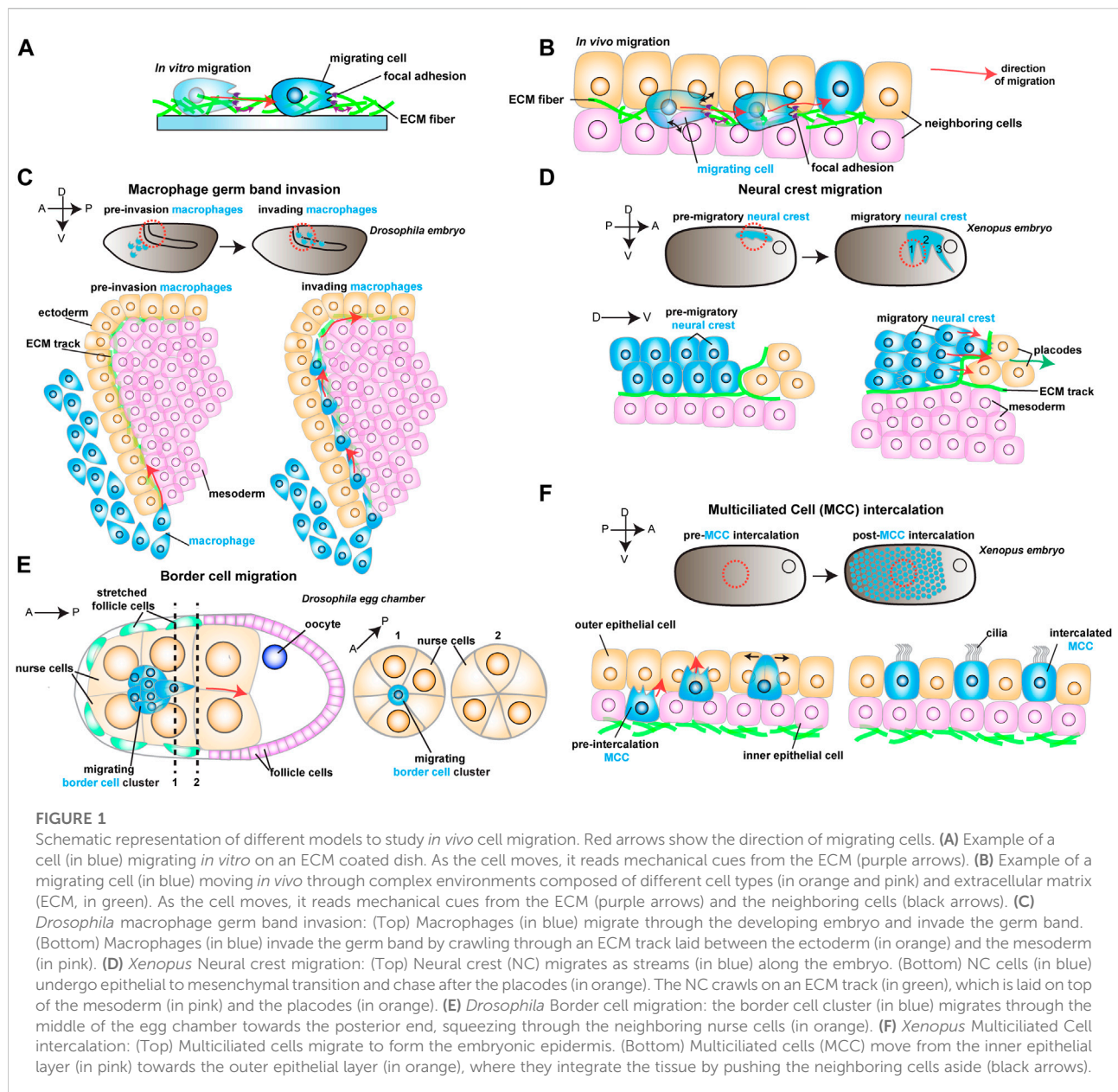


FIGURE 1

Schematic representation of different models to study *in vivo* cell migration. Red arrows show the direction of migrating cells. (A) Example of a cell (in blue) migrating *in vitro* on an ECM coated dish. As the cell moves, it reads mechanical cues from the ECM (purple arrows). (B) Example of a migrating cell (in blue) moving *in vivo* through complex environments composed of different cell types (in orange and pink) and extracellular matrix (ECM, in green). As the cell moves, it reads mechanical cues from the ECM (purple arrows) and the neighboring cells (black arrows). (C) *Drosophila* macrophage germ band invasion: (Top) Macrophages (in blue) migrate through the developing embryo and invade the germ band. (Bottom) Macrophages (in blue) invade the germ band by crawling through an ECM track laid between the ectoderm (in orange) and the mesoderm (in pink). (D) *Xenopus* Neural crest migration: (Top) Neural crest (NC) migrates as streams (in blue) along the embryo. (Bottom) NC cells (in blue) undergo epithelial to mesenchymal transition and chase after the placodes (in orange). The NC crawls on an ECM track (in green), which is laid on top of the mesoderm (in pink) and the placodes (in orange). (E) *Drosophila* Border cell migration: the border cell cluster (in blue) migrates through the middle of the egg chamber towards the posterior end, squeezing through the neighboring nurse cells (in orange). (F) *Xenopus* Multiciliated Cell intercalation: (Top) Multiciliated cells migrate to form the embryonic epidermis. (Bottom) Multiciliated cells (MCC) move from the inner epithelial layer (in pink) towards the outer epithelial layer (in orange), where they integrate the tissue by pushing the neighboring cells aside (black arrows).

importance of physical cues in cell migration has become apparent; the substrate's physical properties in which cells migrate, such as ECM deformability (stiffness) and topography, play vital roles in cell migration (Charras and Sahai 2014; Helvert et al., 2018; Valet, Siggia, and Brivanlou 2022). Similarly, the native environment *in vivo* also exposes migrating cells to diverse mechanical stimuli. However, such environments are much more complex than their *in vitro* counterparts, as tissues are composed of different cell types and multiple ECM components that interact with the migrating cell (Figures 1A,B). Thus, our understanding of

how cells sense and respond to the mechanical properties of their microenvironments *in vivo* is only starting to be defined. In this mini-review, we explore recent discoveries in different models of *in vivo* cell migration through confined environments. We then identify some common features illustrating how migratory behaviors depend on the physical interactions between migrating cells and their surroundings. Defining how such mechanical interplay is regulated will have major implications for understanding how migration shapes fundamental developmental processes, regeneration and cancer.



Cells moving through tissues are physically confined by their neighbors and components of the ECM (Figure 1B). In such crowded microenvironments, migrating cells must squeeze and push through as they move while simultaneously being exposed to various physical cues. We divide these signals into two broad categories: 1) spatial cues, which include the degree of physical constraint cells are exposed to (confinement), the specific features of the environment, such as the available space between neighboring cells (geometry) or how they are connected (topography), and 2) mechanical cues, which rely on the material properties of the substrate such as substrate stiffness to guide cell migration (durotaxis). In the first part of this mini-review, we describe examples of these types of physical information and how they guide cell migration. The second part describes how migrating cells respond to the microenvironment by changing their own mechanical properties. Finally, we provide a unifying perspective on the interplay between the behavior of migratory cells and the physical properties of the tissue through which cells migrate *in vivo*.

## The physical information of the 3D microenvironment

### Cellular confinement, geometry and topography as spatial cues

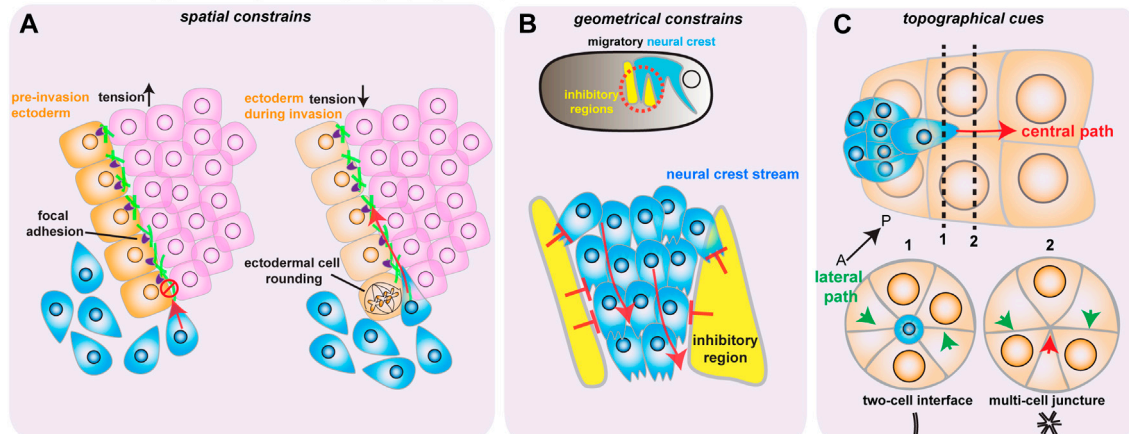
Cell migration through tissue environments proceeds through highly confining spaces. Confined 3D microenvironments present migrating cells with heterogeneous geometries from tight to broader spaces between cells or ECM pores (Figure 1B). While the development of microfabrication techniques has helped understand the impact of confinement *in vitro* (Reversat et al., 2020), the importance of mechanical confinement *in vivo* is still elusive.

There is no more intuitive example of confined migration than immune cells extravasating through vessels or moving through crowded tissues during immune surveillance. An emerging model of how cellular confinement controls immune cell migration *in vivo* is the macrophage invasion of the *Drosophila* germ band (Siekhaus et al., 2010). During *Drosophila* embryonic development, migrating macrophages distribute themselves across the embryo to ensure immune protection. A subset of the migrating macrophages invades the germ band by squeezing through the tightly juxtaposed ectoderm and mesoderm, with the invading macrophages extending protrusions and crawling along an ECM track (Figure 1C) (Ratheesh et al., 2018). Thus, migration through such cell-dense tissue could depend on the confinement and the mechanical features of the environment, concepts that remain poorly understood *in vivo*. Recent studies have identified two complementary mechanisms that promote macrophage migration. First, the ectodermal tissue tension is reduced by a decrease in myosin II contractility, which is triggered by the soluble

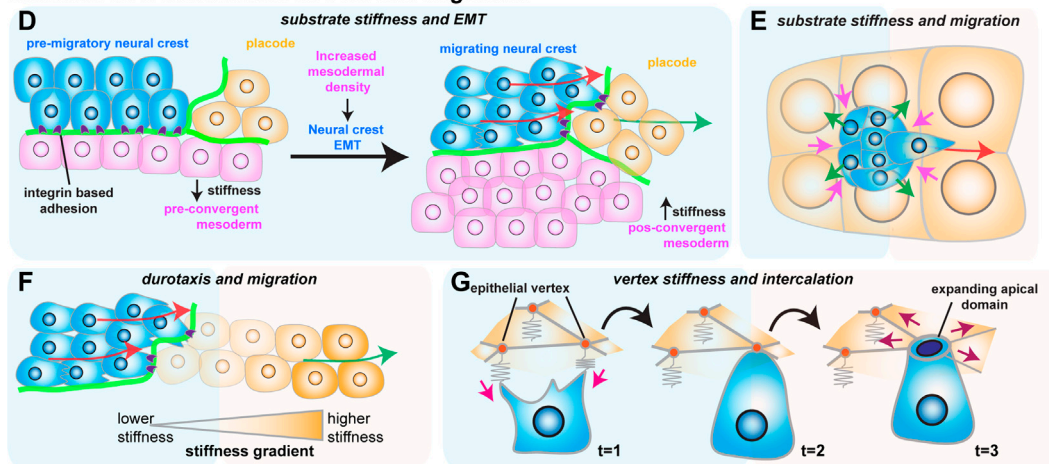
factors released from the amnioserosal tissue neighboring the germ band (Figure 2A) (Ratheesh et al., 2018). This decrease in tissue tension facilitates macrophage invasion, as it enhances the ability of the ectodermal epithelium to deform in response to the invading macrophages. The second mechanism relies on local shape changes of the ectodermal cells at the entrance to the germ band (Akhmanova et al., 2022). As such, ectodermal cells act as gatekeepers to macrophage invasion, and when epithelial cells round up to divide, they form the entry points for macrophage invasion (Figure 2A). Consequently, inhibition of ectoderm cell division greatly blocks macrophage entry into the germ band. However, even in conditions where cell division is largely impaired, the few remaining macrophages still invade the germ band next to dividing or rounding cells, showing that ectoderm cell division is a decisive event for macrophage invasion. Notably, inducing ectoderm cell rounding is itself not sufficient to promote macrophage invasion. Rather, ectoderm cell rounding during division disassembles the focal adhesions (FAs) maintained by the ectodermal cells with the underlying ECM. These FAs impede macrophage entry by blocking the movement of the macrophages' nucleus through the adhesion foci. Similarly, reducing FA components specifically in the ectoderm is sufficient to allow macrophages to invade the germ band, even in the absence of mitotic cell rounding.

While confinement can direct cell movement by controlling the amount of available space, cell migration can also be regulated by dictating where cells can effectively move through geometric constraints. The importance of geometric constraints is nicely illustrated in the migrating cephalic neural crest (NC) progenitors in the *Xenopus* embryo. This collectively migratory population moves along the ventral side of the embryo as it chases the neighboring placodes in well-defined streams (Figure 1D) (Theveneau et al., 2013). These streams rely on constraint imposed by the surrounding tissues (Figure 2B) (Szabó et al., 2016). Although the constraint in itself is not required for cell motility, it ensures directional collective cell migration, relying on the secretion of repellant signals such as semaphorins into the ECM by the neighboring cells. Semaphorins restrict the movement of NC cells by blocking the NC cells' ability to make actin protrusions that provide traction, which avoids NC cell dispersion, keeping cells in the ideal path and ensuring efficient directional migration (Bajanca et al., 2019). Moreover, recent work has defined that the mechanosensitive ion channel Piezo1 in the NC cooperates with surrounding semaphorins, supporting the notion that mechanical cues can control directed cell migration (Canales Coutiño and Mayor, 2021). In this mechanism, Piezo1 is required to partially inhibit actin regulator Rac1 activity in the migrating NCs, which is reinforced by semaphorin signaling from the neighboring tissues. Together, Piezo1 and Semaphorins control protrusion dynamics to optimal levels, avoiding cell dispersion and sustaining directional migration.

### Confinement, geometry and topography as spatial cues



### Stiffness as a mechanical cue for cell migration



### Physical responses of migrating cells

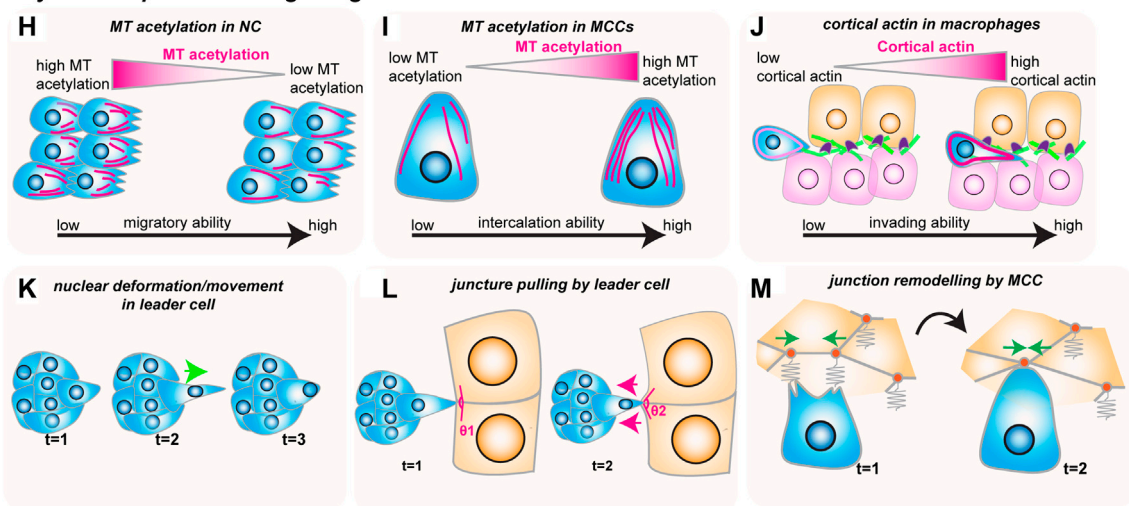


**FIGURE 2**

How mechanical cues impact cell migration *in vivo*. The red arrows show the direction of migrating cells. (A–C) Confinement, geometry and topography as spatial cues. (A) Spatial constraints block macrophage invasion (in blue) by controlling cells' ability to crawl through the ectoderm (in orange) and the mesoderm (in magenta). Decreasing ectodermal tension is paired with ectodermal cell rounding to promote macrophage invasion. Ectodermal cell rounding removes focal adhesions (in purple) that act as an impediment to cell movement. (B) Geometric constraints control stream formation in the neural crest (in blue). Inhibitory signals (in yellow) regulate where NC can move, stopping NC cell dispersion and promoting (Continued)

**FIGURE 2**

collective cell migration. **(C)** Topographic cues determine border cell migration through the central path of the egg chamber (red arrow). The central path provides more space for cluster movement which is energetically favorable, as the multi-cell junctions are easier to unzip than to the lateral paths (green arrows), which are composed of tightly juxtaposed two-cell interfaces. **(D–G)** Stiffness as a mechanical cue for cell migration. **(D)** Increase in mesoderm stiffness induces NC EMT and migration. Convergent-extension movements increase cell density and stiffness of the mesoderm (in pink), which is sensed by the pre-migratory NC (in blue) through their integrin-based adhesions (in purple). **(E)** Nurse cell (in orange) stiffness impacts the migration of the border cell cluster (in blue). The compressive forces from the nurse cells (magenta arrows) are counteracted by the border cells (green arrows). **(F)** NC cells (in blue) interact with the placodes (in orange), which causes the placodes to retreat (green arrow), generating a stiffness gradient that directs cell migration. **(G)** Intercalating MCCs (in blue) pull on the vertices of the neighboring goblet epithelial cells (in orange) to sense vertex stiffness (magenta arrows). The stiffer multicellular vertices act as ideal entry points into the tissue as the increased total line tension favors the opening of the MCCs apical domain (purple arrows). **H–M)** Physical responses of migrating cells. **(H)** Microtubule (MT) deacetylation decreases NC stiffness to promote NC migration (acetylated MTs in magenta). **(I)** MT hyperacetylation promotes MCC intercalation, possibly by increasing cell stiffness (acetylated MTs in magenta). **(J)** Invading macrophages generate a protective cortical actin shell that shields the nucleus from compression. **(K)** In the migrating border cell cluster, the leader cell protrusions are stabilized by the active movement of the nucleus to the base of the protrusion (green arrow). **(L)** Border cells pull on the neighboring junctions of nurse cells to sense the environment (magenta arrows). **(M)** Intercalating MCCs remodel the neighboring goblet cell junctions (green arrows), promoting MCC intercalation.

While the geometrical features of the neighboring tissues can act as restricting cues, the microenvironment can also possess topographical features that serve as guidance signals for cell locomotion. A remarkably instructive system to tackle how topography regulates cell movement is border cell migration during *Drosophila* oogenesis. During ovarian development, the border cells form a cluster of six to ten epithelial cells that migrate towards the oocyte (Figure 1E) (Montell, Yoon, and Starz-Gaiano 2012). During migration, the border cell cluster moves through a highly constraining environment as the cluster squeezes through the surrounding nurse cells, which form the substrate on which cells migrate. Interestingly, while there are several paths border cells can migrate through, the cluster consistently moves through the center of the egg chamber as it advances towards the source of several chemotactic signals (Stuelten, Parent, and Montell 2018). While such signals are essential for the anterior-posterior (AP) movement, chemical cues do not explain why the border cell cluster consistently selects the central track. Recent work has tackled this question by reconstructing egg chambers in 3D and describing all possible paths for border cells inside the egg chamber (Dai et al., 2020). This detailed analysis determined that the central path is unique because it is where contacts (or junctions) between three or more nurse cells are enriched. This particular multiple-cell configuration is more spacious than the optional side paths, which are constituted by tightly juxtaposed two-cell interfaces (Figure 2C). Thus, the extra space provided by the central path originates a favorably energetic environment for the border cells to unzip the neighboring nurse cells (Figure 2C). The preferred central path illustrates how the steric constraints from the environment can direct cell migration.

## Stiffness as a mechanical cue for cell migration

As we have seen, geometrical and topographical features of the environment provide key spatial cues during *in vivo* cell migration. However, the rheological material properties, such as

the substrate stiffness, can also serve as cues for cell movement. Indeed, migrating cells *in vitro* have long been known to respond to their environment's stiffness (Charras and Sahai 2014; Janmey, Fletcher, and Reinhart-King 2020). Until recently, whether migrating cells *in vivo* also react to tissue stiffness had remained an open question. Intriguingly, NC cell migration *in vivo* depends on changes in the mechanical properties of the underlying mesoderm, which becomes stiffer prior to NC migration (Barriga et al., 2018). This increased substrate stiffness is sensed by the pre-migratory NC cells, causing them to undergo epithelial-to-mesenchymal transition (EMT), acquire motility and start migrating by extending actin protrusions that engage with the ECM substrate through focal adhesions (Figure 2D). The stiffening of the mesoderm driving this transition results from the increased cell density underneath the neural crest, as mesoderm cells undergo extensive convergent extension. Blocking convergent extension movements, or decreasing myosin II activity in the mesoderm, inhibits mesoderm stiffening, which blocks NC migration. Interestingly, the influence of substrate stiffness on cell migration is also observed in other model systems—border cell migration also depends on the stiffness of the nurse cells that form the substrate (Aranjuez et al., 2016; Lamb et al., 2021). However, contrary to the NC cells, increasing the myosin II activity in the nurse cells, and consequently their stiffness, blocks border cell migration (Figure 2E). These results suggest that substrate stiffness can act as a key regulator in cell migration and that changes in tissue stiffness elicit different responses from migrating cells that are context dependent.

As we have described, changes in the substrate stiffness control cells' ability to migrate *in vivo*. Indeed, it has long been described that cells *in vitro* migrate along gradients of increasing substrate stiffness, in a process coined as durotaxis (Lo et al., 2000). While durotaxis has been well characterized *in vitro*, and substrate stiffness gradients *in vivo* have also been reported, whether cells migrate across stiffness gradients *in vivo* has long remained elusive (Shellard and Mayor 2021a). However, it has been recently shown that a durotactic gradient cooperates with

chemotactic cues to direct NC migration (Shellard and Mayor, 2021b). As we have seen, NC cells migrate as a cluster along the dorsal-ventral axis as they chase the chemotactic signals secreted by the placodes, and move on ECM tracks laid out by the neighboring placodes and mesoderm (Figure 2D). Once the NC cluster reaches the placode, the two tissues establish repulsive interactions mediated by N-cadherin contacts. This causes the placodes to move away from the NC cells, which continually chase the placodal cells (Theveneau et al., 2013). Yet, during this interaction, NC cells also generate a stiffness gradient (Figure 2F) (Shellard and Mayor, 2021b). As the NC interacts with the retreating placodes through N-cadherin contacts, they cause the placodal cells they contact to soften. This induces the local generation of a stiffness gradient across the placode, which NC cells then sense through integrin-based adhesions (Figure 2F). Similarly to the chemotactic cues, the NC cells then persistently chase the retreating region of higher substrate stiffness. Interestingly, impairing either chemotaxis or durotaxis is sufficient to block proper NC migration, and neither tactic mechanism can overrule the other. It is then the coordinated chemotactic activity of the placodes and the self-generated stiffness gradient that moves the NC along the dorsal-ventral axis in a continuous mechanism of chase-and-run (Shellard and Mayor, 2021b).

While chemical and physical cues cooperate to sustain cell migration, it is unclear whether this is a universal principle. In some cases, mechanical signals might direct cell movement in the absence of clear chemotactic cues. One such example is the addition of multiciliated cells (MCCs) progenitors to the *Xenopus* embryonic epidermis, where no prevalent chemotactic signal has been defined (Stubbs et al., 2006; Werner et al., 2011; Collins et al., 2021). To join the epidermis, hundreds of MCCs execute the multi-step process of radial intercalation (RI) (Figure 1F) (Sedzinski et al., 2016). During RI, MCCs first move from the inner into the outer layer of the epidermis (Figure 1F). Once the MCCs reach the outer epithelium, they move toward the epithelial vertices formed by the outer epithelial cells, which constitute the entry points into the tissue (Figure 2G). Finally, MCCs emerge into the tissue by pushing the neighboring cells apart as they expand their apical domains. It is known that MCC apical emergence is initially dominated by pushing forces exerted by the MCC's actin cortex, while pulling forces exerted by the neighboring epithelial cells contribute to completing the process (Figure 2G) (Sedzinski et al., 2016; Sedzinski et al., 2017; Kulkarni et al., 2021). Modulating the rigidity of the adjacent goblet cells is sufficient to control the final size of the MCC's apical domain (Sedzinski et al., 2016). Thus, apical emergence depends on the fine balance between the mechanical properties of the intercalating cell and its epithelial neighbors. While apical emergence is a mechanical process, it is unclear whether mechanical cues inform MCCs where to

intercalate. Recent work has shown that MCCs actively read the stiffness of the neighboring goblet cells to determine where to integrate (Figure 2G) (Ventura et al., 2021). As MCCs move apically, they extend actin-based protrusions (filopodia) that pull on the epithelial vertices of overlying goblet cells. Interestingly, the epithelial vertices constitute key mechanical hotspots within epithelia, suggesting that intercalating cells could use protrusions to pull and probe the mechanical environment (Higashi and Miller 2017). In silico experiments help explain that the pulling exerted by the MCC can be effectively used to measure the local stiffness of the epithelial vertices, which then determines where the MCCs integrate within the tissue. Vertices with higher stiffness are preferred positions for MCC intercalation because the combined higher line tension from the neighboring goblet cells' junctions enhances apical expansion (Ventura et al., 2021). Thus, intercalating MCCs sense the stiffness of the neighboring cells to determine the ideal positions for cell intercalation.

## The physical responses of migrating cells to their surroundings

We have until now discussed how the surrounding environment's mechanical properties control cell migration. Conversely, migrating cells read such mechanical cues and react to them with their own physical responses. As we shall see, these responses are diverse and range from migrating cells dynamically adjusting their mechanical properties to cells actively remodeling their surrounding environment (Figures 2H–M).

To start with the first example, it is now known that migrating cells fine-tune their mechanical properties in response to changes in the stiffness of the environment. As described above, an increase in mesoderm stiffness is required to induce NC EMT and migration (Barriga et al., 2018). However, recent work has shown that pre-migratory NC cells respond to the increased substrate stiffness by changing their mechanical properties (Marchant et al., 2022). In this mechanism, NC cells activate the mechanosensitive Piezo1 channel, causing NC cells to reduce microtubule (MT) acetylation (Figure 2H). This ultimately changes the mechanical properties of the NC by decreasing NC cell stiffness, which is required for NC migration, as sustaining MT acetylation blocks NC migration. Conversely, inducing a hypoacetylated microtubule network in NCs is sufficient to rescue migration in a non-stiff mesoderm. Thus, NC migration depends not only on changes in the surrounding tissues but also on a dynamic balance between the mechanical properties of the migrating cells and their substrate. This mechanism might not be unique to the neural crest, and a similar mechanism could be at play in other migrating cells. MCC intercalation also depends on the properties of its MT cytoskeleton, and MT hyperacetylation promotes MCC intercalation (Figure 2I) (Collins et al., 2021). How



hyperacetylation determines the mechanical properties of the MCC, and whether this is a response to mechanical constraints from the neighbors, has not been defined. It is likely, however, that hyperacetylation sustains cortical rigidity in the MCCs as they push through their neighbors. Altogether, it is possible that controlling the properties of the MT network could provide a novel general mechanism for regulating the mechanical properties of migrating cells. Other components of the migrating cells' cytoskeleton also play a crucial role in how cells physically respond to the environment. It is now known that the activity of actin bundling protein Fascin in the border cells is required to regulate the myosin II activity of the substrate nurse cells, effectively decreasing their stiffness (Figure 2E) (Lamb et al., 2021). Thus, the migrating border cells can actively fine-tune the stiffness of their substrate *in vivo*, and a complex force balance between the border cells and the nurse cells regulates border cell migration. Similarly, as we have seen, NC cells are able to soften the neighboring placodal cells, allowing them to establish the durotactic gradient that drives them along the dorsal-ventral axis (Figure 2F) (Shellard and Mayor, 2021b). Altogether, it is now clear that migrating cells actively respond to their environment *in vivo* by regulating their intrinsic mechanical properties. Moreover, while the individual mechanical properties of the substrate and the migrating cells are essential, it is the interplay between migrating cells and their substrate (a concept known as mechanoreciprocity) which is key to cell migration through complex tissue environments (Helvert et al., 2018).

As we have seen, the tissue environments through which cells move are highly confined, and migrating cells have to actively deform as they squeeze through the tissue. In this process, cells are particularly challenged by their nucleus, which is the largest and stiffest organelle and often the limiting step when cells migrate in 3D environments (Renkawitz et al., 2019). This forces cells to use strategies to mechanically adapt to such challenges. During macrophage invasion of the germ band, macrophages prepare for the challenging migration through the restrictive environment by forming a protective actin cortex (Belyaeva et al., 2022). This protective shell is required for proper macrophage migration, and it shields the migrating macrophage nucleus from mechanical stress during confinement. Macrophages fail to invade the germ band when the protective actin shell is lost (Figure 2J). A similar challenge is also faced by the migrating border cells. The relatively "spacious" central path border cells take is still smaller than the leading border cell. This requires the leader cell to squeeze its nucleus through the small available spaces (Penfield and Montell, 2021). As a response, the nucleus of the leader border cell deforms as it squeezes through the central path (Figure 2K). During this deformation, however, the leader cell nucleus controls the dynamics of the guiding protrusions. The nuclear movement to the base of the protrusion prevents protrusion collapse and facilitates growth, possibly by counteracting the rearward forces at the protrusion neck. While it can either act as a

mechanical encumbrance or support, the nucleus also acts as a key mechanotransducer. Recent work has shown that nuclear stretching caused by compression, imitating the confinement experienced by cells, can activate myosin II activity and trigger cell migration (Lomakin et al., 2020; Venturini et al., 2020). Altogether, the nucleus is an active player in cell migration in a confined environment, with nuclear deformation mediating many important responses during migration.

Migrating cells also use other strategies to interact with the environment mechanically. As we have seen, actin-based protrusions provide traction during cell locomotion (Figure 1A). However, recently it has been shown how such actin protrusions can act as sensory organs, which actively pull on the neighboring cells (Figures 2G, L). Such actin protrusions pull on the neighboring environment to sense the available space in a possible path, as in the *Drosophila* border cells, or to probe the mechanical properties of the surrounding cells, as in the *Xenopus* MCCs (Dai et al., 2020; Ventura et al., 2021). Another exciting aspect of this phenomenon is how migrating cells can use such actin-based extensions to exert changes in the neighboring environment to promote cell migration. Recent work has defined how during intercalation, MCCs actively form higher-order vertices by inducing the remodeling of the junctions of its neighboring epithelial cells (Ventura et al., 2021). MCCs exert this out of plane remodeling by clutching and pulling the vertices at the ends of a junction, driving junction collapse to form the preferred higher order vertices (Figure 2M). Thus, MCCs can exert forces on the neighboring cells to generate a local environment that favors cell intercalation.

## Conclusion

Cell migration is one of the most fascinating and fundamental biological processes orchestrating our body plan. Understanding the complexity of cell migration *in vivo* requires studying the cellular dynamics locally, right in the microenvironment in which cells naturally reside. How does a heterogeneous microenvironment instruct cell migration? How do migrating cells respond to biomechanical cues presented by the surrounding microenvironment? These questions emphasize the need to consider cell migration as an interplay, a reciprocal interaction between a migrating cell and its surroundings. These interactions are dynamic and evolve over time as both the migrating cells and the microenvironment adapt their mechanical properties to fulfill an overarching developmental program. Furthermore, migrating cells not only read and respond but can also actively remodel the surrounding microenvironment, allowing them to trigger morphodynamic rearrangements efficiently. Recent work has also defined a whole new set of migrating cues, such as cell guidance by electrical gradients and pressure (Barriga and Theveneau 2020; Lennon-Duménil and Moreau 2021). Although these fall beyond the focus of this mini-review, they are incredibly interesting

examples of the diversity of physical cues used by migrating cells to navigate complex environments. Altogether, studies addressing the mechanical interplay between migrating cells and the diverse environments they migrate through *in vivo* will provide important key insights into organ development, tissue homeostasis and disease pathology.

## Author contributions

GV and JS designed and wrote the mini-review. GV designed and made figures.

## Funding

The Novo Nordisk Foundation Center for Stem Cell Medicine (reNEW) is supported by a Novo Nordisk Foundation grant number NNF21CC0073729. GV and JS acknowledge The Novo Nordisk Foundation (NNF19OC0056962) and Leo Foundation (LF-OC-19-000219) for funding support.

## References

- Akhmanova, M., Emtenani, S., Krueger, D., Gyoergy, A., Guarda, M., Vlasov, M., et al. (2022). Cell division in tissues enables macrophage infiltration. *Science* 376 (6591), 394–396. doi:10.1126/science.abj0425
- Aranjuez, G., Burtscher, A., Sawant, K., Majumder, P., and Jocelyn, A. (2016). Dynamic myosin activation promotes collective morphology and migration by locally balancing Oppositional forces from surrounding tissue. *Mol. Biol. Cell* 27 (12), 1898–1910. doi:10.1091/mbc.E15-10-0744
- Bajanca, F., Gougnard, N., Colle, C., Parsons, M., Mayor, R., and Theveneau, E. (2019). *In vivo* topology converts competition for cell-matrix adhesion into directional migration. *Nat. Commun.* 10 (1), 1518. doi:10.1038/s41467-019-09548-5
- Barriga, E. H., Franze, K., Charras, G., and Mayor, R. (2018). Tissue stiffening coordinates morphogenesis by triggering collective cell migration *in vivo*. *Nature* 554 (7693), 523–527. doi:10.1038/nature25742
- Barriga, E. H., and Theveneau, E. (2020). *In vivo* neural crest cell migration is controlled by "Mixotaxis". *Front. Physiol.* 11, 586432. doi:10.3389/fphys.2020.586432
- Belyaeva, V., Wachner, S., Gyoergy, A., Emtenani, S., Gridchyn, I., Akhmanova, M., et al. (2022). Fos regulates macrophage infiltration against surrounding tissue resistance by a cortical actin-based mechanism in drosophila. *PLoS Biol.* 20 (1), e3001494. doi:10.1371/journal.pbio.3001494
- Canales Coutiño, B., and Mayor, R. (2021). The mechanosensitive channel piezo1 cooperates with semaphorins to control neural crest migration. *Development* 148 (23), dev200001. doi:10.1242/dev.200001
- Charras, G., and Sahai, E. (2014). Physical influences of the extracellular environment on cell migration. *Nat. Rev. Mol. Cell. Biol.* 15 (12), 813–824. doi:10.1038/nrm3897
- Collins, C., Kim, S. K., Rosa, V., Mitchell, J. W., Mitchell, B., Han, H., et al. (2021). tubulin acetylation promotes penetrative capacity of cells undergoing radial intercalation. *Cell. Rep.* 36 (7), 109556. doi:10.1016/j.celrep.2021.109556
- Dai, W., Guo, X., Cao, Y., Mondo, J. A., Campanale, J. P., Montell, B. J., et al. (2020). Tissue topography steers migrating *drosophila* border cells. *Science* 370 (6519), 987–990. doi:10.1126/science.aaz4741
- Hannezo, E., Tu, F., Biro, M., and Wallingford, J. B. (2017). Correction: rhoa regulates actin network dynamics during apical surface emergence in multiciliated epithelial cells. *J. Cell. Sci.* 130 (5), 1017. doi:10.1242/jcs.202234
- Helvert, S. v., Storm, C., and Friedl, P. (2018). Mechanoreciprocity in cell migration. *Nat. Cell. Biol.* 20 (1), 8–20. doi:10.1038/s41556-017-0012-0
- Higashi, T., and Miller, A. L. (2017). Tricellular junctions: How to build junctions at the trickiest points of epithelial cells. *Mol. Biol. Cell* 28 (15), 2023–2034. doi:10.1091/mbc.E16-10-0697
- Janmey, P. A., Fletcher, D. A., and Reinhart-King, C. A. (2020). Stiffness sensing by cells. *Physiol. Rev.* 100, 695–724. doi:10.1152/physrev.00013.2019
- Kulkarni, S., Marquez, J., Priya, D., Rosa, V., Mitchell, B. J., and Khokha, M. K. (2021). Mechanical stretch scales centriole number to apical area via piezo1 in multiciliated cells. *eLife* 10. doi:10.7554/eLife.66076
- Lamb, M. C., Kaluarachchi, C. P., Lansakara, T. I., Mellentine, S. Q., Lan, Y., Tivanski, A. V., et al. (2021). Fascin limits myosin activity within *Drosophila* border cells to control substrate stiffness and promote migration. *eLife* 10, e69836. doi:10.7554/eLife.69836
- Lennon-Duménil, A. M., and Moreau, H. D. (2021). Barotaxis: How cells live and move under pressure. *Curr. Opin. Cell. Biol.* 72, 131–136. doi:10.1016/j.ccb.2021.07.006
- Lo, C. M., Wang, H. B., Dembo, M., and Wang, Y. L. (2000). Cell movement Is guided by the rigidity of the substrate. *Biophys. J.* 79 (1), 144–152. doi:10.1016/S0006-3495(00)76279-5
- Lomakin, A. J., Cattin, C. J., Cuvelier, D., Alraies, Z., Molina, M., Nader, G. P. F., et al. (2020). The nucleus acts as a ruler tailoring cell responses to spatial constraints. *Science* 370 (6514), eaba2894. doi:10.1126/science.aba2894
- Marchant, C. L., Malmi-Kakkada, A. N., Espina, J. A., and Barriga, E. H. (2022). Cell clusters softening triggers collective cell migration *in vivo* Nature Materials. doi:10.1038/s41563-022-01323-0
- Montell, D. J., WanYoon, H., and Starz-Gaiano, M. (2012). Group choreography: Mechanisms orchestrating the collective movement of border cells. *Nat. Rev. Mol. Cell. Biol.* 13 (10), 631–645. doi:10.1038/nrm3433
- Penfield, L., and Denise, J. (2021). Nuclear lamins promote protrusion dynamics and collective, confined migration *in vivo*. *bioRxiv*. doi:10.1101/2021.12.16.473064
- Ratheesh, A., Julia, B., Jana, V., Smutny, M., Papusheva, E., Gabriel Krens, S. F., et al. (2018). *Drosophila* TNF modulates tissue tension in the embryo to facilitate macrophage invasive migration. *Dev. Cell* 45 (3), 331–346.e7. doi:10.1016/j.devcel.2018.04.002
- Renkawitz, J., Kopf, A., Stopp, J., de Vries, I., Driscoll, M. K., Merrin, J., et al. (2019). Nuclear positioning facilitates amoeboid migration along the path of least resistance. *Nature* 568 (7753), 546–550. doi:10.1038/s41586-019-1087-5

## Acknowledgments

The authors thank all members of the Sedzinski Lab for comments and suggestions, in particular Mari Tolonen and Raghavan Thiagarajan.

## Conflict of interest

The authors declare that the research was conducted in the absence of any commercial or financial relationships that could be construed as a potential conflict of interest.

## Publisher's note

All claims expressed in this article are solely those of the authors and do not necessarily represent those of their affiliated organizations, or those of the publisher, the editors and the reviewers. Any product that may be evaluated in this article, or claim that may be made by its manufacturer, is not guaranteed or endorsed by the publisher.

- Reversat, A., Gaertner, F., Merrin, J., Stopp, J., Tasciyan, S., Aguilera, J., et al. (2020). Cellular locomotion using environmental topography. *Nature* 582 (7813), 582–585. doi:10.1038/s41586-020-2283-z
- Sedzinski, J., Hannezo, E., Fan, T., Biro, M., and Wallingford, J. B. (2016). Emergence of an apical epithelial cell surface *In Vivo. Dev. Cell.* 36 (1), 24–35. doi:10.1016/j.devcel.2015.12.013
- Sedzinski, J., Hannezo, E., Tu, F., Biro, M., and Wallingford, J. B. (2017). Correction: RhoA regulates actin network dynamics during apical surface emergence in multiciliated epithelial cells. *J. Cell. Sci.* 130 (5), 1017. doi:10.1242/jcs.202234
- SenGupta, S., Parent, C. A., and Bear, J. E. (2021). The principles of directed cell migration. *Nat. Rev. Mol. Cell. Biol.* 22 (8), 529–547. doi:10.1038/s41580-021-00366-6
- Shellard, A., and Mayor, R. (2021a). Durotaxis: The hard path from *in vitro* to *in vivo*. *Dev. Cell.* 56 (2), 227–239. doi:10.1016/j.devcel.2020.11.019
- Shellard, A., and Mayor, R. (2021b). Collective durotaxis along a self-generated stiffness gradient *In Vivo. Nature* 600 (7890), 690–694. doi:10.1038/s41586-021-04210-x
- Siekhaus, D., Haesemeyer, M., Moffitt, O., and Lehmann, R. (2010). RhoL controls invasion and rap1 localization during immune cell transmigration in *Drosophila*. *Nat. Cell. Biol.* 12 (6), 605–610. doi:10.1038/ncb2063
- Stubbs, J. L., Davidson, L., Keller, R., and Kintner, C. (2006). Radial intercalation of ciliated cells during xenopus skin development. *Development* 133 (13), 2507–2515. doi:10.1242/dev.02417
- Stuelten, C. H., Parent, C. A., and Montell, D. J. (2018). Cell motility in cancer invasion and metastasis: insights from simple model organisms. *Nat. Rev. Cancer* 18 (5), 296–312. doi:10.1038/nrc.2018.15
- Szabó, A., Melchionda, M., Nastasi, G., Woods, M. L., Campo, S., Perris, R., et al. (2016). *In Vivo* Confinement promotes collective migration of neural crest cells. *J. Cell. Biol.* 213 (5), 543–555. doi:10.1083/jcb.201602083
- Theveneau, E., Steventon, B., Scarpa, E., Garcia, S., Treppe, X., Streit, A., et al. (2013). Chase-and-run between adjacent cell populations promotes directional collective migration. *Nat. Cell. Biol.* 15 (7), 763–772. doi:10.1038/ncb2772
- Valet, M., Siggia, E. D., and Brivanlou, A. H. (2022). Mechanical regulation of early vertebrate embryogenesis. *Nat. Rev. Mol. Cell. Biol.* 23 (3), 169–184. doi:10.1038/s41580-021-00424-z
- Ventura, G. B., Amiri, A., Thiagarajan, R., Tolonen, M., Doostmohammadi, A., and Sedzinski, J. (2021). Mechanics of cell integration *in vivo*. *bioRxiv*. doi:10.1101/2021.11.18.469090
- Venturini, V., Pezzano, F., Häkkinen, H.-M., Jiménez-Delgado, S., Colomer-Rosell, M., Marro, M., et al. (2020). The nucleus measures shape changes for cellular proprioception to control dynamic cell behavior. *Science* 370 (6514), eaba2644. doi:10.1126/science.aba2644
- Werner, M. E., Hwang, P., Huisman, F., Peter, T., Yu, C. C., and Mitchell, B. J. (2011). Actin and microtubules drive differential aspects of planar cell polarity in multiciliated cells. *J. Cell. Biol.* 195 (1), 19–26. doi:10.1083/jcb.201106110
- Yamada, K. M., and Sixt, M. (2019). Mechanisms of 3D cell migration. *Nat. Rev. Mol. Cell. Biol.* 20 (12), 738–752. doi:10.1038/s41580-019-0172-9



## OPEN ACCESS

## EDITED BY

Alexander Ludwig,  
Nanyang Technological University,  
Singapore

## REVIEWED BY

Pedro Martinez,  
University of Barcelona, Spain  
Dan Bergstralh,  
University of Rochester, United States

## \*CORRESPONDENCE

Patrick O. Humbert,  
p.humbert@latrobe.edu.au

## SPECIALTY SECTION

This article was submitted to  
Morphogenesis and Patterning,  
a section of the journal  
Frontiers in Cell and Developmental  
Biology

RECEIVED 21 August 2022

ACCEPTED 31 October 2022

PUBLISHED 24 November 2022

## CITATION

Wright BA, Kvensakul M, Schierwater B  
and Humbert PO (2022), Cell polarity  
signalling at the birth of multicellularity:  
What can we learn from the first animals.  
*Front. Cell Dev. Biol.* 10:1024489.  
doi: 10.3389/fcell.2022.1024489

## COPYRIGHT

© 2022 Wright, Kvensakul, Schierwater  
and Humbert. This is an open-access  
article distributed under the terms of the  
[Creative Commons Attribution License](#)  
(CC BY). The use, distribution or  
reproduction in other forums is  
permitted, provided the original  
author(s) and the copyright owner(s) are  
credited and that the original  
publication in this journal is cited, in  
accordance with accepted academic  
practice. No use, distribution or  
reproduction is permitted which does  
not comply with these terms.

# Cell polarity signalling at the birth of multicellularity: What can we learn from the first animals

Bree A. Wright<sup>1</sup>, Marc Kvensakul<sup>1,2</sup>, Bernd Schierwater<sup>3</sup> and  
Patrick O. Humbert<sup>1,2,4,5\*</sup>

<sup>1</sup>Department of Biochemistry and Chemistry, La Trobe Institute for Molecular Science, La Trobe University, Melbourne, VIC, Australia, <sup>2</sup>Research Centre for Molecular Cancer Prevention, La Trobe University, Melbourne, VIC, Australia, <sup>3</sup>Institute of Animal Ecology and Evolution, University of Veterinary Medicine Hannover, Foundation, Bünteweg, Hannover, Germany, <sup>4</sup>Department of Biochemistry and Pharmacology, University of Melbourne, Melbourne, VIC, Australia, <sup>5</sup>Department of Clinical Pathology, University of Melbourne, Melbourne, VIC, Australia

The innovation of multicellularity has driven the unparalleled evolution of animals (Metazoa). But how is a multicellular organism formed and how is its architecture maintained faithfully? The defining properties and rules required for the establishment of the architecture of multicellular organisms include the development of adhesive cell interactions, orientation of division axis, and the ability to reposition daughter cells over long distances. Central to all these properties is the ability to generate asymmetry (polarity), coordinated by a highly conserved set of proteins known as cell polarity regulators. The cell polarity complexes, Scribble, Par and Crumbs, are considered to be a metazoan innovation with apicobasal polarity and adherens junctions both believed to be present in all animals. A better understanding of the fundamental mechanisms regulating cell polarity and tissue architecture should provide key insights into the development and regeneration of all animals including humans. Here we review what is currently known about cell polarity and its control in the most basal metazoans, and how these first examples of multicellular life can inform us about the core mechanisms of tissue organisation and repair, and ultimately diseases of tissue organisation, such as cancer.

## KEYWORDS

cell polarity, basal metazoa, multicellularity, asymmetry, signalling, tissue architecture

## Introduction

Cell polarity refers to the intrinsic asymmetric distribution of macromolecules to distinct compartments of a cell to control directionality and coordinated polarisation. Cell polarity is associated with cell behaviours, such as migration and asymmetric cell division (Nelson 2003; Elsum et al., 2012; Butler and Wallingford 2017; Allam, Charnley, and Russell 2018; Stephens et al., 2018). The conservation through evolution of a vast majority of the cell polarity genes from basal metazoans to mammals highlights their significance and relevance in tissue architecture and cell behaviour (Goldstein and Macara 2007;



Simons and Mlodzik 2008; Fahey and Degnan 2010; Elsum et al., 2012; Belahbib et al., 2018). Understanding cell polarity in basal metazoans may help unravel some of the mysteries of multicellularity and key processes that occurred during the transition from unicellular to multicellular organisms. The jump from unicellularity to multicellularity has occurred at least 25 times throughout evolution contributing to a complex tree of species, including: plants, fungi, amoeba and Bilateria to name a few (Grosberg and Strathmann 2007; Rokas 2008).

Advances in the understanding of the genetics of basal metazoans and unicellular organisms have provided opportunities to advance our understanding of signalling pathways that have been considered the main building blocks of multicellularity (Gerhart 1999). Here we extend this framework to include cell polarity signalling. Examination of multicellular events in unicellular organisms can shed light as to how the transition to multicellularity may have occurred and how early forms of cell polarity signalling may have enabled this. For example, Gram-negative bacteria *P. aeruginosa* demonstrates both kin selection (the progressive replication of a single cell to select for traits) (West et al., 2006) and cheating (the differential uptake of resources by certain cells, allowing for some cells to thrive at the cost of others) (Sandoz, Mitzimberg, and Schuster 2007; Dunny, Brickman, and Dworkin 2008). Another example is in the yeast species *S. cerevisiae* where cell polarity proteins *Sro7* and *Sro77*, (homologues of *D. melanogaster* Lgl (Lethal 2) giant larvae)), regulate polarisation of the actin cytoskeleton and vesicle exocytosis (Lehman et al., 1999; Gangar et al., 2005; Hattendorf et al., 2007). There are different hypotheses as to how multicellularity occurred (King 2004; Knoll 2011; Richter and King 2013; Sogabe et al., 2019) of which all fundamentally agree on the significance of cells orientating spatio-temporally to allow for coordinated cell movement, migration, and adhesion.

A key concept in the exploration of multicellularity is co-option—the ability for a trait to switch and thus impact on function (McLennan 2008). Evolutionarily, this occurs in many different contexts and here can be demonstrated by the co-option of genes already present in the genome being redirected to polarising events to support multicellularity. Cell adhesion molecules are considered one of these key co-optive processes (Abedin and King 2010; Harden, Wang, and Krieger 2016), another example being the LAP family of adaptor genes containing leucine rich repeats (LRR) and PDZ domains giving rise to the Scribble cell polarity gene (Santoni et al., 2002). Of note, the choanoflagellate genome (the closest unicellular organism relating to animals) reveals a rich repertoire of adhesion, cell polarity and signalling genes (King 2004; Snell et al., 2006; King et al., 2008).

In this review we will highlight our current knowledge of cell polarity in basal metazoans to further understand the evolution and adaptation of cell polarity signalling. It should be noted that there is still vigorous debate as to the evolutionary order of these lower metazoan animals as to how they relate to the last known

common ancestor of bilaterians. However, this extends outside the scope of this review and we direct the reader to other references that tackle this important issue (see. (Grosberg and Strathmann 2007; Nosenko et al., 2013; Srivastava 2015; Schierwater et al., 2021a)).

## Transitioning to multicellularity: The first animals

Epithelial tissue is a key building block in the development of multicellularity due to the formation of epithelial sheets. ‘True’ epithelia is defined by 1) the presence of polarity between epithelial cells, 2) multiple junctions joining cells together, including: belt, septate, desmosome and tight junction, and 3) the presence of an extracellular matrix (Tyler 2003). The sheet formation acts as a barrier separating compartments of the organism, allowing for the regulation, diffusion and absorption of macromolecules (Tyler 2003; Fahey and Degnan 2012). To achieve such diverse functionality within an organism, epithelial cells need to be highly polarised, which is achieved by the asymmetric compartmentalising of cell polarity constituents (Rodriguez-Boulant and Nelson 1989; Elsum et al., 2012; Ebnet 2015; Wen and Zhang 2018). Basal metazoans are the first multicellular organisms and the ancient relatives to Bilateria, and more broadly the Eumetazoan subkingdom (Schierwater et al., 2021). They all contain examples of epithelial sheet formation, but only cnidarians have examples of true epithelia as explained above (Fahey and Degnan 2010; Rathbun, Everett, and Bergstrahl 2022). The choanocytes in Poriferans (sponges) are considered epithelia-like (Simpson 1984) while the other epithelial cells lack key characteristics, like desmosomes and basal lamina (Fahey and Degnan 2010). Placozoans lack a basal lamina and key junctions associated with ‘true epithelia’. Although extracellular matrix (ECM) constituent genes such as *collagen*, *integrin- $\beta$*  and *laminin*, are present and expressed in Placozoa. The absence of an actual ECM and basal lamina has been a peculiarity in the placozoans (Ringrose et al., 2013). These basal metazoans will be introduced briefly below.

## Placozoa

Phylum Placozoa comprises flat sea-dwelling animals approximately 1–5 mm in diameter and 20  $\mu$ m in height. They are morphologically considered to be one of the simplest animals with no distinguishable organs, nerve or muscle cells, basal lamina or extracellular matrix (Smith et al., 2014; DuBuc, Ryan, and Martindale 2019; Schierwater et al., 2021). The most well-known species of placozoans is *Trichoplax adhaerens*, although a number of other species have been described and studied (Schierwater et al., 2021; Neumann et al., 2022). Structurally, placozoans consist of six

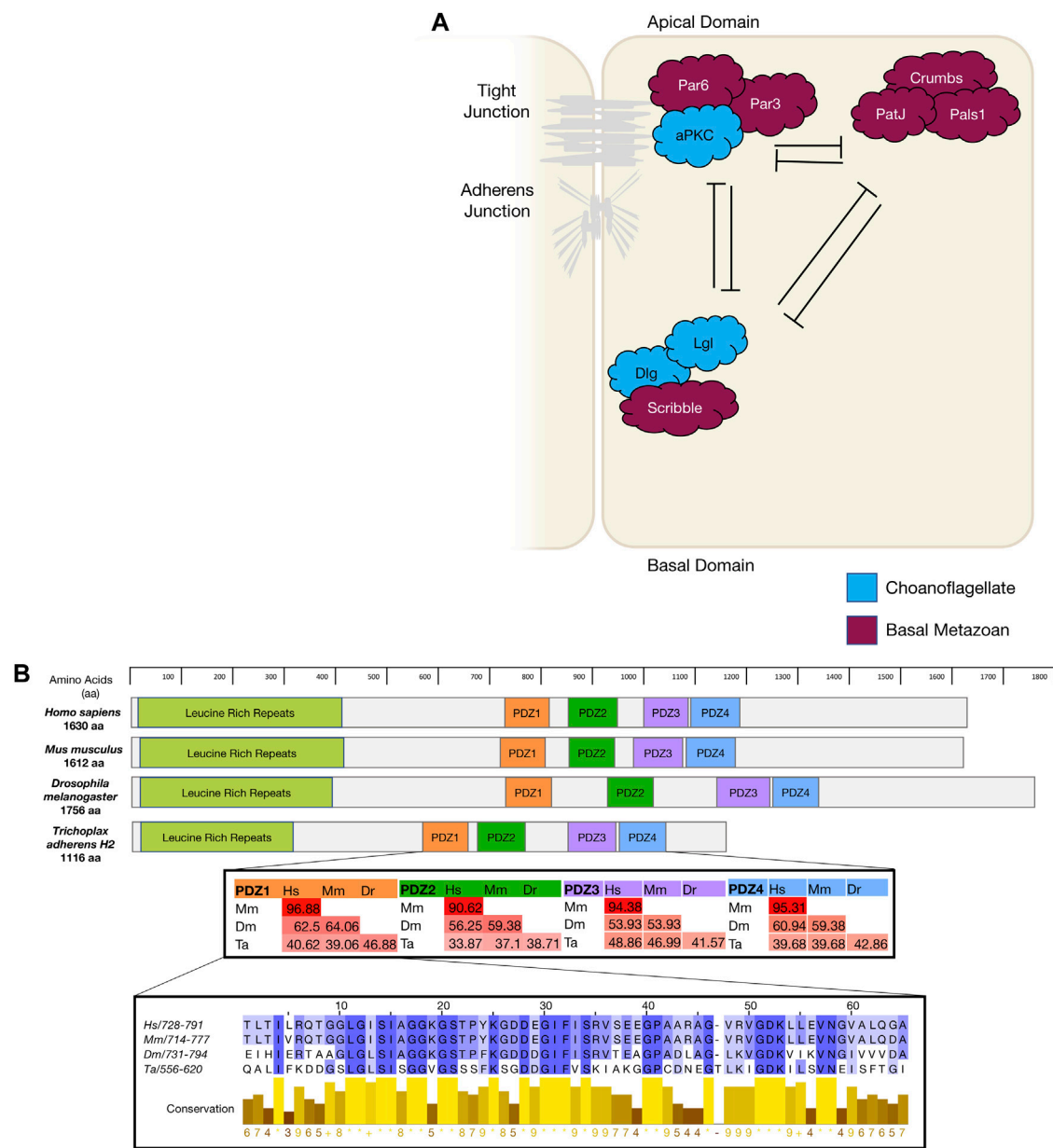
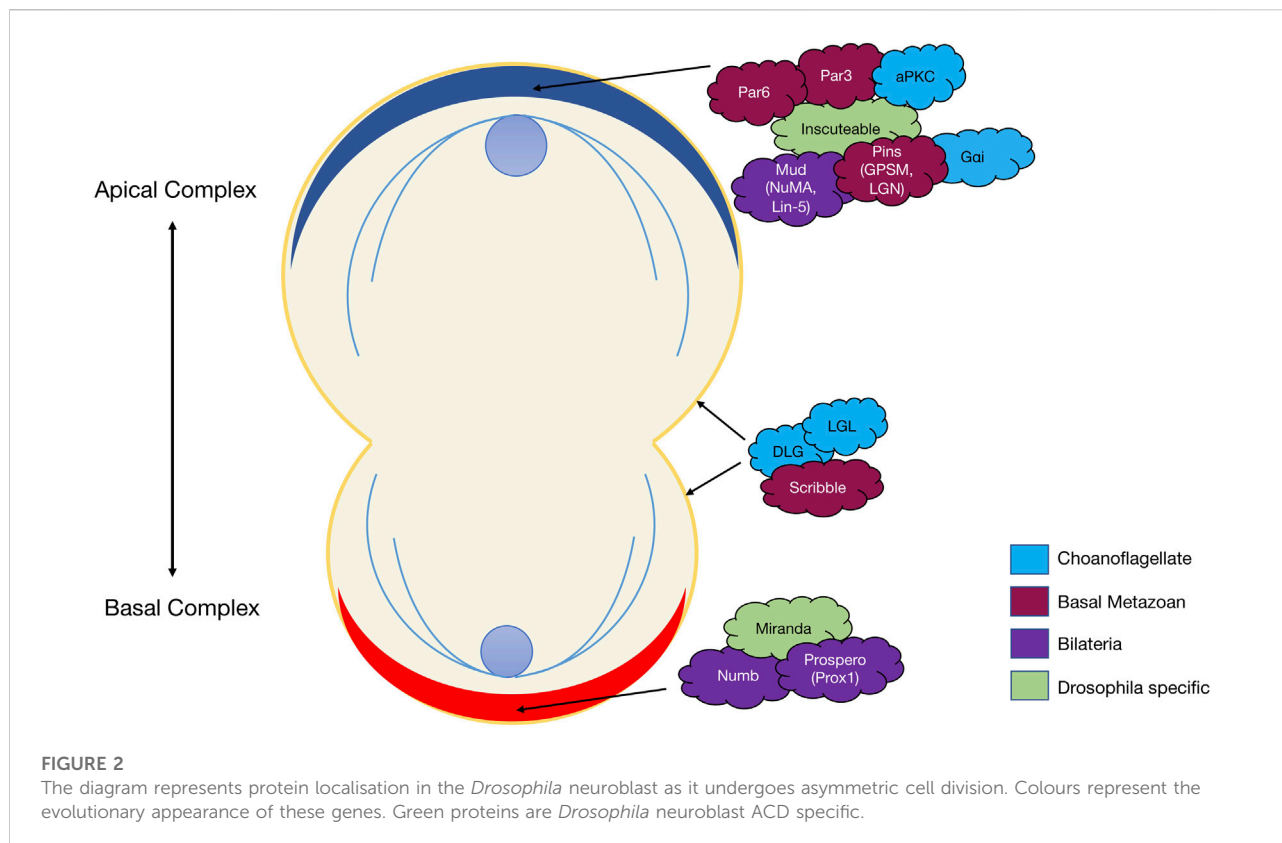


**FIGURE 1**  
(A) The diagram depicts mammalian apico-basal polarity proteins and their interactions and localisation within an epithelial cell and the appearance of these genes in evolution. (B). Using Scribble as an example of gene conservation, a comparison has been made between the gene structure of four animals, a percentage map of key PDZ domains when compared between these four animals. PDZ1 has been expanded as an example of conservation and sequence similarity. Sequences were aligned in Clustal Omega and percentage conservation analysed in Jalview. Colour represented level of conservation. Sequences were sourced from uniprot accessions: *H. sapiens* Q14160-1; *M. musculus* Q80U72-1; *D. melanogaster* Q7KRY7-1; and *T. adherens* A0A369S7Y8.

different cell types, with 80% of the animal comprised of epithelial cells (Smith et al., 2014). Most essential signalling pathways are present in placozoans, including Wnt, Notch, cell adhesion molecules, mitogen-activated protein kinase (MAPK) signalling, NFκB and TGF-β at both the transcriptome and proteome level (Srivastava et al., 2008; Ringrose et al., 2013; Belahbib et al., 2018). Placozoans show a very high regenerative potential including the ability to re-aggregate animals from single cells (A. Ruthmann and Terwelp 1979; Osigus et al., 2022). No placozoan has been identified as having cancer, even when exposed to high levels of radiation (Fortunato et al., 2021).











## Porifera

Porifera, named due to their porous nature, encapsulates a diverse family of sponges. Their body plan consists of a labyrinth of small canals and chambers lined with choanocytes (cilia beating cells) that allows for the flow of water through the animal and the filtration of nutrients and microalgae (Soest et al., 2012). The well-studied marine Porifera *Amphimedon queenslandica* contains key regulatory, transcription, and signalling pathway genes including: Hox, Wnt, Hedgehog, TGF- $\beta$ , Notch, Jak/Stat, MAPK signalling pathway and cell adhesion molecules (Gerhart 1999; Nichols et al., 2006; Adamska et al., 2011; Wu et al., 2022). From a junctional perspective, Porifera have adherens junctions similar to those present in Bilateria, but there is no evidence of septate junctions or basal lamina (Srivastava et al., 2010). In the freshwater sponge *E. muelleri*, focal adhesion-like junctions and adherens junctions have been identified with highly conserved genes such as talin, integrin and focal adhesion kinase (Mitchell and Nichols 2019). Similar to other basal metazoans, sponges have the capacity to regenerate which has been reported to occur through the process of epithelial-to-mesenchymal transition (EMT) (Alexander et al., 2015; Lavrov et al., 2018; Ereskovsky et al., 2021; Wu et al., 2022).

## Ctenophora

Ctenophores more commonly known as comb jellies, consist of over 200 species and differ from other basal metazoans in that they have a characteristic set of eight comb rows that run along their length (Pang and Mark 2008; Tamm 2014). Morphologically, ctenophores consist of an epithelial ectoderm and endoderm with a mesoglea layer containing collagen filaments (Freeman 1977; Harrison and Ruppert 1991; Simmons, Pang, and Martindale 2012). Gene analysis of the ctenophore *M. leidy* reveals a canonical Wnt signalling pathway similar to bilaterians (J. F. Ryan et al., 2013). However, Ctenophores lack key signalling and polarity genes like Scribble and crumbs (Belahbib et al., 2018) and members required for non-canonical Wnt signalling pathway (J. F. Ryan et al., 2013). Similar to placozoans, many ctenophore species examined do not contain a basal lamina (Ringrose et al., 2013). In the ctenophore *M. leidy*, key binding domains such as the groove-binding motif and cytoplasmic binding domain of E-Cadherin showed a lack of conservation compared with Placozoa, Porifera and Bilateria (Belahbib et al., 2018). The analysis of Ctenophores show a lack of gene conservation and it has been suggested this is due to secondary loss (Belahbib et al., 2018). One example is the lack of the MAGUK protein Dlg in ctenophores, which is a highly

TABLE 1 Apico Basal Polarity proteins.

	Species	Gene	Basal Metazoa					Bilateria			References
			Choanoflagellate	Placozoa	Porifera	Ctenophora	Cnidaria	C. elegans	D. melanogaster	M. musculus	
											
Apico-Basal polarity	Scribble		x	.	.	x	.	.	.	.	(1–4)
	Dlg		.	.	.	~	.	.	.	.	(1,5,6)
	Lgl		.	.	.	.	.	.	.	.	(1,5–7)
	Par 3		x	.	.	.	.	.	.	.	(1,5,8,9)
	Par 6		x	.	.	.	.	.	.	.	(1,9)
	aPKC		.	.	.	.	.	.	.	.	(1,10)
	Crumbs		x	.	~	x	.	.	.	.	(1,10)
	Pals1		x	.	~	x	.	.	.	.	(1,5,9)
	PatJ		x	.	.	x	.	.	.	.	(1,9)
	Prospero (Prox1)		x	*	x	x	.	.	.	.	(11–16)
	Numb		x	~	x	~	~	.	.	.	(17)
	Gai		.	.	.	.	.	.	.	.	(18–22)

The table lists the occurrence of polarity genes through evolution based on Choanoflagellate, Basal metazoan and Bilateria classified as . gene present; ~ gene partially present; or x gene not present; \* no data available.

1. Belahbib et al, 2018; 2. Santoni et al, 2002; 3. Elsum et al, 2012; 4. Rathbun et al, 2022; 5. Fahey & Degnan 2010; 6. Yamanaka & Ohno 2008; 7. Richter et al. 2018; 8. Etemad-Moghadam & Kemphues 1995; 9. Tucker & Adams 2014; 10. Seb -Pedr s et al, 2012; 11. B rglin 1994; 12. Doe et al, 1991; 13. Elsir et al, 2012; 14. Larroux et al, 2008; 15. Oliver et al, 1993; 16. Ryan et al, 2006; 17. Gazave et al, 2009; 18. Gotta & Ahringer 2001; 19. Ajduk & Zernicka-Goetz 2016; 20. Bergstr h et al, 2017; 21. Lokits et al, 2018; 22. de Mendoza et al, 2014;

conserved gene present well before basal metazoans e.g. choanoflagellates (Fahey and Degnan 2010; Belahbib et al., 2018; Schiller and Bergstr h 2021).

# Cnidaria

Cnidarians encapsulate over 10,000 species that can be classified into two broad groups–sessile Anthozoa (e.g. the sea anemone *Nematostella vectensis*) and medusozoa (e.g. the freshwater *Hydra vulgaris*) (Technau and Steele 2011; Z.-Q. Zhang 2011). Similar to other basal metazoans, cnidarians have the capacity to regenerate lost or damaged body parts when both chemical or mechanical digestion occurs (P. M. Bode and Bode 1980; Layden, Rentzsch, and R ttinger 2016; R ttinger 2021). Studies of *Hydra* reveal the presence of ECM, cell-cell adhesion molecules, Wnt, hedgehog and notch signalling–which are all present and well conserved (Tucker and Adams 2014). A thorough review on the conservation of cell polarity signalling in Cnidaria has also recently been published (Rathbun, Everett, and Bergstr h 2022).

Core cell polarity signalling complexes in the basal metazoa. Several cell polarity signalling systems have developed through evolution, gaining complexity with evolving form and function of animal structures. In a few instances however, such as ctenophores or *C. elegans*, secondary loss of cell polarity

genes have been observed (Belahbib et al., 2018). Analysis of genomic DNA sequences have identified the central cell polarity regulator complexes Scribble, Par and Crumbs in all basal metazoans (Srivastava et al., 2008; Fahey and Degnan 2010; Riesgo et al., 2014; Tucker and Adams 2014; Belahbib et al., 2018). These cell polarity signalling pathways remain fundamentally unexamined from a functional perspective in the basal metazoans. Here we seek to collate what is known of cell polarity signalling in basal metazoans, including the expression and function of cell polarity proteins, and to highlight the importance of these cell polarity mechanisms throughout evolution.

# The par, crumbs, and scribble modules in apico-basal polarity regulation

Apico-basal polarity is largely specific to epithelial cells and involves the localisation of polarity modules to the apical and basolateral membranes (Figure 1A) (Bilder and Perrimon 2000; Nelson 2003; Margolis and Borg 2005). Apico-basal polarity is considered essential in the formation of epithelial sheet and barrier formation, a concept fundamental to metazoan development. The polarising events of apico-basal localisation within a cell allow for formation of junctions between cells. Notably zonula adherens and tight junctions in vertebrates,



adherens and septate junctions in *D. melanogaster* and apical junctions in *C. elegans* (Alberts et al., 2002; Knust and Bossinger 2002; Guillot and Lecuit 2013). Apico-basal polarity is associated with three modules: Crumbs, Par and Scribble, that were first identified in the model organisms *D. melanogaster* and *C. elegans* (Bilder and Perrimon 2000; Nelson 2003; Margolis and Borg 2005). The spatial localisation of these modules, along with their mutually antagonistic relationship, allows for the establishment of tissue architecture (Figure 1A). Further, it allows for proper epithelial movement, junctional cell interaction, substrate secretion, cell proliferation and apoptosis, and regulation of cell signalling (Elsum et al., 2012; Margolis and Borg 2005; U. Tepass et al., 2001; Nelson 2003; Stephens et al., 2018). Disruptions to these polarity modules have been linked to a loss of tissue architecture, loss of junctional integrity, mislocalisation of other polarity proteins and aberrant cell signalling that can lead to increased cell proliferation and cancer (Bilder 2004; Elsum et al., 2012; Gödde et al., 2014; Stephens et al., 2018).

The par polarity complex first discovered in *C. Elegans* (Kemphues et al., 1988) is considered to be a metazoan innovation (Fahey and Degnan 2010; Belahbib et al., 2018) and is responsible for the first asymmetric division in a zygote by establishing cortical polarity (Figure Figure1A and Figure 2) (Kemphues et al., 1988). The Par complex consists of scaffold proteins well known for their diverse roles in regulating cell polarity. In addition to asymmetric cell division, these proteins play an integral role in regulating many other polarity states including, apico-basal polarity, planar cell polarity and front-rear polarity (Petronczki and Knoblich 2001; Hurd et al., 2003; Goldstein and Macara 2007; Assemet et al., 2008; Etienne-Manneville 2008). The Par complex consists of three interacting proteins, Par3, Par6 and atypical protein kinase C (aPKC) that localise to junctional regions of epithelial cell. This allows for adherens junction and tight junction formation in vertebrates [Figure 1] (Matter and Balda 2003; St Johnston and Ahringer 2010; Wen and Zhang 2018).

Par complex genes have been identified in all the earliest basal metazoans and linked to a variety of polarity signalling contexts that co-evolved through evolution (Table 1) (Macara 2004; Magie and Martindale 2008; Belahbib et al., 2018). Indeed, this is illustrated by the strict evolutionary conservation of the interacting domains of Par proteins and the mechanisms regulating these interactions. For example, the lysine residue in PB1 (Phox and Bem1 binding module) domain of Par6 is responsible for the interaction between Par6 and aPKC, and the aPKC phosphorylation site (S/T) in Par3. This PBM domain remains highly conserved in all basal metazoans (Belahbib et al., 2018). Only a few functional experiments have been undertaken on the Par complex in basal metazoans. In the cnidarian *N. vectensis* functional investigation of the Par complex, a conserved role in maintaining cell-cell adhesion has been demonstrated. *N. vectensis* Par proteins (NvPar-3, NvPar-6, NvaPKC) were shown

to localise within the cnidarian epithelium similarly to that seen in sheet epithelia of bilateria (Salinas-Saavedra et al., 2015; Salinas-Saavedra and Martindale, 2018). *N. vectensis* polyps expressing a dominant negative version of NvPar-3 showed leakage of fluorescent tracer dye demonstrating an ancestral role of the aPKC/Par complex in the maintenance of cell-cell adhesion and the paracellular boundary (SJs) of epithelial cells during animal development (Salinas-Saavedra and Martindale, 2018). Supporting this, knockout of *Nvpar-6* and *Nvpar-3* genes using CRISPR/Cas9 targeting resulted in loss of integrity of ectodermal epithelium including disruption of the cytoskeleton and adherens junctions (as visualised by  $\beta$ -catenin localisation) (Salinas-Saavedra and Martindale, 2018). Clonal studies through single cell blastomere injections of CRISPR/Cas9 targeting *Nvpar-3* showed that the resulting clones of NvPar-3 knockout epithelial cells also lost their structural integrity inducing in this case cell extrusion, thus demonstrating a cell-autonomous role for the Par Complex in regulation of epithelial cell polarity (Salinas-Saavedra and Martindale, 2018). Studies such as these reinforce the notion that these newly established polarity systems in the early metazoans played a critical role in the establishment of multicellularity.

**The Crumbs polarity complex** is well documented as a critical complex in the development and stabilisation of apical adherent and tight junctions (Dow and Humbert 2007; Bazellieres et al., 2009; Bivic 2013; Ebnet 2015). The Crumbs complex consists of two scaffold proteins, Pals1 (Protein associated Lin seven 1) and PatJ (Pals1-associated tight junction), and a transmembrane protein Crumbs (Tepass, 2012). The Crumbs complex proteins are all metazoan developments and first appear in basal metazoans (Belahbib et al., 2018). Crumbs was first discovered in *D. melanogaster* (U. Tepass et al., 1990) and is the central molecule that acts as a scaffold for PatJ and Pals1 (Figure 1A). Genomic analysis revealed that the placozoan *T. adherens*, the cnidarian *N. vectensis*, and the poriferan *A. queenslandica* have conserved domains of Crumbs. Whereas the ctenophore *M. leidyi* most strikingly had no *crumbs* or *crumbs*-like gene that has been identified (Table 1) (Belahbib et al., 2018). Furthermore, analysis of the genomic DNA sequence of *A. queenslandica* revealed multiple *Crumbs*-like coding regions that are either variants of the gene, pseudogenes or truncated forms (Fahey and Degnan 2010). However, there are some questions as to the functional capacity of Crumbs in *A. queenslandica* (Fahey and Degnan 2010; Srivastava et al., 2010; Belahbib et al., 2018). Structurally, Crumbs has extracellular epidermal growth factor (EGF) domains interspersed with laminin repeats and a cytoplasmic tail consisting of two motifs; the FERM-binding motif (FBM) and a Class II PDZ protein binding domain (PBM) essential for the function of Crumbs proteins (Knust, Tepass, and Wodarz 1993; Bivic 2013). Of note, the FBM domain responsible for aPKC binding in higher order species is depleted of two

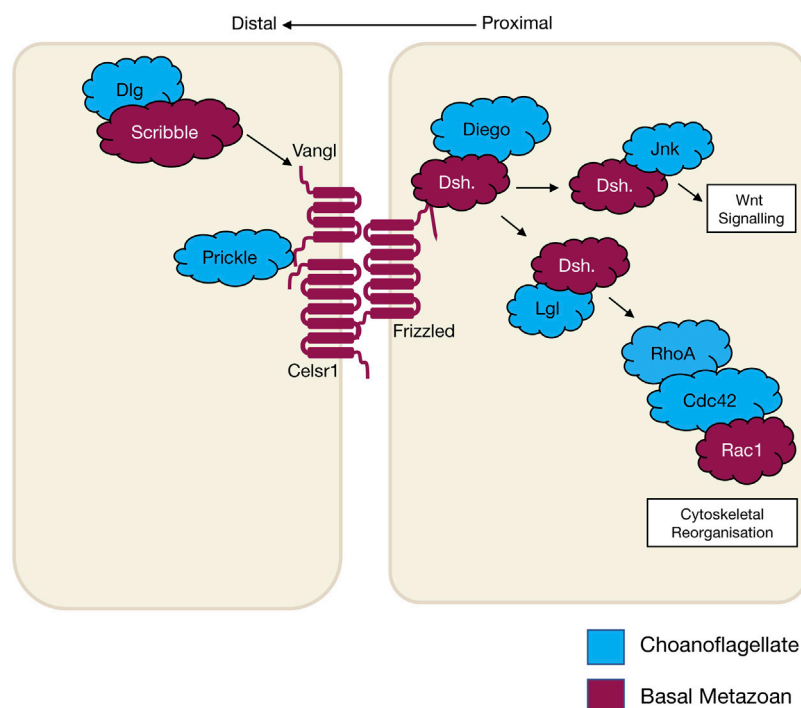


FIGURE 3

The schematic diagram shows core planar cell polarity pathways and their relationship to Wnt signalling and cytoskeletal reorganisation that occurs in wound healing. The different colours represent the evolutionary appearance of these genes.










phosphorylation sites in *T. adherens* and in studied sponges (Belahbib et al., 2018).

Pals1 is a member of the Membrane-Associated Guanylate Kinase (MAGUK) family. The MAGUK family includes cell polarity genes that cumulatively are responsible for the organisation of protein complexes within a cell or at a cell or synaptic junction. Their localisation governs the polarisation of cells and their cytoskeleton filament connections (Mendoza et al., 2010). MAGUK genes extend past the metazoan lineage and have been identified in the choanoflagellate *M. brevicollis* and protist *C. owczarzewski* (Mendoza et al., 2010). The other members of the Crumbs complex Pals1 and PatJ have not been identified in ctenophores and their presence in sponges is unclear. In the sponge *A. queenslandica* a relative of Pals1 gene *MPP5/7*, that is also a member of the MAGUK family, is present and may play a substitutional role in the Crumbs complex (Fahey and Degnan 2010; Bivic 2013).

**The scribble polarity module** consists of a triad of scaffold proteins, Scribble, Lgl (Lethal giant larvae) and Dlg (Discs large), that localise to the basolateral membrane of epithelial cells (Figure 1A). The module has an important role in the control of tissue architecture and morphogenesis, and in tumour suppression (Bilder et al., 2000; Humbert, Russell, and Richardson 2003). Proteins of the Scribble module are major regulators of epithelial apico-basal polarity with broader

roles in other forms of cell polarity (Stephens et al., 2018). Dlg and Lgl have been identified in lower order unicellular species (choanoflagellates and fungi), whereas Scribble is considered a metazoan innovation (Srivastava 2015; Belahbib et al., 2018). Scribble is a member of the LAP (Leucine rich repeat and Post-synaptic density-95/Discs-Large/Zo-1) family. Structurally, Scribble contains 16 Leucine rich repeats (LRR, a highly conserved protein motif that forms an arc-like structure), a LAP-specific domain (a domain related to LRR) and four PSD-95, ZO-1 and Discs large (PDZ) domains that coordinate the majority of Scribble's binding interactions (Figure 1B) (Bilder and Perrimon 2000; Humbert, Russell, and Richardson 2003; Stephens et al., 2018; Bonello and Peifer 2019). A Scribble or Scribble-like gene has not been identified in unicellular organisms and does not appear to be present in the ctenophore *M. leidyi* (Belahbib et al., 2018). In ctenophores, it is thought to be due a secondary loss of the gene, and while no functional studies have been completed, it is postulated that the absence of a Scribble gene may result in variations of polarity complex localisation (Belahbib et al., 2018). As noted above, ctenophores also appear to lack a Dlg gene (Schiller and Bergstrahl 2021). Analysis of different porifera classes identified key polarity proteins, including Scribble, Lgl and Dlg, responsible for cell adhesion and epithelial development (Fahey and Degnan 2010; Riesgo et al., 2014).

TABLE 2 Planar Cell Polarity proteins.

	Species  Gene	Basal Metazoa					Bilateria				References
		Choanoflagellate	Placozoa	Porifera	Ctenophora	Cnidaria	C. elegans	D. melanogaster	M. musculus	H. sapiens	
											
Planar cell polarity	Celsr1 (Flamingo)	✗	•	•	✗	•	•	•	•	•	(1–3)
	Frizzled	✗	•	•	•	•	•	•	•	•	(1,4)
	Dishevelled	✗	•	•	•	•	•	•	•	•	(1,5,6)
	Vangl (Strabismus)	✗	•	•	✗	•	•	•	•	•	(1,4)
	Prickle	•	•	•	•	•	•	•	•	•	(1,7,8)
	Inversin (Diego)	•	✗	•	✗	•	•	•	•	•	(1,9)
	RhoA	•	•	•	•	•	•	•	•	•	(10–12)
	Jnk	•	•	•	*	•	•	•	•	•	(12–18)
	Mapk	•	•	•	*	•	•	•	•	•	(19–23)
	Wnt	✗	•	•	•	•	•	•	•	•	(17,24–27)
	β-Catenin	•	•	•	•	•	•	•	•	•	(20,28)
	α-Catenin	✗	•	•	•	•	•	•	•	•	(28)
	Cdc42	•	•	•	•	•	•	•	•	•	(10,20,29)
	Rac1	*	•	•	✗	•	•	•	•	•	(10,30–32)
	Fat	•	•	•	•	•	•	•	•	•	(33–35)
Dachsous	✗	•	•	•	•	•	•	•	•	(33–35)	
Numb	✗	~	✗	~	~	•	•	•	•	(36)	
Gai	•	•	•	•	•	•	•	•	•	(37–41)	
The table lists the occurrence of polarity genes though evolution based on Choanoflagellate, Basal metazoan and Bilateria classified as • gene present; ~ gene partially present; or ✗ gene not present; * no data available. 1. Schenkelaars et al, 2016; 2. Steimel et al, 2010; 3. Usui et al, 1999; 4. Betschinger & Knoblich 2004; 5. Lee et al, 1999; 6. Walston et al, 2004; 7. Sawa, 2012; 8. Humphries & Mlodzik 2018; 9. Simons & Mlodzik 2008; 10. Beljan et al, 2020; 11. Pillé et al, 2005; 12. King et al, 2008; 13. C. elegans Sequencing Consortium, 1998; 14. Ip & Davis 1998; 15. Kamm et al, 2018; 16. Noselli & Agnès 1999; 17. Philipp et al, 2009; 18. Srivastava et al, 2010 19. Kamm et al, 2019; 20. Richter et al, 2018; 21. Chera et al, 2011; 22. Hammarlund et al, 2009; 23. Widmann et al, 1999; 24. Adamska et al, 2010; 25. Pang et al, 2010; 26. Srivastava et al, 2008; 27. Loh et al, 2016; 28. Alić & Manuel 2010; 29. Melendez et al, 2011; 30. Hakeda-Suzuki et al, 2002 31. Chen et al, 1993; 32. Heasman et al, 2008; 33. Sebé-Pedrós et al, 2012; 34. Zhu et al, 2013; 35. Rock et al, 2005; 36. Gazave et al, 2009; 37. Gotta & Ahringer, 2001; 38. Ajduk & Zernicka-Goetz, 2016; 39. Bergstrahl et al, 2017; 40. Lokits et al, 2018; 41. de Mendoza et al, 2014;.											

Dlg from a structural perspective, contains three PDZ domains, SH3 domain and a GUK domain. As a scaffold protein, Dlg is part of the Post-Synaptic Density (PSD) family. This family is responsible for the maintenance, anchorage and structural localisation of other PSD structures and proteins in relation to neurotransmitter receptors and signalling channels (Sakarya et al., 2007; Alić and Manuel 2010). In metazoan species that do not contain nerve structures, such as Placozoans and Porifera, it was found that these PSD proteins were present and contained near identical interacting domains when compared to their mammalian counterparts. Furthermore, it is suggested that Dlg and other PSD genes like Homer (scaffold protein involved in Ca<sup>2+</sup> signalling and transport) may play significant roles in these metazoan species as Ca<sup>2+</sup> receptors and signalling communicators (Alić and Manuel 2010). The significance of PSD proteins, specifically Dlg, is highlighted by the full conservation of their residues that interact with PDZ domains compared with their human orthologues (Sakarya et al., 2007). Of

note, imaging of Placozoan epithelium using staining with a pan-human Dlg antibody show an identical basolateral cortical staining to that seen for Dlg in Bilateria epithelium suggesting that TaDlg may have a conserved function in the regulation of Trichoplax epithelium (Smith et al., 2014). Lgl is the most ancient gene with homologues found in yeast (Sro7 and Sro77) where it regulates polarised exocytosis (X. Zhang et al., 2005; Grosshans et al., 2006; Müsch et al., 2002). This has been similarly compared to mammalian Lgl in basolateral exocytosis (Müsch et al., 2002). High levels of conservation of polarity genes from the Scribble, Par and Crumbs complexes have been identified in cnidarians when compared to bilateria (Rathbun, Everett, and Bergstrahl 2022).

Planar cell polarity signalling

Planar cell polarity (PCP), also referred to as tissue polarity or the non-canonical Wnt signalling pathway, is the global organisation of cells along a x/y axis in a plane (Figure 3).

PCP signalling is essential for normal tissue development, cell homeostasis, axis determination and tissue morphogenesis (Simons and Mlodzik 2008; Butler and Wallingford 2017). Junctional PCP genes were first identified and have been extensively studied in the fly *D. melanogaster* (Gubb and García-Bellido 1982; Axelrod 2001; Adler 2002; Hale and Strutt 2015). The organisation of six transmembrane proteins on opposing sides of a cell allow for communication and coordinated interactions, including polarising events. The polarising events allow for the asymmetric placement of cilia or hairs and the orientation of the mitotic spindle (Goodrich and David 2011; Schenkelaars et al., 2016; Butler and Wallingford 2017). Downstream from the core PCP signalling, the PCP protein Dishevelled interacts with Lgl, Cdc42, RhoA and Rac1. These interactions aid in cytoskeleton re-organisation, maintaining adherens junctions, and when interacting with Jnk, feeds into Wnt signalling pathway (Figure 3) (Milgrom-Hoffman and Humbert 2018; Wiese, Nüsse, and van Amerongen 2018). On examination of PCP signalling, Frizzled, Dishevelled and Prickle have all been identified in the four basal metazoans, whereas Celsr1 (Flamingo) and Vangl (Strabismus) are not found in ctenophores, nor Inversin (Diego) in porifera (Table 2) (Adamska et al., 2010; Srivastava et al., 2008; Schenkelaars et al., 2016; Belahbib et al., 2018; J. F. Ryan et al., 2013; Momose, Kraus, and Houliston 2012). Phylogenetic analysis of *prickle* and *prickle*-like genes reveals an ancestor of the gene in choanoflagellates. In the basal metazoans placozoa and cnidaria, it diverges from one to two genes—*prickle* and *testin* (Schenkelaars et al., 2016).

Examination of the cnidarian *C. hemisphaerica* larva stages reveal established PCP characteristics of oral-arboreal polarity and the formation of directionally organised cilium in each epithelial cell similar to that described in bilaterians (Momose, Kraus, and Houliston 2012; Milgrom-Hoffman and Humbert 2018). Further, *vangl* mRNA expression levels were evident throughout embryogenesis, elongation and ciliogenesis with enrichment occurring to the axis of the developing hydrozoan (Momose, Kraus, and Houliston 2012). When *vangl* was knocked down in the cnidarian *N. vectensis*, the embryos failed to undergo gastrulation or primary invagination, however this did not impact  $\beta$ -catenin nuclear localisation, which in bilaterians is tightly coupled. Thus cell fate specification of the endoderm may have developed separately to other PCP/Wnt signalling pathways (Kumburegama et al., 2011).

Non-canonical Wnt signalling investigations in the cnidarian *Hydra* revealed specific Wnt pathway genes (*wnt5*, *wnt8*, *frizzled* and *dishevelled*) are all required for correct evagination of the bud and tentacle of the *Hydra*. The upregulation of these genes can be correlated to the activation of Wnt/ $\beta$ -catenin signalling during tissue morphogenesis and development of the *Hydra* pulp (Philipp et al., 2009). Planar cell polarity genes *fat* and *fat*-like genes are associated with cell directional migration and morphogenesis in asymmetric cell division in bilaterians (Matis and Axelrod 2013).










The *Hydra fat* and *dachsous* genes localise to the body of the animals where continuous growth and migration of cells occur supporting the theory of a similar role to that of bilaterians (Brooun et al., 2019). Phylogenetic examination of *frizzled* in a variety of different poriferan, placozoan, cnidarian and ctenophore species show multiple orthologues of *frizzled*. In some porifera and cnidarians, up to four *frizzled* orthologues have been identified, with evidence that the vertebrate paralogue of *frizzled* is an amalgamation of ancestral *frizzled* genes (Schenkelaars et al., 2015). The genes *flamingo*, *inversin* and *vangl* are PCP genes considered to be secondarily lost from the ctenophore *M. leidyi* (Table 2) (J. F. Ryan et al., 2013; Schenkelaars et al., 2016), whereas, *dishevelled*, *frizzled* and *prickle* are present in all metazoans (Srivastava et al., 2008; Schenkelaars et al., 2016). Functional studies relating to specific pathway significance between basal metazoan PCP signalling and its similarities or differences to higher order species are ongoing.

## Asymmetric cell division signalling

Asymmetric cell division (ACD) refers to the specific localisation of cell fate determinants during cell division to establish two different cell characteristics (mother/daughter) (Knoblich 2001). In early cell division in the model organism *D. melanogaster*, asymmetric molecules Par3, Par6, aPKC, Inscuteable, Pins, Gai and Mud localise to the apical cortex of the mitotic spindle, while cell fate factors Numb, Brat, Prospero, Pon and Miranda localise to the basal cortex (Figure 2) (Boyd et al., 1996; Tabuse et al., 1998; Hung and Kempthues 1999; Joberty et al., 2000; Kelsom and Lu 2012). Additionally, in *Drosophila* neuroblasts, the Scribble module proteins Scribble, Dlg and Lgl are important in ACD where they assist in mitotic spindle orientation (Elsom et al., 2012). The asymmetric localisation of these key polarity genes induces separation of the cells in an asymmetric fashion and therefore diversification of tissue types. A failure for polarity proteins to localise to the poles of the mitotic spindle is associated with defects in basal protein targeting, symmetric division, reduced spindle size or inverted neuroblast cell division (Bilder and Perrimon 2000; Albertson and Doe 2003; Neumüller and Knoblich 2009; Royer and Lu 2011). The diversification of ACD has been identified in prokaryote and eukaryotic organisms, basal metazoans and bilaterians (Table 3) (K. R. Ryan and Shapiro 2003; Knoblich 2001). It should be noted that cells at an early embryonic stage have the capacity to divide either asymmetrically, as described above, or symmetrically where two identical daughter cells are formed (Knoblich 2001; Schenkelaars et al., 2017). The selective differential distribution of protein and RNA into daughter cells is the foundation for the development of different tissue or cell types within an organism, referred to as cell fate (Jan and January 1998; Knoblich 2010).



TABLE 3 Asymmetric Cell Division proteins.

	Species	Basal Metazoa					Bilateria			References
		Choanoflagellate	Placozoa	Porifera	Ctenophora	Cnidaria	C. elegans	D. melanogaster	M. musculus	
										
Asymmetric Cell division	Pins (GPSM2/LGN)	~	*	~	x	*	*	*	*	(1–5)
	Prospero (Prox1)	x	*	x	x	x	*	*	*	(6–11)
	Numb	x	~	x	~	~	*	*	*	(12)
	Gai	*	*	*	*	*	*	*	*	(13–17)
The table lists the occurrence of polarity genes though evolution based on Choanoflagellate, Basal metazoan and Bilateria classified as * gene present; ~ gene partially present; or x gene not present; * no data available. 1.Betschinger & Knoblich, 2004; 2.Kraut et al, 1996; 3.Postiglione et al, 2011; 4. Schiller & Bergstrahl 2021; 5. Žigman et al, 2005; 6.Bürglin, 1994; 7. Doe et al, 1991; 8. Elsir et al, 2012; 9. Larroux et al, 2008; 10. Oliver et al, 1993; 11.Ryan et al, 2006; 12. Gazave et al, 2009; 13. Gotta & Ahringer, 2001; 14. Ajduk & Zernicka-Goetz 2016 15. Bergstrahl et al, 2017; 16.Lokits et al, 2018; 17. de Mendoza et al, 2014;										

Asymmetric cell division allows for the development of both germ cells and somatic cells that form different cell lineages and allow for plasticity of the cells in processes, such as reaggregation. In the cnidarian *H. vulgaris*, multipotent interstitial cells have the capacity to differentiate into gametes and almost all somatic cell lines (Bosch 2004; H. R. Bode 1996; Bosch and David 1987). The pliability of cnidarian cells and their capacity to adapt to their environment is remarkable, with the examples of an adult medusa metamorphosis into a polyp (Piraino et al., 1996). Another example is the cnidarian *Podocoryne carnea* that through the process of asymmetric cell division can differentiate medusae formed cells into an unrelated phenotype e.g. Muscle cells to nerve cells (Schmid and Alder 1984; Seipel, Yanze, and Schmid 2003). One of the proteins associated with ACD is Pins (also known as LGN or GPSM2). Pins has been shown to interact closely with Dlg in spindle orientation and this interaction is believed to have evolved in cnidarians (Schiller and Bergstrahl 2021). The placozoan *T. adhaerens* and the sponge *A. queenslandica* do not contain the key linker regions required for GPSM2 to interact with Dlg, however they do contain other key motifs of GPSM2. It is postulated that these conserved regions may still be able to play a part in ACD, cell orientation and division (Schiller and Bergstrahl 2021). In Porifera, during initial embryonic development, asymmetric division of macromeres to micromeres occur while later in embryonic development there is more evidence for higher levels of symmetric cell divisions. In the freshwater sponge *E. fluviatilis* the paralogue gene *Musashi* (a gene required for stem cell maintenance in *Drosophila*) has been identified as being specifically expressed in stem cells and regulates sustainable regeneration. This is the earliest

occurrence of this gene in basal metazoans and of its role in ACD (Okamoto et al., 2012).

Cell junction complexes in the basal metazoa

Adherens junctions

Adherens junctions, also known as Zonula Adherens, form belt-like junctions that act as a conduit between the apical and basal domains of epithelial cells (Figure 4). Adherens junctions are acknowledged as the most common junction in animal epithelia (Oda and Takeichi 2011; Hiroki 2012). Adherens junctions have been identified in placozoans, cnidarians and ctenophores with none so far identified in Porifera (table. 4) (T. J. C. Harris and Ulrich 2010; Salinas-Saavedra and Martindale, 2019). The presence of adherens junctions in placozoans appears crucial for their tissue integrity as no other junctions have been identified placozoans to date (Smith and Reese 2016).

Cadherin-catenin complexes

A major component of adherens junctions are cadherin-catenin complexes. Classical cadherins date back to the Urmetazoan (the hypothetical last common ancestor of all animals or metazoans) and are type I transmembrane proteins that consist of calcium-dependent transmembrane cell adhesion molecules (CAMs) that form adherens junctions associated with cell-cell adhesion, embryonic development,

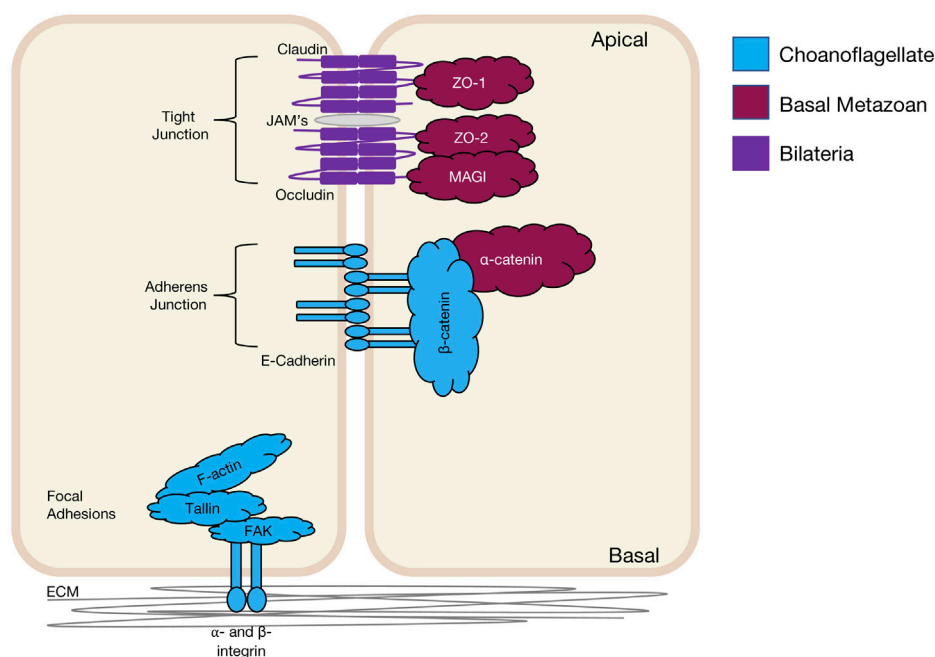


FIGURE 4









Bilateria representation of epithelial cell-cell and cell-ECM junctions and their emergence in evolution. It should be noted that for Claudin, whilst represented as a basal metazoan innovation, it has only been identified in Cnidaria. There are Occludin-like genes present in basal metazoans but it is not known if they have the same functional properties as in Bilateria.

and cell morphogenesis (Hulpiau and van Roy 2011; T. J. C. Harris and Ulrich 2010; King, Hittinger, and Carroll 2003; Gul et al., 2017). The cadherins are a superfamily of proteins containing at least two cadherin repeats and can be classified into three families: Major cadherins, protocadherins and cadherin-related genes (Gul et al., 2017). Placozoans contain cadherin and cadherin-related genes, whereas cnidaria contain multiple genes of all three cadherin families (Gul et al., 2017; Hulpiau, Gul, and van Roy 2013; S. A. Nichols et al., 2012). When examining the current literature of cadherins in the basal metazoans it was found that placozoans, poriferans and cnidarians all have identifiable E-cadherin with necessary binding motifs (Table 4). *M. leidy* (Ctenophora) has E-cadherin motifs but show high levels of divergence that raises doubt to its capacity to bind to known interacting genes such as  $\beta$ -catenin and p120 (Belahbib et al., 2018; Hulpiau and van Roy 2011; S. A. Nichols et al., 2012; Ringrose et al., 2013; Srivastava et al., 2008).

Catenins that form part of adherens junctions can be placed into three sub-families: p120-,  $\alpha$ - and  $\beta$ -, with examples of each subfamily identified in the basal metazoans, with  $\beta$ -catenin being identified in many unicellular organisms (Alié and Manuel 2010; Belahbib et al., 2018). Catenins, including  $\alpha$ - and  $\beta$ -catenin bind filamentous actin (F-actin) within the cell

and cadherins within the adherens junctions to form a semi-permeable barrier between anterior and posterior of the cell (Baum and Georgiou 2011; Gooding, Yap, and Ikura 2004; Tian et al., 2011; Nelson 2008; T. J. C. Harris and Ulrich 2010; Magie and Martindale 2008). A major contributor to adherens junction homeostasis is the presence of  $\beta$ -catenin in higher order metazoans and some basal metazoans. In the ctenophore *M. leidy*,  $\beta$ -catenin does not localise to the cell junctions most likely due to the lack of a cytoplasmic domain essential for  $\beta$ -catenin binding. It was further concluded that this may indicate that the ancestral role of  $\beta$ -catenin was in cell-fate specification associated with Lef/Tcf co-factors that enter the nucleus to regulate canonical Wnt signalling rather than cell adhesion (Salinas-Saavedra and Martindale, 2019). The porifera *A. queenslandica* contain junctional proteins cadherin1 and  $\alpha$ -catenin1-like gene, however within the middle of the gene a stretch sequence has been identified that is not otherwise seen in bilaterian counterparts (Fahey and Degnan 2010). The evidence is still lacking regarding other regulators of adherens junctions, except for the Par complex as discussed previously. Indeed, adherens junctions in the cnidarian *N. vectensis* ectodermal epithelial cells are responsible for the localisation of the Par complex and if disrupted a loss of integrity and loss of solute permeability has been observed (Salinas-Saavedra and Martindale, 2018).

TABLE 4 Junctional proteins.

	Species	Gene	Basal Metazoa					Bilateria			References
			Choanoflagellate	Placozoa	Porifera	Ctenophora	Cnidaria	C. elegans	D. melanogaster	M. musculus	
											
Junctional Proteins	ZO-1 (Polychaetoid)		x	.	.	.	.	.	.	.	(1,2)
	ZO-2		x	.	.	.	.	.	.	.	(1,3)
	β-Catenin		~	.	.	.	.	.	.	.	(4–7)
	α-catenin		x	.	.	.	.	.	.	.	(4,7,8)
	E-Cadherin		.	.	.	~	.	.	.	.	(4,5,9)
	Occludin		x	x	x	*	x	x	~	.	(10–14)
	Claudin		~	~	~	~	~	~	~	.	(11,14–17)
	Magi 1		~	.	.	*	.	.	.	.	(1,18–20)
	F-actin		.	.	.	.	.	.	.	.	(8,21–26)
	Integrin (α- and β-)		.	.	.	.	.	.	.	.	(21,22,26,27)
	Talin		.	.	.	*	.	.	.	.	(21,22,26–28)
	FAK (focal adhesion kinase)		.	.	.	*	.	.	.	.	(22,26,29)
The table lists the occurrence of polarity genes though evolution based on Choanoflagellate, Basal metazoan and Bilateria classified as . gene present; ~ gene partially present; or x gene not present; * no data available.											
1.de Mendoza et al, 2010; 2. te Velthuis et al, 2007; 3.González-Mariscal et al, 2017; 4. Belahbib et al, 2018; 5. Gul et al, 2017; 6.Richter et al, 2018; 7. Alié & Manuel, 2010; 8. Kwiatkowski et al, 2010; 9. Abedin & King, 2008; 10. Fahey & Degnan, 2010; 11. Asano et al, 2003; 12. Carvalho et al, 2001; 13. Srivastava et al, 2010; 14. Magie & Martindale, 2008; 15. Behr et al, 2003; 16. Buzgariu et al, 2015; 17. Ganot et al, 2015; 18. Dobrosotskaya et al, 1997; 19. Lynch et al, 2012; 20. Zaessinger et al, 2015; 21. Mitchell & Nichols, 2019; 22. Sebé-Pedrós et al, 2010; 23. Agosti & Stidwill, 1992; 24. Pang & Martindale, 2008; 25. Thiemann & Ruthmann, 1989; 26. Lo, 2006; 27. Moulder et al, 1996; 28. Reber-Müller et al, 2001; 29.Hsu & Wu, 2010;											

Tight and septate junctions

Tight junctions are attributed to vertebrate species and act as a junctional barrier regulating the diffusion of macromolecules between and through cells (Matter and Balda 2003). Located at the apical region of cells, tight junctions consist of transmembrane signalling proteins, such as Claudin, Occludin, junctional adhesion molecules (JAMs), and adaptor proteins, such as ZO (Zonula Occludin) -1, -2, -3, polarity proteins Par -3, -6, Pals1, PatJ and Magi -1,-2 and -3 (Figure 4) (Fanning et al., 1998; Tsukita, Furuse, and Itoh 2001; Matter and Balda 2003; Niessen 2007; Steed, Balda, and Matter 2010; Hartmann et al., 2020). ZO-1 as a member of the MAGUK family is responsible for junctional organisation and regulation of proteins, such as ZO-2, Occludin and F-actin. These interactions allow linking and binding to the cortical actin cytoskeleton of the cell (Fanning et al., 1998; Itoh et al., 1999). The ZO proteins have been identified in all four basal metazoan lineages (Table 4) (Mendoza et al., 2010). Interestingly, electron microscopy studies have failed to reveal tight junctions in the placozoan *T. adherens*. This is a peculiarity as the genome contains *ZO -1* and *Claudins* that are associated with tight junctions (Mendoza et al., 2010; González-Mariscal et al., 2017; Belahbib et al., 2018).

Although tight junctions are ‘stricto-sensu’ vertebrate specific, genes associated with tight junctions have been identified in invertebrates, basal metazoans and choanoflagellates and hence referred to as ‘claudin-like’ (Ganot et al., 2015). For example, In the cnidarian *Hydra*, 14 claudin-like genes have been identified, with 10 of them specifically in the ectoderm and/or endoderm (Buzgariu et al., 2015) and claudin-like genes in *Drosophila* have been associated with septate junctions (Behr, Riedel, and Schuh 2003). Septate junctions are cell-cell junctions that appear ladder-like under electron microscope and aid in solute diffusion and structural support (Matter and Balda 2003). Septate junctions have been identified in *Hydra*, containing a ladder-like structure that in reaggregation studies forms within hours (Filshie and Flower 1977; Seybold, Salvenmoser, and Hobmayer 2016). A similar structure has also been noted in *Trichoplax* in the proximal cells of the animal that appear ‘ladder-like’ but are periodic in nature. No such junctions have been identified in porifera (Ruthmann et al., 1986; Ganot et al., 2015). Cnidarians display both the required genes and structure to form septate junctions similar to those found in Bilateria (Ganot et al., 2015; Rathbun, Everett, and Bergstrahl 2022). This is not seen in ctenophores, where only claudin-like genes have been identified (Ganot et al., 2015).

## Focal adhesions and integrin complexes

Focal adhesions are protein-rich structures where the integrin transmembrane proteins provide adhesion between cells and the extracellular matrix (ECM) (Figure 4). Like cadherins, integrins also represent signalling hubs (Michael and Parsons 2020). Focal adhesion genes surpass the age of the earliest metazoan lineages, believed to stretch back into the Cambrian time (S. A. Nichols et al., 2012). Whereas, components of the integrin machinery predate the metazoan lineage (Sebé-Pedrós et al., 2010). Integrin receptors that are composed of membrane-anchored heterodimer receptors have been reported in species of marine sponges (Müller 2003). More recently, the focal adhesion proteins, integrin, talin, and focal adhesion kinase (FAK), have been shown to form a complex that localises to the cell-cell junctions and extracellular matrix adhesions in the freshwater sponge *E. mulleri* (Mitchell and Nichols 2019). Of note, focal adhesion associated molecules integrin, vinculin, paxillin, talin and FAK are all found and expressed in *Trichoplax* (Srivastava et al., 2008), although a basement membrane structure does not appear present in these animals suggesting either a secondary loss in Placozoa or an independent gain in the other basal metazoans (Fidler et al., 2017).

## Cell polarity in the basal metazoa and the origin of multicellularity

Here we have reviewed key signalling pathways regulating cell polarity and adhesion in the basal metazoan species and how this relates to the evolution of complex tissues such as epithelial structures. The examination of such pathways not only gives us knowledge into the ancient function of these genes and when they arose, but allows us to examine their role in the advent of multicellularity. A key challenge for a multicellular organism is to organise tissue architecture to drive cellular and organismic function. For the evolution of a multicellular animal to occur, a number of events are required including the development of cell differentiation and adhesive cell interactions within the epithelium, the orientation of division axis, and the ability to reposition daughter cells over long distances so as to establish and maintain a body plan. In addition, to obtain the division of labour that is linked with multicellularity, the process of differentiation that generates various cell types must be properly controlled. Asymmetry and cell polarity provides a universal tool for building multicellular tissue architecture. Although asymmetry can occur by stochastic means, extrinsic cues whether chemical or mechanical are more reliable and provide robustness to generate the asymmetry required for tissue architecture. Cell polarity and cell adhesion mechanisms relay these external cues internally to re-organise cell and tissue

as well as provide a link with transcriptional programs required for tissue morphogenesis.

Apico-basal cell polarity mechanisms first appear in basal metazoans, and based on the simultaneous presentation of multicellularity and these cell polarity constituents, it is reasonable to propose that cell polarity mechanisms played a key role in this process. As discussed, other cell polarity genes are far more ancient and extend back into unicellular organisms. For example,  $\beta$ -catenin's ancestral function appears related to TCF/LEF transcriptional regulation of Wnt signalling rather than junctional polarity and thus provides another example of co-option in cell polarity systems linking nuclear transcriptional programs to newly minted cell adhesion mechanisms (Salinas-Saavedra and Martindale, 2019). Interestingly, of the basal metazoans, ctenophores appear to be outliers at this point in terms of cell polarity mechanisms. The significant cell polarity associated gene loss in ctenophores raises interesting questions as to the alternative mechanisms by which ctenophores control various aspects of cell polarity, tissue organisation and its repair. In addition, the potential role of tight junction proteins in basal metazoans is an interesting enigma and could provide new insights into the evolution of these permeability barriers. As discussed, many basal metazoans produce tight-junction proteins (e.g. *Zo-1*) despite the absence of tight or septate junctions. This may indicate a more ancient divergent function for these genes that has been co-opted for the regulation of tight junctions. Interestingly, Polychaetoid, the *Drosophila* ZO-1 homologue, localises to adherens junctions and provides a link to actin regulation (Takahashi et al., 1998; Wei and Ellis 2001; Choi et al., 2011), pointing to a possible similar role for ZO-1 in basal organisms.

Research in the basal metazoans provides the opportunity to understand the fundamental building blocks of multicellularity and by extension its relationship to key events such as cancer. Indeed, examination of the evolutionary origin of cancer-related protein domains suggests two peaks, one at the time of the origin of the first cell and the other around the time of the evolution of the first multicellular organisms (Domazet-Lošo and Tautz 2010). Importantly, this second peak dubbed “gate-keeper” genes consist of oncogenes and tumour suppressors whose mutations promote tumour progression through altering cell proliferation, inhibiting differentiation or inhibiting cell death. This second peak also corresponds to the advent of the cell polarity signalling pathways in early basal metazoans described in this review. As many of these cell polarity regulators have been linked to tumour suppression in Bilateria (Stephens et al., 2018), examining the mechanisms of cell polarity and tissue architecture regulation in basal metazoans is likely to lead to fundamental insights into the origins of cancer. Almost all bilaterian animals have reported examples of cancer formation (Aktipis et al., 2015). Indeed, sponges and *Hydra* have reported cases of cancer that mimic that of higher order species, such as intrusive proliferation, loss of tissue architecture and a loss of specialised tissue (Hanahan and Weinberg 2000; Aktipis et al., 2015). The advent of multicellularity required new molecular mechanisms that allowed cellular cooperation and suppressed any cellular



conflicts that enhance individual cell fitness to the detriment of the organism (Aktipis et al., 2015; Madan, Gogna, and Moreno 2018; Bowling, Lawlor, and Rodríguez 2019). From this point of view, cancer would represent a breakdown of this multicellular cooperation with over-competitive cells effectively “cheating”, leading to overall loss of fitness of the organism (Rainey 2007; Aktipis et al., 2015). Importantly, cell polarity and tissue architecture regulators play key roles in regulation of cell competition mechanism in Bilateria (Madan, Gogna, and Moreno 2018; Bowling, Lawlor, and Rodríguez 2019; Fahey-Lozano et al., 2019; Baker 2020). We therefore contend that cell competition mechanisms first appeared in basal metazoans and are mechanistically linked to the acquisition of the original cell polarity mechanisms required for the advent of multicellularity. The ability to generate tissue chimaeras in basal metazoans such as *Trichoplax* and *Hydra* (Klimovich, Wittlieb, and Bosch 2019; Schierwater et al., 2021) provides an attractive system to explore how cell competition mechanisms may have first appeared in basal metazoans to both control tissue architecture and enable cancer prevention.

The study of cell polarity and how it helped generate multicellularity in the basal metazoans represents a rich opportunity to identify the original mechanisms that establish and maintain the organisation of tissues. Because of the high conservation in gene function between basal metazoans and Bilateria, these studies are also likely to provide broader insights into regenerative medicine and human cancer. Furthermore, identification of any divergent cell polarity mechanisms between basal metazoan and bilaterians will inform us as to the diversity and evolution of these core cellular mechanisms.

## References

- Abedin, M., and King, N. (2008). The premetazoan ancestry of cadherins. *Science* 319 (5865), 946–948. doi:10.1126/science.1151084
- AbedinKing, M. N. (2010). Diverse evolutionary paths to cell adhesion. *Trends Cell. Biol.* 20 (12), 734–742. doi:10.1016/j.tcb.2010.08.002
- Adamska, M., Degnan, B. M., Green, K., and Zwafink, C. (2011). What sponges can tell us about the evolution of developmental processes. *Zoology* 114 (1), 1–10. doi:10.1016/j.zool.2010.10.003
- Adamska, M., Larroux, C., Adamski, M., Green, K., Lovas, E., Koop, D., et al. (2010). Structure and expression of conserved wnt pathway components in the demosponge *Amphimedon queenslandica*. *Evol. Dev.* 12 (5), 494–518. doi:10.1111/j.1525-142X.2010.00435.x
- Adler, P. N. (2002). Planar signaling and morphogenesis in *Drosophila*. *Dev. Cell.* 2 (5), 525–535. doi:10.1016/S1534-5807(02)00176-4
- Agosti, C., and Stidwill, R. P. (1992). The contributions of microtubules and F-actin to the *in vitro* migratory mechanisms of *Hydra* nematocytes as determined by drug interference experiments. *Exp. Cell. Res.* 200 (1), 196–204. doi:10.1016/S0014-4827(05)80088-6
- Ajduk, A., and Zernicka-Goetz, M. (2016). Polarity and cell division orientation in the cleavage embryo: From worm to human. *Mol. Hum. Reprod.* 22 (10), 691–703. doi:10.1093/molehr/gav068
- Aktipis, C. M., Hibner, U., Hochberg, M. E., Maley, C. C., and Wilkinson, G. S. (2015). Cancer across the tree of life: Cooperation and cheating in multicellularity. *Philos. Trans. R. Soc. Lond. B Biol. Sci.* 370 (1673), 20140219. doi:10.1098/rstb.2014.0219
- Alberts, B., Johnson, A., Lewis, J., Raff, M., Roberts, K., and Walter, P. (2002). *Cell junctions*. 1065–1126.
- Albertson, R., and Doe, C. Q. (2003). Dlg, scrib and Lgl regulate neuroblast cell size and mitotic spindle asymmetry. *Nat. Cell. Biol.* 5 (2), 166–170. doi:10.1038/ncb922
- Alexander, B. E., Achlatis, M., Osinga, R., Harm, G., Cleutjens, P. M., Schutte, B., et al. (2015). Cell kinetics during regeneration in the sponge *halisarca caerulea*: How local is the response to tissue damage? *PeerJ* 3, e820. doi:10.7717/peerj.820
- Alié, A., and Manuel, M. (2010). The backbone of the post-synaptic density originated in a unicellular ancestor of choanoflagellates and metazoans. *BMC Evol. Biol.* 10, 34. doi:10.1186/1471-2148-10-34
- Allam, A. H., Charnley, M., and Russell, S. M. (2018). Context-specific mechanisms of cell polarity regulation. *J. Mol. Biol.* 430 (19), 3457–3471. doi:10.1016/j.jmb.2018.06.003
- Asano, A., Asano, K., Sasaki, H., Furuse, M., and Tsukita, S. (2003). Claudins in *Caenorhabditis elegans*: Their distribution and barrier function in the epithelium. *Curr. Biol.* 13 (12), 1042–1046. doi:10.1016/S0960-9822(03)00395-6
- Assemet, E., Bazellieres, E., Palesi-Pocachard, E., Le Bivic, A., and Massey-Harroche, D. (2008). Polarity complex proteins. *Biochim. Biophys. Acta* 1778 (3), 614–630. doi:10.1016/j.bbame.2007.08.029
- Axelrod, J. D., Werner, E. R., Leitner, S., Grobner, P., and Werner-Felmayer, G. (2001). Nitric oxide synthase is induced in sporulation of *Physarum polycephalum*. *Genes. Dev.* 15 (10), 1299–1309. doi:10.1101/gad.890501
- Baker, N. E. (2020). Emerging mechanisms of cell competition. *Nat. Rev. Genet.* 21 (11), 683–697. doi:10.1038/s41576-020-0262-8
- Baum, B., and Georgiou, M. (2011). Dynamics of adherens junctions in epithelial establishment, maintenance, and remodeling. *J. Cell. Biol.* 192 (6), 907–917. doi:10.1083/jcb.201009141

## Author contributions

BW: writing, editing, data collection and analysis; PH, MK, BS: editing.

## Acknowledgments

The authors would like to thank Sarah Russell and Helena Richardson for their constructive and thorough reading of this manuscript. Many thanks to Yuliya Stepkina for assisting with the figure artwork. We would also like to thank the reviewers for their helpful comments that markedly helped improve this manuscript.

## Conflict of interest

The authors declare that the research was conducted in the absence of any commercial or financial relationships that could be construed as a potential conflict of interest.

## Publisher's note

All claims expressed in this article are solely those of the authors and do not necessarily represent those of their affiliated organizations, or those of the publisher, the editors and the reviewers. Any product that may be evaluated in this article, or claim that may be made by its manufacturer, is not guaranteed or endorsed by the publisher.

- Bazellieres, E., Assemet, E., Arsanto, J. P., Le Bivic, A., and Massey-Harroche, D. (2009). Crumbs proteins in epithelial morphogenesis. *Front. Biosci.* 14, 2149–2169. doi:10.2741/3368
- Behr, M., Riedel, D., and Schuh, R. (2003). The claudin-like megatrachea is essential in septate junctions for the epithelial barrier function in *Drosophila*. *Dev. Cell.* 5 (4), 611–620. doi:10.1016/S1534-5807(03)00275-2
- Belabbib, H., Renard, E., Santini, S., Jourda, C., Borchellini, C., Le Bivic, A., et al. (2018). New genomic data and analyses challenge the traditional vision of animal epithelium evolution. *BMC Genomics* 19 (1), 393. doi:10.1186/s12864-018-4715-9
- Beljan, S., Herak Bosnar, M., and Četković, H. (2020). Rho family of ras-like GTPases in early-branching animals. *Cells* 9 (10), E2279. doi:10.3390/cells9102279
- Bergstrahl, D. T., Dawney, N. S., and Johnston, D. S. (2017). Spindle orientation: A question of complex positioning. *Development* 144 (7), 1137–1145. doi:10.1242/dev.140764
- Betschinger, J., and Knoblich, J. A. (2004). Dare to Be different: Asymmetric cell division in *Drosophila*, *C. Elegans* and vertebrates. *Curr. Biol.* 14 (16), R674–R685. doi:10.1016/j.cub.2004.08.017
- Bilder, D. (2004). Epithelial polarity and proliferation control: Links from the *Drosophila* neoplastic tumor suppressors. *Genes. Dev.* 18 (16), 1909–1925. doi:10.1101/gad.1211604
- Bilder, D., Li, M., and Perrimon, N. (2000). Cooperative regulation of cell polarity and growth by *Drosophila* tumor suppressors. *Science* 289 (5476), 113–116. doi:10.1126/science.289.5476.113
- Bilder, D., and Perrimon, N. (2000). Localization of apical epithelial determinants by the basolateral PDZ protein Scribble. *Nature* 403 (6770), 676–680. doi:10.1038/35001108
- Bivic, A. L. (2013). Evolution and cell physiology. 4. Why invent yet another protein complex to build junctions in epithelial cells? *Am. J. Physiol. Cell. Physiol.* 305 (12), C1193–C1201. doi:10.1152/ajpcell.00272.2013
- Bode, H. R. (1996). The interstitial cell lineage of *Hydra*: A stem cell system that arose early in evolution. *J. Cell. Sci.* 109 (6), 1155–1164. doi:10.1242/jcs.109.6.1155
- Bode, P. M., and Bode, H. R. (1980). formation of pattern in regenerating tissue pieces of *Hydra attenuata*: I. Head-body proportion regulation. *Dev. Biol.* 78 (2), 484–496. doi:10.1016/0012-1606(80)90348-6
- Bonello, T. T., and Peifer, M. (2019). Scribble: A master scaffold in polarity, adhesion, synaptogenesis, and proliferation. *J. Cell. Biol.* 218 (3), 742–756. doi:10.1083/jcb.201810103
- Bosch, T. C. G. (2004). Control of asymmetric cell divisions: Will cnidarians provide an answer? *BioEssays* 26 (9), 929–931. doi:10.1002/bies.20108
- Bosch, T. C. G., and David, C. N. (1987). Stem cells of *Hydra magnipapillata* can differentiate into somatic cells and germ line cells. *Dev. Biol.* 121 (1), 182–191. doi:10.1016/0012-1606(87)90151-5
- Bowling, S., Lawlor, K., and Tristan, A. (2019). Cell competition: The winners and losers of fitness selection. *Dev. Camb. Engl.* 146 (13), dev167486. doi:10.1242/dev.167486
- Boyd, L., Guo, S., Levitan, D., Stinchcomb, D. T., and Kemphues, K. J. (1996). PAR-2 is asymmetrically distributed and promotes association of P granules and PAR-1 with the cortex in *C. Elegans* embryos. *Dev. Camb. Engl.* 122 (10), 3075–3084. doi:10.1242/dev.122.10.3075
- Broun, M., Alexander, K., Bashkurov, M., Pearson, B. J., Steele, R. E., and McNeill, H. (2019). Ancestral role of fat-like cadherins in planar cell polarity. *BioRxiv*.
- Bürglin, T. R. (1994). A *Caenorhabditis elegans* Prospero homologue defines a novel domain. *Trends biochem. Sci.* 19 (2), 70–71. doi:10.1016/0968-0004(94)90035-3
- Butler, M. T., and Wallingford, J. B. (2017). Planar cell polarity in development and disease. *Nat. Rev. Mol. Cell. Biol.* 18 (6), 375–388. doi:10.1038/nrm.2017.11
- Buzgariu, W., S Al Haddad, S. T., Wenger, Y., and Galliot, B. (2015). Multifunctionality and plasticity characterize epithelial cells in *Hydra*. *Tissue Barriers* 3 (4), e1068908. doi:10.1080/21688370.2015.1068908
- Carvalho, A. B., Dobo, B. A., Vbranovski, M. D., and Clark, A. G. (2001). Identification of five new genes on the Y chromosome of *Drosophila melanogaster*. *Proc. Natl. Acad. Sci. U. S. A.* 98 (23), 13225–13230. doi:10.1073/pnas.231484998
- C. elegans Sequencing Consortium (1998). Genome sequence of the nematode *C. Elegans*: A platform for investigating Biology. *Sci. (New York, N.Y.)* 282 (5396), 2012–2018. doi:10.1126/science.282.5396.2012
- Chen, W., Lim, H. H., and Lim, L. (1993). A new member of the ras superfamily, the Rac1 homologue from *Caenorhabditis elegans*. Cloning and sequence analysis of CDNA, pattern of developmental expression, and biochemical characterization of the protein. *J. Biol. Chem.* 268 (1), 320–324. doi:10.1016/S0021-9258(18)54152-1
- Chera, S., Ghila, L., Wenger, Y., and Galliot, B. (2011). Injury-Induced activation of the MAPK/CREB pathway triggers apoptosis-induced compensatory proliferation in *Hydra* head regeneration. *Dev. Growth Differ.* 53 (2), 186–201. doi:10.1111/j.1440-169X.2011.01250.x
- Choi, W., Jung, K. C., Peifer, M., Fanning, A. S., and Beitel, G. J. (2011). The single *Drosophila* ZO-1 protein polychaetoid regulates embryonic morphogenesis in coordination with canoe/afadin and enabled. *Mol. Biol. Cell.* 22 (12), 2010–2030. doi:10.1091/mbc.E10-12-1014
- Dobrosotskaya, I., Guy, R. K., and James, G. L. (1997). MAGI-1, a membrane-associated guanylate kinase with a unique arrangement of protein-protein interaction domains. *J. Biol. Chem.* 272 (50), 31589–31597. doi:10.1074/jbc.272.50.31589
- Doe, C. Q., Chu-LaGriff, Q., Wright, D. M., and Scott, M. P. (1991). The Prospero gene specifies cell fates in the *Drosophila* central nervous system. *Cell.* 65 (3), 451–464. doi:10.1016/0092-8674(91)90463-9
- Domazet-Lošo, T., and Tautz, D. (2010). Phylostratigraphic tracking of cancer genes suggests a link to the emergence of multicellularity in Metazoa. *BMC Biol.* 8 (1), 66. doi:10.1186/1741-7007-8-66
- Dow, L. E., and Humbert, P. O. (2007). Polarity regulators and the control of epithelial architecture, cell migration, and tumorigenesis. *Int. Rev. Cytol.* 262, 253–302. doi:10.1016/S0074-7696(07)62006-3
- DuBuc, T. Q., Ryan, J. F., and Martindale, M. Q. (2019). ‘Dorsal–Ventral’ genes are part of an ancient axial patterning system: Evidence from Trichoplax adhaerens (placozoa). *Mol. Biol. Evol.* 36 (5), 966–973. doi:10.1093/molbev/msz025
- Dunny, G. M., Brickman, T. J., and Martin, D. (2008). Multicellular behavior in bacteria: Communication, cooperation, competition and cheating. *BioEssays* 30 (4), 296–298. doi:10.1002/bies.20740
- Ebnet, K. (2015). *Cell polarity 1: Biological role and basic mechanisms*. Springer International Publishing. doi:10.1007/978-3-319-14463-4
- Elsir, T., Smits, A., Lindström, M. S., and Nistér, M. (2012). Transcription factor PROX1: Its role in development and cancer. *Cancer Metastasis Rev.* 31 (3), 793–805. doi:10.1007/s10555-012-9390-8
- Elsum, I., Yates, L., Humbert, P. O., and Richardson, H. E. (2012). The scribble-dlg-lgl polarity module in development and cancer: From flies to man. *Essays Biochem.* 53, 141–168. doi:10.1042/bse0530141
- Ereskovsky, A., Borisenko, I. E., Bolshakov, F. V., and Lavrov, Andrey I. (2021). Whole-body regeneration in sponges: Diversity, fine mechanisms, and future prospects. *Genes.* 12 (4), 506. doi:10.3390/genes12040506
- Etemad-Moghadam, B., Guo, S., and Kenneth, J. (1995). Asymmetrically distributed PAR-3 protein contributes to cell polarity and spindle alignment in early *C. Elegans* embryos. *Cell.* 83 (5), 743–752. doi:10.1016/0092-8674(95)90187-6
- Etienne-Manneville, S. (2008). Polarity proteins in migration and invasion. *Oncogene* 27 (55), 6970–6980. doi:10.1038/ncr.2008.347
- Fahey, B., and Degnan, B. M. (2010). Origin of animal epithelia: Insights from the sponge genome. *Evol. Dev.* 12 (6), 601–617. doi:10.1111/j.1525-142X.2010.00445.x
- Fahey, B., and Degnan, B. M. (2012). Origin and evolution of laminin gene family diversity. *Mol. Biol. Evol.* 29 (7), 1823–1836. doi:10.1093/molbev/mss060
- Fahey-Lozano, N., Portela, M., Helena, E., and Richardson, H. E. (2019). *Drosophila* models of cell polarity and cell competition in tumorigenesis. *Adv. Exp. Med. Biol.* 1167, 37–64. doi:10.1007/978-3-030-23629-8\_3
- Fanning, A. S., Jameson, B. J., Jesaitis, L. A., and Anderson, J. M. (1998). The tight junction protein ZO-1 establishes a link between the transmembrane protein Occludin and the actin cytoskeleton. *J. Biol. Chem.* 273 (45), 29745–29753. doi:10.1074/jbc.273.45.29745
- Fidler, A. L., Darris, C. E., Sergei, V., Vadim, K., Boudko, S. P., Kyle, L. B., et al. (2017). Collagen IV and basement membrane at the evolutionary dawn of metazoan tissues. *ELife* 6, e24176. doi:10.7554/eLife.24176
- Filshie, B. K., and Flower, N. E. (1977). Junctional structures in *Hydra*. *J. Cell. Sci.* 23 (1), 151–172. doi:10.1242/jcs.23.1.151
- Fortunato, A., Fleming, A., Aktipis, A., and Carlo, C. (2021). Upregulation of DNA repair genes and cell extrusion underpin the remarkable radiation resistance of Trichoplax adhaerens. *PLoS Biol.* 17 e3001471. doi:10.1101/2020.12.24.424349
- Freeman, G. (1977). The establishment of the oral-aboral Axis in the ctenophore embryo. *Development* 24, 237–260. doi:10.1242/dev.42.1.237
- Gangar, A., Rossi, G., Anna, A., Hales, R., and Brennwald, P. (2005). Structurally conserved interaction of Lgl family with SNAREs is critical to their cellular function. *Curr. Biol.* 15 (12), 1136–1142. doi:10.1016/j.cub.2005.05.046
- Ganot, P., Zoccola, D., Tambutti, E., Voolstra, C. R., Aranda, M., Allemand, D., et al. (2015). Structural molecular components of septate junctions in Cnidarians point to the origin of epithelial junctions in eukaryotes. *Mol. Biol. Evol.* 32 (1), 44–62. doi:10.1093/molbev/msu265
- Gazave, E., Pascal, L., Richards, G. S., Brunet, F., Ereskovsky, A. V., Degnan, B. M., et al. (2009). Origin and evolution of the notch signalling pathway: An overview from eukaryotic genomes. *BMC Evol. Biol.* 9 (1), 249. doi:10.1186/1471-2148-9-249
- Gerhart, J. (1999). 1998 warkany lecture: Signaling pathways in development. *Teratology* 60 (4), 226–239. doi:10.1002/(SICI)1096-9926(199910)60:4<226::AID-TERA7>3.0.CO;2-W

- Gödde, N. J., Pearson, H. B., Smith, L. K., and Humbert, P. O. (2014). Dissecting the role of polarity regulators in cancer through the use of mouse models. *Exp. Cell. Res.* 328 (2), 249–257. doi:10.1016/j.yexcr.2014.08.036
- Goldstein, B., and Macara, I. G. (2007). The PAR proteins: Fundamental players in animal cell polarization. *Dev. Cell.* 13 (5), 609–622. doi:10.1016/j.devcel.2007.10.007
- González-Mariscal, L., Miranda, J., Raya-Sandino, A., Domínguez-Calderón, A., and Cuellar-Perez, F. (2017). ZO-2, a tight junction protein involved in gene expression, proliferation, apoptosis, and cell size regulation: ZO-2, a protein with membrane and nuclear functions. *Ann. N. Y. Acad. Sci.* 1397 (1), 35–53. doi:10.1111/nyas.13334
- Gooding, J. M., Yap, K. L., and Ikura, M. (2004). The cadherin–catenin complex as a focal point of cell adhesion and signalling: New insights from three-dimensional structures. *BioEssays* 26 (5), 497–511. doi:10.1002/bies.20033
- Goodrich, L. V., and David, S. (2011). Principles of planar polarity in animal development. *Development* 138 (10), 1877–1892. doi:10.1242/dev.054080
- Gotta, M., and Ahringer, J. (2001). Distinct roles for Galpha and Gbetagamma in regulating spindle position and orientation in *Caenorhabditis elegans* embryos. *Nat. Cell. Biol.* 3 (3), 297–300. doi:10.1038/35060092
- Grosberg, R. K., and Strathmann, R. R. (2007). The evolution of multicellularity: A minor major transition? *Annu. Rev. Ecol. Syst.* 38, 621–654. doi:10.1146/annurev.ecolsys.36.102403.114735
- Grosshans, B. L., Anna, A., Gangar, A., Niessen, S., Yates, J. R., Brennwald, P., et al. (2006). The yeast Lgl family member Sro7p is an effector of the secretory rab GTPase Sec4p. *J. Cell. Biol.* 172 (1), 55–66. doi:10.1083/jcb.200510016
- Gubb, D., García-Bellido, A., and García-Bellido, A. (1982). A genetic analysis of the determination of cuticular polarity during development in *Drosophila melanogaster*. *Development* 68, 37–57. doi:10.1242/dev.68.1.37
- Guillot, C., and Lecuit, T. (2013). Mechanics of epithelial tissue homeostasis and morphogenesis. *Science* 340 (6137), 1185–1189. doi:10.1126/science.1235249
- Gul, I. S., Hulpiau, P., Saeys, Y., and Frans van Roy (2017). Evolution and diversity of cadherins and catenins. *Exp. Cell. Res.* 358 (1), 3–9. doi:10.1016/j.yexcr.2017.03.001
- Hakeda-Suzuki, S., Ng, J., Julia, T., Dietzl, G., Sun, Y., Harms, M., et al. (2002). Rac function and regulation during *Drosophila* development. *Nature* 416 (6879), 438–442. doi:10.1038/416438a
- Hale, R., and Strutt, D. (2015). Conservation of planar polarity pathway function across the animal kingdom. *Annu. Rev. Genet.* Vol. 49, 529–551. doi:10.1146/annurev-genet-112414-055224
- Hammarlund, M., Nix, P., Hauth, L., Jorgensen, E. M., and Bastiani, M. (2009). Axon regeneration requires a conserved MAP kinase pathway. *Science* 323 (5915), 802–806. doi:10.1126/science.1165527
- Hanahan, D., and Weinberg, R. A. (2000). The hallmarks of cancer. *Cell* 100 (1), 57–70. doi:10.1016/S0092-8674(00)81683-9
- Harden, N., Wang, S. H., and Krieger, C. (2016). Making the connection – shared molecular machinery and evolutionary links underlie the formation and plasticity of occluding junctions and synapses. *J. Cell. Sci.* 129 (16), 3067–3076. doi:10.1242/jcs.186627
- Harris, T. J. C., and Ulrich, T. (2010). Adherens junctions: From molecules to morphogenesis. *Nat. Rev. Mol. Cell. Biol.* 11 (7), 502–514. doi:10.1038/nrm2927
- Harrison, F. W., and Ruppert, E. E. (1991). *Microscopic anatomy of invertebrates, placozoa, Porifera, Cnidaria, and ctenophora* 2. New York: Wiley-Liss.
- Hartmann, C., Otani, T., Furuse, M., and Ebnet, K. (2020). Physiological functions of junctional adhesion molecules (JAMs) in tight junctions. *Biochim. Biophys. Acta. Biomembr.* 1862 (9), 183299. doi:10.1016/j.bbmem.2020.183299
- Hattendorf, D. A., Anna, A., Gangar, A., Brennwald, P. J., and Weis, W. I. (2007). Structure of the yeast polarity protein Sro7 reveals a SNARE regulatory mechanism. *Nature* 446 (7135), 567–571. doi:10.1038/nature05635
- Heasman, S. J., and Ridley, A. J. (2008). Mammalian rho GTPases: New insights into their functions from *in vivo* studies. *Nat. Rev. Mol. Cell. Biol.* 9 (9), 690–701. doi:10.1038/nrm2476
- Hiroki, O. (2012). “Evolution of the cadherin–catenin complex,” in *Adherens junctions: From molecular mechanisms to tissue development and disease*. Editor T. Harris (Dordrecht: Springer Netherlands). doi:10.1007/978-94-007-4186-7\_2
- Hsu, T.-Y., and Wu, Y.-C. (2010). Engulfment of apoptotic cells in *C. elegans* is mediated by integrin alpha/SRC signaling. *Curr. Biol.* 20 (6), 477–486. doi:10.1016/j.cub.2010.01.062
- Hulpiau, P., Sahin Gul, I., and Frans van Roy (2013). New insights into the evolution of metazoan cadherins and catenins. *Prog. Mol. Biol. Transl. Sci.* 116, 71–94. doi:10.1016/B978-0-12-394311-8.00004-2
- Hulpiau, P., and van Roy, F. (2011). New insights into the evolution of metazoan cadherins. *Mol. Biol. Evol.* 28 (1), 647–657. doi:10.1093/molbev/msq233
- Humbert, P., Russell, S., and Richardson, H. (2003). Dlg, Scribble and Lgl in cell polarity, cell proliferation and cancer. *BioEssays* 25 (6), 542–553. doi:10.1002/bies.10286
- Humphries, A. C., and Mlodzik, M. (2018). From instruction to output: Wnt/PCP signaling in development and cancer. *Curr. Opin. Cell. Biol.* 51, 110–116. doi:10.1016/j.ceb.2017.12.005
- Hung, T. J., and Kemphues, K. J. (1999). PAR-6 is a conserved PDZ domain-containing protein that colocalizes with PAR-3 in *Caenorhabditis elegans* embryos. *Development* 126 (1), 127–135. doi:10.1242/dev.126.1.127
- Hurd, T. W., Gao, L., Roh, M. H., Macara, I. G., and Margolis, B. (2003). Direct interaction of two polarity complexes implicated in epithelial tight junction assembly. *Nat. Cell. Biol.* 5 (2), 137–142. doi:10.1038/ncb923
- Ip, Y. T., and Davis, R. J. (1998). Signal transduction by the C-jun N-terminal kinase (JNK) — From inflammation to development. *Curr. Opin. Cell. Biol.* 10 (2), 205–219. doi:10.1016/S0955-0674(98)80143-9
- Itoh, M., Furuse, M., Morita, K., Kubota, K., Saitou, M., and Tsukita, S. (1999). Direct binding of three tight junction-associated maguins, zo-1, zo-2, and zo-3, with the cooh termini of claudins. *J. Cell. Biol.* 147 (6), 1351–1363. doi:10.1083/jcb.147.6.1351
- Jan, Y. N., and Jan, L. (1998). Asymmetric cell division. *Nature* 392 (6678), 775–778. doi:10.1038/33854
- Joberty, G., Petersen, C., Gao, L., and Ian, G. (2000). The cell-polarity protein Par6 links Par3 and atypical protein kinase C to Cdc42. *Nat. Cell. Biol.* 2 (8), 531–539. doi:10.1038/35019573
- Kamm, K., Osgus, H. J., Stadler, P. F., DeSalle, R., and Schierwater, B. (2018). Trichoplax genomes reveal profound admixture and suggest stable wild populations without bisexual reproduction. *Sci. Rep.* 8 (1), 11168. doi:10.1038/s41598-018-29400-y
- Kamm, K., Schierwater, B., and DeSalle, R. (2019). Innate immunity in the simplest animals—placozoans. *BMC Genomics* 20 (1), 5. doi:10.1186/s12864-018-5377-3
- Kelsom, C., and Lu, W. (2012). Uncovering the link between malfunctions in *Drosophila* neuroblast asymmetric cell division and tumorigenesis. *Cell. Biosci.* 2 (1), 38. doi:10.1186/2045-3701-2-38
- Kemphues, K. J., Priess, J. R., Morton, D. G., and Cheng, N. S. (1988). Identification of genes required for cytoplasmic localization in early *C. Elegans* embryos. *Cell* 52 (3), 311–320. doi:10.1016/s0092-8674(88)80024-2
- King, N., Hittinger, C. T., and Carroll, S. B. (2003). Evolution of key cell signaling and adhesion protein families predates animal origins. *Science* 301 (5631), 361–363. doi:10.1126/science.1083853
- King, N. (2004). The unicellular ancestry of animal development. *Dev. Cell.* 7 (3), 313–325. doi:10.1016/j.devcel.2004.08.010
- King, N., Westbrook, M. J., Young, S. L., Kuo, A., Abedin, M., Chapman, J., et al. (2008). The genome of the choanoflagellate *monosiga brevicollis* and the origin of metazoans. *Nature* 451 (7180), 783–788. doi:10.1038/nature06617
- Klimovich, A., Wittlieb, J., and ThomasBosch, C. G. (2019). Transgenesis in *Hydra* to characterize gene function and visualize cell behavior. *Nat. Protoc.* 14 (7), 2069–2090. doi:10.1038/s41596-019-0173-3
- Knoblich, J. A. (2001). Asymmetric cell division during animal development. *Nat. Rev. Mol. Cell. Biol.* 2 (1), 11–20. doi:10.1038/35048085
- Knoblich, J. A. (2010). Asymmetric cell division: Recent developments and their implications for tumour Biology. *Nat. Rev. Mol. Cell. Biol.* 11 (12), 849–860. doi:10.1038/nrm3010
- Knoll, A. H. (2011). The multiple origins of complex multicellularity. *Annu. Rev. Earth Planet. Sci.* 39 (1), 217–239. doi:10.1146/annurev.earth.031208.100209
- Knust, E., and Bossinger, O. (2002). Composition and formation of intercellular junctions in epithelial cells. *Sci. (New York, N.Y.)* 298 (5600), 1955–1959. doi:10.1126/science.1072161
- Knust, E., Ulrich, T., and Wodarz, A. (1993). Crumbs and stardust, two genes of *Drosophila* required for the development of epithelial cell polarity. *Dev. Suppl.* 119, 261–268. doi:10.1242/dev.119.Supplement.261
- Kraut, R., Chia, W., Yeh Jan, L., Jan, Y. N., and Jürgen, A. (1996). Role of inscuteable in orienting asymmetric cell divisions in *Drosophila*. *Nature* 383 (6595), 50–55. doi:10.1038/383050a0
- Kumburegama, S., Wijesena, N., Xu, R., and Athula, H. (2011). Strabismus-Mediated primary archenteron invagination is uncoupled from wnt/ $\beta$ -catenin-dependent endoderm cell fate specification in *Nematostella vectensis* (Anchizoa, Cnidaria): Implications for the evolution of gastrulation. *EvoDevo* 2 (1), 2. doi:10.1186/2041-9139-2-2
- Kwiatkowski, V., Stephanie, L., Maiden, S. P., Choi, H. J., Benjamin, J. M., Lynch, A. M., et al. (2010). *In vitro* and *in vivo* reconstitution of the cadherin–catenin–actin complex from *Caenorhabditis elegans*. *Proc. Natl. Acad. Sci. U. S. A.* 107 (33), 14591–14596. doi:10.1073/pnas.1007349107



- Larroux, C., Luke, G. N., Peter, K., Rokhsar, D. S., Shimeld, S. M., and Degnan, B. M. (2008). Genesis and expansion of metazoan transcription factor gene classes. *Mol. Biol. Evol.* 25 (5), 980–996. doi:10.1093/molbev/msn047
- Lavrov, A. I., Bolshakov, F. V., Tokina, D. B., and Ereskovsky, A. V. (2018). Sewing up the wounds: The epithelial morphogenesis as a central mechanism of calcaronian sponge regeneration. *J. Exp. Zool. B Mol. Dev. Evol.* 330 (6–7), 351–371. doi:10.1002/jez.b.22830
- Layden, M. J., Rentzsch, F., and Röttinger, E. (2016). The rise of the starlet sea anemone *Nematostella vectensis* as a model system to investigate development and regeneration. *Wiley Interdiscip. Rev. Dev. Biol.* 5 (4), 408–428. doi:10.1002/wdev.222
- Lee, J.-S., Ishimoto, A., and Yanagawa, S. (1999). Characterization of mouse dishevelled (dvl) proteins in wnt/wingless signaling pathway. *J. Biol. Chem.* 274 (30), 21464–21470. doi:10.1074/jbc.274.30.21464
- Lehman, K., Rossi, G., Adamo, J. E., and Brennwald, P. (1999). Yeast homologues of tomosyn and lethal giant larvae function in exocytosis and are associated with the plasma membrane snare, Sec9. *J. Cell. Biol.* 146 (1), 125–140. doi:10.1083/jcb.146.1.125
- Lo, S. H. (2006). Focal adhesions: What's new inside. *Dev. Biol.* 294 (2), 280–291. doi:10.1016/j.ydbio.2006.03.029
- Loh, K. M., van Amerongen, R., and Nusse, R. (2016). Generating cellular diversity and spatial form: Wnt signaling and the evolution of multicellular animals. *Dev. Cell.* 38 (6), 643–655. doi:10.1016/j.devcel.2016.08.011
- Lokits, A. D., Indrischek, H., Meiler, J., Hamm, H. E., and Stadler, P. F. (2018). Tracing the evolution of the heterotrimeric G protein  $\alpha$  subunit in Metazoa. *BMC Evol. Biol.* 18 (1), 51. doi:10.1186/s12862-018-1147-8
- Lynch, A. M., Grana, T., Couthier, A., Cameron, M., et al. (2012). Theresa grana, elisabeth cox-paulson, annabelle couthier, michel cameron, ian chin-sang, jonathan pettitt, and jeff HardinA genome-wide functional screen shows MAGI-1 is an l1cam-dependent stabilizer of apical junctions in *C. Elegans*. *Curr. Biol.* 22 (20), 1891–1899. doi:10.1016/j.cub.2012.08.024
- Macara, I. G. (2004). Parsing the polarity code. *Nat. Rev. Mol. Cell. Biol.* 5 (3), 220–231. doi:10.1038/nrm1332
- Madan, E., Gogna, R., and Moreno, E. (2018). Cell competition in development: Information from flies and vertebrates. *Curr. Opin. Cell. Biol.* 55, 150–157. doi:10.1016/j.cub.2018.08.002
- Magie, C. R., and Martindale, M. Q. (2008). Cell-cell adhesion in the Cnidaria: Insights into the evolution of tissue morphogenesis. *Biol. Bull.* 214 (3), 218–232. doi:10.2307/25470665
- Margolis, B., and Borg, J. P. (2005). Apical-basal polarity complexes. *J. Cell. Sci.* 118 (22), 5157–5159. doi:10.1242/jcs.02597
- Matis, M., and Axelrod, J. D. (2013). Regulation of PCP by the fat signaling pathway. *Genes. Dev.* 27 (20), 2207–2220. doi:10.1101/gad.228098.113
- Matter, K., and Balda, M. S. (2003). Signalling to and from tight junctions. *Nat. Rev. Mol. Cell. Biol.* 4 (3), 225–236. doi:10.1038/nrm1055
- McLennan, D. A. (2008). The concept of Co-option: Why evolution often looks miraculous. *Evo. Edu. Outreach* 1 (3), 247–258. doi:10.1007/s12052-008-0053-8
- Melendez, J., Grogg, M., and Zheng, Y. (2011). Signaling role of Cdc42 in regulating mammalian physiology. *J. Biol. Chem.* 286 (4), 2375–2381. doi:10.1074/jbc.R110.200329
- Mendoza, A., Seb -Pedr s, A., and Ruiz-Trillo, I. (2014). The evolution of the GPCR signaling system in eukaryotes: Modularity, conservation, and the transition to metazoan multicellularity. *Genome Biol. Evol.* 6 (3), 606–619. doi:10.1093/gbe/evu038
- Mendoza, A., Suga, H., and Ruiz-Trillo, I. (2010). Evolution of the MAGUK protein gene family in premetazoan lineages. *BMC Evol. Biol.* 10 (1), 93. doi:10.1186/1471-2148-10-93
- Michael, M., and Parsons, M. (2020). New perspectives on integrin-dependent adhesions. *Curr. Opin. Cell. Biol.* 63, 31–37. doi:10.1016/j.cub.2019.12.008
- Milgrom-Hoffman, M., and Humbert, P. O. (2018). Regulation of cellular and PCP signalling by the Scribble polarity module. *Semin. Cell. Dev. Biol.* 81, 33–45. doi:10.1016/j.semcdb.2017.11.021
- Mitchell, J. M., and Nichols, S. A. (2019). Diverse cell junctions with unique molecular composition in tissues of a sponge (Porifera). *EvoDevo* 10 (1), 26. doi:10.1186/s13227-019-0139-0
- Momose, T., Kraus, Y., and Houlston, E. (2012). A conserved function for strabismus in establishing planar cell polarity in the ciliated ectoderm during Cnidarian larval development. *Development* 139 (23), 4374–4382. doi:10.1242/dev.084251
- Moulder, G. L., Huang, M. M., Waterston, R. H., and Barstead, R. J. (1996). Talin requires beta-integrin, but not vinculin, for its assembly into focal adhesion-like structures in the nematode *Caenorhabditis elegans*. *Mol. Biol. Cell.* 7 (8), 1181–1193. doi:10.1091/mbc.7.8.1181
- M ller, W. E. G. (2003). The origin of metazoan complexity: Porifera as integrated animals. *Integr. Comp. Biol.* 43 (1), 3–10. doi:10.1093/icb/43.1.3
- M sch, A., Cohen, D., Yeaman, C., James Nelson, W., Rodriguez-Boulant, E., and Patrick, J. (2002). Mammalian homolog of Drosophila tumor suppressor lethal (2) giant larvae interacts with basolateral exocytic machinery in madin-darby canine kidney cells. *Mol. Biol. Cell.* 13 (1), 158–168. doi:10.1091/mbc.01-10-0496
- Nelson, W. J. (2003). Adaptation of core mechanisms to generate cell polarity. *Nature* 422 (6933), 766–774. doi:10.1038/nature01602
- Nelson, W. J. (2008). Regulation of cell–cell adhesion by the cadherin–catenin complex. *Biochem. Soc. Trans.* 36 (2), 149–155. doi:10.1042/BST0360149
- Neumann, J., Tessier, M. S., Kamm, K., Oisig, H. J., Ershel, G., Narechania, A., et al. (2022). Phylogenomics and the first higher taxonomy of Placozoa, an ancient and enigmatic animal phylum. *Front. Ecol. Evol.* doi:10.3389/fevo.2022.1016357
- Neum ller, R. H. A., and Knoblich, J. A. (2009). Dividing cellular asymmetry: Asymmetric cell division and its implications for stem cells and cancer. *Genes. Dev.* 23 (23), 2675–2699. doi:10.1101/gad.1850809
- Nichols, S. A., Dirks, W., Pearce, J. S., and King, N. (2006). Early evolution of animal cell signaling and adhesion genes. *Proc. Natl. Acad. Sci. U. S. A.* 103 (33), 12451–12456. doi:10.1073/pnas.0604065103
- Nichols, S. A., Roberts, B. W., Richter, D. J., Fairclough, S. R., and King, N. (2012). Origin of metazoan cadherin diversity and the antiquity of the classical cadherin–catenin complex. *Proc. Natl. Acad. Sci. U. S. A.* 109 (32), 13046–13051. doi:10.1073/pnas.1120685109
- Niessen, C. M. (2007). Tight junctions/adherens junctions: Basic structure and function. *J. Invest. Dermatol.* 127 (11), 2525–2532. doi:10.1038/sj.jid.5700865
- Noselli, S., and Agn s, F. (1999). Roles of the JNK signaling pathway in Drosophila morphogenesis. *Curr. Opin. Genet. Dev.* 9 (4), 466–472. doi:10.1016/S0959-437X(99)80071-9
- Nosenko, T., Schreiber, F., Adamska, M., Adamski, M., Eitel, M., Hammel, J., et al. (2013). Deep metazoan phylogeny: When different genes tell different stories. *Mol. Phylogenet. Evol.* 67 (1), 223–233. doi:10.1016/j.ympev.2013.01.010
- Oda, H., and Takeichi, M. (2011). Evolution: Structural and functional diversity of cadherin at the adherens junction. *J. Cell. Biol.* 193 (7), 1137–1146. doi:10.1083/jcb.201008173
- Okamoto, K., Nakatsukasa, M., Alexandre, A., Masuda, Y., Agata, K., and Funayama, N. (2012). The active stem cell specific expression of sponge *Musashi* homolog *EflMsiA* suggests its involvement in maintaining the stem cell state. *Mech. Dev.* 129 (1), 24–37. doi:10.1016/j.mod.2012.03.001
- Oliver, G., Sosa-Pineda, B., Geisendorf, S., Spana, E. P., Chris, Q., and Gruss, P. (1993). Prox 1, a prospero-related homeobox gene expressed during mouse development. *Mech. Dev.* 44 (1), 3–16. doi:10.1016/0925-4773(93)90012-M
- Oisig, H. J., Eitel, M., Horn, K., Kamm, K., and Kosubek-Langer, J. (2022). “Studying Placozoa Placozoa WBR Whole-body regeneration (WBR) in the simplest metazoan animal, Trichoplax Adhaerens Trichoplax adhaerens,” in *Whole-body regeneration: Methods and protocols*, edited by Simon Blanchoud and Brigitte Galliot (New York, NY: Springer US). doi:10.1007/978-1-0716-2172-1\_6
- Pang, K., and Mark, Q. (2008). Ctenophores. *Curr. Biol.* 18 (24), R1119–R1120. doi:10.1016/j.cub.2008.10.004
- Pang, K., Ryan, J. F., Mullikin, J. C., and Martindale, M. Q. (2010). Andreas D. Baxeianis, Mark Q. Martindale, and NISC comparative sequencing Program Genomic insights into wnt signaling in an early diverging metazoan, the ctenophore *Mnemiopsis leidyi*. *EvoDevo* 1 (1), 10. doi:10.1186/2041-9139-1-10
- Petronczki, M., and Knoblich, J. A. (2001). DmPAR-6 directs epithelial polarity and asymmetric cell division of neuroblasts in Drosophila. *Nat. Cell. Biol.* 3 (1), 43–49. doi:10.1038/35050550
- Philipp, I., Aufschnaiter, R., Ozbek, S., Pontasch, S., Jenewein, M., Watanabe, H., et al. (2009). Wnt/beta-catenin and noncanonical Wnt signaling interact in tissue evagination in the simple eumetazoan Hydra. *Proc. Natl. Acad. Sci. U. S. A.* 106 (11), 4290–4295. doi:10.1073/pnas.0812847106
- Pill , J. -Y., Denoyelle, C., Varet, J., Bertrand, J. -R., Soria, J., Opolon, P., et al. (2005). Anti-RhoA and anti-RhoC siRNAs inhibit the proliferation and invasiveness of MDA-MB-231 breast cancer cells *in vitro* and *in vivo*. *Mol. Ther.* 11 (2), 267–274. doi:10.1016/j.ymthe.2004.08.029
- Piraino, S., Boero, F., Aeschbach, B., and Schmid, V. (1996). Reversing the life cycle: Medusae transforming into polyps and cell transdifferentiation in turritopsis nutricula (Cnidaria, Hydrozoa). *Biol. Bull.* 190 (3), 302–312. doi:10.2307/1543022
- Postiglione, M. P., J schke, C., Xie, Y., Haas, G. A., Charalambous, C., and Knoblich, J. A. (2011). Mouse inscuteable induces apical-basal spindle orientation to facilitate intermediate progenitor generation in the developing neocortex. *Neuron* 72 (2), 269–284. doi:10.1016/j.neuron.2011.09.022



- Rainey, P. B. (2007). Unity from conflict. *Nature* 446 (7136), 616. doi:10.1038/446616a
- Rathbun, L. I., Everett, C. A., and Bergstrahl, D. T. (2022). Emerging Cnidarian models for the study of epithelial polarity. *Front. Cell. Dev. Biol.* 10, 854373. doi:10.3389/fcell.2022.854373
- Reber-Müller, S., Studer, R., Müller, P., Yanze, N., and Schmid, V. (2001). Integrin and talin in the jellyfish podocoryne carnea. *Cell. Biol. Int.* 25 (8), 753–769. doi:10.1006/cbir.2000.0708
- Richter, D. J., Fozouni, P., Eisen, M. B., and King, N. (2018). Gene family innovation, conservation and loss on the animal stem lineage. *ELife* 7, e34226. doi:10.7554/eLife.34226
- Richter, D. J., and King, N. (2013). The genomic and cellular foundations of animal origins. *Annu. Rev. Genet.* 47 (1), 509–537. doi:10.1146/annurev-genet-111212-133456
- Riesgo, A., Farrar, N., Windsor, P. J., Giribet, G., and Sally, P. (2014). The analysis of eight transcriptomes from all Poriferan classes reveals surprising genetic complexity in sponges. *Mol. Biol. Evol.* 31 (5), 1102–1120. doi:10.1093/molbev/msu057
- Ringrose, J. H., van den Toorn, H. W. P., Eitel, M., Post, H., Neerincx, P., Schierwater, B., et al. (2013). Deep proteome profiling of Trichoplax adhaerens reveals remarkable features at the origin of metazoan multicellularity. *Nat. Commun.* 4, 1408. doi:10.1038/ncomms2424
- Rock, R., Schrauth, S., and Gessler, M. (2005). Expression of mouse Dchs1, Fjx1, and fat-j suggests conservation of the planar cell polarity pathway identified in *Drosophila*. *Dev. Dyn.* 234 (3), 747–755. doi:10.1002/dvdy.20515
- Rodriguez-Boulán, E., and Nelson, W. J. (1989). Morphogenesis of the polarized epithelial cell phenotype. *Science* 245 (4919), 718–725. doi:10.1126/science.2672330
- Rokas, A. (2008). The origins of multicellularity and the early history of the genetic toolkit for animal development. *Annu. Rev. Genet.* 42, 235–251. doi:10.1146/annurev.genet.42.110807.091513
- Röttinger, E. (2021). Nematostella vectensis, an emerging model for deciphering the molecular and cellular mechanisms underlying whole-body regeneration. *Cells* 10, 2692. doi:10.3390/cells10102692
- Royer, C., and Lu, X. (2011). Epithelial cell polarity: A major gatekeeper against cancer? *Cell. Death Differ.* 18 (9), 1470–1477. doi:10.1038/cdd.2011.60
- Ruthmann, A., Behrendt, G., and Wahl, R. (1986). The ventral epithelium of Trichoplax adhaerens (placozoa): Cytoskeletal structures, cell contacts and endocytosis. *Zoomorphology* 106 (2), 115–122. doi:10.1007/BF00312113
- Ruthmann, A., and Terwelp, U. (1979). Disaggregation and reaggregation of cells of the primitive metazoan Trichoplax adhaerens. *Differentiation* 13 (3), 185–198. doi:10.1111/j.1432-0436.1979.tb01581.x
- Ryan, J. F., Pang, K., Schnitzler, C. E., Moreland, R. T., Simmons, D. K., Koch, B. J., et al. (2013). The genome of the ctenophore Mnemiopsis leidyi and its implications for cell type evolution. *Science* 342 (6164), 1242592. doi:10.1126/science.1242592
- Ryan, J. F., Patrick, M., Finnerty, J. R., Kwong, G. K., Mullikin, J. C., and Finnerty, J. R. (2006). The Cnidarian-bilaterian ancestor possessed at least 56 homeoboxes: Evidence from the starlet sea anemone, Nematostella vectensis. *Genome Biol.* 7 (7), R64. doi:10.1186/gb-2006-7-7-r64
- Ryan, K. R., and Shapiro, L. (2003). Temporal and spatial regulation in prokaryotic cell cycle progression and development. *Annu. Rev. Biochem.* 72 (1), 367–394. doi:10.1146/annurev.biochem.72.121801.161824
- Sakarya, O., Armstrong, K. A., Adamska, M., Adamski, M., Wang, I-F., Bruce, T., et al. (2007). A post-synaptic scaffold at the origin of the animal kingdom. *PLoS ONE* 2 (6), e506. doi:10.1371/journal.pone.0000506
- Salinas-Saavedra, M., Dunn, C. W., and Martindale, M. Q. (2015). Par system components are asymmetrically localized in ectodermal epithelia, but not during early development in the sea anemone Nematostella vectensis. *EvoDevo* 6 (1), 20. doi:10.1186/s13227-015-0014-6
- Salinas-Saavedra, M., and Martindale, M. Q. (2018). Germ layer-specific regulation of cell polarity and adhesion gives insight into the evolution of mesoderm. *Elife* 28, e36740. doi:10.7554/eLife.36740
- Salinas-Saavedra, M., and Martindale, M. Q. (2019).  $\beta$ -Catenin has an ancestral role in cell fate specification but not cell adhesion. *bioRxiv*. doi:10.1101/520957
- Sandoz, K. M., Mitzimberg, S. M., and Schuster, M. (2007). Social cheating in *Pseudomonas aeruginosa* quorum sensing. *Proc. Natl. Acad. Sci. U. S. A.* 104 (40), 15876–15881. doi:10.1073/pnas.070563104
- Santoni, M. J., Pontarotti, P., Birnbaum, D., and Borg, J. P. (2002). The LAP family: A phylogenetic point of view. *Trends Genet.* 18 (10), 494–497. doi:10.1016/s0168-9525(02)02738-5
- Sawa, H. (2012). Control of cell polarity and asymmetric division in *C. Elegans*. *Curr. Top. Dev. Biol.* 101, 55–76. doi:10.1016/B978-0-12-394592-1.00003-X
- Schenkelaars, Q., Fierro-Constain, L., Renard, E., and Borchellini, C. (2016). Retracing the path of planar cell polarity. *BMC Evol. Biol.* 16 (1), 69. doi:10.1186/s12862-016-0641-0
- Schenkelaars, Q., Fierro-Constain, L., Renard, E., Hill, A. L., and Borchellini, C. (2015). Insights into frizzled evolution and new perspectives. *Evol. Dev.* 17 (2), 160–169. doi:10.1111/ede.12115
- Schenkelaars, Q., Pralong, M., Kodjabachian, L., Fierro-Constain, L., Vacelet, J., Bivic, A., et al. (2017). Animal multicellularity and polarity without wnt signaling. *Sci. Rep.* 7 (1), 1–11. doi:10.1038/s41598-017-15557-5
- Schierwater, B., Osigus, H. J., Bergmann, T., Blackstone, N. W., Hadrys, H., Hauslage, J., et al. (2021). The enigmatic placozoa Part I: Exploring evolutionary controversies and poor ecological knowledge. *Bioessays* 43 (10), 2100080. doi:10.1002/bies.202100080
- Schiller, E., and Bergstrahl, D. T. (2021). Interaction between Discs large and Pins/LGN/GPSM2: A comparison across species. *Biol. Open* 10, bio058982. doi:10.1242/bio.058982
- Schmid, V., and Alder, H. (1984). Isolated, mononucleated, striated muscle can undergo pluripotent transdifferentiation and form a complex regenerate. *Cell* 38 (3), 801–809. doi:10.1016/0092-8674(84)90275-7
- Sebé-Pedrós, A., Zheng, Y., Ruiz-Trillo, I., and Pan, D. (2012). Premetazoan origin of the hippo signaling pathway. *Cell. Rep.* 1 (1), 13–20. doi:10.1016/j.celrep.2011.11.004
- Sebé-Pedrós, A., Arnau, A. J. R., Lang, F. B., King, N., and Ruiz-Trillo, I. (2010). Ancient origin of the integrin-mediated adhesion and signaling machinery. *Proc. Natl. Acad. Sci. U. S. A.* 107 (22), 10142–10147. doi:10.1073/pnas.1002257107
- Seipel, K., Yanze, N., and Schmid, V. (2003). The germ line and somatic stem cell gene cnivi in the jellyfish Podocoryne carnea. *Int. J. Dev. Biol.* 48 (1), 1–7. doi:10.1387/ijdb.15005568
- Seybold, A., Salvenmoser, W., and Hobmayer, B. (2016). Sequential development of apical-basal and planar polarities in aggregating epitheliomuscular cells of Hydra. *Dev. Biol.* 412 (1), 148–159. doi:10.1016/j.ydbio.2016.02.022
- Simmons, D. K., Pang, K., and Martindale, M. Q. (2012). Lim homeobox genes in the ctenophore Mnemiopsis leidyi: The evolution of neural cell type specification. *EvoDevo* 3 (1), 2. doi:10.1186/2041-9139-3-2
- Simons, M., and Mlodzik, M. (2008). Planar cell polarity signaling: From fly development to human disease. *Annu. Rev. Genet.* 42 (1), 517–540. doi:10.1146/annurev.genet.42.110807.091432
- Simpson, T. L. (1984). *The cell Biology of sponges*. New York: Springer Science & Business Media.
- Smith, C. L., and Reese, T. S. (2016). Adherens junctions modulate diffusion between epithelial cells in Trichoplax adhaerens. *Biol. Bull.* 231 (3), 216–224. doi:10.1086/691069
- Smith, C. L., Varoqueaux, F., Kittelmann, M., Azzam, R. N., Winters, C. A., Eitel, M., et al. (2014). Novel cell types, neurosecretory cells, and body plan of the early-diverging metazoan Trichoplax adhaerens. *Curr. Biol.* 24 (14), 1565–1572. doi:10.1016/j.cub.2014.05.046
- Snell, E. A., M Brooke, N. W. R. T., Casane, D., Philippe, H., and Holland, P. W. H. (2006). An unusual choanoflagellate protein released by hedgehog autocatalytic processing. *Proc. Biol. Sci.* 273 (1585), 401–407. doi:10.1098/rspb.2005.3263
- Soest, R., Boury-Esnault, N., Vacelet, J., Martin, D., Erpenbeck, D., NicoleSantodomingo, J. N., et al. (2012). Global diversity of sponges (Porifera). *PLOS ONE* 7 (4), e35105. doi:10.1371/journal.pone.0035105
- Sogabe, S., Kocot, Kevin M., Say, T. E., Stoupin, D., Roper, K. E., Fernandez-Valverde, S. L., et al. (2019). Pluripotency and the origin of animal multicellularity. *Nature* 570 (7762), 519–522. doi:10.1038/s41586-019-1290-4
- Srivastava, M., Begovic, E., Chapman, J., Putnam, N. H., Hellsten, U., Kawashima, T., et al. (2008). The Trichoplax genome and the nature of placozoans. *Nature* 454 (7207), 955–960. doi:10.1038/nature07191
- Srivastava, M., Simakov, O., Chapman, J., Fahey, B., MarieGauthier, E. A., Mitros, T., et al. (2010). The Amphimedon queenslandica genome and the evolution of animal complexity. *Nature* 466 (7307), 720–726. doi:10.1038/nature09201
- Srivastava, M. (2015). “A comparative genomics perspective on the origin of multicellularity and early animal evolution,” in *Evolutionary transitions to multicellular life: Principles and mechanisms*. Editors I. RuizTrillo and A. M. Nedelcu (Dordrecht: Springer), 269–299.
- St Johnston, D., and Ahninger, J. (2010). Cell polarity in eggs and epithelia: Parallels and diversity. *Cell* 141 (5), 757–774. doi:10.1016/j.cell.2010.05.011
- Steed, E., Balda, M. S., and Matter, K. (2010). Dynamics and functions of tight junctions. *Trends Cell. Biol.* 20 (3), 142–149. doi:10.1016/j.tcb.2009.12.002

- Steimel, A., Wong, L., Ackley, B. D., Garriga, G., and Hutter, H. (2010). The flamingo ortholog FMI-1 controls pioneer-dependent navigation of follower axons in *C. Elegans*. *Development* 137 (21), 3663–3673. doi:10.1242/dev.054320
- Stephens, R., Lim, K., Portela, M., Kvensakul, M., Humbert, P. O., and Richardson, H. E. (2018). The Scribble cell polarity module in the regulation of cell signaling in tissue development and tumorigenesis. *J. Mol. Biol.* 430 (19), 3585–3612. doi:10.1016/j.jmb.2018.01.011
- Tabuse, Y., Izumi, Y., Piano, F., Kemphues, K. J., Miwa, J., and Ohno, S. (1998). Atypical protein kinase C cooperates with PAR-3 to establish embryonic polarity in *Caenorhabditis elegans*. *Dev. Camb. Engl.* 125 (18), 3607–3614. doi:10.1242/dev.125.18.3607
- Takahashi, K., Matsuo, T., Katsube, T., Ueda, R., and Yamamoto, D. (1998). Direct binding between two PDZ domain proteins canoe and ZO-1 and their roles in regulation of the jun N-terminal kinase pathway in *Drosophila* morphogenesis. *Mech. Dev.* 78 (1–2), 97–111. doi:10.1016/s0925-4773(98)00151-8
- Tamm, S. L. (2014). Cilia and the life of ctenophores. *Invertebr. Biol.* 133 (1), 1–46. doi:10.1111/ivb.12042
- Technau, U., and Steele, R. E. (2011). Evolutionary crossroads in developmental Biology: *Cnidaria*. *Development* 138 (8), 1447–1458. doi:10.1242/dev.048959
- Tapass, U. (2012). The apical polarity protein network in *Drosophila* epithelial cells: Regulation of polarity, junctions, morphogenesis, cell growth, and survival. *Annu. Rev. Cell. Dev. Biol.* 28 (1), 655–685. doi:10.1146/annurev-cellbio-092910-154033
- Tapass, U., Tanentzapf, G., Ward, R., and Fehon, R. (2001). Epithelial cell polarity and cell junctions in *Drosophila*. *Annu. Rev. Genet.* 35, 747–784. doi:10.1146/annurev.genet.35.102401.091415
- Tapass, U., Theres, C., and Knust, E. (1990). Crumbs encodes an EGF-like protein expressed on apical membranes of *Drosophila* epithelial cells and required for organization of epithelia. *Cell* 61 (5), 787–799. doi:10.1016/0092-8674(90)90189-1
- Thiemann, M., and Ruthmann, A. (1989). Microfilaments and microtubules in isolated fiber cells of trichoplax-adhaerens (placozoa). *Zoomorphology* 109 (2), 89–96. doi:10.1007/BF00312314
- Tian, X., Liu, Z., Niu, B., Zhang, J., Tan, T. K., Lee, R., et al. (2011). E-Cadherin/ $\beta$ -Catenin complex and the epithelial barrier. *J. Biomed. Biotechnol.* 2011, e567305. doi:10.1155/2011/567305
- Tsukita, S., Furuse, M., and Itoh, M. (2001). Multifunctional strands in tight junctions. *Nat. Rev. Mol. Cell. Biol.* 2 (4), 285–293. doi:10.1038/35067088
- Tucker, R. P., and Adams, J. C. (2014). Adhesion networks of cnidarians: A postgenomic view. *Int. Rev. Cell. Mol. Biol.* 308, 323–377. doi:10.1016/B978-0-12-800097-7.00008-7
- Tyler, S. (2003). Epithelium—the primary building block for metazoan complexity. *Integr. Comp. Biol.* 43 (1), 55–63. doi:10.1093/icb/43.1.55
- Usui, T., Shima, Y., Shimada, Y., Hirano, S., Burgess, R. W., Schwarz, T. L., et al. (1999). Flamingo, a seven-pass transmembrane cadherin, regulates planar cell polarity under the control of frizzled. *Cell* 98 (5), 585–595. doi:10.1016/S0092-8674(00)80046-X
- Velthuis, A. J., Admiraal, J. F., and Bagowski, C. P. (2007). Molecular evolution of the MAGUK family in metazoan genomes. *BMC Evol. Biol.* 7 (1), 129. doi:10.1186/1471-2148-7-129
- Walston, T., Tuskey, C., Edgar, L., Hawkins, N., Ellis, G., Bruce, B., et al. (2004). Multiple wnt signaling pathways converge to orient the mitotic spindle in early *C. Elegans* embryos. *Dev. Cell* 7 (6), 831–841. doi:10.1016/j.devcel.2004.10.008
- Wei, X., and Ellis, H. M. (2001). Localization of the *Drosophila* MAGUK protein polychaetoid is controlled by alternative splicing. *Mech. Dev.* 100 (2), 217–231. doi:10.1016/S0925-4773(00)00550-5
- Wen, W., and Zhang, M. (2018). Protein complex assemblies in epithelial cell polarity and asymmetric cell division. *J. Mol. Biol.* 430 (19), 3504–3520. doi:10.1016/j.jmb.2017.09.013
- West, S. A., Griffin, A. S., Gardner, A., and Diggle, S. P. (2006). Social evolution theory for microorganisms. *Nat. Rev. Microbiol.* 4 (8), 597–607. doi:10.1038/nrmicro1461
- Widmann, C., Gibson, S., Jarpe, M. B., and Johnson, G. L. (1999). Mitogen-activated protein kinase: Conservation of a three-kinase module from yeast to human. *Physiol. Rev.* 79 (1), 143–180. doi:10.1152/physrev.1999.79.1.143
- Wiese, K. E., Nusse, R., and van Amerongen, R. (2018). Wnt signalling: Conquering complexity. *Development* 145 (12), dev165902. doi:10.1242/dev.165902
- Wu, Y. C., Franzenburg, S., Ribes, M., and Pita, L. (2022). Wounding response in Porifera (sponges) activates ancestral signaling cascades involved in animal healing, regeneration, and cancer. *Sci. Rep.* 12 (1), 1307. doi:10.1038/s41598-022-05230-x
- Yamanaka, T., and Ohno, S. (2008). Role of lgl/dlg/scribble in the regulation of epithelial junction, polarity and growth. *Front. Biosci.* 13, 6693–6707. doi:10.2741/3182
- Zaessinger, S., Zhou, Y., Bray, S. J., Tapon, N., and Alexandre, D. (2015). *Drosophila* MAGI interacts with RASSF8 to regulate E-cadherin-based adherens junctions in the developing eye. *Development* 142 (6), 1102–1112. doi:10.1242/dev.116277
- Zhang, X., Wang, P., Gangar, A., Zhang, J., Brennwald, P., TerBush, D., et al. (2005). Lethal giant larvae proteins interact with the exocyst complex and are involved in polarized exocytosis. *J. Cell. Biol.* 170 (2), 273–283. doi:10.1083/jcb.200502055
- Zhang, Z. Q. (2011). Animal biodiversity: An introduction to higher-level classification and taxonomic richness. *Zootaxa* 3148 (1), 7. doi:10.11646/zootaxa.3148.1.3
- Zhu, H., Zhou, Z., Wang, D., Liu, W., and Zhu, H. (2013). Hippo pathway genes developed varied exon numbers and coevolved functional domains in metazoans for species specific growth control. *BMC Evol. Biol.* 13 (1), 76. doi:10.1186/1471-2148-13-76
- Žigman, M., Cayouette, M., Charalambous, C., Alexander, S., Oliver, H., Dunican, D., et al. (2005). Mammalian inscuteable regulates spindle orientation and cell fate in the developing retina. *Neuron* 48 (4), 539–545. doi:10.1016/j.neuron.2005.09.030



## OPEN ACCESS

## EDITED BY

Xinqing Zhao,  
Shanghai Jiao Tong University, China

## REVIEWED BY

Krishna Swamy,  
Ahmedabad University, India  
Ximo Pechuan Jorge,  
Genentech Inc., United States

## \*CORRESPONDENCE

Liedewij Laan  
✉ l.laan@tudelft.nl

RECEIVED 24 October 2022

ACCEPTED 19 June 2023

PUBLISHED 14 July 2023

## CITATION

Kingma E, Diepeveen ET, Iñigo de la Cruz L and Laan L (2023) Pleiotropy drives evolutionary repair of the responsiveness of polarized cell growth to environmental cues. *Front. Microbiol.* 14:1076570. doi: 10.3389/fmicb.2023.1076570

## COPYRIGHT

© 2023 Kingma, Diepeveen, Iñigo de la Cruz and Laan. This is an open-access article distributed under the terms of the [Creative Commons Attribution License \(CC BY\)](#). The use, distribution or reproduction in other forums is permitted, provided the original author(s) and the copyright owner(s) are credited and that the original publication in this journal is cited, in accordance with accepted academic practice. No use, distribution or reproduction is permitted which does not comply with these terms.

# Pleiotropy drives evolutionary repair of the responsiveness of polarized cell growth to environmental cues

Enzo Kingma, Eveline T. Diepeveen, Leila Iñigo de la Cruz and Liedewij Laan\*

Department of Bionanoscience, Kavli Institute of NanoScience, Faculty of Applied Sciences, Delft University of Technology, Delft, Netherlands

The ability of cells to translate different extracellular cues into different intracellular responses is vital for their survival in unpredictable environments. In *Saccharomyces cerevisiae*, cell polarity is modulated in response to environmental signals which allows cells to adopt varying morphologies in different external conditions. The responsiveness of cell polarity to extracellular cues depends on the integration of the molecular network that regulates polarity establishment with networks that signal environmental changes. The coupling of molecular networks often leads to pleiotropic interactions that can make it difficult to determine whether the ability to respond to external signals emerges as an evolutionary response to environmental challenges or as a result of pleiotropic interactions between traits. Here, we study how the propensity of the polarity network of *S. cerevisiae* to evolve toward a state that is responsive to extracellular cues depends on the complexity of the environment. We show that the deletion of two genes, *BEM3* and *NRP1*, disrupts the ability of the polarity network to respond to cues that signal the onset of the diauxic shift. By combining experimental evolution with whole-genome sequencing, we find that the restoration of the responsiveness to these cues correlates with mutations in genes involved in the sphingolipid synthesis pathway and that these mutations frequently settle in evolving populations irrespective of the complexity of the selective environment. We conclude that pleiotropic interactions make a significant contribution to the evolution of networks that are responsive to extracellular cues.

## KEYWORDS

laboratory evolution, adaptation, phenotypic plasticity, fluctuating environment, cell architecture, cell polarity

## Introduction

Polarity establishment, the ability to generate an asymmetric distribution of cellular constituents, plays an important role in many of the biological functions that are observed throughout the tree of life (Piroli et al., 2019). The dynamics of polarity establishment is regulated by an intricate network of molecular interactions, many of which are evolutionary

conserved (Etienne-Manneville, 2004; Thompson, 2013; Chiou et al., 2017). What allows these networks to be versatile while maintaining a relatively high degree of conservation is their ability to generate different responses to various extracellular signals (Dickinson, 2008; Saito, 2010; Waltermann and Klipp, 2010). This feature makes it possible for the polarized appearance of cells to vary between environmental contexts (Granek et al., 2011).

Responsiveness to extracellular signals requires the integration of the polarity network with other molecular networks that either directly or indirectly translate these signals into an intracellular response (Saito, 2010; Waltermann and Klipp, 2010; Granek et al., 2011; Broach, 2012; Mutavchiev et al., 2016; Salat-Canela et al., 2021). An issue of integrated networks is that the decrease in modularity that arises when networks become coupled can frustrate evolvability (Fisher, 1930; Wagner and Altenberg, 1996; Kirschner and Gerhart, 1998; Hartwell et al., 1999; Wagner and Zhang, 2011). Because coupled networks become interdependent, the likelihood that a single mutation affects multiple phenotypic traits, an effect known as pleiotropy (Fisher, 1930; Wagner and Zhang, 2011), increases. Such pleiotropic effects are indeed frequently reported for genes involved in the establishment of cell polarity (Bauer et al., 1993; Zou et al., 2008; Prunskaitė-Hyyryläinen et al., 2014). As antagonistic effects, where a mutation that is beneficial to one trait negatively affects a second trait (Paaby and Rockman, 2013; Austad and Hoffman, 2018; Mauro and Ghalambor, 2020), are considered to be more common than synergistic effects, pleiotropy is generally expected to constrain the number of accessible mutations during evolution in complex environments that select on multiple traits (Fisher, 1930; Waxman and Peck, 1998; Orr, 2000; Welch and Waxman, 2003). In turn, evolution in simple environments may not be constrained by pleiotropic interactions, but can instead lead to the deterioration of networks regulating unused traits (Rose and Charlesworth, 1980; MacLean et al., 2004; Qian et al., 2012; Fraebel et al., 2017). Thus, the molecular details of adaptive evolution of the polarity network are expected to depend on the environment: complex environments only allow mutations that preserve the integrity of coupled networks, while the released constraint in simple environments allows the system to explore alternative evolutionary pathways, but at the cost of the disintegration of unused networks and a loss of the ability to respond to environmental cues. However, whether these theoretical expectations form a general rule for the evolution of pleiotropically connected traits and if exceptions can be identified based on the molecular basis of their pleiotropic interactions is still a point of discussion (Agrawal and Stinchcombe, 2009; Jerison et al., 2020).

An attractive system to study the effect of pleiotropic interactions on the evolution of cell polarity is the yeast *Saccharomyces cerevisiae*. *S. cerevisiae* has adopted asymmetric cell division as its main mode of proliferation and must therefore establish an axis of polarity once per cell cycle (Martin and Arkowitz, 2014; Chiou et al., 2017). In addition, its polarity network is integrated with several different signaling networks to allow different growth modes in response to environmental cues, such as those that signal cell cycle progression (Yoshida and Pellman, 2008), filamentous growth (Cullen and Sprague, 2012) and the activation of stress response pathways (Saito, 2010; Waltermann and Klipp, 2010). Here, we study whether the polarity network can restore its coupling to signaling networks after this

coupling has been lost due to a genetic perturbation and how this restoration depends on selective pressures from the environment. In addition, we discuss whether known connections between the polarity network and other signaling pathways are able to explain our observed patterns of adaptation. To do this, we use a *bem3Δnrp1Δ* strain of *S. cerevisiae* that has been demonstrated to be defective in polarity establishment during vegetative growth. We show that this genetic perturbation also disrupts the responsiveness of the polarity network to an environmental shift that induces cells to change their metabolic program. Using a combination of experimental evolution and whole-genome sequencing, we find that adaptive mutations that restore the responsiveness of the polarity network to this environmental insult emerge frequently and reproducibly in evolving populations and that their occurrence is surprisingly insensitive to the complexity of the environment.

## Results

### Deletion of BEM3 and NRP1 distorts cellular adaptation during the diauxic shift

The combined deletion of *BEM3* and *NRP1* has been shown previously to cause defects in polarity establishment that exceed the summed effects of their individual deletion (Laan et al., 2015), meaning they exhibit epistasis (Phillips, 2008). The existence of epistatic interactions between these mutations suggests a functional relation between Bem3 and Nrp1. This is surprising, because while Bem3 is known as a GTP Activating Protein (GAP) for Cdc42, the master regulator of cell polarity (Etienne-Manneville, 2004), Nrp1 has never been implicated to be involved in polarity establishment before. Instead, based on the current knowledge about its function, Nrp1 is best described as a prion forming protein that localizes to stress granules formed under conditions of glucose stress (Buchan et al., 2008; Kroschwald et al., 2015). This led us to hypothesize that the deletion of *BEM3* and *NRP1* may have consequences for the ability of the polarity network to respond to environmental cues that signal different growth modes.

We tested this hypothesis in the context of the ability of *S. cerevisiae* to perform diauxic growth between glucose and ethanol. In the presence of extracellular glucose, *S. cerevisiae* maintains a rapid mode of growth by alcoholic fermentation of glucose. The ethanol produced during alcoholic fermentation can be used as an alternative energy source when extracellular glucose drops below a critical level, but only in the presence of extracellular oxygen. The transition from the fermentation of glucose to the respiration of ethanol, a growth phase known as the diauxic shift, is characterized by several physiological changes (Galdieri et al., 2010), which includes changes in the polarized distribution of the actin cytoskeleton (De Virgilio and Loewith, 2006; Galdieri et al., 2010).

We qualitatively determined the effects of deleting *BEM3* and *NRP1* on the coupling of (diauxic growth) glucose sensing to cell polarity by imaging *bem3Δnrp1Δ* cells during the diauxic shift (Figure 1A). The diauxic shift was induced by switching from growth media containing glucose as the sole carbon source to one



where ethanol was the sole carbon source using a microfluidic device. A wild-type strain subjected to these conditions displayed the expected behavior, which consisted of rapid growth on glucose followed by a short growth pause at the time of the media switch, after which growth was resumed on ethanol media, but at a slower rate compared to growth on glucose media (Brauer et al., 2005). Overall, *bem3Δnrp1Δ* cells followed the same pattern that we observed for the wild-type cells, but critically failed to produce buds during growth on ethanol media. Instead, isotropic growth was sustained in these cells up to the point where it induced cell death by lysis. Based on the link between polarity defects and an increase in cell size, we deduced that our observations for the *bem3Δnrp1Δ* phenotype are the result of the inability of the polarity network to respond appropriately to the physiological changes that occur during the diauxic shift. Specifically, while *bem3Δnrp1Δ* mutants are generally less fit than the wild-type strain, the cellular defect that leads to a lower fitness differs between conditions of standard vegetative growth and conditions where the cells must respond to the diauxic shift. During vegetative growth (2% glucose in Figure 1A) *bem3Δnrp1Δ* cells proliferate, but do so at a slower rate than wild-type cells. After the media switch (transition from 2% glucose to 3% ethanol in Figure 1A) *bem3Δnrp1Δ* cells enlarge, but are unable to divide.

Next, we quantified the effect of deleting *BEM3* and *NRP1* on the diauxic shift using Optical Density (OD) measurements of population growth in order to obtain growth curves for each strain (Figures 1B, D). The diauxic shift was clearly visible in the growth curves as a transition period between two exponential growth phases with different growth rates. For technical reasons (see Supplementary Figure 1), we used media containing a high glucose concentration (2%) to quantify growth before the diauxic shift and a lower glucose concentration (0.1%) to quantify growth after the diauxic shift. We extracted the growth rate during the exponential phase before and after the occurrence of the diauxic shift by calculating the slope of the linear portion of the growth curve when plotted on a semi-log scale. These values were subsequently converted into their corresponding doubling times ( $T_{PRE-shift}$  and  $T_{POST-shift}$ ). This analysis revealed that *bem3Δnrp1Δ* populations have a significantly longer doubling time than the wild-type both before and after onset of the diauxic shift (Figures 1C, E). While it is expected that the overall fitness defect of *bem3Δnrp1Δ* mutants will lead to longer doubling times both before and after the diauxic shift, we argue based on our microfluidic experiment (Figure 1A) that the physiological cause that leads to a lower doubling time is different between the two conditions. Before the diauxic shift, *bem3Δnrp1Δ* cells divide at a slower rate than the wild-type strain due to a defect in polarity establishment which causes a longer  $T_{PRE-shift}$ . In contrast,  $T_{POST-shift}$  is affected by both the slower division rate and the higher death rate of *bem3Δnrp1Δ* cells as the polarity defect becomes much more severe at the onset of the diauxic shift. In support of this idea, we found that *bem3Δnrp1Δ* populations stop growing at a significantly lower OD than wild-type populations after the diauxic shift (ratio wild-type: *bem3Δnrp1Δ* = 2.25, Figure 1F), while both strains enter the diauxic shift at approximately the same density (ratio wild-type: *bem3Δnrp1Δ* = 1.15, Figure 1F). We therefore interpret these results as indications that the defects in polarity establishment caused by the deletion of *BEM3* and *NRP1* makes the polarity network insensitive to environmental

cues that signal the onset of the diauxic shift. The loss of responsiveness to these cues causes an inability to establish a polarity site when the physiological changes related to the diauxic shift have taken place, leading to prolonged isotropic growth and an increase in cell size.

## Recoupling of polarity establishment to sensing networks does not require a complex environment

We sought to determine whether the environment is the decisive factor that controls the adaptive value of restoring the cellular response to the diauxic shift during evolution. To do this, we took an experimental approach and evolved several parallel wild-type and *bem3Δnrp1Δ* populations in two frequently used set-ups for experimental evolution (Figure 2). In the first set-up, the *batch culture*, nutrient levels vary over time and cells experience periods of glucose depletion several times throughout the experiment (Brauer et al., 2005; Gresham and Dunham, 2014). Mutations that allow cells to correctly coordinate the physiological changes necessary to pass through the diauxic shift with those that regulate polarity establishment are therefore expected to be beneficial during evolution in a batch culture set-up, as this extends the overall number of progeny that a cell can produce before each passage. In the second set-up, the *glucose limited continuous culture*, nutrient concentrations remain constant after a steady state is reached and growth is maintained at a constant rate (Brauer et al., 2005; Gresham and Dunham, 2014). These constant environmental conditions have the consequence that cells do not induce the majority of the cellular responses that are associated with the diauxic shift (Brauer et al., 2005). Thus, the ability to perform diauxic growth appears as a dispensable trait during evolution in a continuous culture. Based on the theoretical assumptions that traits that do not experience selective pressure (1) tend to deteriorate and (2) are unlikely to fix mutations that improve their function during evolution, we expect restoration of diauxic growth by *bem3Δnrp1Δ* populations to emerge only during batch culture evolution.

We evolved a total of 14 *bem3Δnrp1Δ* populations and 2 wild-type populations in the glucose limited continuous culture for 70 generations. The parameter  $T_{PRE-shift}$  was used as a proxy for adaptations that restore the polarity defect caused by the deletion of *BEM3* and *NRP1*, but that do not necessarily improve the ability of the polarity network to respond to cues that signal the onset of the diauxic shift. Alternatively,  $T_{POST-shift}$  was used as a proxy for adaptations that improve the response of cells to the diauxic shift. The values of  $T_{PRE-shift}$  and  $T_{POST-shift}$  of the evolved cell lines were determined by reviving the evolved population from a frozen stock and measuring the change in OD over time in media containing 2% and 0.1% glucose, respectively. This procedure is the same as what was done to determine  $T_{PRE-shift}$  and  $T_{POST-shift}$  for the ancestral wild-type and *bem3Δnrp1Δ* populations (see Figures 1B, D, and the section “Materials and methods”).

Comparison of  $T_{PRE-shift}$  between the evolved populations and their ancestor (Figure 3A) revealed that all evolved populations had either a similar or lower value for  $T_{PRE-shift}$  relative to their

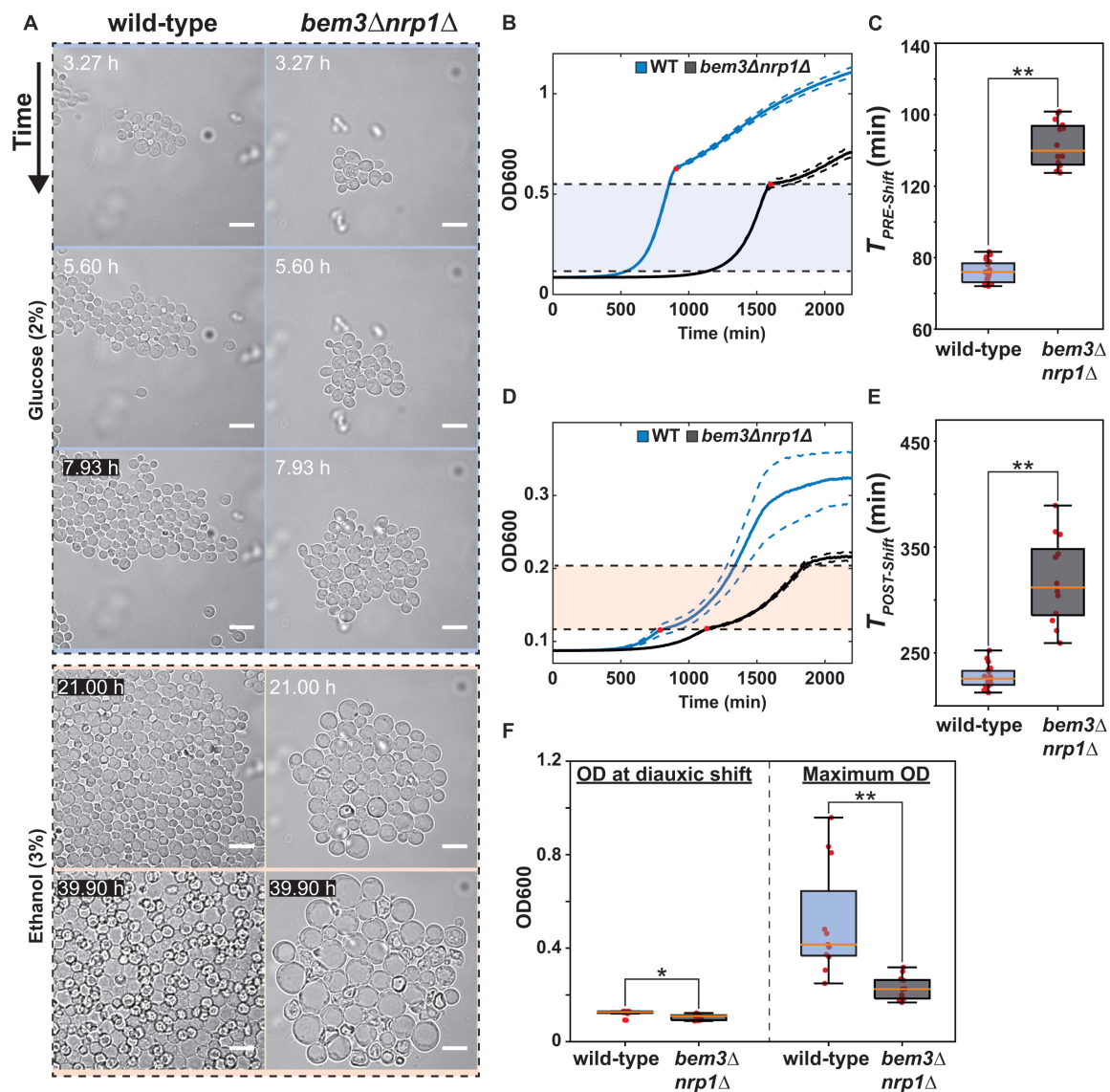
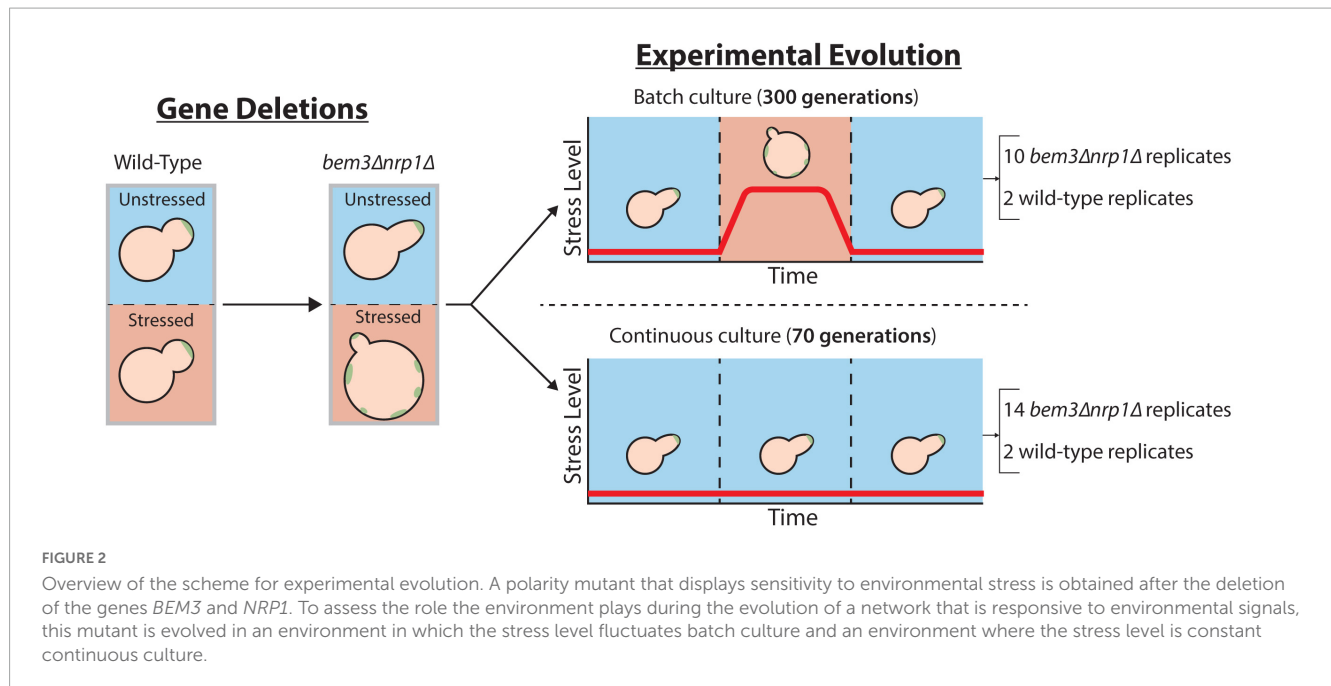


FIGURE 1

Deletion of *bem3Δnrp1Δ* causes defects in pre- and post-diauxic growth. (A) Time-lapse series of the diauxic shift. The WT and *bem3Δnrp1Δ* strain were subjected to a switch from 2% glucose media to 3% ethanol media after 8 h in 2% glucose media. The images show that while the WT strain is able to resume growth, the *bem3Δnrp1Δ* cells increase in size without producing daughter cells. Scale bars represent 10  $\mu$ m (B) Growth curves of a WT (blue) and the *bem3Δnrp1Δ* mutant (black) when grown in 2% glucose media. This data was used to obtain a measure for  $T_{PRE-shift}$ . Red dots indicate the point of diauxic shift, dashed lines represent the Standard Error of the Mean (SEM). (C) Doubling time of the WT strain and the *bem3Δnrp1Δ* mutant during growth before the diauxic shift is entered ( $T_{PRE-shift}$ ). (D) Growth curves of a WT (blue) and the *bem3Δnrp1Δ* mutant (black) when grown in 0.1% glucose media. This data was used to obtain a measure for  $T_{POST-shift}$ . Red dots indicate the point of diauxic shift, dashed lines represent the SEM. (E) Doubling time of the WT strain and the *bem3Δnrp1Δ* mutant during growth after passing through diauxic shift is entered ( $T_{POST-shift}$ ). (F) Comparison of the OD at which the *bem3Δnrp1Δ* mutant and the WT strain enter the diauxic shift and their OD at stationary phase when grown in YP + 0.1% glucose. The plot shows that while both strains enter diauxic shift at around the same density, the final density of the populations differ. \* $p$ -value < 0.05, \*\* $p$ -value < 0.005, Welch t-test.

ancestor. In contrast, we find that for  $T_{POST-shift}$  half of the evolved *bem3Δnrp1Δ* populations (7/14) had a lower doubling time, while the other half (7/14) had a longer doubling time relative to their ancestor, indicating that changes in diauxic growth do not affect fitness in a continuous culture. A similar trend for  $T_{PRE-shift}$  and  $T_{POST-shift}$  was visible for our two evolved wild-type populations. Taken together, these observations support our initial view that a continuous culture selects for faster vegetative growth, but not diauxic growth.

The finding that some of *bem3Δnrp1Δ* populations evolved in the continuous culture show improvements in  $T_{POST-shift}$  could be explained by a possible interdependence of  $T_{PRE-shift}$  and  $T_{POST-shift}$ : improvements in  $T_{PRE-shift}$  may be caused by mutations that increase the overall rate of cell division and these mutations will therefore also lead to improvements in  $T_{POST-shift}$ . However, these mutations do not necessarily also resolve the high death rate of *bem3Δnrp1Δ* mutants at the start of the diauxic shift (Figure 1A), which may be a major factor that determines



$T_{POST-Shift}$ . To verify that a decrease in  $T_{POST-Shift}$  relates to adaptations that resolve the high death rate, we imaged cells from the evolved population with the lowest (fastest growing, CCE1) and highest (slowest growing, CCE2) value for  $T_{POST-Shift}$  during the diauxic shift (Figure 3C) using the same microfluidic set-up we used in Figure 1. In agreement with our expectations, the results showed that the phenotype of CCE1 after switching to ethanol media was qualitatively more similar to that of our ancestral wild-type strain and CCE1 cells were able to resume proliferation after the diauxic shift. Alternatively, the phenotype of CCE2 was more similar to the ancestral *bem3Δnrp1Δ* strain, as CCE2 cells enlarged and were frequently unable to divide after the onset of the diauxic shift.

We evolved 8 *bem3Δnrp1Δ* and 2 wild-type populations in a batch culture with a daily passaging procedure. We initially maintained the same number of generations for evolution as we had done for the continuous culture (70 generations), but after assessing our proxies for fitness we were unable to identify any significant changes in the values of  $T_{PRE-Shift}$  and  $T_{POST-Shift}$  between the evolved populations and their ancestors (see Supplementary Figure 2). We assumed that this is due to the frequent population bottlenecks that occur during the passaging of the populations, which can slow down the rate of adaptation by purging beneficial mutations from the population (Wein and Dagan, 2019). We provide an estimate of the effect of population bottlenecks on the fixation dynamics of beneficial mutations in Supplementary Section 1, which shows that bottlenecks vastly increase the expected number of generations that are required before a beneficial mutation that fixates in the population will emerge. To compensate for this effect of population bottlenecks, we allowed our batch culture experiment to run for an additional 230 generations such that the total number of generations was 300.

We found that all evolved populations grew faster than their ancestors, both before and after the diauxic shift (Figure 3B).

The fact that we do not observe populations that evolve toward a state where the doubling time after the diauxic shift becomes longer suggests that these pathways are inaccessible during evolution in a batch culture. Taken together, these results imply that the environmental variability that exists in the batch culture imposes constraints on the diauxic growth pattern that can be attained during evolution, allowing only those where growth on both nutrients is improved, while the stable environment of the continuous culture releases some of these constraints. As a result, phenotypes that have evolved to perform well during the diauxic shift, presumably through evolutionary repair of the polarity defects caused by deleting *BEM3* and *NRP1*, only reproducibly emerge in a batch culture. However, although the degree of reproducibility is lower, similar phenotypes do frequently evolve in a continuous culture. This indicates that evolutionary constraints imposed by the environment are not sufficient to explain the restoration of the responsiveness of the polarity network to cues of the diauxic shift during evolution.

### Populations with a restored responsiveness to extracellular cues accumulate mutations in genes related to the sphingolipid synthesis pathway

To understand the molecular basis of the different adaptations of  $T_{PRE-Shift}$  and  $T_{POST-Shift}$  we observed in our continuous and batch cultures, we performed Whole Genome Sequencing (WGS) on the 22 evolved *bem3Δnrp1Δ* lines and the 4 evolved wild-type controls and compared them to the genome of their wild-type ancestor (see section “Materials and methods”). We looked for patterns of parallel evolution by restricting our analysis to genes that were mutated in at least 2 different populations evolved in the same environment. This resulted in a total of 88 genes



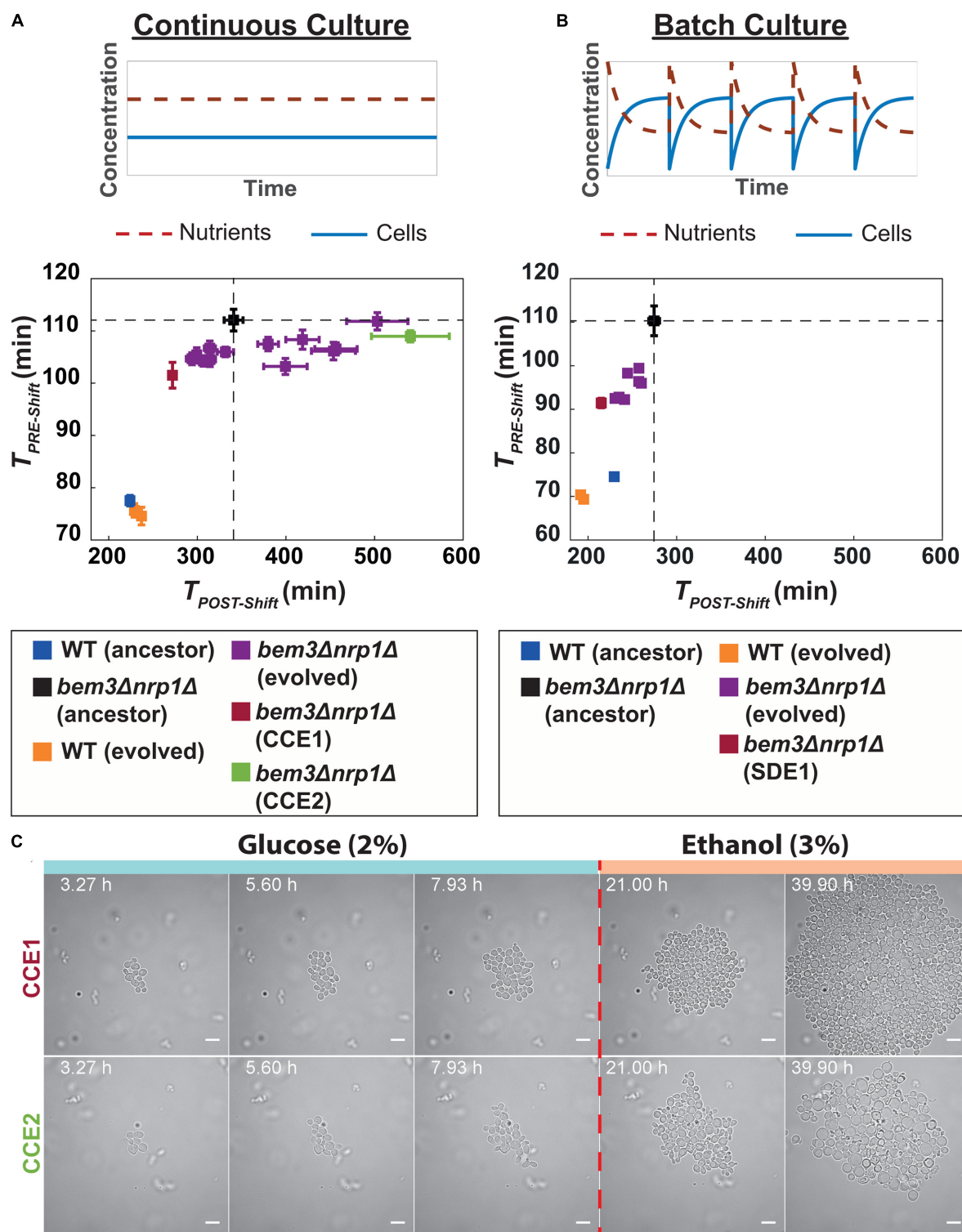


FIGURE 3

Experimental evolution of *bem3Δnrp1Δ* mutants in a constant and variable environment. **(A)** (Top) In a continuous culture, both nutrient concentration and cell density remain constant over time. (Bottom) Scatter plot of  $T_{PRE-Shift}$  against  $T_{POST-Shift}$  for 14 evolved *bem3Δnrp1Δ* lines and 2 wild-type populations after 70 generations of evolution in a continuous culture. Dashed lines indicate the values of  $T_{PRE-Shift}$  and  $T_{POST-Shift}$  of ancestral *bem3Δnrp1Δ* strain. Error bars show the SEM. **(B)** (Top) In a batch culture there are periodic fluctuations over time in nutrient concentration and cell density. (Bottom) Scatter plot of  $T_{PRE-Shift}$  against  $T_{POST-Shift}$  for 8 evolved *bem3Δnrp1Δ* lines and 2 WT lines after 300 generations of evolution in a batch culture. Dashed lines indicate the values of  $T_{PRE-Shift}$  and  $T_{POST-Shift}$  of ancestral *bem3Δnrp1Δ* strain. Error bars show the SEM. **(C)** Time-lapse of evolved lines CCE1 and CCE2 (continuous culture) during a sudden switch from 2% glucose media to 3% ethanol media (dashed red line). The images show that evolved line CCE1 contains cells that have a response to this environmental change that is phenotypically similar to the response of the WT strain. Evolved line CCE2 has a response that resembles the response of the ancestral *bem3Δnrp1Δ*, but with a smaller increase in cell size (see Figure 1A). Scale bars represent 10  $\mu$ m.



that acquired non-synonymous mutations or indels in 2 or more evolved populations (including the wild-type lines).

The most notable environment-specific mutations were the early stop codons in *WHI2* that frequently occurred in the populations evolved in the continuous culture: 12 out of 14 evolved *bem3Δnrp1Δ* and both evolved WT controls had mutated *WHI2*. Disruptive mutations in *WHI2* have also been reported in other experimental evolution studies that used nutrient limited continuous cultures (Kvitek and Sherlock, 2013; Hong and Gresham, 2014) and these mutations therefore likely provide a general advantage during adaptation to nutrient-limiting conditions.

Because we saw the same phenotype emerge in the batch culture and continuous culture (populations that decreased  $T_{POST-Shift}$ ), we questioned whether the molecular basis of these adaptations were similar. In total, 22 genes were mutated in at least 2 of the *bem3Δnrp1Δ* lines evolved in each environment. We grouped these genes according to their Biological Process Gene Ontology (GO) annotation on the Saccharomyces Genome Database. This revealed that populations evolved in a continuous culture had more mutations in genes involved in the stress response, while populations from the batch culture had slightly more mutations in genes related to transcription and translation. We then split the evolved populations into two groups: those that evolved to decrease  $T_{POST-Shift}$  (7/14 populations of the continuous culture and 8/8 populations of the batch culture) and those that evolved to increase  $T_{POST-Shift}$  (7/14 populations of the continuous culture and 0/8 populations of the batch culture). Interestingly, populations with a decreased  $T_{POST-Shift}$  had more mutations in lipid metabolic genes than those that did not decrease  $T_{POST-Shift}$ . Of the 14 *bem3Δnrp1Δ* populations that were evolved in the continuous culture, 6/7 populations with a decreased  $T_{POST-Shift}$  had mutations in the *IPT1*, while we only found mutations in this gene in 1/7 populations with an increased  $T_{POST-Shift}$  (Figure 4). In the batch culture populations, 2/8 had acquired mutations in *IPT1*, while 3/8 had mutations in *SUR1*. Notably, *Ipt1* acts directly downstream of *Sur1* in the pathway for the synthesis of complex sphingolipids (Thevisen et al., 2000; Dickson et al., 2006; Morimoto and Tani, 2015).

Based on this correlation we hypothesize that, after the deletion of *Bem3* and *Nrp1*, the robustness of the polarity module during the diauxic shift can be (partially) restored by changes in the lipid composition of the plasma membrane. Interestingly, this strategy appears to be dominant for repairing the defect caused by the deletion of *BEM3* and *NRP1* regardless of whether diauxic growth is part of the selective environment.

## Discussion

The ability to respond to environmental cues is a crucial factor for the survival of organisms in complex environments. For example, studies have indicated that pathogens increase the likelihood of successfully infecting a host by adjusting their physiology to match the host's circadian rhythm (Kahl Lisa et al., 2022). Here, we used a genetically perturbed strain of *S. cerevisiae* to investigate the contribution of the environment in shaping a polarity network that can translate the extracellular

signals for diauxic growth into an intracellular response. We show that the deletion of *BEM3* and *NRP1* has previously unknown consequences for polarity establishment that diminishes its capacity to respond to these extracellular signals and impedes the ability of cells to successfully navigate through the diauxic shift. Which molecular mechanisms are affected by the deletion of *BEM3* and *NRP1* in such a manner that it leads to the observed phenotype are not addressed in this study. However, the results from several other studies that have looked at the relationship between environmental stress and cell morphology allow us to formulate a hypothesis on how the deletion of *BEM3* and *NRP1* causes the decoupling of cell polarity from diauxic growth. The link between cell morphology and environmental stress is frequently proposed to be a consequence of the loss of polarity of the actin cytoskeleton induced by stress factors (Sivadon et al., 1995; Balguerie et al., 2002; Uesono et al., 2004; Homoto and Izawa, 2018). Failure to repolarize the actin cytoskeleton following environmental stress, either due to the severity of the stress conditions (Homoto and Izawa, 2018) or due to the loss of a genetic component required for repolarization (Sivadon et al., 1995; Balguerie et al., 2002), results in enlarged cells. The similarity of these hypertrophied cells under conditions of environmental stress to the phenotype of *bem3Δnrp1Δ* mutants we observe during a transition from glucose-containing media to ethanol-containing media suggests they are caused by a defect in a similar pathway. Indeed, the depletion of glucose, one of the hallmark cues for entry into the diauxic shift (Brauer et al., 2005), has also been shown to cause the rapid and transient depolarization of actin in wild-type cells (Uesono et al., 2004; Vasicova et al., 2016). The repolarization of actin in the context of glucose depletion depends on the activation of the respiratory metabolism (Uesono et al., 2004), as cells with dysfunctional mitochondria do not repolarize actin (Uesono et al., 2004; Vasicova et al., 2016). Thus, one possibility is that the deletion of *BEM3* and *NRP1* causes defects in respiration. However, we consider this unlikely based on our observation that *bem3Δnrp1Δ* cells are still able to grow, although only isotropically, in media containing ethanol as the only carbon source. In addition, if mitochondrial dysfunction were the cause of the observed phenotype, mutations related to mitochondrial function would be expected to arise during our evolution experiments, but this was not the case.

Instead, our results suggest that the defects in diauxic growth of *bem3Δnrp1Δ* mutants are suppressed by mutations in the sphingolipid synthesis pathway. Interestingly, the genes (*IPT1* and *SUR1*) that were frequently mutated in evolved *bem3Δnrp1Δ* populations with a (partially) restored ability to pass through the diauxic shift are also known to suppress the sensitivities to stress and starvation that arise after the deletion of genes that encode for the amphiphysin-like proteins *Rvs161* and *Rvs167* (Desfarges et al., 1993; Balguerie et al., 2002). *Rvs161* and *Rvs167* have a direct role in regulating the polarity of the actin cytoskeleton (Amberg et al., 1995; Munn et al., 1995; Sivadon et al., 1995, 1997; Breton and Aigle, 1998) and their loss causes defects in the depolarization and repolarization dynamics of actin during stress in an equivalent manner as has been described for glucose stress in the section above (Crouzet et al., 1991; Bauer et al., 1993; Sivadon et al., 1995). Suppression of these defects through the deletion of *IPT1* or *SUR1* has been reported to act by

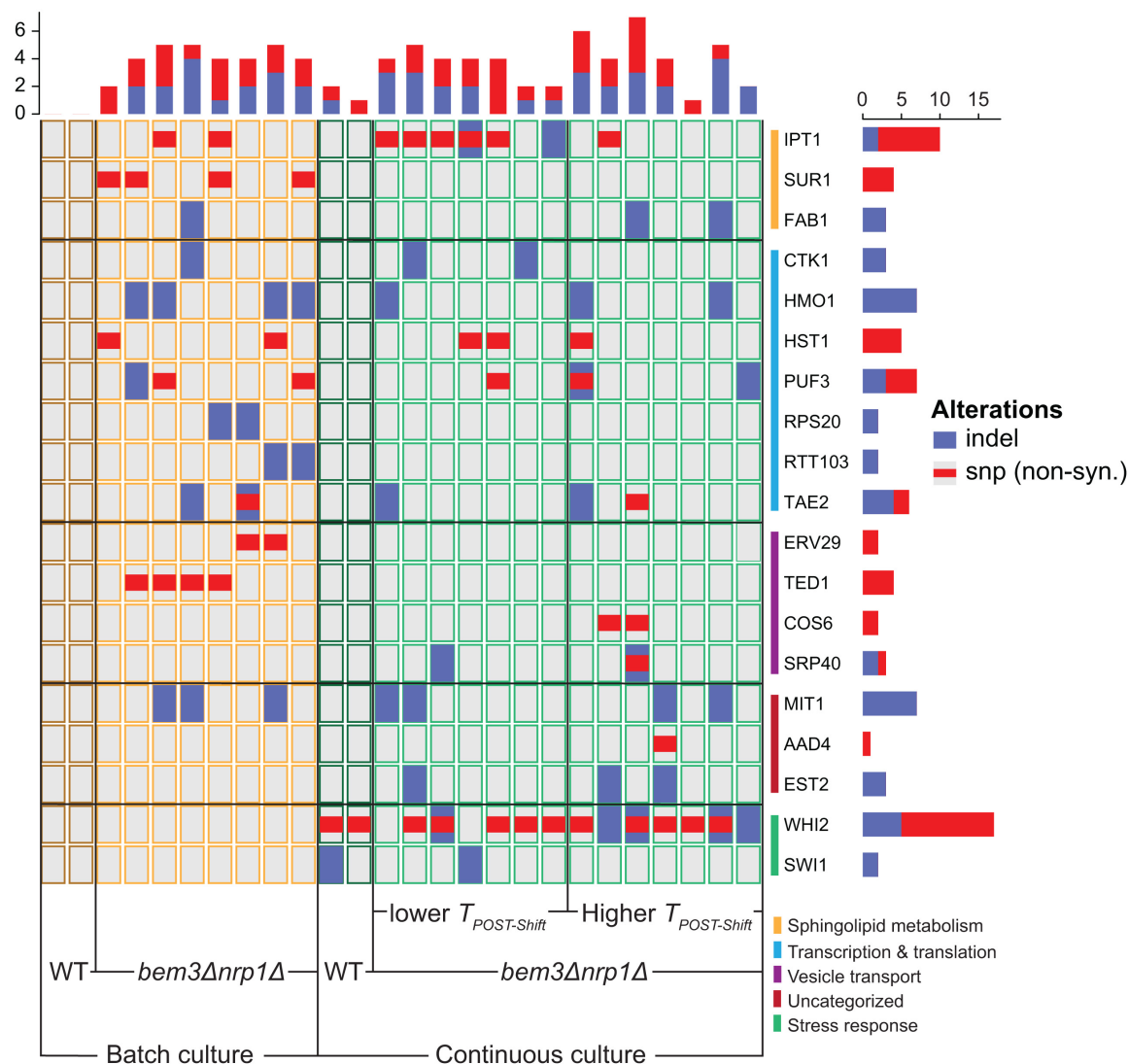


FIGURE 4

The mutational spectrum of different phenotypic subgroups that emerged after experimental evolution of *bem3Δnrp1Δ* populations. The mutant-specific mutations found in each gene for evolved continuous culture lines that decreased their respiration rate, evolved continuous culture lines that increased their respiration rate and evolved batch culture lines. Genes are grouped according to their cellular process GO-term. All genes shown were only mutated in the *bem3Δnrp1Δ* populations and not in the wild-type populations, with the exception of *WHI2* and *SWI1*, which were also found to be mutated in the wild-type populations evolved in the continuous culture.

preventing the full depolymerization of actin under stressful conditions (Balguerie et al., 2002), thereby relieving some of the consequences of an inability to repolarize actin. Extrapolating these findings to *bem3Δnrp1Δ* mutants, this implies that the evolutionary repair of diauxic growth in *bem3Δnrp1Δ* populations acts by directly modulating actin dynamics using sphingolipid synthesis as a control knob. Similarly, the pleiotropic effects resulting from the deletion *BEM3* and *NRP1* are therefore likely a consequence of the dual role of actin in polarized growth and stress response pathways (Ho and Bretscher, 2001; Leadsham et al., 2010; Smethurst et al., 2014) that couples polarity establishment to the diauxic shift.

It remains unclear why the consequences of deleting *BEM3* and *NRP1* are different for the actin dynamics required during vegetative growth and the actin dynamics under stressed

conditions. Much alike to what happens under conditions of stress, the actin cytoskeleton must depolarize and repolarize during the cell cycle to switch between modes of isotropic and polarized growth (Lew and Reed, 1993; Welch et al., 1994; Pruyne and Bretscher, 2000; Ahn et al., 2001; Bi and Park, 2012). However, our results show that polarized growth during the vegetative cell cycle is not strongly affected by the deletion of *BEM3* and *NRP1*, while polarized growth after the stress response of the diauxic shift is strongly diminished. This suggests that cell cycle-related polarization of actin may be regulated by a different pathway than the polarization of actin during the stress response. We find that, despite that they may be regulated by different pathways, the ability to perform polarized growth in both contexts can be restored by mutations in genes related to sphingolipid synthesis. Surprisingly, the fixation of these

mutations that restore both vegetative and diauxic growth does not strongly depend on the complexity of the environment. Instead, we frequently see them emerge in populations evolved under constant conditions where improved diauxic growth appears to have no selective benefit, as is supported by our result that nearly all populations evolved in the continuous culture inactivate *WHI2*, which encodes for a protein that initiates the stress response during nutrient depletion (Sudbery et al., 1980; Saul et al., 1985; Radcliffe et al., 1997; Kaida et al., 2002). Interestingly, a recent study investigating the adaptive response of *Escherichia coli* to different temperature fluctuation regimes also found that the same mutations frequently evolve in parallel in a manner that does not depend on the dynamics of the selective environment (Lambros et al., 2021). A large-scale phenotypic assay revealed that the evolved strains generally became closer to the phenotype of their ancestor under a large number of conditions, leading to the hypothesis that an innate evolutionary response of an organism in a stressful environment is to evolve in such a way that their physiology resembles that of their (fitter) ancestor in unstressed conditions. Overall our results agree with this hypothesis, as we find that genetically perturbed cells frequently evolve to better match the cellular response of their ancestor, even in unseen environmental conditions. Possible explanations for why the fixation of mutations that restore the cellular response to conditions beyond those experienced during adaptation would be preferred are that (1) these mutations might occur more frequently in the population because they constitute mutational hotspots or (2) their fixation is purely driven by the fitness benefit that they confer to vegetative growth and the restored diauxic growth is merely a side effect of a pleiotropic interaction network. In conclusion, our results demonstrate that the evolution of interaction networks that can sense and respond to different environmental signals should not always be interpreted as adaptive, but may instead be a consequence of a strong integration between different interaction networks regulating different cellular functions. Such an integration of different interaction networks may also be able to explain observations of the seemingly purposeless emergence of phenotypic plasticity, the ability of an organisms to adjust its phenotype to its environment, during evolution in constant environmental conditions (Fraebel et al., 2020).

## Materials and methods

### Yeast strains and media preparation

All strains used in this study are derived from the W303 background and are *MATa* haploid cells. We used yLL132a as our WT strain and yLL143a as our *bem3Δnrp1Δ* strain (Laan et al., 2015), which has the same genetic background as yLL132a, but with *BEM3* and *NRP1* replaced with, respectively, the natMX4 (clonNAT-Nourseothricin resistance) and hphMX4 (Hygromycin B resistance) cassettes. For batch culture evolution experiments, standard rich media (10 g/L Yeast Extract, 20 g/L Peptone and 20 g/L Dextrose) was used and was prepared by dissolving 50 g/L from a premixed batch of ingredients (Sigma-Aldrich) in H<sub>2</sub>O. For chemostat evolution experiments the same premix was used,

but supplemented with 19 g/L extra Yeast Extract and 9.5 g/L extra Peptone to obtain a final dextrose concentration of 1 g/L. A total of 0.1 mg/mL Ampicillin was added to the chemostat media as a safeguard against bacterial contamination. Microscopy experiments were performed in Synthetic Complete (SC) media prepared from Complete Supplement Mixture without amino acids, riboflavin and folic acid (750 mg/L), Yeast Nitrogen Base (6.9 g/L) and either Dextrose (2%w/v) or Ethanol (3%v/v) as a carbon source. All media was filter sterilized to avoid degradation of components during autoclaving.

## Experimental evolution of continuous cultures

### Multiplexed chemostat array set-up

We performed our evolution experiments in a dextrose limited chemostat environment by setting up a multiplexed chemostat array of 16 cultures according to the protocol from Miller et al. (2013). YP 0.1%D media was filter sterilized directly into a 10 L glass carboy. During the run, fresh media was provided to the cultures from this carboy by using a peristaltic pump fitted with Marprene tubing. The correlation between rotation speed and media flow rate was empirically determined by measuring the effluent volume at different rotation speeds. Aquarium pumps were used to maintain the positive pressure inside the culture chambers required for the removal of excess culture volume, to keep the cultures aerated and mixed. To minimize evaporation and maintain sterility, air from the pumps was first routed through gas washing bottles and 0.45 μm PTFE filters before entering the culture chambers. The temperature was regulated at 30°C using heat blocks.

### Initialization of multiplexed arrays

We initialized our multiplexed chemostat arrays by allowing the culture chambers to fill with media until the volume exceeded 20 mL. We dissolved cells from a glycerol stock in YP 0.1 %D media and used to inoculate the cultures by aseptically injecting 4 mL into each culture chamber. In total, 14 *bem3Δnrp1Δ* cultures and 2 WT cultures were inoculated using this procedure. With the peristaltic pump turned off and the aquarium pumps turned on, the *bem3Δnrp1Δ* cultures were left to grow for 4 days and the WT cultures were left to grow for 2 days until they reached saturation (batch phase growth). After the cultures reached saturation, the culture volume was set at  $20 \pm 1$  mL while performing the zero time point sampling.

### Sampling regimen

All cultures were sampled twice a week. Samples were taken by replacing the effluent bottles with sterile sampling bottles and collecting the effluent on ice over a period of approximately 2 h. Directly after sampling, 1 mL of each collected sample was mixed with 500 μL glycerol and stored at −80°C. Optical Density (OD) measurements at 600 nm were taken of each sample in 10 mm plastic cuvettes using a photospectrometer (Nanorop 2000C). When necessary, samples were diluted with YP to obtain a final OD of between 0.1 and 1.5. All samples were diluted in the same media used for blanking the photospectrometer. Effluent

volumes were measured daily with a graduated cylinder from which the volume could be read with 0.5 ml precision. On days that sampling took place, the effluent volume of samples was determined after the standard procedure for sampling (glycerol stocks and OD measurements).

### Calculation of dilution rates and generation times

We calculated the dilution rate  $D$  of each sample in our multiplexed chemostat array from the effluent volume using the following formula:

$$D = \frac{V_{\text{Eff}}}{t \cdot V_{\text{Cult}}}$$

Here,  $V_{\text{Eff}}$  is the measured effluent volume,  $t$  is the time that has passed since the last sampling and  $V_{\text{Cult}}$  is the culture volume. At steady state, the growth rate equals the dilution rate [63], allowing the number of generations  $G$  that have passed to be calculated by:

$$G = t \cdot \frac{D}{\ln 2}$$

### Experimental evolution of batch cultures

Batch culture evolution experiments were started with 10 *bem3Δnrp1Δ* and 2 WT cultures. The cultures were derived from a single *bem3Δnrp1Δ* and a single WT liquid culture initiated from a glycerol stock and grown to saturation for 2 days in YP 2 %D in a roller drum (set at 40 RPM) at 30°C. After the cultures reached saturation, 10 μL of each starter culture was diluted into 10 mL of fresh YP 2 %D and were placed back into the roller drum. The cultures were diluted by 10 μL into 10 mL of fresh YP 2 %D every 24 ± 2 h. After each dilution, the OD at 600 nm of the remaining culture was measured using the same procedure as described above for the chemostat evolution experiment. Because batch cultures involve frequent population bottlenecks that can reduce genetic variation and possibly purge beneficial mutations (Gresham and Dunham, 2014; Gresham and Hong, 2014), it might take longer for an adaptive mutation to settle in the population. To compensate for this effect, the number of generations that the populations were evolved in a batch culture setting was increased to 300 generations (an additional 230 generations compared to the populations evolved in a continuous culture).

### Growth curve measurements

Growth curves were obtained by measurements using a plate reader (Tecan Infinite 200 Pro). Cells were inoculated from a glycerol stock in YP 0.1 %D liquid media and grown to saturation for 2 days in a roller drum at 30°C. On the day of the measurement, the saturated cultures were diluted 1000X into either fresh YP 0.1 %D or fresh YP 2 %D, depending on whether we wanted to measure the doubling time before ( $T_{\text{PRE-Shift}}$ ) or after ( $T_{\text{POST-Shift}}$ ) the diauxic shift. A total of 100 μL of this culture was pipetted into each well of a sterile 96-well plate (Nunc™ Edge 2.0, Thermo Scientific™) with the edge moats filled with 1.7 mL of sterile H<sub>2</sub>O. Each plate contained multiple technical replicates of each sample. As a control for contamination and to allow for background subtraction for

downstream processing, 8 wells were filled with blank medium. Measurements were taken during incubation at 30°C in the plate reader using the following protocol: First, the cells were shaken for 1000 s (linear shaking, 1 mm amplitude) without measurement. After this, the absorbance of each well was measured every 7 min with intermittent shaking (260 s, linear, 1 mm amplitude) for 48 h.

### Growth parameter calculations

Doubling times for pre-diauxic ( $T_{\text{PRE-Shift}}$ ) and an post-diauxic ( $T_{\text{POST-Shift}}$ ) growth were extracted from the growth curve measurement in YP 2 %D and YP 0.1 %D, respectively. First, the measured OD values were blanked using the time average value of one of the wells containing blank media. Then, the data was converted to semi-log data by taking the natural logarithm of the blanked OD values. A home written MATLAB script was used to fit a line to the linear portion of the semi-log data to obtain the growth rate during pre-diauxic or post-diauxic growth. These growth rates were converted into doubling times using the following relation:

$$T_d = \frac{\ln 2}{\mu}$$

where  $T_d$  is the doubling time corresponding to the growth rate  $\mu$  obtained from the slope of the linear fit.

### Microscopy and microfluidics

Cells were grown to log phase in SC media containing 2% dextrose. Clumps of cells were dissociated prior to imaging by sonicating (Q500 Sonicator, QSonica) in a sealed Eppendorf tube using a cup horn at 70% amplitude for 2 min (cycle of 30 s pulse on, 15 s pulse off). After sonication, each sample was diluted to the same optical density in fresh Synthetic Complete media containing 2% dextrose. Cells were trapped in a microfluidic culture chamber (CellASIC ONIX Y04C-02, Merck–Millipore) after flushing the culture chambers with fresh media for 20 min using a pressure of 8 psi. Brightfield images were taken with a Nikon Eclipse Ti-E inverted Microscope using a 60x objective (Plan Apo λ 60X oil, NA: 1.40) with 1 min intervals. During imaging, cells were maintained in a constant flow of media using a pressure of 1 psi. Cells were subjected to a media switch by changing from an inlet with SC media containing 2% dextrose to an inlet with SC media with 3% ethanol after 8 h of imaging.

### DNA extraction, Illumina library preparation, and whole genome sequencing

We extracted genomic DNA from liquid cultures grown for two overnights for each of the 16 chemostat samples, 10 serial dilution samples and a non-evolved yLL132a ancestor with the MasterPure Yeast DNA Purification Kit (Epicentre, Madison, WI, USA) following the manufacturer's protocol. We included a RNase



A (Qiagen, Hilden, Germany) treatment step in the protocol and collected DNA in a final volume up to 30  $\mu$ L H<sub>2</sub>O. We pooled up to three extractions per sample using the Genomic DNA clean and Concentrator kit (Zymo Research, Irvine, CA, USA), following the supplied protocol. We eluted DNA in a final volume of 30  $\mu$ L. We assessed DNA quality by 0.8 % agarose gel electrophoresis and quantity by fluorometry using a Qubit 4.0 Fluorometer (Invitrogen, Carlsbad, CA, USA). Samples were individually barcoded and pooled into a single library with the NEB Next Ultra DNA Library Prep Kit (New England Biolabs, Ipswich, MA, USA) and sequenced on a HiSeq machine (Illumina, San Diego, CA, USA) by Novogene (Beijing, China).

## WGS data analysis

We first checked raw paired-end reads (150 bp) for quality with the FASTQC toolkit (version 0.11.7).<sup>1</sup> We removed low quality ends (Quality scores <20; and first 9 bases of all reads), and removed duplicates with the FastX toolkit (version 0.0.14).<sup>2</sup> We downloaded the R64-1-1 *S. cerevisiae* genome from the Saccharomyces Genome Database (SGD)<sup>3</sup> and used it as our reference. We indexed the reference genome with the Burrows-Wheeler Aligner [BWA; version 0.7.17; (Li and Durbin, 2010)], and SAMtools [version 1.8; (Li and Durbin, 2009; Li, 2011)], and generated a dictionary with Picard (version 2.18.5).<sup>4</sup> We mapped sequences from all samples individually to the reference with BWA-MEM sorted and indexed mapped reads into a BAM file with SAMtools. We performed multisample SNP calling and additional indexing with SAMtools and BCFtools (version 1.8). We plotted and checked statistics, e.g., TS/TV and quality of sites and read depth, with BCFtools. These statistics were used to filter out SNPs and Indels with low quality sites (QUAL > 30), low read depth (DP > 20), and variants in close proximity to gaps (SnpGAP 10). We annotated the VCF file with snpEff [version 4.3T; (Cingolani et al., 2012)] with R64-1-1.86. We then retrieved variants (SNPs and indels) of interest through comparison of variants between the reference strain, the ancestor strains, and the evolved strains. We excluded variants that were different between R64 and all our W303 samples, as these merely display differences between the two genetic backgrounds [see e.g., (Ralsler et al., 2012)]. Synonymous variants, variants in non-coding regions, and stop retained variants were excluded. Mutations in telomeric regions and in Long Terminal Repeats (LTRs) were excluded from analysis due to the natural variation that occurs in the genomic sequence of these regions. To find causative mutations, we looked for genes that mutated in at least two evolved lines, excluding those that appeared only in the mutant line(s) from one environment and the wild-type line(s) of the other environment. From the resulting list of genes, genes corresponding to dubious or uncharacterized Open Reading Frames (ORFs) were removed according to their description on SGD. Two genes (*RPS29B* and *ECM33*) had acquired the same

mutation across all 22 parallel evolved *bem3 $\Delta$ npr1 $\Delta$*  lines that swepted the population, suggesting that these mutations were acquired in the ancestor before the different cell lines were split. Although these mutations might have some fitness benefit in the *bem3 $\Delta$ npr1 $\Delta$*  background, they do not explain the adaptation we observe during our evolution experiments and we therefore excluded them from further analysis. We used the OncoPrint function from the ComplexHeatmap package (Gu et al., 2016) available in R (version 4.2.3) to visualize the relevant mutations in our evolved lines as a heatmap.

## Data availability statement

The data presented in this study are available under the CC0 license in the 4TU.ResearchData repository: <https://doi.org/10.4121/01c1cf07-870a-4bc5-8b04-7df0919e0304.v1>.

## Author contributions

LL and EK designed the research and wrote the manuscript. EK, ED, and LI executed the research. All authors contributed to the article and approved the submitted version.

## Funding

LL and EK gratefully acknowledge funding from the European Research Council (ERC) under the European Union's Horizon 2020 research and innovation programme (Grant agreement No. 758132).

## Conflict of interest

The authors declare that the research was conducted in the absence of any commercial or financial relationships that could be construed as a potential conflict of interest.

## Publisher's note

All claims expressed in this article are solely those of the authors and do not necessarily represent those of their affiliated organizations, or those of the publisher, the editors and the reviewers. Any product that may be evaluated in this article, or claim that may be made by its manufacturer, is not guaranteed or endorsed by the publisher.

## Supplementary material

The Supplementary Material for this article can be found online at: <https://www.frontiersin.org/articles/10.3389/fmicb.2023.1076570/full#supplementary-material>

<sup>1</sup> <https://www.bioinformatics.babraham.ac.uk/projects/fastqc/>

<sup>2</sup> [http://hannonlab.cshl.edu/fastx\\_toolkit/](http://hannonlab.cshl.edu/fastx_toolkit/)

<sup>3</sup> [www.yeastgenome.org](http://www.yeastgenome.org) (accessed September, 2018)

<sup>4</sup> <https://broadinstitute.github.io/picard/>

## References

- Agrawal, A. F., and Stinchcombe, J. R. (2009). How much do genetic covariances alter the rate of adaptation? *Proc. Biol. Sci.* 276, 1183–1191. doi: 10.1098/rspb.2008.1671
- Ahn, S. H., Tobe, B. T., Fitz Gerald, J. N., Anderson, S. L., Acurio, A., and Kron, S. J. (2001). Enhanced cell polarity in mutants of the budding yeast cyclin-dependent kinase Cdc28p. *Mol. Biol. Cell* 12, 3589–3600. doi: 10.1091/mbc.12.11.3589
- Amberg, D. C., Basart, E., and Botstein, D. (1995). Defining protein interactions with yeast actin in vivo. *Nat. Struct. Biol.* 2, 28–35. doi: 10.1038/nsb0195-28
- Austad, S. N., and Hoffman, J. M. (2018). Is antagonistic pleiotropy ubiquitous in aging biology? *Evol. Med. Public Health* 2018, 287–294. doi: 10.1093/emph/eoy033
- Balguerie, A., Bagnat, M., Bonneau, M., Aigle, M., and Breton, A. M. (2002). Rvs161p and sphingolipids are required for actin repolarization following salt stress. *Eukaryot Cell* 1, 1021–1031. doi: 10.1128/ec.1.6.1021-1031.2002
- Bauer, F., Urdaci, M., Aigle, M., and Crouzet, M. (1993). Alteration of a yeast SH3 protein leads to conditional viability with defects in cytoskeletal and budding patterns. *Mol. Cell Biol.* 13, 5070–5084. doi: 10.1128/mcb.13.8.5070-5084.1993
- Bi, E., and Park, H. O. (2012). Cell polarization and cytokinesis in budding yeast. *Genetics* 191, 347–387. doi: 10.1534/genetics.111.132886
- Brauer, M. J., Saldanha, A. J., Dolinski, K., and Botstein, D. (2005). Homeostatic adjustment and metabolic remodeling in glucose-limited yeast cultures. *Mol. Biol. Cell* 16, 2503–2517. doi: 10.1091/mbc.e04-11-0968
- Breton, A. M., and Aigle, M. (1998). Genetic and functional relationship between Rvsp, myosin and actin in *Saccharomyces cerevisiae*. *Curr. Genet.* 34, 280–286. doi: 10.1007/s002940050397
- Broach, J. R. (2012). Nutritional control of growth and development in yeast. *Genetics* 192, 73–105. doi: 10.1534/genetics.111.135731
- Buchan, J. R., Muhlad, D., and Parker, R. (2008). P bodies promote stress granule assembly in *Saccharomyces cerevisiae*. *J. Cell Biol.* 183, 441–455. doi: 10.1083/jcb.200807043
- Chiou, J. G., Balasubramanian, M. K., and Lew, D. J. (2017). Cell polarity in yeast. *Annu. Rev. Cell Dev. Biol.* 33, 77–101. doi: 10.1146/annurev-cellbio-100616-060856
- Cingolani, P., Platts, A., Wang le, L., Coon, M., Nguyen, T., Wang, L., et al. (2012). A program for annotating and predicting the effects of single nucleotide polymorphisms, SnpEff: SNPs in the genome of *Drosophila melanogaster* strain w1118; iso-2; iso-3. *Fly (Austin)* 6, 80–92. doi: 10.4161/fly.19695
- Crouzet, M., Urdaci, M., Dulau, L., and Aigle, M. (1991). Yeast mutant affected for viability upon nutrient starvation: characterization and cloning of the RVS161 gene. *Yeast* 7, 727–743. doi: 10.1002/yea.320070708
- Cullen, P. J., and Sprague, G. F. Jr. (2012). The regulation of filamentous growth in yeast. *Genetics* 190, 23–49. doi: 10.1534/genetics.111.127456
- De Virgilio, C., and Loewith, R. (2006). Cell growth control: little eukaryotes make big contributions. *Oncogene* 25, 6392–6415. doi: 10.1038/sj.onc.1209884
- Desfarges, L., Durrrens, P., Juguelin, H., Cassagne, C., Bonneau, M., and Aigle, M. (1993). Yeast mutants affected in viability upon starvation have a modified phospholipid composition. *Yeast* 9, 267–277. doi: 10.1002/yea.320090306
- Dickinson, J. R. (2008). Filament formation in *Saccharomyces cerevisiae*—a review. *Folia Microbiol.* 53, 3–14. doi: 10.1007/s12223-008-0001-6
- Dickson, R. C., Sumanasekera, C., and Lester, R. L. (2006). Functions and metabolism of sphingolipids in *Saccharomyces cerevisiae*. *Progr. Lipid Res.* 45, 447–465. doi: 10.1016/j.plipres.2006.03.004
- Etienne-Manneville, S. (2004). Cdc42 - the centre of polarity. *J. Cell Sci.* 117, 1291–1300. doi: 10.1242/jcs.01115
- Fisher, R. A. (1930). *The genetical theory of natural selection*. Oxford: Clarendon Press.
- Fraebel, D. T., Gowda, K., Mani, M., and Kuehn, S. (2020). Evolution of generalists by phenotypic plasticity. *iScience* 23:101678. doi: 10.1016/j.isci.2020.101678
- Fraebel, D. T., Mickalide, H., Schnitkey, D., Merritt, J., Kuhlman, T. E., and Kuehn, S. (2017). Environment determines evolutionary trajectory in a constrained phenotypic space. *Elife* 6:e24669. doi: 10.7554/eLife.24669
- Galdieri, L., Mehrotra, S., Yu, S., and Vancura, A. (2010). Transcriptional regulation in yeast during diauxic shift and stationary phase. *Omics* 14, 629–638. doi: 10.1089/omi.2010.0069
- Granek, J. A., Kayıkcı, Ö., and Magwene, P. M. (2011). Pleiotropic signaling pathways orchestrate yeast development. *Curr. Opin. Microbiol.* 14, 676–681. doi: 10.1016/j.mib.2011.09.004
- Gresham, D., and Dunham, M. J. (2014). The enduring utility of continuous culturing in experimental evolution. *Genomics* 104(6 Pt. A), 399–405. doi: 10.1016/j.jygeno.2014.09.015
- Gresham, D., and Hong, J. (2014). The functional basis of adaptive evolution in chemostats. *FEMS Microbiol. Rev.* 39, 2–16. doi: 10.1111/1574-6976.12082
- Gu, Z., Eils, R., and Schlesner, M. (2016). Complex heatmaps reveal patterns and correlations in multidimensional genomic data. *Bioinformatics* 32, 2847–2849. doi: 10.1093/bioinformatics/btw313
- Hartwell, L. H., Hopfield, J. J., Leibler, S., and Murray, A. W. (1999). From molecular to modular cell biology. *Nature* 402, C47–C52. doi: 10.1038/35011540
- Ho, J., and Bretscher, A. (2001). Ras regulates the polarity of the yeast actin cytoskeleton through the stress response pathway. *Mol. Biol. Cell* 12, 1541–1555. doi: 10.1091/mbc.12.6.1541
- Homoto, S., and Izawa, S. (2018). Persistent actin depolarization caused by ethanol induces the formation of multiple small cortical septin rings in yeast. *J. Cell Sci.* 131:jcs217091. doi: 10.1242/jcs.217091
- Hong, J., and Gresham, D. (2014). Molecular specificity, convergence and constraint shape adaptive evolution in nutrient-poor environments. *PLoS Genet.* 10:e1004041. doi: 10.1371/journal.pgen.1004041
- Jerison, E. R., Nguyen Ba, A. N., Desai, M. M., and Kryazhinskiy, S. (2020). Chance and necessity in the pleiotropic consequences of adaptation for budding yeast. *Nat. Ecol. Evol.* 4, 601–611. doi: 10.1038/s41559-020-1128-3
- Kahl Lisa, J., Eckart Kelly, N., Morales Diana, K., Price-Whelan, A., and Dietrich Lars, E. P. (2022). Light/dark and temperature cycling modulate metabolic electron flow in *Pseudomonas aeruginosa* biofilms. *mBio* 13, e01407–01422. doi: 10.1128/mbio.01407-22
- Kaida, D., Yashiroda, H., Toh-e, A., and Kikuchi, Y. (2002). Yeast Whi2 and Prs1-phosphatase form a complex and regulate STRE-mediated gene expression. *Genes Cells* 7, 543–552. doi: 10.1046/j.1365-2443.2002.00538.x
- Kirschner, M., and Gerhart, J. (1998). Evolvability. *Proc. Natl. Acad. Sci. U.S.A.* 95, 8420–8427. doi: 10.1073/pnas.95.15.8420
- Kroschwald, S., Maharana, S., Mateju, D., Malinowska, L., Nüske, E., Poser, I., et al. (2015). Promiscuous interactions and protein disaggregases determine the material state of stress-inducible RNP granules. *Elife* 4:e06807. doi: 10.7554/eLife.06807
- Kvitek, D. J., and Sherlock, G. (2013). Whole genome, whole population sequencing reveals that loss of signaling networks is the major adaptive strategy in a constant environment. *PLoS Genet.* 9:e1003972. doi: 10.1371/journal.pgen.1003972
- Laan, L., Koschwanez, J. H., and Murray, A. W. (2015). Evolutionary adaptation after crippling cell polarization follows reproducible trajectories. *Elife* 4:e09638
- Lambros, M., Pechuan-Jorge, X., Biro, D., Ye, K., and Bergman, A. (2021). Emerging adaptive strategies under temperature fluctuations in a laboratory evolution experiment of *Escherichia coli*. *Front. Microbiol.* 12:724982. doi: 10.3389/fmicb.2021.724982
- Leadsham, J. E., Kotiadis, V. N., Tarrant, D. J., and Gourlay, C. W. (2010). Apoptosis and the yeast actin cytoskeleton. *Cell Death Different.* 17, 754–762. doi: 10.1038/cdd.2009.196
- Lew, D. J., and Reed, S. I. (1993). Morphogenesis in the yeast cell cycle: regulation by Cdc28 and cyclins. *J. Cell Biol.* 120, 1305–1320. doi: 10.1083/jcb.120.6.1305
- Li, H. (2011). A statistical framework for SNP calling, mutation discovery, association mapping and population genetical parameter estimation from sequencing data. *Bioinformatics* 27, 2987–2993. doi: 10.1093/bioinformatics/btr509
- Li, H., and Durbin, R. (2009). Fast and accurate short read alignment with Burrows-Wheeler transform. *Bioinformatics* 25, 1754–1760. doi: 10.1093/bioinformatics/btp324
- Li, H., and Durbin, R. (2010). Fast and accurate long-read alignment with Burrows-Wheeler transform. *Bioinformatics* 26, 589–595. doi: 10.1093/bioinformatics/btp698
- MacLean, R. C., Bell, G., and Rainey, P. B. (2004). The evolution of a pleiotropic fitness tradeoff in *Pseudomonas fluorescens*. *Proc. Natl. Acad. Sci. U.S.A.* 101, 8072–8077. doi: 10.1073/pnas.0307195101
- Martin, S. G., and Arkowitz, R. A. (2014). Cell polarization in budding and fission yeasts. *FEMS Microbiol. Rev.* 38, 228–253. doi: 10.1111/1574-6976.12055
- Mauro, A. A., and Ghalambor, C. K. (2020). Trade-offs, pleiotropy, and shared molecular pathways: a unified view of constraints on adaptation. *Integr. Comp. Biol.* 60, 332–347. doi: 10.1093/icb/icaa056
- Miller, A. W., Befort, C., Kerr, E. O., and Dunham, M. J. (2013). Design and use of multiplexed chemostat arrays. *J. Visual. Exp.* 72:e50262. doi: 10.3791/50262
- Morimoto, Y., and Tani, M. (2015). Synthesis of mannosylinositol phosphorylceramides is involved in maintenance of cell integrity of yeast *Saccharomyces cerevisiae*. *Mol. Microbiol.* 95, 706–722. doi: 10.1111/mmi.12896
- Munn, A. L., Stevenson, B. J., Geli, M. I., and Riezman, H. (1995). end5, end6, and end7: mutations that cause actin delocalization and block the internalization step of endocytosis in *Saccharomyces cerevisiae*. *Mol. Biol. Cell* 6, 1721–1742. doi: 10.1091/mbc.6.12.1721

- Mutavchiev, D. R., Leda, M., and Sawin, K. E. (2016). Remodeling of the fission yeast Cdc42 Cell-polarity module via the Sty1 p38 Stress-activated protein kinase pathway. *Curr. Biol.* 26, 2921–2928. doi: 10.1016/j.cub.2016.08.048
- Orr, H. A. (2000). Adaptation and the cost of complexity. *Evolution* 54, 13–20. doi: 10.1111/j.0014-3820.2000.tb00002.x
- Paaby, A. B., and Rockman, M. V. (2013). The many faces of pleiotropy. *Trends Genet.* 29, 66–73. doi: 10.1016/j.tig.2012.10.010
- Phillips, P. C. (2008). Epistasis — the essential role of gene interactions in the structure and evolution of genetic systems. *Nat. Rev. Genet.* 9, 855–867. doi: 10.1038/nrg2452
- Pioli, M. E., Blanchette, J. O., and Jabbarzadeh, E. (2019). Polarity as a physiological modulator of cell function. *Front. Biosci.* 24:451–462. doi: 10.2741/4728
- Prunskaitė-Hyryläinen, R., Shan, J., Railo, A., Heinonen, K. M., Miinalainen, I., Yan, W., et al. (2014). Wnt4, a pleiotropic signal for controlling cell polarity, basement membrane integrity, and antimüllerian hormone expression during oocyte maturation in the female follicle. *FASEB J.* 28, 1568–1581. doi: 10.1096/fj.13-233247
- Pruyne, D., and Bretscher, A. (2000). Polarization of cell growth in yeast. *J. Cell Sci.* 113, 571–585. doi: 10.1242/jcs.113.4.571
- Qian, W., Ma, D., Xiao, C., Wang, Z., and Zhang, J. (2012). The genomic landscape and evolutionary resolution of antagonistic pleiotropy in yeast. *Cell Rep.* 2, 1399–1410. doi: 10.1016/j.celrep.2012.09.017
- Radcliffe, P., Trevethick, J., Tyers, M., and Sudbery, P. (1997). Deregulation of CLN1 and CLN2 in the *Saccharomyces cerevisiae* whi2 mutant. *Yeast* 13, 707–715. doi: 10.1002/(sici)1097-0061(19970630)13:8<707::Aid-yea130<3.0.Co;2-9
- Ralsler, M., Kuhl, H., Ralsler, M., Werber, M., Lehrach, H., Breitenbach, M., et al. (2012). The *Saccharomyces cerevisiae* W303-K6001 cross-platform genome sequence: insights into ancestry and physiology of a laboratory mutt. *Open Biol.* 2:120093. doi: 10.1098/rsob.120093
- Rose, M., and Charlesworth, B. (1980). A test of evolutionary theories of senescence. *Nature* 287, 141–142. doi: 10.1038/287141a0
- Saito, H. (2010). Regulation of cross-talk in yeast MAPK signaling pathways. *Curr. Opin. Microbiol.* 13, 677–683. doi: 10.1016/j.mib.2010.09.001
- Salat-Canela, C., Carmona, M., Martín-García, R., Pérez, P., Ayté, J., and Hidalgo, E. (2021). Stress-dependent inhibition of polarized cell growth through unbalancing the GEF/GAP regulation of Cdc42. *Cell Rep.* 37:109951. doi: 10.1016/j.celrep.2021.109951
- Saul, D. J., Walton, E. F., Sudbery, P. E., and Carter, B. L. A. (1985). *Saccharomyces cerevisiae* whi2 mutants in stationary phase retain the properties of exponentially growing cells. *Microbiology* 131, 2245–2251. doi: 10.1099/00221287-131-9-2245
- Sivadon, P., Bauer, F., Aigle, M., and Crouzet, M. (1995). Actin cytoskeleton and budding pattern are altered in the yeast rvs161 mutant: the Rvs161 protein shares common domains with the brain protein amphiphysin. *Mol. Gen. Genet.* 246, 485–495. doi: 10.1007/bf00290452
- Sivadon, P., Crouzet, M., and Aigle, M. (1997). Functional assessment of the yeast Rvs161 and Rvs167 protein domains. *FEBS Lett.* 417, 21–27. doi: 10.1016/S0014-5793(97)01248-9
- Smethurst, D. G. J., Dawes, I. W., and Gourlay, C. W. (2014). Actin – a biosensor that determines cell fate in yeasts. *FEMS Yeast Res.* 14, 89–95. doi: 10.1111/1567-1364.12119
- Sudbery, P. E., Goodey, A. R., and Carter, B. L. (1980). Genes which control cell proliferation in the yeast *Saccharomyces cerevisiae*. *Nature* 288, 401–404. doi: 10.1038/288401a0
- Thevisen, K., Cammue, B. P. A., Lemaire, K., Winderickx, J., Dickson, R. C., Lester, R. L., et al. (2000). A gene encoding a sphingolipid biosynthesis enzyme determines the sensitivity of *Saccharomyces cerevisiae* to an antifungal plant defensin from dahlia (*Dahlia merckii*). *Proc. Natl. Acad. Sci. U.S.A.* 97:9531. doi: 10.1073/pnas.160077797
- Thompson, B. J. (2013). Cell polarity: models and mechanisms from yeast, worms and flies. *Development* 140, 13–21. doi: 10.1242/dev.083634
- Uesono, Y., Ashe, M. P., and Toh-e, A. (2004). Simultaneous yet independent regulation of actin cytoskeletal organization and translation initiation by glucose in *Saccharomyces cerevisiae*. *Mol. Biol. Cell* 15, 1544–1556. doi: 10.1091/mbc.e03-12-0877
- Vasicova, P., Rinnerthaler, M., Haskova, D., Novakova, L., Malcova, I., Breitenbach, M., et al. (2016). Formaldehyde fixation is detrimental to actin cables in glucose-depleted *S. cerevisiae* cells. *Microb. Cell* 3, 206–214. doi: 10.15698/mic2016.05.499
- Wagner, G. P., and Altenberg, L. (1996). Perspective: complex adaptations and the evolution of evolvability. *Evolution* 50, 967–976. doi: 10.1111/j.1558-5646.1996.tb02339.x
- Wagner, G. P., and Zhang, J. (2011). The pleiotropic structure of the genotype–phenotype map: the evolvability of complex organisms. *Nat. Rev. Genet.* 12, 204–213. doi: 10.1038/nrg2949
- Waltermann, C., and Klipp, E. (2010). Signal integration in budding yeast. *Biochem. Soc. Trans.* 38, 1257–1264. doi: 10.1042/bst0381257
- Waxman, D., and Peck, J. R. (1998). Pleiotropy and the preservation of perfection. *Science* 279, 1210–1213.
- Wein, T., and Dagan, T. (2019). The effect of population bottleneck size and selective regime on genetic diversity and evolvability in bacteria. *Genome Biol. Evol.* 11, 3283–3290. doi: 10.1093/gbe/evz243
- Welch, J. J., and Waxman, D. (2003). Modularity and the cost of complexity. *Evolution* 57, 1723–1734. doi: 10.1111/j.0014-3820.2003.tb00581.x
- Welch, M., Holtzman, D., and Drubin, D. (1994). The yeast actin cytoskeleton. *Curr. Opin. Cell Biol.* 6, 110–119.
- Yoshida, S., and Pellman, D. (2008). Plugging the GAP between cell polarity and cell cycle. *EMBO Rep.* 9, 39–41. doi: 10.1038/sj.embor.7401142
- Zou, L., Sriswasdi, S., Ross, B., Missiuro, P. V., Liu, J., and Ge, H. (2008). Systematic analysis of pleiotropy in *C. elegans* early embryogenesis. *PLoS Comput. Biol.* 4:e1000003. doi: 10.1371/journal.pcbi.1000003

# Frontiers in Cell and Developmental Biology

Explores the fundamental biological processes of life, covering intracellular and extracellular dynamics.

The world's most cited developmental biology journal, advancing our understanding of the fundamental processes of life. It explores a wide spectrum of cell and developmental biology, covering intracellular and extracellular dynamics.

## Discover the latest Research Topics

[See more →](#)

### Frontiers

Avenue du Tribunal-Fédéral 34  
1005 Lausanne, Switzerland  
[frontiersin.org](https://frontiersin.org)

### Contact us

+41 (0)21 510 17 00  
[frontiersin.org/about/contact](https://frontiersin.org/about/contact)

